Department of Civil and Environmental Engineering
Stanford University

Seismic Demands for Performance Evaluation of Steel Moment Resisting Frame Structures

by
Akshay Gupta
and
Helmut Krawinkler

Report No. 132

June 1999

The John A. Blume Earthquake Engineering Center was established to promote research and education in earthquake engineering. Through its activities our understanding of earthquakes and their effects on mankind's facilities and structures is improving. The Center conducts research, provides instruction, publishes reports and articles, conducts seminar and conferences, and provides financial support for students. The Center is named for Dr. John A. Blume, a well-known consulting engineer and Stanford alumnus.

Address:

The John A. Blume Earthquake Engineering Center
Department of Civil and Environmental Engineering
Stanford University
Stanford CA 94305-4020

(650) 723-4150
(650) 725-9755 (fax)
earthquake @ce. stanford.edu
http://blume.stanford.edu

SEISMIC DEMANDS FOR PERFORMANCE EVALUATION OF STEEL MOMENT RESISTING FRAME STRUCTURES

(SAC Task 5.4.3)

by

Akshay Gupta

and

Helmut Krawinkler

The John A. Blume Earthquake Engineering Center
Department of Civil and Environmental Engineering
Stanford University
Stanford, CA 94305-4020

A report on research sponsored by

The SAC Joint Venture

Report No. 132

June 1999

ABSTRACT

The objective of this work is to improve the knowledge base on the seismic behavior of typical steel moment resisting frame structures, considering regions of different seismicity and sets of ground motions of various intensities and frequency characteristics. The emphasis is on behavior assessment and quantification of global and local force and deformation demands for different hazard levels. The research is intended to contribute to progress in the development of performance-based seismic design and evaluation of steel moment resisting frame structures.

The behavior and response of different height structures in Los Angeles, Seattle, and Boston are studied. Analytical methods and models of various complexities are utilized and evaluated for their ability to predict global and local performance. A sensitivity study is performed on the effects of analysis assumptions on demand predictions. System level behavior characteristics and seismic demands are studied from the perspective of performance at different hazard levels. Local behavior characteristics and element deformation demands are evaluated for various designs, with consideration given to subjective design decisions, variations in material properties, and different types of beam-to-column connections. A simplified procedure for estimation of global and local seismic demands is developed to facilitate decision making in the conceptual design process.

This work is concerned only with the behavior of “ductile” structures; fracturing of connections is not considered. The results from this study demonstrate that for ductile code conforming structures the global seismic demands, measured in terms of story drifts, are mostly within the range of acceptable performance at the various hazard levels – with one important exception. This exception occurs when severe ground motions drive a

structure into the stability sensitive range, in which case P-delta effects constitute a potential collapse hazard. Local (element) seismic demands are found to be very sensitive to a multitude of factors, which may result in a concentration of plastic deformation demands in either the beams or the panel zones, or in sharing of demands between these two elements and possibly also the columns.

ACKNOWLEDGEMENTS

This report is a reproduction of the senior author's Ph.D. dissertation. The work reported herein is part of the FEMA sponsored SAC effort intended to understand, quantify, and improve the seismic behavior of steel moment-resisting frame structures with welded connections. Many individuals and research teams have participated in this effort. The cooperate spirit among the team members facilitated coordination and the sharing of information, and made it possible to write individual reports which, in combination, will form a comprehensive knowledge base on SMRF structures.

The authors would like to sincerely thank Professor Allin Cornell for his valuable input to the work. The feedback provided by the SAC management team is much appreciated. Several Stanford students, present and former, have provided assistance and valuable input. In particular, the help provided by Dr. Pasan Seneviratna is much appreciated.

This work was conducted pursuant to a contract with the Federal Emergency Management Agency (FEMA) through the SAC Joint Venture. SAC is a partnership of the Structural Engineers Association of California, the Applied Technology Council, and the California Universities for Research in Earthquake Engineering. The opinions expressed in this report are those of the authors. No warranty is offered with regard to the results, findings and recommendations contained herein, either by FEMA, the SAC Joint Venture, the individual joint venture partners, their directors, members or employees, or the authors of this publication. These organizations and individuals do not assume any legal liability or responsibility for the accuracy, completeness, or usefulness of any of the information, product or processes included in this publication.

TABLE OF CONTENTS

CHAPTER 1

INTRODUCTION

1.1 Motivation for Study

A great number of modern mid- and high rise buildings have steel moment resisting frames (SMRFs) as the primary lateral load resisting system. This type of construction was considered the safest one for earthquake resistance, as steel elements are expected to be able to sustain large plastic deformations in bending and shear. This confidence was greatly shaken when during the 1994 Northridge earthquake more than 150 steel moment resisting frame structures suffered damage, primarily in the form of brittle fractures at welded beam-to-column connections. Structural damage and collapses of steel structures during the 1995 Kobe earthquake further highlighted the severity of the problem. These two events exposed critical issues concerning the seismic behavior of code compliant SMRF structures. The issues can be broadly addressed with the following three questions:

- Why was the observed behavior of SMRF structures so different from what is generally expected from code compliant designs,
- What level of seismic demands can be expected for the very large number of existing SMRF structures in different geographic locations and under different levels of ground shaking, and
- How large is the decrease in structural safety at various seismic hazard levels due to potential connection fractures?

Answers to these questions are needed in order to assess the necessity for corrective actions for existing SMRF structures and to develop improved designs for new structures.

The answers must be based on an in-depth understanding of the basic factors controlling the seismic behavior of SMRF structures. They should provide an estimate of the structural performance and reliability for the very large inventory of existing SMRF structures, in order to facilitate the decision process for the seismic rehabilitation of these structures to acceptable performance levels. Therein lies a great challenge, as even though the majority of SMRF structures conform to conceptually similar seismic design guidelines, there exists a very large variability in designs for these structures caused by prescriptive code procedures and subjective design decisions. Thus, there is a pressing need for a systematic evaluation of SMRF structures in order to better understand and bound the core structural behavior characteristics and address performance expectations at different hazard levels.

Current seismic design codes appear to fulfill their main objective; that to provide adequate life safety in structures. This argument is supported by the absence of structural collapses of SMRF structures in past seismic events in the US. Providing life-safety remains the most critical aspect for any design process, but that by itself is no longer sufficient. Due to changing business and technological trends, buildings are becoming storehouses of critical operations and contents. The socio-economic impact of business interruption or damage may far outweigh the cost of the structural system. Thus, the economic and social implications of unsatisfactory performance of a structure during a seismic event need to be incorporated in future seismic design and evaluation methodologies. The performance demanded from a structure is, therefore, now being related to the function of the structure and to various hazard levels on account of cost-benefit considerations. The development of this new process also requires, as its basic framework, a detailed understanding of the system and element behavior and an estimate of the response (seismic demands) at various hazard levels.

This research draws motivation from the presented issues, and addresses both short-term objectives (related to the solution to the SMRF problems encountered in recent earthquakes) and long-term objectives (related to the development of an improved design and evaluation methodology). The study provides a detailed assessment of behavior, response, and performance of typical ductile SMRF structures, and develops a simplified demand estimation procedure to assist in the evaluation (and conceptual design) of SMRF structures. The study addresses and quantifies issues intrinsic to the development of a performance-based seismic design and evaluation procedure for steel moment resisting frame structures.

1.2 Objectives and Scope

The primary focus of this study is on the development of an in-depth understanding of the inelastic seismic behavior of typical SMRF structures. Important issues having a significant effect on the behavior and response of SMRF structures (e.g., structure P-delta effects, influence of accuracy of analytical modeling on structural response prediction, influence of relative element strength at connections, column force demands, effects of modified beam-to-column connection details, among others) are identified, addressed, and quantified. The seismic demands at the structure and element levels are evaluated for a wide range of SMRF structures (different heights, geographic locations, and design criteria) subjected to suites of ground motions representative of different hazard levels at the various locations. The information generated through nonlinear dynamic analysis is used for performance assessment of these structures, and forms the basis for a simplified seismic demand estimation procedure in which the spectral displacement characteristics of the ground motion are related to the element level inelastic deformation demands for the structure. The information generated on the story level maximum and cumulative drift angle demands is also used for the development of a loading history for experimental investigations of beam-column subassemblies (separate report, Krawinkler et al., 1998).

The behavior, response, and performance assessment is carried out for a set of nine model buildings (3-, 9-, and 20-story buildings, located in Los Angeles, Seattle, and Boston). The structural systems for these buildings have been designed by leading consulting engineering companies and are deemed to be representative of typical design practices followed currently in different parts of the US. At least two designs have been carried out for each building, one according to pre-Northridge practice and one with improved connection details according to FEMA 267 Guidelines (post-Northridge designs). Basic parameters (e.g., configuration, gravity loading, etc.) are common to all locations and are believed to be representative for a great number of existing steel moment resisting frame structures. Thus, seismic evaluation of these structures provides a frame of reference for estimation of seismic demands for typical SMRF structures, and provides basic information for issues to be addressed in current seismic design procedures for improving the performance of new structures. Documentation of the designs of the model buildings is provided in Appendix B.

The structural evaluation is carried out for seven suites of ground motions (3 for Los Angeles, 2 each for Seattle and Boston), representative of hazard levels with a 72 year to 2475 years return period, thereby addressing the behavior and response issues over a wide range of imposed seismic hazard levels. The emphasis is on statistical analysis of seismic demands, however, specific case by case evaluations are also carried out to investigate structural behavior issues in detail. While nonlinear time history analysis, using representative analytical models of the structure, is the basic analysis technique employed for the seismic demand estimation, nonlinear static pushover analysis is employed as a supplemental analysis procedure, especially for behavior evaluation purposes.

The stated objectives of this study necessitated the use of specific structural designs, having the advantage that particular design issues could be addressed in detail. The disadvantage is a loss of generality. However, the tradeoff between generality and "reality" is balanced on account of careful selection of basic design criteria for these structures, and the performed designs being representative of current design practices. The results obtained in this study are, thus, representative for typical steel moment resisting frame structures, and provide partial answers to the three questions asked on page 1. The developed simplified demand estimation methodology is applicable for most steel moment resisting frame structures.

1.3 Outline for Report

In Chapter 2 the issues motivating this study are explored in more detail, within the scope of two larger programs of which this study forms a part. Both programs address the long-term objective of development of a performance-based seismic design and evaluation methodology. One program has as its focus the development of recommendations for improving the reliability of existing and new SMRF structures, while the other has a broader focus on the development of a conceptual seismic design and evaluation methodology.

Chapter 3 summarizes basic behavior and modeling issues for steel moment resisting frame structures at the element and structure levels. Analytical models for the elements (beams, panel zones, and columns) and the structure are discussed, and salient differences between various structural models are identified. The effect of analytical modeling

assumptions on the statistical response of SMRF structures is evaluated in detail in this chapter.

Structure P-delta effects are found to have a potentially severe influence on the response of flexible steel moment resisting frame structures. This issue is investigated in-depth in Chapter 4, using two structures as case studies. The response of the structures is studied under very severe ground motions that induce very large drift demands in the structures. Analytical models of various complexities are evaluated using nonlinear static pushover analysis, nonlinear time history analysis, and "dynamic pushover" analysis, to evaluate the potential for collapse in flexible SMRF structures due to the P-delta effect.

Global and story response parameters for the majority of structures investigated in this study are discussed in Chapter 5. Elastic modal properties, pushover analysis results, and statistical data based on nonlinear time history analysis are presented. The emphasis is on story and roof drift demands and their patterns for structures of different heights, different design details, and in different seismic locations, subjected to varying levels of ground excitation. Cumulative deformation demands and energy demands are also discussed in this chapter. The computed story drift demands are used to assess the performance of these typical structures vis-à-vis currently available guidelines (FEMA 273, 1997). The performance of the structures is also expressed in a probabilistic format using a procedure developed by Cornell (1996a).

Element behavior and deformation demands are discussed in Chapter 6. The major issues relate to the effects of relative element strength on local and global demands. The effect of the use of cover-plated beam flanges and reduced beam sections (RBS) is evaluated. Critical issues controlling the behavior and response of columns (e.g., plastification in columns) and splices is also discussed, as are element level hysteretic energy demands.

Chapter 7 summarizes a simplified demand prediction procedure in which the behavior assessment and demand estimation carried out in the previous chapters is used to develop a formal procedure for relating the elastic spectral displacement demands for the ground motion to the element level inelastic deformation demands for the structure. This process relates the elastic spectral displacement demand at the first mode period of the structure to the roof drift demand for the structure, then to the story drift demands, and finally to the element level deformation demands. The use of nonlinear static

pushover analysis in assisting in this simplified demand estimation approach is explored in-depth in this chapter. Examples evaluating the procedure are also presented.

The computed structural response is affected by a multitude of assumptions at the element and structure level, including strain-hardening , structural damping, and stiffness assumptions. The sensitivity of the computed structural response to various assumptions is evaluated in Chapter 8.

Chapter 9 summarizes the findings of this study, presents conclusions, and identifies issues that need further investigation.

Properties of the ground motions used in this study are summarized in Appendix A, and details and properties pertaining to the structural designs of the model buildings are documented in Appendix B.

CHAPTER 2

SEISMIC DESIGN AND EVALUATION ISSUES

2.1 Introduction

The basic performance objective of designing structures for adequate life-safety while keeping the designs economical has been the backbone of structural engineering practice for many decades. Current design guidelines have served the profession well in fulfilling this basic objective. However, the structural engineering profession has for long also recognized the necessity for seismic designs to provide consistent and predictable performance at various hazard and performance levels. The current design codes and guidelines provide simple seismic design procedures, through the use of empirical factors and simple equations. The performance of the resulting designs, however, cannot be predicted in an equally simple fashion, as the behavior of the structure is a complex interaction of various phenomena, many of which are not adequately captured or represented in the simple design processes.

In addition to the basic performance requirement of life-safety, engineered structures, today, should conform to a variety of different performance objectives depending on the function of the structure. Structures housing critical facilities, operations and businesses, or manufacturing facilities, for which an interruption of operation might result in severe socio-economic consequences need to be designed for different criteria than housing units for which life safety may be the dominant criterion. Thus, a cost-benefit-risk assessment, which considers different hazards and all important tangible and intangible (e.g., business interruption) losses for a facility should control the performance requirements for the structure.

The cost-benefit-risk tradeoff necessitates that structures be designed for different performance objectives, which are linked to the risk associated with the occurrence of different seismic events, i.e., the performance objectives are realizations of generic or user-specified performance levels at different seismic hazard levels. Relations between performance levels and seismic hazard levels for different types of facilities have been proposed in several recent documents [e.g., Vision 2000 (SEAOC, 1995), FEMA 273 (1997), and ATC-40 (1997)].

To implement postulated performance objectives, the seismic design of the structure needs to conform to different structural response states (some of which extend well into the inelastic range), which are related to different hazard levels. Thus, an in-depth knowledge of behavior and response of structures at different levels of seismic excitation, and the ability to predict response with reasonable confidence, become intrinsic for the design of structures in accordance with different performance objectives. In the following section, the work contained in this report is placed in context of a performance based seismic design and analysis framework.

2.2 A Performance Based Seismic Design and Evaluation Framework

The primary objective of performance based seismic engineering is to design, build, and maintain facilities such that they have predictable performance in accordance with pre-defined performance objectives. This process should result in a minimization of earthquake related investment for the structure, over the life of the structure. Many frameworks and guidelines, targeting performance based seismic engineering (PBSE), are available in the literature [e.g., Vision 2000 (SEAOC, 1995), FEMA 273 (1997), ATC-40 (1997), Bertero (1997), Krawinkler (1998), among others], which are similar in concept and vary only in details and terminology.

The basic outline for a PBSE approach is given in Figure 2.1. The process is iterative in nature, and begins with a non-technical definition by the owner for the desired performance (inclusive of special consideration such as vibration control, etc.) of the facility based on a cost-benefit-risk evaluation. This definition needs to be translated into requirements on specific structural response parameters, which control the level of damage to structural and non-structural components, and content. These structure specific technical requirements need to be related to seismic hazard levels, i.e., the

desired performance of the structure is described in terms of various structural response parameters, which may not be the same for different performance levels.

The desired performance at various hazard levels forms the basis for a conceptual design of the structure (structural layout, choice of structural system, preliminary member sizing, etc.). The conceptual design process needs to consider multiple performance levels, with the recognition that different levels could control different aspects of the design. The basis for this design phase is a knowledge base that captures the expected behavior and response of similar structural systems, under seismic excitation of the type expected at the site, for different seismic hazard levels. The knowledge base is founded on experimental and analytical studies, which attempt to capture behavior and response characteristics of similar structural systems and constituent elements as close to reality as possible. Work on the conceptual design development phase is summarized in Nassar and Krawinkler (1991), Bertero and Bertero (1992), Rahnama and Krawinkler (1993), Seneviratna and Krawinkler (1997), among others.

A major challenge in the process of PBSE lies in the ability to evaluate and predict structural and element performance with reasonable confidence. The evaluation of structural response and performance is not only necessary for the design evaluation/modification process, but also for the basic purpose of defining performance levels. The translation of a performance level to an engineering limit state requires a transformation relationship based on the structural system and the severity and characteristics of the seismic input. This transformation function can only be derived from detailed studies, which cover the expected range of structural and seismic characteristics - with due regard to uncertainties. For example, a value of x% story drift can only be related to a collapse prevention performance level for a particular structural system if experimental and analytical studies confirm that beyond x% story drift the stability of the structural system is compromised.

The work discussed in this report focuses on demand evaluation, but its major objective is to increase the knowledge base on which decisions on performance levels and in the conceptual design phase can be based. The emphasis is on the development of an understanding of the behavior, response, and performance of typical steel moment resisting frame structures, designed for different seismic regions, under sets of ground motions representative of different hazard levels.

The framework for this research is outlined in the next section, which also relates the research to a larger project (SAC steel project), the focus of which is on answering the questions asked in Chapter 1. The entire SAC steel project can be seen as a part of the process of development of PBSE as a means for designing economical structures with predictible and reliable performance.

2.2.1 Behavior, Response, and Performance of SMRF Structures

The evaluation of system performance of typical SMRF structures is one of the key objectives of the SAC steel program, which is directed towards reduction of seismic risk for steel moment resisting frame structures. Performance evaluation implies assessment of demands and capacities. The research discussed here is concerned only with the demand side, and assumes that individual elements have unlimited deformation capacity.

Figure 2.2 outlines the framework for this research, wherein the SAC ground motions and model structures form the starting point. Analytical methods and models of different complexities are utilized and evaluated for their ability to predict global and local performance. A sensitivity study is performed on the effects of analysis assumptions on demand predictions. System level behavior characteristics and seismic demands for various hazard levels are studied from the perspective of performance at different levels and with consideration given to design practice in regions of different seismicity. Local behavior characteristics and element deformation demands are evaluated for various designs, with consideration given to subjective design decisions, variations in material properties, and different types of beam-to-column connections. A simplified procedure for estimation of global and local seismic demands is developed to facilitate decision making in the conceptual design process. The research is directed specifically towards the SAC objective of improving the seismic behavior of SMRF structures, but is intended to be also a contribution to progress in the development and implementation of performance-based seismic engineering.

This study focuses on the behavior and demands for ductile SMRF structures with no strength and stiffness degradation in the element characteristics, and disregarding the potential for connection weld fractures. Special ground motion characteristics (e.g., near-fault effects and soft soil effects) are not considered. These aspects are being considered by other research groups within the SAC project. The expectation is that on the

completion of all these studies, significant additions will have been made to the knowledge base needed to understand the behavior and to predict the response of typical steel moment resisting frame structures under ground motions with different characteristics and intensities. This improved knowledge base should permit improved design and evaluation of steel moment resisting frame structures within the context of performance based seismic engineering.

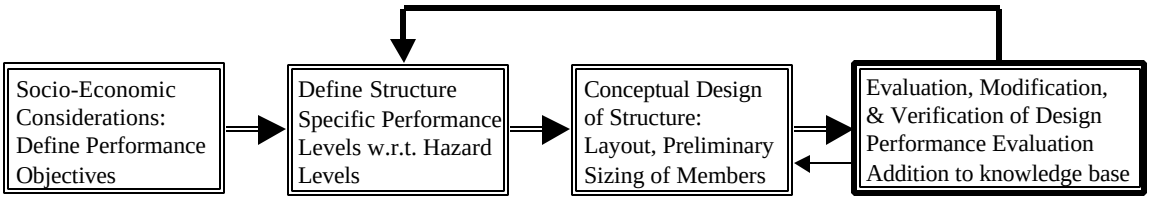

Figure 2.1. Framework for Performance Based Seismic Engineering

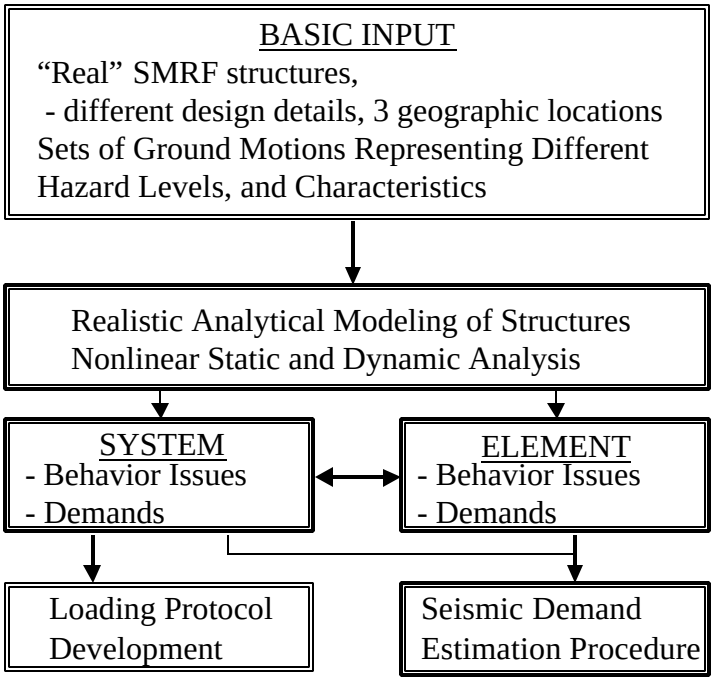

Figure 2.2. Framework for Research Summarized in this Report

CHAPTER 3

MODELING AND ANALYSIS OF STEEL MOMENT RESISTING FRAME STRUCTURES

3.1 Introduction

Structures designed according to current seismic code provisions are expected to deform in the inelastic range when subjected to design level earthquake ground motions. The elements of the structure are thus called upon to dissipate the seismic energy in the form of hysteretic energy. The ability of structural steel as a base material to dissipate large amounts of seismic energy through inelastic deformations makes steel a material ideally suited for structures undergoing seismic excitations. Steel hardens under cyclic loading, i.e., it gains strength as the number of cycles and the deformation amplitude increase, resulting in large hysteresis loops. The cyclic stress-strain response for a typical steel element is shown in Figure 3.1. The specimen exhibits large stable hysteresis loops, and a strength increase of almost 40% above yield on account of cyclic strain-hardening.

The ideal behavior of steel as seen in Figure 3.1, however, may be adversely affected by two phenomena. When steel is subjected to loading in tension, the presence of localized imperfections can result in stress concentrations (and associated high strains) which may cause cracks leading to fracture in the material. The imperfections may be pre-existent in the base material, or may be caused during the erection and fabrication process. Crack propagation occurs when the material is subjected to cyclic loading, and on reaching a critical size the cracks can manifest as fractures, which are associated with a sudden deterioration in strength. The load-deformation response for a steel cantilever beam exhibiting fracture is shown in Figure 3.2. The specimen exhibits a few large stable hysteresis loops, similar to the loops observed in Figure 3.1, followed by a sudden loss in strength.

Undesirable behavior may also be observed when steel elements are loaded in compression. Local or lateral torsional buckling may occur, which results in a gradual decrease in the strength and stiffness of the element. A typical load-deformation response for a cantilever beam, in which local buckling occurred in the beam, is shown in Figure 3.3. The specimen exhibits a large number of stable loops, however, after the initial cycles there is a gradual decrease in strength and stiffness.

Specifications such as the LRFD 1994 (AISC, 1994) and other design guidelines provide explicit criteria which, if followed rigorously, assure that the onset of strength and stiffness deterioration associated with local and lateral torsional buckling is delayed to the extent that it occurs only at large values of strain; values which are typically higher than those expected in a severe earthquake.

Throughout this study two basic assumptions have been made: 1) that all designs use compact sections with adequate lateral bracing provided, so that strength and stiffness deterioration due to local and lateral torsional buckling can be neglected, and 2) that elements do not exhibit any undesirable characteristics under tension, i.e., ductile behavior can be assumed. The assumptions are necessary in order to contain the size of the problem being addressed. Response of models of the type M1 (described in Section 3.4) for the same structures as used in this study, subjected to the same sets of ground motions, but with strength and stiffness deterioration are summarized in Reinhorn and Naeim (1998). A pilot study which addresses the effect of stiffness degradation on the response of a subset of the structures defined in Appendix B, is summarized in Section 8.3. A study focusing on the effects of beam-to-column weld fractures is summarized in Cornell and Luco (1998).

This chapter focuses on a description of the element behavior for the various elements like beams, columns, splices, panel zones, gravity columns, simple (shear) connections, floor slabs, non-structural elements (partition walls, cladding), and beam-to-column welded joints constituting a typical steel moment resisting frame. The emphasis is on representation of the element behavior in a standard nonlinear analysis program (including both geometric nonlinearity and material inelasticity), on evaluation of the interaction between different elements at a typical connection, and on studying the effect of different modeling assumptions on global, story, and element demands.

This chapter also discusses the behavior and modeling of the post-Northridge structures (see Appendix B), which make use of reduced beam sections (RBS) and/or cover plates as per the guidelines laid down in the FEMA 267 (FEMA, 1995) document. The global and story level response of post-Northridge structures, using cover plates on the beam flanges adjacent to the column face, is discussed in Chapter 5. The element level demands are evaluated in Chapter 6. The response for the RBS designs is also discussed in Chapter 6.

The nonlinear static and dynamic response of a subset of the pre-Northridge structures, defined in Appendix B, is discussed in this chapter. The response for three analytical models, ranging from the basic bare frame centerline model to a model that incorporates the strength and stiffness of the panel zones and the contributions from the other elements (shear connections, gravity columns, and floor slabs), is evaluated. The effect of modeling assumptions on element deformation and strength demands is highlighted using the nonlinear pushover response for the different models. The global (roof) and story level drift demands, obtained by subjecting the different models to sets of 20 ground motions representative of a 2/50 (2% probability of being exceeded in 50 years) hazard level, are compared to evaluate the influence of modeling assumptions on the nonlinear dynamic response of the structures. This comparison forms the basis for the selection of representative models for the different structures analyzed in this study and provides a benchmark for all other results obtained in this study and parallel studies [MacRae (1998), Kasai and Maison (1998), Reinhorn and Naiem (1998), and Cornell and Luco (1998)].

3.2 Element Behavior and Modeling

In this section the behavior of the typical elements constituting a steel moment resisting frame structure is discussed. The representation of the element behavior in the standard computer program DRAIN-2DX (Allahabadi and Powell, 1988) using the element modules available in the program is discussed. The approximations introduced due to the limitations of the analysis program are presented and their effect on the response of the structures is discussed. A modified rotational spring element module has been added to the program for the purposes of investigating the effects of stiffness degradation on the response of SMRFs. The results from the pilot study are discussed in Section 8.3.

Computer programs/models which permit more accurate modeling of the element behavior are becoming available [e.g., Ziemian et al. (1992a and 1992b), Liew et al. (1993a and 1993b), Kim and Englehardt (1995), Kilic (1996), Carr (1996)]. However, these programs either address only parts of the problem, have not been rigorously benchmarked, or are too complex and computationally expensive for system response analysis, especially when the size of the problem is large.

A compromise between accuracy and efficiency (and practicality) is usually necessary in the context of the problem being addressed. The focus of this study is on developing a better understanding of the response and assessment of the seismic demands for a wide range of SMRF structures when subjected to a multitude of ground motions. In this context an accurate representation (if possible) of the structure and loading is desirable, but not an overriding issue, especially on account of the many uncertainties involved in the estimation of demands and capacities. The critical requirement is to represent all the major behavioral characteristics of the structure and its constituent elements such that representative behavior for the structure under suitably represented loading can be obtained with reasonable confidence. The different element models, system models and the associated modeling assumptions are discussed next.

3.2.1 Beams

Beams forming part of SMRFs consist of elastic portions and partially or completely plastified regions whose location, length, and strain distribution depend on geometric parameters, boundary conditions, the effect of gravity loading, and the interstory drift demands imposed by the earthquake. For designs in which the effect of the gravity load is significantly smaller than the lateral load effect, the regions of plasticity (if any) are located usually near the face of the column, which is advantageous from the viewpoint of the lateral restraint provided by the columns and disadvantageous from the viewpoint of the high stresses that may be induced in the beam-to-column welded joint.

The behavior of the beam is of the form shown in Figures 3.1 to 3.3, depending on the loading conditions and the physical properties associated with the element. A model capable of representing distributed plasticity, cyclic strain-hardening, strength and stiffness deterioration, and capable of modeling fracture is required to capture the different possible behavior modes of the beam. There is, however, a basic problem

associated with such an element model. The problem is related to the quantification of the deformation level at which the deterioration of properties occurs and the associated rate of deterioration, as both these phenomena are loading history (duration, amplitude, sequence, and number of reversals) dependent. However, under the assumption of compact sections, adequate lateral restraint, and ductile connections these phenomena can be neglected. This assumption, coupled with the lack of availability of analytical programs capable of modeling the element behavior accurately and also performing complex system analysis efficiently, necessitates the use of simpler models which do not compromise too severely on the representation of the behavioral characteristics of the element.

Most engineering analyses adopt a beam model in which the plastified region is represented as a point [Chen and Powell (1982), Allahabadi and Powell (1988), among others]. The moment-rotation relationship is usually represented by a bilinear curve, with the "yield" strength value being equal to the plastic moment capacity given as F_yZ (F_y = material yield strength, Z = plastic section modulus), and constant strain-hardening beyond yield. This representation disguises the level of strains along the beam and the length of the plastified regions. The use of constant strain-hardening ignores the presence of cyclic hardening, permits an increase in strength irrespective of the level of deformation, and does not permit modeling of deterioration due to local instabilities. In this study point plastic hinges with a bilinear moment-rotation relationship with 3% strain-hardening are used to represent beam behavior. The beam is modeled as an elastic element bounded by inelastic rotational springs at the ends. The beam springs are given a very high elastic stiffness and a strength equal to F_y Z of the beam section. The post-yield stiffness is 3% of the elastic flexural stiffness of the beam. The use of rotational springs at the beam ends permits easy modifications in the properties of the beams (strength, post-yield stiffness, incorporation of partially restrained connections, fractures, deterioration, etc.) if required.

Other than the basic assumptions related to the modeling of the beam, as discussed above, the beam behavior represented by the adopted beam model is associated with other uncertainties. These uncertainties arise from, among other sources, the effect of the floor slab (discussed in Section 3.2.4) on the strength and stiffness of the beams, variability associated with the yield strength of the material (discussed in Section 8.5), and system modeling assumptions (discussed in Sections 3.3 and 3.4). Thus, the final representation used is, at best, a reasonable approximation of the true behavior of the

beam element, but for the purposes of the intended series of analyses, is an acceptable approximation. Results obtained from the analysis have to be interpreted in the context of the different assumptions inherent in the modeling.

3.2.2 Columns and Splices

The presence of significant axial force, which distinguishes columns from beams, leads to inelastic strain distributions and moment-curvature relationships that are much more complex for columns than for beams and are greatly affected by the loading history. The behavior of columns has been documented by many researchers [Yura (1971), Chen and Atsuta (1976), SSRC (1988), Duan and Chen (1989), Cai et al. (1991), Nakashima (1991, 1994), Ren and Zeng (1997), among others]. The point hinge concept may become a poor approximation if the axial force is high because then the plastified regions may extend over a significant length of the column. The plastic deformation capacity of columns subjected to bending moments and a significant axial force depends on many parameters and has a great variability (Nakashima 1991, 1994). Because of member P-delta effects the maximum moment may be within the unsupported length of the column rather than at the end. Moreover, column behavior cannot be separated from frame behavior because of structure P-delta effects. The formation of regions of plasticity in columns can be detrimental to the behavior of a system, especially if the plastification occurs in a sufficient number of columns to form a story mechanism.

For these reasons it is beneficial to size structural elements such that significant plastification in columns is avoided. The practice of designing columns such that limited or no plasticity occurs is enforced by the design codes through the "strong column-weak girder/panel zone" concept. If column hinging is limited or avoided, the column interaction equations given in LRFD 1994 should provide adequate protection against undesirable column behavior and it should be acceptable to model inelasticity in columns, if it occurs, by means of point hinges at the column ends. In this study such point hinges are utilized, with the bending strength defined by a bilinear M-P interaction diagram and a strain-hardening of 3% assigned to the moment-curvature relationship. The bilinear M-P interaction under strong-axis bending has a nominal strength equal to the plastic strength for axial loads less than 15% of the axial load capacity followed by a linear relationship thereafter. For weak-axis bending the corner point is taken at 40% of the axial load carrying capacity of the column. Due to constraints imposed by the

analysis program, the 3% strain-hardening has been imposed on the moment-curvature relationship as against the moment-rotation relationship for the beam spring elements. These two representations are not identical. A pilot study carried out to investigate the sensitivity of the response to small variations in the value of strain-hardening for columns showed that the effects are minor for reasonable levels of deformations. Thus, for cases where the columns are not subjected to exceedingly high inelastic deformations the approximate representation of column behavior through a point-hinge plasticity model with 3% strain-hardening on the moment-curvature relationship, and a bilinear M-P interaction is considered to be a reasonable representation.

Welded column splices represent a special problem since welds are susceptible to brittle fracture when overstressed in bending and/or direct tension [Popov and Stephen (1976), Bruneau et al. (1987)]. In this study the state of stress is checked at the splice locations to evaluate the potential of brittle fracture at the splice locations. Explicit modeling of splice fractures has not been included in the analysis. The demands evaluated at the splice locations are summarized in Section 6.3.3.

3.2.3 Panel Zones

The transfer of moments between beams and columns causes a complicated state of stress and strain in the connection area. Within the column portion of the connection, high normal stresses are generated in the flanges and high shear stresses are generated in the panel zone. The forces acting at a connection are shown in Figure 3.4. The possibility exists for the panel zone to yield in shear before the beam(s) framing into the connection reach their flexural capacity. In such cases plastification may occur in the panel zone alone or in both the beam(s) and the panel zone. An experimental result from a test done reported in Krawinkler et al. (1971) for a case in which yielding is limited to shear yielding of the panel zone is shown in Figure 3.5; the panel zone distortion is plotted as a function of the difference in the moments of the beams framing into the connection.

Panel zone shear behavior exhibits very desirable hysteretic behavior per se (as seen in Figure 3.5), characterized by a considerable increase in strength beyond first yielding, significant cyclic hardening, and large stable hysteresis loops. Yielding usually starts at the center of the panel zone and propagates towards the four corners, deforming the panel

zone globally into a parallelogram shape. Because of the desirable hysteretic characteristics of panel zones it is attractive to have these elements participate in the energy dissipation during severe earthquakes. For this reason, design codes have permitted the use of weak panel zones (UBC 1994, Section 2211.7.2) as a means to dissipate the seismic energy by concentrating the inelastic deformations in the panel zones. However, it must be considered that low strength and plastification of panel zones will affect the strength and stiffness of the structure. The lateral displacement caused by panel zone shear deformations is in most cases a significant component of the total story drift, particularly if the panel zone is weak in shear. Moreover, excessive panel zone distortion may have a detrimental effect on the behavior of welded beam-to-column connections. The effect of panel zones on the strength, stiffness, and deformation demands for steel frames has been the subject of much research [Krawinkler and Mohasseb (1987), Tsai and Popov (1990), Liew and Chen (1996), Schneider and Amidi (1998)]. The effect of interaction between the beams, columns, and panel zones is discussed in Section 3.3.

Mathematical models for the behavior of the panel zone in terms of shear force-shear distortion relationships have been proposed by many researchers [e.g., Krawinkler (1971, 1978), Lu et al. (1988), Tsai and Popov (1988), and Kim and Englehardt (1995)] based on either experimental observations or modifications to pre-existent models. The models differ in terms of the representation of the inelastic behavior, but agree well in the representation of the elastic shear stiffness, K_e, and the yield strength in shear, V_y. The monotonic shear force-shear distortion relationship proposed by Krawinkler (1978) is shown in Figure 3.6. This model has been adopted for the representation of panel zone shear behavior in this study. The control values for the model are given as follows:

$$V_y = \frac{F_y}{\sqrt{3}} A_{eff} = \frac{F_y}{\sqrt{3}} (0.95 d_c t_p) \approx 0.55 F_y d_c t_p \tag{3.1}$$

where V_y is the panel zone shear yield strength, F_y is the yield strength of the material, A_{eff} is the effective shear area, d_c is the depth of the column, and t_p is the thickness of the web including any doubler plates. The corresponding yield distortion, γ_y, is given as:

$$g_y = \frac{Fy}{\sqrt{3} \times G} \tag{3.2}$$

The elastic stiffness, K_e, of the panel zone can then be written as:

$$K_e = \frac{V_y}{g_y} = 0.95 d_c t_p G \tag{3.3}$$

where G is the shear modulus of the column material.

Additional shear resistance, which is mobilized primarily after yielding of the panel zone, is attributed to the resistance of the column flanges at the panel zone corners which have to bend in order to accommodate the shear distortion mode of the panel zone. The full plastic shear resistance of the joint, V_p, is estimated using the following equation:

$$V_p = V_y \left(1 + \frac{3K_p}{K_e} \right) \approx 0.55 F_y d_c t_p \left(1 + \frac{3 b_c t_{cf}^{\,2}}{d_b d_c t_p} \right) \tag{3.4}$$

where K_p is the post-yield stiffness, b_c is the width of the column flange, and t_{cf} is the thickness of the column flange. A similar formulation for the plastic shear strength is used in Section 2211.7.2.1 of the UBC 1994. This strength is assumed to be reached at a value of $4g_y$. Beyond $4g_y$ an appropriate value of the strain-hardening can be assumed to fully define the tri-linear shear force-shear deformation relationship of the panel zones; in this study 3% strain-hardening is ascribed to the joint shear – shear distortion.

Equation 3.4 uses a factor of 0.55, whereas LRFD 1994 recommends a factor of 0.60. The lower value is used here for the capacity estimation as the demand on the panel zone, V, is slightly underestimated using the following equation:

$$V = \left(\frac{\Delta M}{d_b} - V_{col} \right) \tag{3.5}$$

where DM (= | $M_{b,l}$ | + | $M_{b,r}$ |) is the net moment transferred to the connection as shown in Figure 3.4, and V_{col} represents the average of the shears in the column above, $V_{col,t}$, and below, $V_{col,b}$, the connection.

The DRAIN-2DX analysis program used for the system analysis does not have an element module that can directly model the behavior of the panel zones. The panel zones are modeled using a combination of the available standard beam-column module and the rotational spring module. The model uses rigid beam-column elements to form a parallelogram of dimensions d_b (depth of beam) by d_c (depth of column). The panel zone shear strength and stiffness can be modeled by providing a trilinear rotational spring in any of the four corners as shown in Figure 3.7; in this study two bilinear springs are superimposed to model the trilinear behavior. The remaining three corners are modeled as simple pin connections.

The boundary elements for the panel zone model are rigid beam-column elements with very high axial and flexural rigidity. The properties for the rotational spring(s) that model the shear strength and stiffness of the panel zone are evaluated using the principle of virtual work applied to a deformed configuration of the panel zone. For a case where the panel zone distorts through an angle g, equating the external and internal work results in the following equation:

$$M_s g = K_s g^2 = (M_{b,l} + M_{b,r}) g - (V_{col,t} + V_{col,b}) g \frac{d_b}{2} \tag{3.6}$$

Representing the shear force, V, in the panel zone as follows

$$V = \left(\frac{M_{b,l} + M_{b,r}}{d_b} \right) - \left(\frac{V_{col,t} + V_{col,b}}{2} \right) = \frac{\Delta M}{d_b} - V_{col} \tag{3.7}$$

simplifies the formulation for the rotational spring stiffness, K_s, to

$$K_s = d_b \left(\frac{V}{g} \right) \tag{3.8}$$

where M_s is the moment in the rotational spring, $M_{b,l}$ and $M_{b,r}$ are the beam moments on either side of the connection, $V_{col,t}$ and $V_{col,b}$ are the column shear forces in the column above and below the connection (see Figure 3.4), and (V/γ) is the panel zone shear stiffness. Thus, by using Equations 3.1 through 3.4, and combining with Equation 3.8, the complete trilinear behavior of the rotational spring is defined. The trilinear spring is further decomposed into two bilinear springs with the following properties for spring 1:

$$K_{1,e} = d_b\left(K_e - K_p\right) = d_b K_e\left(1 - \frac{b_c t_{cf}^{\,2}}{d_b d_c t_p}\right) \tag{3.9}$$

$$K_{1,p} = 0 \Rightarrow \alpha_1 = 0 \tag{3.10}$$

$$\gamma_{1,y} = \gamma_y \tag{3.11}$$

$$M_{1,y} = d_b V_{1,y} = K_{1,e}\gamma_{1,y} = d_b\left(K_e - K_p\right)\gamma_y \tag{3.12}$$

where $K_{1,e}$ is the elastic stiffness, $K_{1,p}$ the post-yield stiffness (equal to zero, i.e., elastic perfectly-plastic spring), α_1 the strain-hardening ratio, $\gamma_{1,y}$ the yield distortion (rotation) angle, and $M_{1,y}$ the moment in the spring at yield. The properties of the second bilinear spring are:

$$K_{2,e} = d_b K_p = d_b K_e\left(\frac{b_c t_{cf}^{\,2}}{d_b d_c t_p}\right) \tag{3.13}$$

$$K_{2,p} = \alpha\left(d_b K_e\right) \tag{3.14}$$

$$a_2 = \frac{K_{2,p}}{K_{2,e}} = a\left(\frac{d_b d_c t_p}{b_c t_{cf}{}^2}\right) \tag{3.15}$$

$$g_{2,y} = 4g_y \tag{3.16}$$

$$M_{2,y} = d_b V_{2,y} = K_{2,e} g_{2,y} = 4 d_b K_p g_y \tag{3.17}$$

where $K_{2,e}$ is the elastic stiffness, $K_{2,p}$ the post-yield stiffness, $g_{2,y}$ the yield distortion (rotation) angle, a the strain-hardening ratio for the panel zone, a_2 the strain-hardening for spring 2, and $M_{2,y}$ the moment in spring 2 at yield. The dynamic shear force-distortion response for a typical joint represented by the model described above is shown in Figure 3.8.

The panel zone behavior can also be modeled through the use of a "scissors" type element [Krawinkler et al. (1995)]. The "scissors" element permits relative rotation between two rigid elements joined at the beam/column centerline. The rotation is controlled by a spring(s) that relates the moment difference in the beams to the spring rotation. The moment difference can be related to the joint shear force, and the spring rotation is equal to the panel zone shear distortion. There are, however, two approximations involved in the "scissors" model. Firstly, the moment at the spring location needs to be estimated assuming mid-point inflection points in the adjoining beams and columns and secondly, the right angles between the panel zone boundaries and the adjacent beams and columns are not maintained, which results in approximations in deflections. The parallelogram model described previously is a more accurate representation of the panel zone and is used in this study, even though it increases the complexity of the model substantially.

3.2.4 Effect of Floor Slabs on Lateral Stiffness

Experimental studies by many researchers [Kato et al. (1984), Lee and Lu, (1989), Tagawa et al. (1989), Leon et al. (1997), among others] have shown that the interaction between the floor slab and the steel girder results in, among other effects, an increase in

the strength and stiffness of the beam. The extent of the composite action is, however, dependent on many different factors like thickness of slab, effective width of slab, strength of concrete, capacity of shear studs, and reinforcement in the slab. Thus, it may not be possible to accurately capture/estimate the effect of composite action in a structure. In this study the contribution of the floor slab is only accounted for in 1) the increase in stiffness of the beams, and 2) the strength of the simple (shear) connections (Section 3.2.6). The effect of the floor slab on the strength of the beams forming part of the moment resisting frame, and on the panel zone, has been neglected as the effect is usually small and its estimation, being dependent on a suite of factors, cannot be carried out with confidence.

Different equations [e.g., Kato et al. (1984)] are available in the literature for estimating the effective width of the floor slab for estimating the stiffness contribution from the slab under lateral loading. For simplicity, the following approach has been adopted, which compromises between different recommendations for calculating the effective width, B, of the slab:

$$B = b_f + 0.2L \text{ (for interior beam spans)} \tag{3.18}$$

$$B = b_f + \min\left[0.1L, \text{overhang}\right] \text{ (for exterior beam spans)} \tag{3.19}$$

where b_f is the flange width of the steel girder and L is the span of the girder. Using the above definition for the effective width of slab, the positive (slab in compression) and negative (slab in tension) effective moment of inertia is calculated using the approach proposed by Kato et al. (1984). For beams forming part of the perimeter moment resisting frames (exterior spans) the stiffness under compression is found to be about two times the stiffness of the bare steel beam. The effective stiffness under tension, however, is found to be very similar to the stiffness of the bare beam on account of the small reinforcement in the floor slabs (typically a wire mesh is provided).

The effective moment of inertia of the composite sections varies over the span of the girder. Due to limitations of the analysis program this variable moment of inertia cannot be adopted. An average of the effective inertia in compression and tension is ascribed to the beam section for model M2A (discussed in Section 3.4). This procedure is at best

approximate, but given the uncertainties involved with an accurate assessment, it has to serve as an acceptable approximation. A pilot study did show that the beam end rotations do not differ significantly whether this average moment of inertia is used or a linear variation is assumed over the span of the girder. Overall, the stiffness of the SMRF beams is increased by 30-60% depending on the beam section.

3.2.5 Beam-to-Column Joints

The welded beam-to-column joints in this study are taken to be fully restrained (FR) joints, defined as joints which result in less than 5% contribution to the frame displacements (FEMA 273). Thus, the beam-to-column joints are assumed to have infinite strength and stiffness. A study with the same set of structures as defined in Appendix B, but employing partially restrained (PR) connections is summarized in Kasai and Maison (1998). Another study on the effects of brittle fracture around beam-to-column joint welds is summarized in Cornell and Luco (1998).

3.2.6 Other Contributions to Lateral Strength and Stiffness

There are many other contributions to the strength and stiffness of steel moment resisting frame structures, which are typically ignored in analysis. These contributions come from the gravity columns, orthogonal moment resisting frame columns, simple (shear) connections, and non-structural elements such as partition walls and exterior cladding. Limited experimental and analytical information exists on the behavior and contribution of many of these elements to the structures strength and stiffness, and consequently the process of including the effects of these elements on the structural response is associated with many simplifying and judgmental assumptions. While some of these effects may be minor, especially in the inelastic range, the effect of others on the strength and stiffness of the structure can result in significant changes in the system response, as shown in Sections 3.5 and 3.6.

Gravity Columns

In typical modern steel frame design, the moment resisting frames are located on the perimeter of the structure. This design practice results in the presence of many interior frames which are designed to carry only gravity loads. Thus, the number of the gravity columns can be higher than the number of columns that form part of the MRF.

Furthermore, if 2-dimensional analysis is carried out, the effect of the columns forming part of the orthogonal MRF is usually not taken into consideration. All these columns have to follow the deflected shape of the moment frames, which may generate significant shear forces. This is particularly true in the first story for structures with basements where columns continue to the base of the structure, resulting in the boundary conditions at ground level being identical for all the different columns.

Shear (Simple) Connections

Interior (gravity) frames are typically designed to carry only gravity loads. A usual assumption in analysis is that the shear connections, i.e., connections using shear tabs and no flange connections, can be treated as ideal pin connections with no bending resistance. Limited experimental studies [Astaneh (1989, 1993), Leon et al. (1997)] carried out to quantify the response of these shear connections show that the bending resistance is not negligible, especially when including the effect of the floor slab. The quantification of the bending resistance is, however, hampered by the many different controlling factors, like strength of bolts in shear and bearing, strength of shear tab, properties of the slab, among many others. Nevertheless, the effect of these shear connections should not be ignored because the number of simple connections may be much larger than the number of FR connections and cumulatively may contribute significantly to the strength of the structure, especially if many FR connections fracture.

Modeling of Interior (Simple) Frames

Modeling of all interior frames can substantially add to the size of the problem. In this study, the effect of all gravity and orthogonal MRF columns, beams forming part of the simple frames, and simple connections is modeled through an equivalent one bay frame attached to the primary moment resisting frame with rigid link elements. This representation does not add significantly to the size of the problem and also does not introduce any major approximations to the model. The properties of the elements forming the equivalent frame are described next.

The columns of the equivalent bay have the following properties at each story level: The moment of inertia is equal to half the sum of moment of inertia of all gravity columns and orthogonal MRF columns, with the correct bending axis represented. A similar procedure is adopted for the axial capacity of the equivalent columns. The bending strength at all column ends is, also, half the sum of the strength of all gravity

columns and orthogonal MRF columns, calculated about the representative axes. The base of the columns at story 1 for the 3-story structures, which have no basement and hence gravity columns are pinned at the base, is modeled using a rotational spring having a strength representative of the strength of the orthogonal MRF columns at the base of story 1.

The beams connecting the two columns of the equivalent bay are modeled as elastic elements with rotational springs at both ends. The elastic beam is given a stiffness which is equal to the sum of the stiffness of all the beams forming part of the interior frames at that floor level.

Rotational springs are used to model the equivalent strength and stiffness of all the simple (shear) connections. Each spring represents the cumulative strength of half the number of simple connections. Based on judgement backed by limited experimental information, the shear connections in this study are given a strength of 40% of the plastic strength of the bare beam under compression and 20% under tension. The elastic stiffness is obtained by setting the elastic rotation as 0.02 radians under compression and 0.01 radians under tension. To study the sensitivity of the response to these assumptions, the response with the springs having 20% of plastic strength of the bare beam in compression and 10% in tension has also been studied. The expectation is that this range provides the upper and lower bounds for the strength and stiffness of the shear connections.

Non-structural Elements

Exterior cladding, partition walls, and other non-structural elements also affect the response of the structure. The effect of all these contributions on the strength of the structure is expected to be minor, but the effect on stiffness, especially in the elastic range may be significant. Limited sensitivity analyses have been performed by approximating the effects of these non-structural elements on the elastic stiffness of the structure. The general conclusion is that conventional models that ignore the contribution of these elements to the elastic stiffness will overestimate the deformation demands for SMRF structures. A sensitivity study, employing period shifts to represent the increases elastic stiffness is discussed in Section 8.6.

3.3 Interaction Between Elements at a Typical Connection

The stress and deformation demands at a typical SMRF beam-to-column connection depend strongly on the relative strength of the elements constituting the connection, namely the beam(s), column(s), and panel zone, assuming that the medium connecting the beam to the column is representative of a fully restrained joint. If the beam is the weak element, it develops a plastic hinge and the joining media transfer the beam bending strength, with appropriate strain-hardening, to the column. For a welded beam flange joint this implies transfer of (a) very high horizontal normal stresses generated by axial yielding and strain-hardening of the beam flange, (b) high shear stresses due to concentration of shear stresses in the beam flange near the column face, and (c) possibly high normal stresses due to local bending of the beam flange in the region along the cope hole. If the column is the weak element, it develops a plastic hinge and the beam may remain in the elastic range even under severe earthquake loading. For a welded beam flange joint this implies very high vertical normal stresses and strains in the column flange near the weld root. If the panel zone is the weak element and it yields in shear, neither the beam nor the column may reach their yield strength. For a welded beam flange joint this implies a state of stress and strain that may be controlled by localized yielding of the column flange due to large shear distortions in the joint panel zone. The following discussion is based on an evaluation of current design criteria which attempt to control the state of relative stress at a beam-to-column connection.

3.3.1 Strong Column-Weak Beam/Panel Zone Criterion

The design intent in highly seismic areas is to prevent the formation of plastic hinges in columns by forcing the plastification to occur either in the beams or the panel zone. Different design documents [UBC (1994, 1997), FEMA 267] provide equations which attempt to ensure that the column strength is higher than the strength of either the beam(s) or the panel zone. However, under certain conditions, even when the design guidelines are followed, plastification in the columns can occur. For instance, both beams and panel zones gain strength on account of strain-hardening, thus, if the strength of the column is only slightly higher than that of the weaker element, the possibility exists that the column may also yield at some drift demand level. Furthermore, designs are usually based on nominal strength of steel which is very different from the expected strength of the material (SSPC, 1994). For example, A36 steel, typically used for beams, has an expected mean yield strength of 49.2 ksi (against a nominal yield strength of 36

ksi), whereas A-572 steel, typically used for columns, has an expected mean yield strength of only 57.6 ksi (against a nominal yield strength of 50 ksi). Thus, the designed beam in actuality may be relatively stronger than the column. The strength of beams is further increased on account of the floor slab. The intent of this discussion is to show that these different conditions and many others may result in very different (and possibly undesirable) states of stress at a connection.

3.3.2 Beam Strength vs. Panel Zone Strength

Most present seismic design codes do not place restrictions on the relative strength of beams and joint panel zones, except for a basic design shear strength requirement for panel zones at the design load level. Since beam sizes are often controlled by stiffness requirements, it can be expected that in many practical cases the panel zones are the weak elements and much or maybe all the plastification at beam-to-column connections will be limited to panel zone shear deformations and the associated plastification in the columns flanges at the panel zone corners. Furthermore, differences between the nominal and expected strength of steel will, as in the case of columns, make the panel zones relatively weaker than the beams. Excessive panel zone shear distortions (and perhaps severe plastic hinging in columns) may have a detrimental effect on the behavior of welded joints.

Design practices have been changing insofar that very weak panel zones are discouraged (FEMA 267), though the guidelines stop short of prescribing a lower bound for the strength other than the basic strength requirement at the design force level. Thus, designs may still have inelastic deformations concentrated solely in the panel zones or beams, or distributed in some proportion between the panel zones and beams. The second option is more desirable as then neither element is called upon to dissipate excessively large amounts of seismic energy.

Behavior and Modeling of Post-Northridge Connections

Guidelines such as FEMA 267 (1995), published after the Northridge earthquake, recommend design practices aimed at forcing of the plastic hinge in the beam away from the face of the column. Designs using the FEMA 267 guidelines are termed as “post-Northridge” designs. The movement of the plastic hinge away from the column face is induced by either increasing the capacity of the beam at the column face by addition of

cover plates onto the beam flanges, and/or by reducing the strength of the beam at a distance away from the face of the column by reducing the beam flange material (reduced beam sections). Other techniques, like use of haunches or ribs, are aimed at similar outcomes.

The modeling of the post-Northridge connections needs to consider the following different features: 1) the plastic hinge is located at a distance away from the face of the column and may have a strength which is different from the strength of the bare beam (case of reduced beam sections), 2) there is an additional element with varying strength and stiffness properties between the location of the plastic hinge and the face of the column, 3) the beam between the location of the two plastic hinges (on either end of the beam) may have a varying stiffness for reduced beam sections (RBS), and 4) a (minor) possibility exists for an additional plastic hinge formation at the face of the column. The analytical model for a typical post-Northridge connection (a typical bay is shown in Figure 3.9) employs the following simplifying assumptions, 1) the zone of plasticity away from the column face is approximated as a point plastic hinge with strength equal to that of the bare beam section (for cover plated designs) or the reduced beam section, 2) the element between the column face and the plastic hinge is modeled as a beam-column element with a uniform stiffness, I_1, equal to the average of the stiffness at the face of the column and the stiffness at the location of the plastic hinge, and a strength equal to the strength at the face of the column, and 3) the beam between the two plastic hinge locations has uniform stiffness I_b.

The model described above and shown in Figure 3.9 is capable of representing all the major behavioral characteristics of the typical connection, within the framework of the basic assumptions discussed previously. The location of the plastic hinges and the strength of the reduced sections are determined as per the FEMA 267 recommendations coupled with the design details for the cover plates and the reduced beam sections.

3.3.3 Sensitivity of Predictions

From the discussion on the different element behavioral characteristics and the interactions between the different elements, the conclusion can be drawn that the distribution of inelastic demands to individual elements may be very sensitive to the assumptions in modeling and the relative strength of elements. Even with the design

guidelines being followed to the letter, the uncertainty associated with strength of material, fracture, effect of floor slabs on strength and stiffness, and other factors may result in conditions not directly accounted for in the design. The impact of the sensitivity needs to be minimized through analyses that bound the behavior of the elements. Analytical models which represent the major behavioral characteristics of the elements need to be used in order to obtain a reasonable representation of the system behavior. The rest of this chapter focuses on system level modeling and evaluation of effects of different modeling assumptions on the system and element level demands. Detailed results for force, deformation, and energy demands, at the global and story level, using representative models (discussed in Section 3.4) for the structure are presented in Chapter 5. The element level demands for the structures are presented in Chapter 6. The sensitivity to various modeling assumptions concerning strain-hardening, damping, and strength of material are presented in Chapter 8.

3.4 Modeling of the Structure

The structures are modeled as 2-dimensional frames that represent half of the structure in the north-south direction (see Appendix B). The frame is given half the seismic mass of the structure at each floor level. The seismic weight and mass properties for the different structures are also given in Appendix B.

Three basic analytical representations are used in this chapter to evaluate the effect of different modeling assumptions on local (element) deformation and force demands and global (roof) and story drift demands. The characteristics of these different analytical models are as follows:

Model M1: A basic centerline model of the bare moment resisting frame. The beams and columns extend from centerline to centerline. The strength, stiffness, dimensions, and shear distortions of panel zones is neglected. Moments in beams and column are computed at the connection centerline as against at the faces of columns and beams, which results in a high estimates of moments. The element modeling is as described in Sections 3.2.1 and 3.2.2.

Model M2: Bare moment resisting frame model in which panel zone dimensions (depth of beam by depth of column), strength, stiffness, and shear distortions are considered. Shear strength and stiffness properties, and modeling of panel zones are as discussed in Section 3.2.3. Columns and beams have clear span length.

Model M2A: Model M2 with estimates of all (A) other "dependable" contributions to strength and stiffness. All gravity columns and the weak axis columns of the orthogonal SMRFs are included in the model as discussed previously. The effect of the floor slab on the stiffness of all beams is considered. All simple (shear) connections are included, using the simplified model described in Section 3.2.6. Model M2A(1) denotes a model in which the positive (top in compression) and negative bending strengths at the shear connection are taken as $0.4M_p$ and $0.2M_p$, respectively, and Model M2A(2) denotes a model in which these values are $0.2M_p$ and $0.1M_p$.

Model M1 is perhaps the most commonly used model in structural engineering analyses. It is a widely used practice to ignore the effects of joint shear distortion and shear strength on the lateral stiffness and strength of SMRFs, and to perform analysis with centerline dimensions of beams and columns. In stiffness (or lateral displacement) calculations the argument is that the use of centerline dimensions compensates for the disregard of panel zone shear deformations and that stiffness estimates based on bare frame properties are only approximations because of the disregard of non-structural contributions. In strength calculations the argument is that an accurate evaluation of strength is desirable but not critical in the evaluation of seismic performance. The other factors usually cited for not employing a model M2 type of representation is the complexity associated with the modeling and the associated increase in computational effort.

In stiffness calculations the use of centerline dimensions gives a very distorted picture of the relative importance of beam versus column stiffness in drift control. If centerline dimensions are used for columns rather than clear span dimensions, the contributions of the column flexural deformations to interstory drift can easily be overestimated by a factor of two or more, as the contribution of the columns to the story drift is proportional to the cube of the column length. This is especially true for perimeter moment resisting

frames where the beam depths are usually large, resulting in a significant difference between the clear span dimension and centerline span dimension for the columns.

In strength calculations the disregard of the panel zone shear strength may give a very distorted picture of the locations of plastified regions in a SMRF. Panel zones that fulfill present code design requirements may be so weak in shear that they yield long before the plastic moment capacity of the beams framing into the column is attained. In such cases the possibility exists that all plastic deformations are located in panel zones and the beams never attain their bending strength and remain essentially elastic in severe earthquakes. The stable hysteretic behavior of the panel zones might indicate that concentrating all the inelastic deformations in the panel zones is not detrimental to system response. However, in view of recently observed failures at welded beam-to-column joints, it becomes an important issue to find out where plastification around the joint area occurs. If panel zones are called upon to dissipate all the energy imparted to a structure in a severe earthquake, they may have to undergo very large inelastic shear distortions. This may not cause undesirable behavior within the panel zone, but may create problems at welds since very large panel zone shear distortions will cause very high strains at the corners where beam flanges are welded to the column flanges. This behavior has led to weld fractures in the experimental study reported by Krawinkler et al. (1971).

Improvements beyond model M2 are seldom used on account of the uncertainty and complexity associated with estimating and modeling the effects of the other elements. When the structure is not subjected to severe demands, this approximation may not be very critical in most cases, but when the structure is subjected to severe earthquake loads these seemingly small effects can result in a significant change in the response of the structure. The effects of using model M2A versus the bare frame models are discussed in sections 3.5 and 3.6. The effect of modeling improvements on system level response is investigated in detail for the LA 20-story structure in Chapter 4. The response of this structure is very sensitive to second order effects.

All pre-Northridge structures and the redesigned structure R1-LA9 (see Appendix B) are represented using both bare frame models, M1 and M2. Both models are used for the following reasons: 1) to highlight the difference in response between the two bare frame models at the global and story level, and especially the element level, and 2) model M1 provides a benchmark for comparison with other analysis results from parallel studies

carried out to investigate specific issues (referenced previously). The reference model for this study is model M2, as the model permits a reasonably accurate representation of the moment resisting frame. The modeling of post-Northridge structures necessitates the use of model M2 as a bare minimum, to estimate the effects of moving the plastic hinge away from the face of the column on the panel zone and consequently the connection. Thus, for the analysis of all post-Northridge structures (discussed in Chapters 5 and 6), only model M2 has been adopted.

Unless specifically mentioned, all models use 3% strain-hardening as defined in the discussion on element modeling, strength properties are based on expected strength of material, and 2% Rayleigh damping is enforced at the first mode period and a period of 0.2 seconds, except for the 20-story structures where the damping is controlled at the first mode period and the fifth mode period of the structure.

Representation of Gravity and Seismic Loading

The moment resisting frames oriented in the north-south direction are modeled. The orientation of the floor beams is also north-south, resulting in uniformly distributed gravity loads on the beams of the MRF and concentrated loads on the columns from the orthogonal beams. The uniformly distributed loads are applied to the model as fixed end effects. The concentrated loads transferred from the orthogonal beams to the columns are modeled as nodal loads. The basements for the 9- and 20-story structures are modeled as typical stories, however, the basement floor(s) and the ground floor are restrained against lateral displacement. The seismic excitation is applied at all the laterally restrained degrees of freedom simultaneously.

Representation of P-delta Loads

Two-dimensional analytical models of the type M1 and M2 represent only the perimeter frames and ignore the presence of the interior (gravity) frames. However, what cannot be ignored are the P-delta effects caused by vertical loads tributary to the interior frames, which are transferred to the MRF through the rigid floor slab. Thus, for the structures under study, each moment resisting frame has half the structure weight (dead load plus 20 psf live load) contributing to the P-delta effect for that frame.

The potential importance of P-delta effects (specifically addressed in Chapter 4) on the seismic response of flexible SMRF structures necessitates the consideration of these

effects in all nonlinear static and dynamic analysis cases. These effects are considered by attaching an elastic "P-delta column" to the 2-dimensional model with link elements. The P-delta column is loaded with all the vertical loads tributary to the simple frames at each floor level. This imaginary column is given a very high axial stiffness and a negligible bending stiffness. The column can thus take on the deflected shape of the moment frames without attracting any bending moments. The analysis program uses a geometric stiffness matrix, assuming a cubic shape function, based on the axial force in the columns under gravity loads only, which is added to the tangent stiffness matrix for the element in order to model the structure P-delta effects. Details concerning the procedure adopted in the analysis program are given in Allahabadi and Powell (1988). This representation for the P-delta effects in the program is a reasonably good approximation for small deflection levels.

3.5 Nonlinear Static Analysis

The pushover analysis is an evaluation method in which force and deformation demands are estimated from a nonlinear (geometric nonlinearity) static, incremental, inelastic (material nonlinearity) analysis. Static lateral loads are applied using predetermined or adaptive patterns that represent approximately the relative inertia forces generated at locations of substantial masses. The structure is pushed under these loads to specified displacement levels at which the global, story, and element level strength and deformation demands are computed. Extensive research [e.g., Lawson et al. (1994), Krawinkler and Seneviratna (1998)] has been carried out to evaluate the applicability of this analysis technique under different conditions. In somewhat different formats the pushover analysis is implemented in recent seismic guidelines for retrofitting of existing building structures [FEMA 273 (1997), ATC-40 (1996)].

This pushover analysis has been shown to provide a reasonable estimate of the deformation response for structures that respond primarily in the first mode. More often than not the pushover will detect only one weakness in the structure and will ignore other weaknesses that may exist but are not exposed by the specified lateral load pattern. However, the biggest advantage of the pushover analysis lies in its ability to provide information regarding inelastic behavior characteristics of the structure which cannot be studied in detail from a time history analysis (see Chapter 4).

In this study, pushover analysis for all structures has been carried out using the design load pattern suggested in the FEMA 222A (NEHRP 1994) document. The governing equation for the load pattern is given as:

$$C_x = \frac{w_x h_x^{\,k}}{\sum_{i=1}^{n} w_i h_i^{\,k}} \tag{3.20}$$

where C_x is the normalized load at floor level x, w_i and w_x are the seismic weights at floor i and x respectively, h_i and h_x are the heights from the ground level to floor i and x, and k is a period-dependent factor. In this study, a k value of *2* has been used for all pushover analyses. Note that $k=1$ results in a triangular pattern.

The remainder of this chapter addresses the global, story, and element level response obtained for the Los Angeles 3-, 9-, and 20-story and the Seattle 3-story pre-Northridge structures. The demands obtained for the three analytical models, M1, M2, and M2A are compared for each of the four structures.

3.5.1 Global and Story Level Response

The global pushover plots, i.e., the normalized base shear (base shear normalized by structure seismic weight, or V/W) versus roof drift angle (roof displacement normalized by structure height) response for the different models M1, M2, and M2A, for four structures are shown in Figures 3.10 to 3.13. The first mode period for the different structures and analytical models is given in Table 3.1.

The global pushover curves for the LA 3-story structure in Figure 3.10 show that there is very little difference in the response of models M1 and M2. The elastic stiffness of the two models is almost identical, indicating that the effect of using clear span dimensions is balanced by the flexibility of the panel zones. Both models exhibit almost the same strength because yielding is primarily confined to the beams, even for model M2. The slightly higher effective strength of model M2 is attributed to the clear span of the beams, which effectively makes the beams stronger compared to beams with centerline spans in model M1. The models exhibit an elastic - almost perfectly plastic

response because the P-delta effect closely balances out the 3% strain-hardening. In comparison to the bare frame models, the M2A models show significantly higher elastic stiffness and strength. The difference in global response between the two M2A models is, however, very minor.

The response of the different models for the Seattle 3-story structure, shown in Figure 3.11, appears to follow similar patterns as those observed for the LA 3-story structure. However, there are important differences. Firstly, models M1 and M2 exhibit a clear negative post-yield stiffness. The reason is that the P-delta effect reduces the post yield stiffness by about 6% which, when coupled with a strain-hardening of 3%, results in a negative post-yield stiffness of about –3%. The presence of a negative post-yield stiffness has serious ramifications on the dynamic response of the structure (see Chapter 4). Model M1 attains the negative post-yield stiffness right after system yield. Model M2 yields earlier than model M1, because many panel zones yield before the beams, but attains a negative post-yield stiffness at a much higher global drift (at 0.045 drift angle as against 0.017 drift angle for model M1). This small difference in the static response results in a significant difference in the dynamic response, as is shown later and discussed in detail in Section 4.4. For models M2A, which are significantly stronger and stiffer than the bare frame models, the onset of a negative post-yield stiffness is delayed to a global drift of about 0.060.

The response of the different models for the LA 9-story structure, presented in Figure 3.12, shows similar trends as observed for the 3-story structures. For model M1 the negative stiffness starts at a relatively small global drift of about 0.025. However, in the time history responses discussed later this global drift is attained under only a few ground motions, resulting in the P-delta effect not being as critical a factor in the dynamic response of the LA 9-story structure, especially for the improved models M2 and M2A.

Figure 3.13 shows the global pushover curves for the different models of the 20-story structure in Los Angeles. Model M1 exhibits a small strength plateau after yield, followed by a very steep negative slope on account of severe P-delta effect. Model M2 and Models M2A show similar behavior except that the width of the strength plateau increases with an improvement in the analytical model. The behavior and response for these and additional models for the LA 20-story is discussed in detail in Chapter 4, and is therefore not addressed in depth in this chapter.

For all four structures the effect of the variation in strength and stiffness of the simple connections (model M2A(1) versus model M2A(2)) on the response of the structure is very small. The effect on dynamic response is equally small, indicating that the bending resistance of simple connections is not a very important issue - unless early fracture at welded connections occurs, a condition which is not evaluated in this study. From here on the use of the term model M2A refers to model M2A(1).

3.5.2 Element Level Demands

The major difference in response between model M1 and models M2 and M2A is anticipated at the element level where the distribution of demands between the beams, columns, and panel zone can change significantly depending on the relative strength of the elements framing into a connection. The values (maximum values obtained during analysis) for element plastic deformation demands, obtained from a pushover analysis at a global drift value of 4%, for the Seattle 3-story structure are shown in Figure 3.14 for models M1, M2, and M2A. The numbers in italics at the right side of the frame denote the story drift angles at the global drift value of 4%.

All three models exhibit column yielding only at the base. Model M2A has the lowest plastic deformation demands for the columns, between the different models. This observation ties in with the story 1 drift for model M2A being the lowest, which is primarily on account of the strength and stiffness contribution from the orthogonal MRF and gravity columns. Figure 3.14b shows that almost all the panel zones yield in model M2, and in some locations the panel zones take up almost all the plastic deformation demand, with the beam response being essentially elastic. This observation is in sharp contrast to the observations for model M1 (Figure 3.14a), in which all the plastic deformation demands are concentrated in the beams. Thus, neglecting the presence of the panel zones in an analytical model would not only present a severely distorted picture of the demands imposed on the beams, but may also suggest a misleading state of stress at the beam-to-column welded joint, which is a critical issue in light of the weld fracture problem. The presence of higher deformation demands on one end of the beam as against the other is on account of gravity load effects, which increase the demands on one side and reduce them on the other.

Figure 3.15 shows the envelope values for the element plastic deformation demands, at a global drift of 4%, for the three models for the LA 3-story structure. The beams in the LA structure are the weaker elements as compared to the panel zones, which are relatively strong account of very heavy column sections. The beams, thus, account for most of the plastification. The interior panel zones on floors 2 and 3 do yield and take up some of the plastic deformation demand. The difference between the element deformation demands for model M1 and M2, is however, not as drastic as the difference observed between the Seattle models.

A comparison of element plastic deformation demands between the different models, at a typical interior connection on the second floor of the Seattle 3-story structure, as a function of the story 1 drift angle is shown in Figure 3.16. "Beam Fl.2[l]" denotes the beam on floor 2 (Fl.2) framing into the connection from the left [l]. The figure clearly shows that for the M2 models the plastic deformations are concentrated in the panel zones and the panel zones yield much before the beams, and that the panel zones in model M2A yield before the panel zones in model M2. Because the response of the beams framing from the left side and right side of the connection is similar, only the response of the beam framing from the left side is shown. The figure also shows the variation of the plastic deformation demands at the base of the interior column (referred to a Col.St.1.[b], i.e., base of column in story 1 as a function of the story drift. The curves indicate that the relationship between the plastic deformation at the base of the column and the story drift is insensitive to the analytical model.

Figure 3.17 shows the variation in the element forces (normalized to their yield values) as a function of the story drift angle for the same connection as presented in Figure 3.16. The figure presents the force demands for the panel zone, and the moment demands for the top of the column framing from below (Col.St.1[t]), the bottom of the column framing from above (Col.St2.[b]), and the beam framing from the left into the connection. The force demands on the panel zones for models M2 and M2A are similar. The difference between the beam force demands is small, however the force demands are close to the yield value, thus even a small difference in force demands results in a large difference in plastic deformation demands as seen in Figure 3.16. The normalized moment demands for the column end framing into the connection, though less than 1.0, show a significant difference between the three different models.

This short discussion indicates that the state of stress and the distribution of the plastic deformation demands around a connection is severely affected by the assumptions in the analytical model. A model that represents the essential characteristics of all basic elements is intrinsic to understanding the response of the structure. As will be shown in the following section, the overall effect of the different models can also result in significant changes in the dynamic story drift demands. The rest of the discussion focuses on global and story drift demands obtained from nonlinear dynamic analysis for the various models.

3.6 Nonlinear Dynamic Analysis

As structures designed according to current design codes are expected to deform well into the inelastic region, a nonlinear dynamic analysis is necessary to capture the response of the structure to severe ground motion and obtain reasonable estimates for the demands on the structure. This analysis method is the most accurate method provided the structure (and constituent elements) and the seismic input to the structure can be modeled to be representative of reality. This report refers extensively to inelastic time history analysis results, but all results must be evaluated in the context of the assumptions made. The main objective is to improve the understanding of the seismic response of SMRF structures. The presented quantitative information, in this chapter and subsequent chapters, depends on modeling assumptions discussed in this chapter and on the choice of ground motion records, which are discussed in Appendix A.

Global (Roof) and Story Level Response

The minimum, median[1], 84th percentile (defined as the median multiplied by the exponent of the standard deviation of the natural log values of data points), and maximum global (roof) drift angle demands for the different models of the four structures are given in Table 3.2. Also given in the table are the standard deviations associated with the natural log values for the global drift demands (termed as the "dispersion" in the data set); these values may be taken, approximately, to be representative of the coefficient of

[1] Median is defined as the geometric mean (exponential of the average of the natural log values) of the data points, and is given as (for n data points):

$$\hat{x} = \exp\left[\frac{1}{n}\sum_{i=1}^{n}\ln x_i\right]$$

variation (COV) in the data set (Shome et al., 1997). The median and 84th percentile story drift angle demands for the different models of the LA 3-story, Seattle 3-story, and the LA 9- and 20-story structures are compared in Figures 3.18 to 3.21, respectively. The story drift angle values are marked as points between the bounding floors, and are connected by straight lines. The drift demands are obtained by subjecting the different models of the structures to sets of 20 ground motions representative of a 2/50 hazard level for the two locations (see Appendix A).

The global drift demands for models M1 and M2 of the LA 3-story structure are almost identical and higher than the demands for model M2A. The improvement in the model beyond a bare frame representation is effective in reducing the demands for ground motions that shake the structure more severely. This observation is also evident from Figure 3.22, which shows the individual global drift demands for the 20 records for the three models for the structure. The reduction in peak demands also translates into a decrease in the scatter in the data set, as reflected in a reduction in the standard deviation value. However, the reduction in drift demands from model M2 to model M2A occurs in only 13 of the 20 records, the other 7 records show higher demands. The major reduction is observed for records LA37-40, records for which the spectral displacement demand at the first mode period of model M2A is significantly lower than the demand at the first mode period for the bare frame models (Figure A.6, Appendix A). In general, the variation in global drifts between the different models can be traced to similar variations in spectral displacement demands.

The benefit of improved modeling at the global level, shown in Table 3.2, is similar to the benefit observed at the story level, Figure 3.18. The distribution of story drifts over the height of structure also does not differ by much between the three models. Again, the effect of improved modeling is more pronounced at the 84th percentile level than at the median level. The element deformation demands also do not change by much because the panel zones are relatively strong and yield only after significant yielding occurs in the beams, an observation that is anticipated on the basis of a comparison between the element demands shown in Figures 3.15a and 3.15b.

The models for the Seattle 3-story structure show a significant reduction in demands not only from the bare frame models to model M2A, but also from model M1 to model M2. The large reduction at the 84th percentile is essentially on account of the reduction in drift demands for two records, SE27 and SE31, and to a smaller extent for records SE25

and SE33, as shown in Figure 3.23. The reason for the large differences in response of the different models is the existence of a negative post-yield stiffness in the models and the value of global drift at which it is attained (see Figure 3.11). For model M1 even relatively weak ground motions push the structure into the range of negative stiffness, whereas only a few of the stronger ground motions succeed in pushing model M2, and especially model M2A, to the large displacement values at which the models attain a negative post-yield stiffness.

At the story drift demand level, the Seattle 3-story structure shows similar but more pronounced trends as the LA 3-story structure, insofar that the improvements in the models result in lower drift demands, as shown in Figure 3.19. However, the distribution of demands over height, and the extent of difference in drift demands between the various models, is quite different from the LA 3-story structure. The cause for the differences is the negative post-yield stiffness in the Seattle 3-story models. The issue related to response of structures having a negative post-yield stiffness, using the Seattle 3-story structure as a case study, is explored in detail in the next chapter.

The global drifts for the LA 9- and 20-story structures also decrease with an improvement in the analytical model, though the reduction is not as large as observed for the Seattle 3-story structure. An exception is the response of the LA 20-story structure under the LA30 ground motion; model M1 exhibits collapse whereas the global drift demand for model M2 is 0.043, and for model M2A is only 0.022. The behavior and response of the LA 20-story structure is discussed in depth in the next chapter dealing with the effect of P-delta on the response of flexible SMRFs.

For the LA 9-story structure the decrease in story drift demand as models are being improved (from M1 to M2A) is significant only at the 84^{th} percentile level, as shown in Figure 3.20. The reason is that only for a few ground motions the less accurate models (particularly model M1) get driven in the range of negative stiffness, whereas this does not occur for model M2A. A similar response, following the same reasoning, is observed for the LA 20-story structure as shown in Figure 3.21. For the taller structures the effect of improvement in modeling is significant in the lower stories of the structure, where the post-yield stiffness may be negative (see Chapter 4). For the upper stories the effect of improvement in modeling is comparatively much less as a major part of the seismic energy is being dissipated in the lower stories of the structures.

The general conclusion to be drawn is that the effect of modeling accuracy on global and story drift demands can be very important if a change in basic mechanism occurs or the range of negative post-yield stiffness is entered. If the latter occurs, the drift becomes very sensitive and can be greatly amplified, particularly if the ground motions have a long strong motion duration (several of the Seattle records, Appendix A).

3.7 Conclusions

An accurate representation of the elements in a structural model is desirable, but often not critical, or possible, in view of the uncertainties involved in the estimation of demands and capacities, and limitations of currently available system level analysis tools. What is critical is to detect weaknesses in a structure and to obtain reasonable bounds on force and deformation demands that the structure is expected to undergo. To this end, reasonable models that represent the important behavioral aspects of the different elements, albeit in a simplified fashion (e.g., no cyclic strain-hardening or degradation) are useful in developing an understanding of the system behavior and quantifying the demands on the system components. If this goal can be achieved with a thoughtful and carefully evaluated 2-D analysis it may be more useful than the execution of a complex 3-D analysis in which a thoughtful evaluation often is very difficult to achieve because of the complexity of currently available 3-dimensional analysis tools. Clearly, this does not hold true if torsional effects become important.

The presented results and conclusions must be interpreted in the context in which they have been obtained, regarding the strength and stiffness characteristics of the structures, the assumptions related to the modeling and analysis, and particularly the characteristics of the ground motions, as very high intensity ground motions have been used for evaluating the global and story level drift demands. It is likely that the effect of the different improvements to the basic models seismic demands may not be as significant for low intensity ground motions. The general conclusions drawn from the discussions in this chapter are summarized next.

- Gross approximations in analytical models for the structures, like model M1 which neglects the presence of panel zones, can result in very erroneous predictions of the demands at the element level, and for certain structures also at the system level.

- An analytical model for the panel zone is defined, which uses standard element routines found in almost all nonlinear structural analysis programs (beam–column and rotational spring). The developed panel zone model permits a realistic representation of the behavior of the panel zone.

- The distribution of plastic deformation demands at a typical connection is found to be very sensitive to the relative strength of the members framing into the connection. Within the same code designed structure (even when the strong column concept is followed) the distribution of element demands between beams and panel zones may vary significantly from one connection to another.

- The incorporation of all reliable contributions besides the moment frames (floor slabs, gravity columns, simple connections, etc.) may have a substantial impact on the response of the structural model. The effect is much more pronounced in cases in which the system is subjected to high levels of ground shaking and/or is subject to severe P-delta problems.

- The response of the models is not very sensitive to the value ascribed to the strength of the simple connections. The influence of these simple connections can become more important in the event of fractures in the moment resisting connections.

- The response of the structures may become very sensitive if the range of negative post-yield stiffness is entered. For this reason, modeling assumptions related to strain-hardening in elements may assume critical importance in the response for certain structures (see Section 8.2).

- The nonlinear static analysis (pushover analysis) is very helpful in rationalizing the dynamic response of the structure.

From the discussion on element behavior and on interaction between different elements, and the observations from the static and dynamic analysis of the different models for the four structures, it is concluded that a model which incorporates the strength, stiffness, and shear yielding of the panel zones is intrinsic to developing an understanding of the response of steel moment resisting frame structures. A model that incorporates the panel zones, within the basic modeling assumptions, is a quite accurate model for an SMRF. The improvements beyond model M2 can also be very important to

the response of the structure and should be contemplated if they can be incorporated with confidence. Mostly M2 models are being used for the analyses described in the subsequent chapters, but M1 models are also evaluated in order to provide a benchmark reference.

Table 3.1 First Mode Periods of LA 3-, SE 3-, LA 9-, and LA 20-story Structures, Different Analytical Models

Structure	Analytical Model		
	Model M1	Model M2	Model M2A
LA 3-story	1.03	1.01	0.85
SE 3-story	1.36	1.36	1.15
LA 9-story	2.34	2.24	1.97
LA 20-story	3.98	3.74	3.45

Table 3.2 Statistical Values for Global Drift Angle Demands for Various Structures, Different Analytical Models; 2/50 Sets of Ground Motions

Structure	Analytical Model	Global (Roof) Drift Angle				
		Maximum	84th Percentile	Median	Minimum	Std. Dev. of Logs
LA 3-story	Model M1	0.1114	0.0657	0.0401	0.0168	0.49
	Model M2	0.1095	0.0658	0.0393	0.0152	0.52
	Model M2A	0.0734	0.0511	0.0339	0.0167	0.41
SE 3-story	Model M1	0.4251	0.1070	0.0506	0.0216	0.75
	Model M2	0.2054	0.0726	0.0408	0.0190	0.58
	Model M2A	0.0749	0.0504	0.0350	0.0195	0.37
LA 9-story	Model M1	0.0687	0.0408	0.0256	0.0138	0.47
	Model M2	0.0558	0.0392	0.0252	0.0142	0.44
	Model M2A	0.0551	0.0358	0.0237	0.0107	0.41
LA 20-story	Model M1		0.0236	0.0143	0.0078	0.50
	Model M2	0.0432	0.0247	0.0146	0.0080	0.53
	Model M2A	0.0383	0.0218	0.0137	0.0078	0.47

Note: Statistical values for LA 20-story model M1 are based on 19 records. The model collapsed under record LA30 (see Chapter 4).

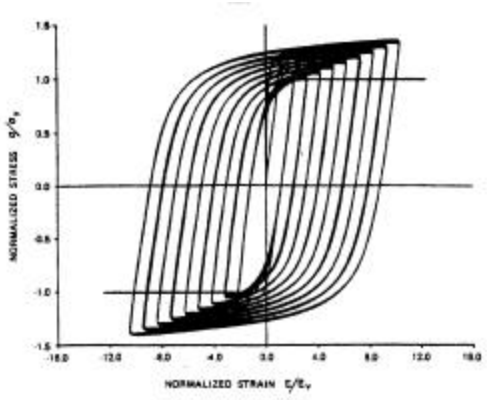

Figure 3.1 Cyclic Stress-Strain Diagram of Structural Steel
[from Krawinkler et al. 1983]

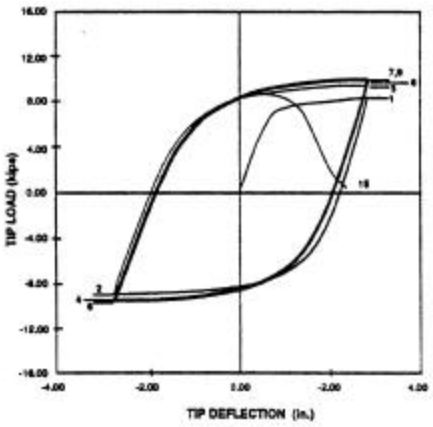

Figure 3.2 Load-Deformation Response Showing Rapid Deterioration
[from Krawinkler et al. 1983]

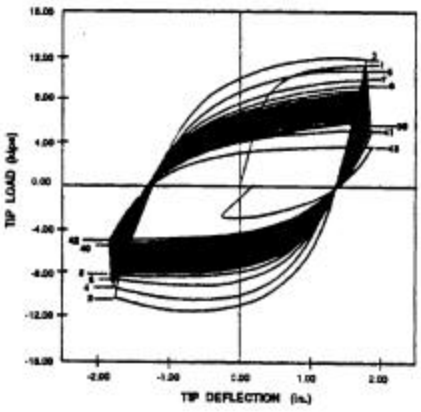

Figure 3.3 Load-Deformation Response Showing Gradual Deterioration
[from Krawinkler et al. 1983]

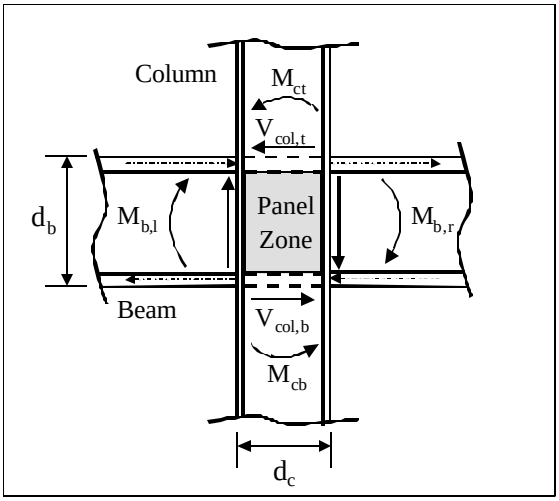

Figure 3.4 Moments and Shear Forces at a Connection due to Lateral Loads

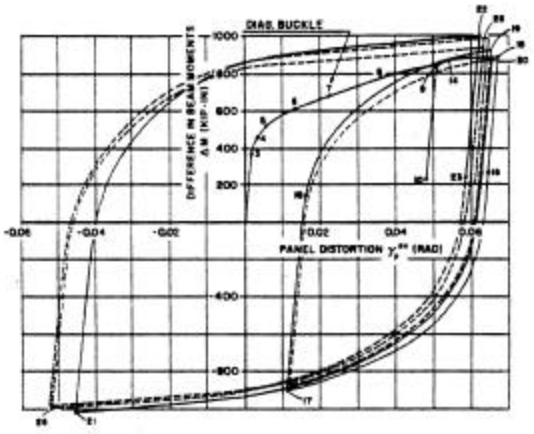

Figure 3.5 Shear Distortion Response for a Panel Zone
[from Krawinkler et al., 1971]

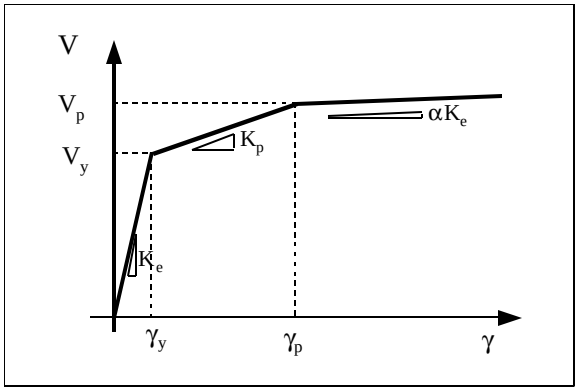

Figure 3.6 Trilinear Shear Force-Shear Distortion Relationship for Panel Zone
[from Krawinkler, 1978]

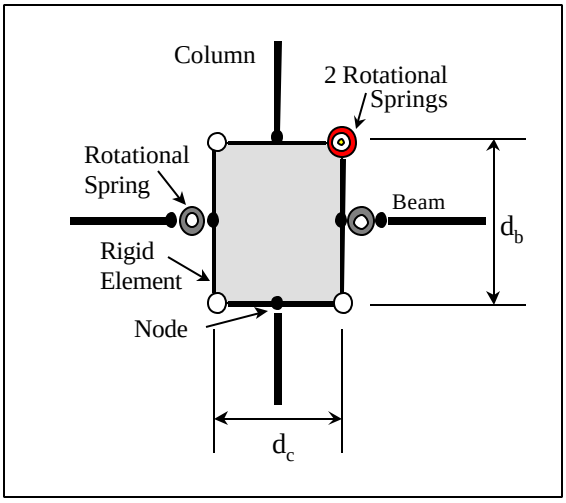

Figure 3.7 Analytical Model for Panel Zone

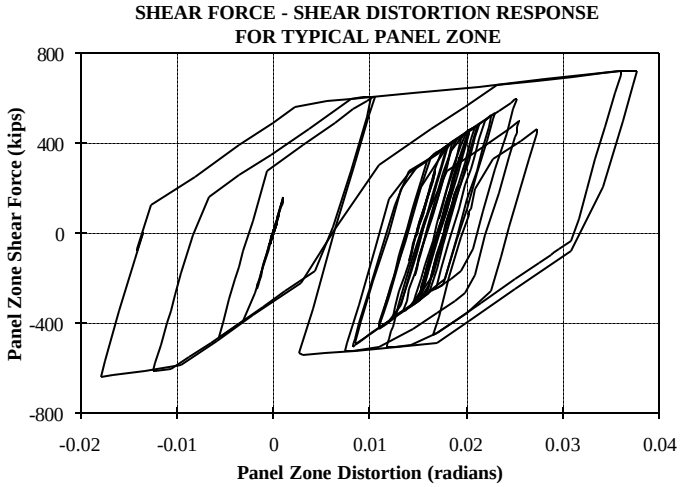

Figure 3.8 Shear Force-Shear Distortion Response for a Typical Panel Zone

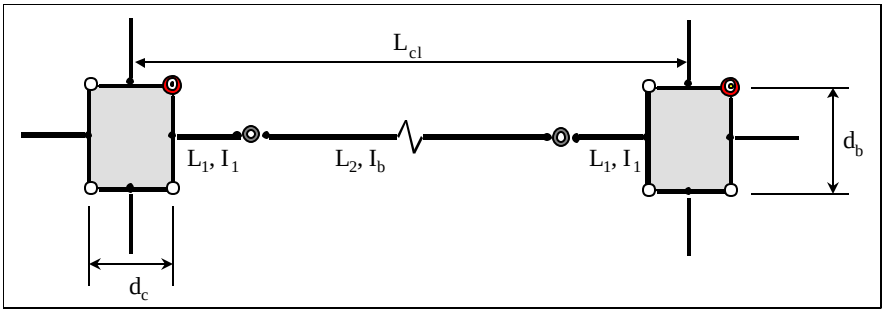

Figure 3.9 Analytical Model for Typical Bay in a Post-Northridge Structure

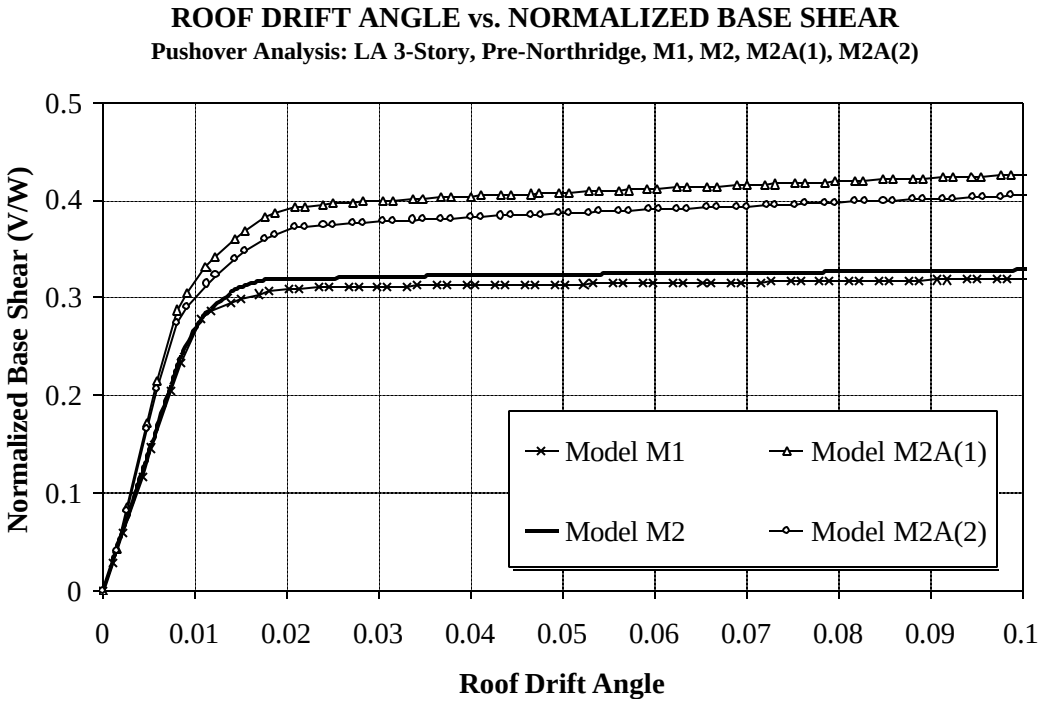

Figure 3.10 Global Pushover Curves for LA 3-story Structure, Different Models

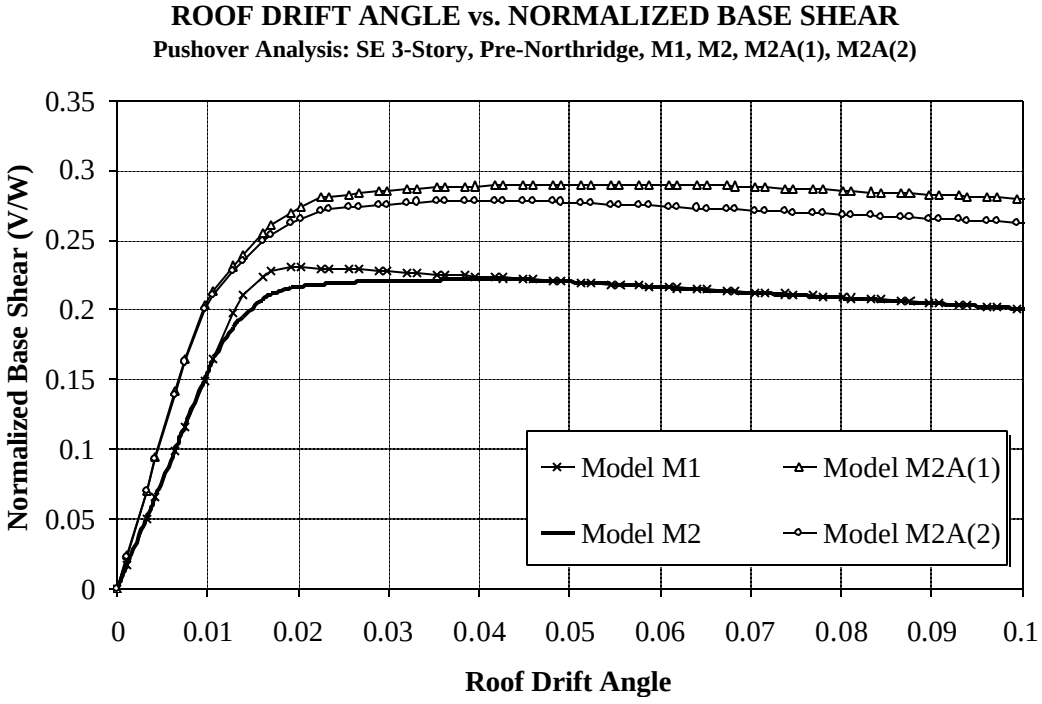

Figure 3.11 Global Pushover Curves for Seattle 3-story Structure, Different Models

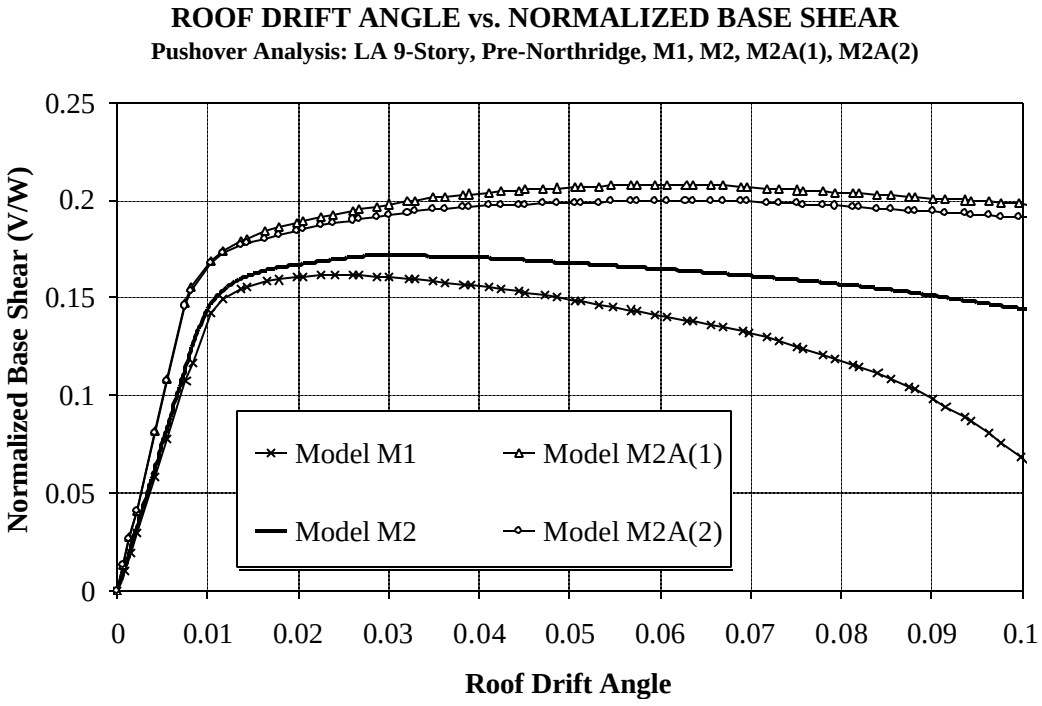

Figure 3.12 Global Pushover Curves for LA 9-story Structure, Different Models

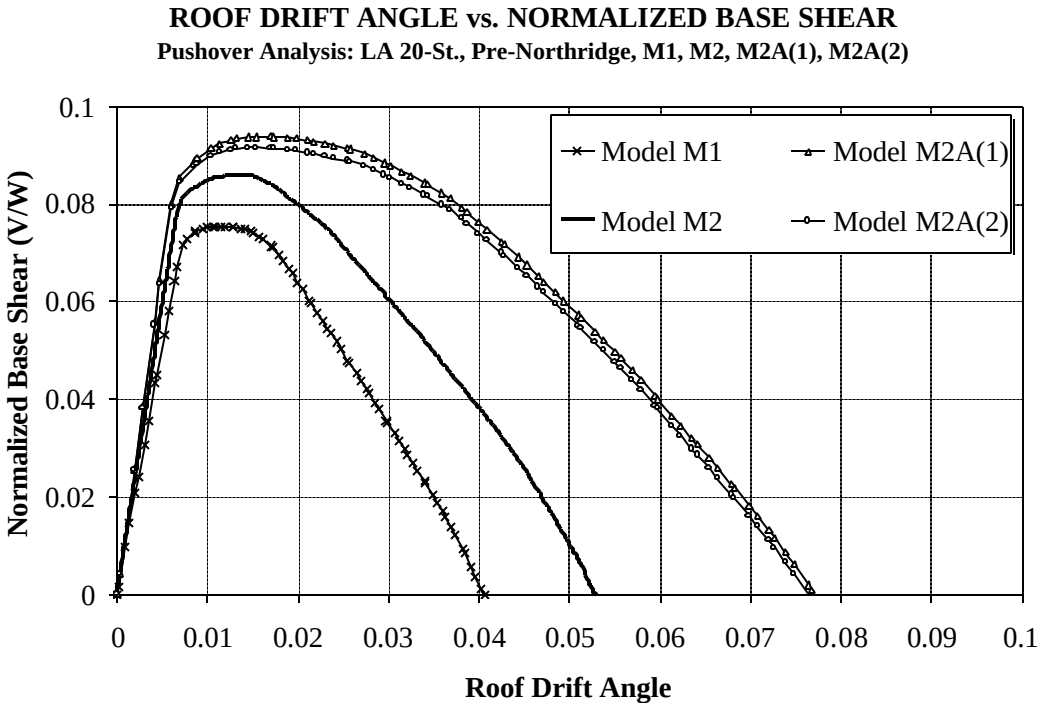

Figure 3.13 Global Pushover Curves for LA 20-story Structure, Different Models

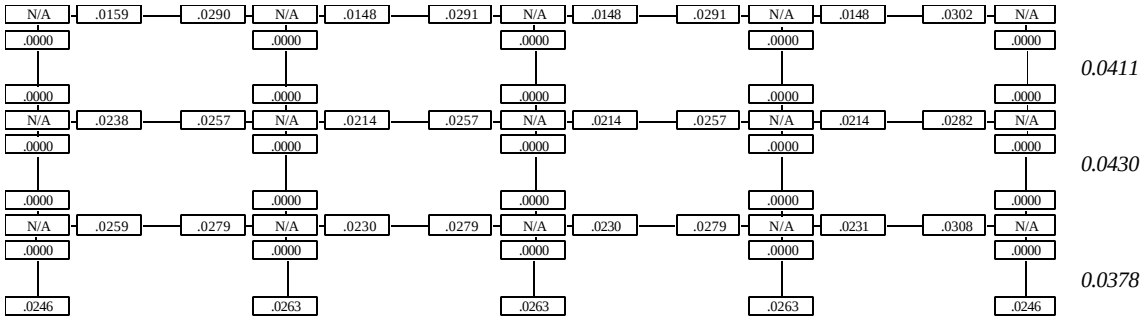

(a) Model M1

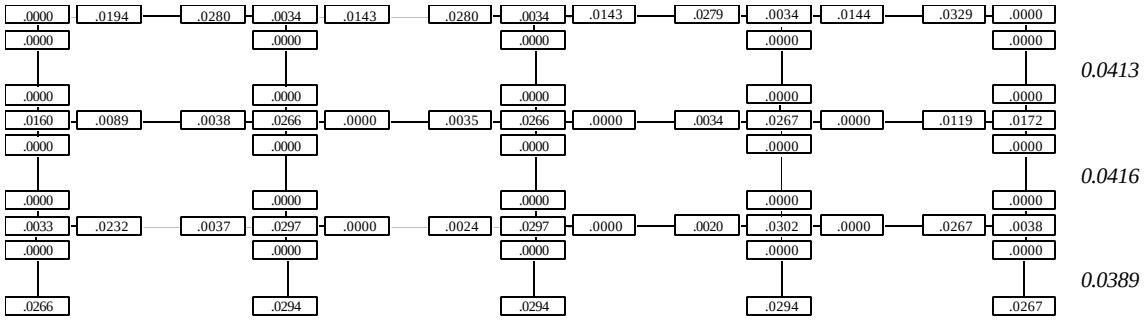

(b) Model M2

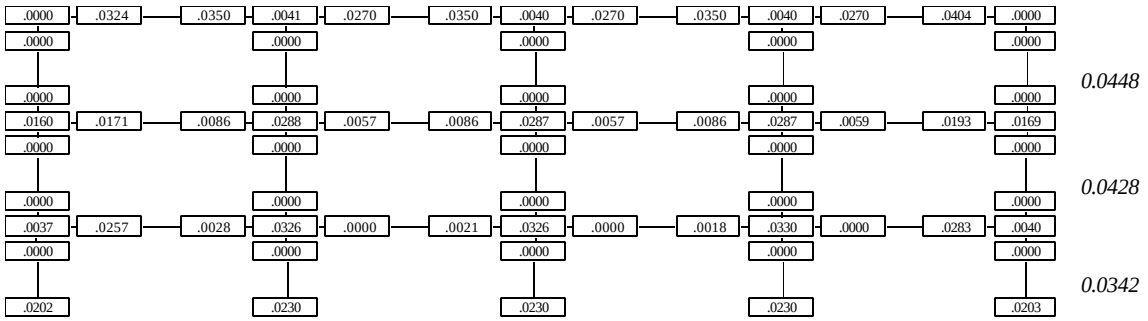

(c) Model M2A

Figure 3.14 Element Plastic Deformation Demands at Global Drift of 4%, for Seattle 3-story Structure, Different Models; Pushover Analysis

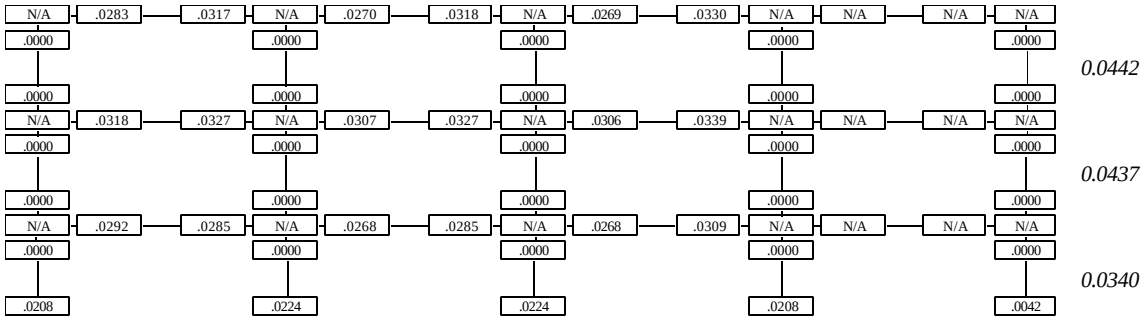

(a) Model M1

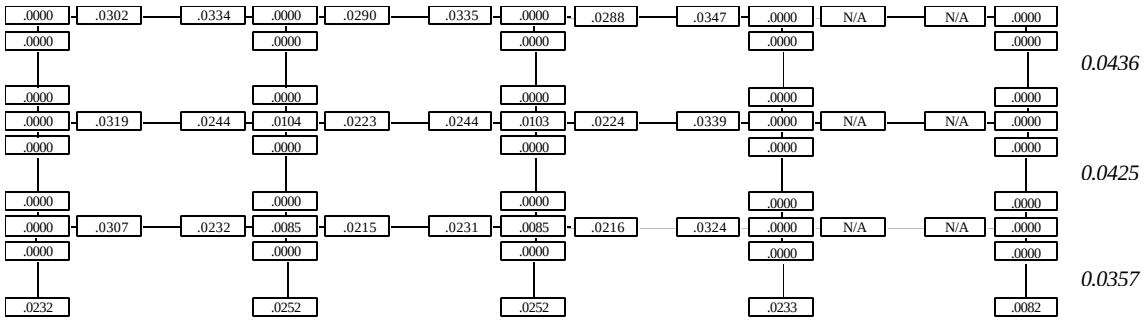

(b) Model M2

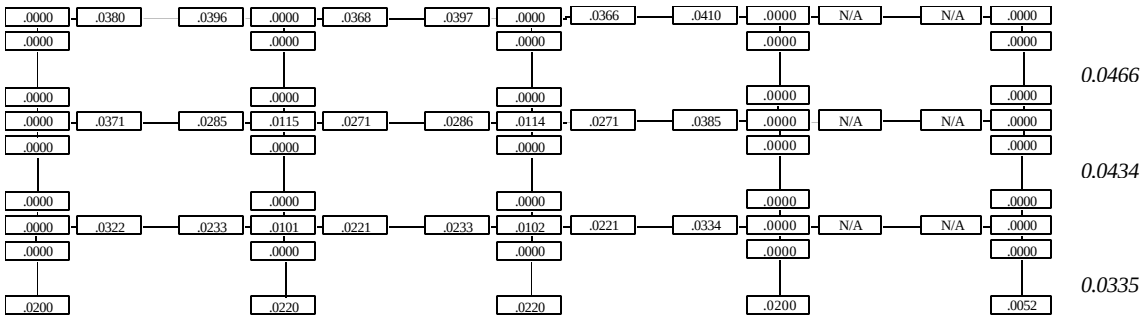

(c) Model M2A

Figure 3.15 Element Plastic Deformation Demands at Global Drift of 4%, for LA 3-story Structure, Different Models; Pushover Analysis

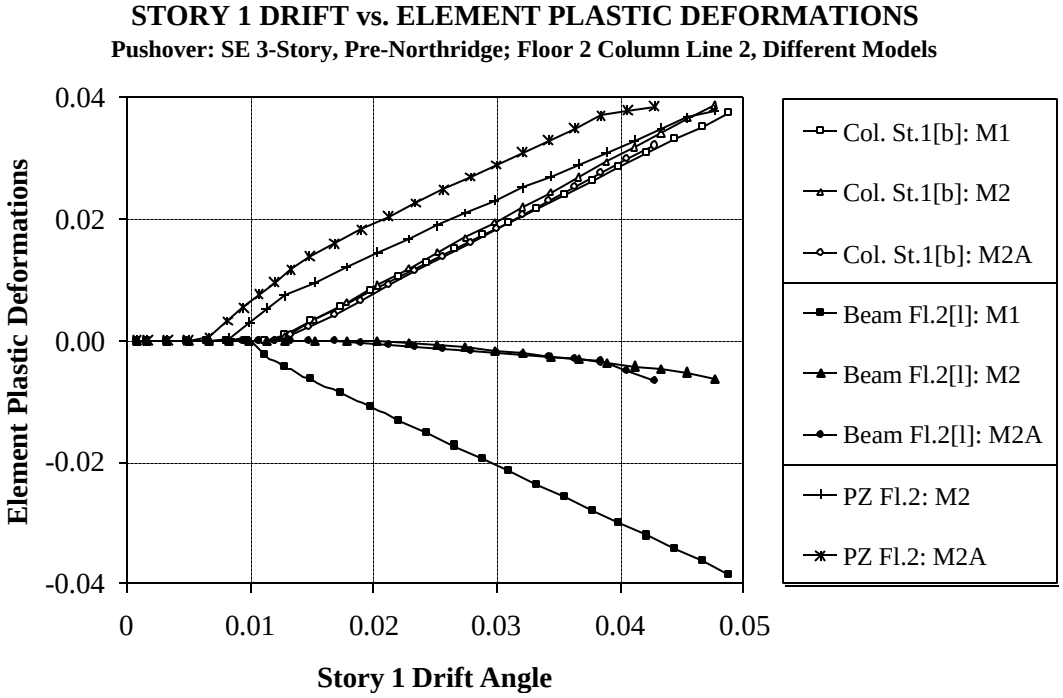

Figure 3.16 Element Plastic Deformations Versus Story 1 Drift Angle, Seattle 3-story Structure, Different models; Pushover Analysis

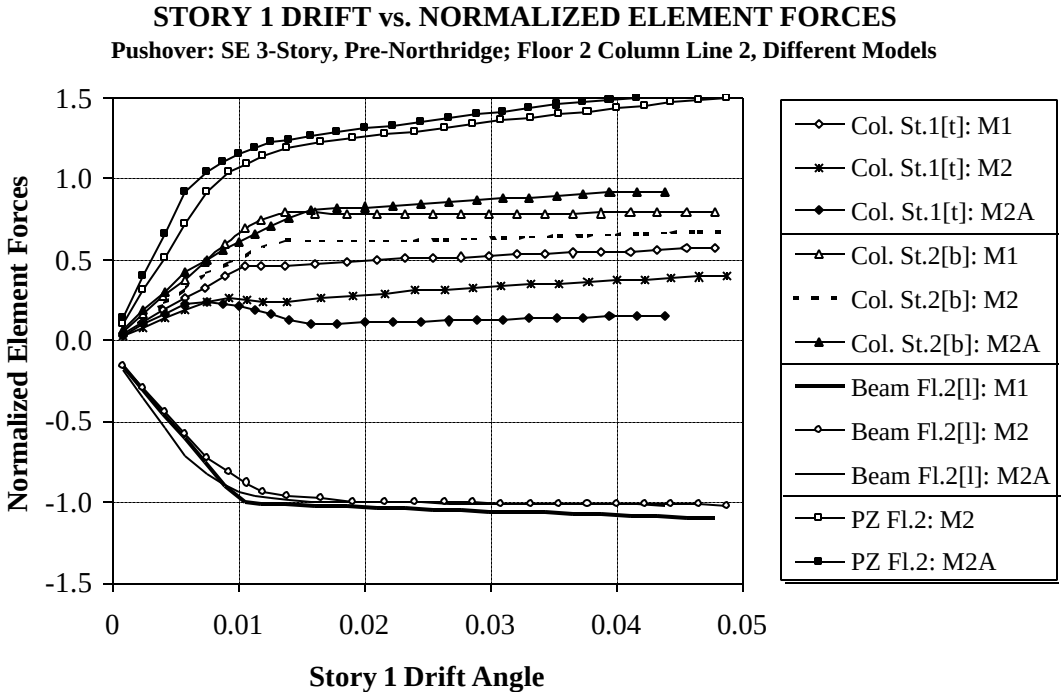

Figure 3.17 Element Force Demands Versus Story 1 Drift Angle, Seattle 3-story Structure, Different Models; Pushover Analysis

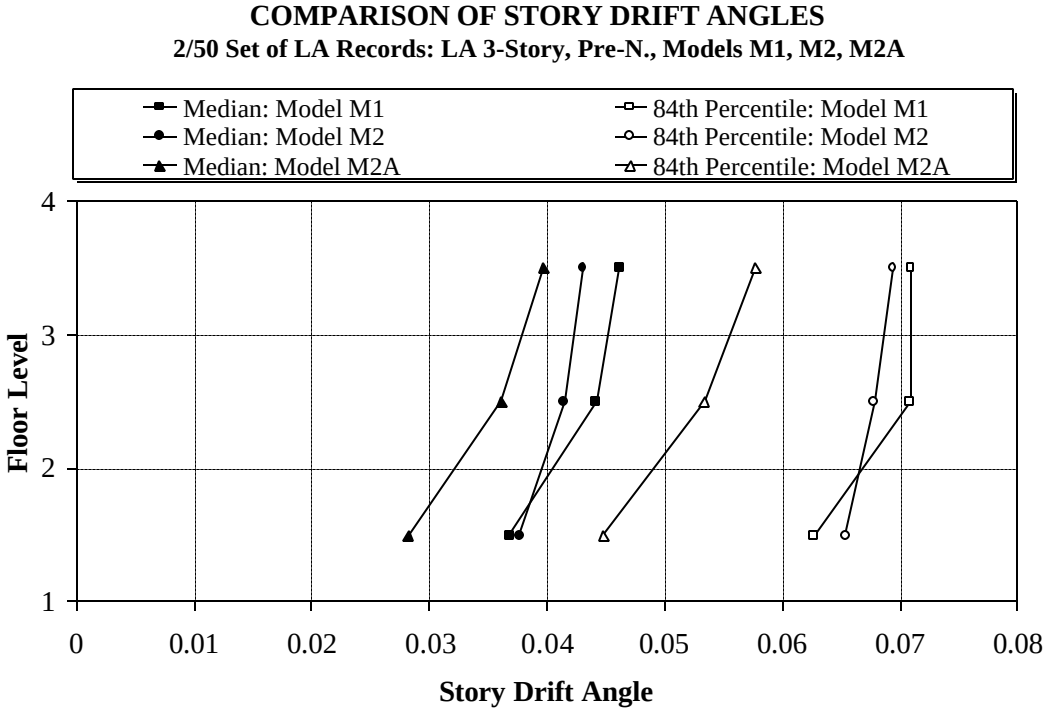

Figure 3.18 Median and 84th Percentile Values of Story Drift Demands for LA 3-story Structure, Different models; 2/50 Set of Ground Motions

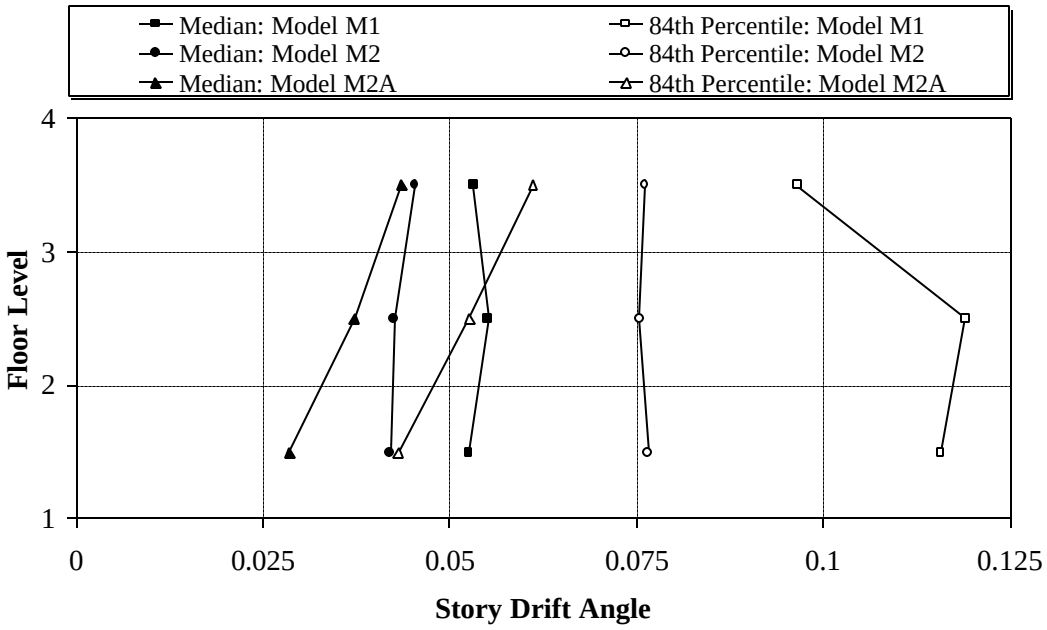

Figure 3.19 Median and 84th Percentile Values of Story Drift Demands for Seattle 3-story Structure, Different models; 2/50 Set of Ground Motions

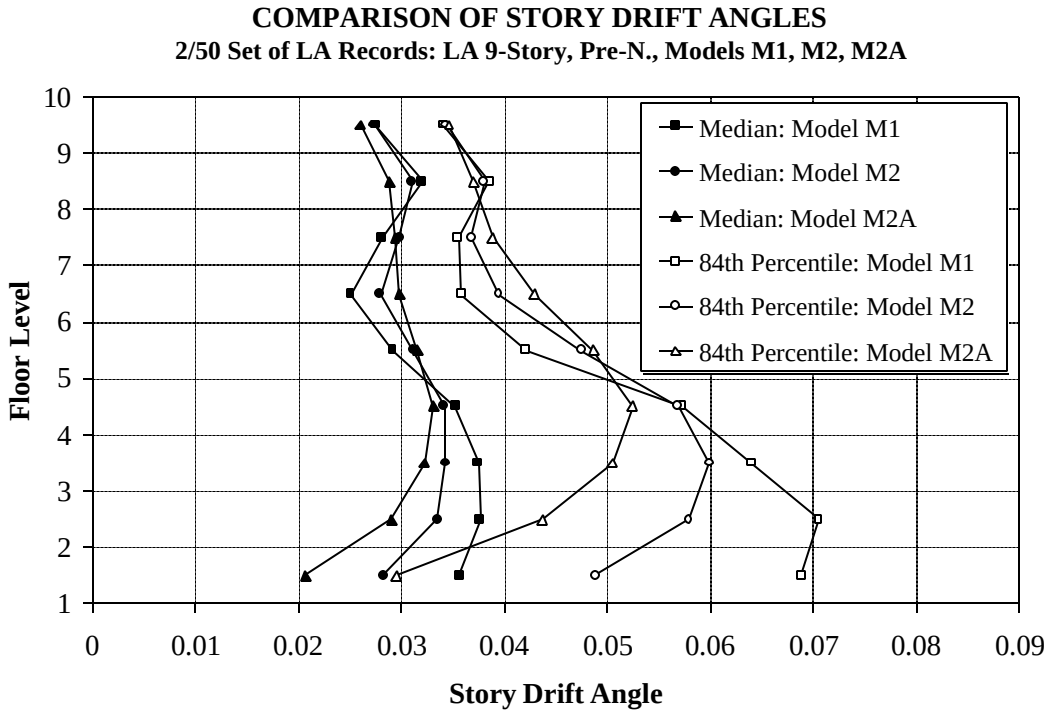

Figure 3.20 Median and 84th Percentile Values of Story Drift Demands for LA 9-story Structure, Different Models; 2/50 Set of Ground Motions

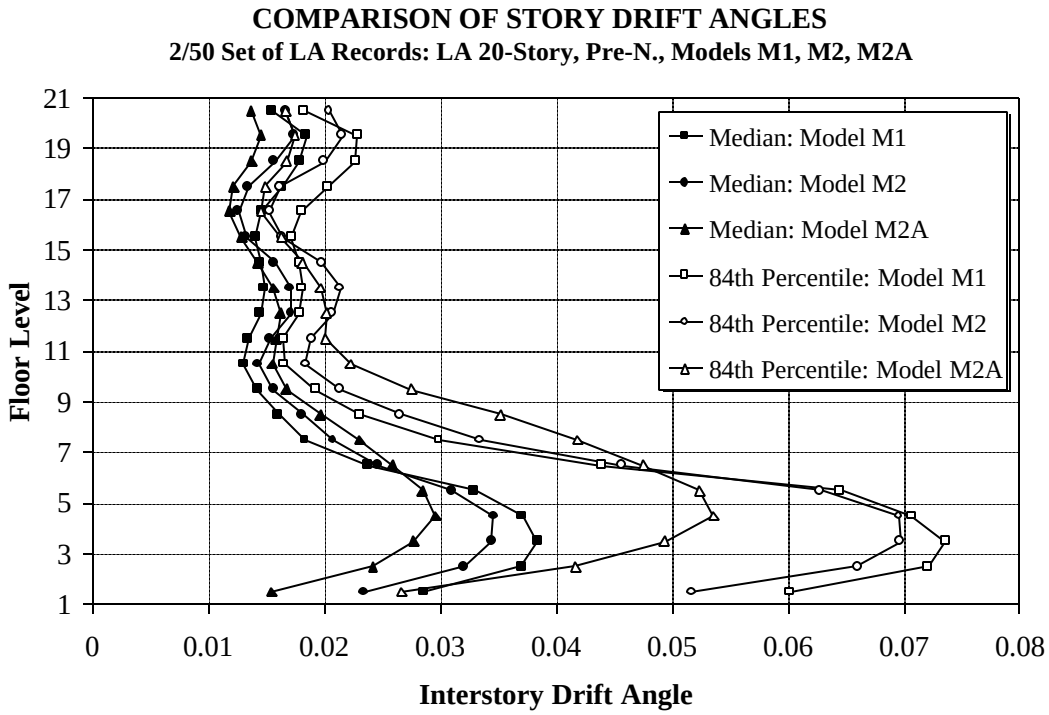

Figure 3.21 Median and 84th Percentile Values of Story Drift Demands for LA 20-story Structure, Different Models; 2/50 Set of Ground Motions

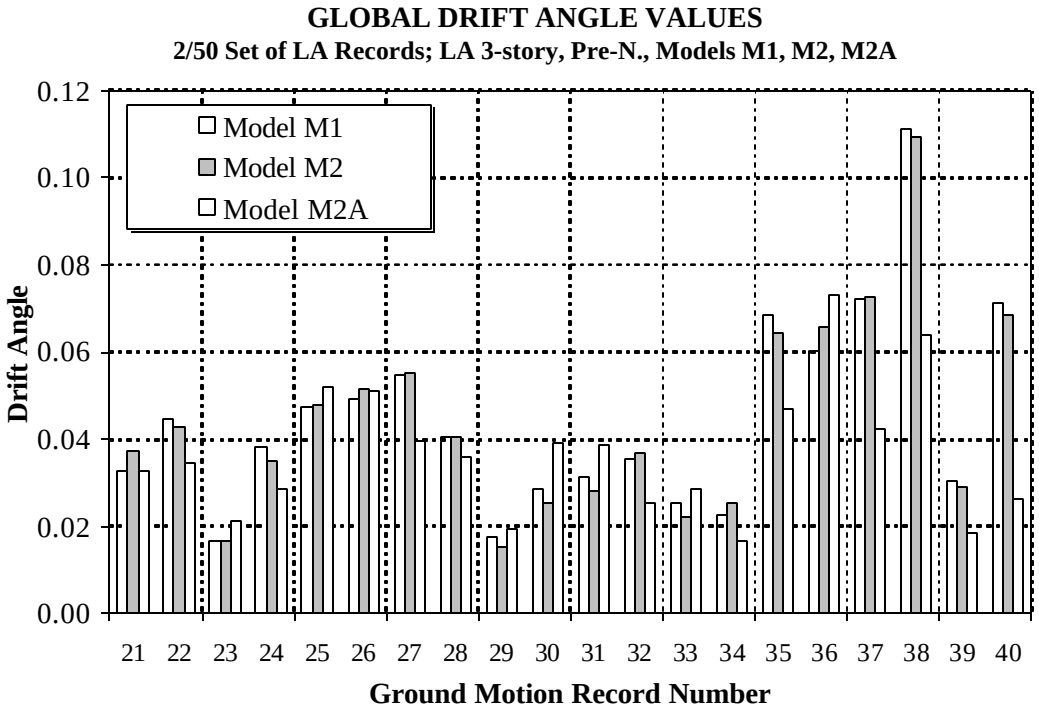

Figure 3.22 Global Drift Angle Values for LA 3-story structure, Different Models; 2/50 Set of Ground Motions

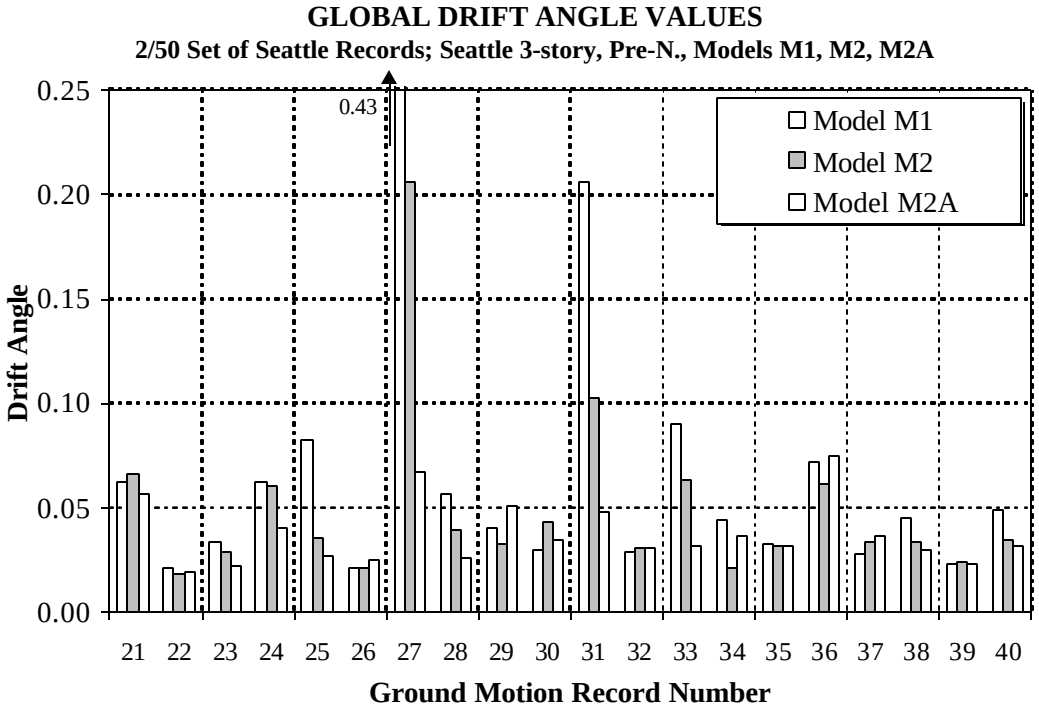

Figure 3.23 Global Drift Angle Values for Seattle 3-story Structure, Different Models; 2/50 Set of Ground Motions

CHAPTER 4

P-DELTA EFFECTS FOR FLEXIBLE STRUCTURES

4.1 Introduction

This chapter focuses on the effect of structure P-delta on the response of single-degree-of-freedom (SDOF) systems and two multi-degree-of-freedom (MDOF) steel moment resisting frame buildings. For MDOF structures the P-delta effect, caused by the cumulative gravity loads above a story level acting on the deflected shape, is dependent on the properties of individual stories. The effective lateral load resistance of the story is approximately reduced by the amount $P_i q_i$, where P_i is the sum of the gravity loads acting above story i and q_i is the story drift angle. This P-delta effect can be very severe for steel moment resisting frame structures as these structures are usually quite flexible and may be subjected to large lateral displacements. For certain cases where the vertical load on a story is high and the story is subjected to large displacement demands, progressive increase in displacements can occur resulting in a loss of stability for the structure.

The P-delta effect for SDOF systems is evaluated for a wide range of periods, over different strength levels, and for different intensities of the P-delta effect, using nonlinear dynamic analysis. The effect on the response is represented in terms of displacement amplification ratios. The collapse potential of MDOF structures is evaluated using different models of increasing complexities for the Los Angeles 20-story pre-Northridge structure and analyzing using static pushover analysis, elastic and inelastic time history analysis, and dynamic pushover analysis. Another case study using the Seattle 3-story pre-Northridge structure is presented to highlight the potential for unstable behavior due to the structure P-delta effect even for low-rise structures. The feasibility of using SDOF systems to represent the P-delta effect for MDOF structures is investigated.

The effect of using an improved analytical model of the MDOF structure, as against a simpler model, on the static and dynamic response has been presented in the previous chapter. In cases where the simple bare frame models (models M1, and M2) may show unstable behavior due to the P-delta effect, the use of a model which is representative of the strength and stiffness of the entire structure becomes more critical to ascertain the actual collapse potential of the structure. The assumptions made in the analytical modeling of the structures (e.g., strain-hardening, damping, etc.), as described in the previous chapter, are also adopted for all the models used here to evaluate the effect of P-delta on the response of the two case study structures.

4.1.1 Code Provisions for P-Delta Effects

According to Section 1628.9 of the UBC 1994, P-delta effects need not be considered when either the ratio of the secondary moment to the primary moment in a story is less than 0.10, or when the story drift is less than $0.02/R_w$ for structures in seismic zones 3 and 4. A similar formulation is adopted by NEHRP 1994 under Section 2.3.7.2. The formulation can be expressed in terms of the stability coefficient q as follows:

$$q = \frac{P_i \Delta_i}{V_i h_i} \tag{4.1}$$

where P_i is the total vertical load acting above floor level i, Δ_i is the design story drift occurring when the story shear is equal to the design shear V_i, and h_i is the height of story i. NEHRP 1994 also prescribes an upper limit for the stability factor, which for steel moment resisting frame structures is approximately equal to the 0.10 limit. For structures having the stability factor greater than this limit the guidelines suggest that the structure may be potentially unstable and should be redesigned.

The provisions given in the UBC and NEHRP guidelines for the stability check of the structure are based only on the elastic stiffness of the structure. One of the reasons given in NEHRP 1994 for estimating P-delta effects using the elastic stiffness is based on the apparent lack of stability related failures, the credit for which is ascribed to the overstrength in a structure. The overstrength in a structure (which may vary significantly from one design to another) may reduce the intensity of the displacements, however, dynamic P-delta effects in an inelastic structure may still result in unacceptable performance of the structures, as will be shown later in this chapter. Furthermore, the

stability coefficient values are based on studies carried out using SDOF systems (e.g., Bernal, 1987), which may not be good indicators for the P-delta effect at the story level, an issue which is investigated in this study. The expectation is also that the response of the MDOF structure, which responds inelastically during a design event, will be more severely affected by P-delta effects than the response of the same structure responding in the elastic range.

4.2 P-delta Effect for SDOF Systems

In a static sense the P-delta effect can be visualized as an additional lateral loading that causes an increase in member forces and lateral deflections, reduces the lateral load resistance of the structure, and may cause a negative slope of the lateral load-displacement relationship at large displacements. For a bilinear SDOF system with mass m and height h the P-delta effect can be represented as illustrated in Figure 4.1. A dimensionless parameter $q = mg/(Kh)$ [identical to the stability coefficient] can be used to describe the decrease in strength and stiffness. The elastic stiffness K is reduced to $(1-q)K$ and the post-elastic stiffness $a'K$ is reduced to $(a' - q)K$. In this formulation a' is the strain-hardening ratio of the system without P-delta effects, and $(a' - q)$ is the ratio with P-delta effects, which is denoted here as the effective strain-"hardening" ratio a. If $q > a'$, then a becomes negative and for such a case the system reaches a state of zero lateral resistance (termed as "collapse") at a displacement of D_c. The maximum lateral strength of the system with P-delta, $V'_{y,}$ is the strength of the system without P-delta reduced by a factor of $(1-q)$.

From a dynamic perspective the structure P-delta effect may lead to a significant amplification in displacement response if a is negative and the displacement demands are high enough to enter the range of negative lateral stiffness. This is illustrated in Figure 4.2, which shows the dynamic response of an SDOF system whose hysteretic behavior is bilinear but includes P-delta effects that lead to a negative post-yield stiffness $aK = -0.05K$. The presence of the negative stiffness leads to drifting (ratcheting) of the displacement response, which may bring the SDOF system close to collapse. Using the set of 20 LA 2/50 ground motion records (see Appendix A), mean values of the displacement amplification ratio (displacement for $a = -0.03$ normalized by displacement for $a = 0.0$) for different strength reduction factors R (R = elastic strength demand over yield strength) and a period range from 0 to 5.0 seconds are shown in Figure 4.3. The

displacement amplification depends strongly on the yield strength (*R*-factor) and the period of the SDOF system. Particularly for short period systems with low yield strength the amplification can be substantial. The diagrams are terminated at the last period of stability, i.e., for shorter periods at least one record did lead to a complete loss of lateral resistance. The displacement amplification for the systems with a decreased value of a = -0.05 (increased P-delta effect) is shown in Figure 4.4. The response of the system is found to be extremely sensitive to the level of P-delta effect, as shown by the significant increase in the displacement amplification factor and the increased instability observed for the systems (the curves are stopped at longer period values).

4.3 Case Study 1: The Los Angeles 20-Story Structure

The value of the stability coefficient for the 20-Story pre-Northridge structure designed for Los Angeles conditions is evaluated and found to be less than 0.10 for all stories. The values are obtained from a static analysis using a base shear based on the bare frame period of the centerline model (model M1), and distributed over the height of the structure following the UBC load pattern. Thus, based on a static elastic analysis the P-delta effects do not indicate any potential for unstable behavior of the structure. Use of a stability coefficient value of 0.10, would only result in the story displacements being amplified by a factor of 1.11. The structure, even with the amplified displacements, satisfies the code drift requirements. The inelastic response of different structural models to static and dynamic loading is presented in the following sections.

4.3.1 Static Pushover Analysis for Model M1

The normalized base shear versus roof drift angle (displacement of the roof normalized with the height of the structure) response for model M1, with and without P-delta effects being considered is shown in Figure 4.5. The model in which P-delta effects are not being considered (model M1-NPD) has a hardening post-yield stiffness which is maintained even at large drifts. The elastic stiffness of the model for which P-delta effects are considered (model M1) is only slightly smaller (indicating that the value of q is not large) than for model M1-NPD resulting in very similar elastic response of the two models. The post-yield global response of the model is, however, radically different exhibiting only a short strength plateau (till 1.5% roof drift) followed by a rapid decrease

in lateral load resistance, shown by the negative slope of the curve. The structure reaches a state of zero lateral resistance at the relatively small global (roof) drift value of 4%.

As mentioned previously, the P-delta effect is caused by the vertical forces acting above a story level on the story displacement. The global pushover curve only shows an aggregation of the effects over the different stories of the structure. The response of the lower ten stories of the structure, in terms of the normalized story shear versus story drift angle (story drift normalized with story height), is shown in Figure 4.6 for model M1. The lower five stories exhibit similar negative post-yield stiffness values, which are approximately equal to –6% of the elastic story stiffness. The negative post-yield stiffness arises on account of the Pd/h (or Pq) "shear" which counteracts the 3% strain-hardening that would exist without P-delta. The absolute sum of the strain-hardening stiffness without P-delta effects, and the post-yield stiffness (as percentages of the elastic stiffness), approximately yields the value of the stability coefficient. Thus, from the elastic analysis itself an estimate of the post-yield stiffness of the story can be obtained. The elastic analysis will, however, not be able to estimate the strength at, and the width of, the post-yield plateau.

The story shear versus story drift response curves presented in Figure 4.6 indicate that the lower stories reach a state of zero lateral resistance around 16% story drift and that the model would collapse if the displacement demands exceeded this value. The figure also seems to indicate that stories 6 through 10 reach a collapse limit at much smaller drifts, however, this is a misleading indication as these stories are recovering the effective stiffness (unloading with elastic stiffness) as the structure is pushed to larger displacements (beyond 1.5% global drift). Thus, even as the structure is experiencing increasing displacements, only the lower five stories have corresponding increasing displacements; the other stories are backing up. The response of the model at different points during the pushover analysis under the given load pattern is shown in Figure 4.7. This figure shows that beyond a global drift value of approximately 1.5%, the stage at which the structure attains a negative post-yield stiffness, the deflected profile above story 5 is straightening out whereas the lower five stories have increasing displacements. At the incipient collapse global drift of 4%, almost the entire roof drift is constituted by the lower five stories whereas the upper 15 stories have negligible drift.

The amplification of drifts in the lower stories and the corresponding de-amplification in the upper stories, as the structure is pushed to increasing roof displacements, is

quantitatively represented in Figure 4.8. This figure shows the relative contribution of different stories (represented as the ratio of the story drift angle to the global drift angle) to the global drift. In the elastic range the contribution of all the stories is about the same, but large differences are observed in the inelastic range. The rapid increase of drift in the lower 5 stories is evident, and at near collapse level the contribution of the upper thirteen stories is almost zero.

The results presented in Figures 4.5 through 4.8 are based on a pushover analysis using the NEHRP 1994 design load pattern with k = 2.0. The global pushover response is relatively insensitive to the applied load pattern (see Section 7.2.3). The story level pushover results are typically more sensitive to the load pattern adopted. However, if the chosen pattern is representative of seismic loading on the structure, then drastic changes are not expected in the observed response. From a design perspective it is most helpful to understand the behavioral characteristics of the structure from the pushover analysis in order to evaluate the influence of P-delta effects on the response of the structure.

4.3.2 Dynamic Response for Model M1

The potential importance of P-delta effects on the seismic response of flexible steel moment resisting frame structures, as indicated by the static pushover analysis, necessitates the use of nonlinear time history analysis to better evaluate the response of the structure under time varying loads.

The model M1 for the structure was subjected to the set of 20 ground motions representative of a 2/50 year hazard level (LA21-40, see Appendix A). Collapse (defined as the state when one story cannot resist any lateral loads) of the model was observed for the ground motion record LA30 (Tabas, Iran). The acceleration, velocity, and displacement time history of the record are shown in Figure 4.9. The record exhibits clear pulse type characteristics and drives the lower stories in the model to story drifts in excess of 15% at around T = 17.5 seconds, during the second pulse which follows the largest pulse in the ground motion. The time histories of story drifts for the lower six stories are shown in Figure 4.11. The first pulse drives the story drifts in the range of 6-7%, at which level the stories have clearly attained the negative post-yield stiffness shown in Figure 4.6. Once on the negative post-yield slope, the reversal in the loading pulse is incapable of inducing a complete recovery in the story drifts. The next pulse, which is smaller in magnitude, drives the stories farther into the range of unstable

behavior, reaching the stage of negligible lateral resistance and collapse at around 15% story drifts. Story 6 shows a better recovery of drift with reversal in loading as compared to the other 5 stories, which is also indicated by the pushover analysis.

The dynamic analysis results presented so far indicate that a collapse potential exists for the analytical model M1, which is a very simple representation of a complex three dimensional structure. If the model were to be representative of the structure, then the analysis points out an alarming problem since the structure was designed in accordance with the UBC 1994 requirements, and in addition has a strength, which is much more than required by the code (design base shear = 0.03W whereas the strength at the plateau level is 0.075W, see Figure 4.5).

4.3.3 Static and Dynamic Response of Improved Models

As pointed out in the previous chapter, the bare frame centerline model M1 is a poor representation of the structure. Improvements to the model have been made in the form of models M2, and M2A, as described in Section 3.4. In addition to these three models for the structure, different models focusing on contributions from additional elements (for example, contributions from the interior columns only), as well as approximate quantification of contributions, which cannot be estimated accurately (for example, non-structural components), are evaluated to ascertain the relative and combined contribution of different elements to the dynamic response of the structure. Elastic time history analysis, including P-delta effects, are also carried out to ascertain the extent to which elastic analysis is able to capture the effect of P-delta on the response of the structure. The following different models are investigated:

M1 : basic centerline model of the bare moment resisting frame

M1FW : model M1 with the contribution of all the columns not part of the moment resisting frame modeled as an equivalent column (“flag pole” F); the interior columns are assumed to bend about their weak axis (W). The columns of the orthogonal moment resisting frame are also included. For structures with basements, the effect of the interior columns can be quite significant in the first story as the columns continue into the basements.

M1FS : same as model M1FW, but all the interior columns are bending about the strong (S) axis. The orientation of the orthogonal moment resisting frame columns is taken as per the design.

M1A : model M1 with all (A) reliable contributions as described in Section 3.2.2. The interior columns are modeled as bending about their weak axis.

M2 : model for bare moment resisting frame, including strength and stiffness of panel zones

M2L : model M2 with a limit (L) on the gain in strength of beams due to strain-hardening. The beams are assumed to attain a maximum strength of 1.2 times the plastic strength at 2% plastic rotation. The strain-hardening of the elements is adjusted accordingly.

M2A : model M2 with all reliable contributions

M2AL : model M2A with the limited strength of beam springs as described for model M2L.

M2AK : model M2A with the stiffness (K) of beams and columns (not panel zones) increased by 50% (in elastic and inelastic range) to account for non-structural components. The effect of increasing the stiffness only in the elastic range is presented under section 8.6.

M1-NPD : model M1 with no (N) P-delta (PD) effects

M1E-PD : elastic (E) model M1 with P-delta effects

M1E-NPD : elastic model M1 with no P-delta effects

The first mode periods, corresponding elastic spectral acceleration values for two ground motions (LA30 and LA36), and the global drift angle values obtained from time history analysis of the different models under the two records are tabulated in Table 4.1. The acceleration, velocity, and displacement time histories for the second record (LA36, see Appendix A) are shown in Figure 4.10. This record also exhibits clear pulse type characteristics. This record is chosen as large story displacement demands for the 20-story structure were observed for this record also.

Depending on the model, the first mode period of the structure varies anywhere between 3 and 4 seconds, which is a significant variation in the period for a structure. Correspondingly the elastic spectral acceleration at the first mode period for the different models is significantly different. The elastic displacement spectra for the two ground motions used in this case study are shown in Figure 4.12. While the LA30 ground

motion shows a rapid increase in the displacement demands for systems having a period greater than 3.5 seconds, the LA36 ground motion shows almost constant displacement demands over a period range of 2 to 5 seconds. The displacement demand is almost identical between the two ground motions at the first mode period of the basic model M1.

Static Response

The roof drift angle versus normalized base shear response for many of the models is shown in Figure 4.13. The improvements in the strength and post-yield stiffness of the improved models as compared to the basic M1 model are evident. The addition of the interior columns to the centerline bare frame model M1 (models M1FW and model M1FS) does not influence the effective strength of the structure by much, however, the strength plateau is widened considerably. The widening of the strength plateau results in the structure attaining a negative post-yield stiffness at a higher drift value and thereby increasing the global drift level associated with the collapse (about 8% as against approximately 4%) condition for the structure. Addition of all other reliable contributions to the M1 model (model M1A) increases the elastic stiffness, and the strength at the plateau level slightly as compared to models M1FW and model M1FS. The post-yield behavior of the model M1A is, however, very similar to the behavior of the model M1FW.

Model M2, which is a more realistic representation of the bare frame moment resisting frame, shows improved behavior as compared to the bare frame centerline model M1. The differences in the behavior are in terms of a slightly higher elastic stiffness, higher effective strength at the yield level, and a higher global drift value associated with the collapse level. Addition of all other reliable contributions to the M2 model (model M2A) results in an increase in the effective strength, and an increase in the width of the strength plateau. These improvements are further enhanced if model M2AK is used. The global static pushover analysis results show that a wide range of behavior is observed depending on the modeling assumptions. Of the models used, Model M2A is the most reliable (least number of judgmental assumptions) model of the structure, and exhibits a response which is far superior to the response of the bare frame centerline model M1.

The normalized story shear versus story drift response for story 2 (used as a representative story for the P-delta sensitive region of the structure) of the different

models is shown in Figure 4.14. Differences observed at the global response level are observed at the story level as well. The story drift at which dynamic instability occurs increases from 0.16 (or 16%) for model M1 to 0.235 (or 23.5%) for model M2A. Figure 4.15 shows the contribution of story 2 drift to the global drift for the different models. The contribution of different stories to the global drift becomes less non-uniform (individual stories differ less from the global drift) as the model is improved.

Dynamic Response

Dynamic analysis of the different models is carried out with record LA30, for which collapse was observed for model M1. The time history of response for story 2 drift for the different models (excluding models M2L and M2AL) is shown in Figures 4.16a and 4.16b. If P-delta effects are ignored (model M1-NPD) the response is drastically different from the response of model M1. The stories recover drift with the reversal in the loading during the first pulse, and the subsequent response oscillates about the mean position with only a small offset. The maximum story drift of about 5% and negligible residual drift (offset from mean position at end of record) are well within tolerable limits for highly nonlinear response cases.

The response of model M2, which has only slightly higher effective strength and wider strength plateau as compared to model M1 causes the peak drift during the first loading pulse to be slightly lower and permits a larger recovery of drift during the load reversal in the pulse. This small increase in reversal results in the subsequent pulse being unable to drive the story to drifts nearing the point of collapse (around 0.20). However, by the end of the second pulse the story is well into the negative post-yield stiffness region and even the subsequent small ground motion excitations result in a progressive increase (ratcheting) in the drift of the story, close to a value of 0.15. Thus, even though the model does not “collapse”, it is clearly in a precarious state with any increase in load or decrease in capacity being capable of pushing it further towards collapse. This observation is reinforced by the collapse condition encountered for model M2L.

The addition of the interior columns to model M1 (models M1FW and M1FS) changes the response of the models in a similar manner as observed for model M2, wherein the amplitude of the first excursion is reduced, resulting in better recovery of drift, and the inability of subsequent smaller ground motion excitations to push the model to collapse. Model M1A shows peak and residual drifts of about 5%. By far the best

behavior is observed for model M2A, the peak story drift is 4.2% and the residual drift is approximately 2%. Full drift recovery (crosses the mean position) occurs during the load reversal of the first loading pulse, and the response is similar to that of model M1-NPD, even though P-delta effects are being considered for model M2A. The response of model M2AK is better than the response of model M2A, but not very substantially as neither model is being pushed onto the range of significant negative post-yield stiffness. The response of model M2AL is also found to be only slightly different from the response of model M2A.

The width of the strength plateau is a critical parameter controlling the response of the models. Based on this plateau width, the first loading pulse can either drive the structure firmly onto the region of negative post-yield stiffness from where recovery of drift is difficult and the structure ratchets towards collapse, or can drive it not too far onto the negative post-yield slope from where the recovery of drift is still possible and the structure has a well contained response. Thus, even small differences in the strength and stiffness of the model can result in a drastic difference in the response of the structure once an individual story attains the negative post-yield stiffness. The presence of the second loading pulse immediately following the first largest pulse in the ground motion and its ability to drive the structure severely compounds the P-delta effect for this structure under this particular ground motion.

The response of the elastic models, with and without P-delta effects (models M1E-PD and M1E-NPD), is very similar to one another. The model with P-delta effects shows slightly larger amplitudes, but both responses oscillate in a symmetric pattern about the mean position resulting in zero residual drifts.

The maximum story drift angle envelopes for all the models, based on a time history analysis using the LA30 ground motion, are shown in Figure 4.17. The results for model M1 are not shown owing to the predicted collapse conditions. For model M2 the story drifts are as high as 0.15, which is clearly outside the acceptable range of story drifts. For model M2A, however, the maximum story drift is 0.051 and occurs in story 4. The improved model is thus far from a P-delta collapse state. It is only a coincidence that the story drift angle envelope for model M1-NPD is very similar to the envelope for model M2A. Overall, the use of an improved model can change the entire perspective regarding the potential for P-delta collapse for the structure.

Even though large variations are observed in the dynamic response of the different models, the pattern of deformation over height is similar. This pattern shows larger story drifts in the bottom stories, a sharp decrease around the sixth story level, and small story drifts in the middle and top stories. This pattern is a consequence of not only the P-delta effects, which are more severe for the lower stories, but is also a function of characteristics of the ground motion which induces large inelastic deformations in the structure. The elastic models (models M1E-PD and M1E-NPD) are, however, unable to capture the deformation pattern over the height of the structure and predict close to uniform drifts for all the stories. Not much difference is observed between the story drift response of the elastic model with P-delta effects and the elastic model without P-delta effects. This observation suggests that inelasticity magnifies the P-delta effects on the response of a structure. In addition, the elastic analysis severely under-predicts the deformation demands in the lower stories, and over-predicts demands in the upper stories. These observations based on the elastic analysis question the advocacy of the concept that elastic analyses can be used as indicators of inelastic behavior of a structure.

The story drift angle envelopes for the models, based on a time history analysis using the LA36 ground motion, are shown in Figure 4.18. The trends in terms of reduction in peak drifts with improvements to the model, and distribution of drift demands over height are similar to the trends observed for the models under the LA30 ground motion. The elastic analysis results are again drastically different from the inelastic analysis results. However, there are also some very critical differences. Firstly, the centerline bare frame model M1 did not collapse, even though the spectral displacement demand for both the records at the first mode period of model M1 is the same. The maximum story drifts for model M1 are even smaller than the drifts for model M2 under the LA30 record. The most significant difference between the response to the two ground motions is in the effect of the modeling improvements on the maximum drift demands. The story drift demands for model M2A under record LA36 are not significantly lower from the demands for model M1, and the difference between the response of the two models is much less than the difference observed for the same two models under the LA30 record. Even for model M2A, the maximum story drift demand is 0.105 occurring in story 4, as against a maximum story drift demand of 0.051 in story 4 for model M2A under the LA30 ground motion. Clearly, even with improved modeling, the simulated record LA36 brings this 20-story structure closer to collapse (or results in undesirable high drift demands) than the Tabas record. The simple centerline bare frame model M1 would, however, imply the opposite conclusion.

The global drift angle demands (Table 4.1) follow the trends observed at the story level. A large variation in demands at the roof level is observed for the models when subjected to LA30, which is as expected from the change in first mode period for the different models and the corresponding spectral displacement demand. Following the same reasoning, the global drift demands under LA36 do not change significantly except for the cases where either P-delta effects are not considered or where the elastic response for the structure is computed.

4.3.4 Dynamic Pushover Analysis

An understanding of the behavior of the different models can also be obtained from an analysis process, which is referred to as the "dynamic pushover analysis". For this analysis, which consists of a series of time history analysis, the analytical model of the structure is subjected to different intensities of the same ground motion, and the peak value of the response parameter of interest (in this case the maximum story drift over the height of the structure) is recorded from each analysis. The increase in ground motion intensity, caused by a simple scalar multiplication of the ground motion time history with a "scale factor" is carried out till the critical parameter reaches an unacceptable value. The scale factor at which this unacceptable performance is observed can be taken as a measure of the "capacity" of the structure for resisting this specific ground motion within a specified performance range. The procedure and some sample studies are documented in [Wen and Foutch (1997), Luco and Cornell (1998)].

The results from the dynamic pushover analysis for the different models subjected to the Tabas (LA30) ground motion record are shown in Figure 4.19. The figure presents the maximum story drift over the height of the structure as a function of the scale factor used for the ground motion time history. Often the y-axis is represented in terms of the spectral acceleration of the ground motion at different intensities, however, since the models have different first mode periods, a representation employing the spectral acceleration would not uniformly show the effect of an increase in the ground motion intensity on the different models. Hence, the y-axis is represented in terms of the scale factor. A value of 1.0 represents the ground motion as shown in Figure 4.9.

If a value of 0.05 (or 5%) maximum story drift is taken as the limit state for acceptable performance, then the model M1 reaches the limit at a scale factor of 0.62. The model M2A would fail the same performance limit at a scale factor of about 1.0. If

the performance criterion was based on very high story drift values, then the models M1 and M2A would fail the performance test at scale factor values of 0.8, and 1.4 respectively. The important conclusion from the results is that the capacity of the structure in resisting the Tabas ground motion is consistently about 70% higher if the more realistic model M2A is used, as against the basic centerline bare frame model M1.

The change in response of the individual stories for model M2A, with increasing severity of the ground motion is shown in Figure 4.20. At a low scale factor of 0.2, the response is elastic as shown by a straight line drift envelope, where all the stories have almost equal drift demands. As the intensity of the ground motion is increased, there is a clear movement of the higher drift demands towards the lower stories, where the severity of the P-delta effect is the maximum. The nonlinearity in the P-delta effect is visible through the much higher increase in story drift demands from similar increases in the intensity of the ground motion.

4.3.5 Conclusions from the Case Study

The case study discussed in Section 4.3 considers the P-delta effect on the response of a flexible 20-story steel moment resisting frame, designed for Los Angeles conditions according to the Uniform Building Code 1994. Different models ranging from a bare frame centerline model (model M1) to a model incorporating the effects of panel zones, effects of slabs, effects of interior columns, and the effects of shear connections (model M2A) have been studied under two ground motions to evaluate the collapse potential of the different models, on account of the structure P-delta effect. The important observations and conclusions from the case study are as follows:

- The potential for P-delta induced collapse (or of attaining undesirable levels of drift demands) exists for flexible structures. The lateral load resisting system, which resists the P-delta effect from the entire structure as the interior simple frames transfer the P-delta effect through the rigid floor diaphragm, designed according to the present code requirements may be insufficient to provide adequate safety against collapse or excessive drifts when subjected to extreme ground motion excitations.

- The seismic response of the structure is heavily dependent on the modeling assumptions and the ground motion characteristics. If large P-delta effects (due to

high gravity loads and/or high displacement demands) are expected, then the need exists to employ the best possible mathematical representation of the structure in order to realistically assess the importance of P-delta effects.

- The incorporation of strength and stiffness from elements other than the elements forming the main lateral load resisting system may improve the seismic behavior of the structure significantly.

- The width of the strength plateau plays a critical role in the response of the model to severe ground motions. Best inelastic behavior is observed if the structure remains on the strength plateau and does not move into the negative post-yield stiffness region. Thus, one of the considerations during design should be concerning the extension of the plateau width. This may be achieved by using different beam sections (therefore strengths) on a floor level. This will result in all the beams not form plastic hinges at about the same instance, thereby delaying the formation of a mechanism. Another possible solution to the P-delta problem exists in the form of a flexible secondary system (like the gravity columns), which add to the stiffness of the structure after the primary system has yielded, thereby widening the stable strength plateau region of the global pushover curve.

- Elastic analysis even when including the P-delta effects will not be able to represent the effects of P-delta on the inelastic system response, neither in terms of maximum response of critical parameters, nor in terms of the distribution of demands over the height of the structure.

- The use of the elastic stability coefficient q, such as the one used by the UBC and NEHRP '94, does not provide adequate protection against the occurrence of a negative post-yield stiffness and excessive deformations. In general, if the stability coefficient q is greater than the strain-hardening ratio for individual elements, then a negative post-yield stiffness will develop at formation of a mechanism.

- The use of static pushover analysis is very useful in understanding the behavior of the structure as represented through different models. The analysis identifies the effect of different modeling improvements on the strength and stiffness of the structure (at global and story level), the drift levels at which the negative post-yield

stiffness is attained, and the drift level associated with instability. This information is most helpful in rationalizing the inelastic dynamic response of the models.

- The P-delta effect is a story level problem and needs to be addressed at that level. Displacement amplification factors obtained using single-degree-of-freedom systems may not be able to predict the amplification of demands at the story level.

- Model M2AK, which has increased stiffness on account of approximate representation of non-structural components, exhibits the best behavior as compared to other models. Sensitivity to increase in stiffness in the elastic range due to the non-structural elements is presented in Section 8.6.

The above stated conclusions have to be interpreted within the context in which they are obtained. A two dimensional representation of a complex three dimensional system has been used with many inherent assumptions. The assumptions include use of concentrated plasticity elements, use of constant strain-hardening of 3% for all inelastic elements irrespective of the magnitude of inelastic deformations (except for models M2L and M2AL), disregard for cyclic hardening, no strength and stiffness deterioration in element behavior (sensitivity to stiffness degradation is summarized in Section 8.3), and assumption of ductile connections with no weld fracture problems. The models may not be an accurate representation of reality, but the presented results, which are obtained under a combination of favorable and unfavorable assumptions, indicate that there is a potential for P-delta induced collapse hazard (or unacceptable behavior in the form of excessive deformations) that needs to be considered explicitly and more realistically than is done in the current design process.

4.4 Case Study 2: The Seattle 3-Story Structure

The 3-story pre-Northridge design for Seattle also exhibits a potential collapse hazard on account of P-delta effects. The model M1 and model M2 representation for the structure, using 3% strain-hardening for all elements, attain a negative post-yield stiffness at 1.7% global drift and 4.5% global drift respectively. The global pushover curves for the two models for the Seattle structure, clearly showing the negative post-yield stiffness, are presented in Figure 4.21. For model M2, on account of distribution of yielding between panel zones and beams, the negative post-mechanism stiffness is reached at a

global drift value which is much higher than the drift value at yield, as compared to model M1 which attains negative post-yield stiffness soon after yield.

The Seattle 3-story structure is more flexible (first mode period is 1.36 seconds) than the Los Angeles 3-story structure (first mode period is 1.01 seconds) as it is designed for a lower base shear demand (seismic zone factor of 0.3 for Seattle as against 0.4 for Los Angeles). The stability coefficient (inversely proportional to the elastic stiffness) is much larger for the Seattle structure than the Los Angeles structure, as both the structures have identical vertical loading. Thus, the P-delta effect, which for the Los Angeles 3-story structure results in a post-yield stiffness of approximately 0% (see Figure 3.10, stability coefficient is about 0.03), for the Seattle structure results in a negative post-yield stiffness of about -3% (stability coefficient is approximately 0.06).

Ground Motion Characteristics

The set of ground motion records representative of a 2% probability of being exceeded in the next 50 years for Seattle does contain records which drive the models of the structure onto the negative post-yield stiffness region. Ground motion records for which important results in the context of P-delta effects were obtained are the two orthogonal components of the Olympia 1965 ground motion (designated SE27 and SE28, see Appendix A). The scaled acceleration, velocity, and displacement time histories for the two ground motions are shown in Figures 4.22 and 4.23. The records were scaled by a factor of 10 to attain spectral acceleration values compatible with the 2475 year return period hazard for Seattle conditions. The scaling, thus resulted in relatively strong ground motions.

The elastic displacement spectra for the two ground motions are shown in Figure 4.24. From the displacement demand values at the first mode period of the two models the expectation is that both the bare frame models will be pushed far enough to attain the negative post-yield stiffness. Since the first mode period lies in a region where the slope of the spectra is very steep, the displacement demands for the two models are expected to increase with elongation of the period (due to nonlinear response) of the models.

Dynamic Response of Models M1 and M2

The drift demands obtained from an inelastic time history analysis, using model M1 and model M2, are in the range of expected demands (based on the elastic displacement

spectra) for SE28. However, the inelastic demands obtained under the SE27 record are almost an order of magnitude larger than the inelastic demands obtained under the SE28 record. This is for two components of the same ground motion, which have very similar peak ground motion characteristics as well as similar spectral characteristics. The global drift time history of response of models M1 and M2 subjected to the two records is shown in Figures 4.25 and 4.26, respectively. As expected, model M2 shows relatively better behavior as compared to model M1 though the response of the two models under the SE27 ground motion is clearly in the unacceptable range.

The cause of the exceedingly high drift demand observed under the SE27 ground motion is the second pulse that immediately follows the first pulse in the ground motion. The two pulses are clearly seen in the ground motion displacement time history (Figure 4.22). The first pulse drives the two models into the negative post-yield stiffness range, partial recovery of drift occurs and then the second pulse drives the models into very high drift ranges (around 10%) from where on the structure ratchets in one direction, for the full duration of motion, with each small cycle of loading progressively increasing the displacement of the structure. The other ground motion, SE28, does not drive the structure very far in the first cycle of loading, recovery of drift occurs, and the structure responds cyclically to the rest of the ground motion with a very small offset.

The loss in lateral load resistance of the structure can be seen from Figure 4.27, which shows the effective strength for story 1 (measured by the story shear) as a function of the lateral displacement for story 1, for model M1. The story shear is defined as the net external loading that the story is capable of resisting (or sum of all applied lateral loads above that story level), as against the "equivalent" story shear, which is the sum of the external loading plus the representation of P-delta effects as externally applied forces. The story shear is obtained in an approximate manner by subtracting, over the entire time history, the P-delta component ($P\Delta/h$, at each time step) from the "equivalent" story shear (as given by the analysis program). Figure 4.27 resembles a single-degree-of-freedom system with bilinear characteristics and a negative post-yield stiffness ($\alpha \approx -0.03$), similar to Figures 4.1 and 4.2.

Clearly, the obtained drift demand value of about 0.50 (or 50%) is a byproduct of the inherent assumptions in the models used for analysis. Stiffness degradation, strength deterioration, and possible fracture of welded connections would occur at much smaller drift values, indicating a collapse potential. On the other hand, the analytical models (M1

and M2) are bare frame models and disregard many contributions to strength and stiffness.

Table 4.2 compares the global drift angles obtained using elastic analysis (with and without P-delta; models M1E-PD and M1E-NPD), the demands obtained using inelastic time history analysis and model M1-NPD (without P-delta), and the inelastic global drift angle demands for model M1. The drift demands observed for the elastic models are as expected from the elastic spectral displacement demands, with higher demands being observed for the SE28 record than for the SE27 record. The elastic analysis also shows a symmetric response about the mean position ($q+$ values are similar in magnitude to the $q-$ values), even with P-delta effects included. The use of inelastic models changes the values and patterns of the deformation demands significantly as compared to the elastic models; the response becomes much less symmetric (the inelastic models subjected to severe P-delta effects tend to ratchet on one side) coupled with, for SE27, a drastic increase in the demands for model M1. For SE28, the maximum inelastic global demands are lower than the maximum elastic demands, which is not unexpected as for systems not influenced by severe P-delta effects, the inelastic global demands are shown to be smaller than the elastic demands (depending on the period, and level of inelasticity - Seneviratna and Krawinkler 1997, also see Chapter 7).

The case study involving the Seattle 3-story structure has been presented to show that the potential for P-delta induced collapse or unacceptable behavior exists even for low-rise structures, and that the P-delta effects need to be better considered in the design process.

The results using SE27 may not be representative of "reality" on account of the severe scaling of the ground motion, and the use of analytical models, which do not include many tangible and intangible contributions. However, the average deformation demands for the structure based on all the 20 records in the set, are also very severe; 84^{th} percentile story drift demands are of the order of 0.08. Thus, there exists a potential for unacceptable behavior if the structure attains negative post-yield stiffness and is subjected to severe ground shaking. Since the results are very sensitive to the structural models, analysis techniques, and the ground motion characteristics, an inelastic time history analysis is required to understand the P-delta problem for a structure. Guidelines to safeguard against the possibility of P-delta induced problems need to be developed, in the context of nonlinear behavior of structures.

4.5 Conclusions

The study discussed in this chapter is concerned with the evaluation of P-delta effects on the response of flexible steel moment resisting frame structures. The P-delta effects can result in a potential collapse hazard or unacceptable behavior for such structures. Two case studies, one involving a 20-story structure designed according to UBC 1994 for Los Angeles conditions, and the other a 3-story structure designed according to UBC 1994 for Seattle conditions, have been presented to highlight the P-delta effect on these structures. Sensitivity of results to analysis techniques, modeling assumptions, structural characteristics, and ground motion characteristics has been evaluated. Furthermore, the feasibility of representing the P-delta effect for MDOF structures using SDOF systems is evaluated.

The results presented in this chapter are based on simple models of the structures, with inherent assumptions associated with these models. While effects such as strength and stiffness deterioration, or weld fractures, will increase the potential for P-delta related problems, cyclic strain hardening and distributed plasticity models will improve the behavior by delaying the onset of the negative post-yield stiffness. However, the case studies have highlighted the potential for P-delta induced unacceptable behavior in code designed SMRF structures, presented ways to better understand and address the P-delta problem for existing structures, and reinforced the need for explicitly considering P-delta effects in the context of inelastic behavior for future designs. The following important conclusions can be derived from the two case studies and the evaluation for the SDOF systems:

- Elastic analysis will not disclose the potential for P-delta related problems for structures which are expected to respond inelastically. Inelastic static analysis is very useful for understanding the behavior of the inelastic structure but by itself will not be able to capture the dynamic P-delta effects, which are very sensitive to the ground motion characteristics once negative post-yield stiffness has been attained. Inelastic time history analysis is required to ascertain the full potential of P-delta related problems for a structure.

- Current design guidelines need revisions to incorporate the effect of P-delta on inelastic systems, in order to mitigate the hazard associated with P-delta effects for flexible SMRF structures. The use of the elastic stability coefficient is found to be

inadequate to capture the P-delta effect in inelastic systems. The elastic stability coefficient, however, can be used to estimate the extent of negative post-yield stiffness ($\alpha' - q$) that the structure might experience.

- The design modifications can take the shape of increased elastic stiffness (reduced $\alpha' - q$) or specific procedures which ensure a wider strength plateau after yielding in the structure. The second option may be introduced by using different section properties over a floor level to delay the formation of a mechanism. Another option is to provide a flexible back-up system, which increases the stiffness of the structure especially after the primary system has yielded, thereby delaying the onset of negative post-yield stiffness in the structure.

- The SDOF systems clearly show that the response is very sensitive to structural period and the slope of the negative stiffness region. The potential for unstable behavior exists especially for short period systems with low yield strength. Even code designed MDOF structures, like the Seattle 3-story structure, which have significant overstrength and a "low" negative post-yield stiffness value (as compared to a q value of 0.10), harbor the potential for unstable behavior under rare seismic events. Amplification factors derived on the basis of SDOF systems may underestimate the amplification at the story level in MDOF structures.

- The inelastic response of the structure in the negative post-yield region is very sensitive to the structural characteristics, thereby requiring an accurate model to better estimate the P-delta effect on the structure. The strength associated with the plateau region and the width of the plateau, which critically affect the response, are severely affected by the type of analytical model used to represent the structure.

- The duration of the ground motion assumes importance from the viewpoint of progressive increase in displacements towards one side for the structure, once the structure reaches the negative slope. The Seattle ground motions have a very long strong-motion duration compared to the Los Angeles ground motions, which are characterized more by the pulse type behavior. Even with a "small" negative slope, the Seattle 3-story model is progressively driven to collapse.

The effect of P-delta on the response of the structure is contingent on a multitude of structural and ground motion characteristics which makes the "prediction" of the

intensity of the effect very difficult, requiring a case by case evaluation. The level of expected displacement demands can be estimated using approximate procedures such as the one described in Chapter 7. If the expected displacement is estimated to be in the range of potential P-delta problems, a detailed nonlinear dynamic analysis is necessary.

Table 4.1 First Mode Periods, Spectral Acceleration at First Mode Periods, and Global Drift Angles for LA 20-story Structure

Model	First Mode Period	Spectral Acceleration (g's)		Global Drift Angle	
		LA30	LA36	LA30	LA36
M1	3.98	0.495	0.496	Collapse	0.040
M1FW	3.97	0.493	0.498	0.035	0.039
M1FS	3.95	0.487	0.500	0.027	0.040
M1A	3.56	0.376	0.671	0.024	0.041
M2	3.73	0.423	0.584	0.043	0.039
M2L	3.73	0.423	0.584	Collapse	Collapse
M2A	3.45	0.373	0.730	0.022	0.038
M2AL	3.45	0.373	0.730	0.022	0.040
M2AK	3.07	0.445	0.952	0.020	0.034
M1-NPD	3.81	0.446	0.545	0.025	0.030
M1E-PD	3.98	0.495	0.496	0.034	0.034
M1E-NPD	3.81	0.446	0.545	0.030	0.036

Table 4.2 Global Drift Angles for Seattle 3-story Structure

	SE27		SE28	
Model	θ+	θ-	θ+	θ-
M1	0.4184	0.0166	0.0200	0.0557
M1-NPD	0.0652	0.0249	0.0318	0.0375
M1E-PD	0.0459	0.0461	0.0712	0.0609
M1E-NPD	0.0422	0.0428	0.0600	0.0486

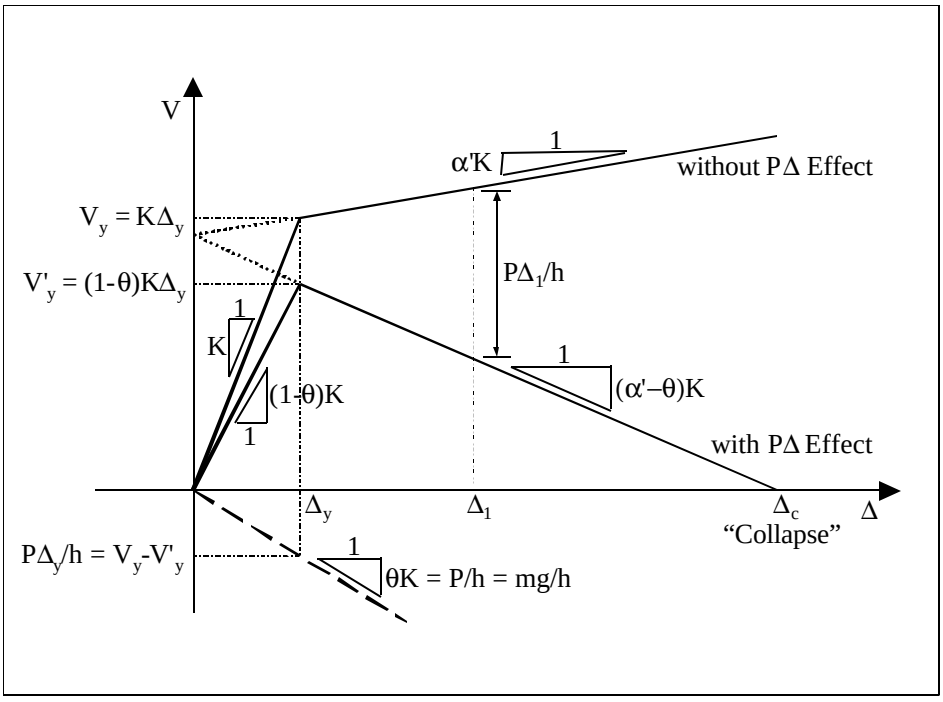

Figure 4.1 SDOF Lateral Force - Displacement Relationship without and with P-Delta

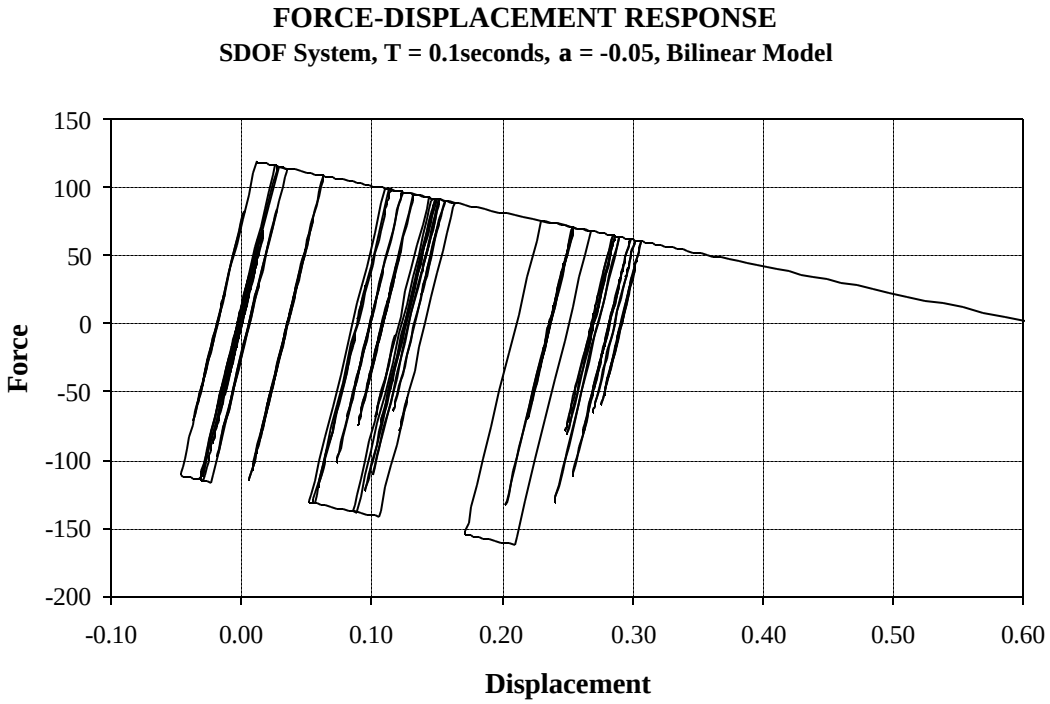

Figure 4.2 Dynamic Lateral Force - Displacement Response of SDOF System with T = 0.1 and a = -0.05.

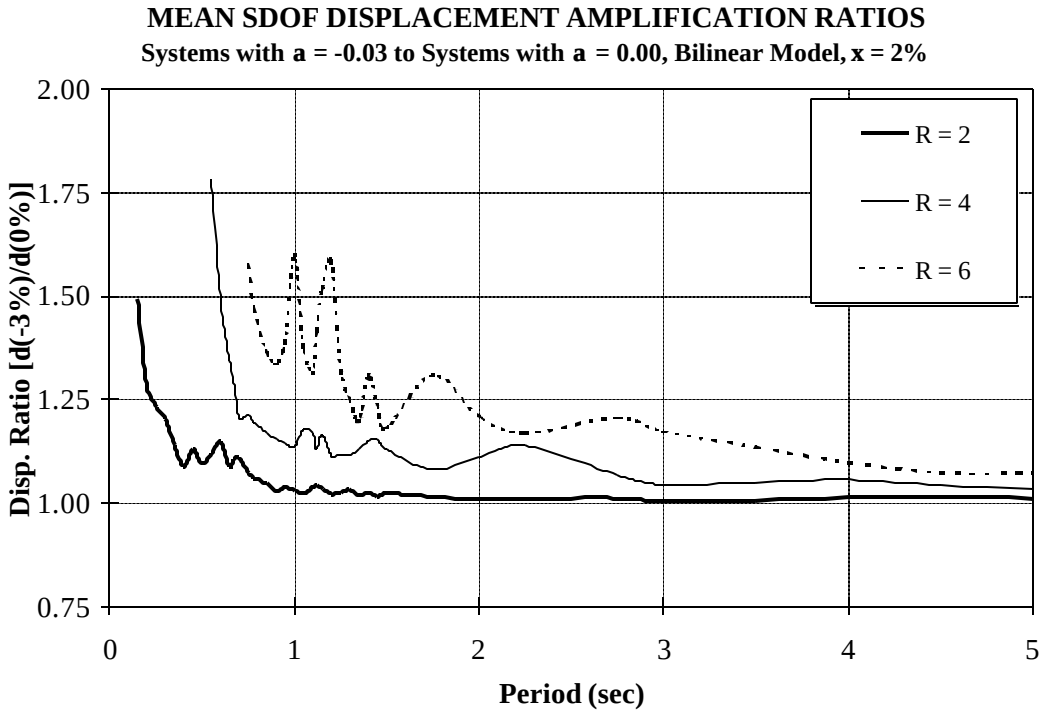

Figure 4.3 Mean SDOF Displacement Amplification Ratios for α = -0.03; Bilinear Model

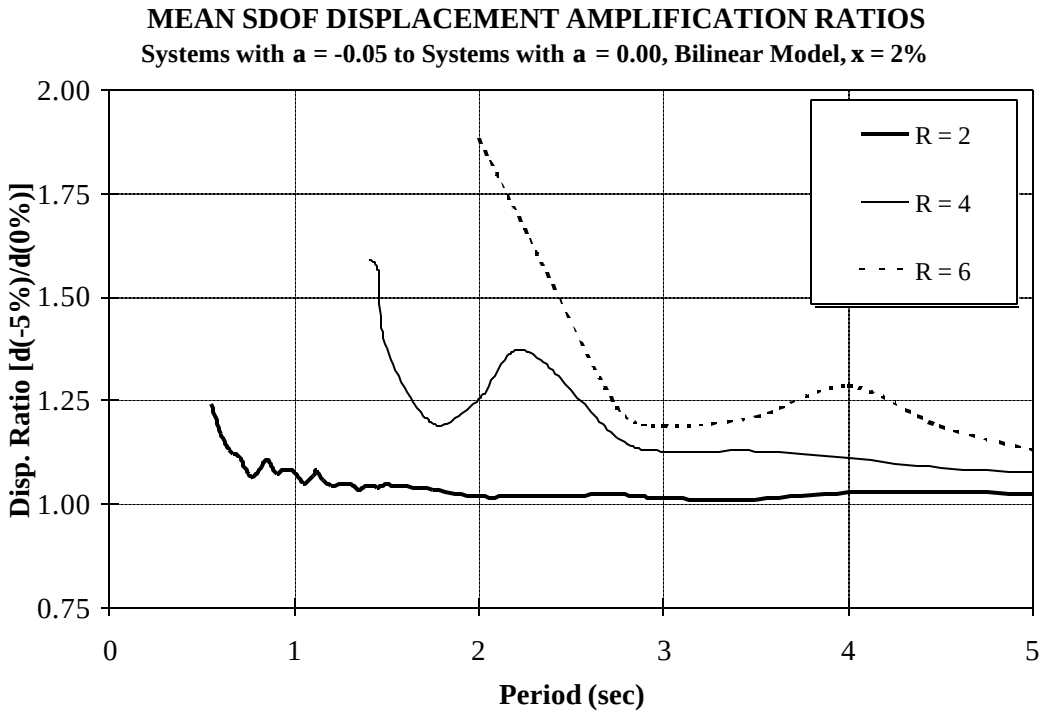

Figure 4.4 Mean SDOF Displacement Amplification Ratios for α = -0.05; Bilinear Model

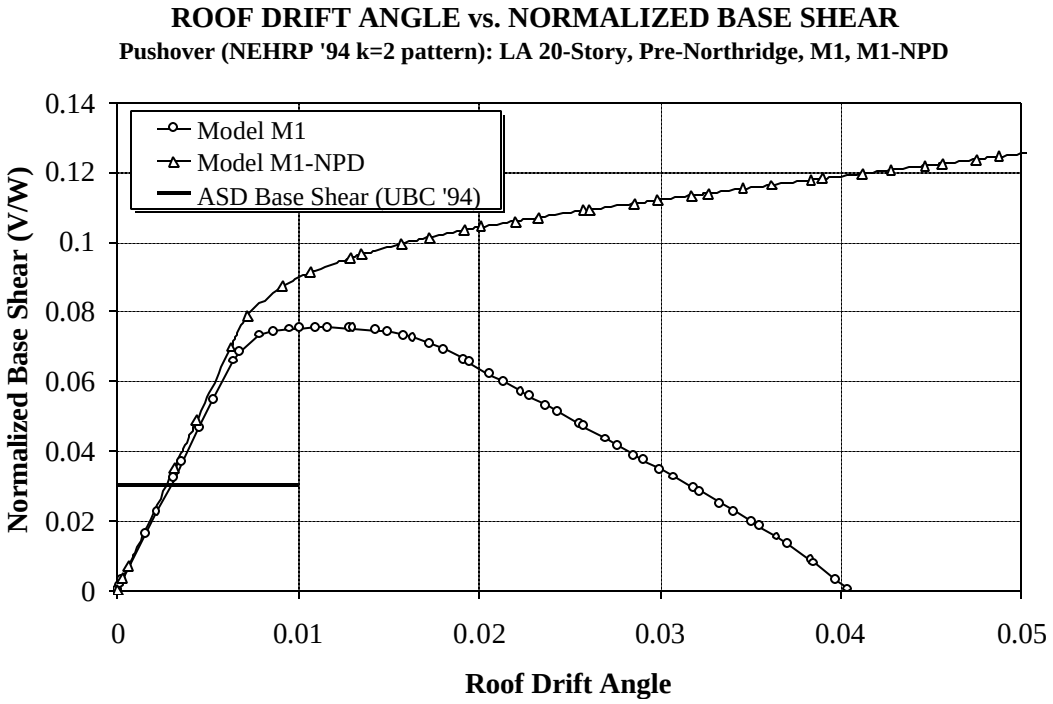

Figure 4.5 Global Pushover Curves for Model M1 of LA20-story Structure, without and with P-delta

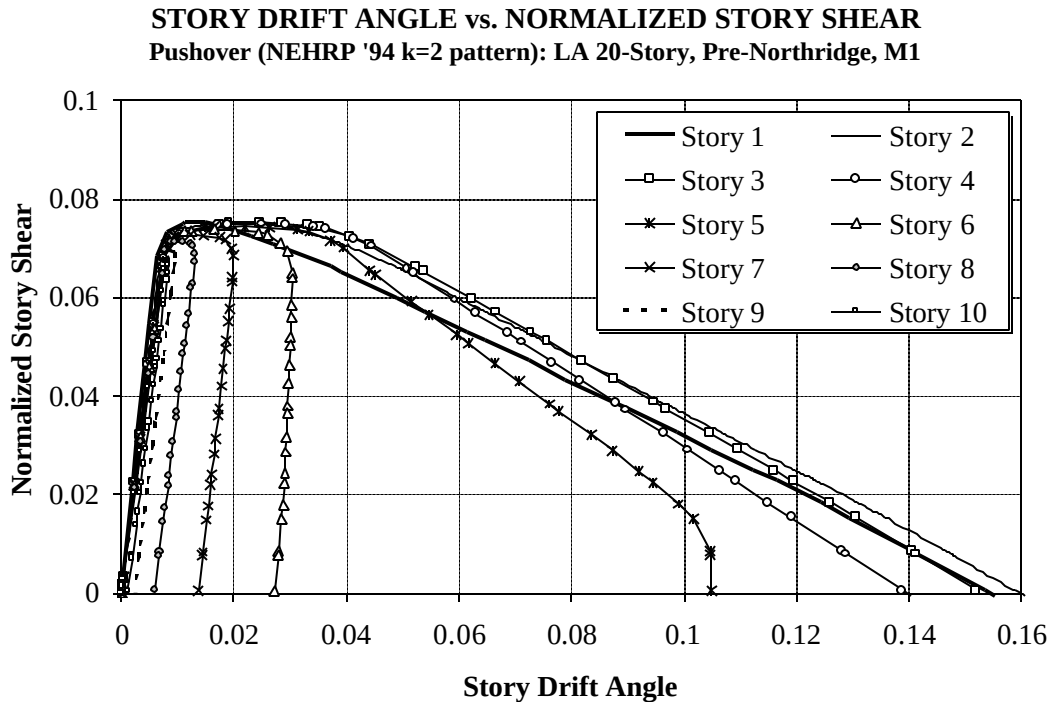

Figure 4.6 Story Shear versus Story Drift Diagrams for Model M1 of LA 20-story Structure; Pushover Analysis

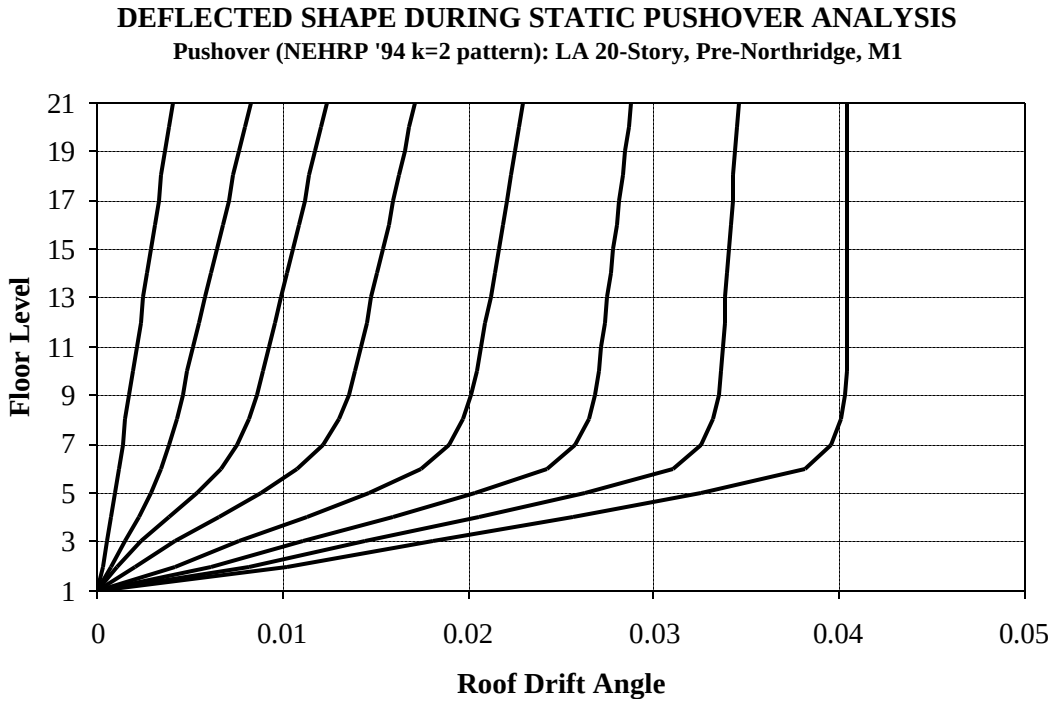

Figure 4.7 Deflected Shapes for Model M1 of LA 20-story Structure from Pushover Analysis

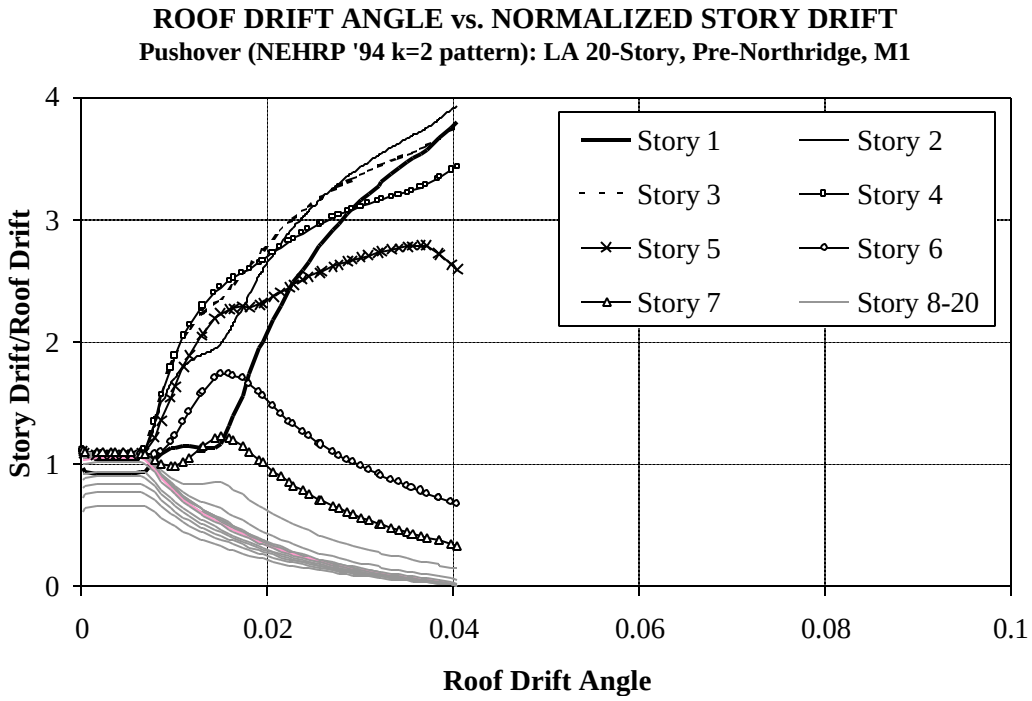

Figure 4.8 Ratios of Story Drift Angle to Roof Drift Angle, Plotted Against Roof Drift Angle, for Model M1 of LA 20-story Structure

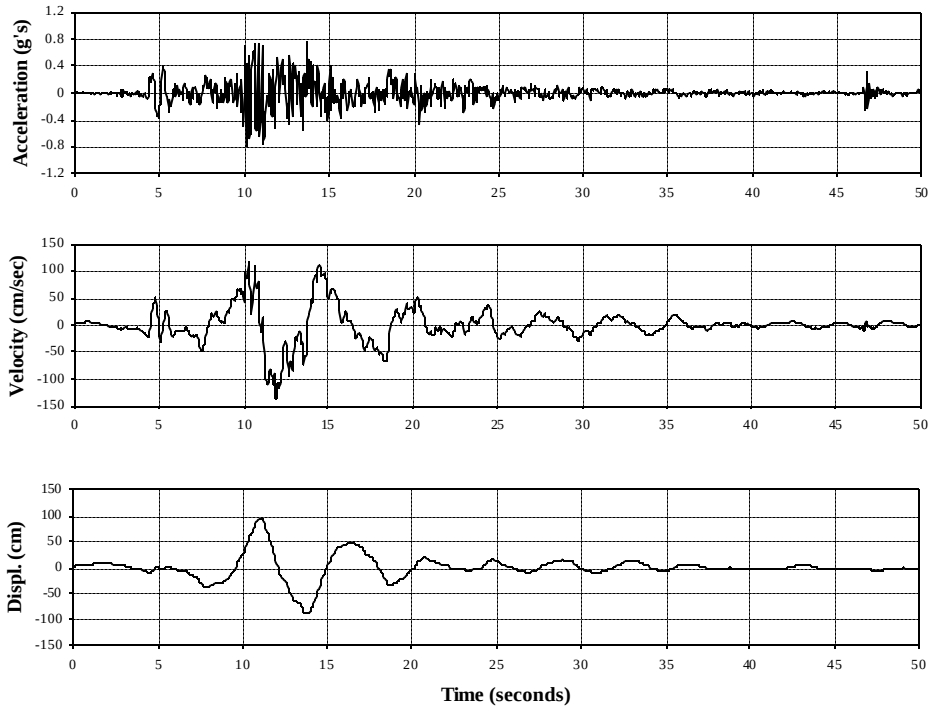

Figure 4.9 Time History of Record LA30 (Tabas) Used for P-delta Study of LA 20-story Structure

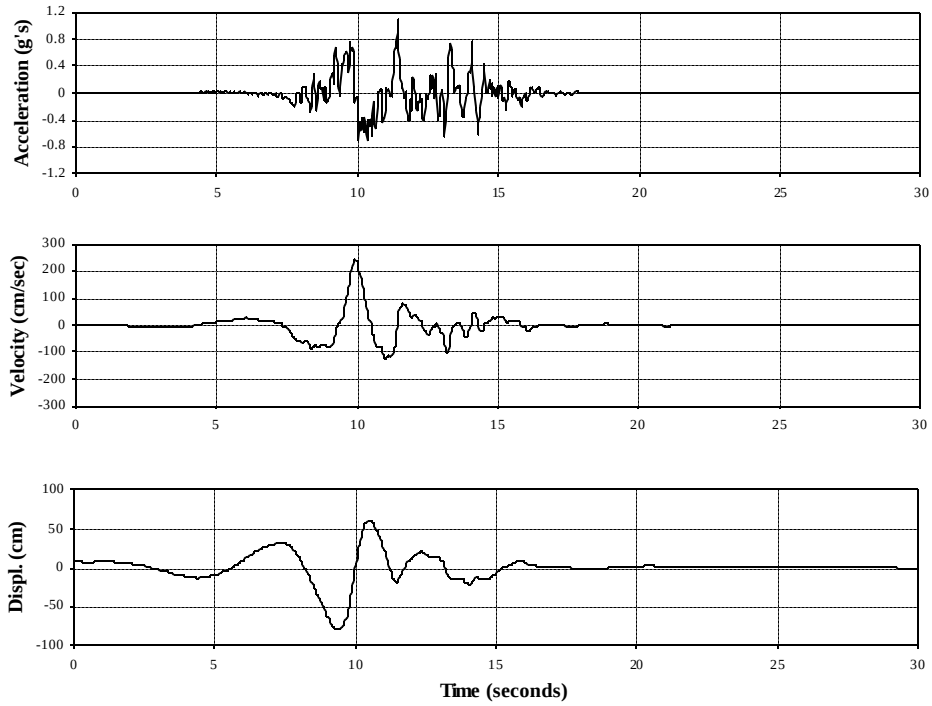

Figure 4.10 Time History of Record LA36 (Simulated) Used for P-delta Study of LA 20-story Structure

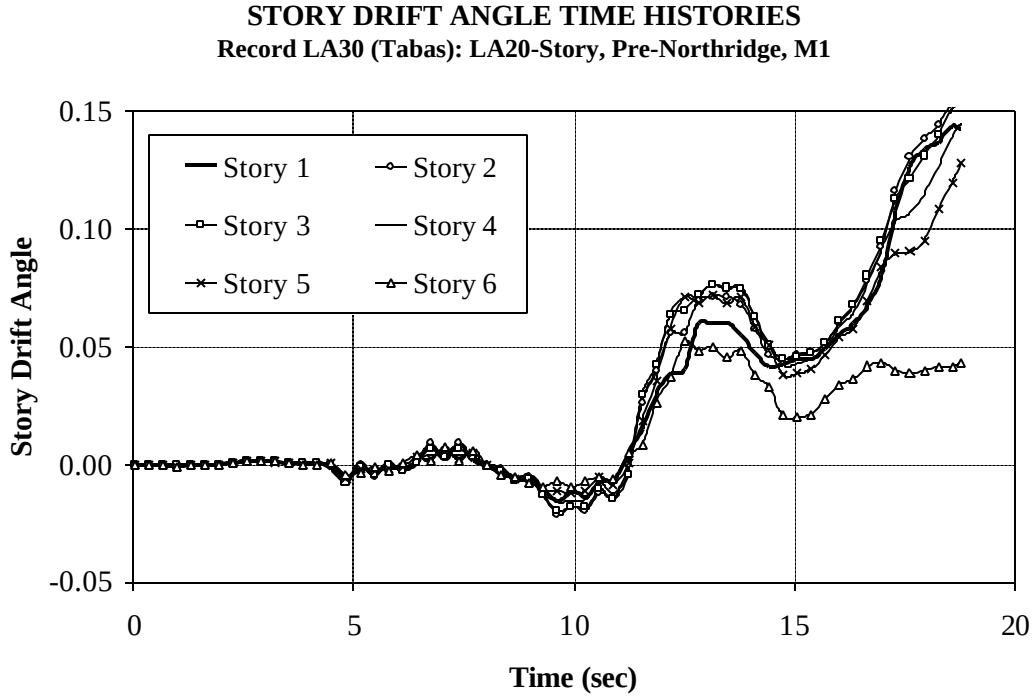

Figure 4.11 Story 1-6 Drift Angle Time Histories for Model M1 of LA 20-story Structure; LA30 (Tabas) Ground Motion

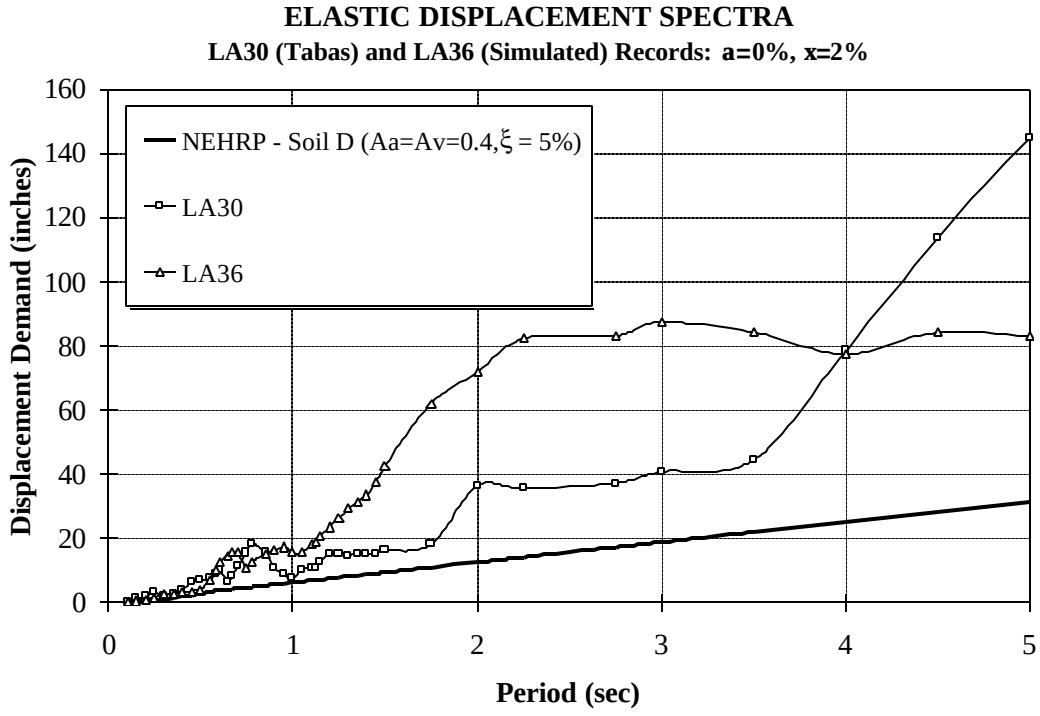

Figure 4.12 Elastic Displacement Spectra for Ground Motions Used for P-delta Study of LA 20-story Structure

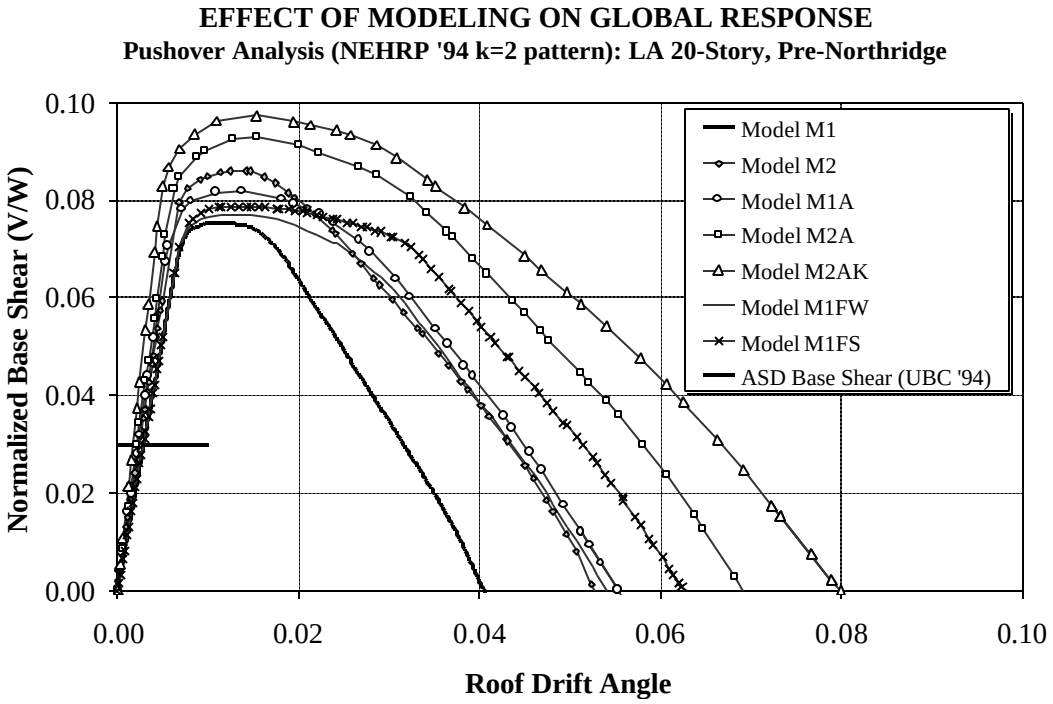

Figure 4.13 Global Pushover Curves for Various Models of LA 20-story Structure

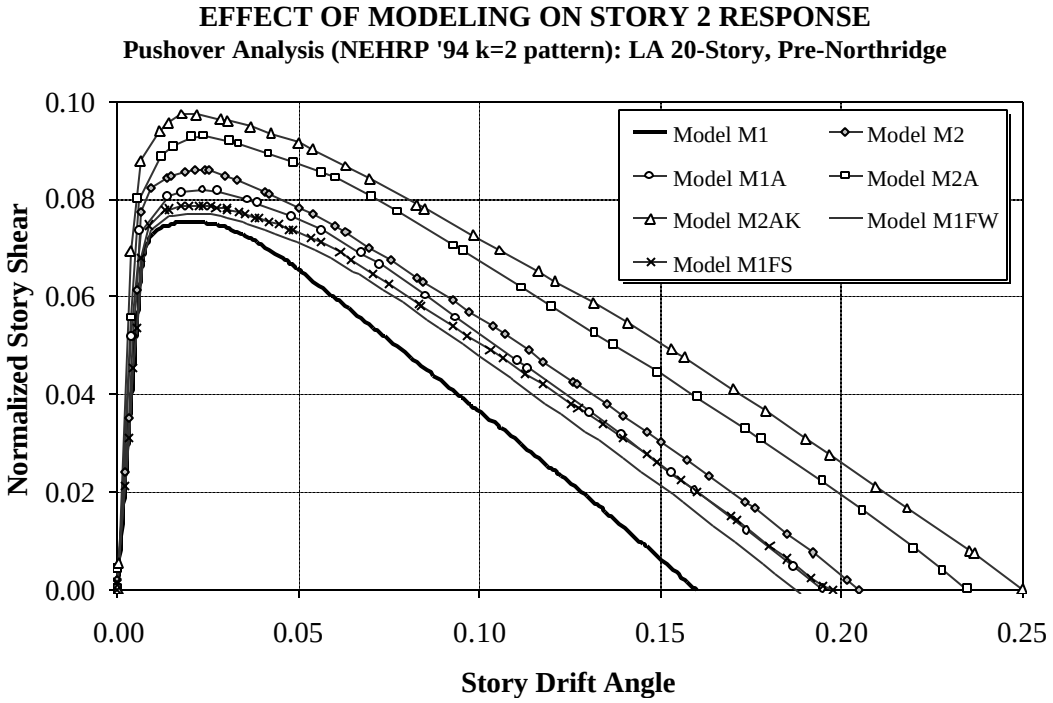

Figure 4.14 Story 2 Shear versus Roof Drift Diagrams for Various Models of LA 20-story Structure

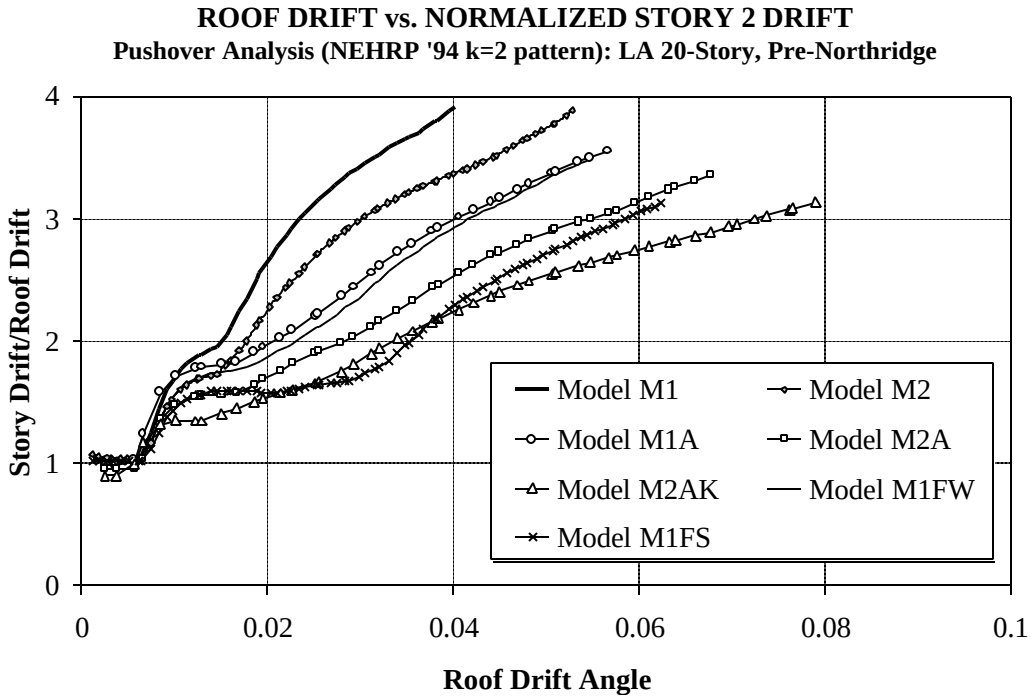

Figure 4.15 Ratios of Story 2 Drift Angle to Roof Drift Angle, Plotted Against Roof Drift Angle for Various Models of LA 20-story Structure

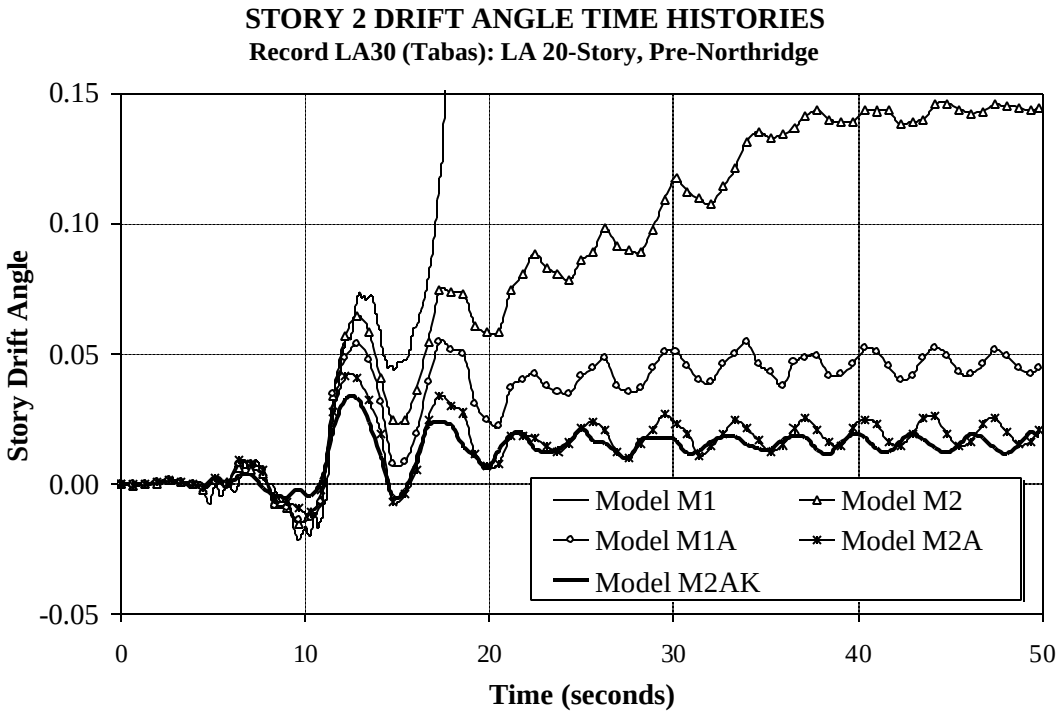

Figure 4.16a Time Histories of Story 2 Drift Angle for Various Models of LA 20-story Structure; LA30 (Tabas) Ground Motion

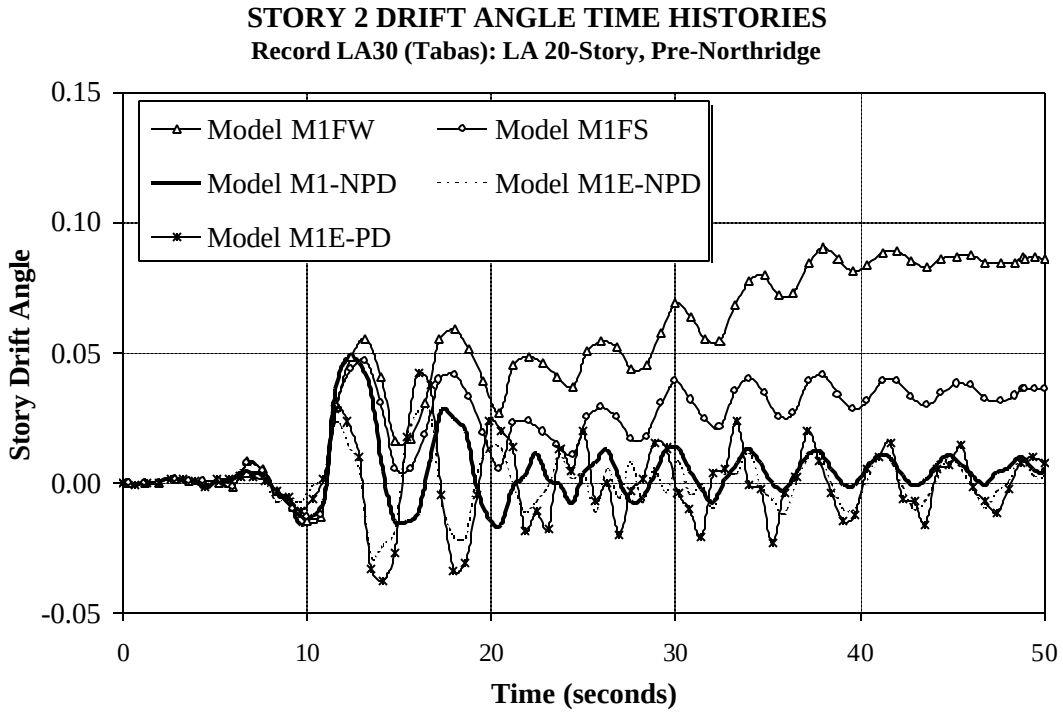

Figure 4.16b Time Histories of Story 2 Drift Angle for Various Models of LA 20-story Structure; LA30 (Tabas) Ground Motion

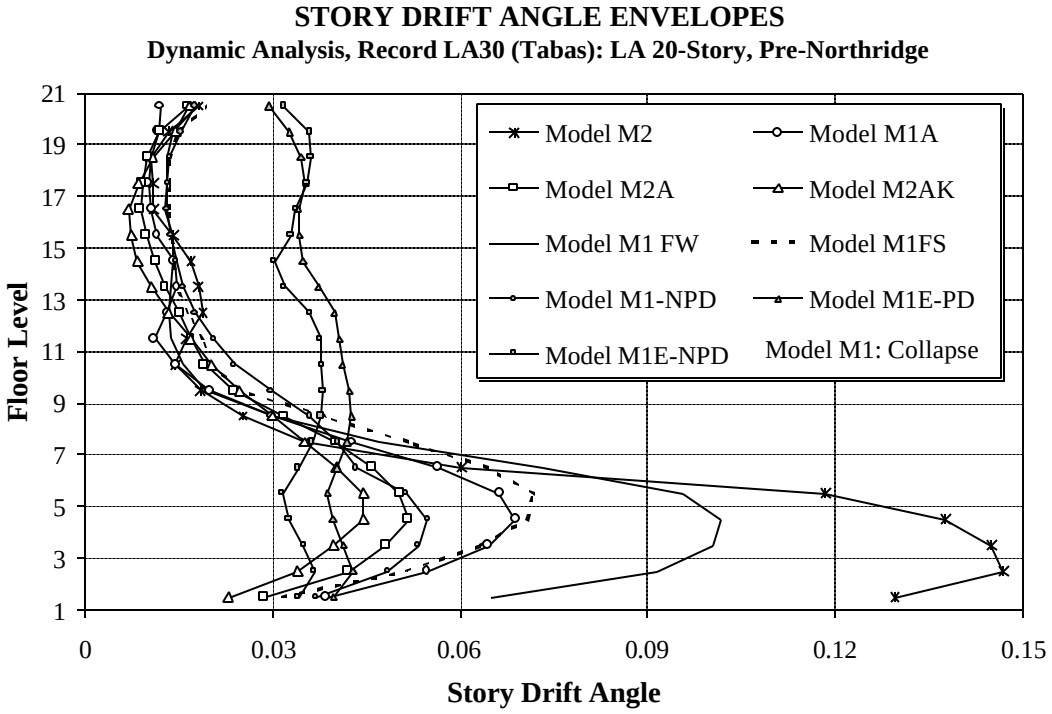

Figure 4.17 Maximum Story Drift Angles for Various Models of LA 20-story Structure; LA30 (Tabas) Ground Motion

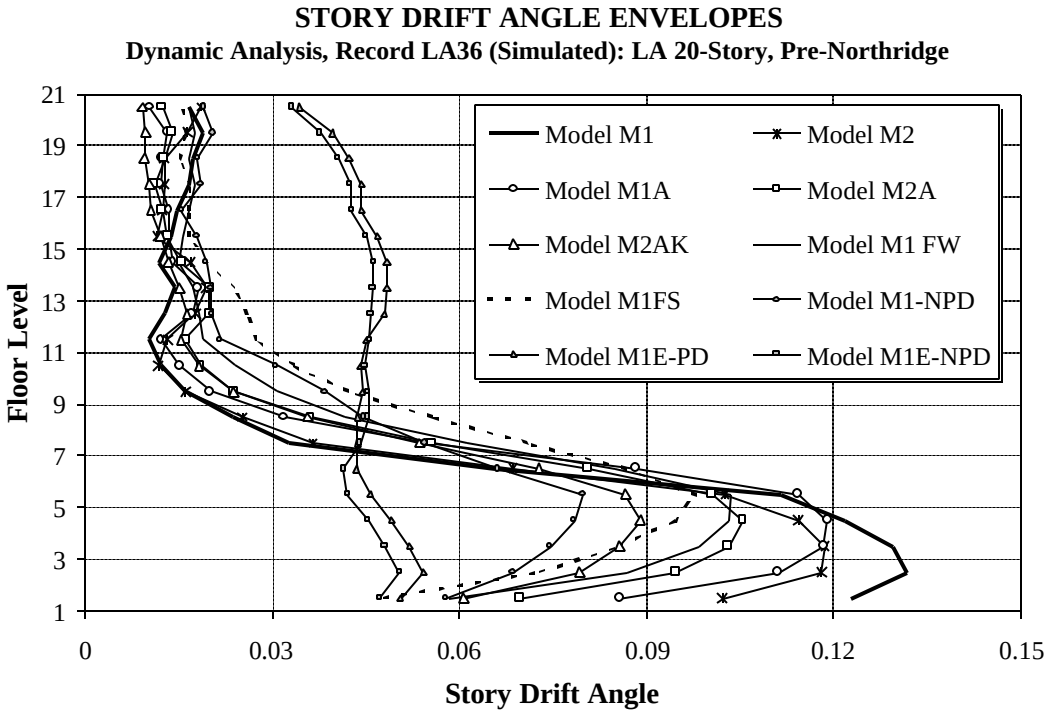

Figure 4.18 Maximum Story Drift Angles for Various Models of LA 20-story Structure; LA36 (Simulated) Ground Motion

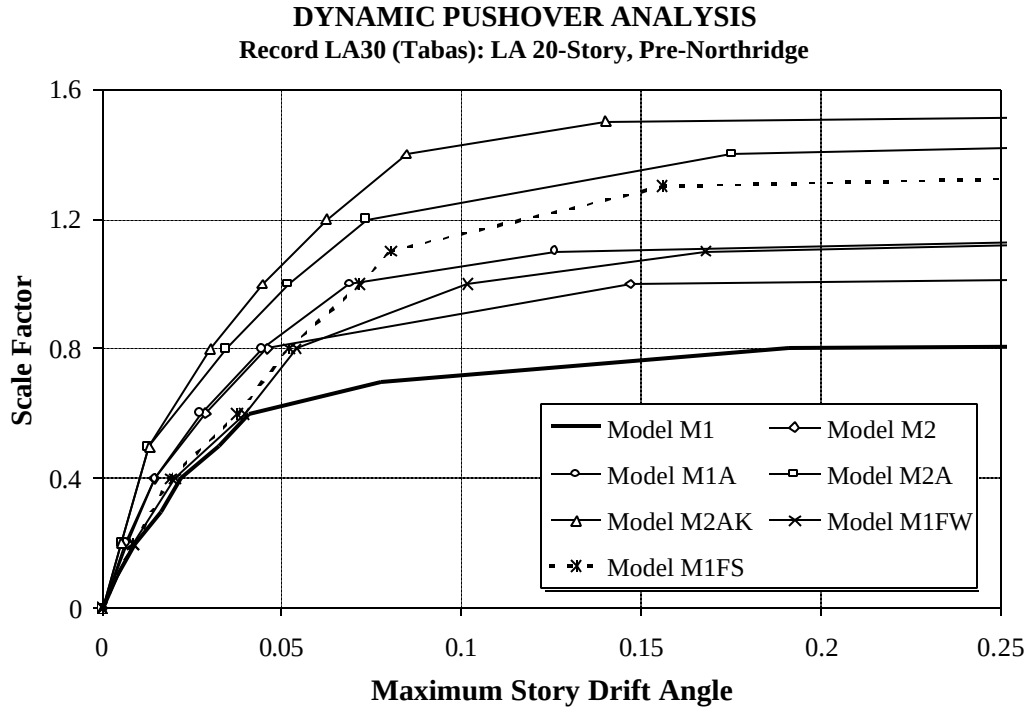

Figure 4.19 "Dynamic Pushover Analysis" for Various Models of LA 20-story Structure; LA30 (Tabas) Ground Motion

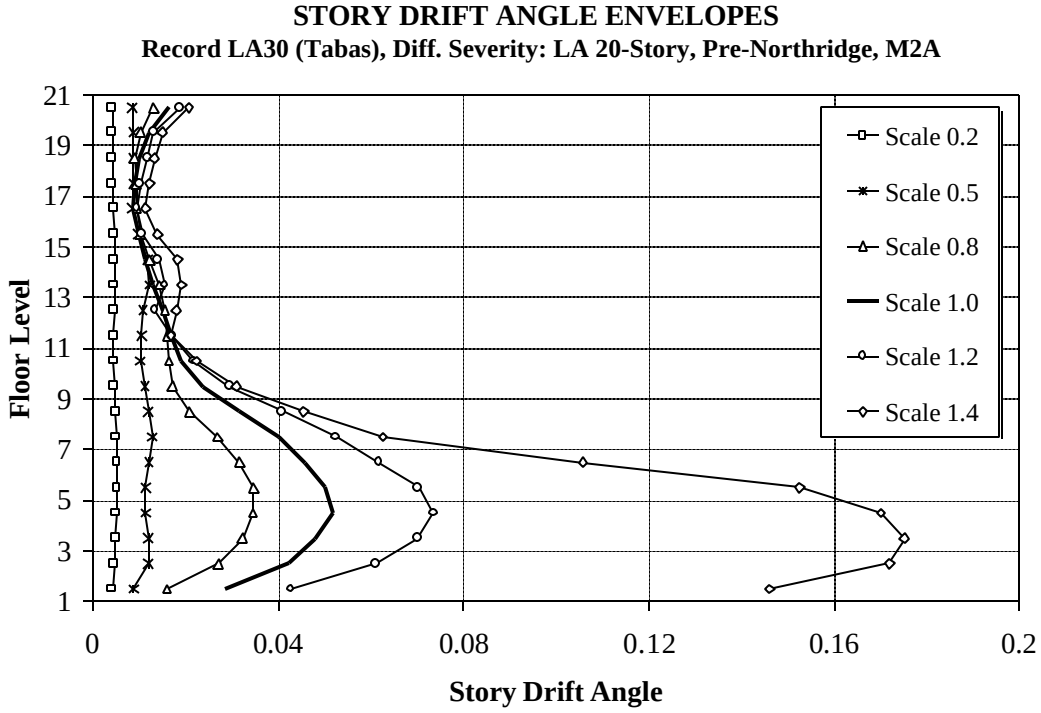

Figure 4.20 Change in Maximum Story Drifts with Increasing Ground Motion Severity, Model M2A of LA 20-story Structure; LA30 (Tabas) Ground Motion

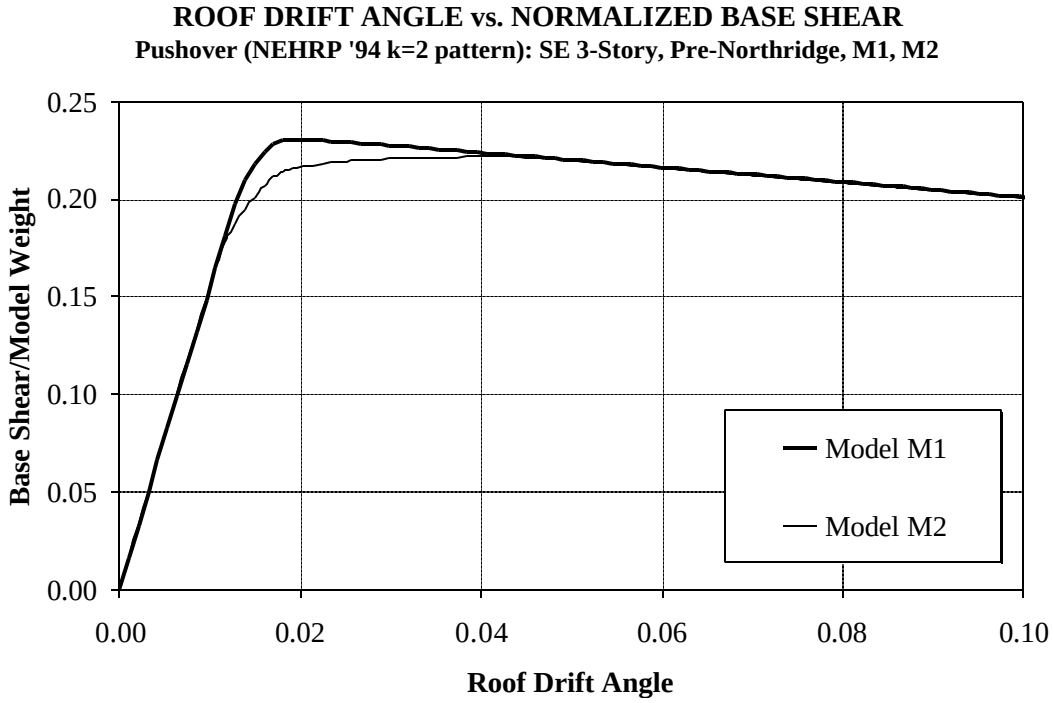

Figure 4.21 Base Shear versus Roof Drift Diagrams for Model M1 and M2 of Seattle 3-story Structure

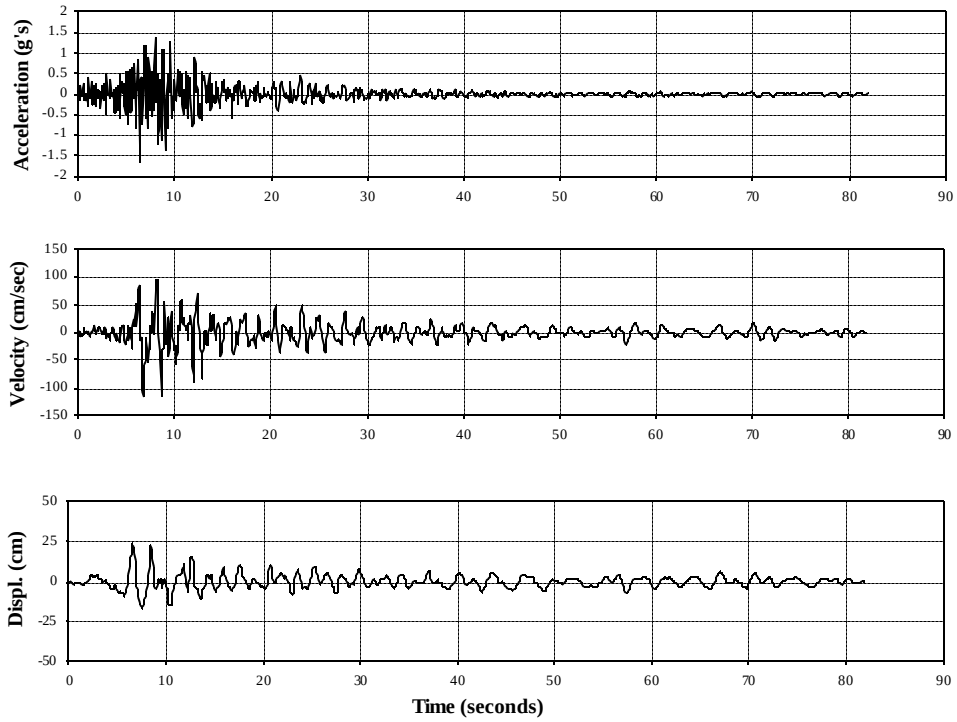

Figure 4.22 Time History of Record SE27 Used for P-delta Study of Seattle 3-story Structure

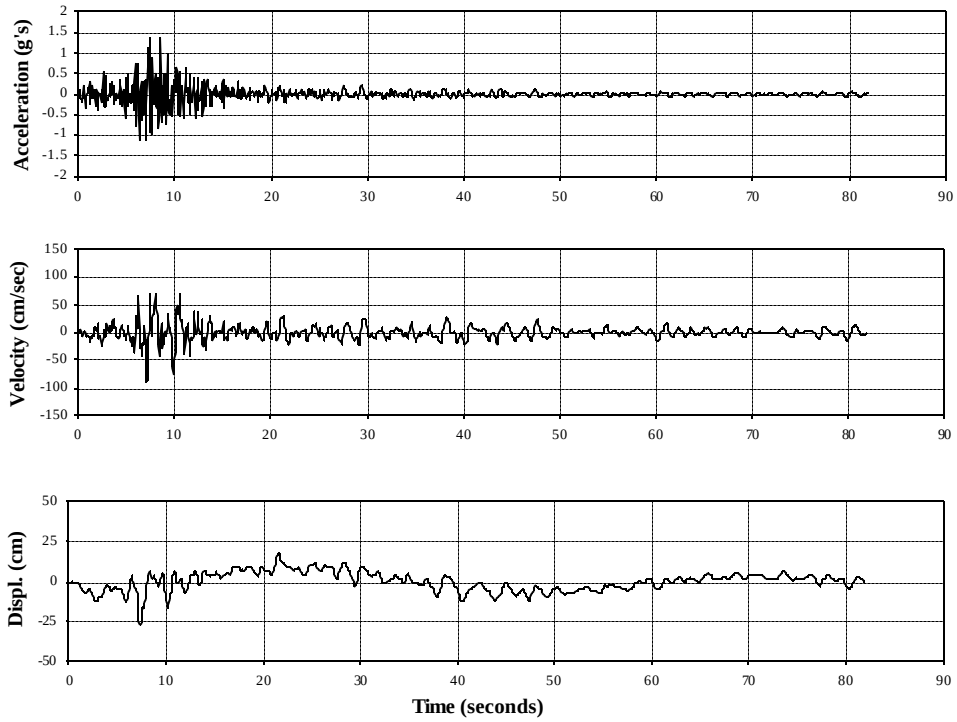

Figure 4.23 Time History of Record SE28 Used for P-delta Study of Seattle 3-story Structure

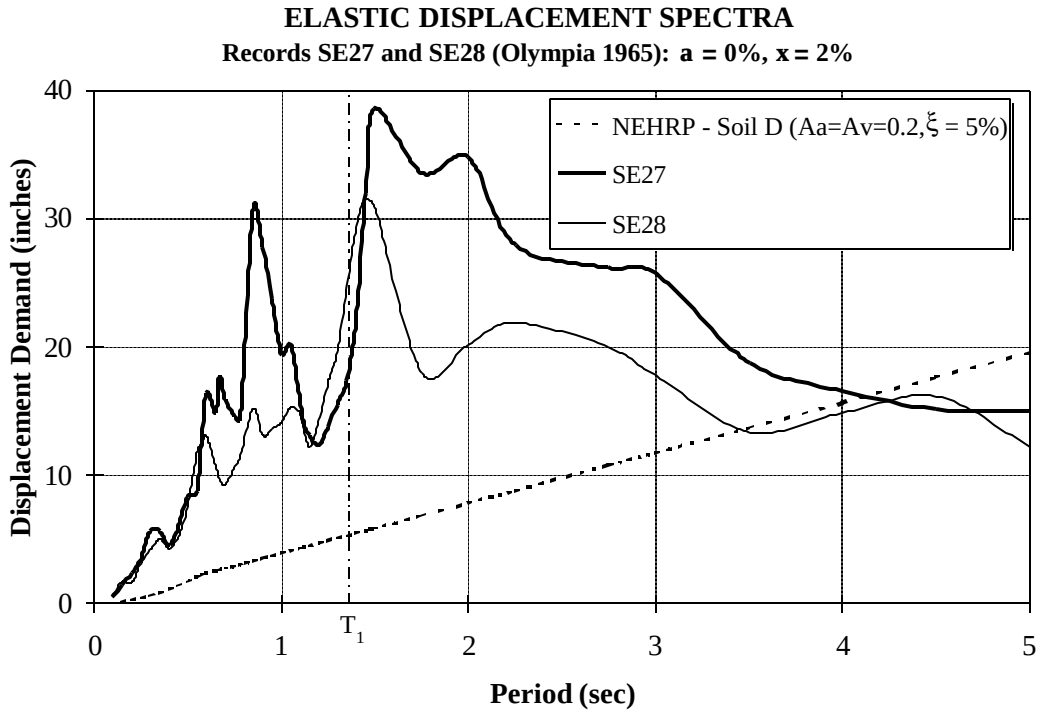

Figure 4.24 Elastic Displacement Spectra for SE27 and SE28 Ground Motions Used for P-delta Study of Seattle 3-story Structure

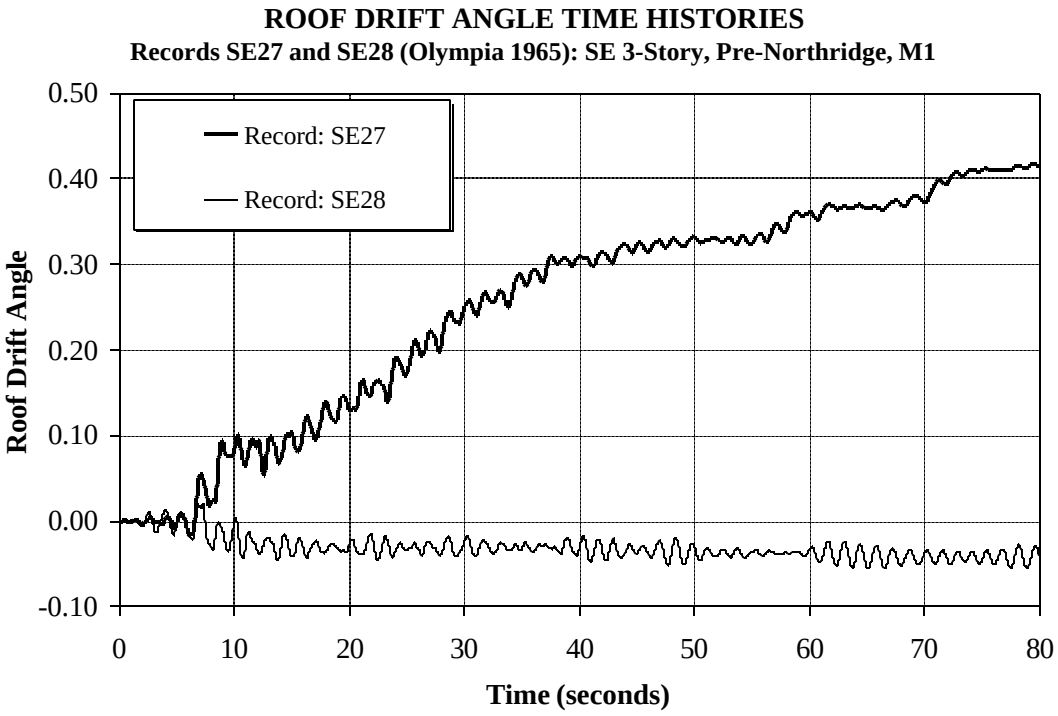

Figure 4.25 Roof Drift Angle Time Histories for Model M1 of Seattle 3-story Structure; SE27 and SE28 (Olympia 1965) Ground Motion

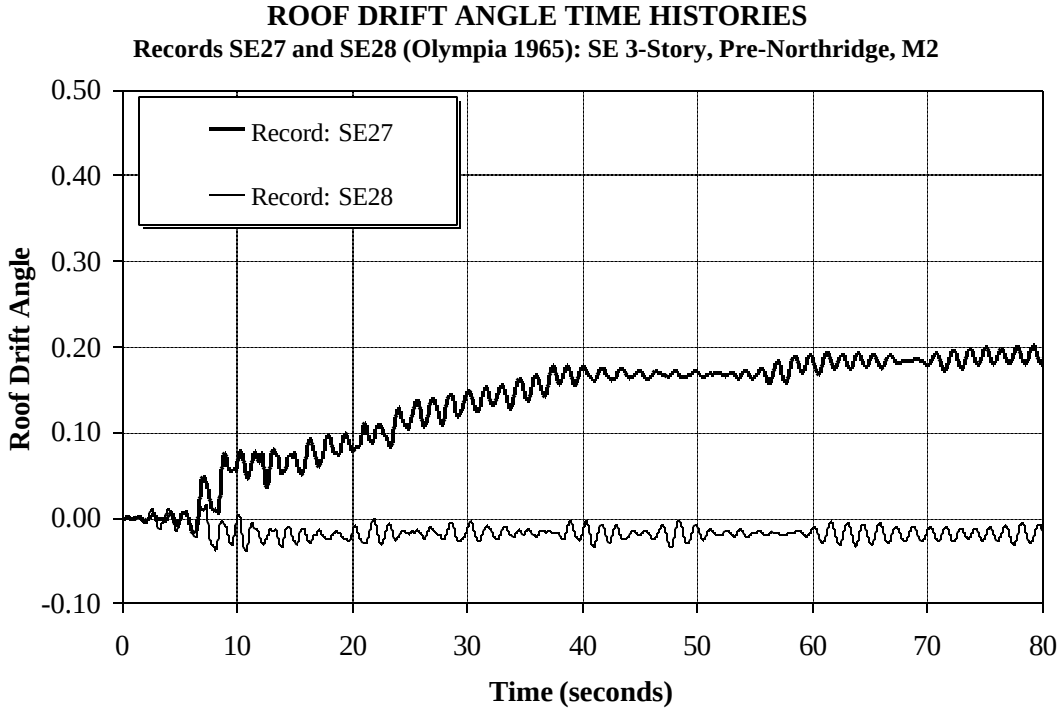

Figure 4.26 Roof Drift Angle Time Histories for Model M1 of Seattle 3-story Structure; SE27 and SE28 (Olympia 1965) Ground Motion

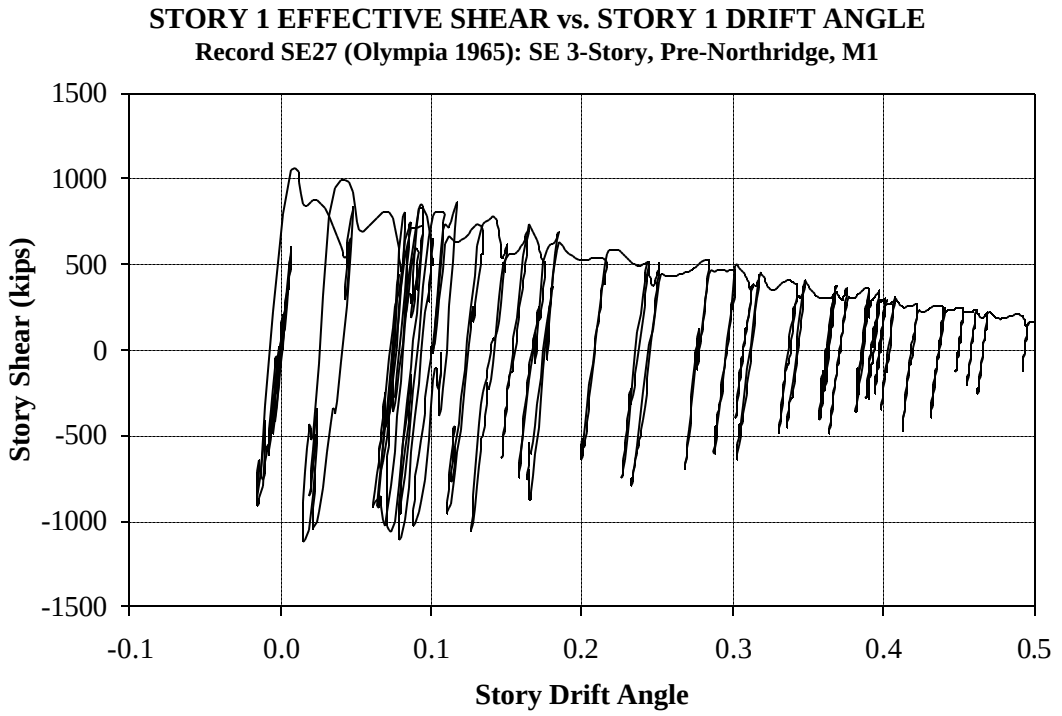

Figure 4.27 Story 1 Shear versus Story 1 Drift Angle Response for Model M1 of Seattle 3-story Structure; SE27 (Olympia 1965) Ground Motion

CHAPTER 5

GLOBAL AND STORY DRIFT, STRENGTH, AND ENERGY DEMANDS

5.1 Introduction

The quantification of seismic demands for steel moment resisting frame structures (SMRFs) has been the subject of much analytical research [e.g., SAC 95-04 (1995) which describes studies on SMRFs subjected to the Northridge earthquake and references work by many researchers], as has been the quantification of demands for generic frame structures [Nassar and Krawinkler (1991), Seneviratna and Krawinkler (1997)]. The goal of the latter studies has been the development of a basic understanding of inelastic effects in frame structures and development of simplified procedures for addressing these effects in the design and analysis processes.

This chapter focuses on the quantification of seismic demands at the structure level for 3-, 9-, and 20-story steel moment resisting frame structures located in Los Angeles (seismic zone 4), Seattle (seismic zone 3), and Boston (seismic zone 2A). Documentation of the designs for these structures is given in Appendix B. The behavior and response of these structures is studied by subjecting representative nonlinear analytical models of the structures (models M1 and M2, see Section 3.4) to sets of ground motions (20 records per set) representative of different hazard levels (10/50 years and 2/50 years, and for Los Angeles additionally 50/50 years; see Appendix A) for each location. Nonlinear static analysis (pushover analysis) is used to identify behavior characteristics of the structure that cannot be obtained from time history analysis but are important in understanding and rationalizing dynamic response.

The structural demand parameters used to develop an understanding of the behavior, and to quantify the response of the structure, include the global (roof) and story drift angle (maximum and residual), strength quantities (base and story shear forces and overturning moments), and energy demands (total input, hysteretic). The overstrength of the designs, as compared to code (UBC 1994) seismic requirements, is also identified. A performance evaluation for all these structures is carried out using two different procedures; 1) the story drift angle demands obtained from nonlinear dynamic analysis are compared to characteristic values given in documents such as FEMA 273 (FEMA, 1997) and Vision 2000 (SEAOC, 1995), and 2) by representing the demands on the structures in a probabilistic format in the form of drift and ductility hazard curves using an approach by Cornell (1996a).

The response of structures with post-Northridge type connection details (design information is given in Appendix B) is studied by subjecting the bare frame analytical model M2 to the sets of ground motions representative of a 2475 (2/50) year hazard level for the different seismic locations. The structures designated as "post-Northridge" have beam cover plates designed in accordance with the FEMA 267 guidelines (FEMA, 1995). The response of other post-Northridge designs, such as reduced beam section (RBS) designs, is discussed in Chapter 6. The analytical modeling of post-Northridge connections has been summarized in Section 3.3.2. The results of pre- and post-Northridge designs are presented together in order to permit a direct comparison between the responses of structures designed using conventional pre-Northridge beam-to-column connections and structures designed with the intent to reduce the potential for fractures at the welded beam-to-column connections. The emphasis in this chapter is on the global and story drift demands, element force and deformation demands are evaluated in Chapter 6.

The study summarized here is an attempt to assess seismic demands for SMRF structures designed in accordance with standard practice and prevailing code criteria and guidelines [UBC (1994), BOCA (1993), FEMA 267 (1995)]. A detailed evaluation of the seismic demands for similarly designed structures (in terms of guidelines/criteria/codes followed) in different seismic areas has been carried out. The focus is on issues related to modeling of structures, distribution of demands as a function of the hazard level and characteristics, variation in demands with period of the structure, and different design details (e.g., pre-Northridge versus post-Northridge). The results presented in this and the next chapter are used later to develop relationships between global drift and story

drift, and story drift and element plastic deformation demands. These relationships are then tied back to the elastic spectral displacement demands at the first mode period of the structures. The developed simplified demand estimation procedure is presented in Chapter 7. Sensitivity of the response to different structural parameters is discussed under Chapter 8.

5.2 Nonlinear Static Response

The response of the structures is first studied using nonlinear static analysis (pushover analysis, Section 3.5). This analysis technique permits an estimation for the overstrength, identification of locations of potential weaknesses and irregularities (if any), assessment of force demands on brittle elements, assessment of completeness and adequacy of load path, and an estimate of the inelastic strength and deformation demands for flexible elements. The pushover analysis is used to develop a better understanding of the behavior of the structure and for rationalization of the nonlinear dynamic response of the structure. The emphasis is not on projecting the pushover analysis technique as an alternative for nonlinear dynamic analysis, but on using it as supplemental analysis to gain more insight into the behavior of the structure. The load pattern used for the pushover analysis has been discussed in Section 3.5.

The structural response comparisons are carried out location by location, and for each location on a structure by structure basis. The response of the pre-Northridge bare frame models M1 and M2 is compared, followed by a comparison between the pre-Northridge and post-Northridge designs represented by the bare frame model M2.

5.2.1 Response of LA Structures

The global pushover curves (base shear divided by structure seismic weight versus roof displacement divided by structure height) for the LA 3-, 9-, and 20-story structures are shown in Figures 5.1 to 5.3, respectively. The design seismic base shear level according to the UBC ’94 is also marked on the figures to provide an estimate for the effective overstrength in the structures.

The three figures show similar behavior patterns, with the pre-Northridge M2 models showing an improved behavior compared to the pre-Northridge M1 models. The panel

zones in these designs are relatively strong compared to the beams framing into the connection, thus, in most cases the initial yielding takes place in the beams. However, with increased inelasticity in the beams the panel zones also yield, affecting the distribution of inelastic demands and the post-mechanism behavior between models M1 and M2. The improved model M2 shows higher strength because the effective strength of the beams is increased on account of the clear span dimensions used in this model compared to the centerline dimensions used in model M1. The elastic stiffness of models M1 and M2 differs somewhat, depending on the compensating effect of the two errors introduced in model M1 by using centerline dimensions but ignoring the flexibility of the panel zones.

The post-Northridge structures, in general, show a higher effective strength due to the addition of the cover plates onto the beam flanges. The post-mechanism response is mostly similar to the post-mechanism response for the pre-Northridge M2 models. The similarity in response of the pre-Northridge and post-Northridge structures (models M2) is to be expected as the basic designs, in terms of beam and column sections, do not differ significantly (see Appendix B for a documentation of the different designs).

A feeling for the distribution of drift demands over the height of the structures (from the static pushover analysis) can be obtained from Figure 5.4, which shows the ratio of the maximum story drift angle (over height) to the roof drift angle, at particular values of the roof drift angle. For the 20-story structure the roof drift of 0.025 (or 2.5%) corresponds to a negative post-yield stiffness, see Figure 5.3. For the 3- and 9-story structures the distribution of demands over the height does not vary much and is almost identical for the pre- and post-Northridge designs. The story drift distribution for the 20-story structure is, however, significantly affected by the design as well as the analytical model. The improved behavior of post-Northridge structure is ascribed to the increased effective strength coupled with the change in redistribution of relative demands at the connection level. The change in the roof drift angle from 1.5% to 2.5% for the 20-story structure results in a substantial increase in the ratio of the maximum story drift to global drift, for all designs and models, reinforcing that the demands for few stories increase disproportionately when second order effects become significant (see Chapter 4).

The relative values of the design strength (UBC ’94; allowable stress design) of the structures and the effective strength capacity provide an idea of the overstrength in the structures. The 3- and 9-story structures show an effective strength of about 4 times the

design strength, while the 20-story structure shows an "overstrength factor" of about 3. The structures are significantly stronger than needed by the design strength requirements, on account of the designs being controlled by stiffness requirements (drift control), and the use of materials whose expected yield strength is significantly higher than the nominal strength values used in design (refer Section 8.5).

5.2.2 Response of Seattle Structures

The global pushover response for the Seattle 3-, 9-, and 20-story structures is shown in Figures 5.5 to 5.7, respectively. Many of the trends observed in the response of the LA structures hold true for the Seattle structures, with the M2 models showing improved behavior and the post-Northridge structures showing higher effective strength. However, the Seattle 3-story pre-Northridge structure exhibits a small negative post-yield stiffness, which was not noticed in the LA 3-story structure. This seemingly small difference in stiffness has a large effect on the dynamic response if the ground motion is large enough to drive the structure into the range of negative post-yield stiffness (see Section 4.4). The negative post-yield stiffness is not present in the 3-story post-Northridge structure, which has a higher elastic stiffness and about 40% more strength than the pre-Northridge structure. The difference is attributed to the use of significantly larger sections in the post-Northridge design (see Appendix B). The consequence of the lack of negative stiffness is that the maximum drift demands for the Seattle 3-story post-Northridge structure in the most severe 2/50 ground motions are much smaller than for the pre-Northridge structure.

Model M1 for the Seattle 20-story structure shows a response similar to that of the model M1 for the LA 20-story structure, insofar that there is very rapid loss in lateral load resistance after about 2% roof drift, on account of development of a weak story. However, the Seattle structure is not pushed to that drift demand range by any of the ground motions (see Section 5.4.2) and thus, the presence of the large negative post-yield stiffness has no consequences on the computed dynamic response. The M2 models for the pre- and post-Northridge structures show a greatly improved behavior. Model M1 develops a story mechanism in the first story, whereas no story mechanism is formed in the M2 models because of redistribution of demands, resulting in much improved behavior.

The effect of the weak story can also be observed from Figure 5.8, which shows the maximum story drift normalized with roof drift angle, at particular values of the roof drift angle. A comparison between the results for the 20-story structures at 1% and 2.5% roof drift angle clearly shows that the drift contribution of one story (in this case, the first) in model M1 increases very rapidly and becomes more than 6 times as large as the average drift. For all M2 models the story drifts are well distributed over the height of the structure, as evidenced by the low values of the ratios even at a large roof drift angle value.

Significant overstrength is observed for all Seattle structures, because of drift requirements and because the design for the 20-story structure is mostly controlled by wind forces.

5.2.3 Response of Boston Structures

The global pushover response of the Boston structures is very different from the response of the LA and Seattle structures. The global pushover curves for the 3-, 9-, and 20-story structures are shown in Figures 5.9 to 5.11. The most significant difference is observed between the response of the pre-Northridge models M1 and M2. Only for the Boston structures do the M2 models show a lower effective strength than the M1 models. This is attributed to the presence of very weak joint panel zones in the Boston structures; neither UBC ’94 nor BOCA ’93 has a minimum strength requirements (in addition to the basic ASD requirement) for panel zones in structures located in seismic zones 1 and 2. Thus, in the M2 models the panel zones yield much earlier than the beams, resulting in a much lower effective strength than the M1 models.

The post-Northridge structures show a much higher strength, and in the case of the 3-story structure, also higher elastic stiffness. The significant increase in strength is attributed to compliance of the post-Northridge designs with the FEMA 267 guidelines, which specify a minimum strength requirement for panel zones irrespective of the seismic zone in which the structure is located. Other than the 3-story structure, these differences between the models M1 and M2, and between the pre- and post-Northridge structures are not very important because of the very low seismic demand imposed by the Boston ground motions. As is shown later in Sections 5.3 and 5.4.3, the spectral displacement demands in the long period ranges are very low and consequently the 9- and

20-story structures remain mostly elastic under almost all ground motions. Model M1 for the 9-story structure develops a weak story mechanism at about 1.7% global drift angle, however, the maximum calculated dynamic roof drift angle demand is only 1.2%. Thus, the dynamic response of the different designs and models is not expected to be significantly different.

For the selected pushover load pattern the contributions of the individual stories to the roof drift in the elastic range are rather uniform, as can be seen from the ratios of maximum story drift angle to roof drift angle, which are shown in Figure 5.12. The ratios are all close to unity.

The design of the 9- and 20-story structures is controlled by wind effects. As a result there is a perception of much overstrength. This may be a misconception, as shown in Figure 5.10. Accounting for the low shear strength of the panel zones, which is often not considered in design evaluation, the actual overstrength may be rather low (see 9-story pre-Northridge model M2). In fact, the overstrength may essentially disappear if the design is controlled by seismic loads and the panel zone shear strength is ignored, as seen in the response of the 3-story pre-Northridge model M2 in Figure 5.9.

5.2.4 Comparisons Across Regions

The modal characteristics of the different structures and analytical models are listed in Table 5.1. Since the mass of the structures of a particular number of stories is kept constant between the different regions, a comparison of the first mode periods reflects the differences in the elastic stiffness of the structures. Model M2 shows a higher stiffness than model M1, suggesting that the flexibility of the panel zones does not balance fully the increase in stiffness due to use of clear span rather than centerline dimensions. The first mode period (and therefore the elastic stiffness) of the post-Northridge structures is similar to the period for the corresponding pre-Northridge model M2 structures for LA and Seattle. The post-Northridge Boston structures have a higher stiffness on account of explicit design requirements for the panel zones.

All the structures are very flexible, with even the LA 3-story structure having a bare frame period of about 1.0 seconds. The Seattle 3-story structure has a stiffness which is about 60% of the stiffness of the LA structure. The Boston 3-story is exceedingly

flexible with a period of 1.9 seconds (or a stiffness which is 30% of that of the LA 3-story). The structures become more flexible for lower seismic zones, except in the case of the 20-story structures whose design in Seattle and Boston is controlled by wind effects. The Seattle structure has a stiffness which is almost equal to that of the LA structure, while the Boston 20-story structure shows a significantly higher stiffness. The first mode effective mass and modal participation factors are similar between different models and regions, for same number of stories.

The global lateral load – displacement response of the different structures can be compared directly from the presented pushover curves, considering that all structures are subjected to the same load pattern. An expectation may be that for a given configuration (same geometry and gravity loading) the global strength and stiffness properties decrease or increase in accordance with the seismic base shear coefficient for the location. This expectation is met sometimes, but not in general. There are many real and perceived issues that affect lateral strength and stiffness. Subjective design decisions vary greatly from office to office and between individual engineers. Such subjective decisions may greatly affect the relative strength of members (e.g., strong versus weak panel zones, see Section 6.2), which in turn may greatly affect the strength and stiffness properties. The importance of wind effects compared to seismic effects depends strongly on location as well as shape of the structure. Last but certainly not least, the analytical model used to predict response will have a great effect on perceived strength and stiffness. The differences between M1 and M2 models have been emphasized in the previous chapter, as well as here. The beneficial effects of other reliable contributions have been described in Chapter 3.

Caution is necessary against a hasty summary assessment of relative strength and stiffness of SMRFs as a function of height (number of stories) and geographic location. There are too many variables to consider. The following illustrative example reiterates the differences in assessment of strength and stiffness of the structures on account of assumptions in the analytical models for the structure. Figures 5.13 and 5.14 show the global pushover curves for the 20-story structures in LA, Seattle and Boston, for the M1 and M2 models, respectively. The M2 models for the three structures show comparable strength. The Seattle and Boston structures show desirable post-yield characteristics, insofar that negative post-yield stiffness is not attained for the levels of drift expected for these structures. The drift associated with zero lateral load resistance for the LA structure is higher for the M2 model. The Seattle M1 model shows very undesirable post-yield

behavior. The M1 models for the Boston structures indicate a significantly higher strength compared to the M2 model. Thus, very different estimates for the strength and stiffness of SMRF structures may be obtained based on the analytical model, and other assumptions (see Chapter 8). This distinction can be very important for cases where the structure response is severely affected by the analytical model, e.g., the M1 model for the LA 20-story "collapsed" under LA30 ground motion while the M2 model did not.

From an engineering perspective what needs to be answered is how important it is to provide reasonably accurate predictions of the global load – displacement response. The answer depends on the performance level of interest and on the importance of the information contained in the global pushover curve for seismic design and earthquake response. Some of these issues are addressed later in this chapter.

5.3 Spectral Characteristics of the Sets of Ground Motions Used in Dynamic Analysis

The seismic demand predictions obtained from time history analysis need to be evaluated in the context of the ground motions used in the analysis. Comprehensive documentation on the sets of ground motions is contained in Appendix A. The figures shown in this section present spectral displacement data that is needed to understand structure drift data in this chapter and in Chapter 7. The importance of the displacement spectra for assessing drift demands is discussed in Chapter 7, where it will be shown that spectral displacements can be used with good confidence to predict drift demands for a majority of elastic as well as inelastic structures. Here the spectral displacements are used to illustrate the spectral frequency characteristics and severity of the ground motions in relation to design "expectation" as represented by the NEHRP provisions.

Figures 5.15 to 5.17 present median elastic displacement demands for the SAC ground motions used in this study. The definition of the median is given in Section 3.6. Overlaid on the graph is the NEHRP '94 design displacement spectrum for soil profile D. A direct comparison of the NEHRP spectrum with the median spectra must be done with caution as the NEHRP spectrum is for 5% damping, whereas the median spectra are for a damping value of 2% of critical, which is the damping used in all the dynamic analysis in this study.

Figure 5.15 shows that for periods of interest for the LA structures (approximately 1.0, 2.25, and 3.75 seconds) the median 2/50 spectrum greatly exceeds the NEHRP design spectrum level. The median 10/50 spectrum matches the design spectrum rather well, except at long periods. The median 50/50 median spectral displacement demand is between 30-80% of the design level demand. The median spectral displacement demand for the three sets of ground motions is virtually constant beyond a period of about 3 seconds, indicating that changes in the stiffness of the structure in that region will not influence the deformation demands on the structure, as also observed in Chapter 4 for the 20-story structure under the LA36 record.

Figure 5.16, which shows the median displacement demand spectra for the Seattle sets of ground motions, indicates that the Seattle demands are comparable to the LA demands for the 3-story structure, but they become clearly smaller for the longer period structures. The Seattle spectral displacement demands are almost constant after about a period of 1.5 seconds. In the long period range (greater than 2.5 seconds) the Seattle median displacement demands are about half of the demands for LA, and the 10/50 demands fall significantly below the design level. It appears that the long duration records generated in the Seattle subduction zone area create relatively smaller long period displacement demands than the short duration near-fault records that dominate the rare LA events.

The median elastic displacement demands for Boston, shown in Figure 5.17, are well below the design level demands at all periods of interest (between 2.0 and 3.0 seconds). The displacement demands decrease for periods exceeding about 1.5 seconds and become very small at long periods. These small displacement demands dominate the response of the Boston 9- and 20-story structures. With such small displacement demands it is no surprise that these structures respond essentially elastic to the postulated ground motions. It is not within the context of this report to assess ground motion "reality", but it must be emphasized that the very large difference between the median displacement demands of the selected ground motions and the design level demands at long periods have an overpowering effect on the conclusions to be drawn on demands for long period SMRFs in the Boston area.

Figure 5.18 shows the measure of dispersion (standard deviation of the log values of the data) of spectral displacement demands for the different sets of ground motions for the different locations. All sets of ground motions are associated with a large scatter,

particularly in the long period range of interest in this study, and particularly for the Boston records. This large scatter in the input has a direct bearing on the response of the structure and needs to be considered carefully when interpreting the results from the nonlinear dynamic analysis, which are discussed next.

5.4 Drift Demands Under Nonlinear Dynamic Analysis

There is wide consensus that for moment resisting frames the interstory drift demand, expressed in terms of the story drift angle δ/h (δ being the interstory drift, h the height of the story) is the best measure of performance at the story level. The story drift angle is a global parameter in the sense that it can be related to the roof drift angle and therefore to the spectral displacement demand (see Chapter 7), and local in the sense that it provides good estimates of the element force and deformation demands (see Chapter 7). For the structures studied here most of the story drift is "shear drift" caused by flexural deformations in beams and columns and shear distortions in the panel zones, whereas the "flexural drift" component due to axial deformations in the columns is small.

The global (roof) drift angle demands and the story drift angle demands are evaluated for the sets of ground motions discussed in the previous section. For each story and each set of ground motions the median value and the measure of dispersion (standard deviation of log values of data) are computed. Assuming a lognormal distribution, the value of median multiplied by the exponent of the measure of dispersion corresponds to the 84^{th} percentile of the distribution. This percentile is reported in some cases to provide information on the range of data. In the following discussion the response of the M1 and M2 models of the pre-Northridge structures and of the M2 model of the post-Northridge structures is evaluated.

The median roof drift angle demands (expressed as a percentage, e.g., 0.03 radians is expressed as 3%) and the corresponding measures of dispersion for the different structures and analytical models are summarized in Table 5.2. These global demands are relatively high for the 3-story structures but decrease significantly for the 9- and particularly the 20-story structure. In part this is attributed to the fact that period and number of stories are nonlinearly related, but in part it is also attributed to the peculiar shape of the median displacement spectra, which exhibit a cap on the spectral displacement at relatively low periods (see Figures 5.15 to 5.17).

5.4.1 Drift Demands for LA Structures

The roof drift angle data for the LA structures indicate that the demand is not sensitive to the analytical model or the design characteristics (pre-Northridge versus Post-Northridge). The roof drift angle demand is very high for the 3-story structure. The demands are associated with a scatter that is similar to the scatter observed in the elastic spectral displacement demands at the first mode period (Figure 5.18). The reported values for model M1 of the 20-structure subjected to the 2/50 ground motion set are based on 19 records since the model "collapsed" under record LA30, see Chapter 4.

The medians of the maximum story drift angle demands over the height of the 3-, 9-, and 20-story structures, for models M1 and M2 of pre-Northridge designs and model M2 of the post-Northridge design, subjected to the different sets of LA ground motions are shown in Figures 5.19 to 5.21, respectively. The story drift demands for the 3-story structure (Figure 5.19) do not vary significantly over the height of the structure and are similar to the roof drift demands. The difference between the demands for models M1 and M2 or between the pre- and post-Northridge designs is not significant.

The 50/50 set of ground motions results in an almost uniform distribution of median story drift demands over the height of the 9- and 20-story structures. Some higher mode effects in the response of the structures are evident from the higher story drift demands observed for the top stories of the structures. The effect of higher modes is also seen in the response of the structures to the 10/50 set of ground motions. The maximum story drift demands are, consequently, higher than the maximum roof drift demand.

The 2/50 set of ground motions imposes high demands on the structures, causing significant P-delta effects for the 20-story structures. The lower stories median demands are more than twice the roof drift demand. The 20-story post-Northridge structure shows improved response as compared to the pre-Northridge design, on account of the higher strength and better strength balance between adjacent stories. This improvement in response is anticipated on the basis of the pushover analysis results shown in Figure 5.4, where the post-Northridge structure shows lower story drift amplification for the same level of roof drift, as compared to the pre-Northridge design.

Figure 5.22 shows the measure of dispersion of the story drift demands for the M2 models of the pre- and post-Northridge 20-story structures, for the three different sets of

ground motions. The high intensity 2/50 set of ground motions has a very large dispersion (0.6-0.8) associated with the demands in the lower six stories, and a low dispersion associated with the upper ten stories of the structure. This large dispersion is attributed to the presence of near-fault ground motions in the 2/50 set of records, which impose demands that depend strongly on the pulse-type characteristics of the motions. In addition, some of the records drove the structure into the range of negative stiffness, causing severe P-delta effects. Combined, the two effects result in a large dispersion, which is significantly larger than the dispersion of the spectral displacement around the first mode period (see Figure 5.18).

5.4.2 Drift Demands for Seattle Structures

The median roof drift angle demands for the Seattle structures, shown in Table 5.2, indicate that in most cases the demands for Seattle are smaller, and in some cases much smaller, than the demands for the LA structures for similar hazard levels. The exception is the 3-story structure, for which the pre-Northridge M1 model has a larger demand than the LA structure for the 2/50 set of records, whereas the pre-and post-Northridge M2 models have about the same demands. The latter observation is in line with expectations derived from the elastic displacement spectra (Figures 5.15 and 5.16). The large median roof drift of the M1 model is attributed to the early attainment of a negative post-yield stiffness (Figure 5.5) that greatly amplifies P-delta effects (see Section 4.4).

The effect of modeling for the 3-story structure is seen also in the median story drift angles presented in Figure 5.23. The modeling makes little difference at the 10/50 hazard level but has a pronounced effect at the 2/50 level at which the 3-story M1 model gets driven into the range of negative stiffness under most of the ground motions. Since the Seattle 9- and 20-story structures are not driven into the range in which P-delta effects become significant, the response of the structures is stable with moderate story drift demands, except for some of the upper stories in which higher mode effects increase the drift demand, see Figures 5.24 and 5.25. The concentration of drift demands in the upper stories is attributed in part also to the design characteristics, particularly for the 20-story structure. The design of the 20-story structure was controlled by wind effects, which results in a story shear strength distribution that favors lower stories compared to upper ones. Thus, upper stories are relatively weak and yield relatively early.

The argument that the large drifts in the upper stories can be attributed more to the relative story strength rather than the frequency characteristics of the ground motions is supported by the results presented in Figure 5.26. This figure shows the median story drifts of the Seattle 20-story pre-Northridge M2 model subjected to the LA 2/50 set of records, and the median story drifts of the LA 20-story pre-Northridge M2 model subjected to the Seattle 2/50 set of records. The Seattle structure still shows the bulge in story drifts near the top of the structure. The large drifts in the bottom stories is traced back to two ground motions that induce exceedingly large (about 22%) story drifts in the lower stories. Removal of those two records from the data set significantly reduces the drift demand in the lower stories but does not much affect the demand in the upper stories. The LA structure when subjected to the Seattle 2/50 set of records does not show the bulge in story drifts near the top of the structure.

5.4.3 Drift Demands for Boston Structures

Table 5.2 shows that the Boston structures exhibit rather low roof drift demands, particularly the 20-story structures. This does not imply that the response is confined to the elastic range. The story drift demands for the 3-, 9-, and 20-story structures are shown in Figures 5.27 to 5.29, respectively. The response of the 9- and 20-story structures is dominated by higher mode effects, which is no surprise since the elastic spectra show very little energy content in the long period range. As a consequence, the story drift angle demands are significantly higher than the roof drift angle demand, especially for the taller structures. In the top story of the 20-story structure the median drift angle demand is 3 to 4 times the demand in the lower stories for the 2/50 set of records. Several of the 2/50 records did cause yielding in the top stories. For the 3-story structure yielding was observed under many of the 2/50 ground motions.

The response of the 20-story pre-Northridge model M2 for one of the Boston 2/50 ground motions is shown in Figure 5.30. This figure shows the drift angle time history for stories 1 and 20, and the roof of the structure. The higher mode effects on the response of the 20^{th} story, and the high drift angle demand, compared to the roof and story 1, are evident. The roof drift response is in the first mode for this ground motions with cycles at about 3 seconds, which is the first mode period of the structure.

5.4.4 Assessment of Drift Demands

The results presented for the different structures (and analytical models) in different seismic locations, in terms of global and story drift demands under suites of different intensity ground motions, coupled with the behavioral characteristics exposed by the pushover analysis, assist in providing a basic understanding of the behavior of different structures and of their response in relation to design and ground motion characteristics. The presented data can form a basis for performance assessment at different hazard levels, provided that (a) these structures are representative of typical SMRFs in these seismic locations, (b) the employed ground motion records are representative of the specified hazard levels, and (c) the analytical models employed in the analysis are realistic representations of the structure.

Presuming that these conditions are fulfilled, a number of important observations and conclusions can be derived from the results of the analysis. To facilitate interpretation of the results, summary representations of the drift demand data are provided in Figures 5.31 to 5.36. Figures 5.31 to 5.33 present, at a consistent scale, medians and 84^{th} percentiles of story drift angle demands obtained by subjecting the M2 models of the nine pre-Northridge structures to the various sets of ground motions (50/50, 10/50, and 2/50 hazard levels). Figures 5.34 to 5.36 show the same results, but using story ductility values rather than absolute drift angles. The yield story drift angles used for normalization are obtained from the pushover analysis; they vary between 0.007 and 0.013, depending on span, number of stories, location in structure (story), and location of structure (geographic region). These yield values are not unique quantities; they depend on the applied load pattern in a static analysis and vary throughout the time history in a dynamic analysis. Thus, the presented ductility values are indicators rather than exact values; they are presented primarily to provide an idea of the extent of inelastic behavior.

The following general observations and conclusions can be derived from the presented results:

- The 50/50 ground motions in LA (72 year return period) induce drift angle demands of about 1% in average, but in some events the demands may become larger than 2%. These records cause very small inelastic behavior in average, but ductility demands larger than 2 are noted in some events and locations.

- For LA and Seattle the 10/50 ground motions cause drift demands of about 2% in average; except for the 20-story structures where the demands are clearly lower. In some cases the demands approach 3%. The demands for Seattle are often but not always somewhat smaller than for Los Angeles. A clear decrease in demands for Seattle compared to Los Angeles is not evident, particularly for the 3-story structure.

- In rare events, represented by the 2/50 set of records, all LA structures and the 3-story Seattle structure may experience very high drift demands. For a few ground motions drift angles in excess of 10% are computed. The median drift demands are in the order of 4%.

- The drift demands are associated with a large scatter. This scatter is usually somewhat larger than the scatter observed in the spectral displacement at the first mode period. This increase in scatter is due to higher mode effects and P-delta effects. The latter becomes important if the ground motion is sufficiently severe to drive a story into the range of negative lateral stiffness. If this occurs, the drift demands get amplified, which may result in extremely large outliers in drift demands. This increases the scatter, but also points out the potential for collapse due to P-delta. The extremely large outliers in drift demands may not be adequately represented by the reported statistical values (median and measure of dispersion). Their magnitude, which is a matter of concern, is seen only in graphical representations of individual data points such as those presented in Figures 5.39 and 5.42.

- The main reason for the very large 84^{th} percentile values of drift demand for the Seattle 3-story and LA 20-story structures is the P-delta effect. This effect affects the two structures differently. The LA 20-story structure experiences a small number of very large excursions due to the pulse-type nature of some of the near-fault records contained in the 2/50 set. The Seattle 3-story structure experiences many excursions due to the long strong motion duration of some of the Seattle 2/50 records. These repeated excursions cause "ratcheting" once the structure enters the range of negative stiffness.

- For the LA and Seattle 3-story structures the distribution of story drift over the height of the structure is rather uniform. These structures vibrate primarily in the

first mode. For the 9-story structures the distribution over height is also rather uniform although higher mode effects are becoming evident in the Seattle structure. For the LA 20-story structure the drift distribution over height is also rather uniform for small and moderate ground motions, but a clear drift bulge in the bottom stories is evident once the ground motions are sufficiently severe to cause significant P-delta effects. For the Seattle 20-story structure the drift demands show a clear bulge in the top stories, which is caused primarily by the relatively weak shear strength of the top stories due to wind design considerations.

- The drift demands seem to decrease with the height of the structure, with the 20-story structures showing (relatively) the lowest demands. This observation does not hold true if the structure is subjected to very severe ground shaking and is affected by high P-delta effects, as is the case for the LA 20-story structure.

- The performance of the code designed steel moment resisting frame structures used in this study is deemed to be in fair agreement with general expectations for conventional design events (10/50 ground motions) and more frequent events. However, for rare events (2/50 ground motions) larger than expected inelastic deformations may be experienced and the potential for unacceptable performance is not negligible.

- Except for very severe ground motions, the story ductility demands for all LA and Seattle structures are in the range of 5 or less.

- Under the ground motions representing a 2/50 event the drift angle and ductility demands for the Boston 3-story structure are in the order of 0.01 to 0.02 and 1.5 to 2.5, respectively. These demands may necessitate detailing for ductility.

- The Boston 9- and 20-story structures are subjected to ground motions whose spectral displacement demands at the first mode period are much smaller than those represented by the NEHRP spectrum. As a consequence, the first mode effects for these structures are small. Nevertheless, yielding in the upper stories is observed in several of the analyses of the 9 and 20-story structures due to higher mode effects. Story ductility demands higher than 2 are computed in some cases. This yielding occurs even though the structures have significant overstrength due to wind effects that control the design.

- For the post-Northridge designs with cover plates the drift demands are very similar to, and in general slightly smaller than, the drift demands for the pre-Northridge structures. The reason is that the beam and column sections used in the pre- and post-Northridge designs are very similar and some lateral strength is gained by strengthening the beam sections close to the column faces. This does not mean that the deformation demands at the element level are always similar, because the relative strength of beams and panel zones may change due of the strengthening of the beams (see Chapter 6).

Again, this assessment of drift demands is based on a few representative structures, modeled in a certain manner (M2 models), and subjected to specific sets of ground motions. As was discussed in Section 3.6, the computed drift demands are somewhat smaller (and in extreme cases significantly smaller) if other contributions to lateral strength and stiffness are considered in the analytical model (M2A model). On the other hand, constant strain-hardening of 3%, as is assumed at all levels of inelastic response, is likely too low for small inelastic deformations and certainly too high at the very large drift levels observed in some cases. Issues related to the ground motion representation, which include record selection (there are several pulse-type near-fault records in the LA 2/50 set and several very long strong motion duration records in the Seattle 2/50 set), orientation of components with respect to fault, record scaling, and matching with spectral values are addressed in Somerville et al. (1997). A brief description is also given in Appendix A. The results and conclusions need to be interpreted in the context of these assumptions and with due regard to the significant scatter associated with the demand estimates.

The statistical representation of demands pays very little attention to outlier data points in the response of the structures. These outlier values may, however, be very important for a performance assessment of these SMRF structures. Using the story drift demand results from the dynamic analysis of the different structures, a semi-quantitative performance assessment that takes advantage of drift limits suggested in currently available guidelines is carried out in the next section. A probabilistic representation of the drift and ductility hazard is also discussed.

The focus of the remainder of this chapter is on M2 models of the pre-Northridge structures. For the parameters discussed in this chapter the results for the M2 model of

the pre-Northridge structures may be taken as representative for the post-Northridge structures as well.

5.5 Performance Evaluation of SMRF Structures

Significant advances have been made towards answering questions on seismic performance of structures; documents such as Vision 2000 (SEAOC, 1995) and FEMA 273 (1997) provide a framework for a performance-based seismic engineering approach, outline analysis procedures to facilitate the performance evaluation of structures, and provide qualitative and quantitative definitions for seismic hazard and structural (and component) performance levels. Furthermore, procedures are becoming available for quantifying the performance of structures in a probabilistic format [Luco and Cornell (1998), Wen and Foutch (1997), Collins et al. (1996), Cornell (1996a)], permitting a better estimate for design demands associated with different performance objectives for the structure. The probabilistic demand estimates, coupled with information on capacities of elements and of the structure, can then be used to determine probabilities of exceeding certain performance levels. The results of such a performance evaluation can be used for retrofit purposes (if applied to existing structures), to modify preliminary designs in order to conform to specific performance requirements, and as indicators for the modifications needed in design provisions in order to improve the current state of design and performance assessment procedures.

The performance evaluation summarized next focuses on the use of the story drift (maximum and residual) as the basic parameter for performance assessment. The residual story drift is the permanent drift (offset from original position) of the story at the end of the seismic excitation. Story drift is the only parameter used in this discussion because the intent is to evaluate the performance of the structures according to current guidelines and procedures. The importance of cumulative damage effects, however, cannot be ignored and is briefly addressed in Section 5.5.3.

5.5.1 Performance Assessment Based on Presently Recommended Drift Limits

The SEAOC Vision 2000 and FEMA 273 documents define, qualitatively, different structural performance levels in terms of the damage sustained by the structure. For example: an immediate occupancy state of the structure would imply very light damage

as shown by minor local yielding and negligible residual drifts, while a collapse prevention limit state may be associated with extensive inelastic distortion of the beams, columns, or panel zones, with the structure having little residual strength and stiffness (from FEMA 273). The different performance levels are associated with different levels of ground motion hazard expressed in terms of return periods; for instance, under a frequent event, defined as a 43 year return period event, the structure should remain fully operational (from SEAOC Vision 2000). Both documents define similar performance levels and associated hazard levels, with some differences in terminology.

Acceptable limits of maximum and residual story drifts for various structural systems, associated with different performance levels, are given in these two documents. The documents emphasize that the values provided are only indicative of the range of drift values that the particular type of structure may sustain when responding within the different performance levels. Thus, the drift limits should only be used as indicators (and not strict design or evaluation limits) for structural performance. For SMRF structures, FEMA 273 recommends the following drift values: 1) immediate occupancy: 0.7% transient (or maximum) with negligible residual, 2) life-safety: 2.5% transient with 1% residual, and 3) collapse prevention: 5% transient and 5% residual. FEMA 273 also provides component level force and deformation acceptance values, related to the analysis procedure used to evaluate the structure. The emphasis in this section is at the story level.

The values suggested in FEMA 273 can be used as one set of guidelines by which the performance of a SMRF structure may be judged. The judgment may be preliminary and incomplete since the emphasis is on a "maximum" value parameter without regard to cumulative damage. In the following discussion the FEMA 273 values are used to obtain an estimate of the range of performance that the nine structures exhibit under different seismic hazard levels.

The maximum story drifts over the height of the structure (maximum drift in any story for a record), and the maximum residual drifts for the three pre-Northridge LA structures are shown in Figures 5.37 to 5.39 for the 50/50, 10/50, and 2/50 sets of LA ground motions. The figures show the 20 data points corresponding to the 20 records in each set, i.e., representative of one hazard level. The median and 84^{th} percentile values for the responses are shown by solid dash marks.

The results for the 50/50 set of records indicate that for a short return period of 72 years the structures respond between the immediate occupancy (IO) and the life-safety (LS) level. One of the ground motions in this set of records drives the 3-, and 9-story structures into the range between LS and collapse-prevention (CP) limits. The 20-Story structure shows the best performance of the three structures, with no outliers, lowest median value for the maximum story drift, and low scatter in the response. The residual drift values are well contained for the three structures, especially the 9- and 20-Story structures.

The relative performance pattern changes somewhat under the 10/50 ground motion hazard. All structures show outliers, with many records driving the response between the LS and CP levels, however no record drives the structures beyond the CP level. The residual drifts increase significantly, indicating increased inelastic deformations coupled with a more one-sided response. This trend is amplified in the results for the 2/50 ground motion hazard; there are clear outliers for all the three structures with the story drift demands exceeding 10%, which is likely unsustainable by the physical system constituting a typical SMRF. On the other hand, some ground motions in the 2/50 set result in response values similar to those observed in the 50/50 and 10/50 sets. The maximum residual drifts for the outliers in the 2/50 set follow closely the maximum story drift demands, indicating a one-sided response typical of structures subjected to near-fault pulse-type ground motions, which dominate the hazard at the 2/50 level for LA. The presence of the outliers in the response is of concern, as it is difficult to assess the likelihood of their occurrence and of the associated collapse potential.

The residual drift is often used as an indicator of the "damage" to the structure. There is value to this parameter, but it must be understood that residual drift may be a misleading indicator of the inelasticity that occurs in a structure. A cyclic pulse may cause significant inelasticity but low residual drift, whereas a half pulse of much smaller amplitude may cause much larger residual drift. For illustration of this point, the drift response of the third story of the 3-story LA structure for two ground motions is shown in Figure 5.40. Clearly, the ground motion inducing higher inelasticity in the structure has a lower residual drift on account of the cyclic nature of the predominant pulse.

The drift demands for the Seattle structures under the 10/50 and 2/50 sets of records are shown in Figures 5.41 and 5.42. The demands exhibit a clear trend with the height of the structure, with the 20-story structure having the smallest demands. For the 10/50 set

of records the demands for the 9- and 20-story structures are in the IO-LS range, indicating satisfactory performance. For the 3-Story structure the demands for some records fall into the LS-CP range, which may be unsatisfactory for a 10/50 hazard level. For the 2/50 set of records the drift demands for the 3-story structure exceed the CP limit of 0.05 for several records, and for one record the demand reaches an unrealistic value of 0.23. This indicates unacceptable performance. The reason for these large drift demands is the long strong motion duration of the records, which leads to "ratcheting" (progressive increase of displacements towards one side) of the response once the range of negative post-yield stiffness is attained. Some records also drive the 9-story structure beyond the CP level. The 20-story structure, however, performs in the LS-CP range, which should be acceptable at a 2/50 hazard level.

The maximum drift demands for the Boston structures under the 10/50 and 2/50 sets of records are shown in Figures 5.43 and 5.44, respectively. Under the 10/50 ground motions all three structures exhibit very small, if any, demands on inelastic behavior, indicating that the structures perform within the IO range. Under the 2/50 ground motions the drift demands in most cases are lower than the LS limits and in no case approach the CP limit. Thus, the performance of all Boston structures can be judged as satisfactory at all hazard levels, which is no surprise considering that wind effects control the design process for the 9- and 20-story structures. However, this performance assessment is based on the assumption that the deformation capacities of the Boston structures are comparable to those in higher seismic regions.

5.5.2 Story Drift and Ductility Hazard Curves

The performance assessment, as carried out in the previous section, indicates relative performance of different structures and compares predicted demands to indicative limit values suggested in current guidelines. The presented graphs also point out the presence of outliers in the response. However, the presented information does not provide any formal probabilistic estimate for the recurrence interval of the story drift demands.

Formal procedures for relating the calculated demand for a response parameter to the probability of occurrence of that demand have been proposed in the literature (Cornell 1996a, Wen 1995). The different methodologies relate the spectral hazard to a structural response parameter (usually interstory drift), in order to estimate the hazard associated

with the structural parameter. The methodologies differ in approach and extent of their applicability, but essentially provide a means to estimate the probability of exceeding predefined limits on a response parameter associated with specific levels of performance. In this study, the procedure proposed by Cornell (1996a) and described in Luco and Cornell (1998) is used to assess the annual probability of exceeding a particular story drift demand value.

The procedure is briefly summarized as follows. For given sets of records associated with specific return periods, say the 10/50 and 2/50 record sets, a period specific seismic hazard curve is developed (in the absence of site specific hazard curves) using the median spectral acceleration at the first mode period of the structure, S_a, and fitting a curve of the form of Equation 5.1 to obtain the parameters k_0 and k. Then a relationship between the drift demand q and the first mode spectral acceleration S_a is developed by fitting a curve of the form of Equation 5.2 to nonlinear time history analysis results in order to obtain the parameters a and b. Then a correction factor is calculated that accounts for the variability in the demand for a given spectral acceleration, using Equation 5.3. Finally, the drift hazard is calculated using Equation 5.4, which is obtained by substituting Equation 5.2 into Equation 5.1 and multiplication with the correction factor. If the correction factor is not used, the result amounts to relating the median demand value to the recurrence probability associated with the set of ground motions.

$$H(S_a) = k_0 S_a^{-k} \tag{5.1}$$

$$q = a S_a^{\,b} \tag{5.2}$$

$$C_{f1} = \exp[\frac{1}{2} k^2 (s_{\ln q \,|\, Sa} / b)^2] \tag{5.3}$$

$$H(q) = k_0 [(q/a)^{\frac{1}{b}}]^{-k} \times C_{f1} \tag{5.4}$$

The relationship between the spectral acceleration and the drift demand, given by Equation 5.2, is developed best for a specific story rather than for the maximum drift demand over the height of the structure. The reasons are that a stable relationship of the form of Equation 5.2 can be developed between spectral acceleration and global (roof)

drift demand for a structure, and a relationship can also be developed between global drift and story drift [see Chapter 7, Collins (1995), Miranda (1997)]. The two steps can be combined to relate the spectral acceleration to a particular story drift. The relationship between the global drift and the story drift changes significantly over the height of the structure, especially for tall structures where higher mode effects are significant (see Chapter 7). For this reason, the probabilistic assessment discussed here is carried out for a particular story. Furthermore, for cases in which higher mode effects are significant, the *"b"* value from Equation 5.2 becomes small (much less than 1) and consequently the correction factor may become large (greater than 10), at which point the procedure becomes less attractive.

The probabilistic performance assessment is illustrated here for the third story of all three story structures, the third story of the LA 9-story structure, and the fourth story of the LA 20-story structure. These particular stories have been selected because the highest median drift demands are observed for these stories. The ground motion hazard curves are developed using the median spectral accelerations of the 10/50 and 2/50 sets of records at the first mode period of the structures.

The values of the parameters k_0, k, a, b, and C_{f1} are given in Table 5.3. The hazard curves for the spectral accelerations corresponding to the first mode period of the three 3-story structures and of the three LA structures are shown in Figures 5.45 and 5.46, respectively. The median spectral acceleration values for the different sets of records are marked on the graphs. The curves are plotted, in general, between the minimum and maximum spectral acceleration values obtained for all the records in the sets, but in no case they are extended below an annual probability of 0.0001 (10000 year return period). As expected, based on the seismicity of the different regions, the slope of the hazard curve is steepest for LA.

The resulting drift hazard curves for story 3 of the 3-story structures are shown in Figure 5.47. Clearly, the Boston structure has the lowest drift hazard, which follows from the low spectral acceleration hazard at the first mode period of the 3-story Boston structure. The LA 3-story structure exhibits a higher drift hazard for larger values of annual probability of exceedence, whereas the Seattle 3-story structure exhibits a higher drift hazard at low values of annual probability. The cross-over of the drift hazard curves occurs at an annual probability of exceedence at which the first mode spectral acceleration hazards differ by a factor of about 2 (see Figure 5.45), which is on account

of the negative post-yield stiffness in the Seattle 3-story structure that causes accelerated drift amplification as the seismic input increases. The implication of the cross-over is that for large return periods the expected drift demand for the Seattle 3-story structure is significantly larger than for the LA 3-story structure. This is a consequence of structural properties (negative post-yield stiffness) in addition to ground motion characteristics (long strong motion duration).

A somewhat different picture is obtained if hazard curves are developed for story ductility (story drift normalized by drift at first yield) rather than story drift. The Seattle structure has a higher yield drift of 1.3% compared to roughly 1.0% for the LA structure, thus, for the same drift demand the ductility demand is higher for the LA structure, as shown in Figure 5.48. Consequently, if the damage estimate is based on ductility values, then the LA structure exhibits a higher "damage" potential for return periods up to about 5000 years.

The story drift hazard curves and ductility hazard curves for the three different height structures in LA are presented in Figures 5.49 and 5.50. The annual probability of exceedance associated with the drift demand is highest for the 3-story structure, till about 9% drift demand values (not shown because of the low annual probability of exceedance); for larger drift demands the hazard would be higher for the 9-, and 20-story structures. The 9- and 20-story structures exhibit almost identical drift hazard curves even though the response of the 20-story structure contains several outlier values, which are not observed for the 9-story structure. This discrepancy arises on account of the goodness of fit of the drift data to the spectral acceleration, as per Equation 5.2. The correction factor does capture the larger error in fit for the 20-story structure, reflected in a higher value (1.82 for 20-story as against 1.35 for 9-story), but applies this factor as a constant irrespective of the drift demand level. Thus, the presence of the outliers in the response of the 20-story structure is not evident in this representation. The ductility hazard curves shown in Figure 5.50 indicate a larger hazard for the 20-story structure, on account of the lower yield story drift value of 0.7% compared to 1.0% for the 3- and 9-story structures.

The procedure proposed by Cornell provides a convenient vehicle for evaluating performance in a probabilistic format. The process discussed in this section is only the first step towards performance assessment. Acceptable values for demands, which may be viewed as drift capacities, still need to be defined. The advantage of the drift hazard

curves is that they express the drift demand expectations that need to be met at various return periods. These expectations can be used to identify the deformation capacities that need to be achieved through proper detailing. There are potential shortcomings that need to be addressed in the implementation of this procedure. Due to the form of the equations used, and the necessary step of fitting a "best-fit" curve through data points, the outlier points may not be adequately reflected in the final representations. Furthermore, for cases in which the correction factor becomes very large, like for story drifts strongly influenced by higher mode effects, the procedure may not be very effective.

5.5.3 Cumulative Deformation Demands

Performance assessment of structures based solely on maximum value parameters may not present a complete picture of the distribution of damage in a structure. Experimental investigations have shown that structural damage is a function of not only the maximum values but also of the cumulative values of inelastic deformations, i.e., the structure has a memory of the inelastic deformations it experiences. There are many models [McCabe and Hall (1989), Chung et al. (1987), Park et al. (1984), Krawinkler and Zoheri (1983), among others], which assess the cumulative damage to particular types of elements and/or structures. The focus in this section (and in Section 6.4, where element cumulative deformation and energy demands are discussed) is not on using any of these indices to "measure" damage, but to show that ignoring cumulative inelastic effects may present a misleading picture for performance assessment of structures.

The issue is illustrated using the pre-Northridge LA and Seattle 9-story structures. The maximum value response parameters used are the following:

1. story drift angle demands: basic parameter being used for performance assessment of SMRF structures,
2. maximum total range of story drift angle demand: defined as the sum of the maximum positive drift angle and the absolute value of the maximum negative drift angle, and
3. maximum plastic drift range: defined as the maximum total range from which twice the story yield drift is subtracted.

These maximum value parameters are compared to a cumulative story drift angle parameter, defined as the sum of all plastic deformation ranges for a story during the time

history. The ranges are counted using the simplified rain-flow cycle counting method (described in Fuchs and Stephen, 1980, also see Krawinkler et al., 1983).

The median values of maximum and cumulative parameters, for the LA 9-story subjected to the 2/50 set of LA ground motions, are shown in Figure 5.51. All the maximum value parameters indicate a similar distribution of demands over the height of the structure. The cumulative plastic deformation demands, however, are larger for the upper three stories of the structure. This behavior is attributed to the increased number of inelastic cycles that are experienced by the upper stories due to higher mode effects. For example, the number of total cycles increased from 15 in story 1 to 25 in story 9 with the inelastic cycles increasing from 4 to 8. The effect can be more clearly seen from Figure 5.52, where the different parameter values are normalized to the value of the parameter in story 1. If maximum story drift capacity was assumed to be the same for all stories of this structure, then all the stories indicate similar levels of performance. Using cumulative deformation capacity as a measure of performance, however, indicates the upper stories to be more critical. Thus, the identification of the "critical" story of the structure is seen to vary with the choice of the response parameter.

The difference between the maximum value parameters and the cumulative plastic deformations is amplified for the Seattle 9-story structure, as seen in Figure 5.53, and from the normalized values in Figure 5.54. The reason is the influence of significant higher mode effects, which, when coupled with the very long duration of the Seattle ground motions, results in a very large number of inelastic cycles in the upper stories. In the top story the median value of the cumulative plastic deformation demand is almost 3 times the demand observed for the LA structure. This observation also suggests that the relative performance assessment between different regions may be affected by the choice of the response parameter. This issue is revisited in Section 5.7 when comparing the energy demands for the different structures.

The relationship between cumulative plastic story drift demand and maximum drift demand depends strongly on the structure height (number of stories), the location of the story (top versus bottom story), and the type of ground motion (e.g., pulse-type versus long duration), see Krawinkler and Gupta (1997). In the performance evaluation process, the demands obtained from the analysis are being compared to the capacity obtained from experimental investigations. Thus, in an experimental capacity evaluation program much attention needs to be paid in the applied loading history to the great variation in the ratio

of cumulative to maximum demand. This is a challenging task on account of the many variables affecting the relationship.

5.6 Evaluation of Global Force Parameters

The inelastic components of story drift are a direct function of the provided story shear strength and its relation to the elastic strength demands imposed by ground motions. An issue of interest for design is the relationship between a "shear strength reduction factor", defined as the ratio of elastic shear demand to provided shear strength, and the associated ductility ratio. Both quantities can be expressed at the story level, and both quantities can be evaluated for the cases studied in this project. Similarly, overturning moment (OTM) demands, which control axial loads in exterior columns, can be assessed from the results of this study. As a representative example, the story shear force and OTM results for the M2 model of the LA 20-story structure subjected to the 2/50 set of ground motions are discussed here.

Base and Story Shear Demands

In order to permit an assessment of the effects of P-delta on the effective story strength, the following two definitions are used here for story shear forces:

Story (or Base) Shear Force: This term is defined as the sum of column shear forces in a story, ΣV_c, which for static loading is equal to the sum of all horizontal loads applied to the structure above the story under consideration. Thus, the normalized values shown in the global pushover curves (Figures 5.1 to 5.3, 5.5 to 5.7, and 5.9 to 5.11) reflect the base shear that can be resisted at a given lateral displacement (this shear force may decrease after the development of a mechanism because of P-delta effects).

Equivalent Story (or Base) Shear Force: This term is defined as a quantity that incorporates, in an approximate manner, the effect of P-delta on the effective story (base) shear resistance. It is defined as $\Sigma V_c + P\delta/h$, with the second term representing the P-delta effect. In a pushover analysis the equivalent shear force will always increase with increasing story drift unless member strength deterioration is built into the analytical model. In a pushover analysis that includes P-delta effects the equivalent shear (sum of

the applied loads plus Pδ/h) will be similar to story shear (sum of applied loads) from an analysis that ignores the P-delta effect. Qualitatively, this is shown in Figure 4.1.

No attempts are made here to correlate computed story shear forces with design shear forces because of the multitude of factors (including expected strength of material, subjective design decisions, member selection, stiffness and/or wind controlled design) that introduce overstrength in the structure (Osteraas and Krawinkler, 1990). But an illustration is provided here of the differences between actual and equivalent shear forces and of the often made observation that the dynamic story shear forces (obtained from time history analysis) may be significantly higher than the story shear strengths obtained from a static pushover analysis.

A comparison of story shear forces over the height of the 20-story LA structure is shown in Figure 5.55. The figure shows the median equivalent shear force values ($\Sigma V_c+P\delta/h$) from dynamic analysis under the set of 2/50 ground motions, and the actual (ΣV_c) and equivalent ($\Sigma V_c+P\delta/h$) shear strength estimates obtained from a pushover analysis at the median roof drift demand of the 2/50 set of ground motions. The pushover analysis significantly under-estimates the dynamic story strengths of the structure and also does not capture the distribution of story shear strength over the height of the structure very well. The differences are largest for the upper stories of the structure. The reason for the differences is that the pushover analysis uses a fixed lateral load pattern over the height (in this case the NEHRP 1994 k=2 pattern), which results in a fixed pattern of inelasticity over the height, whereas during the dynamic response of the structure the distribution of shear forces over the height may be very different on account of higher mode effects and dynamic interaction between adjacent stories.

Figure 5.55 shows also the median elastic dynamic story shear demands, which are about 3 times as high as the median shear forces from inelastic dynamic analysis. This factor is rather constant over the height of the structure, indicating a constant "strength reduction factor" of 3 over the height of the structure. It is a matter of interest, but one that is not pursued here in detail, to relate this strength reduction factor to the story drift ductility factors whose median values are shown in Figure 5.34. This figure indicates a median ductility demand of about 4 in the lower stories in which P-delta effects are important, but a median ductility demand of less than 3 in most of the other stories.

A comparison of base shear values for the LA 20-story structure is shown in Figure 5.56. The curves for actual (ΣV_c) and equivalent ($\Sigma V_c + P\delta/h$) base shear versus roof drift angle are shown. The maximum dynamic equivalent base shear demand values obtained from dynamic analysis using the 10/50 and 2/50 sets of LA ground motions, are overlaid as circles on the figures. The shear demands are normalized with the seismic weight of the structure. The maximum strength demands during dynamic analysis are graphed against maximum roof drift angle value for convenience, however, the maximum strength demand and maximum roof drift may not occur at the same time, thus the data points may move to the left of the position they are shown at. This however, does not change the basic information contained in the graph, which is that the dynamic base shear strength of the structure is consistently higher than the strength predicted by the pushover analysis.

Thus, the pushover analysis will provide a low value for the base shear and story shear strengths. Furthermore, on account of being tagged to a fixed load pattern, the pushover analysis cannot capture the distribution of strength demands over the height of the structure. It is also observed that the story shear strength distribution depends on the ground motion characteristics. These conclusions are based on the response of the 20-story LA structure. The 3-, and 9-story structure show similar response, and in general, the results can be taken as being reflective of SMRF behavior.

Base and Story Overturning Moments

Two issues concerning overturning moment (OTM) demands in steel moment resisting frame structures are discussed in this section. The first issue relates to the question whether an overturning moment reduction factor should be applied in the design process, i.e., whether it is justified to reduce the design overturning moment below the value obtained from the design story shear forces. The reason often quoted for this reduction is that maximum story shear forces do not occur simultaneously. The second issue relates to the adequacy of using the pushover analysis for determining the OTM demands on the structure, as this would provide a convenient way to ascertain the axial forces induced in the columns. These issues are discussed using the LA 20-story structure as an example, with results presented in Figures 5.57 and 5.58. In both figures the OTM is normalized to the seismic weight of structure multiplied by the height of structure.

Figure 5.57 presents results obtained by assuming that the structure behaves elastically. The curve with data points represents the median story OTMs obtained from time history analyses. The bold line curve represents the pushover story OTMs obtained by pushing the structure to a base shear value equal to the median base shear from the time history analyses, whereas the light line curve represents the story OTMs obtained by pushing the structure to the median roof drift of the time history analyses. The following observations and conclusions can be made from these curves:

- Since the lateral load pattern for both pushover curves is identical, the two curves differ by a constant factor, which represents the difference between the base shear associated with median dynamic drift (0.256W) and the median dynamic base shear (0.396W). This difference is significant, which shows that the relationship between dynamic roof drift and dynamic base shear is poorly represented by the pushover lateral load pattern. This is no surprise since for this structure the roof drift is controlled by first mode displacements whereas the story shear forces are controlled by a combination of modal contributions.

- The dynamic median story OTMs have a different distribution over height than the OTMs from the pushover load pattern. In the upper stories they are larger than the OTMs from both pushover analyses, but in the lower stories they are significantly smaller than the OTMs from the pushover to a base shear equal to the median dynamic base shear. The latter reason is often used to advocate an OTM reduction factor. Even for structures with unlimited story shear strength (elastic behavior in all earthquakes) such a reduction factor is questionable since it would severely underestimate the OTMs in upper stories.

- For the reason discussed next, the relationship between elastic shear force demands and OTM demands is a matter of intellectual curiosity but not one that is very relevant for design of SMRF structures – unless there is assurance that the structure is strong enough to resist earthquakes in the elastic range.

The magnitude of story shear strength is a design decision under control of the designer. As long as flexural ductility is available in beams or columns (or shear distortion ductility is available in panel zones), low story shear strengths that lead to inelastic behavior in the ductile elements can be tolerated, within limits. The same does not hold true for OTMs, because OTMs cause axial forces in columns. Columns are

critical elements of the gravity load path and must maintain stability even in the most severe earthquake. Since column ductility under compressive forces is very questionable, overloads that may lead to column buckling must be prevented. Thus, the axial force design of columns must be based on capacity design criteria using the maximum OTM an earthquake can conceivably generate. This can only be accomplished by explicit consideration of inelastic behavior based on the shear strength of individual stories.

Nassar and Krawinkler (1991) have concluded that for inelastic structures whose story strengths are tuned to the design lateral load pattern, simultaneous yielding in stories is very likely and thus, maximum OTMs should be based on story shear strengths without application of an overturning moment reduction factor. Figure 5.58 provides support for this conclusion. It shows the median normalized OTM demands from time history analysis of the inelastic LA 20-story structure (with P-delta), together with OTMs obtained from a pushover analysis at the median roof drift demand level under the 2/50 set of records, with and without P-delta effects. The pushover OTM predictions match well with the time history results for the lower stories, but provide low predictions for the upper stories. The primary reason is the previously stated observation that the pushover underestimates the dynamic story shear strengths.

A comparison of the base OTM demand from a pushover analysis and dynamic analysis case is shown in Figure 5.59. The circles represent the maximum dynamic base OTM values from the dynamic analysis, graphed against the maximum roof drift angle demand, for each record of the 10/50 and 2/50 set of ground motions (the two maxima may not occur at the same time, thus the data points may move to the left of their shown position). The pushover analysis reasonably represents the dynamic base OTM demand except at large drift demands, where the pushover under-predicts the dynamic demand. The primary reason is again that the pushover under-predicts the dynamic story shear strengths. The few low values observed for the time history analysis around 0.01 roof drift angle are primarily due to the maximum roof drift angle not corresponding to the maximum base OTM demand, thus, the true position of the points is to the left of their current position.

An interesting result is the higher base OTM demand exhibited at large roof drifts by the structure without P-delta effects. This indicates that the effective lever arm of the P-delta OTMs is smaller than the lever arm of the applied loads.

In conclusion, the pushover analysis will, in general, provide a good prediction of the base overturning moment and a low prediction of the OTMs in the upper stories. There is no evident reason to apply an overturning moment reduction factor to the results obtained from the pushover analysis.

5.7 Energy Demands

Energy parameters are believed to provide additional insight into damage potential on account of their cumulative nature. The hysteretic energy, or the energy dissipated through inelastic deformations, has been shown to be representative of cumulative damage (Nassar and Krawinkler, 1991). Furthermore, relationships have been developed, which indicate that the percentage of the seismic input energy to the structure dissipated as hysteretic energy is a stable parameter [Seneviratna and Krawinkler, (1997), Fajfar, (1996)] for both SDOF and MDOF structures. Design philosophies have been proposed based primarily on energy concepts [e.g., Bertero (1997), Bertero and Uang (1992)], however, these design concepts are at the research level and need to be formalized for general acceptance. The focus of this section is to evaluate the energy demands for "real" structures, and evaluate the applicability of previously proposed energy based relationships to "real" structures, and augment the state of knowledge for developing energy based design and evaluation criteria.

The first relationship to be evaluated is between the seismic input energy to an SDOF system having a period equal to the first mode period of the MDOF system, and the input energy to the inelastic MDOF structure. Seneviratna and Krawinkler (1997) have shown that the ratio of the input energy for the MDOF system to the input energy for the SDOF system increases non-linearly with increasing the period of the structure. At a period of about 2 seconds, for design level ground motions, they evaluated the mean ratio to be about 1.6 with a standard deviation of about 0.35 for generic SMRFs. The ratio was not affected significantly by the level of inelasticity in the structure, but significantly affected by the characteristics of the mean elastic response spectrum.

The median of ratios of the MDOF total dissipated energy (hysteretic plus damping, which can be taken as the total input energy) to the input energy for the first mode period SDOF system (assuming full mass participation in the first mode), for the 10/50 and 2/50 sets of ground motions, for the LA and Seattle structures are shown in Table 5.4. Figure

5.60 shows the elastic response spectra for the four sets of ground motions. The following patterns are identified from the median values of the ratios between the MDOF and the SDOF input energy:

1. The values increase drastically with an increase in period, showing a clear non-linear relationship.
2. The values are significantly higher for the Seattle ground motions than for the LA ground motions. This is because the Seattle ground motions have a relatively low energy content at the first mode period of the structure. On account of larger contributions from the higher modes, the energy ratio is much higher for the Seattle structures than the LA structures.
3. The results are in line with expectations based on Seneviratna and Krawinkler's (1997) study, which documented this effect for generic frames till a period of 2.05 seconds.

The second relationship evaluated is between the seismic input energy to the structure and the percentage dissipated through inelastic deformations, i.e., as hysteretic energy (or HE). This ratio has been shown to be affected by the ground motion characteristics, period of the structure, and the level of inelasticity in the structure. However, the ratio has been observed to be quite stable between SDOF and MDOF structures. The values of this ratio for the LA and Seattle structures are given in Table 5.5. The values for the LA structures under the 10/50 set of records are in good agreement with the values shown by Seneviratna and Krawinkler for generic frame structures under similar intensity ground motions. The ratios are also in good agreement with equivalent ratios obtained at the SDOF level. The increase in the ratio for the 2/50 set is expected on account of the increased inelasticity in the structure.

The Seattle 10/50 ground motions show a low value for the ratio on account of the limited inelasticity in the structure; furthermore, the duration of the records is very long and the response for the most part is elastic, thus, the energy is primarily dissipated through damping. The value is also associated with a very large scatter. The ratio increases significantly for the 2/50 set of SE ground motions and has a reduced scatter, again, on account of more uniform yielding in the structure. Similar ratios are observed for the SDOF systems. Thus, the results confirm that the fraction of input energy dissipated as hysteretic energy can be well estimated using SDOF information.

From a perspective of identifying the location of damage in structure, the quantity of interest is the percentage of the total structure HE dissipated at the different floor levels. This quantity is obtained by summing the HE dissipated in each element framing into a floor and normalizing by the value of the structure hysteretic energy. The distribution of HE over the height of the Seattle and LA 9-story structures, under 2/50 sets of ground motions, is shown in Figures 5.61 and 5.62, respectively. The figures show the individual data points for each floor, as well as the median and 84^{th} percentile values.

The distribution of HE at a floor level is associated with very large scatter. The base (floor 1) of the structure does not yield under a few records, there no statistical values are calculated. For the Seattle structure, the concentration of HE is in the upper floors, which is to be expected from Figure 5.53. The comparison between the cumulative deformation figures and HE figures must be done with caution as 1) the HE is at the floor level while the cumulative deformation is at the story level, and 2) the energy capacity is lower for the upper floors of the structure due to lighter beam and column sections. Thus, the HE and cumulative deformation graphs need not be similar.

The distribution of HE over the height of the LA 20-story structure, shown in Figure 5.63, indicates that the P-delta effects control the energy dissipation. The concentration of HE is in the lower floors where the P-delta effect is maximum. The lower five floors dissipate about half the structure hysteretic energy. However, some local concentrations are also observed in the middle and upper floors of the structure indicating the influence of higher mode effects.

The following conclusions can be drawn from this brief discussion on energy demands for typical steel moment resisting frame structures:

1. The seismic input energy to the MDOF structure may be much larger than the input energy to the first mode SDOF system. The amplification is highly non-linear, showing a rapid increase with an increase in the period of the structure.
2. The relationship between the input energy and the dissipated energy is quite stable and can be adequately ascertained from SDOF systems. The relationship is not strongly influenced by the period (in the range of these structures), but is affected by the intensity of ground motions (extent of inelasticity).
3. The distribution of hysteretic energy dissipation over the height of the structure is strongly controlled by the strength characteristics of the structure and the ground

motion characteristics. Where higher mode effects are significant the concentration of energy is in the upper floors, and where P-delta effects are predominant the concentration is in the lower stories.

Even though energy based design or structural evaluation is not a well formalized or accepted process, an evaluation of the energy parameters for the structure permits a better understanding of the behavior and response. Caution must be exercised when comparing absolute HE values or normalized HE values, as the energy capacity of the floors is not the same over the height of the structure.

Table 5.1 Modal Characteristics for pre-Northridge (Models M1 and M2) and post-Northridge (Model M2) Structures

FIRST MODE CHARACTERISTICS

Period (seconds)

	LA			SEATTLE			BOSTON		
	3-Story	9-Story	20-Story	3-Story	9-Story	20-Story	3-Story	9-Story	20-Story
Pre-Northridge Model M1	1.03	2.34	3.98	1.36	3.17	3.92	1.89	3.33	3.19
Pre-Northridge Model M2	1.01	2.24	3.74	1.36	3.06	3.46	1.97	3.30	3.15
Post-Northridge Model M2	1.02	2.21	3.65	1.30	3.06	3.52	1.62	3.17	2.97

Modal Mass %age

	3-Story	9-Story	20-Story	3-Story	9-Story	20-Story	3-Story	9-Story	20-Story
Pre-Northridge Model M1	82.8	83.5	80.4	82.6	81.1	77.1	83.6	85.0	75.0
Pre-Northridge Model M2	82.9	82.1	80.1	82.8	80.1	78.0	83.3	82.9	75.2
Post-Northridge Model M2	83.4	82.2	80.1	88.9	80.3	75.8	83.1	75.8	74.1

Participation Factor

	3-Story	9-Story	20-Story	3-Story	9-Story	20-Story	3-Story	9-Story	20-Story
Pre-Northridge Model M1	1.27	1.36	1.37	1.27	1.36	1.44	1.26	1.35	1.46
Pre-Northridge Model M2	1.30	1.38	1.36	1.29	1.37	1.42	1.28	1.37	1.45
Post-Northridge Model M2	1.30	1.37	1.38	1.28	1.39	1.43	1.28	1.42	1.43

SECOND MODE CHARACTERISTICS

Period (seconds)

	LA			SEATTLE			BOSTON		
	3-Story	9-Story	20-Story	3-Story	9-Story	20-Story	3-Story	9-Story	20-Story
Pre-Northridge Model M1	0.33	0.88	1.36	0.43	1.13	1.40	0.59	1.22	1.17
Pre-Northridge Model M2	0.30	0.84	1.26	0.41	1.06	1.30	0.57	1.22	1.17
Post-Northridge Model M2	0.30	0.82	1.26	0.41	1.10	1.28	0.49	1.17	1.04

Modal Mass %age

	3-Story	9-Story	20-Story	3-Story	9-Story	20-Story	3-Story	9-Story	20-Story
Pre-Northridge Model M1	13.5	10.6	11.5	13.3	12.6	13.7	12.9	10.1	14.6
Pre-Northridge Model M2	13.7	11.1	11.3	13.5	13.0	12.5	13.3	10.9	13.9
Post-Northridge Model M2	13.2	11.2	11.8	9.6	12.4	14.1	13.4	14.3	13.3

Participation Factor

	3-Story	9-Story	20-Story	3-Story	9-Story	20-Story	3-Story	9-Story	20-Story
Pre-Northridge Model M1	0.40	0.52	0.56	0.39	0.52	0.65	0.39	0.52	0.72
Pre-Northridge Model M2	0.45	0.56	0.56	0.41	0.55	0.64	0.42	0.57	0.71
Post-Northridge Model M2	0.43	0.55	0.57	0.39	0.55	0.64	0.41	0.65	0.71

THIRD MODE CHARACTERISTICS

Period (seconds)

	LA			SEATTLE			BOSTON		
	3-Story	9-Story	20-Story	3-Story	9-Story	20-Story	3-Story	9-Story	20-Story
Pre-Northridge Model M1	0.17	0.50	0.79	0.22	0.61	0.82	0.31	0.73	0.69
Pre-Northridge Model M2	0.14	0.47	0.74	0.18	0.56	0.76	0.27	0.71	0.69
Post-Northridge Model M2	0.14	0.46	0.72	0.15	0.57	0.74	0.23	0.67	0.63

Modal Mass %age

	3-Story	9-Story	20-Story	3-Story	9-Story	20-Story	3-Story	9-Story	20-Story
Pre-Northridge Model M1	3.7	3.6	3.4	4.1	3.6	4.3	3.5	3.1	4.7
Pre-Northridge Model M2	3.4	4.1	3.5	3.7	3.9	4.3	3.4	3.8	4.7
Post-Northridge Model M2	3.4	3.9	3.1	1.5	4.3	4.4	3.6	6.7	5.7

Participation Factor

	3-Story	9-Story	20-Story	3-Story	9-Story	20-Story	3-Story	9-Story	20-Story
Pre-Northridge Model M1	0.26	0.25	0.32	0.28	0.26	0.34	0.25	0.24	0.42
Pre-Northridge Model M2	0.26	0.27	0.34	0.27	0.28	0.34	0.25	0.28	0.43
Post-Northridge Model M2	0.25	0.27	0.32	0.16	0.28	0.34	0.26	0.34	0.47

Table 5.2 Statistical Global (Roof) Drift Angle Demands for pre- and post-Northridge Structures (Models M1 and M2); Different Sets of Ground Motions

- The drift angle values are presented as percentages, e.g., 0.0393 radians = 3.93%

LA 3-STORY	**MEDIAN**			**STD. DEV. OF LOG VALUES**		
	50/50 Set	10/50 Set	2/50 Set	50/50 Set	10/50 Set	2/50 Set
Pre-Northridge Model M1	1.11	1.96	4.01	0.42	0.33	0.49
Pre-Northridge Model M2	1.11	1.87	3.93	0.41	0.32	0.52
Post-Northridge Model M2			3.91			0.51
LA 9-STORY						
Pre-Northridge Model M1	0.76	1.37	2.56	0.32	0.29	0.47
Pre-Northridge Model M2	0.74	1.35	2.52	0.33	0.26	0.44
Post-Northridge Model M2			2.46			0.42
LA 20-STORY						
Pre-Northridge Model M1	0.40	0.84	1.44*	0.44	0.36	0.50*
Pre-Northridge Model M2	0.39	0.84	1.46	0.43	0.32	0.53
Post-Northridge Model M2			1.47			0.42

SEATTLE 3-STORY	**MEDIAN**			**STD. DEV. OF LOG VALUES**		
	50/50 Set	10/50 Set	2/50 Set	50/50 Set	10/50 Set	2/50 Set
Pre-Northridge Model M1		1.61	5.06		0.35	0.75
Pre-Northridge Model M2		1.55	4.08		0.34	0.58
Post-Northridge Model M2			3.70			0.41
SEATTLE 9-STORY						
Pre-Northridge Model M1		0.94	1.95		0.31	0.59
Pre-Northridge Model M2		0.94	1.70		0.30	0.49
Post-Northridge Model M2			1.85			0.53
SEATTLE 20-STORY						
Pre-Northridge Model M1		0.53	0.91		0.37	0.39
Pre-Northridge Model M2		0.52	0.82		0.34	0.40
Post-Northridge Model M2			0.85			0.41

BOSTON 3-STORY	**MEDIAN**			**STD. DEV. OF LOG VALUES**		
	50/50 Set	10/50 Set	2/50 Set	50/50 Set	10/50 Set	2/50 Set
Pre-Northridge Model M1		0.34	1.02		0.35	0.30
Pre-Northridge Model M2		0.34	0.94		0.42	0.31
Post-Northridge Model M2			1.08			0.32
BOSTON 9-STORY						
Pre-Northridge Model M1		0.13	0.36		0.57	0.61
Pre-Northridge Model M2		0.13	0.38		0.56	0.59
Post-Northridge Model M2			0.42			0.53
BOSTON 20-STORY						
Pre-Northridge Model M1		0.07	0.21		0.51	0.51
Pre-Northridge Model M2		0.08	0.20		0.48	0.50
Post-Northridge Model M2			0.20			0.44

* Values based on 19 records only. The model "collapsed" under LA30 ground motion

Table 5.3 Values of Different Parameters For Development of Drift Hazard Curves for LA, Seattle, and Boston Structures

	T1	k_0	k	a	b	C_{f1}
LA 3-Story	1.01	0.001308	3.132	0.0264	0.8371	2.44
LA 9-Story	2.24	0.000177	2.365	0.0418	0.8415	1.35
LA 20-Story	3.74	0.000016	2.789	0.0922	0.9829	1.82
Seattle 3-Story	1.36	0.000400	1.742	0.0433	0.7195	1.48
Boston 3-Story	1.97	0.000015	1.420	0.0725	0.7072	1.34

Table 5.4 Median Values for Ratio of MDOF Input Energy to SDOF Input Energy at First Mode Period of MDOF LA and Seattle Structures; 10/50 and 2/50 Sets of Ground Motions

	LA			SEATTLE		
	3-Story: T1=1.01	9-Story: T1=2.24	20-Story: T1=3.74	3-Story: T1=1.36	9-Story: T1=3.06	20-Story: T1=3.46
10/50 Set of Ground Motions	0.88	3.49	5.47	1.19	6.91	10.47
2/50 Set of Ground Motions	0.98	2.89	4.57	1.33	6.68	12.36

Table 5.5 Median Values for Ratio of MDOF Hysteretic Energy to MDOF Input Energy for LA and Seattle Structures, Under 10/50 and 2/50 Sets of Ground Motions

	LA			SEATTLE		
	3-Story: T1=1.01	9-Story: T1=2.24	20-Story: T1=3.74	3-Story: T1=1.36	9-Story: T1=3.06	20-Story: T1=3.46
10/50 Set of Ground Motions	0.64	0.61	0.62	0.31	0.39	0.25
2/50 Set of Ground Motions	0.83	0.83	0.80	0.76	0.68	0.63

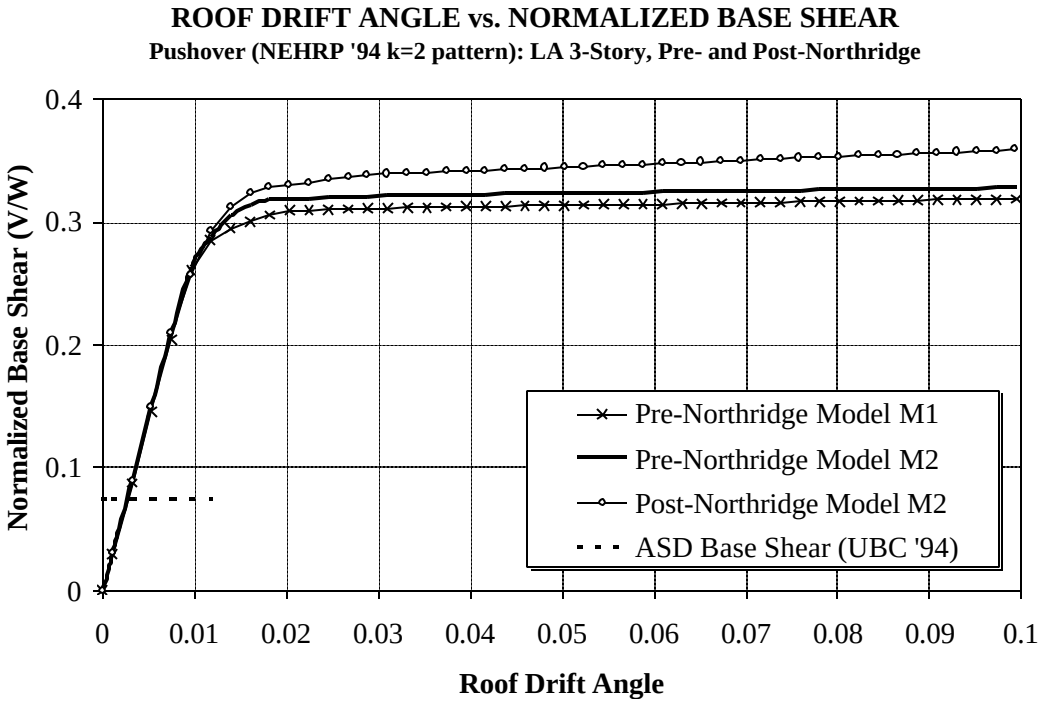

Figure 5.1 Global Pushover Curves for LA 3-story Structures

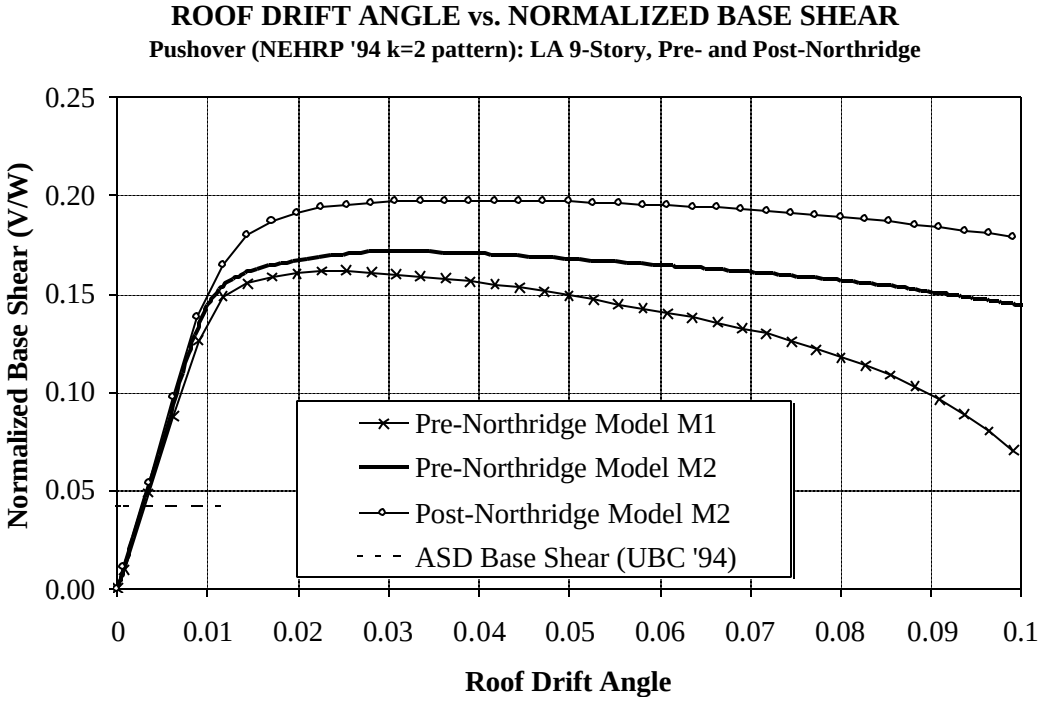

Figure 5.2 Global Pushover Curves for LA 9-story Structures

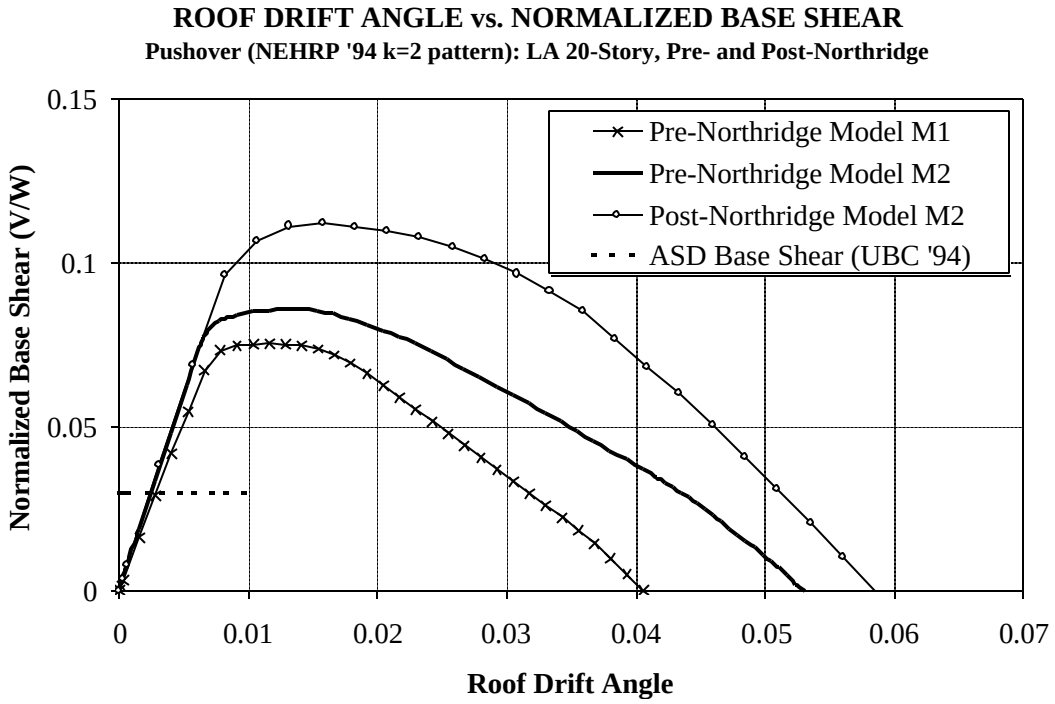

Figure 5.3 Global Pushover Curves for LA 20-story Structures

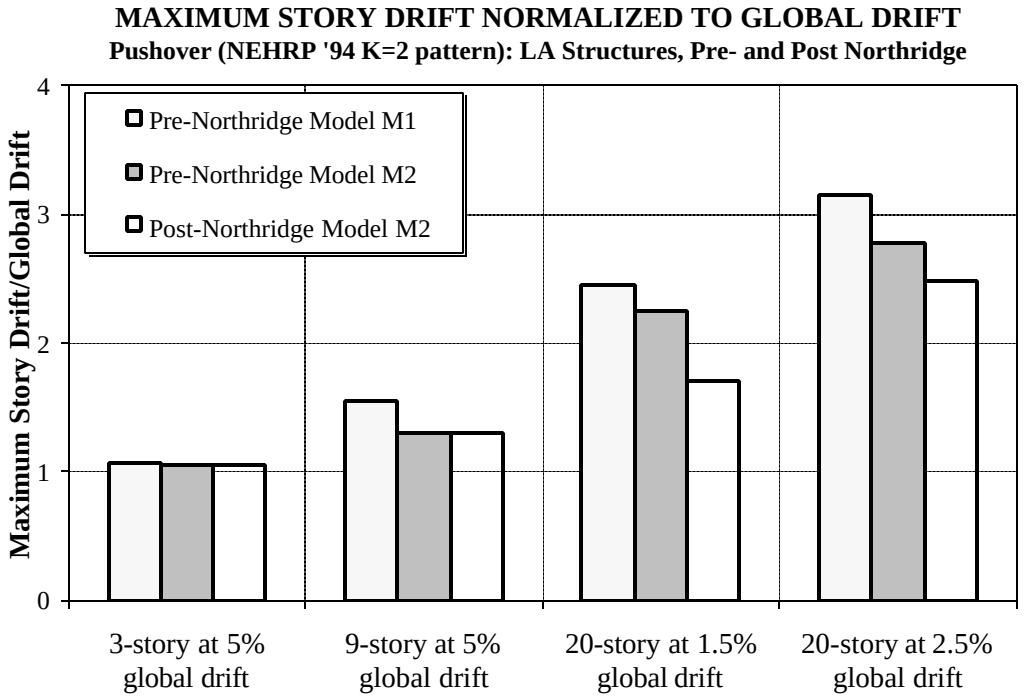

Figure 5.4 Ratio of Maximum Story Drift Angle to Roof Drift Angle at Particular Roof Drift Demand Levels for LA Structures, Pushover Analysis

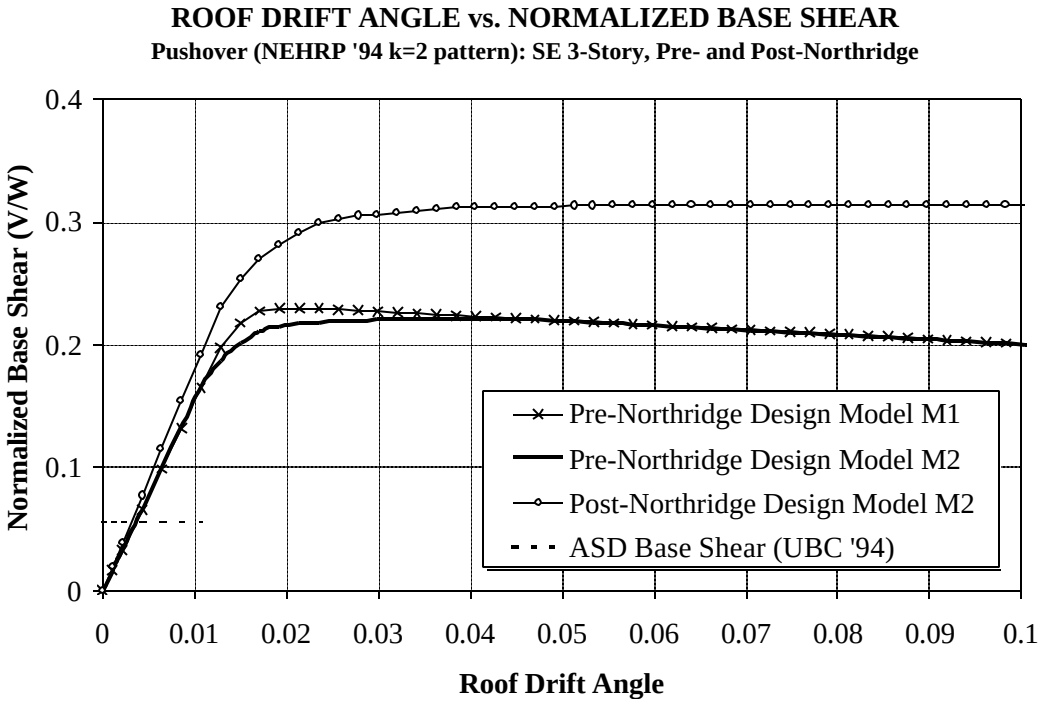

Figure 5.5 Global Pushover Curves for Seattle 3-story Structures

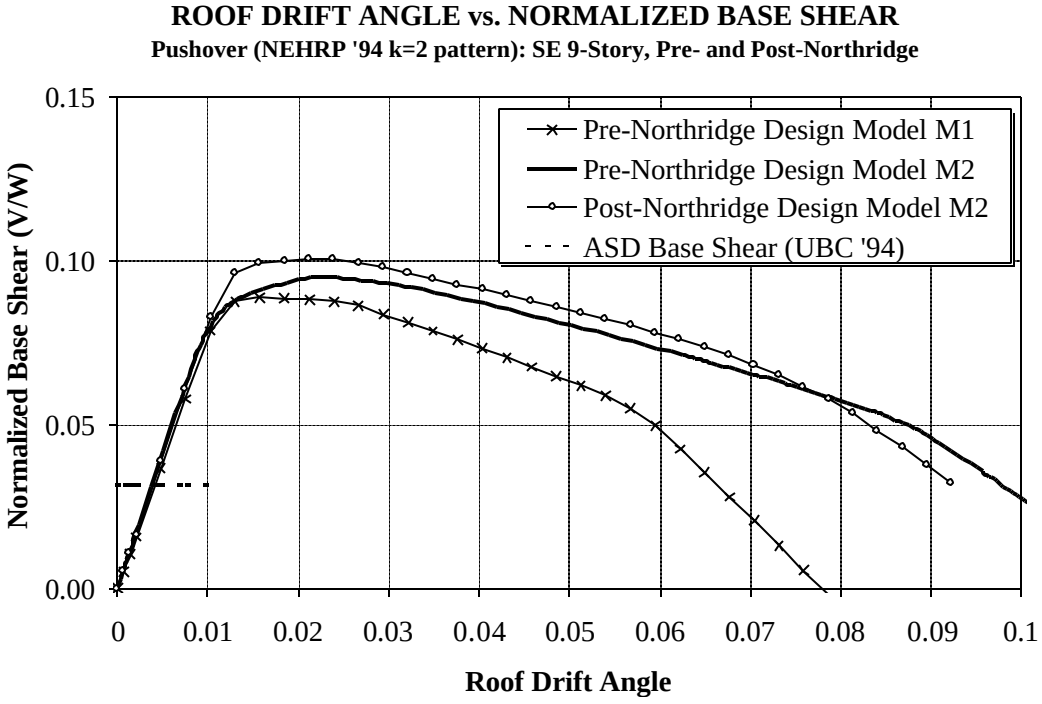

Figure 5.6 Global Pushover Curves for Seattle 9-story Structures

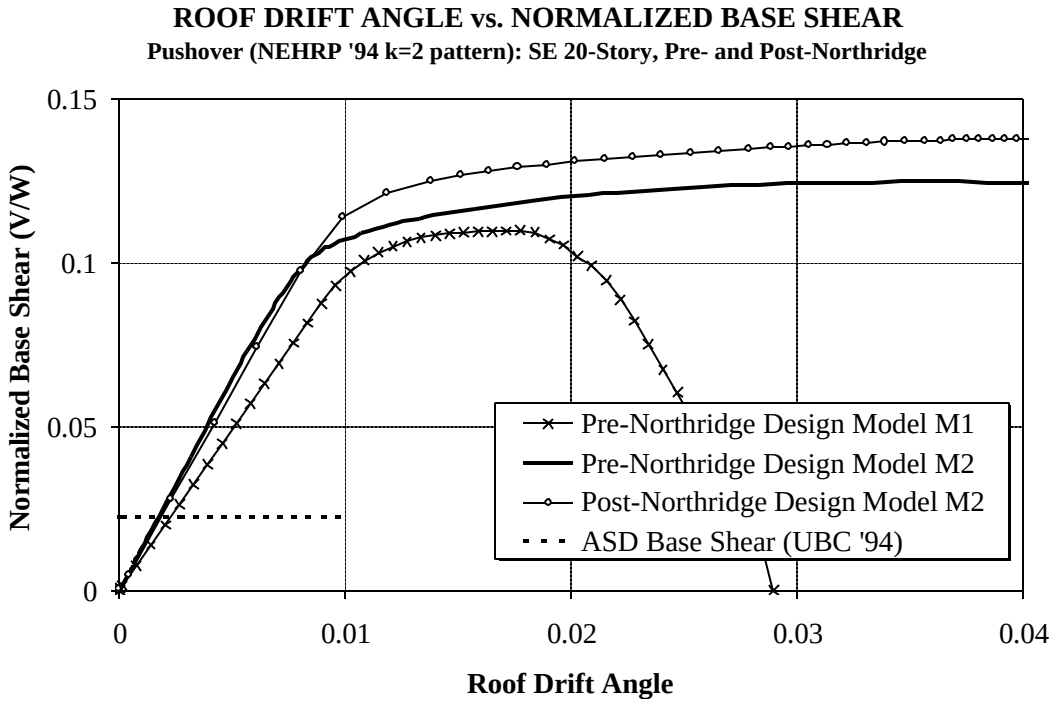

Figure 5.7 Global Pushover Curves for Seattle 20-story Structures

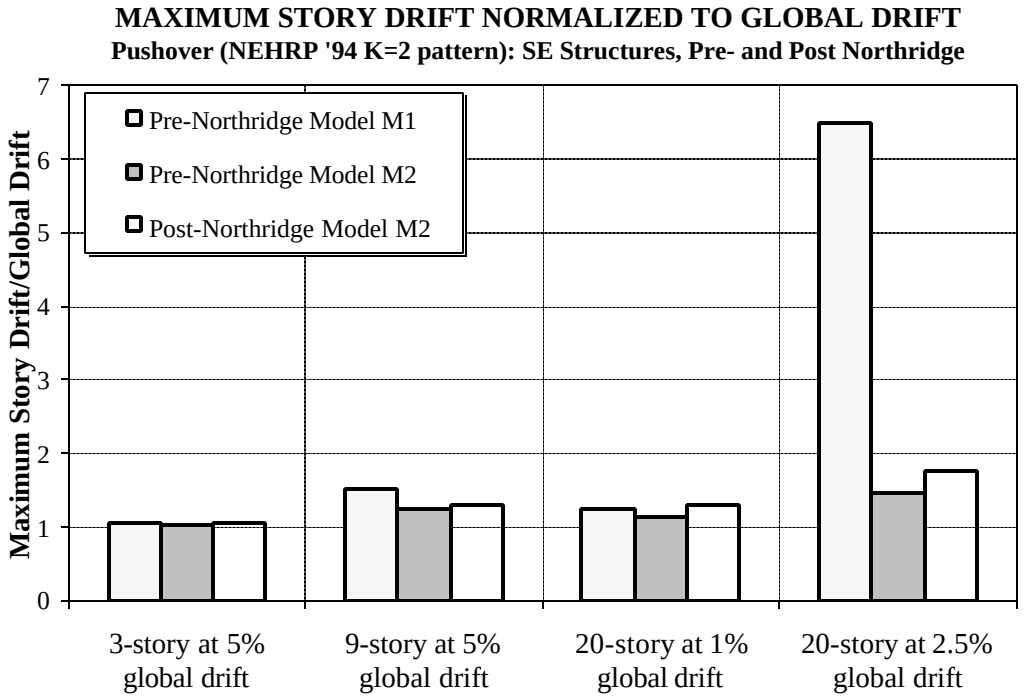

Figure 5.8 Ratio of Maximum Story Drift Angle to Roof Drift Angle at Particular Roof Drift Demand Levels for Seattle Structures, Pushover Analysis

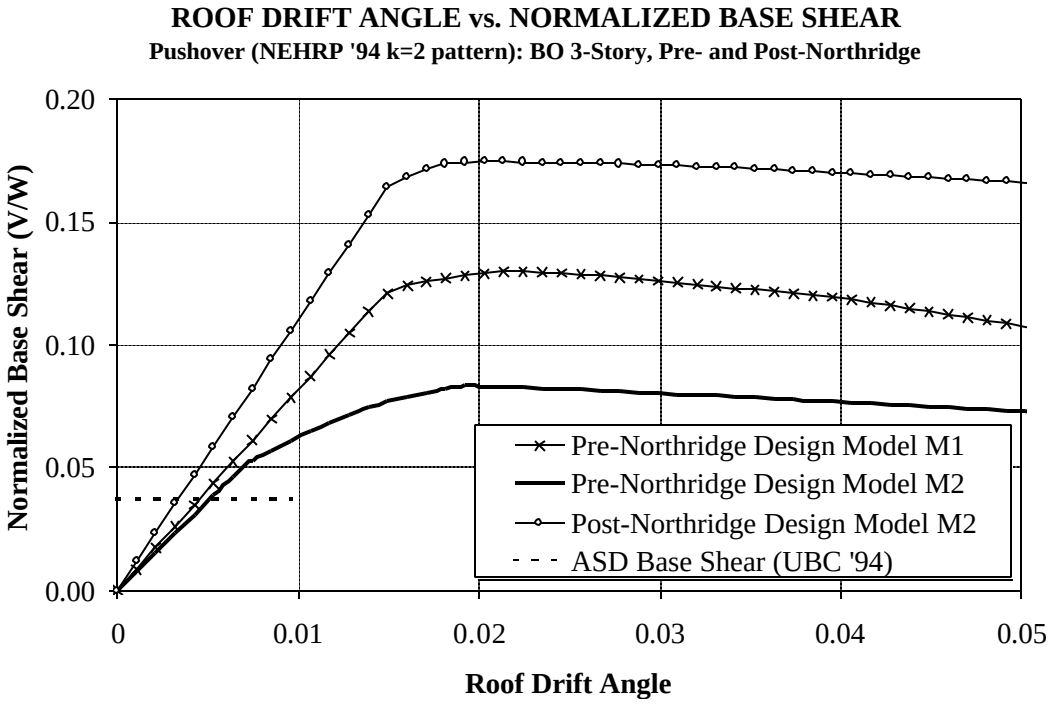

Figure 5.9 Global Pushover Curves for Boston 3-story Structures

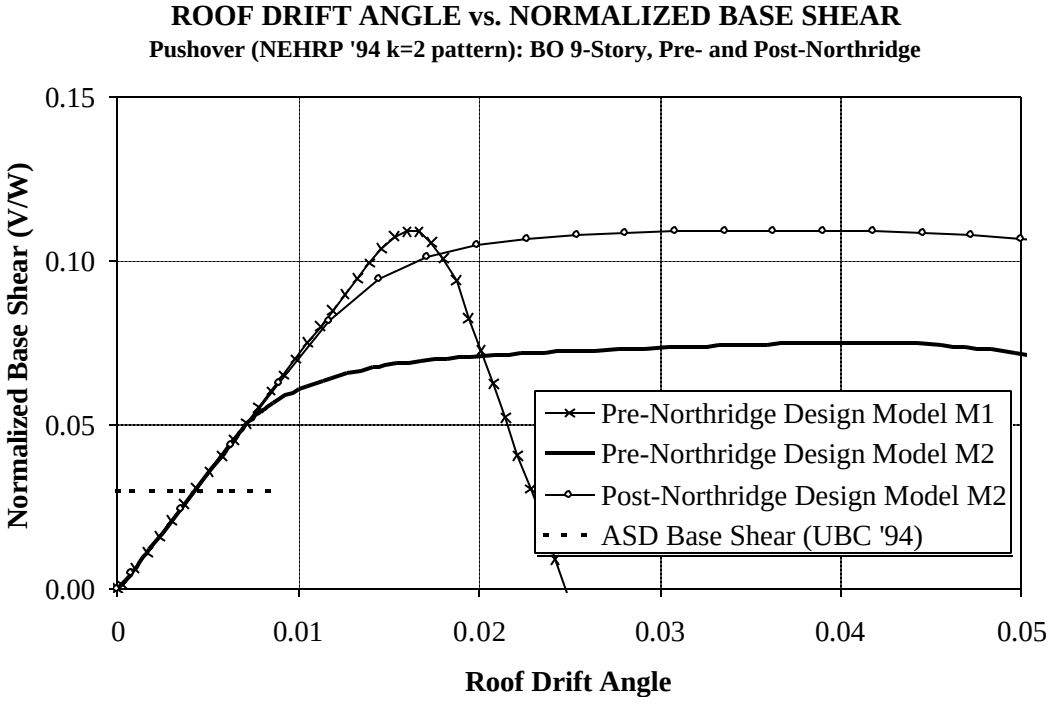

Figure 5.10 Global Pushover Curves for Boston 9-story Structures

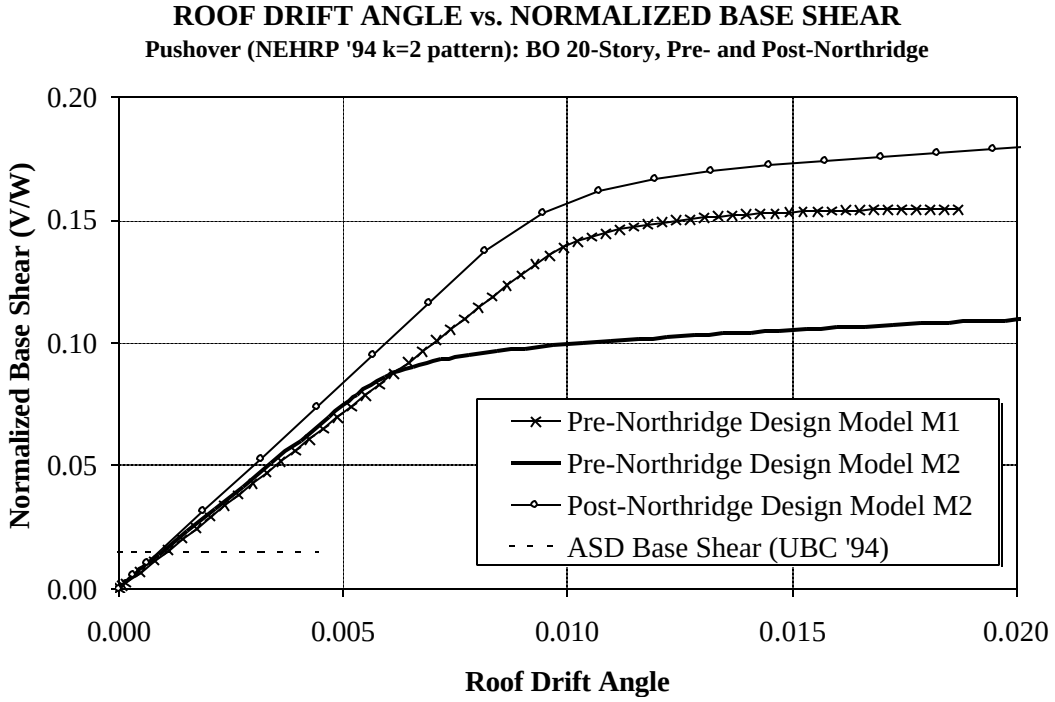

Figure 5.11 Global Pushover Curves for Boston 20-story Structures

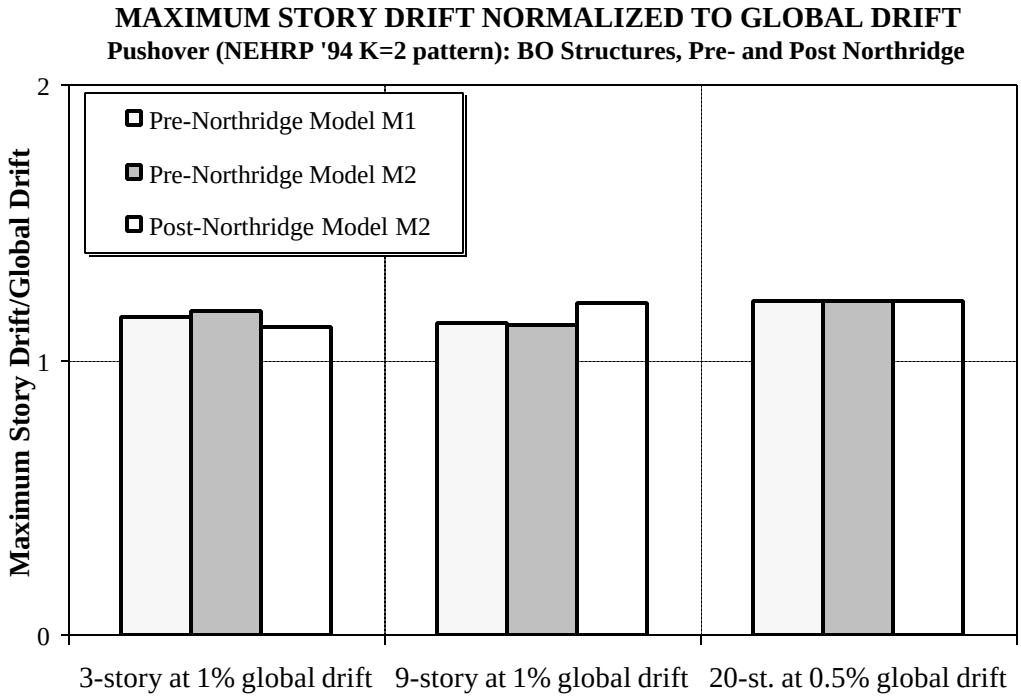

Figure 5.12 Ratio of Maximum Story Drift Angle to Roof Drift Angle at Particular Roof Drift Demand Levels for Boston Structures, Pushover Analysis

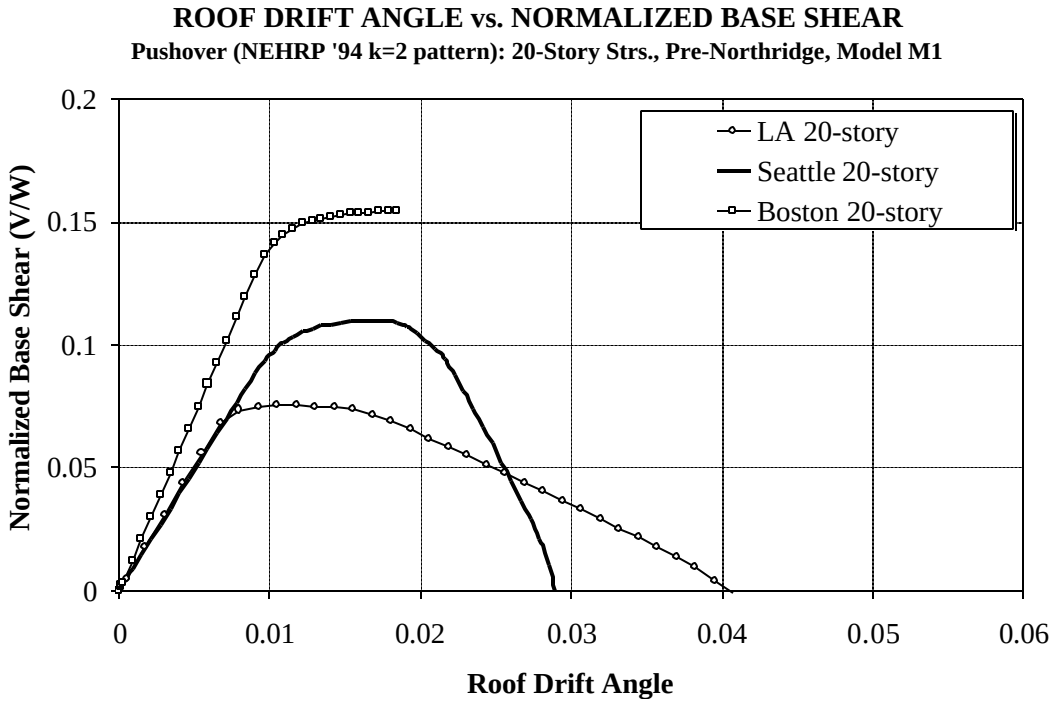

Figure 5.13 Global Pushover Curves for 20-story LA, Seattle, and Boston Structures; Model M1 (Centerline Model)

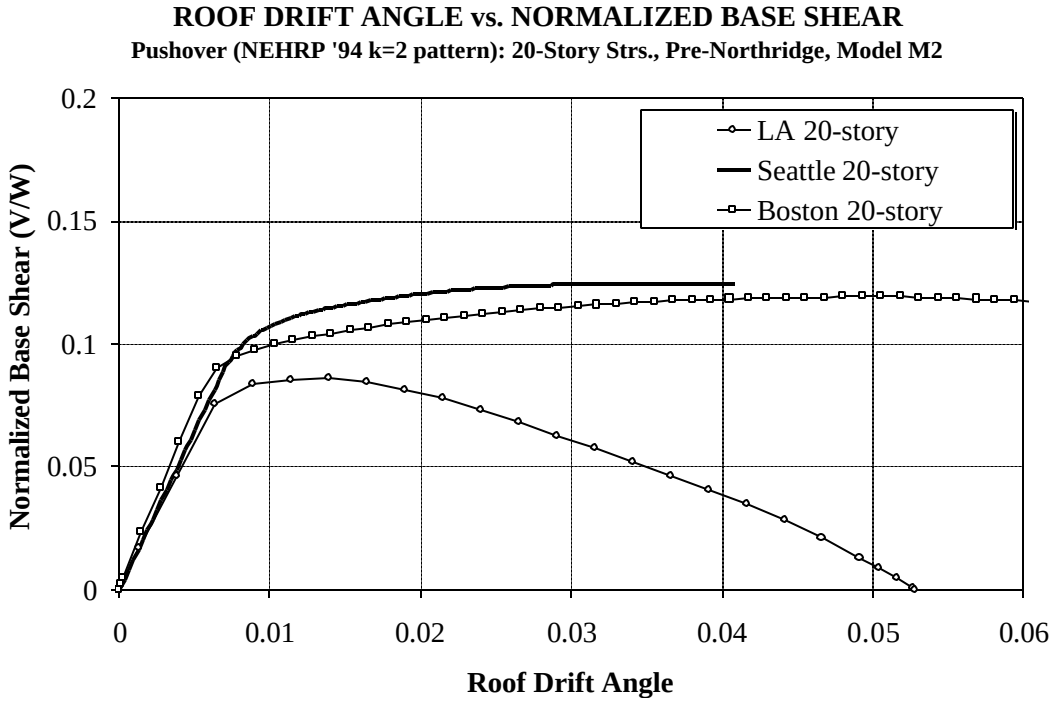

Figure 5.14 Global Pushover Curves for 20-story LA, Seattle, and Boston Structures; Model M2 (Clear Span Model with Panel Zones)

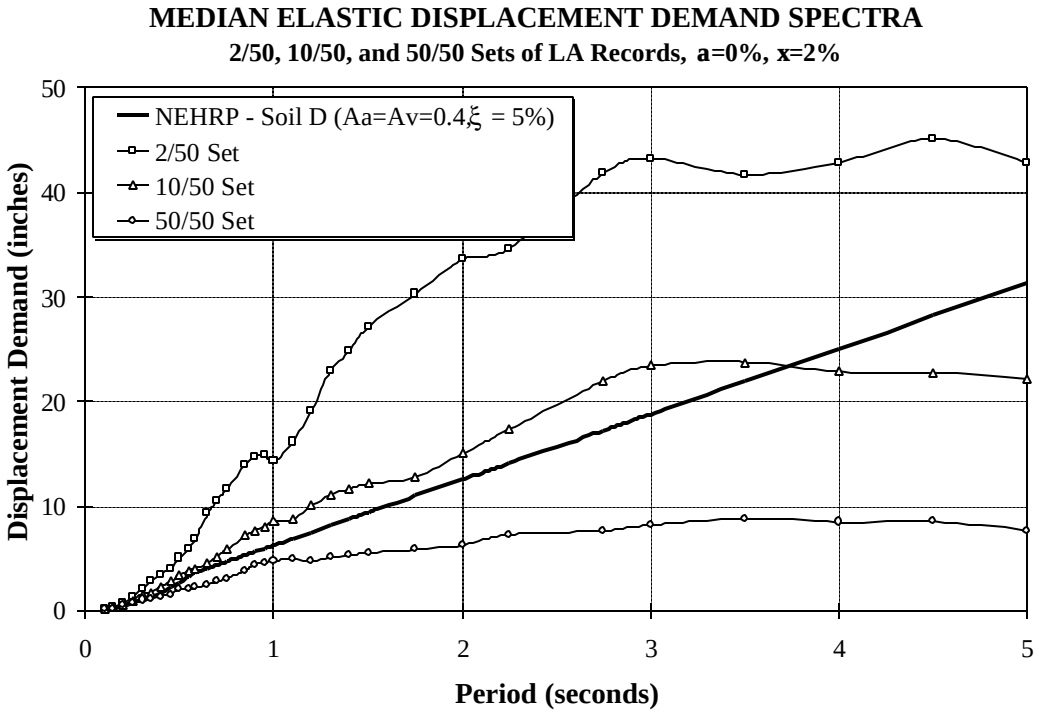

Figure 5.15 Median Values of Elastic Spectral Displacement Demands for LA 50/50, 10/50, and 2/50 Sets of Ground Motions

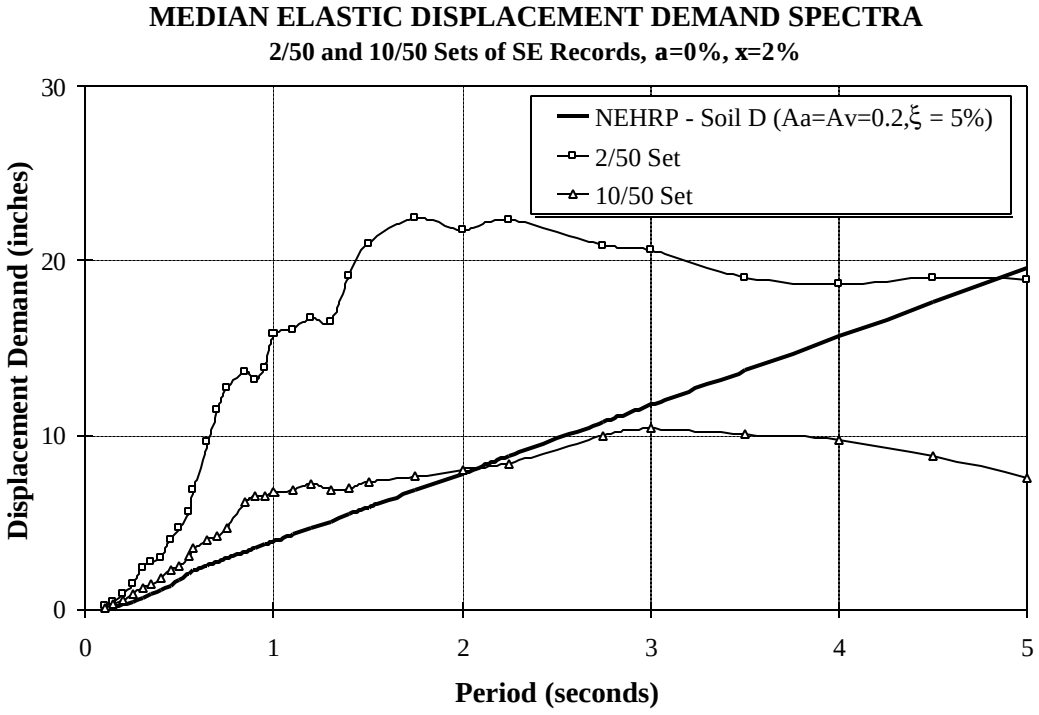

Figure 5.16 Median Values of Elastic Spectral Displacement Demands for Seattle 10/50 and 2/50 Sets of Ground Motions

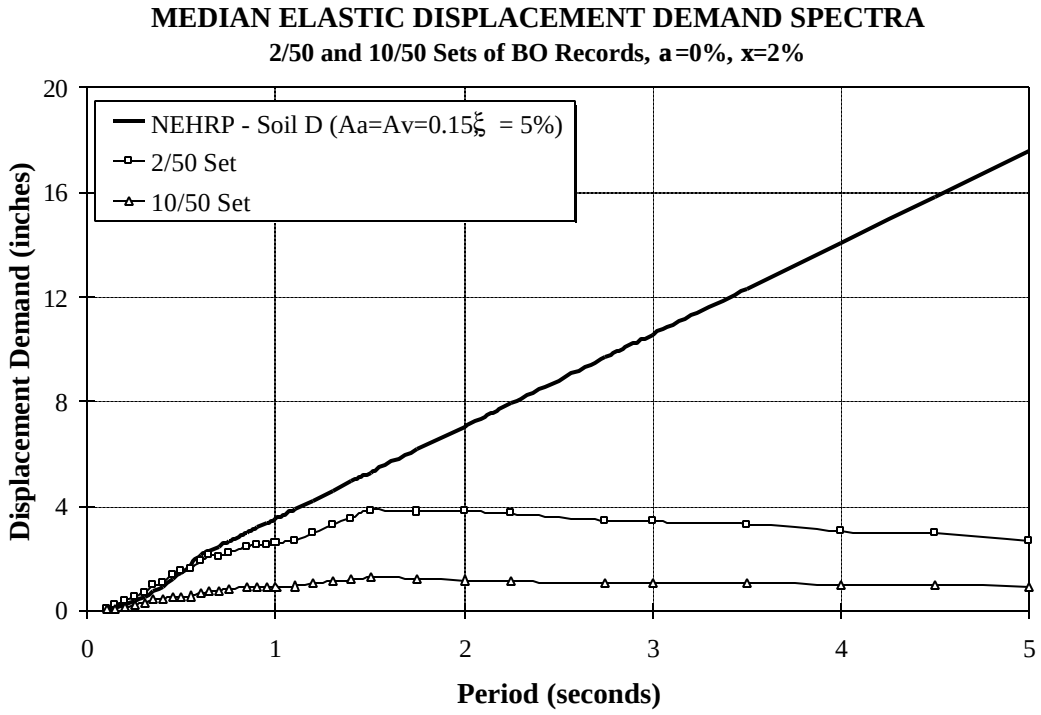

Figure 5.17 Median Values of Elastic Spectral Displacement Demands for Boston 10/50 and 2/50 Sets of Ground Motions

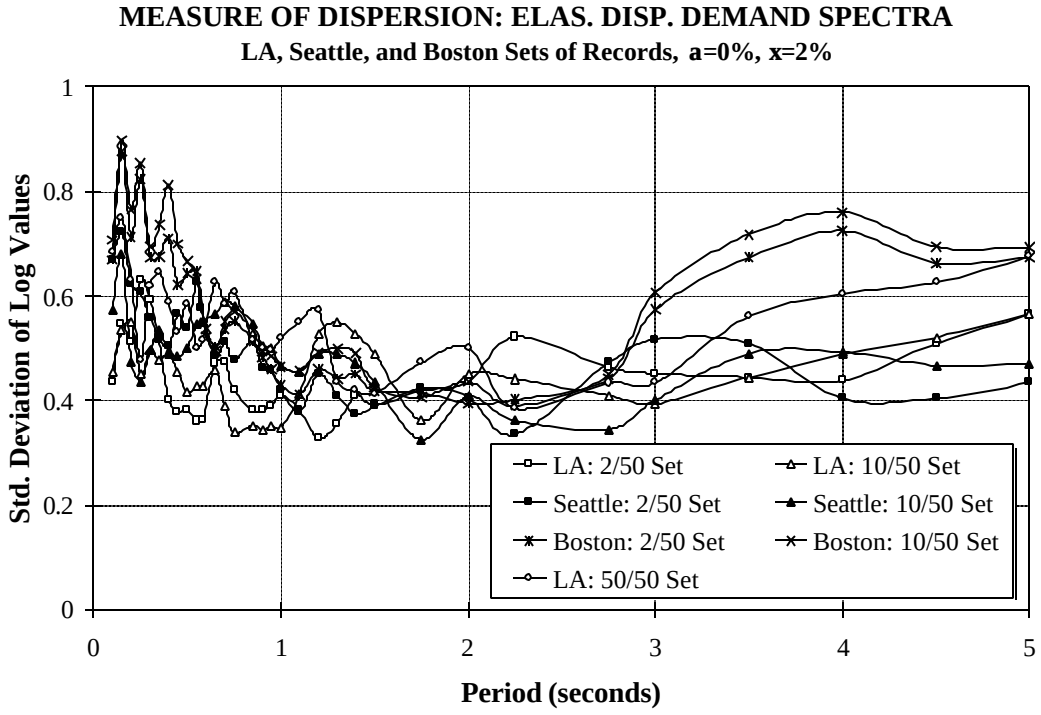

Figure 5.18 Measure of Dispersion of Elastic Spectral Displacement Demands for LA, Seattle , and Boston Sets of Ground Motions

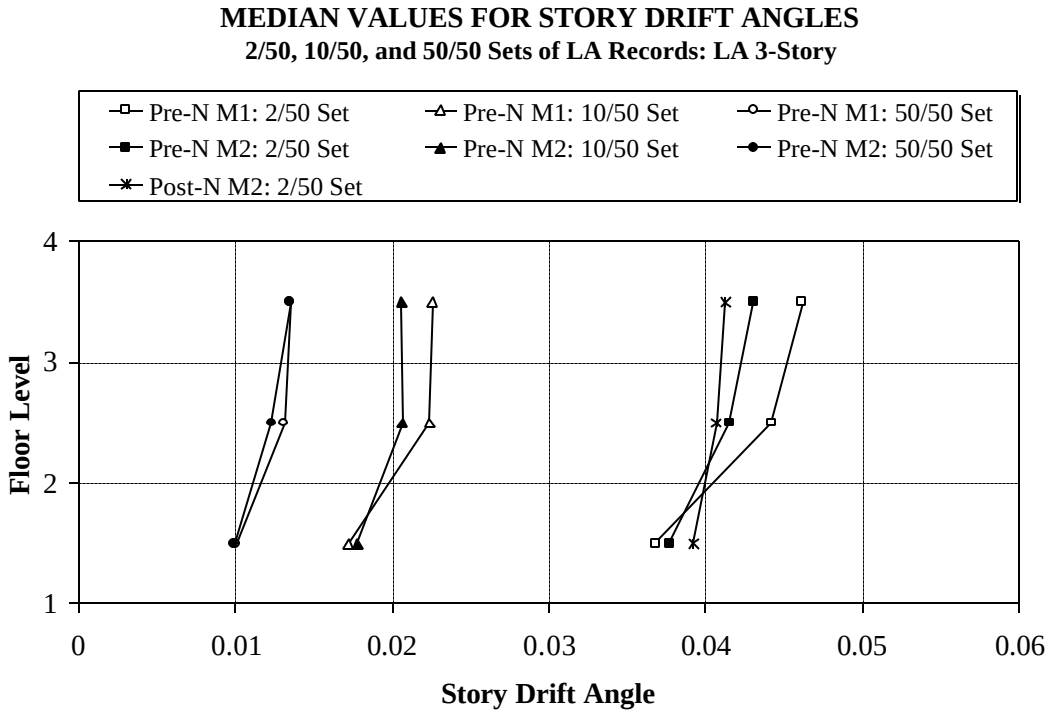

Figure 5.19 Median Values of Story Drift Angle Demands for LA 3-story Structures; 50/50, 10/50, and 2/50 Sets of Ground Motions

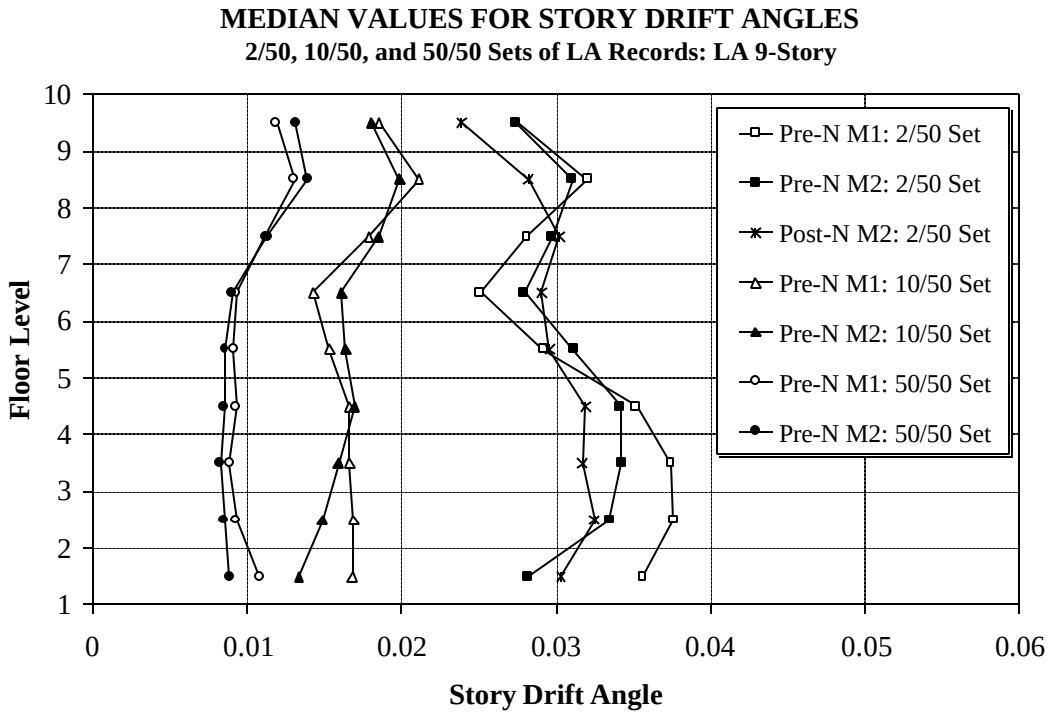

Figure 5.20 Median Values of Story Drift Angle Demands for LA 9-story Structures; 50/50, 10/50, and 2/50 Sets of Ground Motions

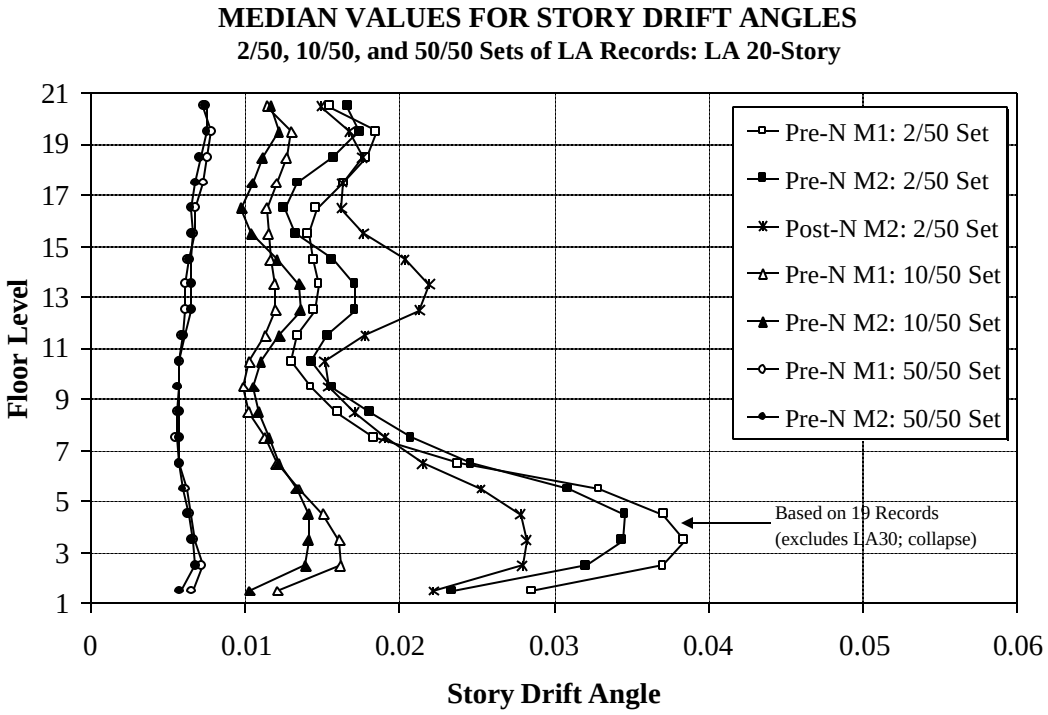

Figure 5.21 Median Values of Story Drift Angle Demands for LA 20-story Structures; 50/50, 10/50, and 2/50 Sets of Ground Motions

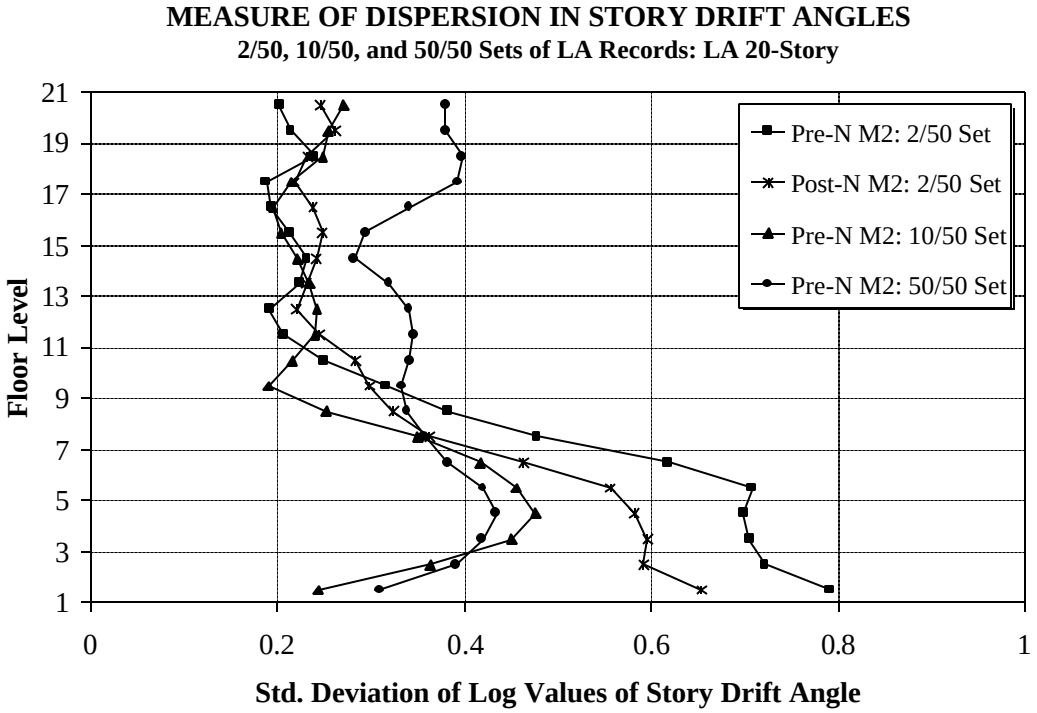

Figure 5.22 Measure of Dispersion of Story Drift Angle Demands for LA 20-story Structures; 50/50, 10/50, and 2/50 Sets of Ground Motions

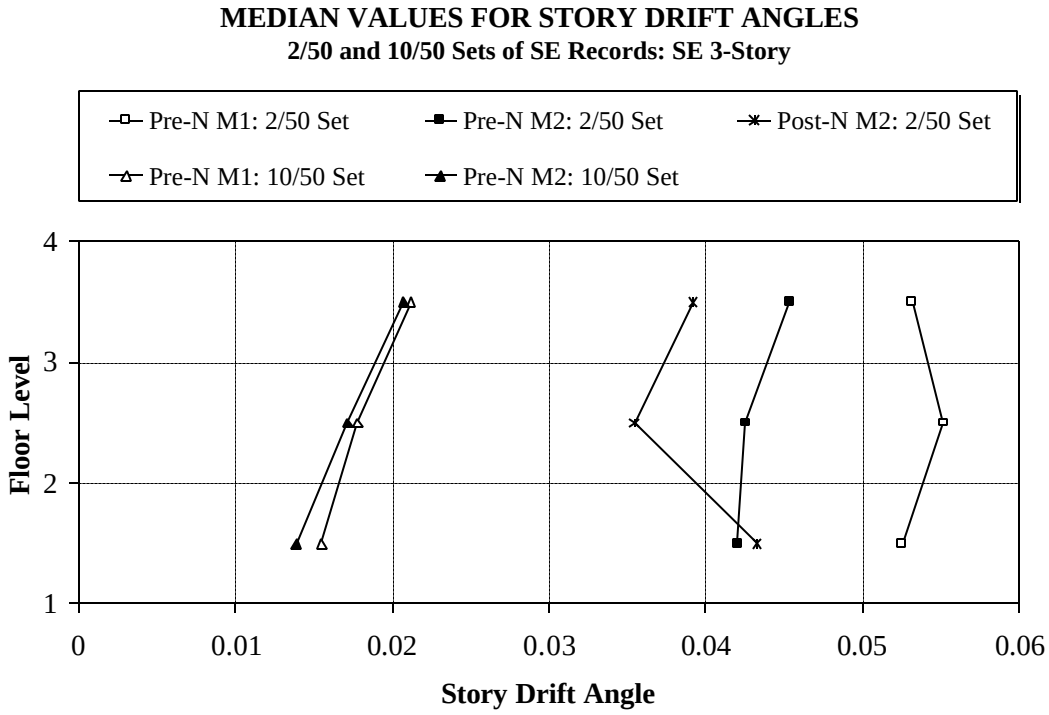

Figure 5.23 Median Values for Story Drift Angle Demands for Seattle 3-story Structures; 10/50 and 2/50 Sets of Ground Motions

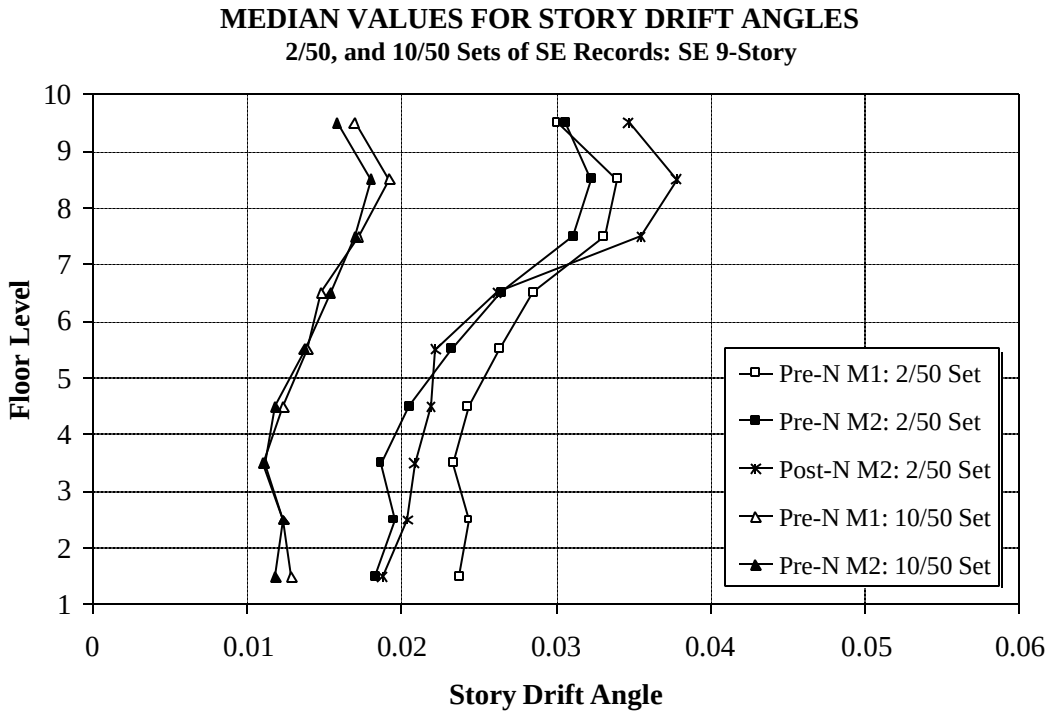

Figure 5.24 Median Values for Story Drift Angle Demands for Seattle 9-story Structures; 10/50 and 2/50 Sets of Ground Motions

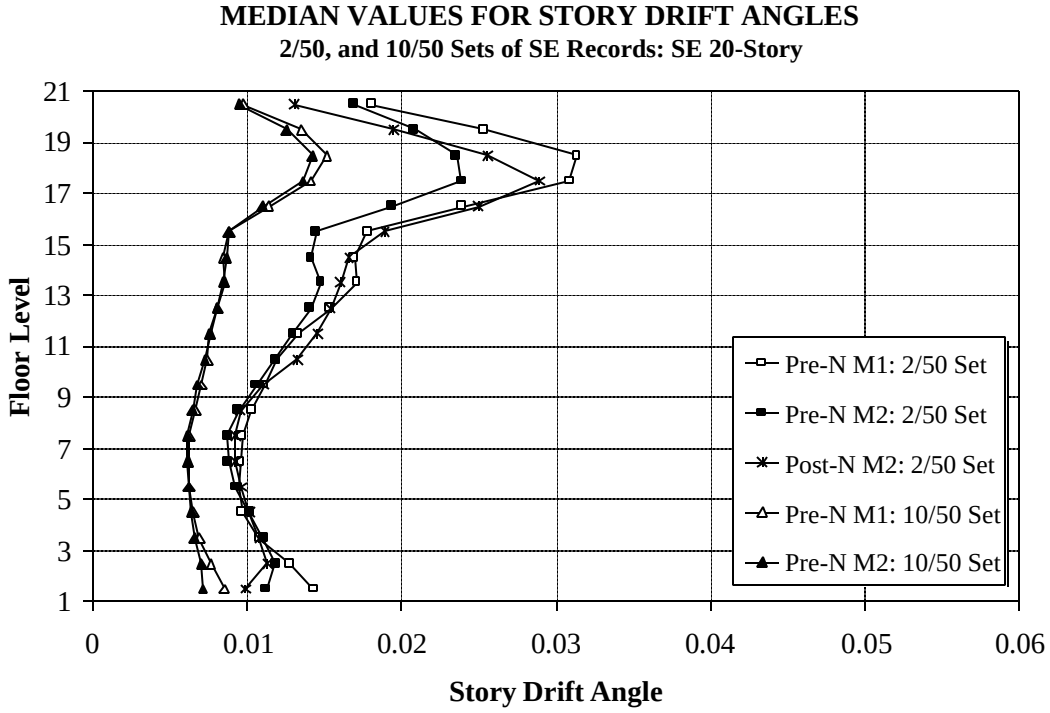

Figure 5.25 Median Values for Story Drift Angle Demands for Seattle 20-story Structures; 10/50 and 2/50 Sets of Ground Motions

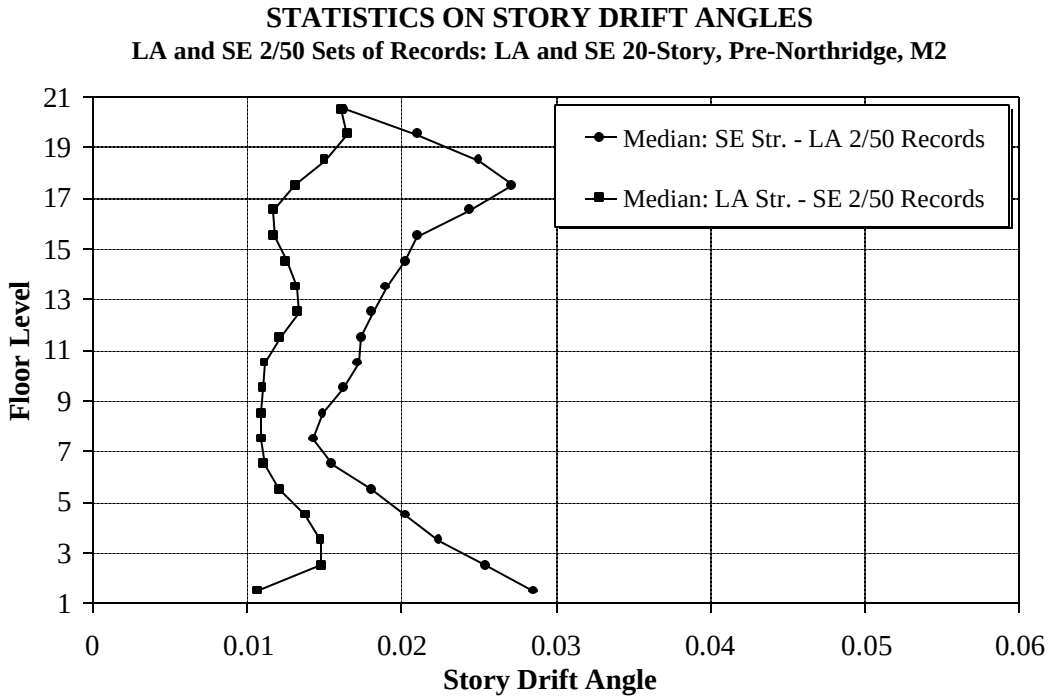

Figure 5.26 Median Values of Story Drift Angle Demands for 20-story LA Structure Subjected to SE Records and Vice Versa; 2/50 Sets of Ground Motions

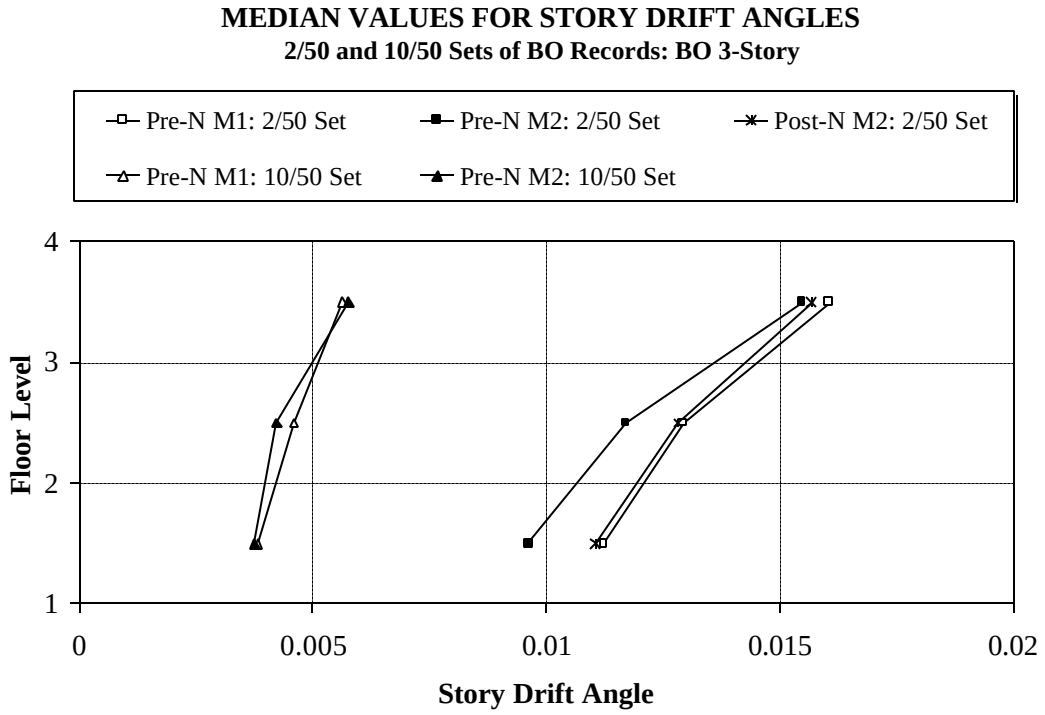

Figure 5.27 Median Values of Story Drift Angle Demands for Boston 3-story Structures; 10/50 and 2/50 Sets of Ground Motions

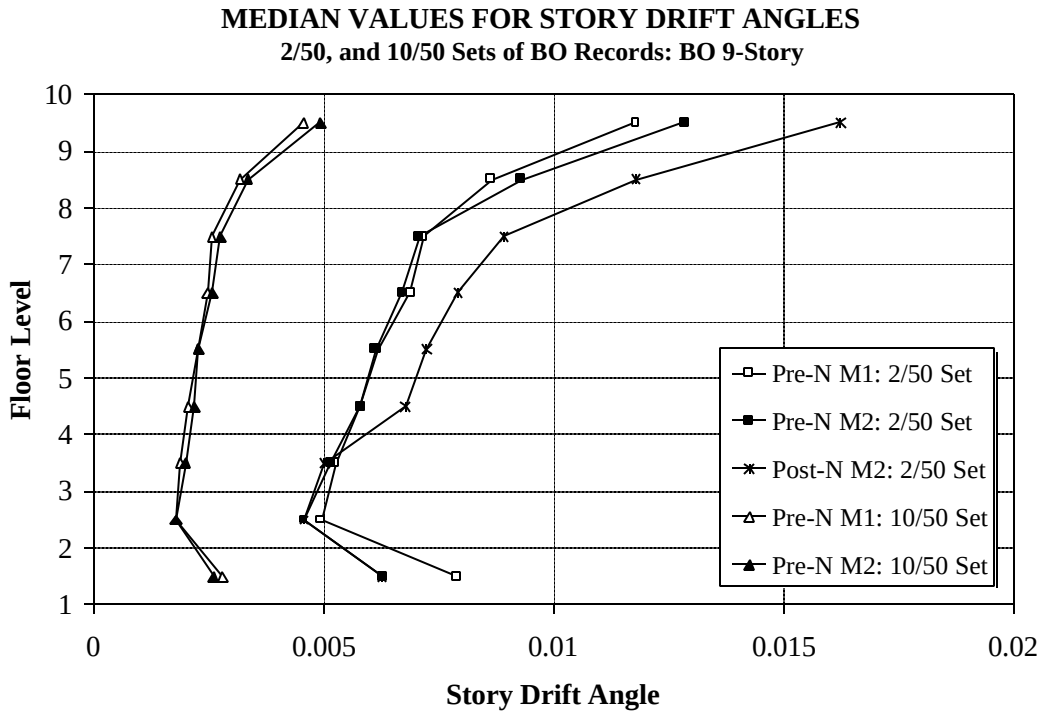

Figure 5.28 Median Values of Story Drift Angle Demands for Boston 9-story Structures; 10/50 and 2/50 Sets of Ground Motions

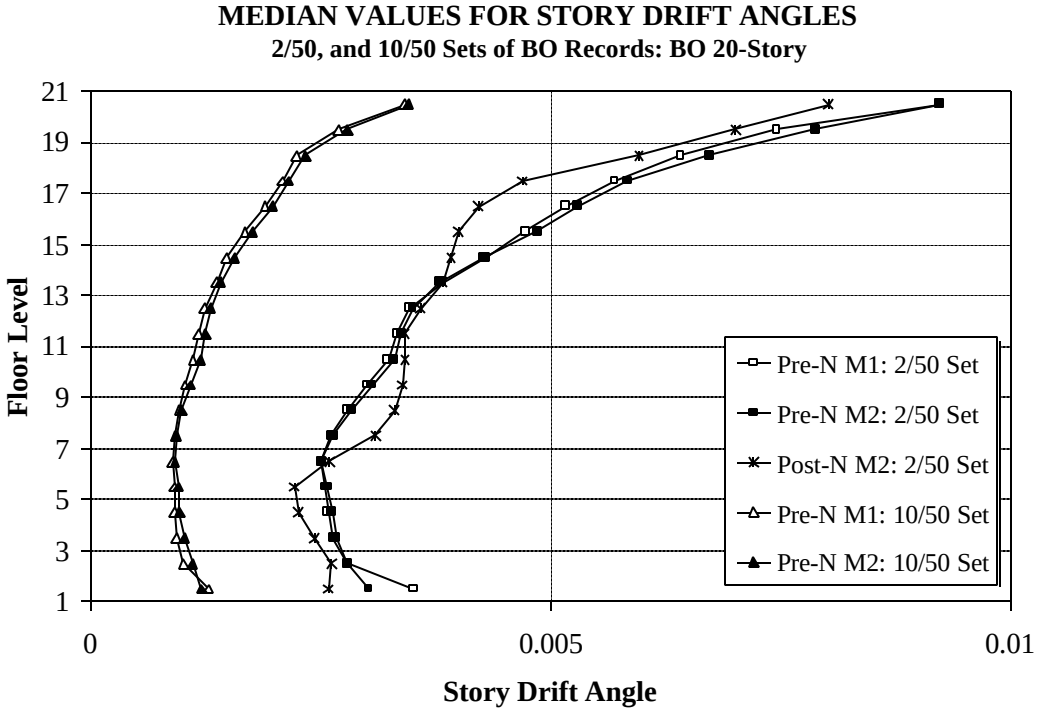

Figure 5.29 Median Values of Story Drift Angle Demands for Boston 20-story Structures; 10/50 and 2/50 Sets of Ground Motions

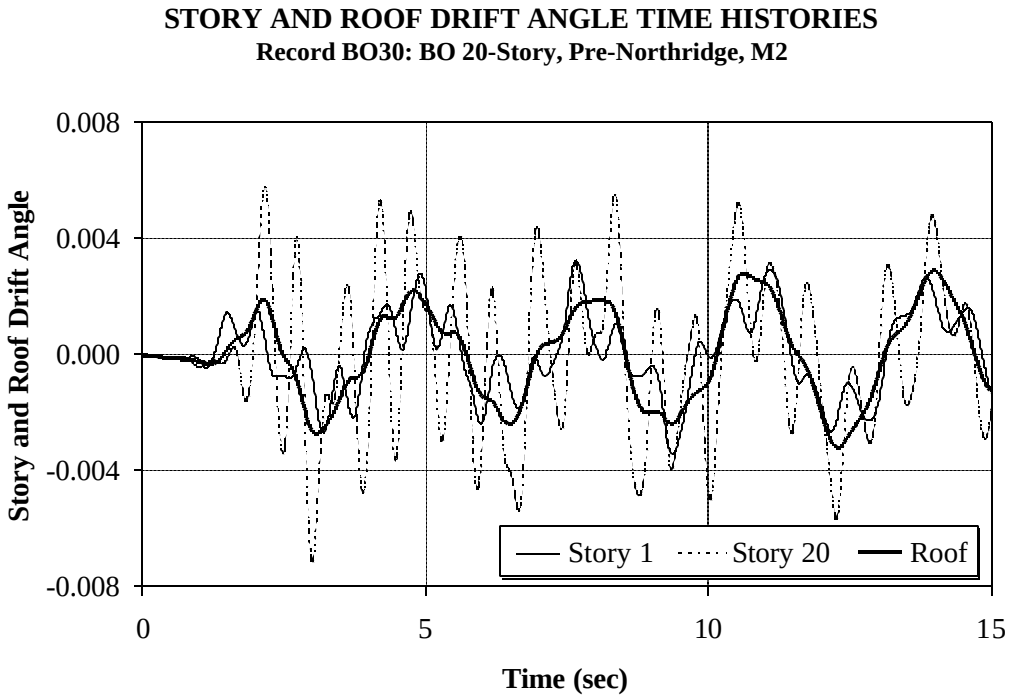

Figure 5.30 Displacement Time Histories for Boston 20-story pre-Northridge Structure; BO30 Record, Showing Presence of Significant Higher Mode Effects

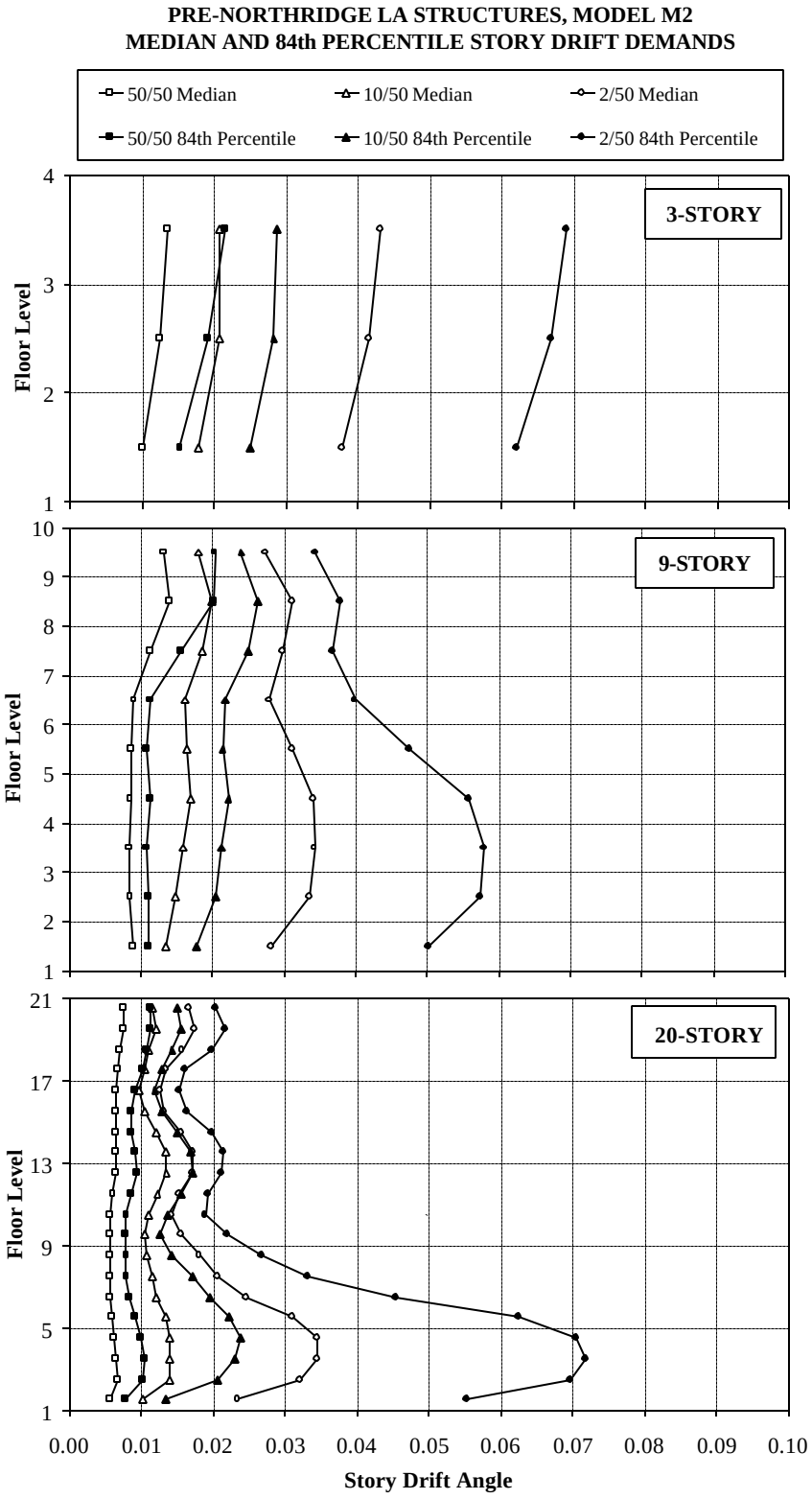

Figure 5.31 Median and 84th Percentile Story Drift Angle Demands for LA Structures, Model M2; 50/50, 10/50, and 2/50 Sets of Ground Motions

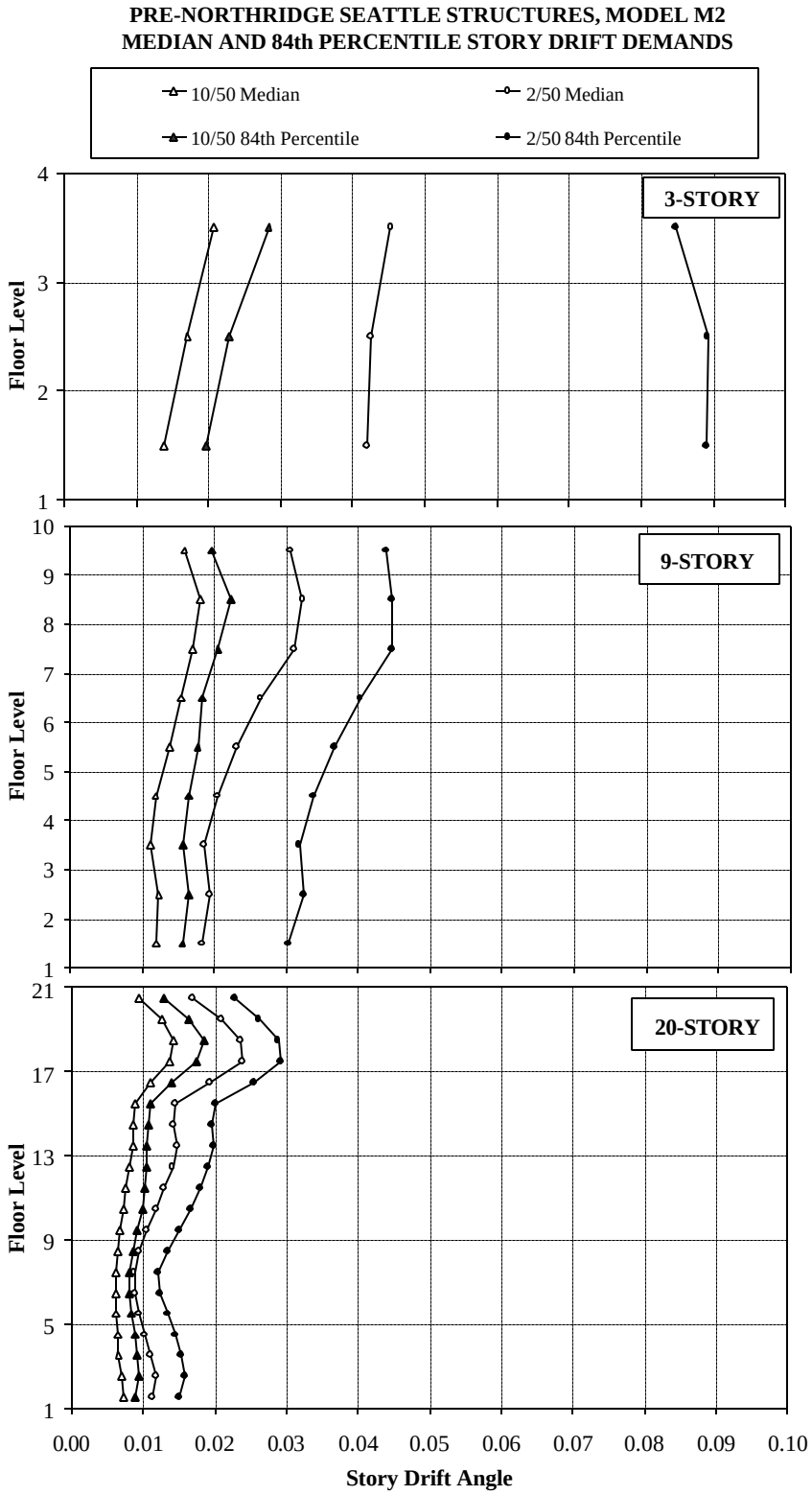

Figure 5.32 Median and 84th Percentile Story Drift Angle Demands for Seattle Structures, Model M2; 10/50 and 2/50 Sets of Ground Motions

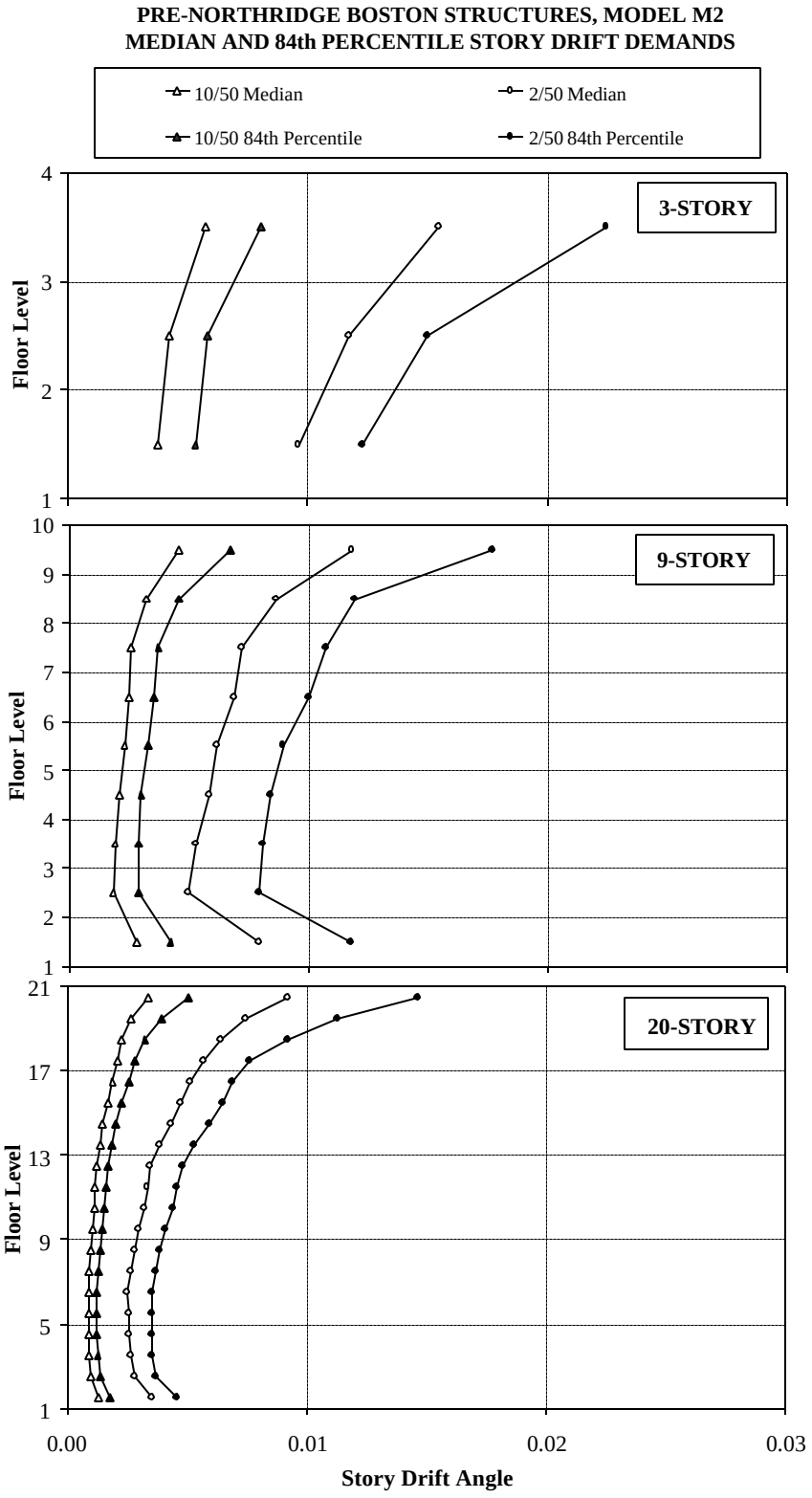

Figure 5.33 Median and 84th Percentile Story Drift Angle Demands for Boston Structures, Model M2; 10/50 and 2/50 Sets of Ground Motions

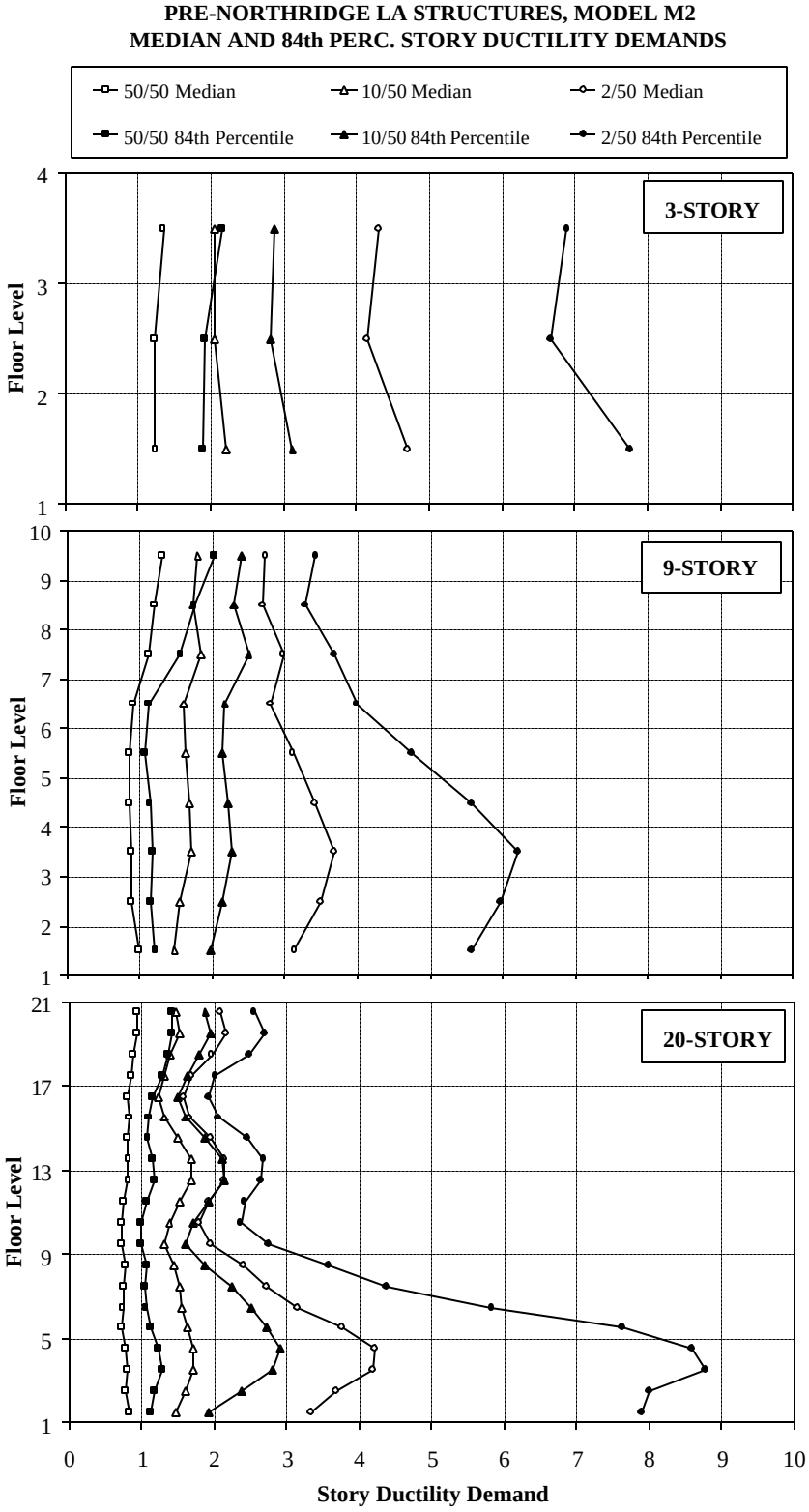

Figure 5.34 Median and 84th Percentile Story Ductility Demands for LA Structures, Model M2; 50/50, 10/50, and 2/50 Sets of Ground Motions

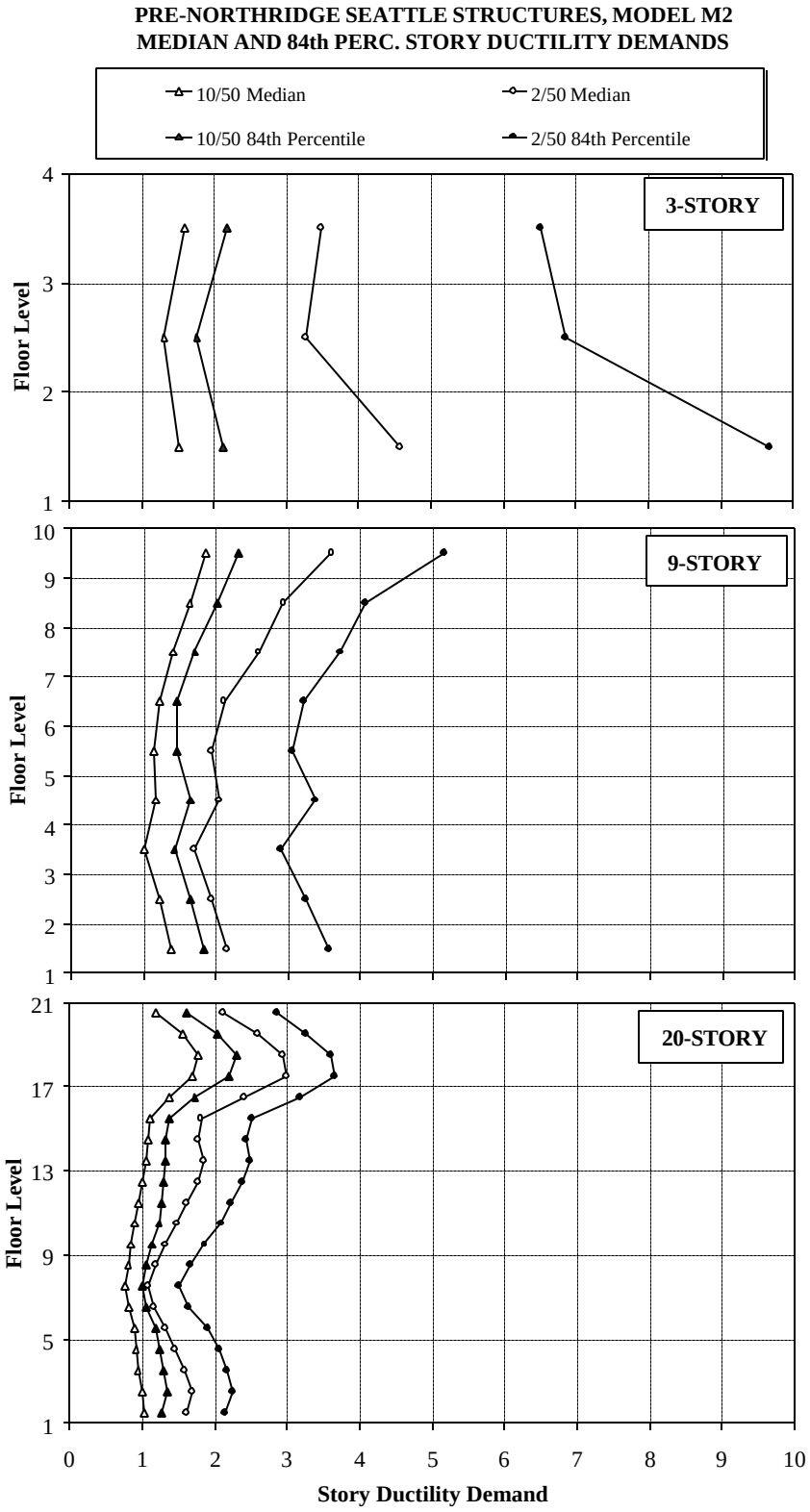

Figure 5.35 Median and 84th Percentile Story Ductility Demands for Seattle Structures, Model M2; 10/50 and 2/50 Sets of Ground Motions

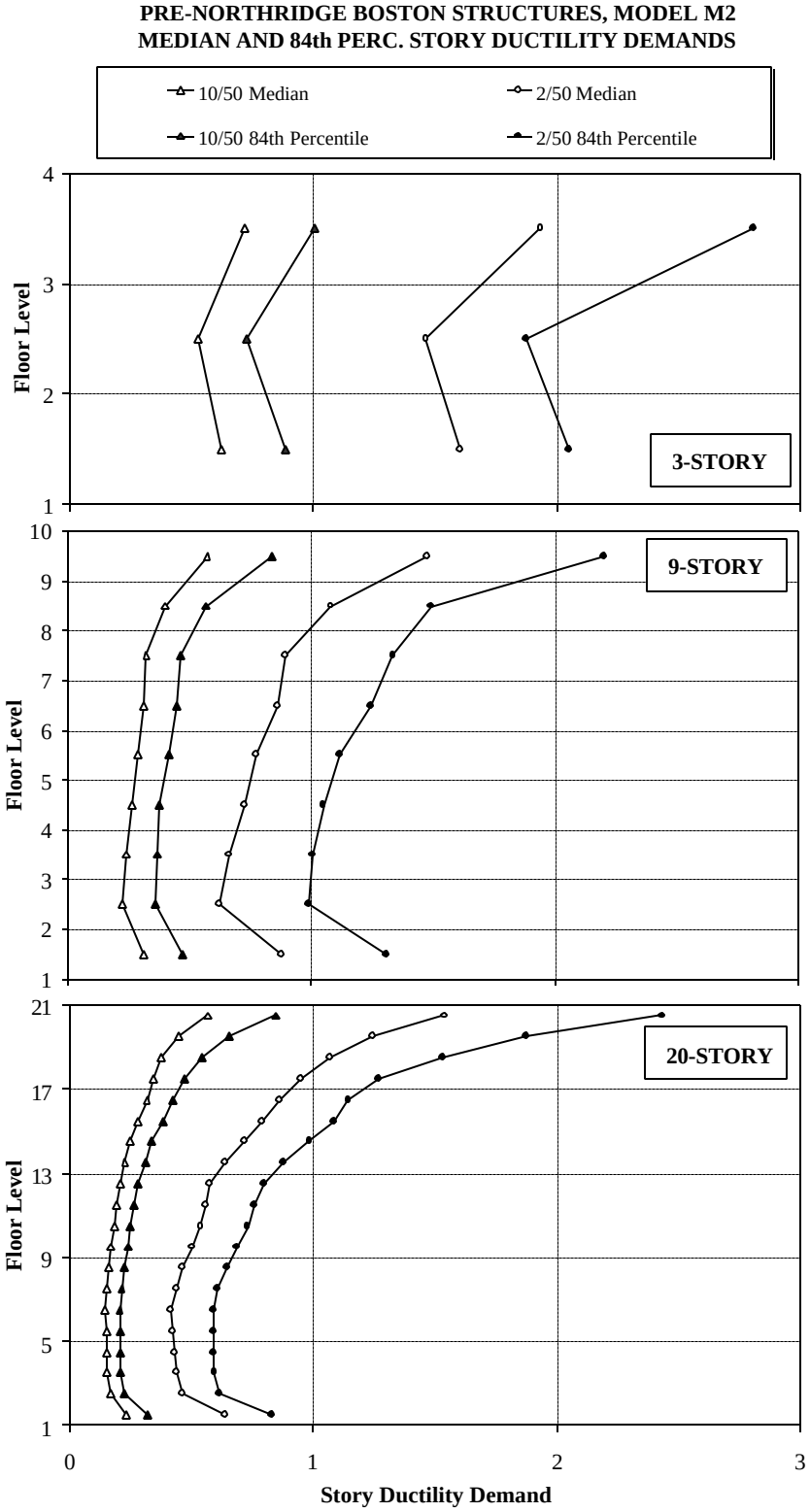

Figure 5.36 Median and 84th Percentile Story Ductility Demands for Boston Structures, Model M2; 10/50 and 2/50 Sets of Ground Motions

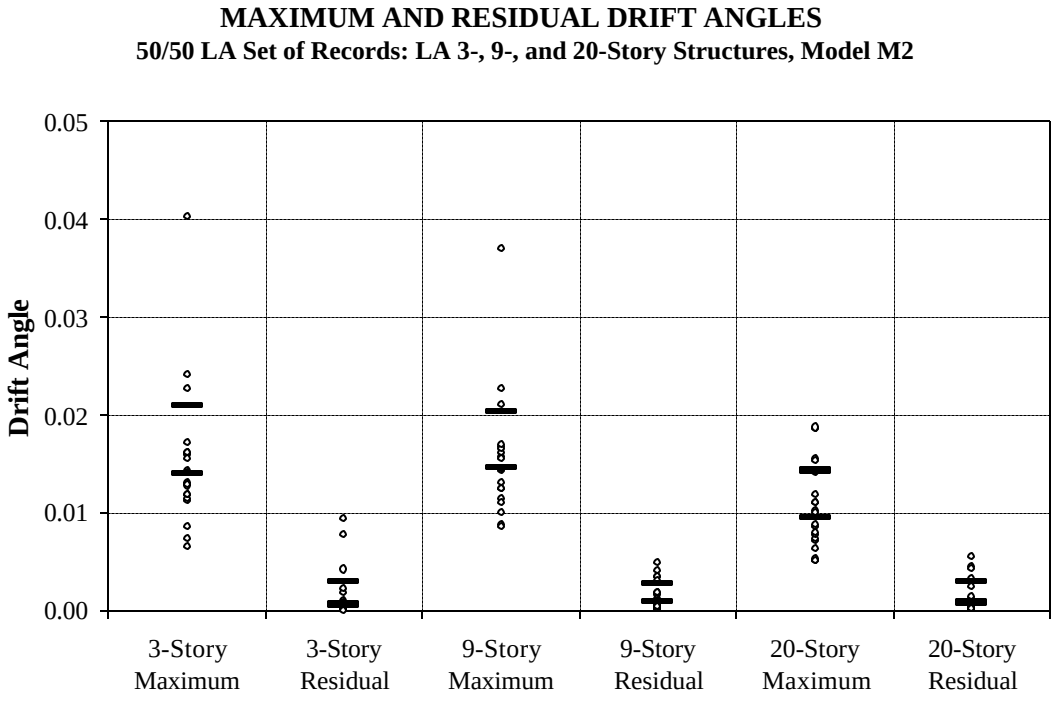

Figure 5.37 Maximum and Residual Story Drift Angle Demands for LA Structures; 50/50 Set of Ground Motions

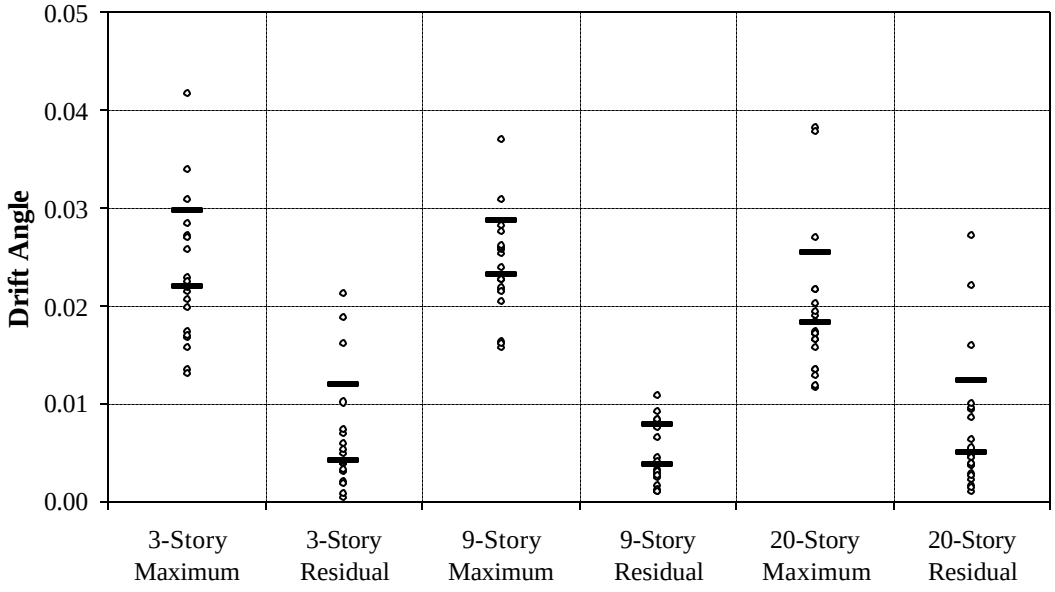

Figure 5.38 Maximum and Residual Story Drift Angle Demands for LA Structures; 10/50 Set of Ground Motions

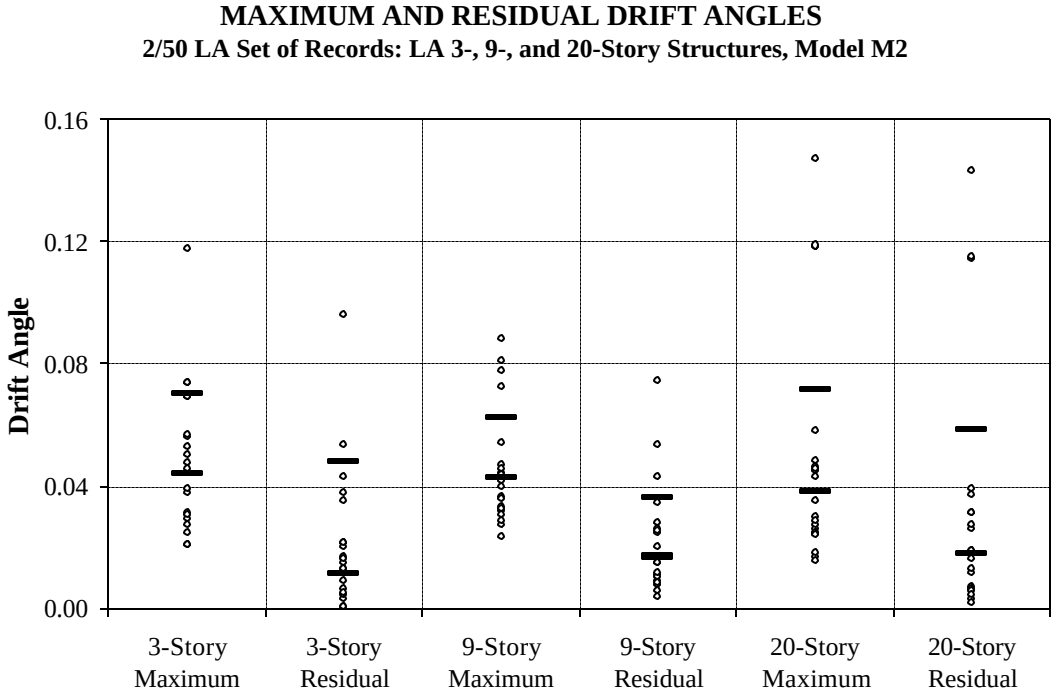

Figure 5.39 Maximum and Residual Story Drift Angle Demands for LA Structures; 2/50 Set of Ground Motions

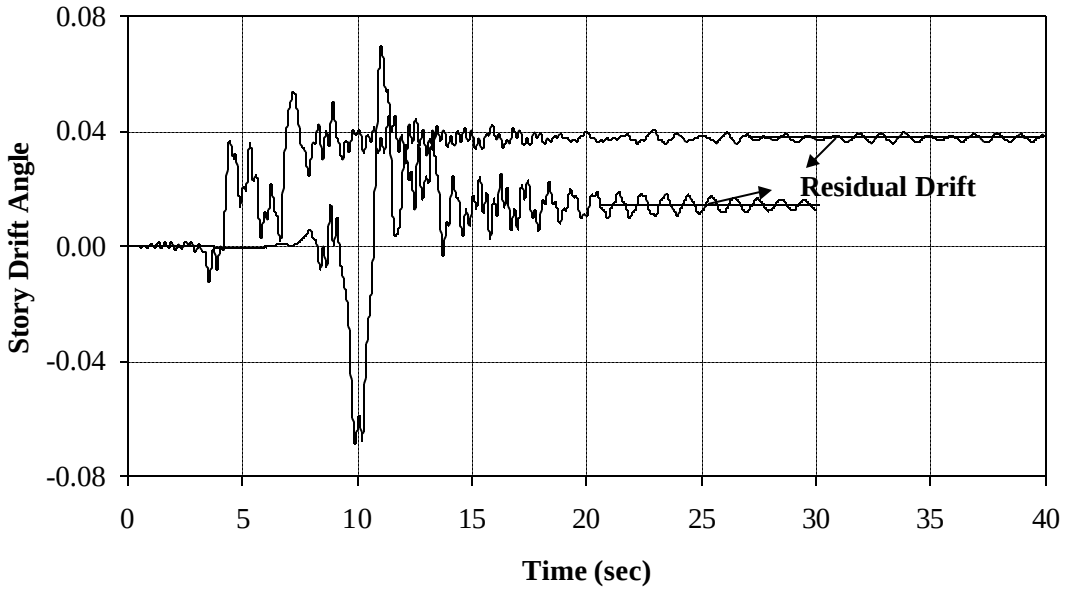

Figure 5.40 Comparison of Residual Story Drift Angle Demands for LA 3-story Structure Under Two Records From 2/50 Set of Ground Motions

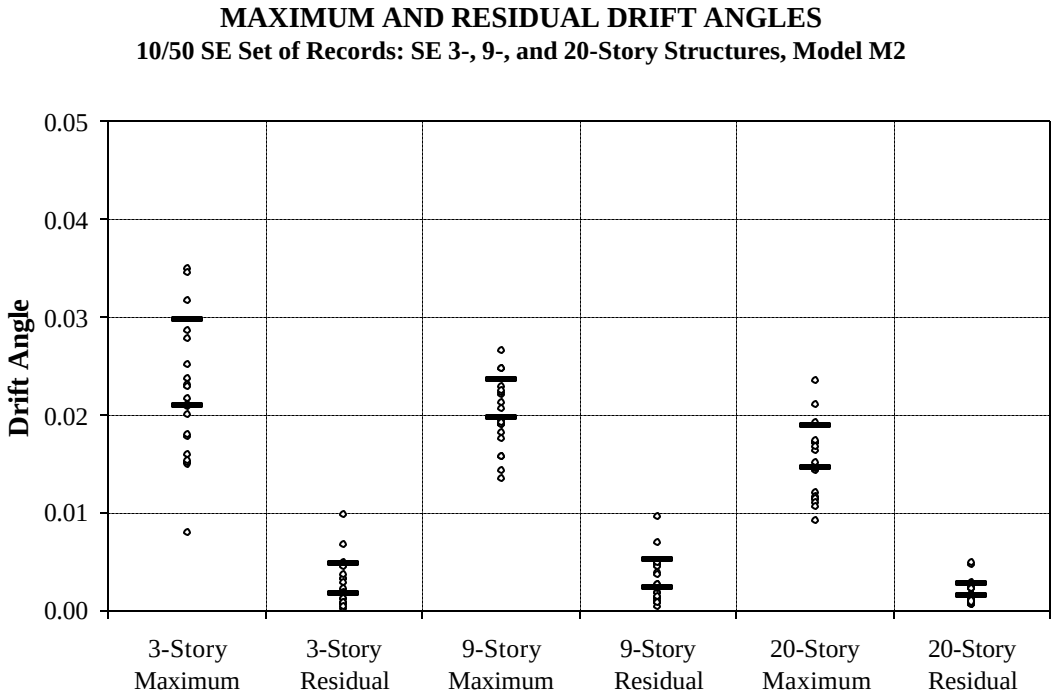

Figure 5.41 Maximum and Residual Story Drift Angle Demands for Seattle Structures; 10/50 Set of Ground Motions

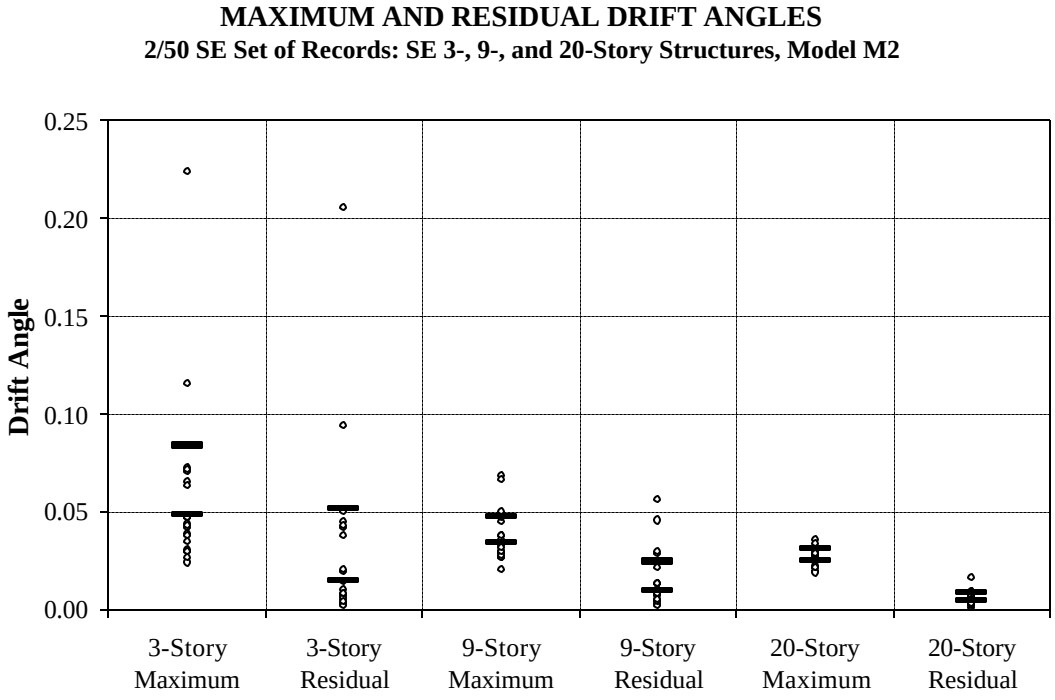

Figure 5.42 Maximum and Residual Story Drift Angle Demands for Seattle Structures; 2/50 Set of Ground Motions

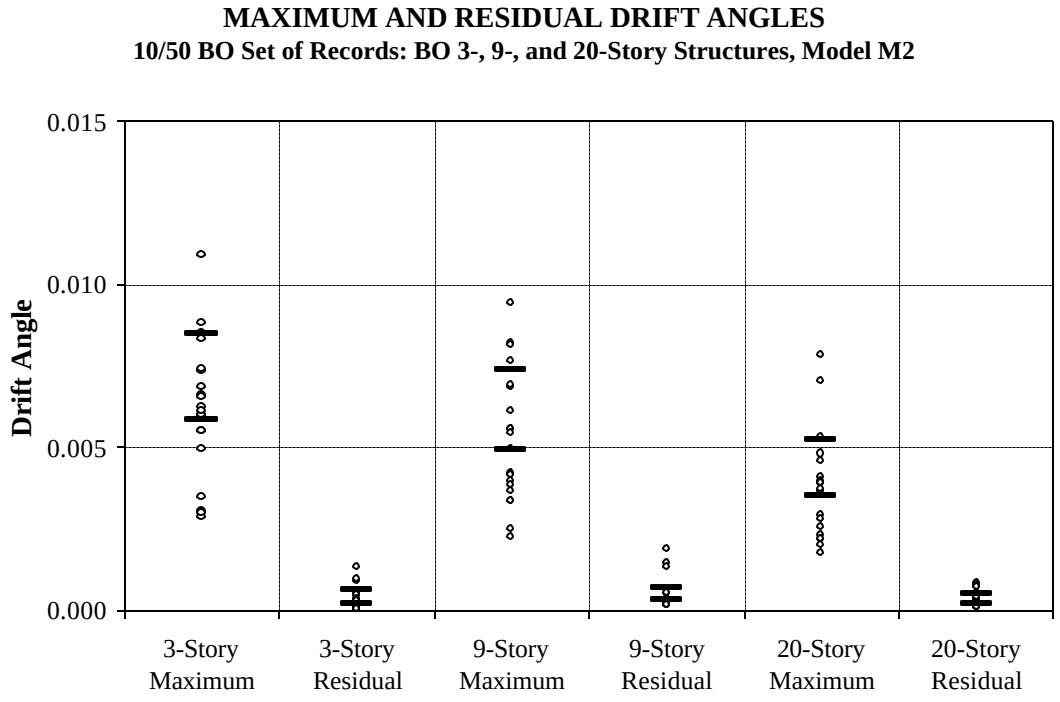

Figure 5.43 Maximum and Residual Story Drift Angle Demands for Boston Structures; 10/50 Set of Ground Motions

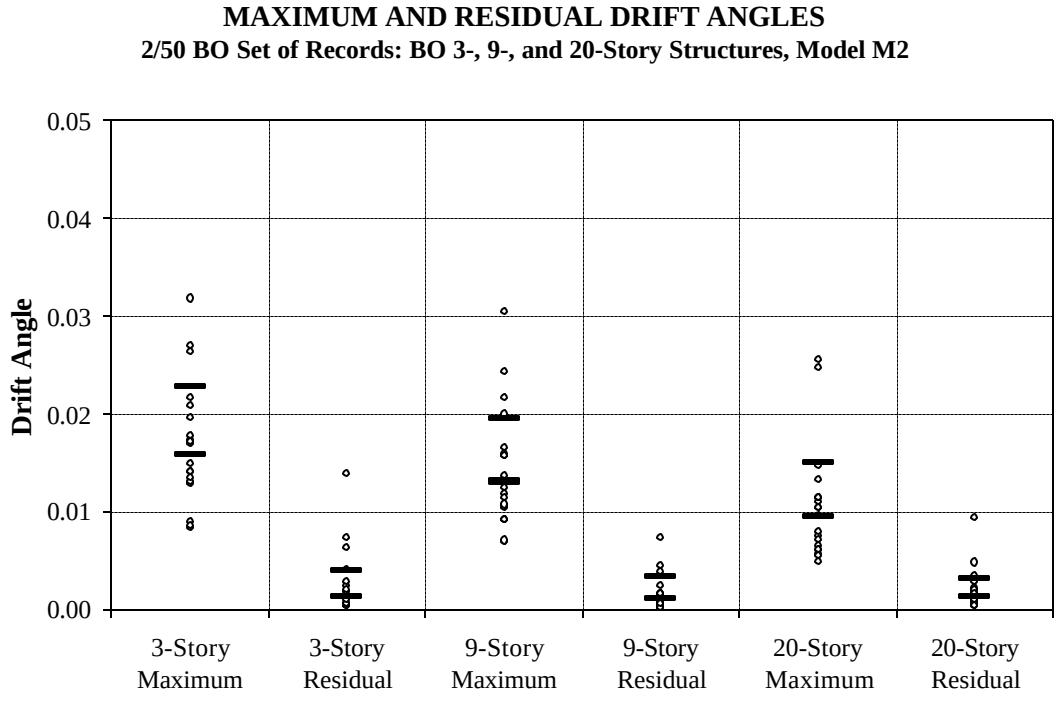

Figure 5.44 Maximum and Residual Story Drift Angle Demands for Boston Structures; 2/50 Set of Ground Motions

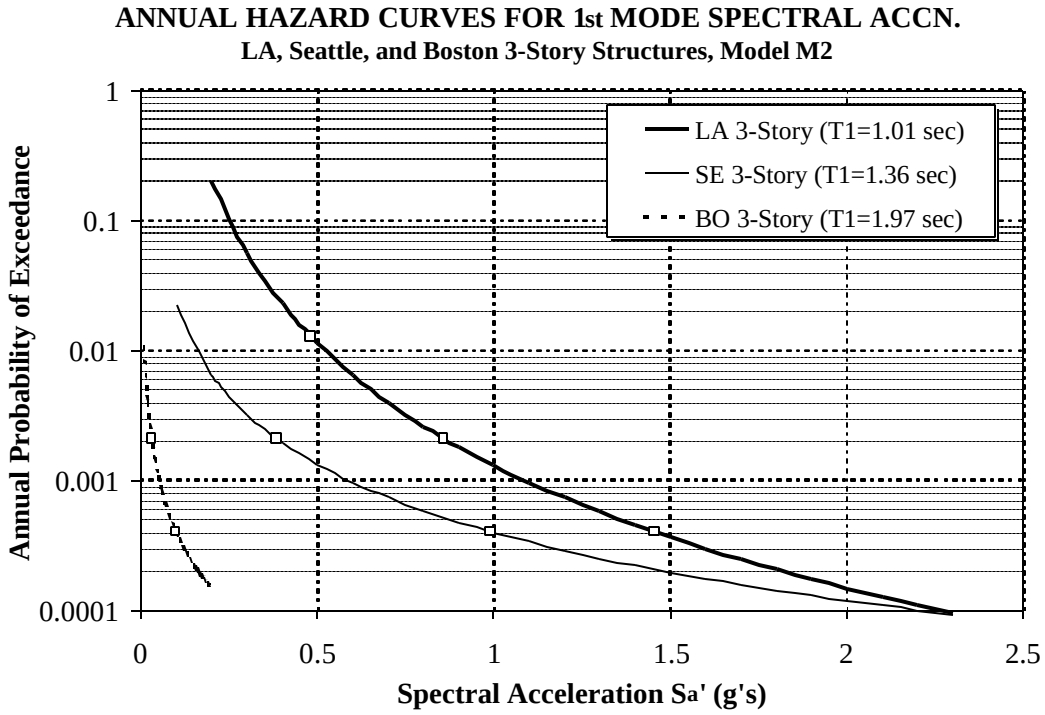

Figure 5.45 Annual Hazard Curves for 1st Mode Spectral Acceleration for LA, Seattle, and Boston 3-story Structures

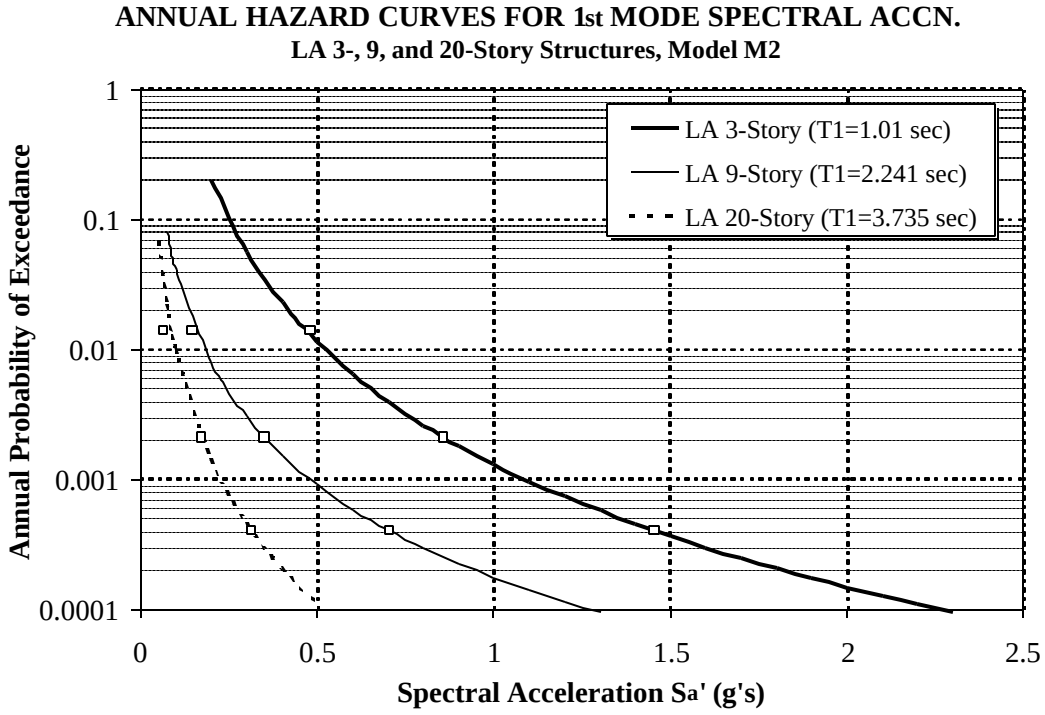

Figure 5.46 Annual Hazard Curves for 1st Mode Spectral Acceleration for LA 3-, 9-, and 20-story Structures

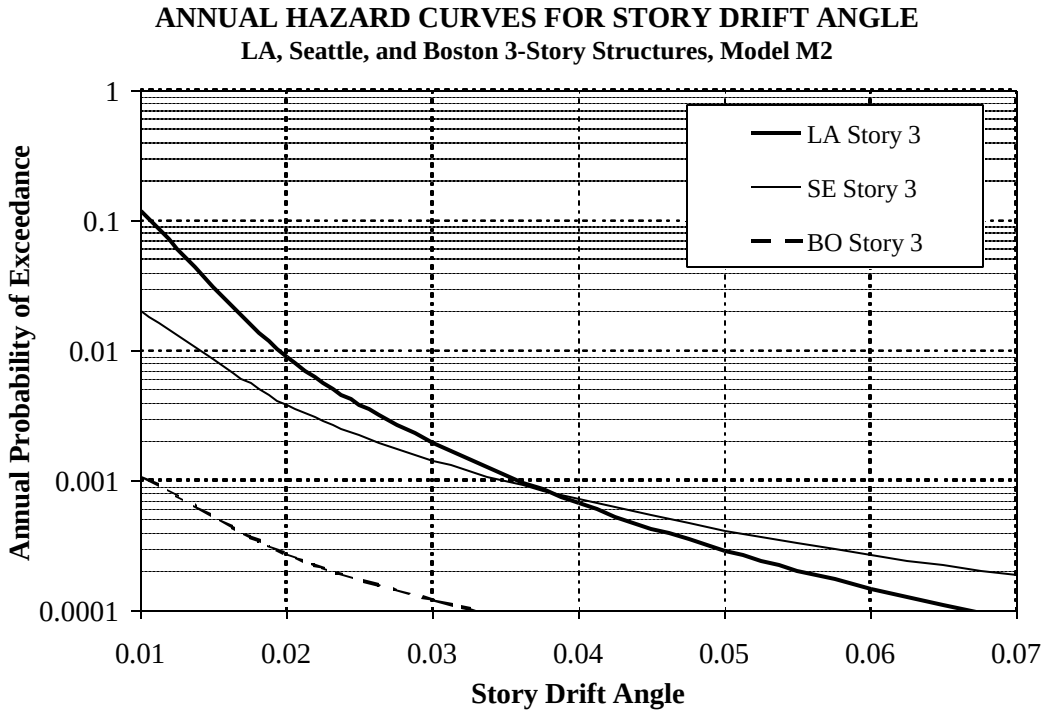

Figure 5.47 Annual Hazard Curves for Story 3 Drift Angle Demand for LA, Seattle, and Boston 3-story Structures

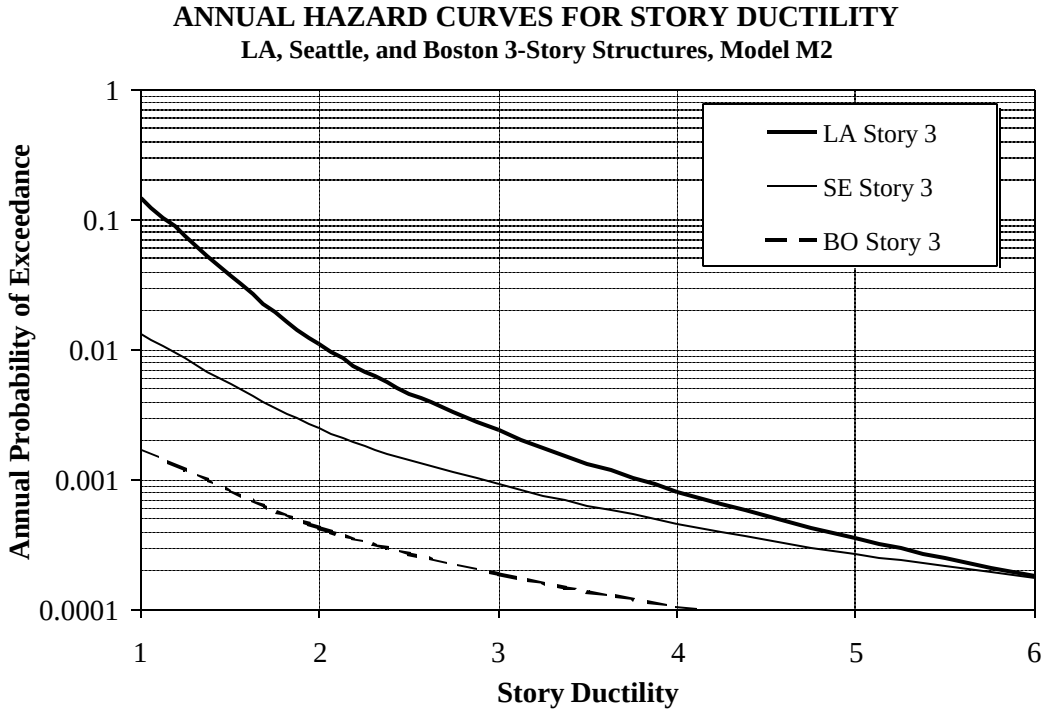

Figure 5.48 Annual Hazard Curves for Story 3 Ductility Demand for LA, Seattle, and Boston 3-story Structures

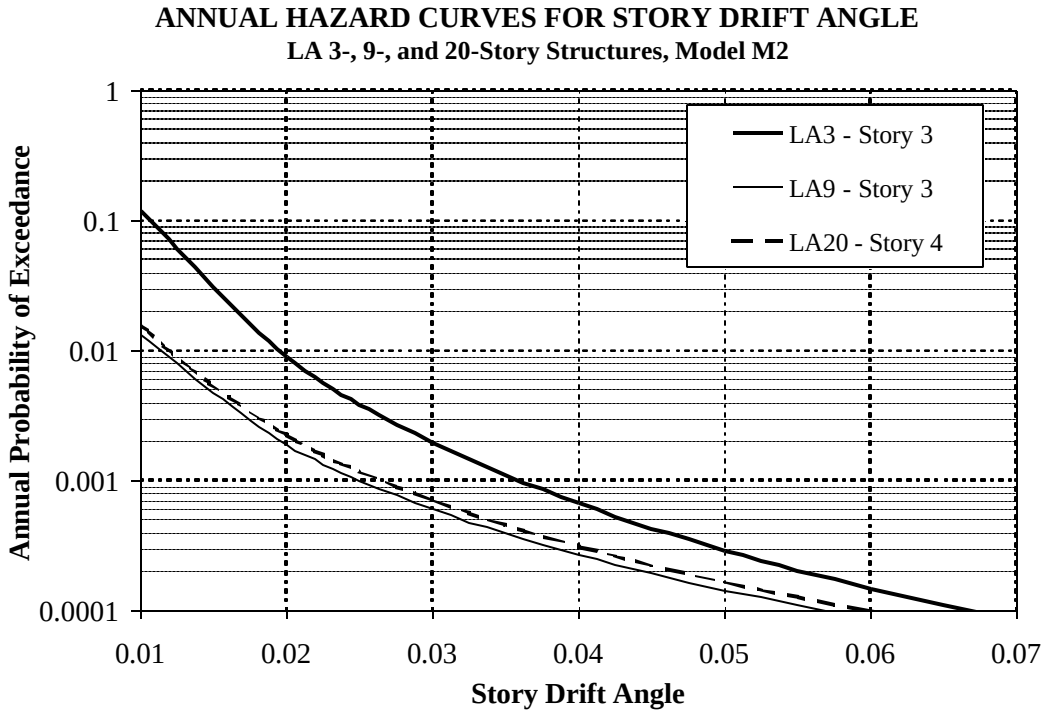

Figure 5.49 Annual Hazard Curves for Story Drift Angle Demand for LA 3-, 9-, and 20-story Structures

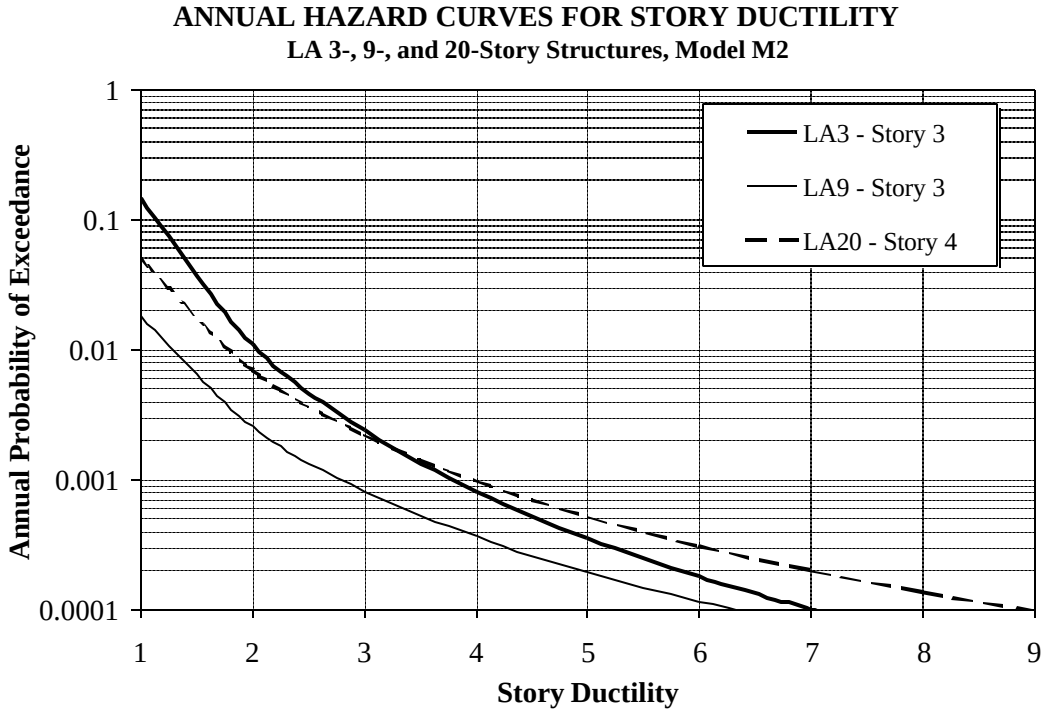

Figure 5.50 Annual Hazard Curves for Story Ductility Demand for LA 3-, 9-, and 20-story Structures

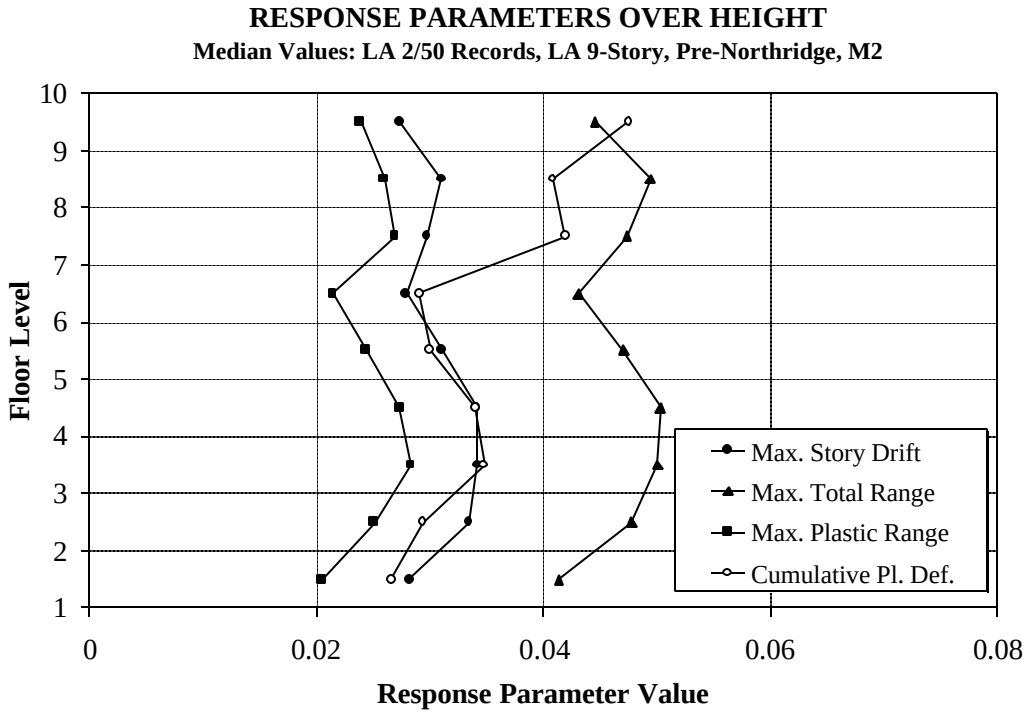

Figure 5.51 Median Values of Maximum and Cumulative Response Parameters for LA 9-story Structure; 2/50 Set of Ground Motions

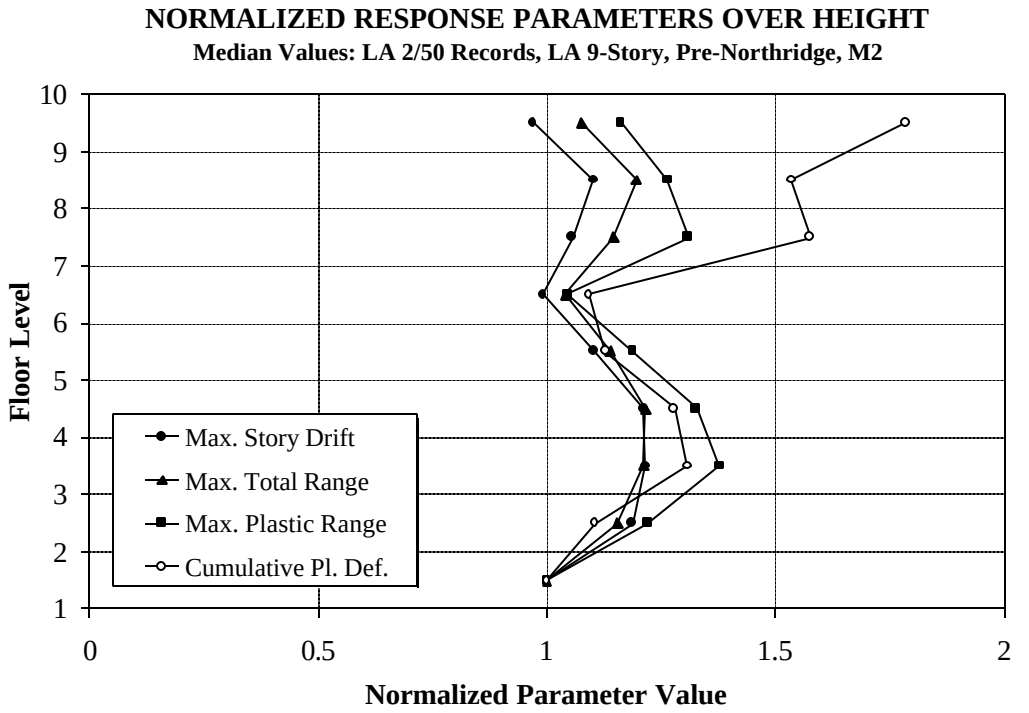

Figure 5.52 Median Values of Normalized Maximum and Cumulative Response Parameters for LA 9-story Structure; 2/50 Set of Ground Motions

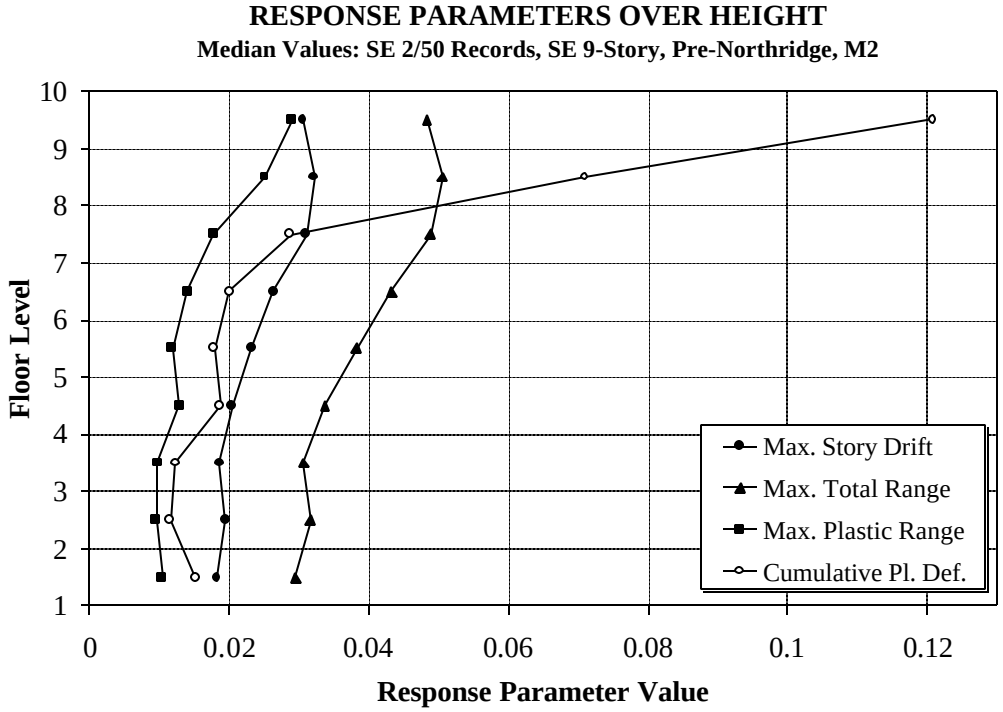

Figure 5.53 Median Values of Maximum and Cumulative Response Parameters for Seattle 9-story Structure; 2/50 Set of Ground Motions

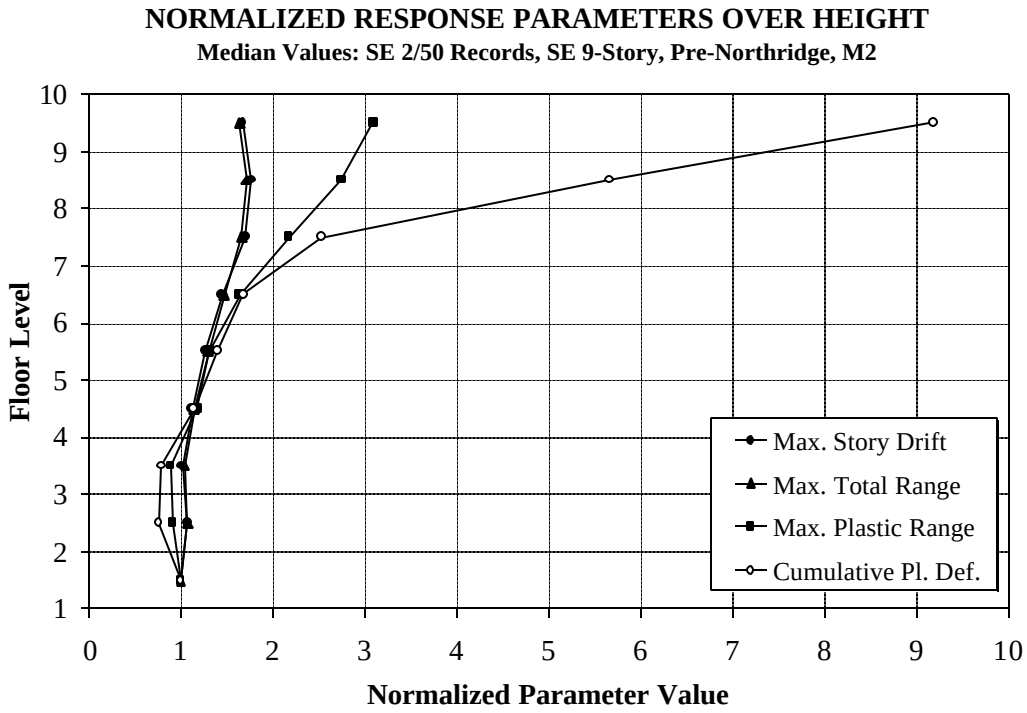

Figure 5.54 Median Values of Normalized Maximum and Cumulative Response Parameters for Seattle 9-story Structure; 2/50 Set of Ground Motions

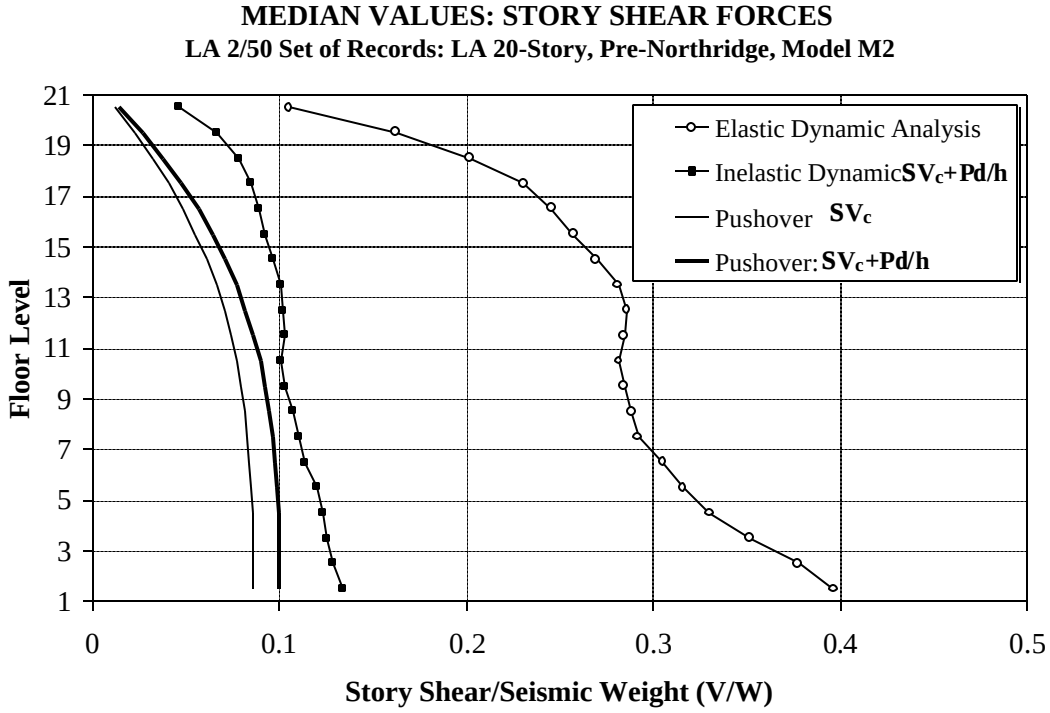

Figure 5.55 Median Values of Base and Story Shear Forces for LA 20-story Structure; 2/50 Set of Ground Motions, and from Pushover Analysis

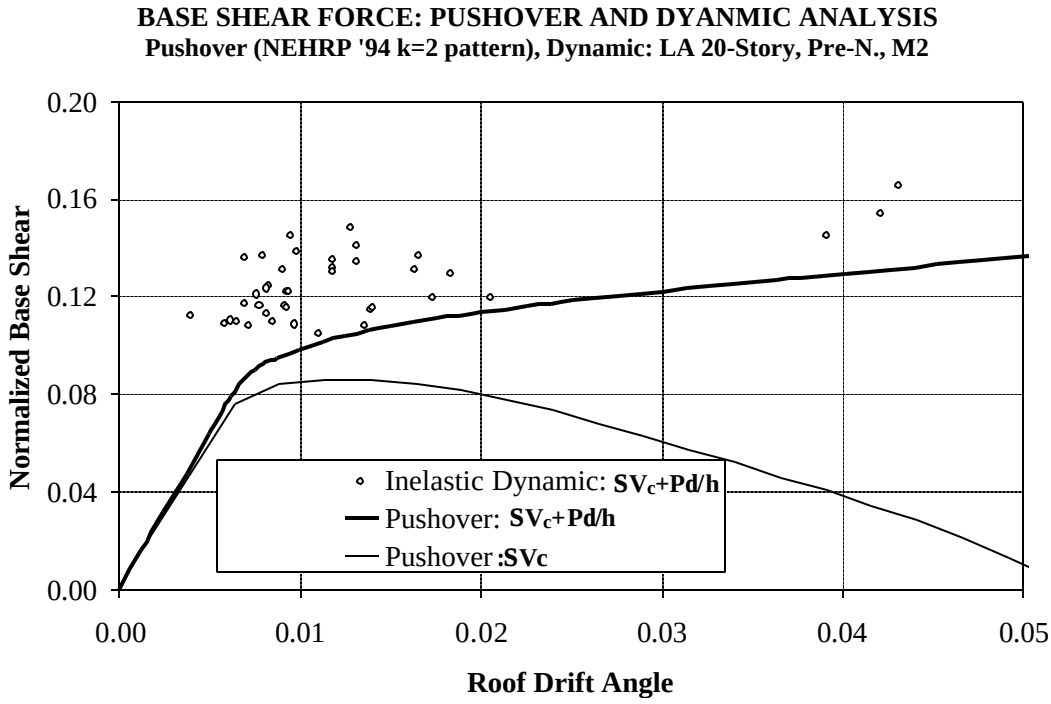

Figure 5.56. Maximum Base Shear Forces Under 10/50 and 2/50 Sets of Ground Motions, compared to Base Shear From Pushover Analysis, for LA 20-story Structure

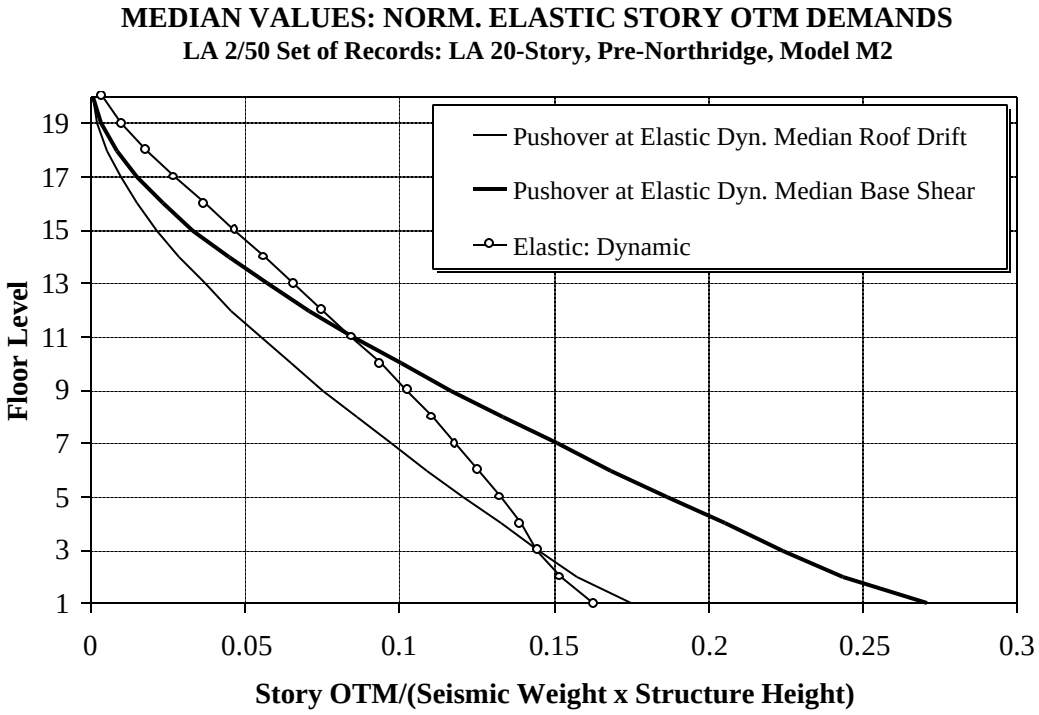

Figure 5.57. Median Story OTM Demands Under 2/50 Sets of Ground Motions, Compared to Demands From Pushover Analysis, for Elastic LA 20-story Structure

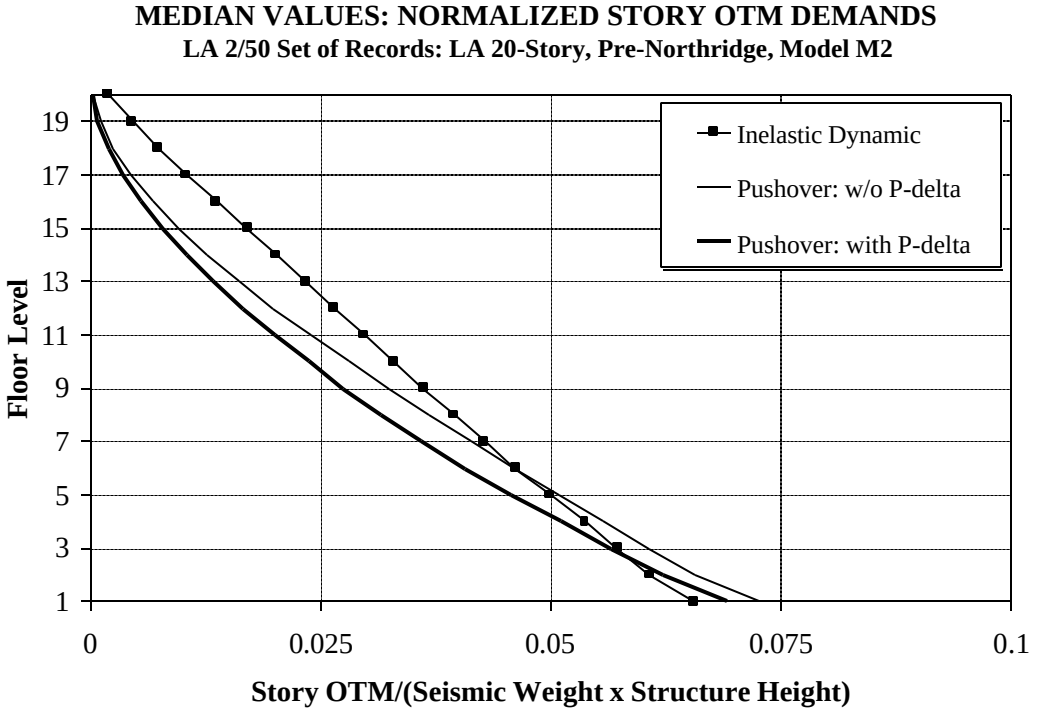

Figure 5.58. Median Story OTM Demands Under 2/50 Sets of Ground Motions, Compared to Demands From Pushover Analysis, for Inelastic LA 20-story Structure

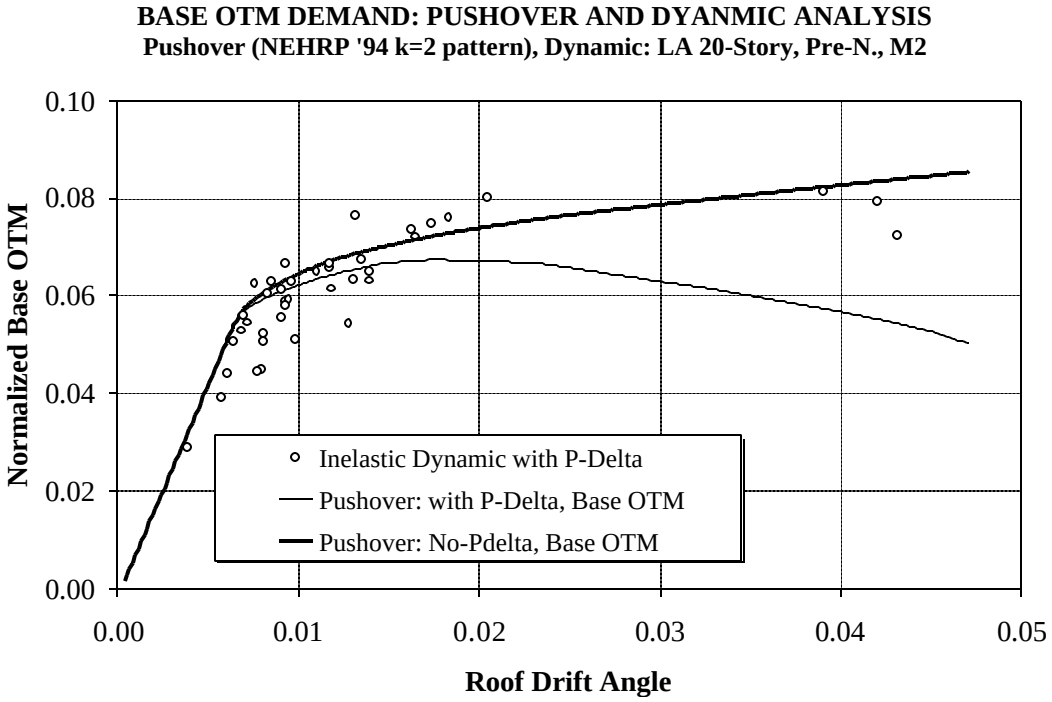

Figure 5.59. Base OTM Demands Under 10/50 and 2/50 Sets of Ground Motions, compared to Demands From Pushover Analysis, for Inelastic LA 20-story Structure

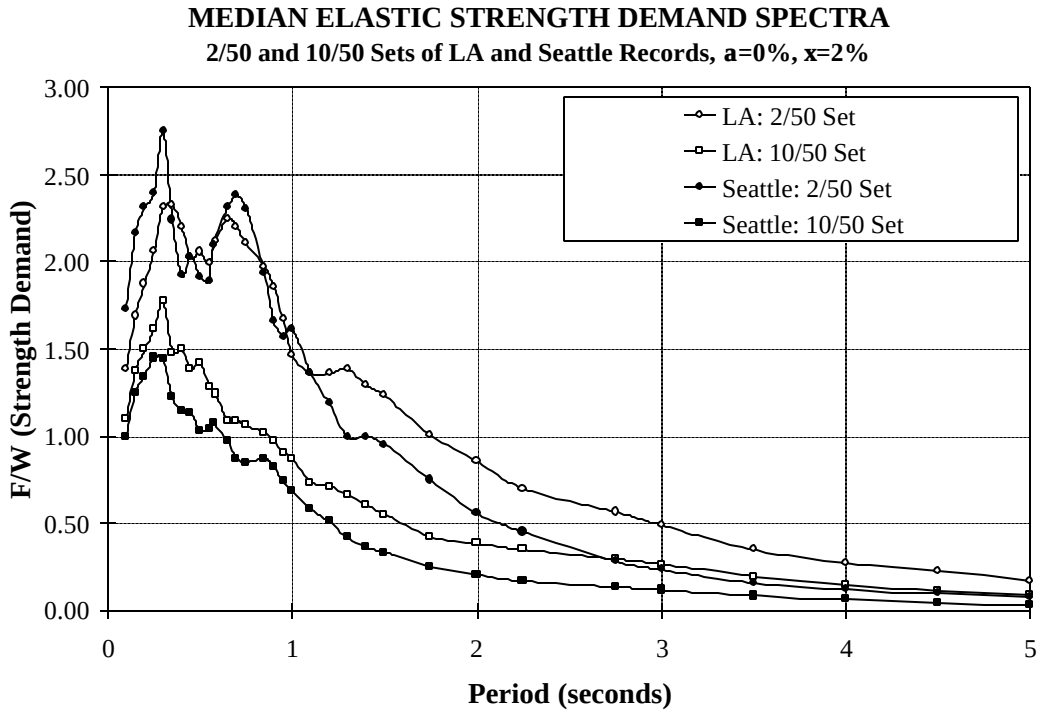

Figure 5.60 Comparison of Median Elastic Spectra for LA and Seattle 10/50 and 2/50 Sets of Ground Motions

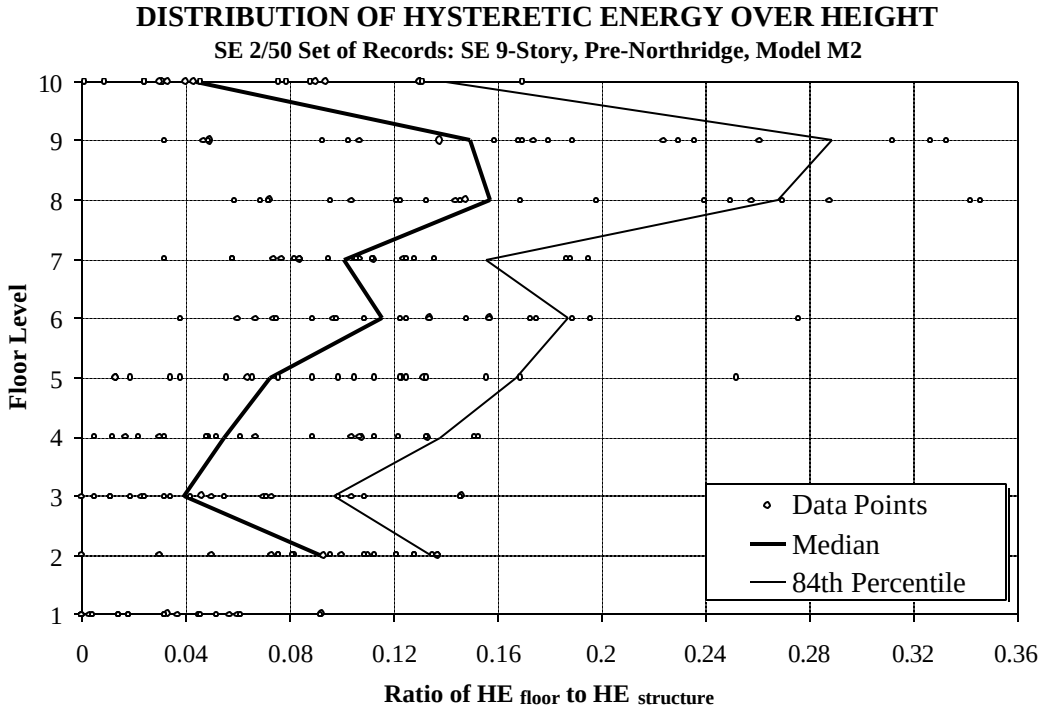

Figure 5.61 Distribution of Hysteretic Energy Demands Over the Height of 9-story Seattle Structure; 2/50 Set of Ground Motions

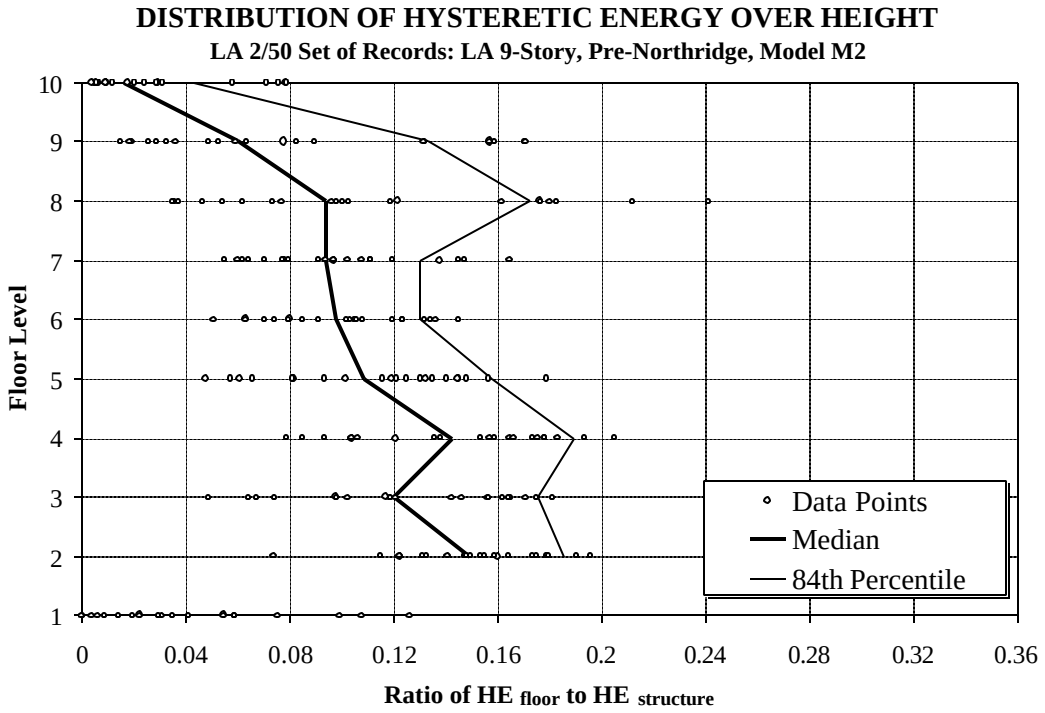

Figure 5.62 Distribution of Hysteretic Energy Demands Over the Height of 9-story LA Structure; 2/50 Set of Ground Motions

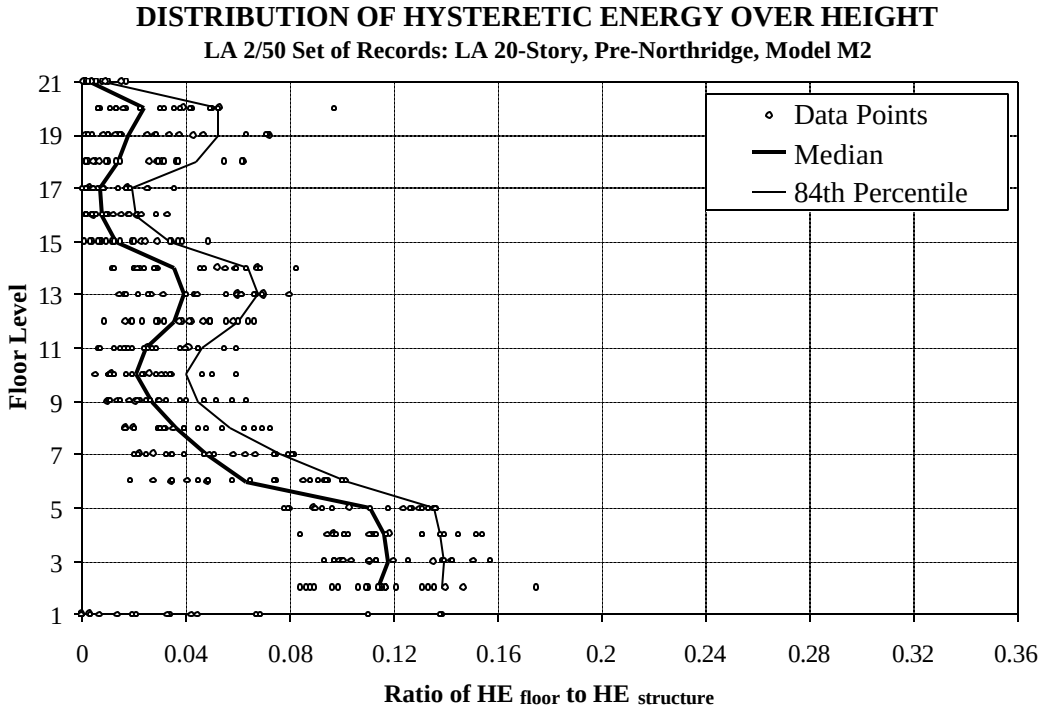

Figure 5.63 Distribution of Hysteretic Energy Demands Over the Height of 20-story LA Structure; 2/50 Set of Ground Motions

CHAPTER 6

ELEMENT DEFORMATION, FORCE, AND ENERGY DEMANDS

6.1 Introduction

The behavior and response of the structures has so far been discussed primarily in terms of global parameters i.e., roof and story drift angle demands. However, the system is the sum of its parts, and the behavior and response of the system is controlled by the element level behavior and the interaction between different elements. Thus, an in-depth evaluation of the element behavior and response is intrinsic to developing a holistic understanding of the behavior and response of the structure. Furthermore, capacity information is usually available at the element level through experimental investigations, thus any performance evaluation carried out at the system level has to implicitly have the element performance as its basis.

The focus of this chapter is on the identification of the critical issues controlling the behavior and response of elements at beam-to-column connections, and then on the evaluation of the influence of these issues on the dynamic response of the structure and constituent elements. The issues concerning beams and panel zones addressed in this chapter are the design decisions for connections (e.g., choice of section properties resulting in strong column/weak beam or strong column/weak panel zone design), effect of material strength (e.g., nominal strength versus expected strength) on relative distribution of demands between the beams and panel zones, and use of pre-Northridge standard connections versus post-Northridge connections (e.g., cover-plated beam flanges and reduced beam sections). Another important issue relates to the analytical model used to evaluate the element level demands. Here the emphasis is on presenting the range of

element level response that is calculated for the same structure, depending on the accuracy of the analytical model.

Even though standard design practices follow a strong column-weak beam/panel zone design criterion, there exists a potential for plastic hinging in the columns due to the movement of the inflection point on account of global bending of the columns, and/or higher mode effects [Park and Paulay, (1975), Bondy, D. K. (1996)]. The moment distribution over the column could change to the extent that the column bends in single curvature. This particular issue is investigated in this chapter. Additionally, the demands at column splice locations and for columns at the ground level are evaluated. Another critical issue for column behavior addressed in this chapter relates to axial forces induced in the columns (especially the exterior columns) due to the overturning moment demand for the structure.

The behavior issues for the beams, panel zones, and columns are addressed using static pushover analysis for selected structures and information obtained from time history analysis. The distribution of plastic deformation demands between the beams and panel zones is also tied back to the story drift demands presented in the previous chapter. An approximate method for the estimation of element level deformation demands from story drift demands is presented in Section 7.4.

The energy issues discussed in the previous chapter focused on the distribution of the structure hysteretic energy demand among the individual floors. In this chapter the distribution of this floor energy demand among the constituent elements is discussed and related to the cumulative plastic deformation demands for the elements. Furthermore, normalized element hysteretic energy demands are used, which provide a better framework for comparison between different elements and similar elements at different locations in a structure.

The aforementioned issues are studied using the LA and Seattle 9-story structures, the LA 20-story structure, and a redesign for the LA 9-story structure. The conclusions drawn are, however, applicable to the entire set of model buildings used in this study and some conclusions can be generalized for steel moment resisting frames.

6.2 Behavior and Demands for Beams and Panel Zones

The primary issues affecting the distribution of demands between beams and panel zone at a beam-to-column connection, which are discussed in detail in this section are the following:

Subjective Design Decisions

The relative strength of the elements at a connection is often governed by the strong column criterion, whereby of the three elements – beam(s), panel zone, and column – either the beam(s) or the panel zone has to be weaker than the column to "ensure" that plastification does not occur in the column. Thus, the first subjective decision concerns the choice for the weaker element; beam or panel zone. Another subjective decision concerns the relative strength between the beam and the panel zone, depending on which the entire plastification could be concentrated in the weaker element or shared between the two elements. Finally, the decision concerning the relative strength between the weaker element and the column could result in the column developing a plastic hinge if the force increase in the weaker element due to strain-hardening (coupled with other factors discussed below) is large enough to increase the column demand beyond its yield strength limit.

Material Strength

The mechanical properties of steel vary on account of many factors related to the chemical properties and the manufacturing process. The Structural Shape Producers Council (SSPC, 1994) studies show that there is a large variability in the properties of commonly used steels. For example, A36 steel has a nominal yield strength of 36 ksi, however, test data have shown that the mean yield strength is 49.2 ksi (37% higher than nominal) with a standard deviation of 4.9 ksi. Similarly, A572 Gr. 50 steel has a nominal yield strength of 50 ksi as against an expected strength of 57.6 ksi (15% higher than nominal) with a standard deviation of 5.1 ksi. This difference between nominal and expected values has a direct effect on the behavior of connections if beams and columns are made of different steels (all LA designs). Thus, even though the design intent (based on nominal strength) may have been to have beams weaker than the columns, the actual behavior may cause the relative strengths to be much closer and in some cases could result in the column being the weaker element.

Pre- and Post-Northridge Connections

The focus in this study is on fully restrained (FR) connections, which can be of two basic types; standard pre-Northridge connections or post-Northridge connections. Under the post-Northridge category, the choice can be between cover-plated beam flange connections, reduced beam sections, use of haunches or fins, among many others. In this study the cover-plated beam flange connections and the reduced beam section (RBS) connections are studied, along with the pre-Northridge standard connections. A description of these fully restrained connections and their analytical modeling is given in Chapter 3.

The issues related to the behavior of elements at a connection are discussed using the static pushover analysis for the LA and Seattle 9-story structures. Three different designs for the Seattle structure are studied; a pre-Northridge design, and two post-Northridge designs – one using cover-plated beam flange connections and the other using reduced beam sections. The LA 9-story structure (and a redesigned structure R1-LA9, see Appendix B) is used to evaluate the issues related to strength of material and the difference between pre-Northridge and cover-plated designs (reinforcing the observations from the Seattle structure). The analytical modeling issue is evaluated using the redesigned LA 9-story structure (R1-LA9). The seismic demands are evaluated using the 2/50 sets of ground motions for the respective sites. Unless stated differently, all analyses are carried out using a model M2 representation and expected yield values for steel strength.

6.2.1 Behavior Issues Studied Through Static Pushover Analysis

In seismic SMRF structures the customary design intent is to assign relative member strengths in a fashion that forces inelastic deformations into beams and panel zones and protects the columns from plastic hinging. This "strong column" concept is implemented in the UBC seismic provisions [UBC (1994)] through the following design requirement. At beam-to-column connections at least one of the following two conditions needs to be satisfied (with exceptions as noted in UBC Section 2211.7.5):

$$\frac{\sum Z_c\left(F_{yc} - f_a\right)}{\sum Z_b F_{yb}} \geq 1.0 \;\; or \;\; \frac{\sum Z_c\left(F_{yc} - f_a\right)}{1.25\sum M_{pz}} \geq 1.0 \qquad (6.1)$$

The subscripts *b* and *c* refer to beams and columns, respectively, and f_a is the axial stress in the column. SM_{pz} is the sum of beam moments associated with panel zone shear strength. The numerator is an estimate of the sum of the bending strengths of the columns above and below the connection, and the denominator is an estimate of the sum of the maximum moments that can be transferred from the beams to the columns. The first criterion applies when the beams are weaker than the panel zone, and the second criterion applies when the panel zone is the weak element. In the 1997 UBC the equations are modified in details but not in concept.

The exceptions, and also the rule as expressed in Equation 6.1, permit plastic hinging in columns in many cases, as will be shown in Section 6.3. Even if plastic hinging in the columns is prevented, there is no assurance that energy in a severe earthquake will be dissipated through plastic hinging in beams. In many code designs the panel zones will yield in shear before beams attain their yield strength. The 1994 UBC does not place restrictions on the relative strength of beams and panel zones, except for the basic shear strength design requirement for panel zones, which is applied at 1.85 times the code seismic forces at the allowable stress level. In the 1997 UBC the design requirement is slightly more stringent. Since beam sizes are often affected significantly by gravity loading and/or stiffness requirements, it can be expected that in many practical cases the panel zones are the weak elements and much or maybe all the plastification at beam-to-column connections is limited to panel zone shear deformations and the associated plastification in the columns flanges at the panel zone corners.

Effects of Subjective Design Decisions on Behavior and Deformation Demands

Table 6.1 shows the relative strength of the elements at an interior beam-to-column connection for the pre-Northridge LA 9-story structure. The strength quantities for the different elements are calculated as follows:

Column Strength	$= \Sigma M_p$ of columns at connection
Beam Strength	$= \Sigma M_p$ of beams framing into column
Panel Zone Yield Strength	$= 1.30 \times V_y d_b$
Panel Zone Plastic Strength	$= 1.30 \times V_p d_b$

These quantities identify, approximately, the lateral bending strength at the connection provided by the column, two girders, and the panel zone. The panel zone

strength incorporates the shear strengths V_y and V_p (Equations 3.1 and 3.4), and a factor of 1.30 to account approximately for the reduction in panel zone shear due to the shear force in the column. The strength of the elements is normalized by the strength of the weakest of the elements (beam, column, and yield strength of panel zone). Plastification is expected to occur first in the element with relative strength of 1.0. Other elements are expected to undergo plastification only if the relative strength value is not significantly larger than 1.0. Also shown in the table are the column and girder sections for the frame.

The original LA 9-story design has very large columns and is about 20% stiffer than required by the UBC (drift control was based on the code empirical period equation rather than the period of the bare frame). A redesign for the structure was performed using the computer tool BERT (Fuyama et al. 1993), to conform closer to minimum code requirements. In this redesign all strength and drift requirements of the UBC 1994 are satisfied and emphasis is placed on the criterion that drift control is better achieved by increasing girder sections rather than column sections. The column sizes could be significantly reduced at the expense of a small increase in girder sections. The section properties for the redesign (referred to as R1-LA9) are listed in the lower portion of Table 6.1. The redesigned frame is about 23% lighter than the LA 9-story frame.

The LA 9-story values show that for most floors the plastification will start in the panel zones and that the beams will yield soon after, except on floor 7 where significant plastification in the panel zone will occur before the beams yield. Thus, for all floors (except floor 7) the beams and panel zones are expected to share the plastic deformation demands. The relative column strength is large for all the cases. The redesigned structure shows a very different pattern, with the panel zones being significantly weaker than the beams. Thus, the beams are not expected to yield in this design. This difference is on account of the significantly reduced column sections, which still satisfy the "strong-column" concept by satisfying the second criterion in Equation 6.1. The relative strength values for R1-LA9 also show that the beams are now stronger than the columns, an issue which is discussed in Section 6.2.3.

The global pushover curves for the two structures are shown in Figure 6.1. The LA 9-story structure is stiffer and much stronger than the redesigned structure. Both designs show desirable inelastic response characteristics insofar that they exhibit a wide inelastic strength plateau, which suggests that the structures are not severely affected by P-delta effects. Figure 6.2 shows the element deformation demands for the two designs under the

pushover analysis at a roof drift angle of 0.03 (from the basement to floor 7). The element plastic deformation demands are shown in boxes, for an exterior and an interior column line. The corresponding story drift demands are shown in italics outside the frame.

As expected, based on the relative strength values given in Table 6.1, on the interior column line for the LA 9-story structure most of the plastic deformations are concentrated in the beams, with small plastification in the panel zones. The relative values for deformations in beams and panel zones are very different on account of the difference in post-yield stiffness between the beams (fixed at 3%) and panel zone (function of beam and column sections - is usually of the order of 10-15%). Thus, even though the panel zones yield prior to the beams on most floors, the beams have a higher rate of plastification with increase in applied load as compared to the panel zones. Significant plastification in the panel zone is only observed at floor 7, where the panel zones are much weaker than the beams, and consequently there is no plastification in the beam ends framing into the interior columns. On the exterior column line, the panel zones are relatively stronger than the beam framing into the connection and consequently all the plastification is concentrated in the beam. The redesigned structure has all the plastic deformations concentrated in the panel zones at the interior column line, and even at the exterior column line the panel zones undergo significant plastification.

Both the LA 9-story structure and the redesigned R1-LA9 structure conform to the strength and stiffness requirements of the UBC ’94, though the difference in column sections is very significant. However, based on the design decisions the global strength and stiffness are different, and the element behavior at the connections is very different. While one structure has a concentration of plastic deformations in the beams, the other has all the plastic deformations in the panel zones. Also, for the LA 9-story structure, the distribution of plastic deformation demand between the beam and panel zone varies from floor to floor (e.g., floor 7 has all plastic deformations in the panel zone, while floor 4 has all the plastic deformations in the beams). This illustrative example shows that there is a wide range of element behavior that can be expected from code designed structures, and the often made assumption of having all (or most) plastic deformations in the beams may not hold true.

Values for beam and panel zone plastic deformation demands need to be compared with caution as the relationship between beam plastic deformation and story drift is

different from the relationship between panel zone plastic deformation and story drift (see Section 7.4).

Effect on Material Strength on Behavior and Demands

The relative element strength values based on nominal yield strength of material, for the two LA 9-story designs, are shown in Table 6.1, alongside the values based on the expected yield strength of material. Since the LA structures use A36 steel for beams and A572 Gr. 50 steel for columns, the panel zone strength decreases by a small amount (50 ksi as against 57.6 ksi) but the beam strength decreases by a large amount (36 ksi as against 49.2 ksi) if nominal yield strength properties are used. Thus, the beams become relatively weaker than the panel zones and yield first also in the LA 9-story structure. The difference between the relative strength of the beams and panel zones reduces as compared to the relative strength values based on expected strength properties, thus for most floors there will be a more uniform distribution of demands. For the redesigned structure, however, the reduction in steel yield strength does not change the pattern of yielding because the beams are significantly stronger than the panel zones.

The global pushover curves for the LA 9-story structure and the redesigned structure, with nominal strength of steel, are shown in Figure 6.3. The response of the structures is similar to the response observed for the structures with the expected strength properties, as shown in Figure 6.1. The only difference observed is a reduction in the relative strength of the structures. The LA 9-story structure undergoes a larger reduction in strength as for this structure the strength of the yielding elements (beams) is affected severely, while for the redesigned structure the strength of the yielding elements (panel zones) is not affected much.

Figure 6.4 shows the element plastic deformation demands at an exterior and an interior column line for the two designs with nominal yield strength properties, corresponding to a roof drift of 0.03 under a static pushover. As expected from the relative strength values shown in Table 6.1, the plastic deformations for the LA 9-story are more concentrated in the beams and the panel zone plastic deformations are lower as compared to the values for the structure with expected strength of steel (Figure 6.2a). There is, however, no difference for the element deformation patterns (only panel zones yield at interior column line) in the redesigned structure.

The story drift distribution over height for the LA 9-story structure with expected strength properties is very similar to the story drift distribution over height for the structure with nominal strength properties. Thus, even though the pattern of yielding at the connection is changing on account of the change in material strength properties, the effect at the story level demands is virtually negligible. This observation reinforces the conclusion concerning the difference between element performance and system performance; the same system performance level may induce different levels of element performance depending on the design decisions and the variability in the material properties. This conclusion is based on static pushover behavior. The effect under dynamic loading is evaluated in Section 6.2.3.

Effect of Connection Types on Element Behavior and Deformation Demands

Seismic design of structures in regions of high seismicity has relied heavily on the use of fully-restrained welded beam-to-column connections. Many of these connections fractured in a brittle mode during the 1994 Northridge earthquake. One reason for these fractures is ascribed to the high stresses developed at the column face due to the plastification in the beams framing into the connection. A remedial measure, based on limited experimental investigations, was proposed in FEMA 267 (1995) with the intent to move the location of the plastic hinge away from the face of the column.

Three basic connection types are evaluated; the pre-Northridge standard connection and post-Northridge connections using either cover-plated beam flanges, or reduced beam sections (RBS). The effect of using the pre-Northridge versus the cover-plated post-Northridge connection detail on the story dynamic drift demands has been discussed in the previous chapter. The median story drift demands for the two types of structures were found to be very similar. The influence of the connection design details on the element deformation demands at a connection is evaluated next. The evaluation is performed using three designs for the Seattle 9-story structure. The design details are summarized in Appendix B.

The global pushover curves for the three designs are shown in Figure 6.5. The RBS design shows a lower effective strength on account of the lower strength of the beam sections (the maximum permissible flange area reduction of 50% has been used in this design). The RBS design also shows a wider strength plateau.

The element plastic deformation demands at an interior column line, for the three designs, at a roof drift angle of 0.03 under static pushover, are shown in Figure 6.6. The corresponding story drift demands are shown in italics. The distribution of story drift demands is significantly different for the RBS design, while the pattern is similar between the pre-Northridge and the cover-plated post-Northridge design. There is a clear shift of demands towards the upper stories for the reduced beam design structure. This indicates that the relative strength profile of the structure changes on account of the RBS design (upper stories get relatively weaker), and the pushover captures this weakness in the upper stories.

The beam and column sections are different (though not significantly, see Appendix B) between the different designs, however, the panel zone doubler plate thickness changes significantly (e.g., at locations where quarter inch doubler plates are used in pre-Northridge designs, half inch doubler plates are used in the post-Northridge cover-plated design). For this reason the cover-plated post-Northridge design shows a higher concentration of beam plastic rotation demands. The RBS design also shows a concentration of the plastification in the beams, with little or no plastification in the panel zones.

A clearer picture of the relative distribution of demands at an interior column line on the sixth floor of the three designs is obtained from Figures 6.7 to 6.9. The figures show the element plastic deformation demands as a function of the roof drift angle during a static pushover analysis. The adjacent story drift demands, which are not significantly different between the three designs, are also shown on the figures. The beam section is a W27X94 and the column section is a W24X207 for all three designs. The cover-plated post-Northridge design also has a 0.375 inch doubler plate welded to the panel zone.

For the range of roof drift angles shown, the plastic deformation demands are concentrated mostly in the panel zone for the pre-Northridge structure (Figure 6.7), well distributed between the panel zone and the beam for the cover-plated post-Northridge structure (Figure 6.8), and mostly concentrated in the beam for the RBS design (Figure 6.9). Thus, depending on the type of connection used for the design of the same structure, the relative distribution of element deformation demands at the connection can vary significantly.

Figure 6.10 shows the force demands for a beam and the panel zone (shear force demand multiplied by the beam depth) at an interior column line on the sixth floor for the three designs, during the pushover analysis. The force demand for the beam in the pre-Northridge and cover-plated post-Northridge design is almost identical, however, the panel zone demand is much higher in the post-Northridge design. Thus, the doubler plates used in the design are required to offset the increase in the force demand. The RBS design shows a lower force demand for the beam (on account of lower strength) and correspondingly a lower force demand on the panel zone.

Summary on Behavioral Characteristics of Elements at FR Connections

The discussion has shown that the behavior at beam-to-column welded fully-restrained connections, in terms of the relative distribution of force and deformation demands between the elements framing into the connection, can vary significantly based on a multitude of factors. Three factors are discussed; subjective design decisions, which control the size of beam and column sections based on the choice of the design criterion (weak beam or weak panel zone), the variability in the material strength properties (discussed in terms of difference between nominal and expected yield strength of steel), and the basic choice of the type of connection used for the structure.

While all the factors identified affect the local behavior at the connection severely, the effect on the system level response is usually not as significant, with the exception of the designs using the reduced beam section details. For similar story drift demand levels, different combinations for the distribution of plastic deformation demands ranging from full concentration in the beams to no yielding in the beams with all plastification in the panel zones can be obtained based on the factors identified. Thus, the factors identified may result in different element performance levels for the same system performance level. Also, the differences are not confined to different types of designs (e.g., pre-Northridge versus post-Northridge), but may be existent within the same design.

The identification of the behavioral characteristics has so far been based on static pushover analysis. The issue of interest is to evaluate and quantify the effect of these different local behavior patterns on the dynamic response of the structures, at both the element level and the system level. The focus of the next section is on the dynamic response of the same structures, obtained by subjecting the structures to sets of 2/50 hazard level ground motion records (see Appendix A).

6.1.2 Effects of Relative Element Strength on Seismic Demands

The modal characteristics for the different structures are given in Table 6.2. The redesigned LA 9-story (R1-LA9) structure is more flexible than the original 9-story LA structure. The different designs for the Seattle 9-story structure have very similar modal characteristics. The dynamic response of these structures is studied next.

Effects of Subjective Design Decisions and Material Strength on Seismic Demands

The median and 84th percentile story drift angle demands for the pre-Northridge LA 9-story structure with expected and nominal material strength properties are shown in Figure 6.11. Figure 6.12 shows the story drift angle demands for the redesigned LA 9-story structure. The demands for the redesigned structure (unless specifically mentioned in the figure legend) are based on 18 records of the set of 20 (LA35 and LA36 are excluded) as the redesigned structure with nominal strength properties "collapsed" under these two ground motions.

Figures 6.11 and 6.12 show that the story drift demands are similar between the original design and the redesigned weaker structure, irrespective of the material strength properties. The primary difference observed is in terms of the distribution of story drift over the height of the structure, with the redesigned structure showing a more uniform distribution. The conclusion appears to be that the drift demands are not sensitive to the relative distribution of demands between the beams and panel zones, and also to the strength of the structure. The conclusion regarding the strength of the structure is, however, valid only if the demands are not large enough to drive the structure into the range of significant post-yield negative stiffness. For example, the redesigned structure with nominal strength properties "collapsed" under two very severe ground motions (LA35 and 36; elastic spectral displacement demand at first mode period of the structure is about 80 inches, compared to a median demand for the 20 records of only about 40 inches). The reduction in strength of the structure and the reaching of the steep negative post-yield slope at a lower global drift (comparing Figures 6.1 and 6.3) contribute to the "collapse" of the redesigned structure with nominal strength properties. The redesigned structure with expected strength properties did not "collapse" under these two ground motions.

Beams and panel zones on floor 1 (ground floor) for the 9-story structures did not yield under a majority of records of the 2/50 sets as the plastification was concentrated in

the columns (see Section 6.3.3). Thus, Figures 6.13 to 6.16 and Figures 6.19 and 6.20 show the statistical values for element deformation demands only from floor 2 to floor 10 (roof).

The statistical values for the beam plastic rotations for the beam end framing into an exterior column, for the LA 9-story structure, are shown in Figure 6.13. The panel zones at the exterior column line do not yield under any of the 20 ground motions. Values for a beam end framing into an interior column are shown in Figure 6.14. The plastic deformation demand values for the panel zone at the interior column line are shown in Figure 6.15. The beams framing into the interior column of the redesigned structure do not yield under any of the ground motions, with the entire plastic demand being concentrated in the panel zones. The statistical values for the panel zone deformation demands at the interior column line for the redesigned structure are shown in Figure 6.16. At the exterior column line of the redesigned structure, the plastic deformation demands are distributed between the beams and panel zones. The following general conclusions can be drawn from these figures:

- For cases in which the plastic deformation demands are concentrated at the beam ends (Figure 6.13), the distribution of demands over the height follows a pattern similar to the story drift demands, and the demands are lower than the story drift demands by a value approximately equal to the story yield drift angle. For cases in which the concentration of plastic demands is in the panel zones (Figure 6.16), the demands are also in a pattern similar to the story drift demands. For these structures the panel zone plastic deformation demands are comparable to the story drift demand values (see Section 7.4).

- The plastic deformation demand pattern for an element may vary significantly over the height of the structure, as observed from Figures 6.14 and 6.15, and between different designs, depending on the design decisions. The nature of the deformation patterns between the beams and panel zones is complementary and related to the story drift demand.

- The effect of change in material strength properties is not very significant for the two structures evaluated, as one has relatively weak beams (original LA 9-story structure) and the other weak panel zones (redesigned LA 9-story structure). For structures in which the strength of the beam and panel zone is comparable, a change

in the material strength can change the relative distribution of demands significantly. An idea to this effect can be obtained from Figure 6.15; locations where the panel zone median plastic deformation demands reflected little (or no) plastification with nominal strength of material, there the panel zones have finite (or higher) plastic deformation demands when expected strength of material is used. For cases in which the change in strength properties results in the development of an undesirable post-yield mechanism, the dynamic response of the structure can be affected very significantly (e.g., the two collapse cases for the redesigned structure).

- For a given story drift demand, pushover analysis captures localized behavior well and is able to indicate the relative distribution of demands between the beams and panel zone.

Effect of Connection Types on Element Seismic Demands

The median and 84th percentile story drift angle demand values for the three designs for the Seattle 9-story structure, when subjected to the 2/50 set of Seattle ground motions, are shown in Figure 6.17. While there is no significant difference between the response of the pre-Northridge and cover-plated post-Northridge structures, the RBS design shows higher story drift demands, especially at the 84th percentile level. The difference in response is traced back to two ground motions (SE27 and SE31). Both these ground motions result in a global drift angle demand, for the RBS design, of almost 2.5 times the drift angle demand for the cover-plated post-Northridge design, as can be seen for record SE31 in Figure 6.18, which shows the roof drift response history for the two structures. The response is similar to the response observed for the P-delta sensitive Seattle 3-story structure (Figures 4.25 and 4.26). The pushover analysis in this case, however, indicated that the cover-plated design would attain the negative post-yield stiffness before the RBS design. The conclusion is that for this particular case the reduced strength (and corresponding change in yielding patterns) of the structure plays an important role in the dynamic response.

Statistical values for the beam plastic rotation demands for the different designs at an exterior and an interior column line are given in Table 6.3. Except for the reduced beam section design, the beams did not yield under all the records in the set. The number of records in which the response of the beams was elastic is given in the column under "No Yield". For cases in which the beams did not yield in 3 or more records of the set of 20

records the median is reported as the 10^{th} smallest value of the data set, and the 17^{th} smallest (4^{th} largest) value is taken as the 84^{th} percentile value. The results are associated with a very large scatter, thus comparisons between the statistical values need to be carried out with caution. Pictorially, the median beam plastic rotation demands at an interior column are shown in Figure 6.19. The corresponding total (elastic plus plastic) shear distortion demands for the panel zones are given in Table 6.4, and the median demands at an interior column line shown in Figure 6.20. The panel zones at the exterior column lines remain elastic in the three designs.

The presented results confirm that the distribution of local demands is design specific, and that the distribution of demands is well captured by the pushover analysis, in terms of indicating the elements in which the plastic deformation demands are concentrated.

6.1.3 Effect of Analytical Modeling on Evaluation of Local Seismic Demands

The effect of analytical modeling on the system level response has been discussed in detail in previous chapters, with the conclusion that a representation which accounts for the basic elements of the steel frame (e.g., model M2) is necessary for a realistic estimation of demands. Requirements for modeling improvements beyond that level are case specific. The effect of modeling accuracy on the evaluation of local seismic demands for the redesigned LA 9-story structure is discussed briefly in this section.

The global pushover curves for the two bare frame models (M1 – centerline model, and M2 – including panel zones) are shown in Figure 6.21. The centerline model M1 exhibits a higher lateral load resistance than model M2 (similar to the response for the Boston 9-story structure, Figure 5.10) but also predicts a rapid decrease in lateral resistance around a roof drift of about 0.03. This difference in response can be explained as follows: the columns in the structure are weaker than the beams but stronger than the panel zones, thus, first yielding in model M1 occurs at a higher lateral load, but the yielding in the columns results in undesirable story yield mechanisms, which lead to the rapid decrease in resistance. What must be emphasized here is that these story mechanisms are fiction rather than reality, and are obtained only because the centerline model is a poor representation of reality.

The effect of ignoring the panel zones in the analytical model on the dynamic response of the structure is shown in Figure 6.22, which shows the element plastic deformation demands under a single ground motion. Model M2 shows a concentration of severe deformation demands in the panel zones with the beams remaining elastic. For the centerline model, however, the plastification is concentrated in the columns. The use of such a model predicts collapse of the structure in 10 out of the 20 ground motions in the 2/50 set. This discussion reconfirms that representation of all the basic elements in the frame is intrinsic for determining the demands imposed on the elements as well as the system.

An important issue to note is that for the redesigned structure (model M2) with expected strength properties (and also the original LA 9-story structure with nominal strength properties – not shown in the figure), there are instances of plastic rotations in the columns at locations other than the ground floor. This response is observed even though the relative strength ratios for the columns (as given in Table 6.1) are of the order of 2.0. Strain-hardening in the plastified beams and panel zones causes an increase in the column end moments, but by far not enough to cause yielding in the columns. The important issue, which largely accounts for column yielding but is ignored in code designs, is the fact that column moments above and below the connection can be very different because of global bending at large displacements. This issue, and other issues concerning the columns are discussed in the next section.

6.3 Behavior and Demands for Columns, Splices, and Rotations at Base

The code criterion (based on elastic response of elements) given by Equation 6.1 assumes that the column moments above and below the connection are about equal. This is a reasonable assumption only if the inflection points are located at the mid-height of the columns. This assumption is usually violated in the first story due to the difference in end conditions between the top and bottom of the column, and may also not be applicable when a significant difference in interstory drift demands exists between adjacent stories, a condition which may develop on account of severe P-delta effects (in lower stories), or higher mode effects (in upper stories), or story strength irregularities. This issue is discussed in detail in Section 6.3.1. The development of plastic hinges in the columns may be detrimental to the response of the frame, especially if a story mechanism is formed. The plastification at the column ends will affect also the state of stress and strain

at the beam-to-column connection and, therefore, the likelihood and direction of fracture at beam-to-column welds.

A critical issue controlling the behavior of columns is the axial force demand imposed on the columns. For tall structures the overturning moment (OTM) demands may induce severe axial forces in the exterior columns, and due to the shear lag effect the interior columns may also be affected. Furthermore, the axial forces due to the OTM, if very high, may offset the gravity loads and induce tension in the columns. The axial forces transferred to the columns due to the OTM are discussed Section 6.3.2, with the emphasis being on the first story column demands. Also discussed in that section are the corresponding rotations at the base of the columns (at ground level).

Other than the basic beam, panel zone, and column elements, another "element" whose behavior and response requires specific attention is the column splice, as column splices are also susceptible to brittle fracture when overstressed in bending and/or direct tension [Bruneau et al. (1987), Popov and Stephen (1976)]. The connection between the two columns can be either bolted, welded, or a combination of the two. The 9- and 20-story designs under investigation in this study use partial penetration welded column splices; there are no splices in the 3-story structures. The combination of the bending moment and axial force demand on the splices is evaluated in Section 6.3.3.

6.3.1 Plastic Hinging at Column Ends

The primary cause of plastic hinge formation in columns is attributed to the shift in the inflection point from the mid-height of the column towards one end of the column. This movement of the inflection point can result in the column moments above and below the connection being significantly different, which may cause plastic hinging if the moment capacity of the column (reduced for axial load effects) is exceeded. This column behavior issue is investigated next, using the pre-Northridge LA 20-story structure represented by the M2 analytical model.

The movement of the inflection point in the column can be observed from Figures 6.23 and 6.24. Figure 6.23 shows the moment values at the top and base of the interior column in story 5, as a function of the story drift during the pushover analysis. Initially the moment values are almost equal, indicating an inflection point at mid-height. The

mid-height inflection point is also seen in Figure 6.24 – line 1, which shows the column moment diagram during the pushover analysis. With increasing story drift demand the bending moment demand at the base of the column decreases (thus, moving the inflection point closer to the base) and at large story drift demands the column goes into single curvature (reflected by a change in the sign of the moment at the base of the column). The movement of the inflection point towards the base of the column is marked on lines 2 to 5 in Figure 6.24. Line 6 shows the column in single curvature. The column end at the top of the story reaches its unreduced (for axial load effects) strength at a story drift demand of about 0.05 radians, forming a plastic hinge.

Thus, even though the design is based on the "strong-column" concept and the strength of the column is much higher than the strength of the beam (by a factor of about 2.3), the possibility exists for a plastic hinge formation in the column. A similar behavior, in terms of the difference between the moments in the column at the top and base of the story, can be observed for story 4 and stories 6 to 8 from Figure 6.25a, which shows the element force demands at a roof drift angle of 0.03 radians during the pushover analysis, for all the elements at an exterior and an interior column line in the lower 9 stories of the structure. The bottom two stories in the figure represent the two-story basement in the structure.

This discussion is based on the observed response of the structure under static loads. Dynamic interaction between different stories and higher mode effects may amplify the severity of the problem as has been indicated by [Bondy, K. D. (1996), Park and Paulay (1975)] primarily for concrete frame structures. The New Zealand Concrete Structures Standard 1995 (NZS, 1995) does recognize this issue and recommends a magnification factor for the design column moments.

The primary cause of excessive bending moment demand in columns in particular stories, which are shown in Figure 6.25a for the LA 20-story structure, is attributed to global bending of the column. In code designs the column strength is proportioned according to Equation 6.1, which focuses only on the relative strength of the column vis-à-vis the beam and/or panel zone. However, even if the beams do not transfer any moment demand to the column (e.g. a gravity column) or after the beams have developed plastic hinges the deflected shape of the column has to follow the deflected shape of the structure, which may result in additional bending moments in the column. Depending on the deflected shape of the structure and the corresponding force distribution over the

height, the moments at the top and base of the column in a story may be significantly different. These moments can be greatly amplified at particular story levels where a large difference exists between the story drift angle demands for adjacent stories ("kink" in deformed shape of structure), as has been observed for the LA 20-story structure (see Figure 5.21) and to a smaller extent in the LA 9-story structure (Figure 5.20) due to the concentration of the P-delta effect in a few lower stories of the structures. Higher mode effects and undesirable design characteristics, like story strength discontinuities, may also cause large differences in the story drift demands between adjacent stories. The former is observed in the top stories of the Seattle and Boston 9- and 20-story structures (Figures 5.24-5.25 and 5.28-5.29).

The maximum element plastic deformation demands at an exterior and an interior column line for the LA 20-story structure, under two ground motions (LA30 and LA36) of the 2/50 set, are shown in Figures 6.26a and 6.26b, respectively. Plastic hinges in the columns are observed in stories 5 and 6 under the LA30 ground motion and stories 2 to 7 and also story 14 (not shown in the figure) under the LA36 record. Fifteen out of the 20 2/50 LA ground motions induced plastic hinges in the columns. While many of the records had column plastification concentrated in stories 5 to 8, some plastification in upper stories of the structure was also observed. Even under the 10/50 ground motions 4 out of the 20 records caused a few columns to develop plastic hinges. Formation of plastic hinges in the columns was also observed in the LA 3- and 9-story structures, and in the Seattle structures, primarily under the 2/50 set of ground motions. For the Seattle 20-story structure the column plastic hinging was confined to stories 16 to 18, where kinks in the story drift demand patterns are observed (see Figure 5.25).

In conclusion, the seismic code criterion presently employed to prevent plastic hinge formation in the columns in steel moment resisting frame structures is found to be inadequate. The formation of these plastic hinges is attributed to the additional column moments generated due to the global bending behavior of the columns. These additional column moments can be significant if the story drift demands between adjacent stories are very different on account of P-delta effect, higher mode effects, or story strength discontinuities. These additional moments result in the column moments being significantly different at the top and base of the column, which implies that columns may form plastic hinges, but only at one end of the column. While this behavior does not outright result in a story mechanism, the inelasticity in the beams coupled with the column plastic hinging can result in undesirable structural response.

Many of the SAC structures were found to develop plastic hinges in the columns under design level and more severe levels of ground shaking. In most cases the potential for column hinging and discontinuities in story drifts was exposed in a pushover analysis. Thus, a pushover analysis of the structure may be used as an indicator for likelihood and location of column plastic hinging. However, the general caveats associated with the pushover analysis, mentioned in Section 3.5 and in the selected studies referenced in that section, need to be carefully considered for all cases.

Redistribution of Force and Deformation Demands During Pushover Analysis

The following discussion points out a potential problem in the evaluation of demands from a pushover analysis. The force and deformation demands during a displacement controlled static pushover analysis are expected to increase for all elements with increasing displacement of the control point. Thus, the maximum values for the element force and deformation demands are expected to occur at the instance of maximum roof displacement. This expectation may not hold true under the following two conditions.

The first condition pertains to the system attaining a negative post-yield stiffness due to structure P-delta effects. For such cases the applied lateral load decreases with an increase in roof drift, once the structure is pushed onto the negative post-yield slope of the force-displacement curve. The drift demands for a few stories, which contribute disproportionately to the roof drift, increase while the drift demands for the other stories decrease. The LA 20-story provides a good example, showing a decrease in drift demands in the upper 14 stories as the roof displacement is increased to large values (see Figure 4.7). In such cases, the maximum demands for the upper stories do not occur concurrently with maximum roof displacement.

The second condition is on account of the change in column moments due to global bending. This case is illustrated in Figure 6.27, which shows the moment demands for the beam and column ends at an exterior connection on floor 5 of the LA 20-story structure. The moment demands are graphed as a function of the roof drift (control point in pushover analysis). In the elastic range, the demands for beams and columns increase, with the demands at the two ends of the column being almost identical. Subsequent to the beam yielding, however, the moment demand at the column end above the connection decreases, while the demand at the column end below the connection continues to increase.

Thus, an evaluation of maximum demands from a pushover analysis may necessitate the extraction of envelope values (maximum values during the entire analysis). Figure 6.25b shows the envelope values for column and beam moments and the panel zone shear at an exterior and interior column line, for the LA 20-story structure pushed till a roof drift of 0.03 radians. The corresponding values at the 0.03 radian roof drift value are shown in Figure 6.25a. The story drift angle demands are identical between the two figures for the lower six stories, however, the story drift angle envelope values are higher for the other 14 stories (not all stories are shown in the figure), and consequently the force demands are also higher. Even for the lower six stories the moment demands in the columns (specifically the column ends at the base of the stories) are different between the two figures, on account of the issues discussed previously.

6.3.2 Column Axial Force Demands in First Story

Axial forces due to gravity and overturning moment (OTM) may decrease the bending moment capacity of the columns, thereby increasing the likelihood of plastification in the columns. The contribution from the OTM can also result in the exterior columns being subjected to tensile axial forces at medium to high drift demand levels, which may have an adverse effect on the behavior of column splices (discussed later). Thus, an evaluation of axial force demands imposed on the columns is essential in the design and evaluation process for SMRFs.

The overturning moment demands at the structure level have been discussed in Section 5.6, with the conclusion that the pushover analysis is able to represent the base OTM demand reasonably well, while it may not be able to properly capture the distribution of the demands over the height of the structure on account of the fixed load pattern. The fact that the base OTM demands from the pushover analysis are close to the dynamic base OTM values, permits the use of the pushover analysis to assess the axial force transferred to the first story columns on account of the structure overturning moment. This evaluation is carried out for the three LA structures. Statistical values for the three LA structures, under the 2/50 set of ground motions, are also evaluated.

The variation of the axial force (normalized to the yield force of the column) with the base shear (normalized to seismic weight of structure) for the two exterior columns and the two columns next to them, for the LA 3-, 9-, and 20-story structures, is shown in

Figures 6.28 to 6.30, respectively. The base shear value provides a direct reference for the first order OTM demand as the lever arm is a fixed quantity (0.86H for 3-story, 0.79H for 9-story, and 0.77H for 20-story, where H is the structure height) on account of the predetermined load pattern.

The overturning moment in the 3- and 9-story structures is resisted almost entirely by axial forces in the exterior columns. For the 20-story structure the columns next to the exterior columns also resist part of the overturning moment, on account of the shorter span of the beams (20 feet as against 30 feet for the 3- and 9-story structures).

For the 3-story structure, since the global pushover curve is elastic-almost perfectly plastic, the axial force demands in the exterior columns increase linearly until global yielding occurs, and increase thereafter due to P-delta effects (the last point on the curves represents a roof drift demand of 10%) even though the applied lateral load does not increase. The reversal in the curves for the 9- and 20-story structures is associated with global yielding and the subsequent reduction in the applied load on account of the negative post-yield stiffness. This reduction in lateral loads is not fully balanced by P-delta effects, resulting in a reduction in axial force. The exterior columns in all three structures are expected to be subjected to tensile axial forces at low levels of lateral loads.

Statistical values for the axial force demands under the 2/50 set of ground motions for the three structures are given in Table 6.5. None of the interior columns experiences tension under any of the ground motions, as is also indicated by the pushover analysis. The column axial force dynamic demands for all the structures are also well represented by the pushover analysis. The minor differences observed, especially in the 20-story structure, can be explained on the basis of similar minor differences observed between the base OTM demands predicted from the pushover analysis and the dynamic analysis (see Figure 5.59). The dynamic compressive axial force demand on the exterior column of the LA 9-story is significantly higher than that predicted by the pushover analysis. This is only on account of the unsymmetrical configuration of the structure (right most bay has only the left end as moment resisting). If the loads in the pushover were applied from the right side, then the maximum axial compressive load would be higher in the left exterior column compared to the value shown for the right exterior (and next to right exterior) column in Figure 6.29.

Another feature of the column dynamic axial force demands is the low scatter, which indicates that the relationship between OTM and base shear is very stable if the ground motion is strong enough to mobilize the base shear strength of the structure.

In conclusion, high axial compressive force demands are to be expected in the columns in the first story of taller structures, which may significantly reduce the bending strength of the columns. This reduction in strength contributes to the formation of plastic hinges in the columns. Furthermore, significant axial tensile forces are also to be expected in tall structures, which needs to be considered in the design of column splices. The behavior of the frames is close to shear building behavior with most of the overturning moment demand being resisted by axial forces in the exterior columns. The pushover analysis presents a convenient means for estimating the axial force demands in the columns. For frames that are not symmetric, the analysis should be carried out with loads applied from one side and then from the other side to ascertain the extent of compressive and tensile axial force demands in the columns.

6.3.3 Plastic Rotation Demands at Base of First Story Columns

The primary cause for the formation of plastic hinges in the columns was ascribed to the movement of the inflection point in the column from mid-height towards one end of the column due to global bending. Because the first story columns are fully restrained (3-story structures) or continue into the basement (9- and 20-story structures) the point of inflection will move closer to the top of the first story. Furthermore, the first story columns are subjected to high axial forces due to gravity loads and overturning moments, which may reduce the bending moment capacity of the columns significantly, as discussed previously. These characteristics, coupled with the high shear force demands in the first story, result in a high likelihood of plastic hinge formation at the base of the columns in the first story. The emphasis in this section is on estimating the level of plastic rotation demands to be expected at these column locations for the different structures.

The statistical values for the plastic hinge rotation demands for the three LA structures are given in Table 6.6. The 10^{th} smallest value (of the 20 data points) has been reported as the median, and the 17^{th} smallest value as the 84^{th} percentile for cases in which the column remained elastic under more than 2 records. The bases of the first

story columns (exterior and interior columns) for the 3- and 9-story structures form plastic hinges under almost all the records, whereas for the 20-story structure the column base, especially for the exterior column, remains elastic under many ground motions. The plastic rotation demands are associated with very high scatter, and cover a range from zero to more than 0.12. The normalized (w.r.t. unreduced moment capacity) moment demands are tabulated alongside the plastic deformation demands.

Results for the column rotation demands from pushover analysis at the median global drift demand for the structures are also presented in Table 6.6. The results indicate that the pushover is able to predict the median demands for the 3-story structure, but the large scatter in the time history analysis results, especially for the taller structures, makes any meaningful assessment of the pushover predictions difficult.

In conclusion, under severe ground motions the first story columns of the structures are expected to experience a combination of high compressive axial force demands, and bending moment demands at the base of the columns. Thus, the bases of the columns are expected to form plastic hinges, and in some cases undergo significant plastic rotation.

6.3.4 Moment and Axial Force Demands at Column Splices

Typically, column splices are located near the mid-height of the story, which places splices close to where columns are expected to have an inflection point. This results in a low design bending moment demand on column splices. However, as discussed in the previous section and shown in Figures 6.23 and 6.24, the inflection point in a column may be substantially displaced from the mid-height position, and the bending moment demands at splice locations may be much higher than anticipated in design. For the 9- and 20-story structures evaluated in this study the splices are located at 6 feet above the floor centerline. The focus of this section is on the estimation of bending moment and axial force demands for column splices, using pushover analysis for the LA 20-story structure, and on relating these demands to statistical values based on information from time history analysis.

The bending moment (normalized to unreduced plastic strength of the column) and corresponding axial force demand (normalized to yield force of the column) for the splices located on the exterior columns in story 5 of the LA 20-story structure, as a

function of the story 5 drift, are shown in Figure 6.31. Similar values for the columns next to the exterior columns (interior) are shown in Figure 6.32. Also marked on the figures, with dashed lines are the median and 84th percentile story 5 drift demand values for the structure under the 2/50 set of LA ground motion records.

The exterior and interior column splices are subjected to low bending moment demands (M/Mp less than 0.1) for median level (based on set of 2/50 ground motions) story drift demand values, however, at larger story drift demands the bending moment demand increases sharply. This is on account of the accelerated change in the column bending moment diagram at large story drift demands (see Figure 6.23). A value of 0.45 for the normalized bending moment demand at the splice is attained when the column goes into single curvature, with a plastic hinge forming at the top of the column. For this story the interior columns deform in single curvature at a story drift angle of approximately 0.06 radians, which the story experiences in 3 out of the 20 ground motion records.

The normalized axial force demands differ significantly between the exterior and interior column splices. The exterior left (direction of applied loading) column splice is subjected to tension forces at very low drift demand values, attains a peak value of about 0.30 and subsequently reduces on account of the unloading of the structure due to the structure being pushed into the negative post-yield range of the force-displacement curve. The exterior right column splice and the interior column splices are subjected only to net compression forces. The pushover analysis indicates that these particular column splices, and the splices in the second story, are subjected to a combination of significant bending moment and axial force demands for story drift demands in the range of those experienced under the 2/50 set of ground motion records.

Previous discussions have shown that while the axial forces in the columns at the base level are reasonably well estimated by the pushover analysis, the bending moment demands may be underestimated. Also, Figure 5.58 indicates that the pushover, in general, underestimates the overturning moment demand in all but the bottom stories of the structure on account of the load pattern. In general, the difference between the pushover estimates for story overturning moment (consequently column axial forces) and story shear force (consequently column bending moment demand), and force demands from dynamic analysis increases over the height of the structure. Thus, for story 5 the

pushover is expected to provide non-conservative estimates for both axial force and bending moment demands.

Statistical values for the dynamic force demands under the 2/50 set of ground motions, at an exterior and an interior column splice in story 5, normalized to the plastic bending strength and axial load capacity, are given in Table 6.7. The three different force demand values for any particular record do not occur at the same instance of time during the time history and may not even be for the same splice location (left column splice versus right column splice), thus, these values represent the upper bounds for the observed individual force demands for exterior and interior column splices in that particular story.

The column splices in story 5, and by extrapolation in story 2, are subjected to high levels of bending moment and axial force demands. The splices on the exterior columns are also subjected to significant tensile axial loads. The combined bending moment and axial force demand resulted in the splices in story 5 reaching the reduced strength of the column in only 1 out of the 20 ground motions. The pushover analysis permits convenient evaluation for the combined state of stress at the splices, but for certain cases may severely underestimate the demands. Much more detailed analytical and experimental research, which is outside the scope of this work, is required to properly understand and quantify the behavior and response of these potentially weak elements.

6.4 Cumulative Deformation and Energy Demands

As discussed briefly in Section 5.5.3, cumulative deformation demand parameters represent a measure of the damage to the structure, and may present a very different picture of the performance of the structure as compared to the performance observed using maximum deformation demands. Another potential measure of damage to a structure is the energy dissipated through inelastic deformations, as discussed in Section 5.8. The focus in these two sections (5.5.3 and 5.8) was on the global and story level cumulative deformation and energy demands. This section supplements the previous discussions by addressing element level cumulative deformation and energy demands. The emphasis is only on identification of the important issues. Results for the LA and Seattle 9-story structures are presented in support of the arguments.

The results obtained at the story level in terms of the difference between the maximum value parameters and the cumulative plastic deformations are reinforced by similar evaluations at the element level. Representative results from the LA 9-story structure are shown in Figures 6.33 to 6.35. These figures show the median and 84th percentile values over the height of the structure, for the maximum plastic rotation and cumulative plastic rotation demands for the beam end framing into an exterior column, the beam end framing into an interior column, and the panel zone in the interior column, respectively. The cumulative beam plastic rotation demands at an exterior beam end for different designs for the Seattle 9-story structure are shown in Figures 6.36 (maximum plastic deformation demands are shown in Figure 6.19). All the demands are for the 2/50 sets of ground motions for the respective sites.

These figures indicate that the distribution of cumulative plastic deformation demands over the height of the structure (and the relative magnitude of demands between different stories) can be quite different from distributions over height of the maximum plastic deformation demands. This is primarily on account of the varying number of cycles, which is a function of the characteristics of the ground motions (duration, energy content at predominant period versus at higher mode periods).

The element performance assessment may also change depending on the parameter evaluated. For example, the peak (over height) median value for the interior beam end plastic rotation is 0.024 radians (rotational ductility of about 4) for the LA 9-story structure, while the peak panel zone plastic deformation is only slightly smaller at 0.021 radians (deformation ductility of 6). The corresponding cumulative deformation demand values are 0.067 radians for the beam, and almost 50% higher at 0.092 radians for the panel zone. This difference may not be very critical as panel zones are, in general, very ductile elements and possess high cumulative deformation capacity. However, this example highlights the importance of also evaluating cumulative deformation values in order to obtain a better understanding of the response of the structure, as maximum value parameters only tell part of the story. The FEMA 273 (1997) guidelines relate element maximum deformation demands to performance levels, but no such guidelines exist for element cumulative deformation demands. Assessment of cumulative deformation demands may be critical for inelastic structures subjected to long duration ground motions and significant higher mode effects, which may result in a large number of inelastic excursions.

Energy Demands

The structure hysteretic energy demands and the contribution of different floors to the hysteretic energy have been discussed in Section 5.7. This section focuses on disaggregation of the floor hysteretic energy demands into the constituent element energy demands. The distribution of floor hysteretic energy to the columns, beams, and panel zones at each floor level for the LA 9-story structure, for the 2/50 set of ground motions, is shown in Figures 6.37 to 6.39, respectively. At the base level almost the entire hysteretic energy dissipation, which varies from 0 to 13% of the structure hysteretic energy, takes place in the columns. Under several ground motions some hysteretic energy dissipation in the columns is observed also for the middle stories of the structure. This reinforces the observation concerning plastic hinging in columns (due to global bending) in the 9-story structure, even though the columns are much stronger than the other elements (beams and panel zone) at the connections.

The hysteretic energy dissipation in the beams and panel zones is compatible with the observations made previously on the cumulative plastic deformation demands for these elements. The demands may be concentrated in beams or in panel zones or distributed between the two elements. The scatter in the normalized floor element energy data is low as indicated by the small difference between the median and 84^{th} percentile values. This is in contrast to the observation for the maximum and cumulative plastic deformation demands (Figures 6.33 to 6.35). The reason for the low scatter is that the sum of the element energy demands adds up to the floor energy demand, and therefore the variability associated with fractions is low in comparison with the variability of individual energy terms.

The energy demands discussed so far and in Chapter 5 have related the structure hysteretic energy to the floor hysteretic energy to the hysteretic energy for a group of particular type elements (beams, panel zones, and columns). The conclusion is that the distribution of structure energy over height is a function of the structural and ground motion characteristics, and the distribution amongst element types at a floor level depends on the relative strengths of the elements.

The energy dissipated by element types (columns, beams, panel zones) can be disaggregated further into energy demands for individual elements. To facilitate a comparison between energy demands on different elements at a floor level, or between

the same element at different floor levels, it is convenient to define a normalizing measure for the dissipated hysteretic energy in each element. An appropriate quantity is the normalized hysteretic energy, NHE, which can be defined for each element as follows:

$$NHE_{col} = \frac{\sum q_{p,c} \times M_{p,c}}{\left(M_{p,c}{}^2 \times h \Big/ 6EI_c \right)}$$

$$NHE_{beam} = \frac{HE_b}{\left(M_{p,b}{}^2 \times L \Big/ 6EI_b \right)} \qquad (6.2)$$

$$NHE_{pz} = \frac{HE_{pz}}{V_{p,pz} \times g_p \times d_b}$$

where the subscripts *c*, *b*, and *pz* refer to column, beam, and panel zone, respectively. M_p is the (unreduced) plastic moment capacity of the beam or column, g_p is the elastic panel zone distortion corresponding to the plastic panel zone shear strength V_p, (see Section 3.2.3), *I* is the moment of inertia, *E* is the elastic modulus, *HE* is the area under the moment-rotation (or shear force-shear distortion) curve for the beam and panel zone elements, and *h* and *L* are the clear span dimensions for the column and beam, respectively.

The normalization values for the beams and columns are approximate, as the assumption is made that the elements deform in perfect double curvature, which as discussed previously does not hold true in many cases, especially for the columns. However, since the emphasis is on a relative assessment of cumulative demands (represented as *NHE*), and the columns yield primarily at the base level, the approximation is considered acceptable. The element NHE is, in concept, similar to the cumulative plastic deformation demand (Figures 6.33 to 6.35) in a normalized form, i.e., it closely represents the cumulative ductility demand.

Median and 84th percentile values of *NHE* for beam ends framing into an exterior column and an interior column, and for a panel zone at an interior column, for the LA 9-

story structure under the 2/50 set of ground motions, are shown in Figures 6.40 and 6.41, respectively. The median NHE value for the exterior and interior column bases is approximately 1.9, with an 84th percentile value of 6.5, values that are relatively small in comparison to the beam and panel zone *NHE* values. This indicates that the cumulative plastic ductility demands for the column bases are not very large. At the median level, the maximum cumulative ductility demand for the panel zone is higher than the corresponding value for the beams. The beam ends framing into an exterior and an interior column have comparable values, except for cases in which significant yielding occurs in the interior panel zones.

The advantage of normalizing the energy dissipation demands at the element level is illustrated as follows. For the LA 9-story structure, floor 3 dissipates about twice as much hysteretic energy as floor 9 (see Figure 5.62). The beams dissipate about 85% of the floor 3 hysteretic energy while only dissipating about 60% for floor 9 (see Figure 6.38). Thus, the beams on floor 3 dissipate almost 3 times the energy being dissipated by the floor 9 beams. The beam *NHE* values at the two floors are, however, almost identical because of the larger beam size used at floor 3. This suggests that the cumulative rotational ductility is similar for the two sets of floor beams. The *NHE* values, thus, provide a reference for relative performance assessment for different elements, and for similar elements at different locations in a structure.

The primary issue that has been addressed in this section relates to the distribution of floor hysteretic energy demands to the elements constituting the floor, and the evaluation of relative energy demands between individual elements. The main conclusion from this brief discussion is that different structural parameters provide different measures for the structural response, and that cumulative demand parameters need to be addressed specifically in order to obtain a comprehensive understanding of the response of the structure.

6.5 Conclusions

The emphasis of this chapter was on an in-depth evaluation of the element (beam, column, panel zone, column splices) behavior and response. Critical issues concerning the behavior of the elements were identified and discussed, as was the influence of different element behavior characteristics on structural response. The issues were

primarily addressed using the static pushover analysis, however, the adequacy of using the pushover analysis was checked for each issue through comparison with results obtained from nonlinear dynamic analysis. The issues addressed, and the conclusions which may be drawn from the presented results, are as follows:

- Subjective design decisions, which enter in the selection for the member sections, may result in strikingly different element behavior at typical connections of SMRFs. The differences are not confined to different designs, but exist between different floors of the same design. The plastic deformation demand can be concentrated almost entirely in the beams, entirely in the panel zones, or can be distributed between the two elements. If the plastic deformation demands are fully concentrated in beams, the demands are comparable to the plastic story drift angle. For cases of concentration in the panel zones, the panel zone plastic distortion is relatively larger because of the different relationship between panel zone distortion and story drift. Thus, for the same level of story drift angle, the element plastic deformation value can be different, depending on the relative strength of the members at the connection. A formal relationship between the beam and panel zone deformations and the story drift is presented in Section 7.4.

- Material Strength Properties: The use of different materials for beams and columns may result in a change in relative strength properties at a connection. If the change is severe enough to result in one member becoming relatively much weaker (e.g., say columns) compared to design intent, then the response could be affected severely. Otherwise a change in material properties results only in a somewhat different distribution of demands at the connections.

- Connection Types: Three basic connection types are studied, the standard pre-Northridge connection, the cover-plated beam flange connection, and the reduced beam section (RBS) connection. The choice of the connection type (along with member selection, and material strength) controls the distribution of demands between the elements at the connection. The RBS designs were found to have a concentration of plastic rotation demands in the beams. The use of cover-plated beam flanges forces additional force demands onto the panel zone, which need to be offset with doubler plates unless much larger deformation demands in the panel zones can be tolerated.

- In most cases, the changes in distribution of element plastic deformation demands at typical connections do not have a pronounced effect on the structure level response. However, if the choice of member properties, material strength, or connection type, induces a severe weakness in the structure, the structure level response may change drastically. For example, the reduced global strength of the RBS design induces very high deformation demands under two records, and the model M2 of the redesigned structure experiences collapse under two records when nominal strength properties are used.

- Analytical Modeling: Using centerline dimensions and ignoring panel zone shear distortions (model M1) may provide very misleading information on local and global demands. An analytical model that incorporates the basic properties of all the structural elements of the steel moment resisting frame is intrinsic to the evaluation of element and structure response. For designs in which the panel zones are the weaker elements, ignoring the panel zones may force the plastic hinging in the columns and may indicate undesirable story mechanisms, which may result in erroneous response evaluation for the structure.

- Plastic Hinging in Columns: Even though current seismic design guidelines enforce the strong-column weak beam/panel zone concept, the possibility exists that plastic hinges will form in the columns. The larger the drift demand, the larger is the chance for plastic hinge formation in the column. Plastic hinging in columns was observed for all the taller structures, even where the strength of the columns was more than twice the strength of the weaker element at the connection. The cause of plastic hinging in the columns is attributed to the movement of the inflection point from mid-height to one end (typically the upper end) of the column due to global bending (bending of the column in the deflected shape of the structure), especially after the adjoining beams form plastic hinges. The additional column moments add to the moment at the top of the column and reduce the moment at the base of the column. This movement of the inflection point is amplified if a large difference exists in the story drift demands between adjacent stories, which may arise due to a strength irregularity in a particular story or due to P-delta effects or higher mode effects. The possibility of the column deforming in single curvature exists, especially at large drift demands.

- Axial Force in Columns: The overturning moments, especially for tall structures, induce high axial force demands in the exterior columns of the SMRF structure. The axial forces may be high enough to result in significant reductions in the bending moment capacity of the columns. Significant tensile axial forces are induced in the columns of tall structures.

- Plastic Hinge Rotation at Column Base: The reduction in column moment capacity, a high inflection point due to different boundary conditions, and high shear forces in the first story result in the formation of plastic hinges at the base of the columns, and significant plastic rotation can be expected under severe ground motions.

- Column Splices: The column splices in tall structures can be expected to be subjected to severe force demands. The interior column splices are subjected to high bending moment demands (due to movement of the inflection point), especially if the column attracts high shear forces, and axial compressive forces induced by the gravity loading. The exterior column splices are subjected to both high bending moment demands and high axial compressive or tensile forces, which needs to be considered in the design of column splices.

- The pushover analysis provides a very convenient tool for behavior evaluation of structures, especially at the element level, and for rationalization of response calculated from nonlinear dynamic analysis. However, the procedure has many shortcomings, particularly for tall structures, and should be used primarily as a support tool to facilitate understanding of the element and structural behavior. The analysis identifies many critical issues clearly, like columns deforming in single curvature, high axial forces in splices, relative distribution of demands between different elements at a connection, location of weakness in the structure, but may not be able to predict the absolute demand values with acceptable accuracy. An important issue to note is that the maximum values for deformations and force demands do not necessarily occur at the peak roof drift level. Redistribution coupled with second order effects may result in the maxima occurring at lower than peak values for the control point deflection.

- Cumulative Deformation and Energy Demands: The demand evaluation at the floor level is found to reinforce the conclusions drawn at the structure level, in terms of the variation in demand patterns over height and the differences in demands

patterns between single-valued parameters (e.g., maximum drift) and cumulative parameters. Depending on the various issues discussed previously, the concentration of demands could be in any or all the elements at a connection. The use of only single-value parameters might result in a misleading picture of the structural response. For example, for a case in which similar levels of element plastic deformation demands were observed for a beam and a panel zone, the corresponding cumulative plastic deformation for the panel zone was 50% higher than that for the beam. A disaggregation of the structure hysteretic energy into individual element hysteretic energy is presented, with the conclusion that the element energy demands need to be normalized to some common parameter to develop a clearer understanding of the relative energy demands between different elements. The columns at the base of the structure may be called upon to dissipate a significant portion of the structure energy.

The inelastic deformation demands imposed on elements at a beam-to-column connection depend on global strength and stiffness considerations as well as on the relative strength of the elements at the connection. Customary expectation is that in severe earthquakes inelastic deformations are concentrated in plastic hinge regions of the beams, that some shear yielding may occur in the panel zone, and that columns remain elastic. This chapter has demonstrated that the actual distribution of deformation demands is sensitive to design decisions and assumptions, material strength properties, and connection type, and that a realistic analytical model, which accounts for the limited shear strength of the panel zones, is needed to predict the element demands. Furthermore, columns, which are expected to behave elastically, may develop plastic hinges even though the strong column concept is followed rigorously.

Table 6.1 Relative Strength of Elements at Interior Column Line for LA 9-story and Redesigned 9-story Structure with Expected and Nominal Strength Properties

LA 9-Story (LA9)

	Exterior Column	Interior Column	Girder	Relative Strength Based on Expected Yield Strength of Steel				Relative Strength Based on Nominal Yield Strength of Steel			
				Column	Beam	PZ, yield	PZ, plast.	Column	Beam	PZ, yield	PZ, plast.
Floor 2	W14X370	W14X500	W36X160	1.97	1.00	1.04	1.46	2.34	1.00	1.23	1.73
Floor 3	W14X370	W14X455	W36X160	1.90	1.08	1.00	1.38	2.08	1.00	1.10	1.51
Floor 4	W14X370	W14X455	W36X135	2.15	1.00	1.12	1.55	2.55	1.00	1.33	1.84
Floor 5	W14X283	W14X370	W36X135	1.95	1.15	1.00	1.33	2.01	1.00	1.03	1.37
Floor 6	W14X283	W14X370	W36X135	1.95	1.15	1.00	1.33	2.01	1.00	1.03	1.37
Floor 7	W14X257	W14X283	W36X135	1.97	1.58	1.00	1.27	1.97	1.34	1.00	1.27
Floor 8	W14X257	W14X283	W30X99	2.37	1.16	1.00	1.32	2.41	1.00	1.02	1.35
Floor 9	W14X233	W14X257	W27X84	2.65	1.13	1.00	1.33	2.77	1.00	1.05	1.39
Floor 10	W14X233	W14X257	W24X68	1.61	1.00	1.08	1.49	1.91	1.00	1.28	1.76

Redesigned 9-Story (R1-LA9)

	Exterior Column	Interior Column	Girder	Relative Strength Based on Expected Yield Strength of Steel				Relative Strength Based on Nominal Yield Strength of Steel			
				Column	Beam	PZ, yield	PZ, plast.	Column	Beam	PZ, yield	PZ, plast.
Floor 2	W14X283	W14X311	W36X210	1.90	2.25	1.00	1.28	1.90	1.89	1.00	1.28
Floor 3	W14X211	W14X233	W36X150	1.98	2.26	1.00	1.23	1.98	1.90	1.00	1.23
Floor 4	W14X211	W14X233	W36X150	1.98	2.26	1.00	1.23	1.98	1.90	1.00	1.23
Floor 5	W14X193	W14X193	W36X150	2.01	2.81	1.00	1.20	2.01	2.37	1.00	1.20
Floor 6	W14X193	W14X193	W36X135	2.03	2.48	1.00	1.20	2.03	2.09	1.00	1.20
Floor 7	W14X145	W14X145	W36X135	2.04	3.40	1.00	1.15	2.04	2.87	1.00	1.15
Floor 8	W14X145	W14X145	W33X118	2.20	3.00	1.00	1.17	2.20	2.53	1.00	1.17
Floor 9	W14X90	W14X90	W33X118	2.17	4.89	1.00	1.11	2.17	4.12	1.00	1.11
Floor 10	W14X90	W14X90	W24X68	1.50	2.89	1.00	1.15	1.50	2.44	1.00	1.15

Table 6.2 Modal Characteristics for LA and Seattle 9-story Structures with Different Design Details

Original LA 9-Story Structure

	Mode 1	Mode 2	Mode 3
Period (seconds)	2.241	0.836	0.467
Modal Mass %age	82.1	11.1	4.1

Redesigned LA 9-Story Structure

	Mode 1	Mode 2	Mode 3
Period (seconds)	2.666	0.985	0.574
Modal Mass %age	82.1	11.3	3.8

Seattle Pre-Northridge Structure

	Mode 1	Mode 2	Mode 3
Period (seconds)	3.055	1.057	0.556
Modal Mass %age	80.1	13.0	3.9

Seattle Post-Northridge Structure: Cover-plated Design

	Mode 1	Mode 2	Mode 3
Period (seconds)	3.063	1.095	0.566
Modal Mass %age	80.3	12.4	4.3

Seattle Post-Northridge Structure: Reduced Beam Section (RBS) Design

	Mode 1	Mode 2	Mode 3
Period (seconds)	3.099	1.112	0.601
Modal Mass %age	79.6	13.0	4.3

Table 6.3 Statistical Values for Beam Plastic Rotation Demands at Exterior and Interior Column Line, for Seattle 9-story Structures with Different Design Details; 2/50 Set of Ground Motions

Pre-Northridge Design

	Beam End At Exterior Column						Beam End At Interior Column					
	Maximum	84th Percentile	*Median*	Minimum	Std. Dev. Of Logs	No Yield	Maximum	84th Percentile	*Median*	Minimum	Std. Dev. Of Logs	No Yield
Floor 2	0.0525	0.0226	*0.0103*	0	0.78	2	0.0253	0.0017	*0.0003*	0		7
Floor 3	0.0516	0.0212	*0.0072*	0	1.08	2	0.0349	0.0076	*0.0008*	0		7
Floor 4	0.0528	0.0204	*0.0058*	0	1.26	1	0.0247	0.0015	*0*	0		13
Floor 5	0.0525	0.0161	*0.0119*	0		5	0.0274	0.0040	*0*	0		10
Floor 6	0.0556	0.0262	*0.0103*	0.0018	0.93	0	0.0291	0.0026	*0.0002*	0		8
Floor 7	0.0547	0.0297	*0.0151*	0.0038	0.67	0	0.0473	0.0234	*0.0132*	0.0038	0.57	0
Floor 8	0.0532	0.0335	*0.0188*	0.0048	0.58	0	0.0349	0.0242	*0.0142*	0.0046	0.53	0
Floor 9	0.0581	0.0332	*0.0174*	0.0047	0.65	0	0.0490	0.0313	*0.0203*	0.0101	0.43	0
Floor 10	0.0567	0.0323	*0.0140*	0.0	0.84	1	0.0414	0.0254	*0.0119*	0.0015	0.76	0

Post-Northridge Design

	Maximum	84th Percentile	*Median*	Minimum	Std. Dev. Of Logs	No Yield	Maximum	84th Percentile	*Median*	Minimum	Std. Dev. Of Logs	No Yield
Floor 2	0.0605	0.0248	*0.0101*	0	0.90	2	0.0385	0.0112	*0.0013*	0		6
Floor 3	0.0602	0.0195	*0.0079*	0		3	0.0415	0.0086	*0.0009*	0		7
Floor 4	0.0640	0.0276	*0.0096*	0	1.06	1	0.0549	0.0254	*0.0092*	0	1.02	2
Floor 5	0.0598	0.0369	*0.0091*	0	1.41	2	0.0444	0.0178	*0.0043*	0		4
Floor 6	0.0574	0.0408	*0.0078*	0.0001	1.65	0	0.0420	0.0183	*0.0072*	0		5
Floor 7	0.0563	0.0370	*0.0172*	0.0031	0.76	0	0.0448	0.0284	*0.0121*	0.0020	0.85	0
Floor 8	0.0703	0.0443	*0.0266*	0.0102	0.51	0	0.0627	0.0420	*0.0270*	0.0133	0.44	0
Floor 9	0.0860	0.0435	*0.0230*	0.0069	0.64	0	0.0697	0.0395	*0.0223*	0.0059	0.57	0
Floor 10	0.0851	0.0452	*0.0162*	0	1.03	1	0.0693	0.0347	*0.0152*	0	0.82	1

Post-Northridge Special Design (RBS)

	Maximum	84th Percentile	*Median*	Minimum	Std. Dev. Of Logs	No Yield	Maximum	84th Percentile	*Median*	Minimum	Std. Dev. Of Logs	No Yield
Floor 2	0.0627	0.0408	*0.0133*	0.0013	1.12	0	0.0531	0.0385	*0.0117*	0.0011	1.19	0
Floor 3	0.0660	0.0460	*0.0126*	0.0005	1.29	0	0.0574	0.0403	*0.0130*	0.0009	1.13	0
Floor 4	0.0738	0.0404	*0.0148*	0.0021	1.01	0	0.0547	0.0318	*0.0102*	0.0008	1.14	0
Floor 5	0.0802	0.0433	*0.0193*	0.0050	0.81	0	0.0651	0.0388	*0.0161*	0.0021	0.88	0
Floor 6	0.0809	0.0462	*0.0220*	0.0078	0.74	0	0.0615	0.0367	*0.0175*	0.0047	0.74	0
Floor 7	0.0768	0.0483	*0.0221*	0.0048	0.78	0	0.0673	0.0445	*0.0225*	0.0063	0.68	0
Floor 8	0.0722	0.0484	*0.0283*	0.0149	0.54	0	0.0538	0.0372	*0.0228*	0.0105	0.49	0
Floor 9	0.0763	0.0522	*0.0323*	0.0135	0.48	0	0.0632	0.0486	*0.0329*	0.0168	0.39	0
Floor 10	0.0751	0.0555	*0.0330*	0.0098	0.52	0	0.0682	0.0542	*0.0347*	0.0143	0.45	0

Table 6.4 Statistical Values for Panel Zone Total Shear Deformation Demands at Exterior and Interior Column Line, for Seattle 9-story Structures with Different Design Details; 2/50 Set of Ground Motions

Pre-Northridge Design

	Panel Zone At Exterior Column					Panel Zone At Interior Column				
	Maximum	84th Percentile	*Median*	Minimum	Std. Dev. Of Logs	Maximum	84th Percentile	*Median*	Minimum	Std. Dev. Of Logs
Floor 2	0.0022	0.0021	*0.0019*	0.0017	0.06	0.0376	0.0244	*0.0134*	0.0029	0.60
Floor 3	0.0026	0.0025	*0.0023*	0.0017	0.09	0.0285	0.0177	*0.0101*	0.0024	0.56
Floor 4	0.0023	0.0022	*0.0020*	0.0017	0.06	0.0408	0.0240	*0.0131*	0.0033	0.60
Floor 5	0.0024	0.0022	*0.0020*	0.0018	0.06	0.0391	0.0247	*0.0146*	0.0064	0.52
Floor 6	0.0024	0.0023	*0.0021*	0.0020	0.05	0.0388	0.0271	*0.0179*	0.0092	0.42
Floor 7	0.0025	0.0023	*0.0022*	0.0020	0.05	0.0174	0.0110	*0.0078*	0.0033	0.34
Floor 8	0.0025	0.0023	*0.0023*	0.0021	0.04	0.0183	0.0126	*0.0094*	0.0058	0.29
Floor 9	0.0024	0.0022	*0.0021*	0.0019	0.06	0.0067	0.0037	*0.0030*	0.0027	0.20
Floor 10	0.0025	0.0024	*0.0023*	0.0021	0.04	0.0129	0.0083	*0.0053*	0.0028	0.44

Post-Northridge Design

	Maximum	84th Percentile	*Median*	Minimum	Std. Dev. Of Logs	Maximum	84th Percentile	*Median*	Minimum	Std. Dev. Of Logs
Floor 2	0.0029	0.0027	*0.0025*	0.0019	0.09	0.0307	0.0195	*0.0104*	0.0024	0.63
Floor 3	0.0039	0.0029	*0.0026*	0.0020	0.13	0.0296	0.0189	*0.0100*	0.0025	0.64
Floor 4	0.0023	0.0022	*0.0021*	0.0017	0.06	0.0161	0.0065	*0.0041*	0.0023	0.45
Floor 5	0.0027	0.0025	*0.0024*	0.0021	0.06	0.0240	0.0130	*0.0078*	0.0029	0.52
Floor 6	0.0028	0.0026	*0.0025*	0.0022	0.06	0.0245	0.0154	*0.0096*	0.0040	0.47
Floor 7	0.0029	0.0027	*0.0026*	0.0024	0.05	0.0198	0.0129	*0.0092*	0.0049	0.34
Floor 8	0.0024	0.0022	*0.0021*	0.0020	0.04	0.0051	0.0032	*0.0028*	0.0026	0.15
Floor 9	0.0028	0.0027	*0.0025*	0.0023	0.05	0.0174	0.0087	*0.0054*	0.0029	0.48
Floor 10	0.0067	0.0037	*0.0029*	0.0026	0.23	0.0185	0.0096	*0.0057*	0.0027	0.52

Post-Northridge Special Design (RBS)

	Maximum	84th Percentile	*Median*	Minimum	Std. Dev. Of Logs	Maximum	84th Percentile	*Median*	Minimum	Std. Dev. Of Logs
Floor 2	0.0029	0.0025	*0.0023*	0.0021	0.10	0.0154	0.0064	*0.0036*	0.0026	0.57
Floor 3	0.0044	0.0031	*0.0025*	0.0021	0.21	0.0177	0.0073	*0.0038*	0.0025	0.64
Floor 4	0.0029	0.0025	*0.0023*	0.0020	0.11	0.0292	0.0158	*0.0086*	0.0036	0.61
Floor 5	0.0024	0.0021	*0.0019*	0.0018	0.09	0.0248	0.0126	*0.0065*	0.0030	0.65
Floor 6	0.0025	0.0022	*0.0020*	0.0018	0.09	0.0290	0.0154	*0.0084*	0.0034	0.61
Floor 7	0.0029	0.0026	*0.0024*	0.0022	0.08	0.0182	0.0078	*0.0041*	0.0027	0.64
Floor 8	0.0026	0.0023	*0.0021*	0.0019	0.09	0.0270	0.0173	*0.0104*	0.0053	0.51
Floor 9	0.0021	0.0019	*0.0018*	0.0016	0.08	0.0128	0.0073	*0.0041*	0.0027	0.58
Floor 10	0.0017	0.0016	*0.0015*	0.0014	0.06	0.0029	0.0027	*0.0026*	0.0024	0.06

Table 6.5 Statistical Values for Exterior and Interior Story 1 Column Axial Force Demands for LA 3-, 9-, and 20-story Structures; 2/50 Set of Ground Motions

		EXTERIOR		INTERIOR	
		Compression	Tension	Compression	Tension
LA 3-Story	Median	0.111	-0.043	0.047	0.000
	84th Percentile	0.115	-0.047	0.048	0.000
LA 9-Story	Median	0.230	-0.114	0.076	0.000
	84th Percentile	0.250	-0.130	0.077	0.000
LA 20-Story	Median	0.401	-0.186	0.243	0.000
	84th Percentile	0.462	-0.239	0.258	0.000

Table 6.6 Statistical Values for Plastic Rotation and Bending Moment Demands at Base of Story 1 Columns, LA 3-,9-, and 20-story Structures; 2/50 Set of Ground Motions, and Pushover Analysis

EXTERIOR COLUMN

Plastic Rotation Demands

	Maximum	84th Percentile	*Median*	Minimum	Std. Dev. Of Logs	No Yield
LA 3-Story	0.0913	0.0567	0.0272	0	0.74	1
LA 9-Story	0.0672	0.0446	0.0088	0	1.63	2
LA 20-Story	0.1080	0.0238	0	0		10

Moment/Mp (unreduced)

Maximum	84th Percentile	*Median*	Minimum	Std. Dev. Of Logs
1.28	1.17	1.09	0.99	0.06
1.18	1.12	1.03	0.80	0.08
1.20	1.10	0.78	0.43	0.34

INTERIOR (NEXT TO EXTERIOR) COLUMN

Plastic Rotation Demands

	Maximum	84th Percentile	*Median*	Minimum	Std. Dev. Of Logs	No Yield
LA 3-Story	0.0976	0.0658	0.0257	0.0015	0.94	0
LA 9-Story	0.0681	0.0389	0.0109	0	1.27	2
LA 20-Story	0.1219	0.0308	0.0117	0		5

Moment/Mp (unreduced)

Maximum	84th Percentile	*Median*	Minimum	Std. Dev. Of Logs
1.30	1.18	1.11	1.00	0.06
1.18	1.12	1.03	0.83	0.08
1.46	1.22	1.02	0.71	0.18

PUSHOVER ANALYSIS AT MEDIAN ROOF DRIFT ANGLE DEMAND

Plastic Rotation Demands

	Exterior Column	Interior Column
LA 3-Story	0.0235	0.0252
LA 9-Story	0.0000	0.0000
LA 20-Story	0.0000	0.0000

Moment/Mp (unreduced)

Exterior Column	Interior Column
1.07	1.08
0.93	0.96
0.58	1.00

Table 6.7 Statistical Values for Axial Force and Bending Moment Demands for Splices in Story 5 of LA 20-story Structure; 2/50 Set of Ground Motions

Force Demands for Splices in Story 5

		Maximum	84th Percentile	*Median*	Minimum	Std. Dev. Of Logs
Story 5 Drift Angle		0.1185	0.0628	0.0309	0.0099	0.71
Exterior Column	M/Mp	0.47	0.32	0.21	0.11	0.43
	P(compression)/Py	0.70	0.65	0.59	0.44	0.10
	P(tension)/Py	-0.37	-0.30	-0.25	-0.19	0.19
Interior Column	M/Mp	0.78	0.55	0.38	0.22	0.39
	P(compression)/Py	0.34	0.32	0.30	0.27	0.06
	P(tension)/Py	0.00	0.00	0.00	0.00	0.00

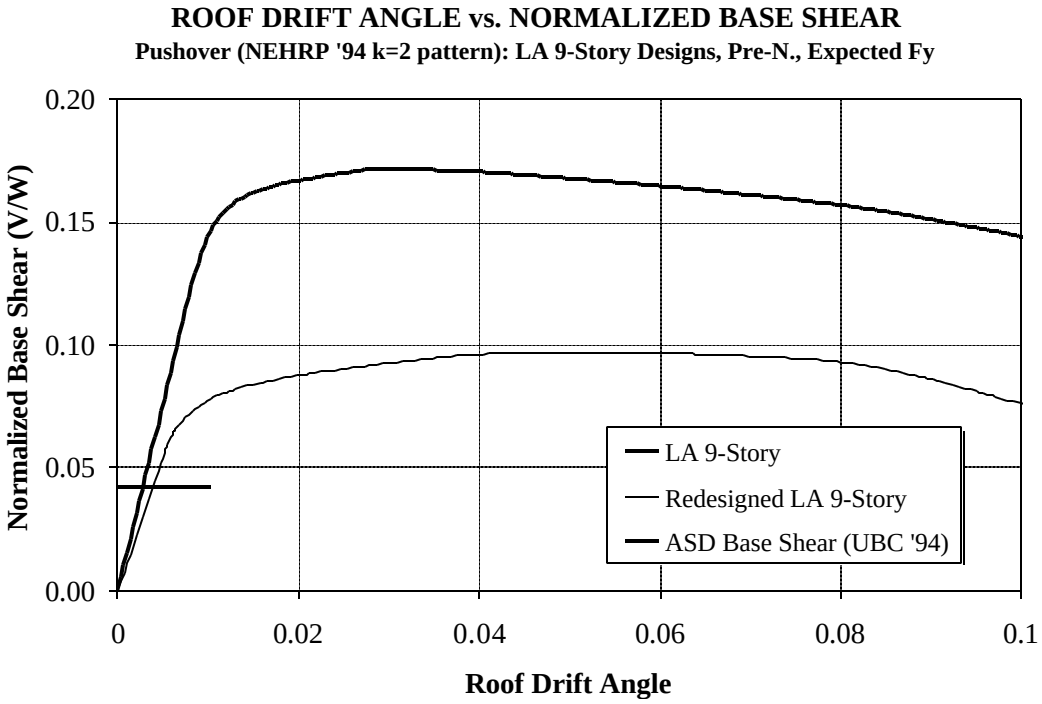

Figure 6.1 Global Pushover Curves for LA 9- and Redesigned 9-story Structure, with Expected Strength Properties

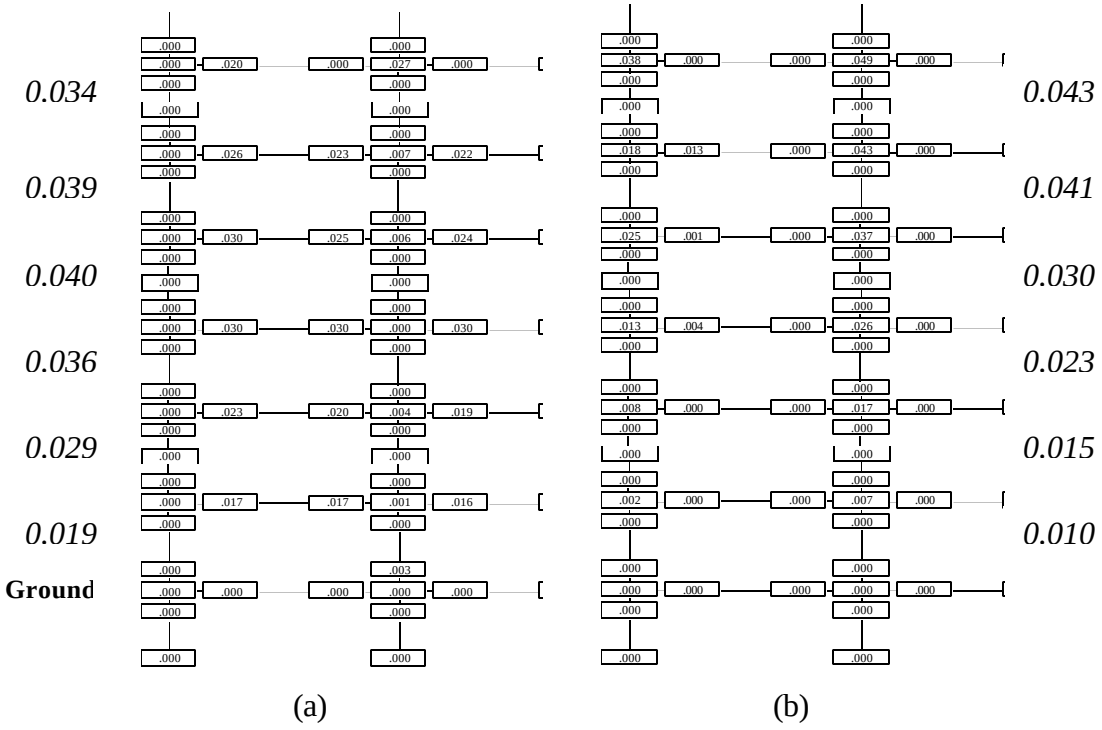

Figure 6.2 Story and Element Deformation Demands at 3% Roof Drift Angle, for (a) LA 9- and (b) Redesigned 9-story Structure, Expected Strength; Pushover Analysis

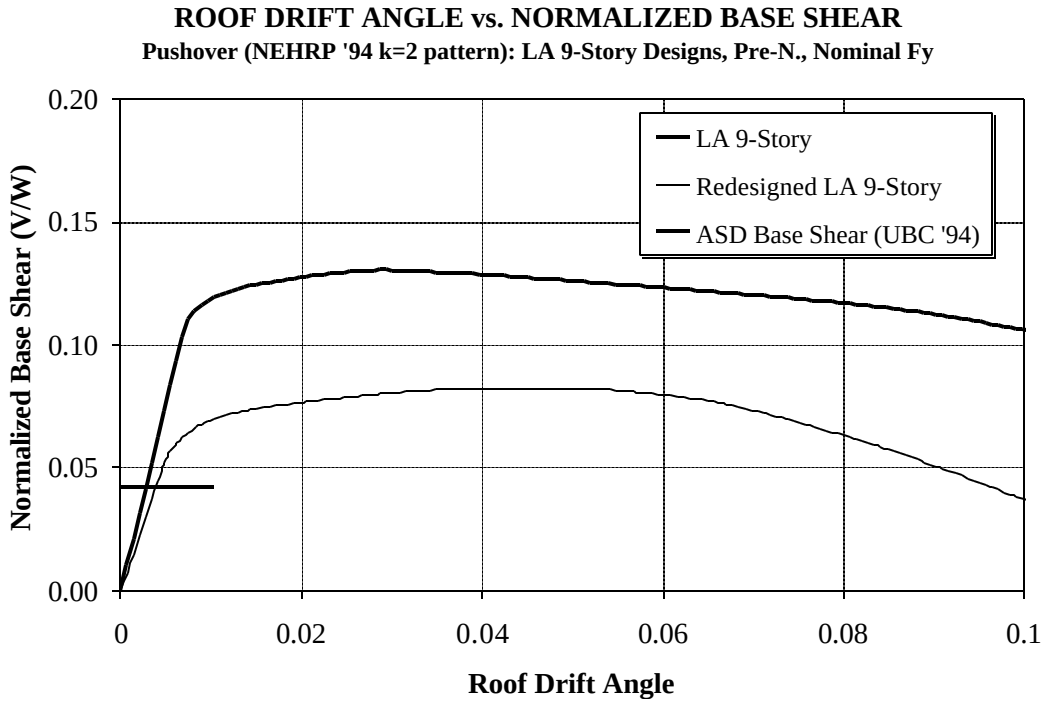

Figure 6.3 Global Pushover Curves for LA 9- and Redesigned 9-story Structure, with Nominal Strength Properties

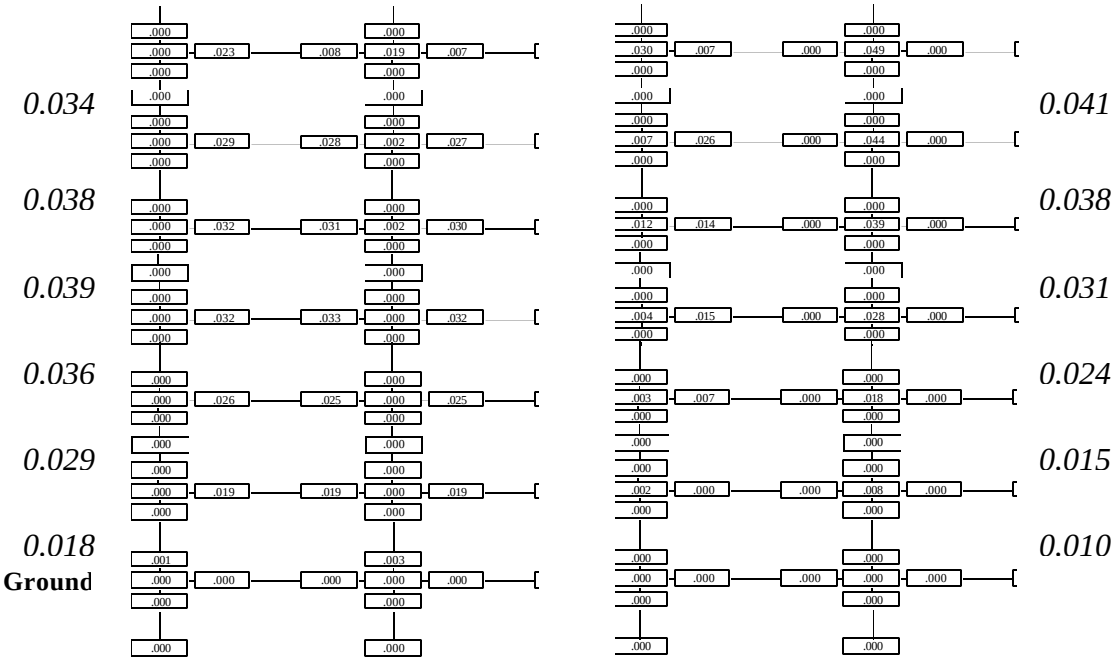

Figure 6.4 Story and Element Deformation Demands at 3% Roof Drift Angle, for (a) LA 9- and (b) Redesigned 9-story Structure, Nominal Strength; Pushover Analysis

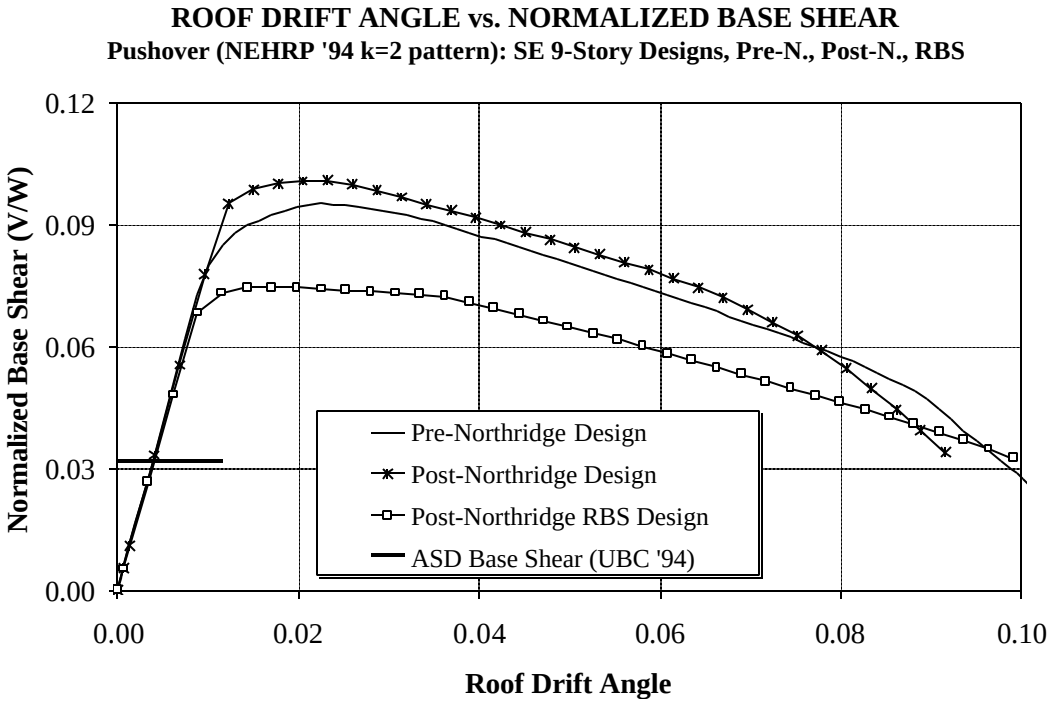

Figure 6.5 Global Pushover Curves for Seattle 9-story Structures, with Different Design Details

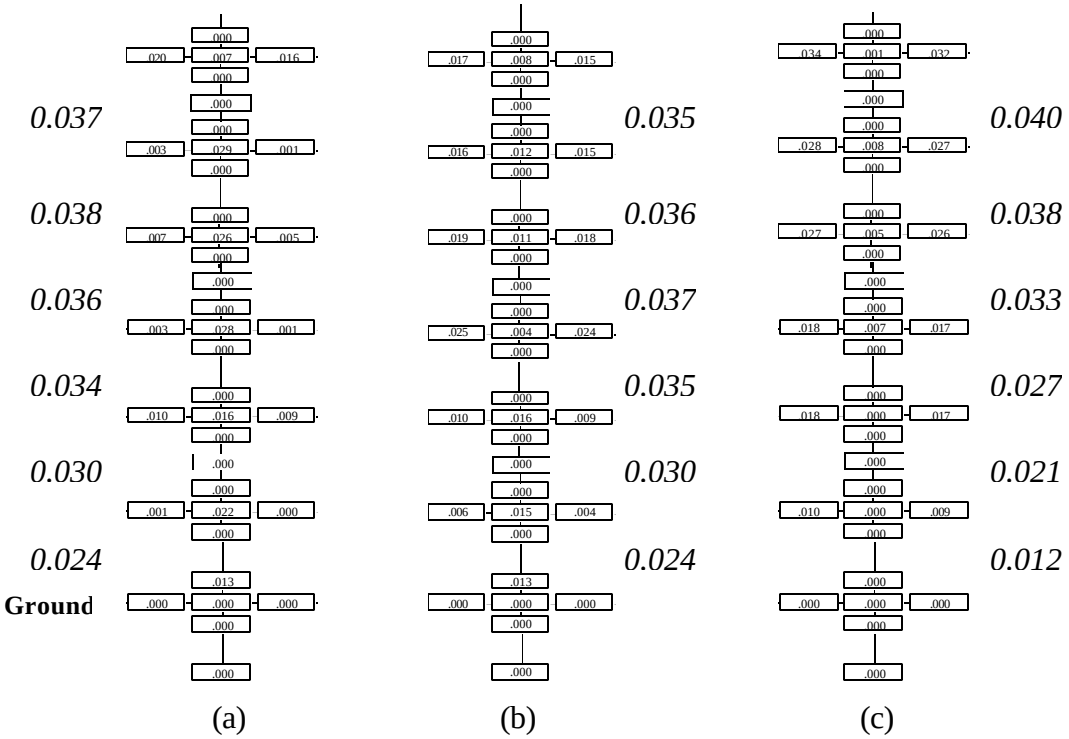

Figure 6.6 Story and Element Deformation Demands at 3% Roof Drift Angle, for Seattle 9-story Str. (a) Pre-N., (b) Cover-Plated Post-N., (c) RBS; Pushover Analysis

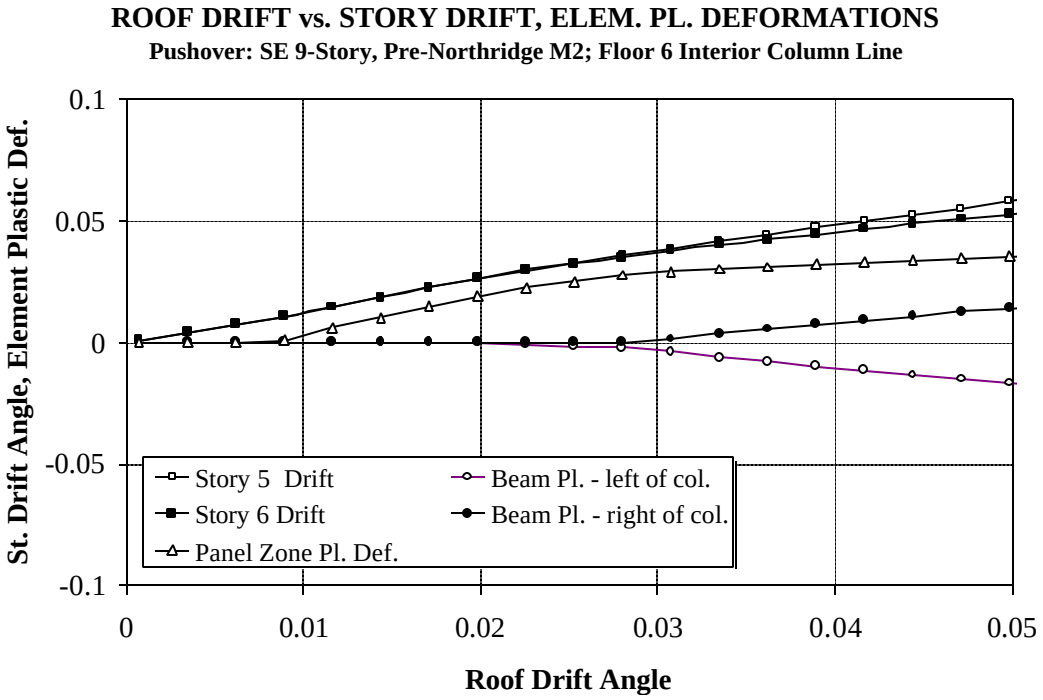

Figure 6.7 Variation of Story and Element Deformation Demands with Increasing Roof Drift Angle for Seattle 9-story Pre-N. Structure; Pushover Analysis

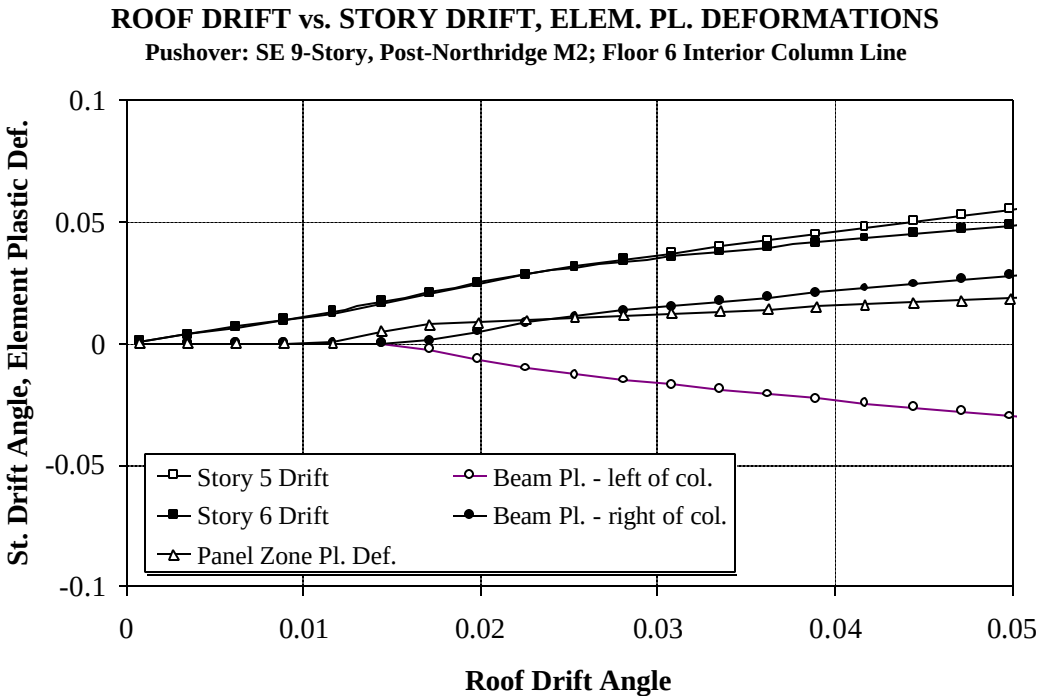

Figure 6.8 Variation of Story and Element Deformation Demands with Increasing Roof Drift Angle for Seattle 9-story Cover-Plated Post-N. Structure; Pushover Analysis

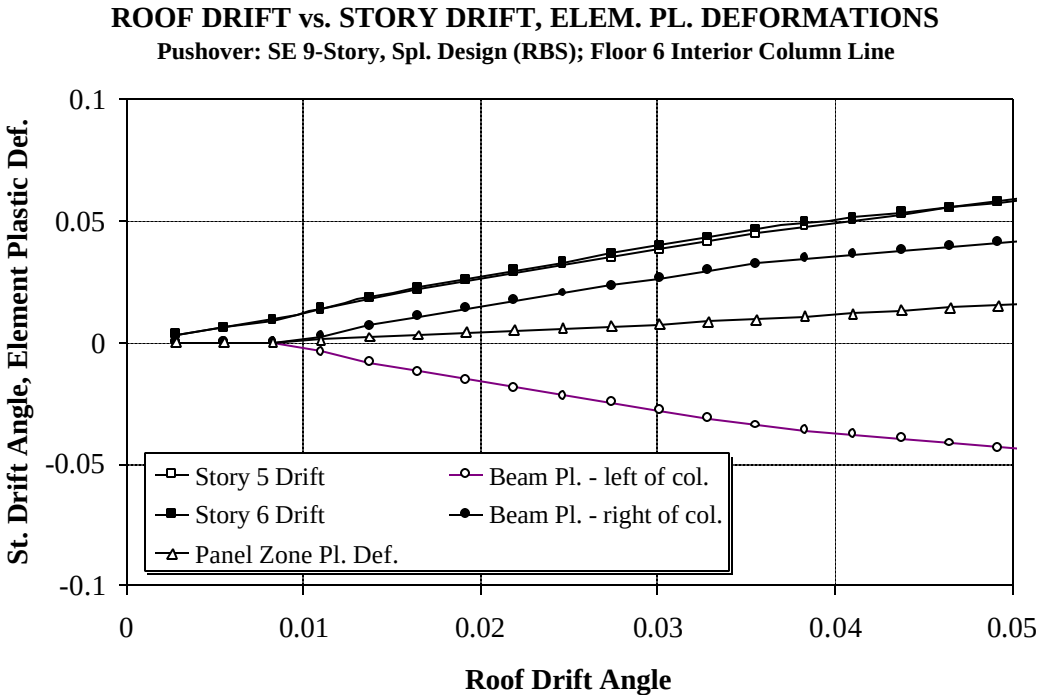

Figure 6.9 Variation of Story and Element Deformation Demands with Increasing Roof Drift Angle for Seattle 9-story RBS Design; Pushover Analysis

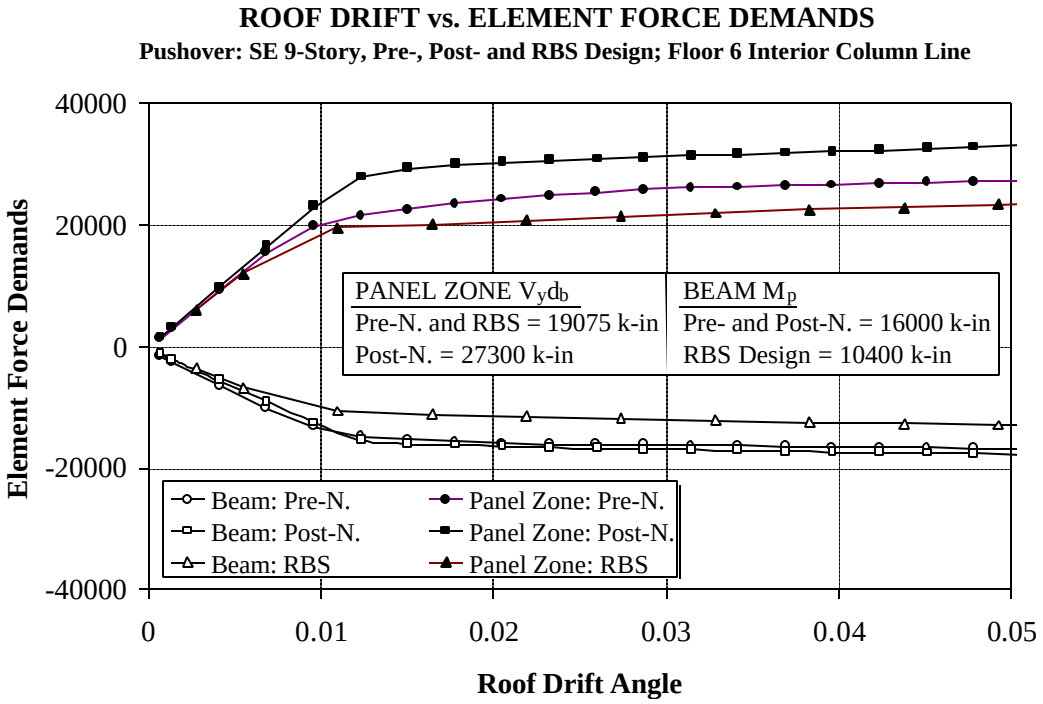

Figure 6.10 Variation of Element Force Demands with Increasing Roof Drift Angle for Seattle 9-story Pre-N., Cover-Plated Post-N., and RBS Design; Pushover Analysis

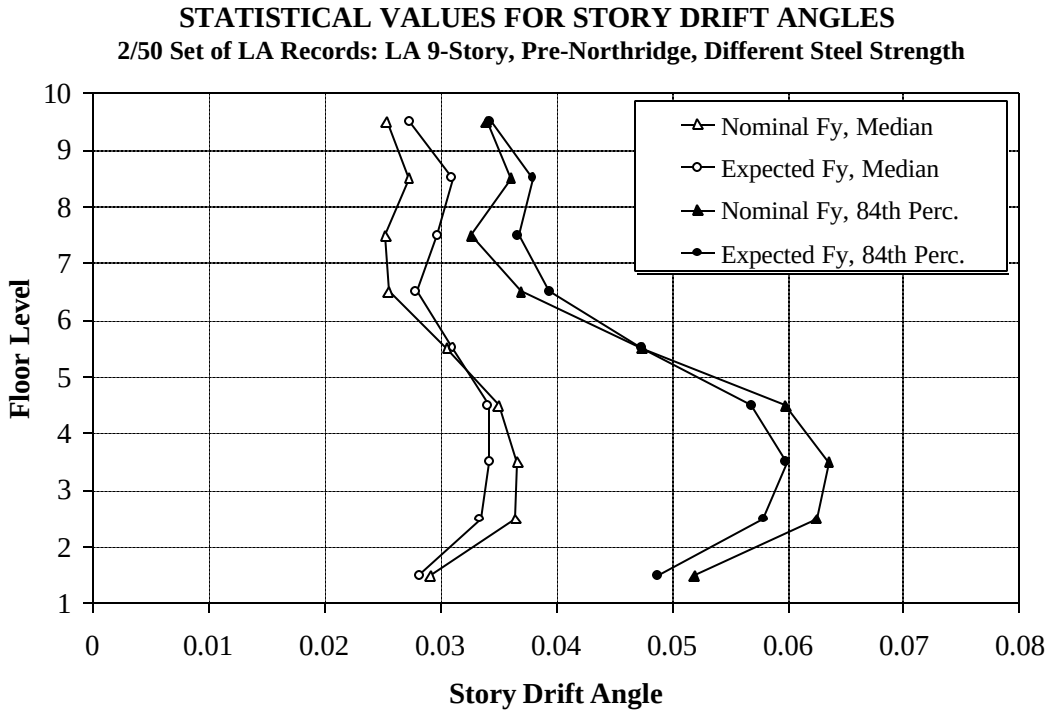

Figure 6.11 Story Drift Angle Demands for LA 9-story Structure with Expected and Nominal Strength Properties; 2/50 Set of Ground Motions

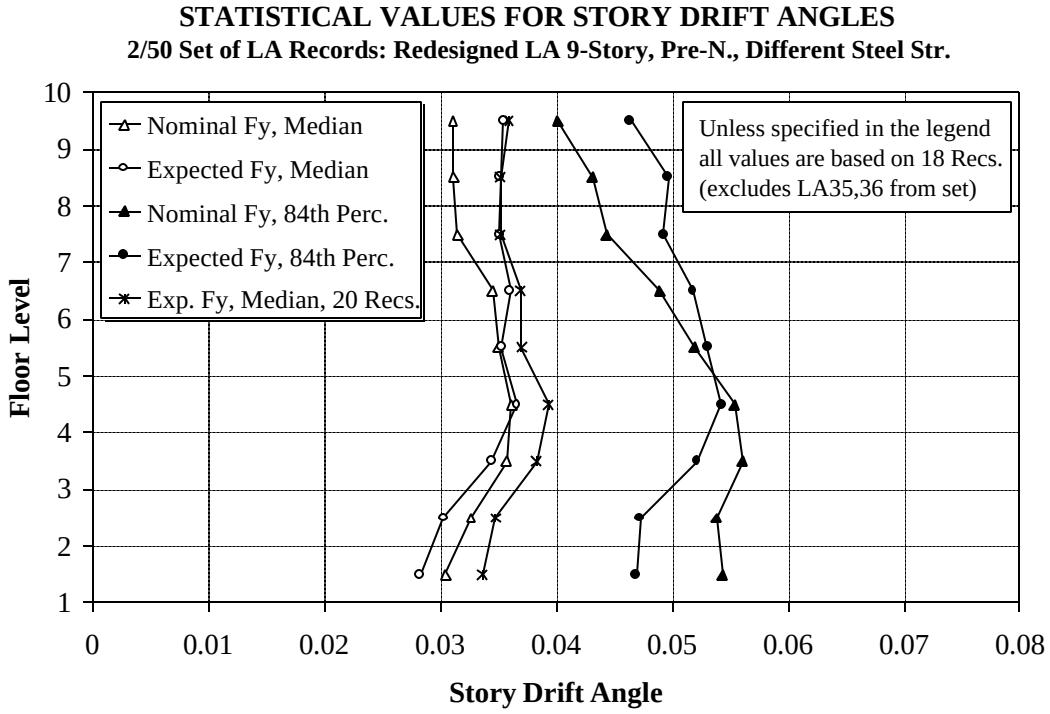

Figure 6.12 Story Drift Angle Demands for Redesigned LA 9-story Structure with Expected and Nominal Strength Properties; 2/50 Set of Ground Motions

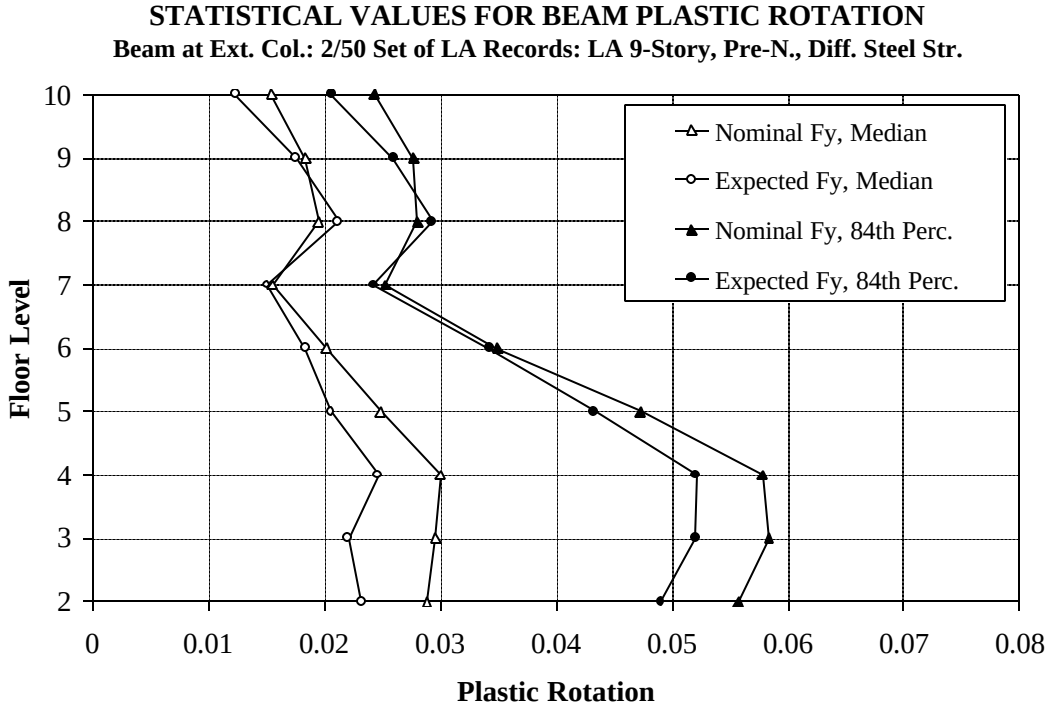

Figure 6.13 Beam (@ Exterior Col.) Plastic Rotation Demands for LA 9-story Structure with Expected and Nominal Strength Properties; 2/50 Set of Ground Motions

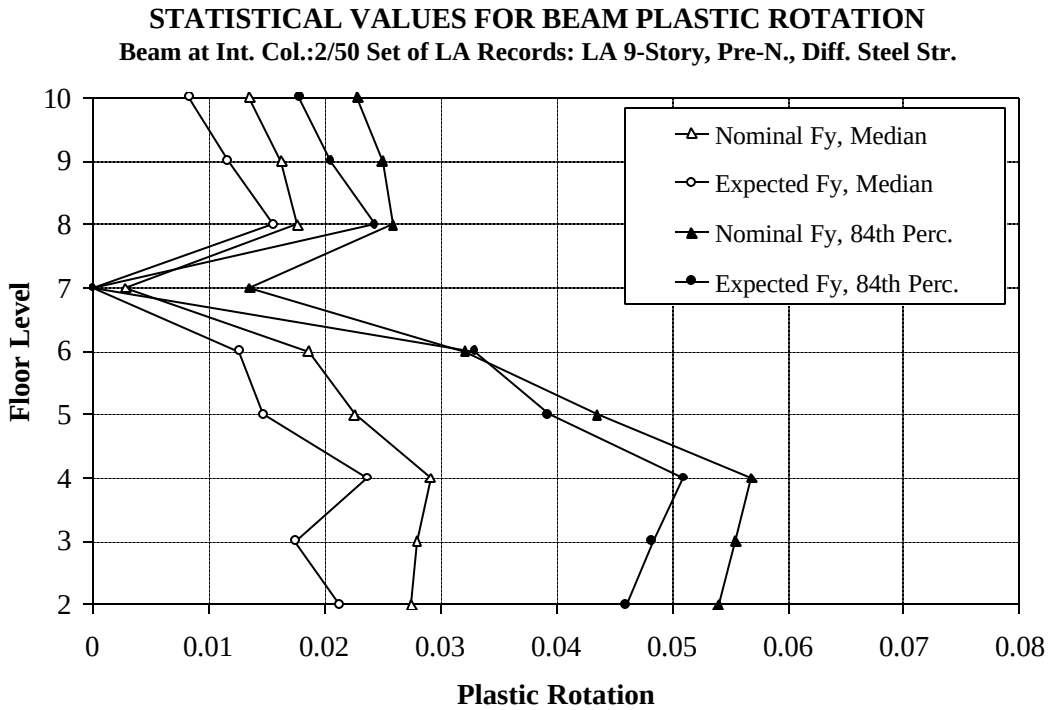

Figure 6.14 Beam (@ Interior Col.) Plastic Rotation Demands for LA 9-story Structure with Expected and Nominal Strength Properties; 2/50 Set of Ground Motions

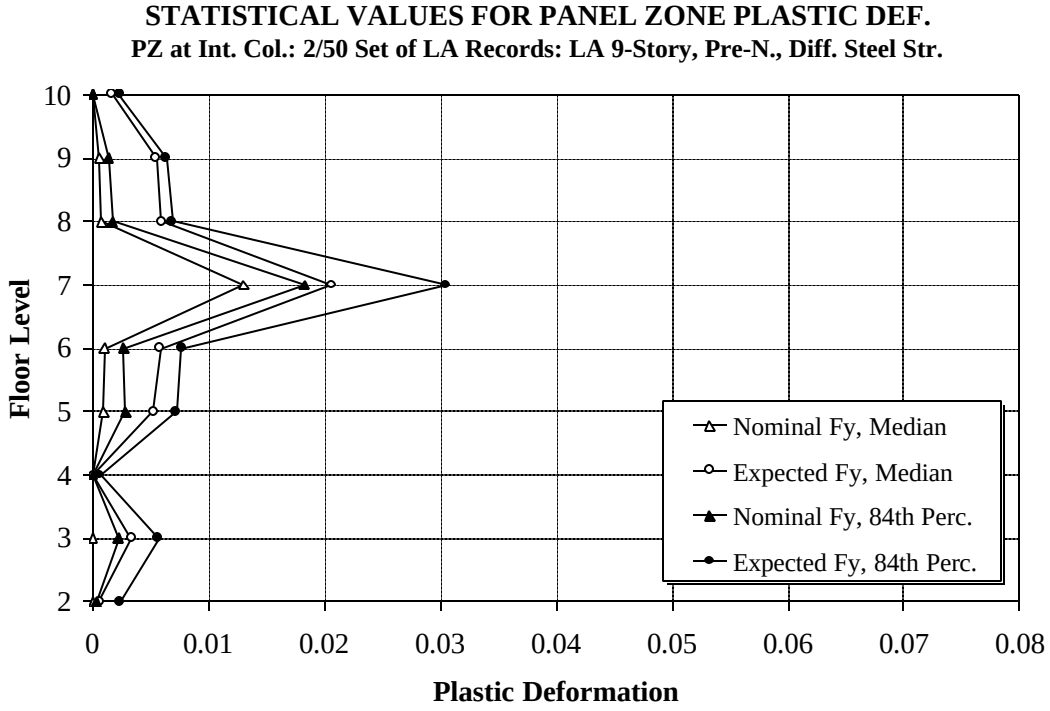

Figure 6.15 Panel Zone (@ Interior Col.) Plastic Deformation Demands for LA 9-story Structure with Expected and Nominal Strength Properties; 2/50 Set of Ground Motions

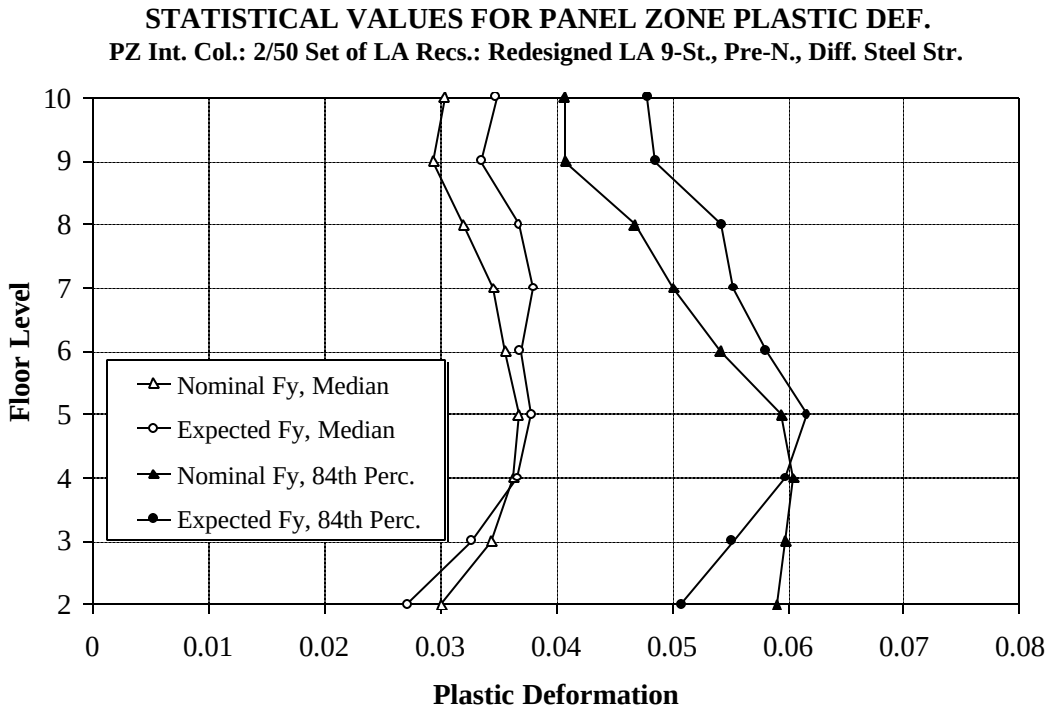

Figure 6.16 Panel Zone (@ Interior Col.) Plastic Deformation Demands for Redesigned LA 9-story Str., with Exp. and Nominal Strength Properties; 2/50 Set of Ground Motions

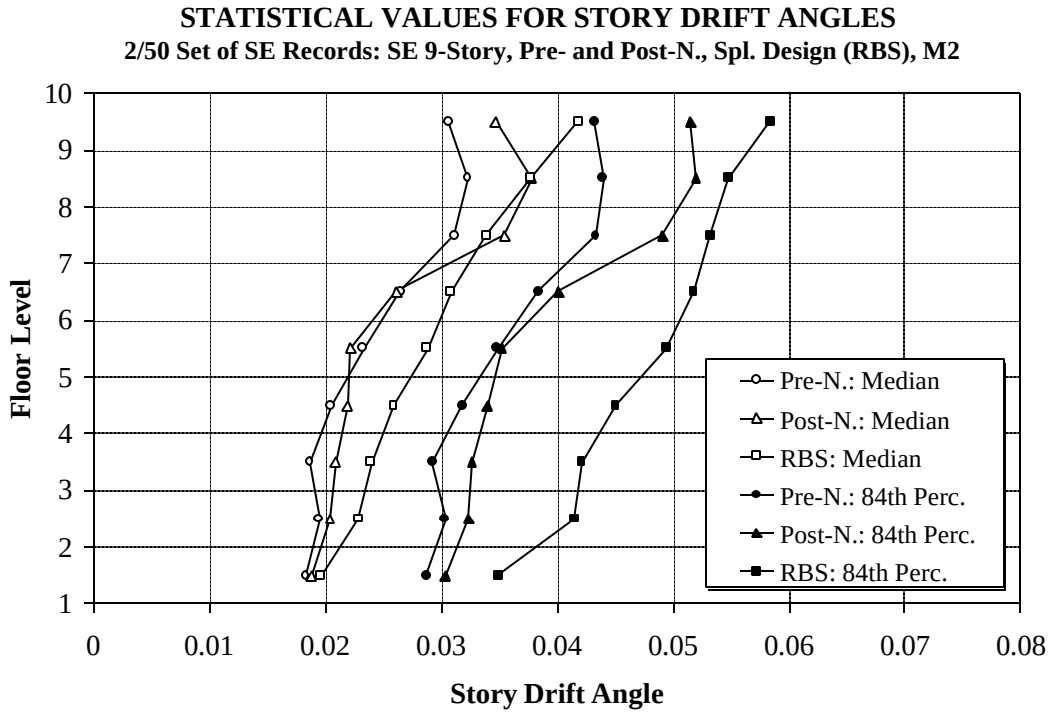

Figure 6.17 Story Drift Angle Demands for Seattle 9-story Pre-N., Cover-Plated Post-N., and RBS Design; 2/50 Set of Ground Motions

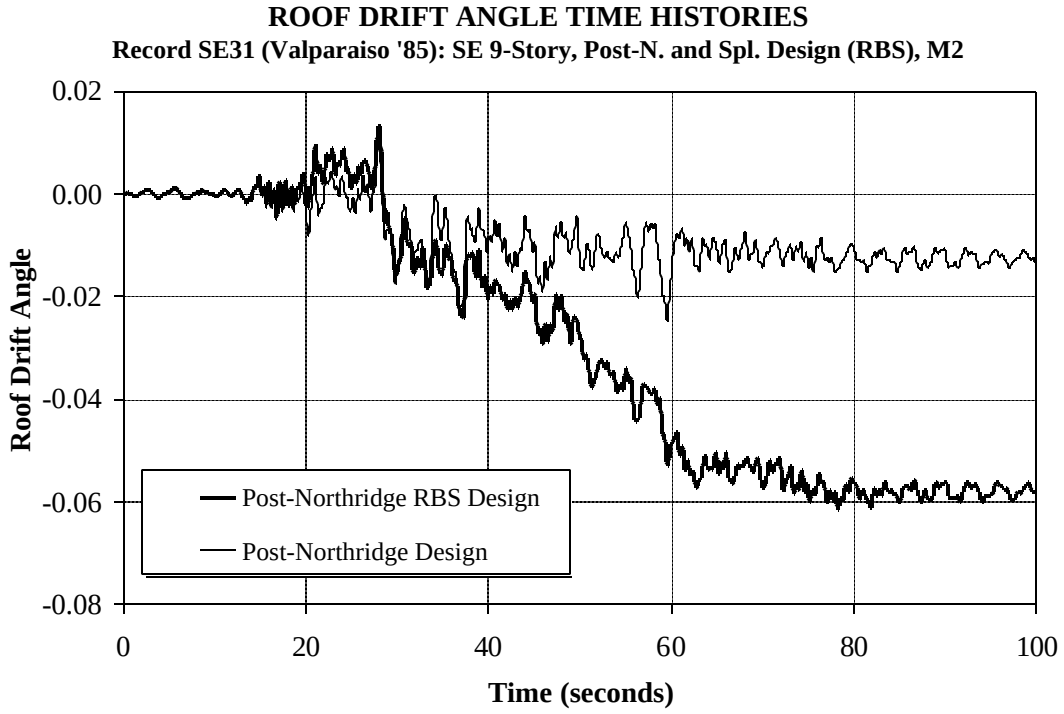

Figure 6.18 Roof Drift Time History of Response of Seattle 9-story Cover-Plated Post-N. and RBS Design; SE31 Ground Motion

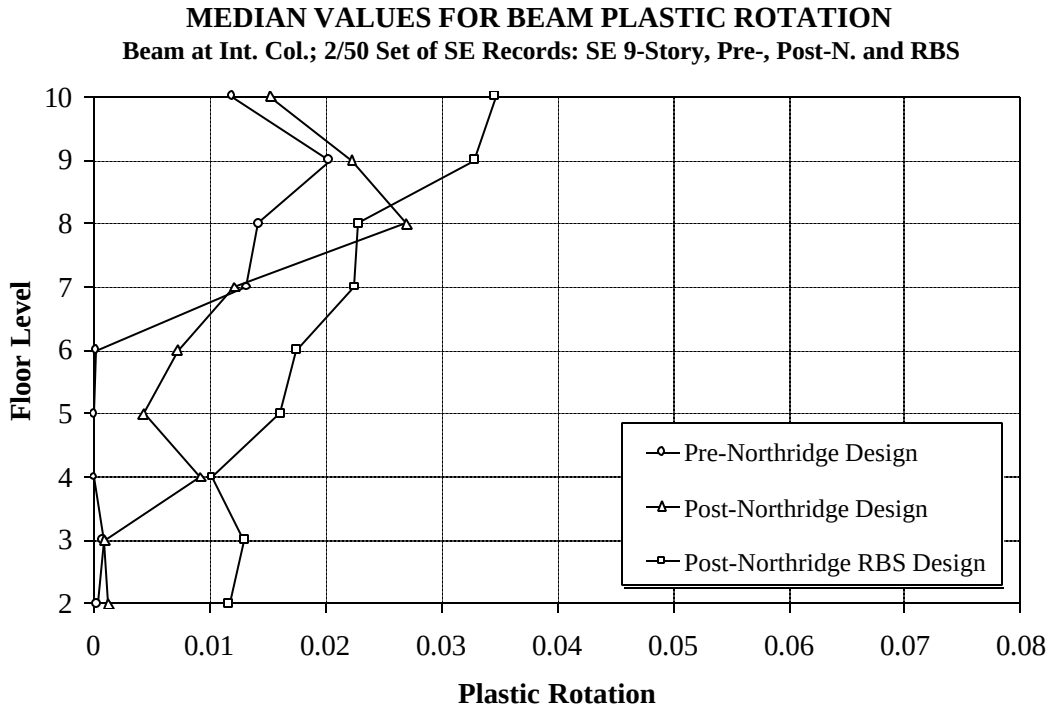

Figure 6.19 Beam (@ Interior Col.) Plastic Rotation Demands for Seattle 9-story Pre-N., Cover-Plated Post-N., and RBS Design; 2/50 Set of Ground Motions

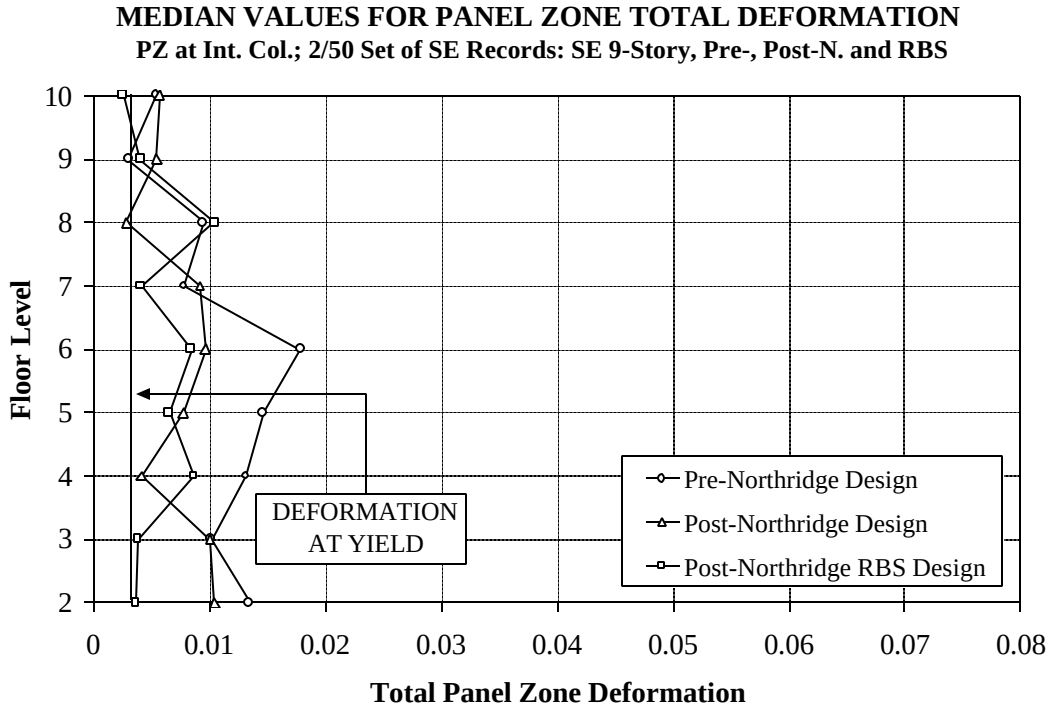

Figure 6.20 Panel Zone (@ Interior Col.) Total Deformation Demands for Seattle 9-story Pre-N., Cover-Plated Post-N., and RBS Design; 2/50 Set of Ground Motions

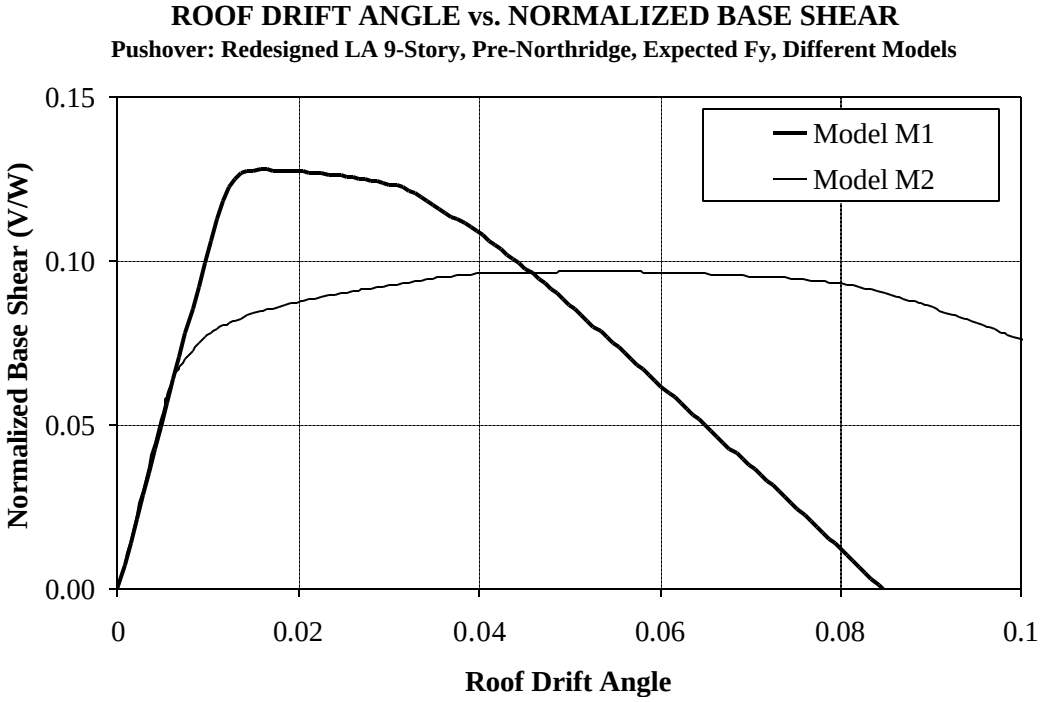

Figure 6.21 Global Pushover Curves for Redesigned LA 9-story Structure, for Different Analytical Models (M1 and M2)

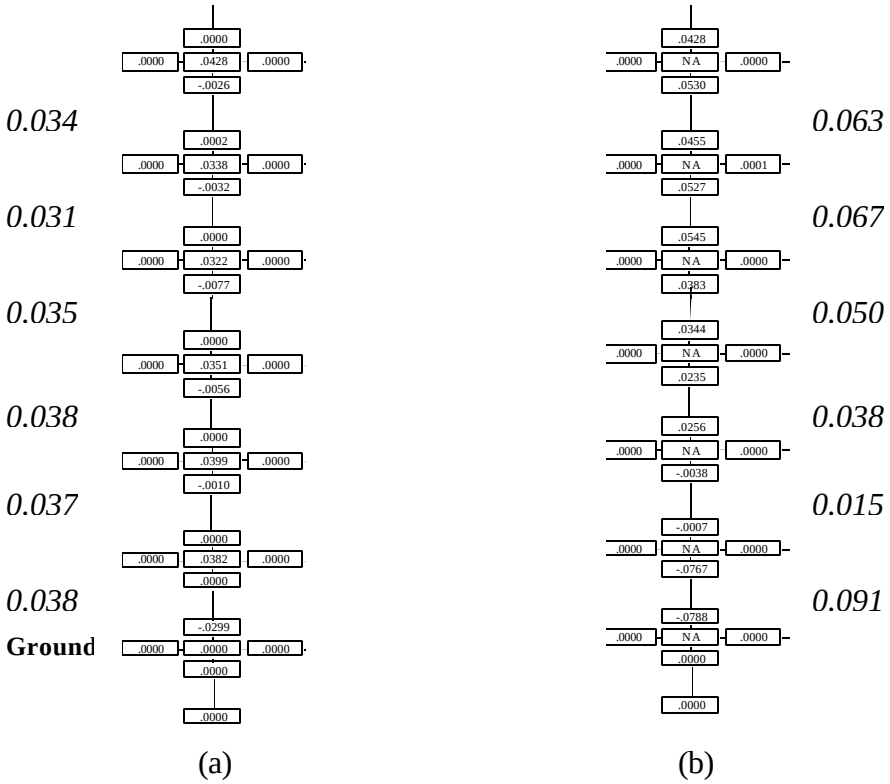

Figure 6.22 Story and Element Plastic Deformation Demands for Redesigned LA 9-story Structure (a) Model M2 and (b) Model M1; LA28 Ground Motion

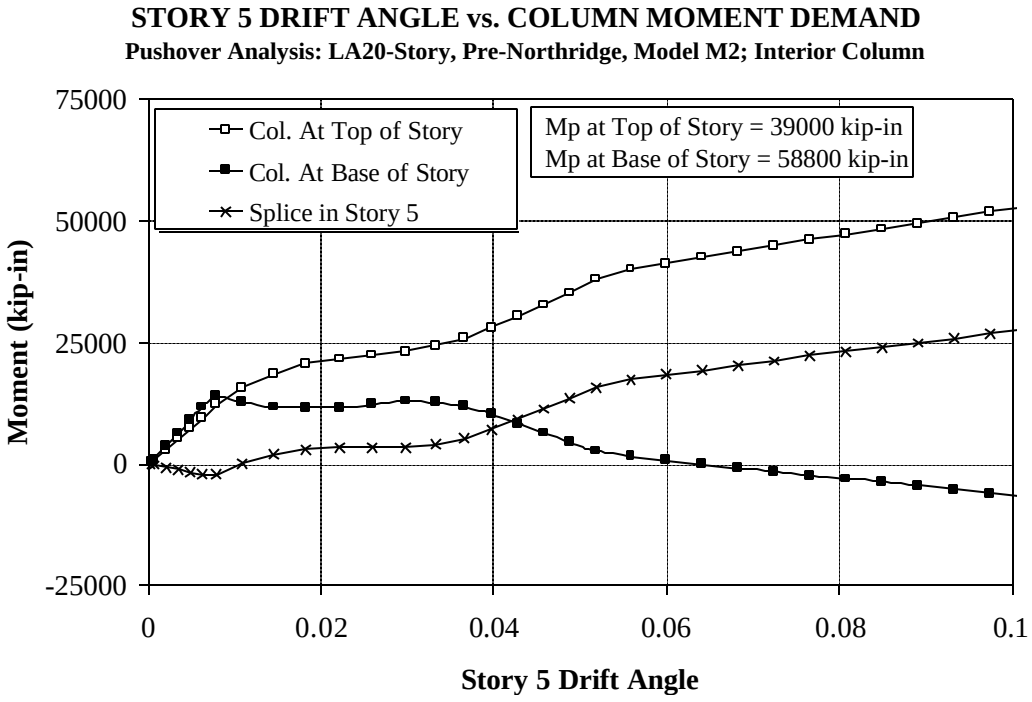

Figure 6.23 Variation of Bending Moment at Top and Base of Story 5 Interior Column with Increasing Story Drift, LA 20-story; Pushover Analysis

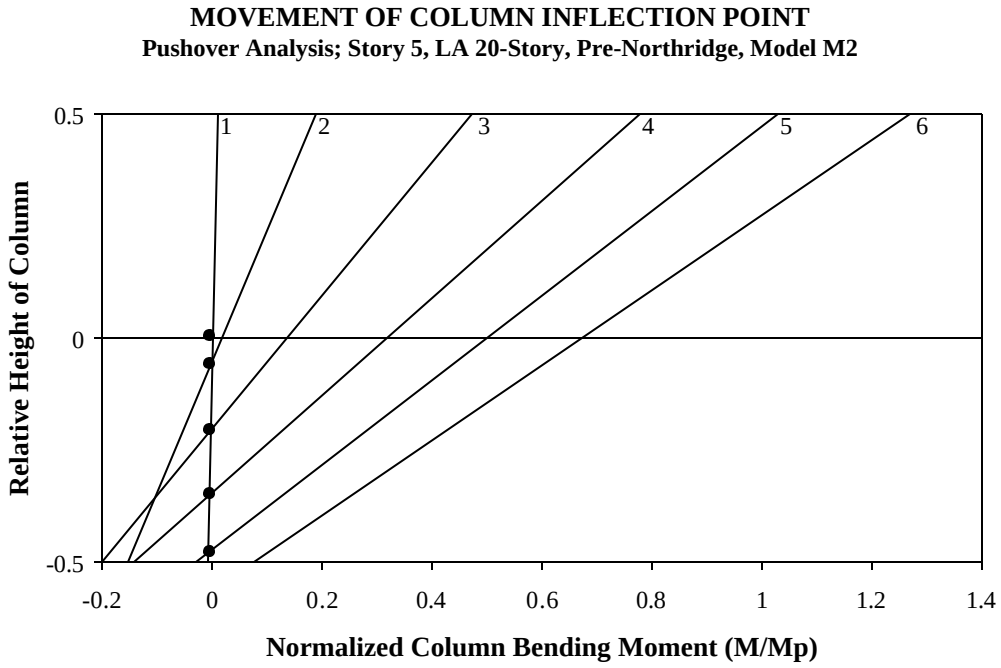

Figure 6.24 Movement of Column Inflection Point in Story 5 with Increasing Story Drift, LA 20-story; Pushover Analysis

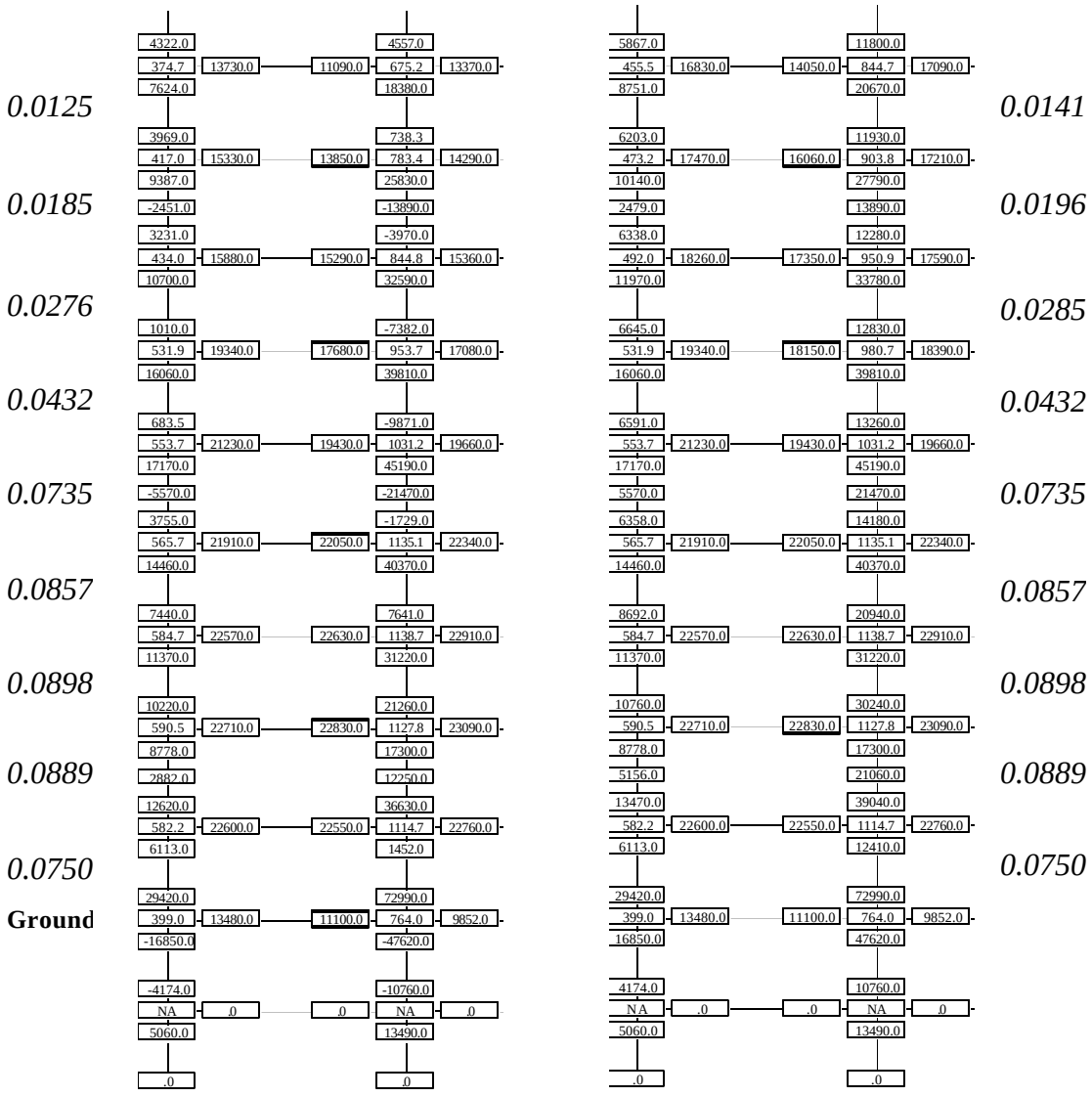

Figure 6.25 Element Force Demands and Story Drift Demands, LA 20-story Structure (a) at 0.03 roof drift, (b) envelope values till 0.03 roof drift; Pushover Analysis

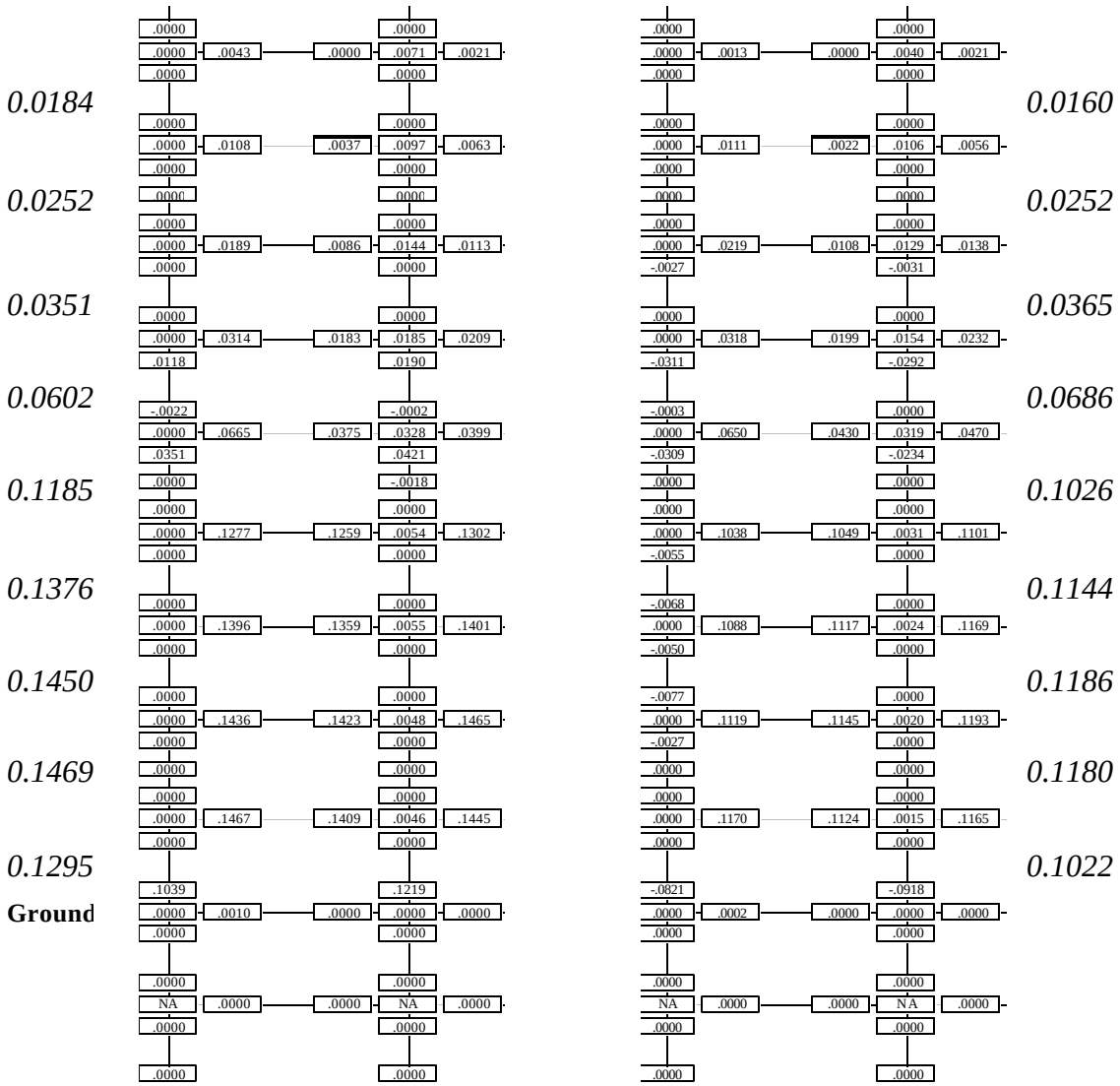

Figure 6.26 Element Plastic Deformation Demands and Story Drift Demands, LA 20-story Structure (a) LA30 (Tabas) Record, (b) LA36 (Simulated) Record

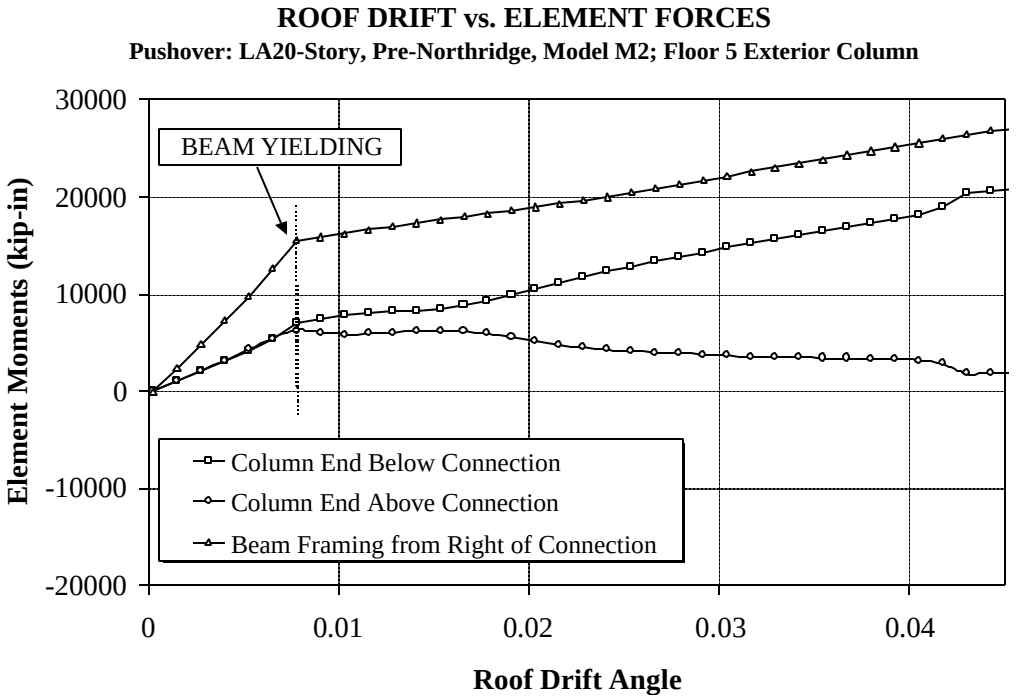

Figure 6.27 Change in Column Bending Moment Demand Above and Below Connection with Yielding in Beam, Exterior Column Line; Pushover Analysis

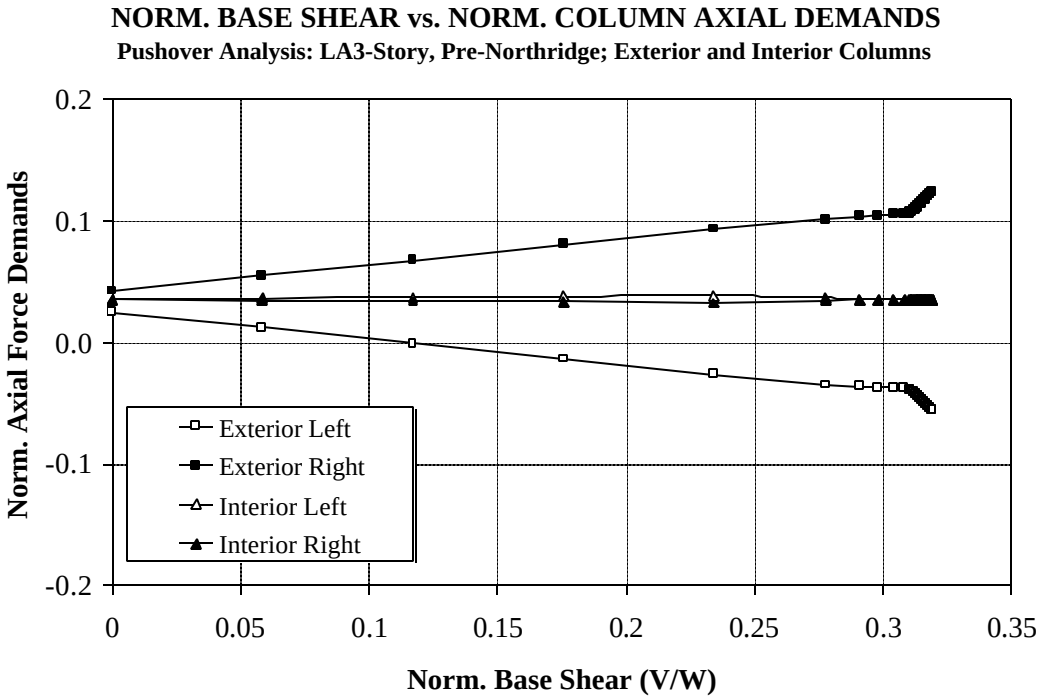

Figure 6.28 Variation of Story 1 Column Force Demands with Base Shear Demand, LA 3-story Structure; Pushover Analysis

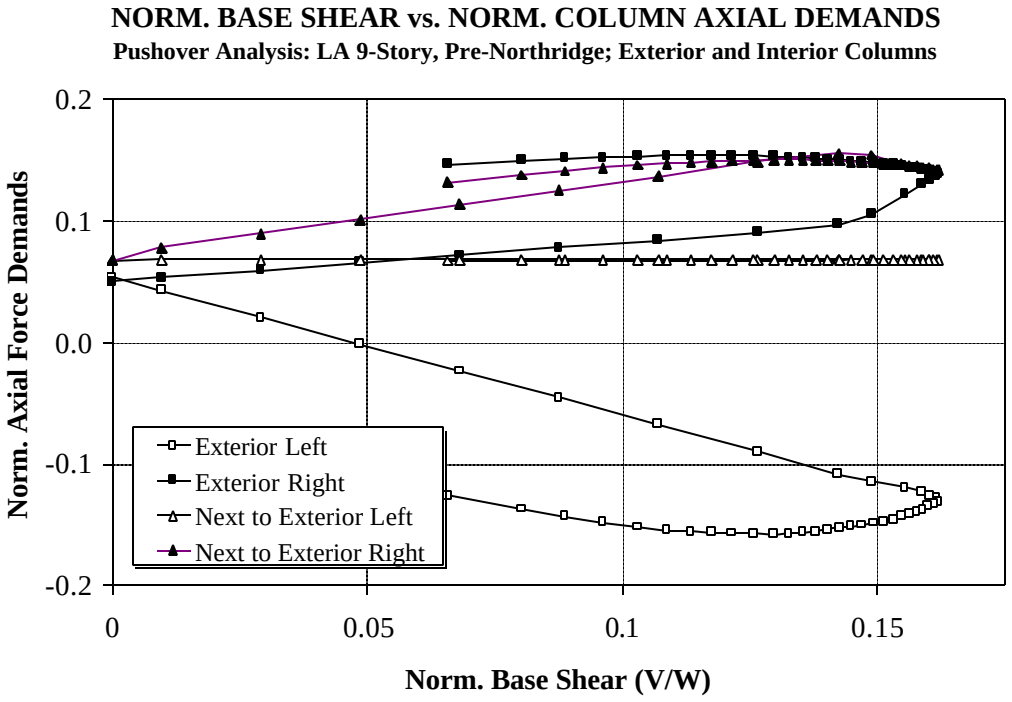

Figure 6.29 Variation of Story 1 Column Force Demands with Base Shear Demand, LA 9-story Structure; Pushover Analysis

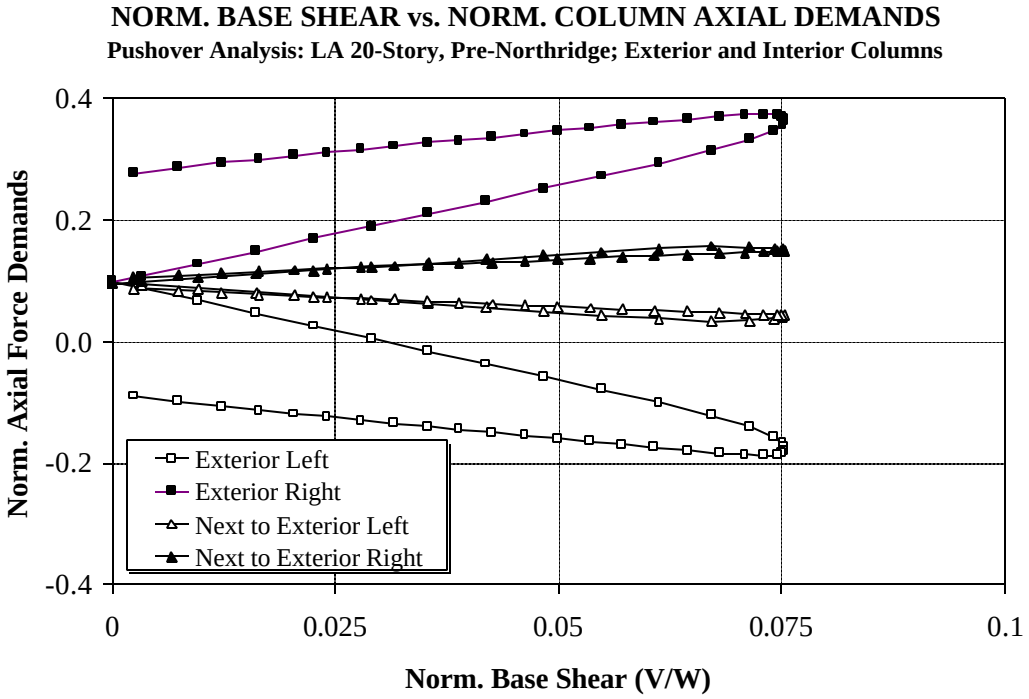

Figure 6.30 Variation of Story 1 Column Force Demands with Base Shear Demand, LA 20-story Structure; Pushover Analysis

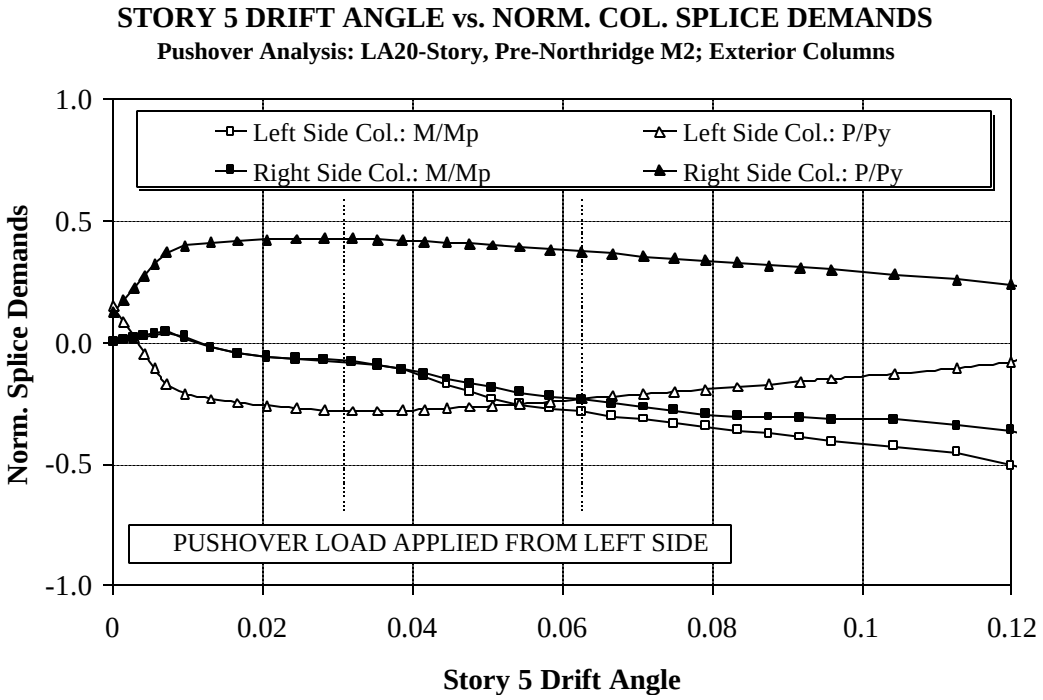

Figure 6.31 Variation of Normalized Force Demands for Exterior Column Splices in Story 5 with Increasing Story 5 Drift; LA 20-story; Pushover Analysis

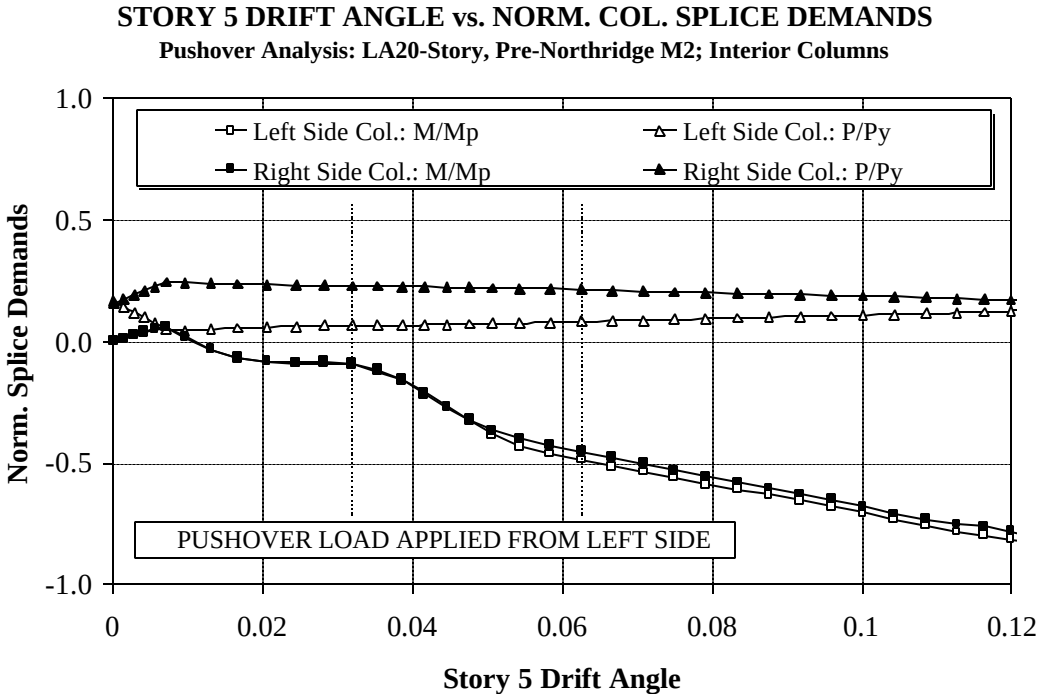

Figure 6.32 Variation of Normalized Force Demands for Interior Column Splices in Story 5 with Increasing Story 5 Drift; LA 20-story; Pushover Analysis

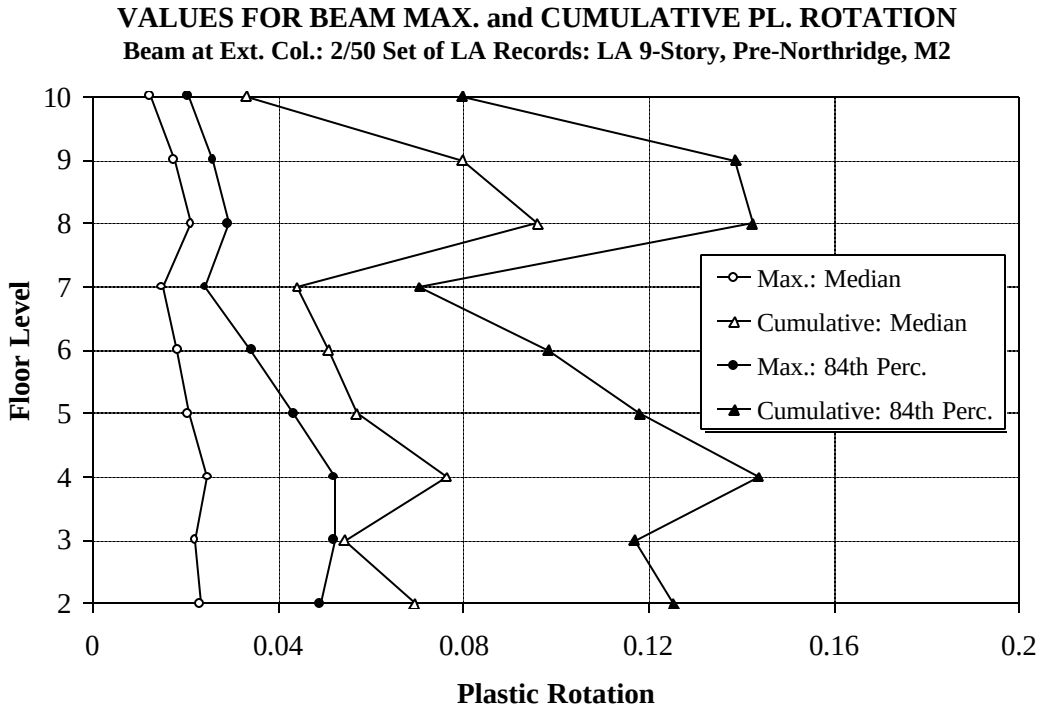

Figure 6.33 Statistical Values for Exterior Beam End Maximum and Cumulative Plastic Rotation Demands, LA 9-story Structure; 2/50 Set of Ground Motions

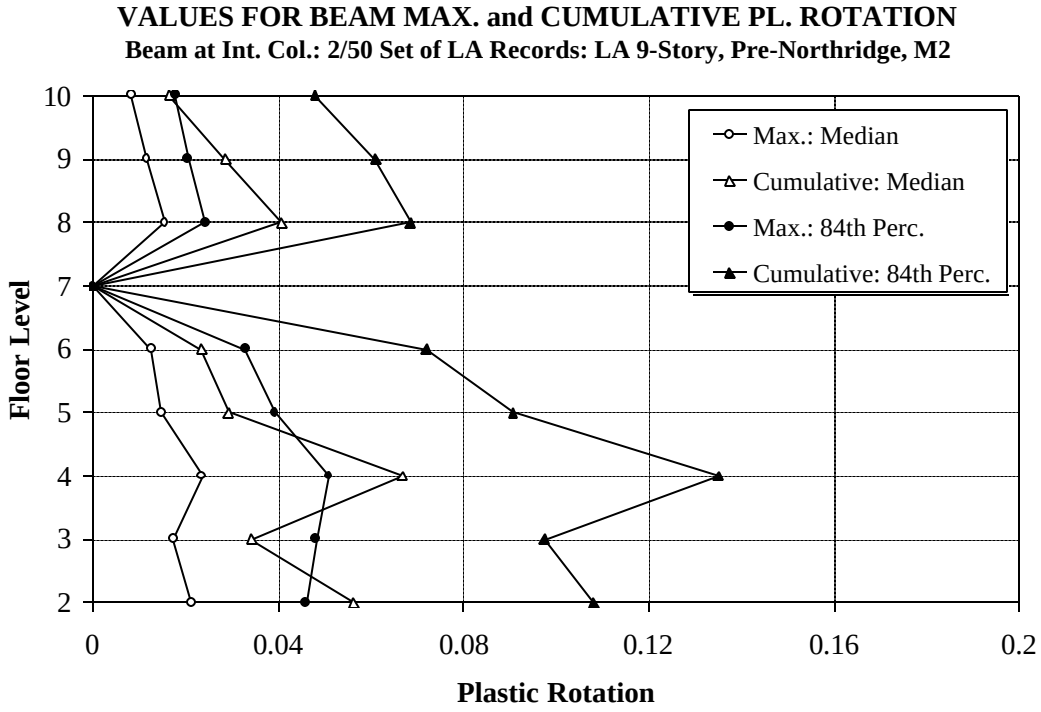

Figure 6.34 Statistical Values for Interior Beam End Maximum and Cumulative Plastic Rotation Demands, LA 9-story Structure; 2/50 Set of Ground Motions

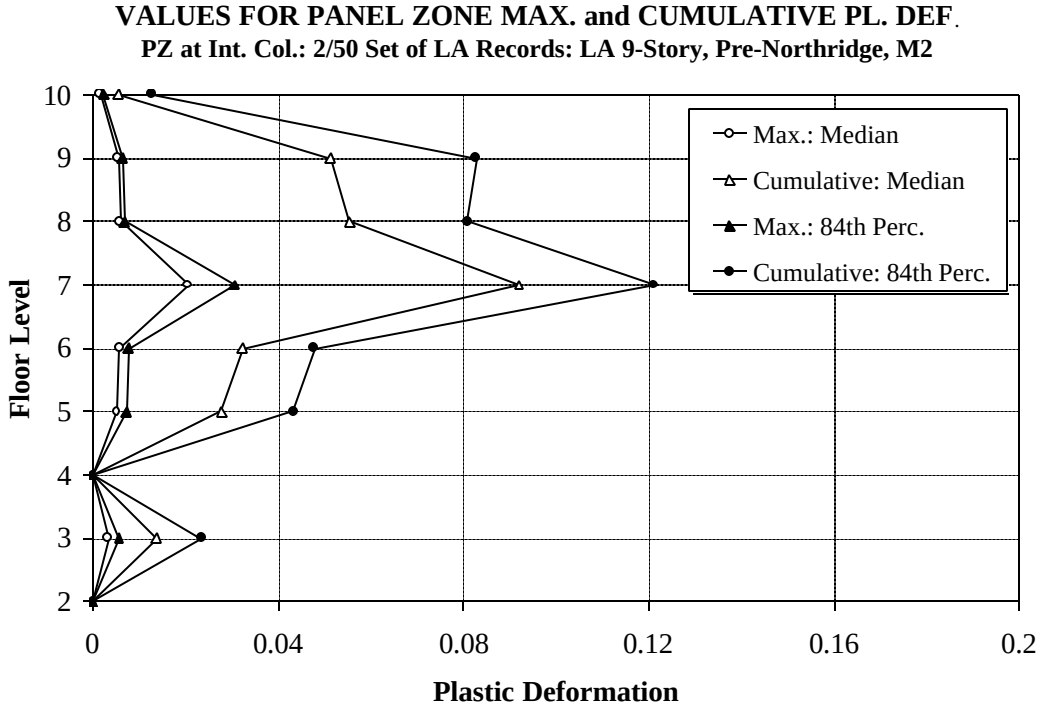

Figure 6.35 Statistical Values for Interior Panel Zone Maximum and Cumulative Plastic Deformation Demands, LA 9-story Structure; 2/50 Set of Ground Motions

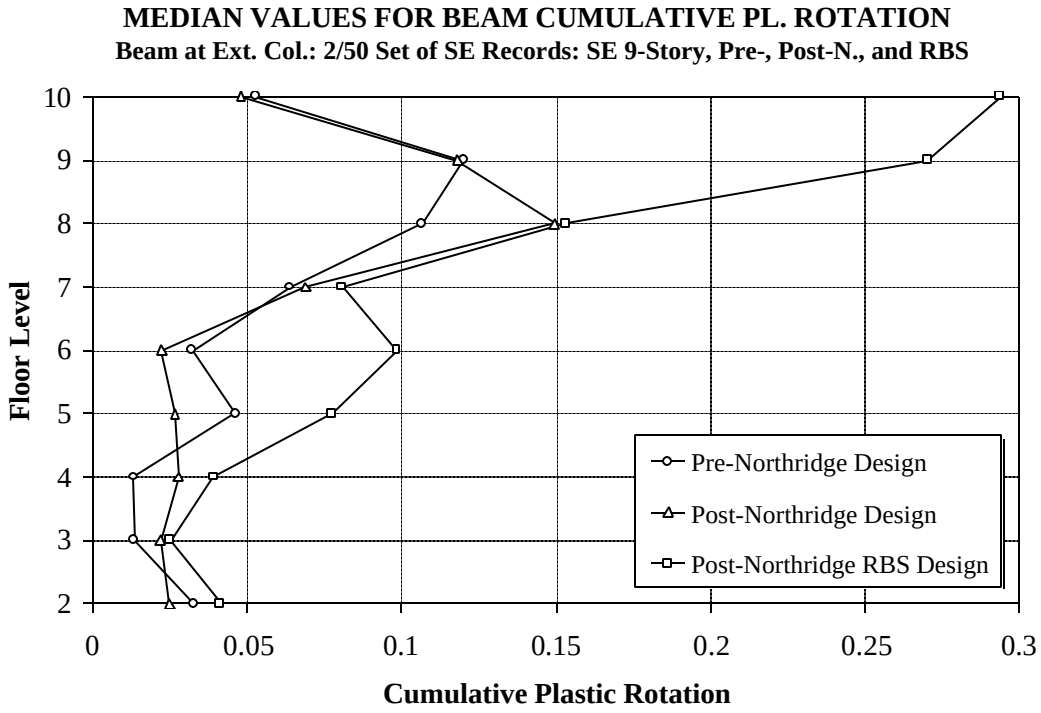

Figure 6.36 Statistical Values for Exterior Beam End Cumulative Plastic Rotation Demands, SE 9-story Structure, Different Designs; 2/50 Set of Ground Motions

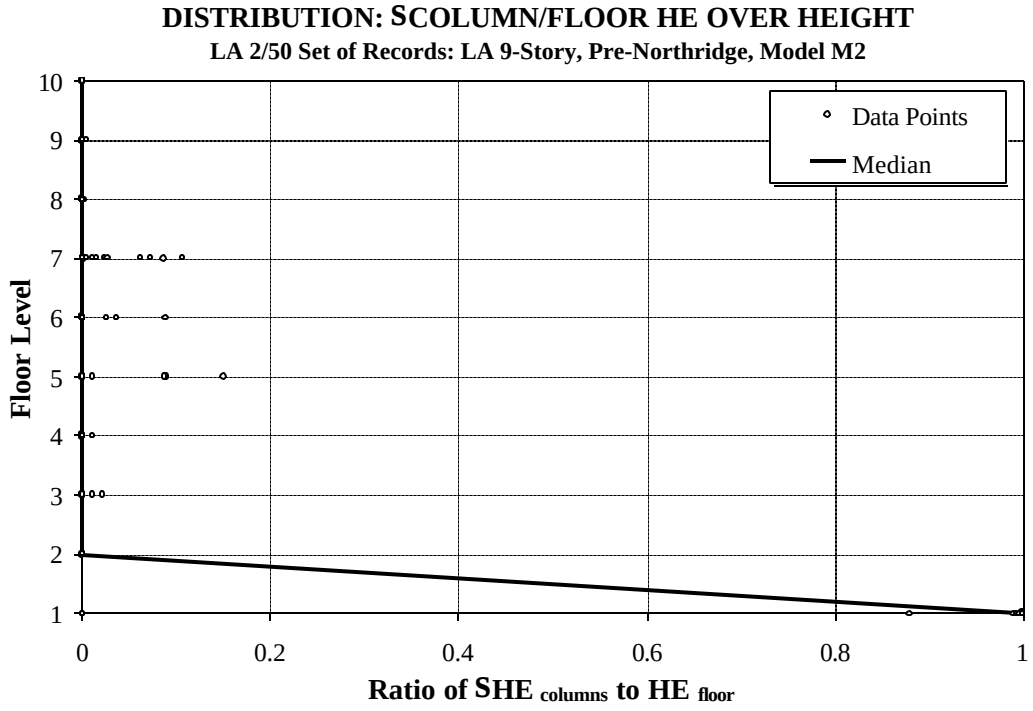

Figure 6.37 Median Values and Data Points for Fraction of Floor Hysteretic Energy Dissipated by Columns at Floor Level; LA 9-story Structure; 2/50 Set of Ground Motions

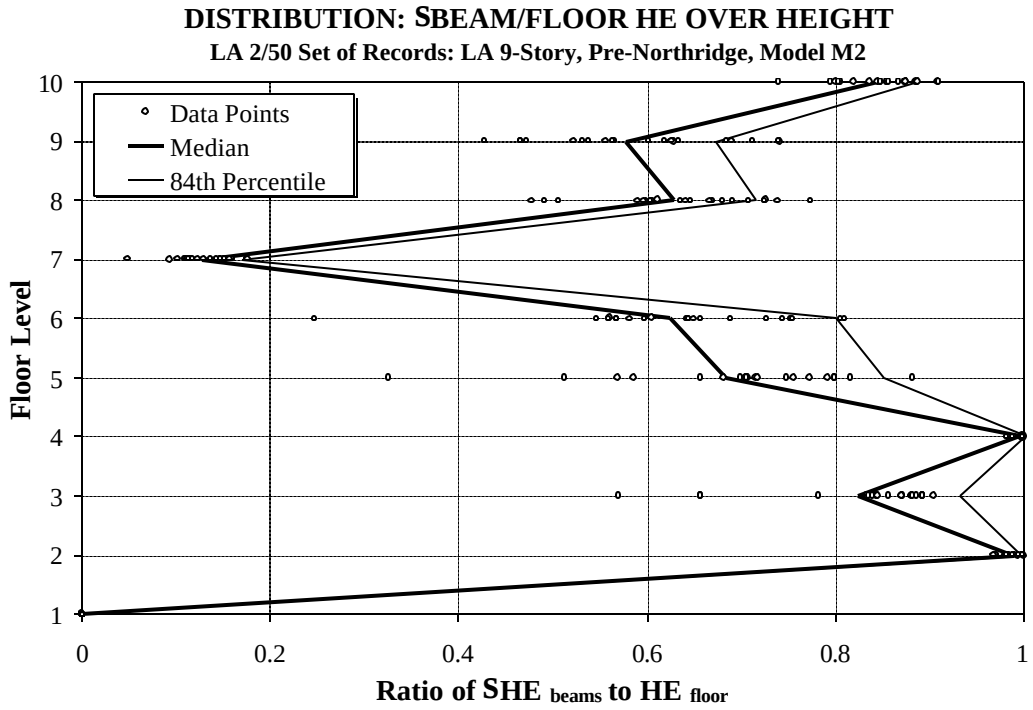

Figure 6.38 Statistical Values and Data Points for Fraction of Floor Hysteretic Energy Dissipated by Beams at Floor Level; LA 9-story Structure; 2/50 Set of Ground Motions

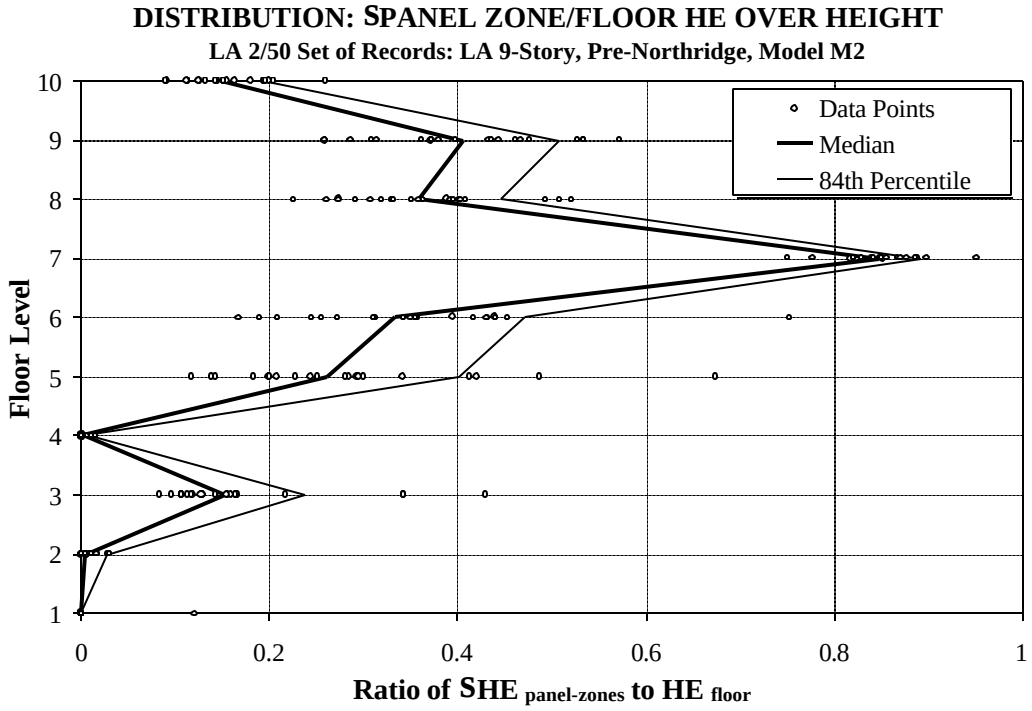

Figure 6.39 Statistical Values and Data Points for Fraction of Floor Hysteretic Energy Dissipated by Panel Zones at Fl. Level; LA 9-st. Structure; 2/50 Set of Ground Motions

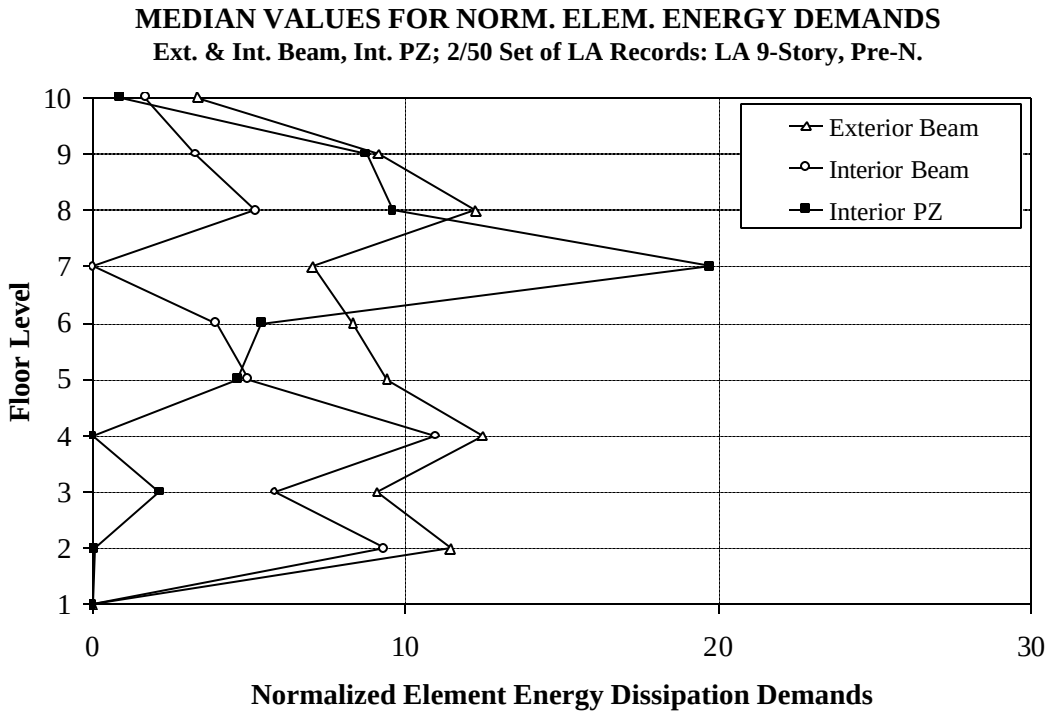

Figure 6.40 Median Values for Normalized Element Energy Dissipation Demands, LA 9-story Structure; 2/50 Set of Ground Motions

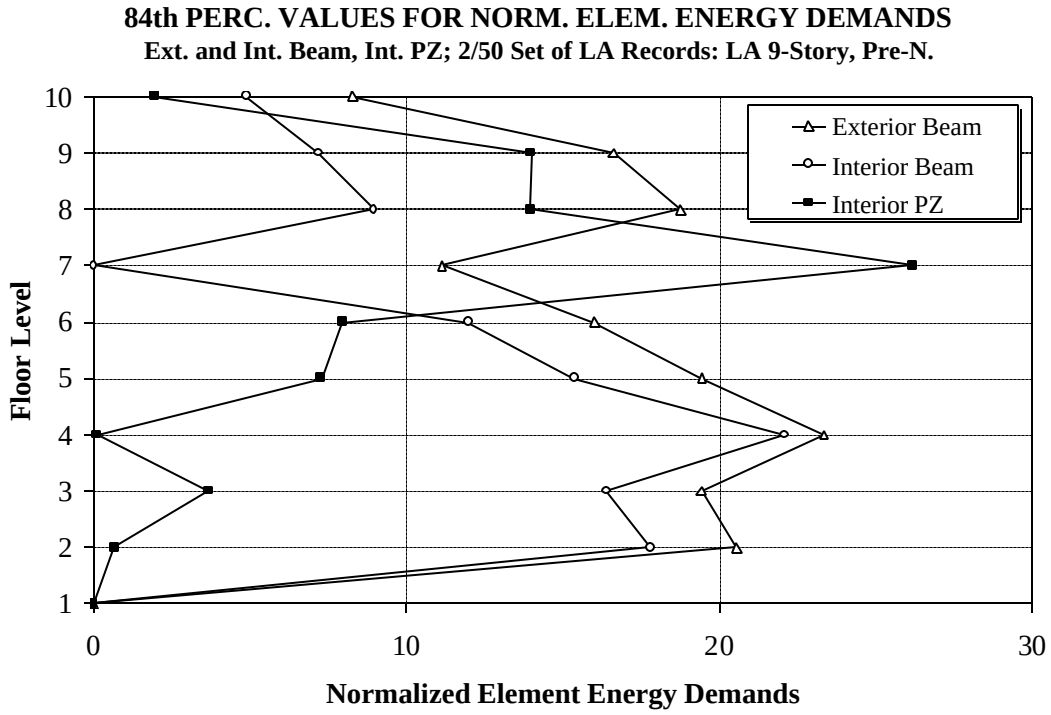

Figure 6.41 84th Percentile for Normalized Element Energy Dissipation Demands, LA 9-story Structure; 2/50 Set of Ground Motions

CHAPTER 7

ESTIMATION OF SEISMIC DEFORMATION DEMANDS

7.1 Introduction

The results presented in the previous chapters have shown that a nonlinear dynamic analysis is intrinsic to the process of quantifying the seismic demands on SMRF structures. Chapter 3 has also shown that the response of the structure may be very sensitive to the assumptions in the analytical model, and Chapter 4 has highlighted the importance of analysis and modeling accuracy in quantifying the response for P-delta sensitive structures. For essentially regular cases, however, the effort involved with the complicated modeling and analysis may not be warranted. Furthermore, in engineering practice the need is often to obtain quick approximate estimates for the system response, for various practical reasons. Thus, a simplified procedure for performance evaluation (estimation of seismic demands to be compared to capacities) of structures is desirable.

This chapter focuses on the development and testing of a simplified procedure for estimation of seismic deformation demands for steel moment resisting frame structures. The procedure uses elastic spectral information coupled with basic structural properties to obtain estimates for roof drifts, story drifts, and ultimately element (beams, panel zones) plastic deformation demands. The procedure is outlined in Figure 7.1 with the different modification factors or process being the following:

1. MDOF modification factor, α_{MDOF}: a factor that transforms elastic spectral displacement demand at the first mode period of the structure to global (roof) elastic drift demand for the multi-degree-of-freedom structure, neglecting P-delta effects

2. Inelasticity modification factor, α_{INEL}: a factor that transforms the roof elastic drift to the roof inelastic drift, without P-delta effects
3. P-delta modification factor, $\alpha_{P\Delta}$: a factor that transforms the inelastic roof drift demand to include structure P-delta effects
4. Story drift modification factor, α_{ST}: a factor or process that relates the story drift demand to the global drift demand
5. Element deformations modification function, α_{ELM}: a function that relates the story drift demand to the element plastic deformation demands

The simplified estimation of seismic deformation demands for MDOF steel and concrete structures has been the subject of much study [Fajfar and Fischinger (1988), Nassar and Krawinkler (1991), Qi and Moehle (1991), Collins (1995), Wen (1995), Seneviratna and Krawinkler (1997), Wen and Han (1997), Miranda (1997), FEMA 273 (1997)]. Though the studies differ in their approach and/or final goal (reliability assessment, code calibration, demand estimation), the common ground is the use of simplified elastic or inelastic SDOF (or 2-DOF) systems coupled with either pushover analysis or use of closed form solutions for simplified systems and loading conditions.

The study summarized in this chapter builds upon this expanse of information and extends the procedure to include P-delta effects and provide a series of steps to relate elastic spectral displacements to the element plastic deformation demands for steel MRF structures. The factors and processes identified in this procedure are based on extensive nonlinear dynamic analysis of a multitude of structures (using representative analytical models) of varying heights and located in different seismic locations. The structures are subjected to many suites of ground motions which are representative of different hazard levels at the different seismic locations. An important feature of the proposed procedure is its direct compatibility with the conceptual design procedure being developed by Krawinkler et al. (1991, 1997). Thus, the simplified procedure can be utilized for conceptual design and, in part, verification of the design.

In summary, the procedure provides a simplified means for the estimation of seismic deformation demands which, when coupled with estimates of capacities, yield information on the performance of the structure. The procedure may be useful for addressing parts of the conceptual design process, wherein the starting point is a targeted deformation demand at the element or story level from which the strength and stiffness requirements for the structure can be estimated.

The procedure has many limitations, which will be pointed out at appropriate places. For one, it is based on two-dimensional modeling of regular structures, which eliminates up front the consideration of irregularities in elevation and in plan. The latter implies that torsion is not an issue.

7.2 Estimation of Roof Drift Demand

The estimation of the inelastic roof drift demand inclusive of P-delta effects for the multi-degree-of-freedom system is carried out in three steps. The first step is concerned with the transformation of the elastic spectral displacement demand at the first mode period of the structure to the MDOF elastic roof drift demand without P-delta effects. The second step involves the transformation of the elastic roof drift demand to the inelastic demand, and the third step involves modification of the inelastic demand to include structure P-delta effects.

Time history analysis results from which appropriate modification factors can be derived are shown in Figures 7.2 to 7.18. Results are presented for all the Los Angeles, the 3-story Seattle, and the 9- and 20-story Boston pre-Northridge structures, using the previously discussed M2 models. Data points are shown for the 10/50 and 2/50 ground motion responses, using different symbols. For the Los Angeles structures different symbols are used also for the ten 2/50 recorded motions and the ten 2/50 simulated motions because in specific cases clear differences are observed in the responses to these two types of ground motions. Statistical data for LA structures are presented for four sets of records in order to evaluate modification factors based on all 40 records, the 20 10/50 records, the 20 2/50 records, and the 10 recorded 2/50 records, i.e., eliminating the 10 simulated 2/50 records. It should be noted that most of the Los Angeles 2/50 records are near-fault records (albeit rotated by 45 degrees with respect to the fault-normal direction) with pulse-type characteristics, which are particularly distinct in the 10 simulated records.

7.2.1 Step 1: Estimation of Elastic Roof Drift Demand Without P-Delta Effects

The expectation is that the roof displacement demand for an elastic MDOF system can be computed rather accurately by an appropriate combination of modal

displacements. For ground motions that do not have unusual characteristics it can be expected that the roof displacement is controlled by first mode vibrations. If this is the case, the transformation from the elastic spectral displacement demand at the first mode period, S_d, to the roof elastic drift demand should be closely related to first mode participation factor for the structure.

The relationships between the normalized spectral displacement at the first mode period of the structure (S_d/H, H being the height of the structure) and the elastic roof drift angle demand normalized by S_d/H, for the LA 3-, 9-, and 20-story pre-Northridge structures are shown in Figures 7.2 to 7.4. The ordinate represents the modification factor α_{MDOF}. The relationships have been obtained using elastic displacement spectra (see Appendix A) and maximum roof drifts from elastic time history analysis with the M2 models. The median values, the associated dispersion (written as the Std. Dev. of Logs), and the first mode participation factor for the structures are given on the figures.

The results for the 3-story structure, presented in Figure 7.2, show that the elastic roof drift demand can be related accurately to the normalized spectral displacement demand through the first mode participation factor. The transformation using the first mode participation factor is independent of the intensity of the ground motions, as shown by the very small scatter (dispersion value of 0.05) in the results. The simulated ground motions (LA31-40) also follow the same trend. Similar results are obtained for the Seattle 3-story pre-Northridge structure.

As the height of the structure is increased to 9- and 20-stories, the dispersion associated with the results increases and the median values exceed the first mode participation factor, indicating increased higher-mode participation. The results shown in Figure 7.3 for the LA 9-story structure indicate a well contained response, except for one outlier. This outlier is caused by record LA31, which has a spectral displacement demand of 14.1 inches at the first mode period, while the spectral displacement demand at the second mode period is 21.2 inches. The influence of higher modes is reflected in the median amplification factor being about 10% larger than the first mode participation factor. Again, the statistical values are virtually independent of the severity of the ground motions, and of the presence of the 10 simulated ground motion records.

The response of the LA 20-story structure shows similar trends as observed for the 9-story structure, as can be seen by comparing Figures 7.3 and 7.4. The only difference is a

clearer pattern of higher amplification factors at lower displacement demand levels. This is reflected in the slightly larger median value of the MDOF modification factor for the 10/50 set of ground motions compared to the 2/50 set (1.58 versus 1.51). This difference suggests that higher mode effects contribute more to the response under the lower intensity ground motions (10/50 set) than to the response under severe ground motions (2/50 set).

The importance of higher mode effects on elastic roof displacements is clearly visible in the response of the Boston 9- and 20-story structures, as shown in Figures 7.5 and 7.6. There is a clear pattern between the magnitude of the spectral displacement demand and the normalized roof drift demand. The amplification increases with decreasing first mode spectral displacement demand. An inspection of the displacement spectra shows that for many of the Boston records the spectral displacement at higher mode periods is clearly larger than that at the first mode period.

In conclusion, a good but usually low estimate of the roof displacement of elastic MDOF systems is the first mode spectral displacement multiplied by the first mode participation factor - **unless higher mode displacements are large**. The latter holds true for most of the Boston records. The so obtained estimate is reasonable also for the near-fault records contained in the LA 2/50 set of records. For such records this conclusion cannot be generalized because studies by others have shown that fault-normal components of near-fault records may be greatly affected by higher mode effects if the structure period is significantly larger than the period of the pulse contained in the near-fault record (Alavi and Krawinkler, 1998).

Thus, with the exceptions noted, the roof drift demand for elastic MDOF structures without P-delta effect, $q_{el,no\text{-}PD,MDOF}$, can be predicted using the following simple equation:

$$q_{el,no-P\Delta,MDOF} = \alpha_{MDOF} \times \left(S_d / H \right) \tag{7.1}$$

An estimate of α_{MDOF} is given as:

$$\alpha_{MDOF} = \begin{bmatrix} 1)\ PF_1 \text{ for low - rise structures} \\ 2)\ 1.1 \times PF_1 \\ \quad \text{for medium - and high - rise structures} \end{bmatrix} \tag{7.2}$$

where PF_1 is the first mode participation factor, and the factor 1.1 gives some credit to higher mode effects in long period structures. For ground motions with large higher-mode spectral displacements this approach results in a poor approximation for the roof drift demand. Appropriate modal combinations should be used in such cases; it was not investigated whether an SRSS combination is adequate. The values obtained in this study are in good agreement with other studies referenced previously.

An important consideration in this process is the estimation of the first mode period of the structure. Present design codes usually provide very low values for the period of SMRF structures, which may result in a severe underestimation of the S_d values. For period determination for the purpose of obtaining drift estimates, an eigenvalue analysis with the best estimate of the stiffness of the structure is the preferred approach.

7.1.2 Step 2: Estimation of Inelastic Roof Drift Demand Without P-Delta Effects

For structures responding in the inelastic range, the elastic roof drift demand estimated in Section 7.2.1 needs to be modified to represent the inelasticity in the structure. This modification is carried out using the factor α_{INEL}.

The effect of inelasticity on the response of a structure can be studied at the SDOF level or the MDOF level. For bilinear SDOF systems the median values (using the 10/50 and 2/50 sets of LA ground motions) of the factor α_{INEL} as a function of the period of the SDOF system, for ductility ratios of 2 and 4, are as shown in Figure 7.7. In the short period range the median inelasticity factor is sensitive to the level of inelasticity, and a rapid amplification of demands for very short period systems is evident. However, in the range of periods applicable to most steel structures the median SDOF inelasticity factor is almost independent of the level of inelasticity in the system and of the period of the system, and has a value less than 1.0. Furthermore, the median is insensitive to the ground motion set, with the value for the 2/50 set of ground motions being very similar to

the value for the 10/50 set. Even though not shown, the response to the Seattle sets of ground motions is very similar to the response to the LA sets of ground motions.

The inelasticity factor is, however, associated with significant dispersion as seen from Figure 7.8. The dispersion increases with the level of inelasticity in the system, but is not much affected by the period of the system. Removal of the simulated ground motions from the data set did not much affect the results for periods greater than 1.0 second, but reduced the median inelasticity factor and the associated dispersion at 1.0 second and lower periods. The maximum effect is felt in the neighborhood of 1.0 second period, which can be attributed to the process of generation of simulated records (Somerville et al., 1997). Different methods were employed for ground motion generation in the short and long period ranges, with the period of 1.0 seconds being the dividing line.

Data points for the inelasticity factor of the LA 3-, 9-, and 20-story M2 models subjected to the 10/50 and 2/50 ground motion sets are presented in Figures 7.9 to 7.11. The figures show the ratio of inelastic roof drift to elastic roof drift (definition for a_{INEL}) plotted against the elastic roof drift angle demand. For the 3-story structure the median inelasticity factor for all 40 records is 0.87, but the associated dispersion is quite high at 0.43 (see Figure 7.9). There are several outliers, mostly from the simulated 2/50 records. Considering only the 20 2/50 records, the dispersion is even larger (0.56), but removing the 10 simulated records from this set reduces the dispersion to 0.39. The dispersion for the 20 10/50 records alone is rather small (0.21), and the medians for the complete 10/50 set and the stripped 2/50 set (with the 10 simulated motions removed) are almost identical (0.80 vs. 0.79). Thus, the results show consistent behavior with acceptable dispersion if only the recorded ground motions are used.

Figures 7.10 and 7.11 show inelasticity factor values for the LA 9- and 20-story structures, respectively. For very low roof drift demand, the factor is close to unity, which is to be expected as the response is almost linear. The median values for the two structures are about the same, with the dispersion for the 9-story being slightly higher than for the 20-story. The statistical values for either of the structures is only slightly affected by the removal of the simulated ground motions from the data set. For both structures the lowest median values for a_{INEL} are obtained for the 2/50 record set, which indicates a slight decrease of the inelasticity factor for highly inelastic systems.

The trend of a decreasing inelasticity factor with an increase in roof drift demand is discernible in all three structures (disregarding the response to the 10 simulated motions). The reason is believed to be the concentration of drift demands in one or few particular stories, which leads to a reduction in roof inelastic drift demand. Although this trend is not very strong, it is noticeable and indicates a dependence of the inelasticity factor on the extent of inelasticity, which is not noted in the SDOF information presented in Figure 7.7.

Based on the observations summarized here, and similar information from other studies that used generic representations for MDOF systems (e.g., Seneviratna and Krawinkler, 1997), the value for the inelasticity factor of structures with periods greater than about 1.0 seconds subjected to 10/50 and 2/50 ground motions can be estimated as follows:

$$a_{INEL} = \begin{bmatrix} 1)\ 0.80, \text{ or} \\ 2)\ \text{as obtained from SDOF inelastic analysis, or} \\ 3)\ 1.00, \text{ conservatively} \end{bmatrix} \tag{7.3}$$

These estimates are mean value estimates. It appears that the estimates are rather insensitive to the design details of the structure and to the ground motion characteristics, provided that the ground motions are of the type contained in the 10/50 and 2/50 sets.

For systems with a first mode period significantly shorter than 1.0 seconds, at least an SDOF system analysis is recommended. An equation relating the inelasticity factor to the period and ductility of the SDOF system, for firm alluvium sites, is given in Miranda (1997).

In the context of presently used professional guidelines it is of interest to compare the roof inelastic drift values obtained from time history analysis of the LA structures with predictions used for the nonlinear static procedure recommended in the FEMA 273 document (FEMA 273, 1997). The FEMA document recommends to estimate the roof inelastic displacement (without P-delta effects) as the product of first mode elastic spectral displacement and two coefficients C_0 and C_1. C_0 may be taken as the first mode participation factor PF_1, and C_1 may be taken as 1.0 for the period range of the LA

structures. Thus, the product amounts to PF_1, which varies within the narrow range of 1.30 and 1.38 for the three LA structures. Using the procedure outlined here, the product $a_{MDOF} \times a_{INEL}$ corresponds to the product $C_0 \times C_1$. Data points and statistical values of $a_{MDOF} \times a_{INEL}$ are presented in Figures 7.12 to 7.14 for the three LA pre-Northridge structures. Disregarding the simulated records, the median values of this product are between 1.0 and 1.15, and the dispersion is between 0.12 and 0.39. Thus, the median values of the data points are consistently lower than the values predicted from the FEMA-273 approach. The differences come primarily from the fact that the inelasticity factor is taken as 1.0 in the FEMA 273 approach, whereas it is approximately 0.8 for the LA structures. If this 0.8 factor is incorporated in the predictions, then the match between predictions and computed median values is very good.

This match between FEMA 273 predictions and the LA structure response data is encouraging, particularly if it is considered that the inelasticity factor is intentionally ignored in the FEMA 273 approach if it is smaller than 1.0, for reasons discussed in Section 7.3. In conclusion, the roof displacement of inelastic but "essentially regular" frame structures can be predicted with reasonable confidence from the spectral displacement of the first mode elastic SDOF system – if no significant P-delta effects are present.

7.1.3 Step 3: Estimation of P-Delta Effects on Inelastic Roof Drift Demand

The effects of P-delta on the response of flexible structures has been discussed in detail in Chapter 4. The P-delta effect also introduces complications in the estimation of roof drift demands, particularly for structures that attain a negative post-yield stiffness (e.g., the LA 20-story and the SE 3-story structures).

The effect of P-delta on the inelastic roof displacement is represented by the factor a_{PD}, defined as the ratio of the inelastic roof displacement with and without P-delta effects. Data and statistical values of this factor for the three LA structures and the 3-story Seattle structure are presented in Figures 7.15 to 7.18.

For structures that do not attain a negative post-yield stiffness, e.g., the LA 3-story structure, the effect of P-delta on the inelastic roof displacement is well contained. In most cases P-delta leads to an increase and in some cases to a decrease in roof

displacement, depending on the frequency content of the ground motion. P-delta always reduces the effective lateral stiffness and thus increases the effective period, leading to a shift in the ground motion frequency content affecting the structure. For the LA 3-story structure, in which the P-delta effect results in the reduction of the post-yield stiffness from about 3% to about 0% of the elastic stiffness, the increase in roof displacement is as high as 25% for specific records (see Figure 7.15). However, the median increase is very small and the P-delta factor is insensitive to the severity of ground motions and the level of drift demands.

The P-delta factor for the LA 9- and 20-story structures is shown in Figures 7.16 and 7.17, respectively. Both figures show similar trends which can be summarized as follows:

- The response is well contained even when P-delta effects are included, provided the ground motion does not drive the structure into the range of negative post-yield stiffness (roof drift angle of approximately 0.035 for the 9-story and 0.015 for the 20-story structure),
- there is no clear pattern to the P-delta factor when the range of negative post-yield stiffness is entered (stability sensitive range), because the response becomes very sensitive to ground motion characteristics (e.g., at a roof drift demand without P-delta of about 0.022 the 20-story structure exhibits P-delta factors of 0.61, 0.96, and 1.95 for three different records), and
- the dispersion associated with the 2/50 set of ground motions is larger than the dispersion for the 10/50 set of ground motions.

The response for the Seattle 3-story structure, shown in Figure 7.18, shows similar trends as observed for the LA 20-story structure. When the drift demands without P-delta exceed the value associated with the onset of negative stiffness (around 0.045), some records result in a very high value of the P-delta factor whereas others do not.

The conclusion from the presented results is that P-delta is a ground motion sensitive effect. When the range of negative post-yield stiffness is not entered, P-delta effects may increase or decrease the roof drift demands, but the P-delta factor is small in average and for the cases studied does not exceed 1.3 for individual ground motions. When the negative stiffness range (stability sensitive range) is entered, drift amplifications may become very large, and only a time history analysis will tell the amount of amplification.

Thus, a small α_{PD} factor can be used for the former case, and the latter case should be prevented whenever possible.

The solution to this problem is to provide a structural system that will not enter the range of negative stiffness for the range of ground motions anticipated at the site. This can be achieved with a back-up system that assures positive post-yield stiffness even after a mechanism has formed in the primary lateral load resisting system. The need for such a back-up system can be assessed from a pushover analysis that evaluates the lateral stiffness at the roof displacement associated with the most severe ground motion anticipated at the site (see Chapter 4).

Results presented earlier indicate that a pushover analysis is a rather reliable means of detecting the drift demand associated with the onset of negative post-yield stiffness. There are two considerations associated with this procedure; the first concerned with the choice of load pattern, and the second concerned with the choice of analytical model to be used for the pushover analysis.

Load patterns considerations are illustrated in Figures 7.19 and 7.20, which show the model M2 global (roof) pushover curves for the two P-delta sensitive structures, the LA 20-story and the Seattle 3-story structure, respectively. The curves are obtained for three different load patterns. In addition to the NEHRP pattern (see Section 3.5) used in this study, a triangular pattern including the UBC '94 roof load, and a uniform load pattern are used to evaluate the sensitivity of the response to the applied load pattern. For both structures the uniform load pattern leads to higher strength but to a smaller drift associated with onset of negative stiffness, compared to the two other load patterns. Since P-delta sensitivity is observed only at drifts larger than the onset drifts predicted by the NEHRP or triangular load patterns, the use of either one of these two patterns is recommended for this purpose. These two patterns demand higher shear strength in the lower stories, which are usually the critical ones for P-delta control.

The second consideration relates to the analytical model to be used for the pushover analysis. The influence of modeling assumptions on the drift associated with onset of the negative post-yield stiffness is discussed in Section 3.5.1. An M1 model of the bare moment frames alone will generally provide the lowest estimate of this reference drift. Such a model may be adequate if it shows that the P-delta sensitive range in not entered at the maximum anticipated roof displacement. Otherwise more refined models will have

to be used, with preference given to a model that accounts for all dependable contributions to lateral strength and stiffness (M2A model).

To summarize, the inelastic roof drift angle for an MDOF structure inclusive of P-delta effects can be obtained, in concept, as follows:

$$q_{inel,P\Delta,MDOF} = a_{MDOF} \times a_{INEL} \times a_{P\Delta}\left(S_d / H\right) \tag{7.4}$$

The different modification factors have been discussed and in part quantified. The assumptions and conditions under which these factors have been developed need to be carefully considered in any application. In general, these factors are believed to be applicable for regular steel moment frame structures whose roof displacement is not greatly affected by higher modes, and which are subjected to ground motion records of the types used in this study.

7.1 Global Drift to Story Drift Relationships [a_{ST}]

The distribution of story drifts over the height of the structure, and therefore the relationship between story drifts and global drift, is strongly dependent on the structural and ground motion characteristics. An attempt to draw general quantitative conclusions beyond the range of structures and ground motions used in this study is not intended. The objectives of this section are to add to the existing data base from many studies, to search for patterns that will assist in understanding inelastic dynamic behavior, to provide information on the range of expected story drifts for regular SMRF structures subjected to sets of ground motions with different return periods, and to evaluate the utility of the pushover method for predicting story drifts given that the roof drift is known. Nevertheless, the objective is also to contribute to the mission of relating story drifts to roof drifts, so that with more time and effort the important task of closing the loop between global drift (which can be predicted with good confidence), story drifts, and element deformation demands, can be accomplished. This task is an essential part of the evolving process of performance based seismic design.

7.1.1 Estimation of the Ratio of Maximum Story Drift to Roof Drift

This section focuses on estimating the ratio of maximum story drift to roof drift occurring anywhere over the height of the structure, i.e. no distinction is made between the maximum drift being in the 19th story for one record and being in the 2nd story for another record. For the structures studied the maximum story drift angle mostly occurs in the upper stories in cases in which the response is greatly affected by higher mode effects, and in the lower stories in cases in which the response is controlled by P-delta effects. There are exceptions, such as in the response of long period structures to pulse-type near-fault ground motions, where the story drift is largest in the upper stories for small ductility demands but migrates to the lower stories if the ductility demands become high (Krawinkler and Alavi, 1998).

Figure 7.21 shows the median values for the ratio of maximum story drift to roof drift for the 9 pre-Northridge structures for all the sets of ground motions. The ratio is calculated for each record separately and the statistics is performed on these computed ratios. Figure 7.22 shows the associated dispersion in the data for the different structures and record sets. The following patterns can be identified from the presented results:

1. For all three locations the median values increase with an increase in the height (number of stories) of the structure.
2. For any given structure height, the medians are lowest for Los Angeles and highest for Boston.
3. Structures whose response is controlled by higher mode effects (e.g., Boston structures) show relatively large amplification values. The dispersion associated with these values is also very large (around 0.70). The maximum story drift angles for these structures were observed to occur mostly in the upper stories.
4. The median values are not very sensitive to the intensity of the ground motions (record sets). This pattern is somewhat surprising, particularly for the LA 20-story structure. For this structure the maximum story drifts under the 50/50 records occur mostly in the upper stories, whereas under the 2/50 records they occur mostly in the lower stories. The dispersion, however, differs greatly between the records sets and is very high if the maximum drift is in the upper stories.

The general patterns, which likely can be generalized to other regular SMRF structures, are that the median ratios of maximum story drift to roof drift are small (in the

order of 1.2) for low-rise structures, increase to about 2.0 for mid-rise-structures (9-story) and increase further to about 2.5 to 3.0 for tall structures (20-story) – except for structures in a location in which the ground motions are such that the response is dominated by higher mode effects, such as in Boston. There, the median ratios and the dispersions become significantly larger.

7.1.2 Variation of the Ratio of Story Drift to Roof Drift Over Height of Structure

The median values of the ratio of maximum story drift to roof drift for individual stories are presented in Figures 7.23 to 7.25 for the 3-, 9-, and 20-story structures in the three locations. The values are shown for the 10/50 and 2/50 sets of ground motions. The following patterns can be identified from these figures:

1. The distributions over height are somewhat similar in shape to the story drifts distributions presented in Figures 5.31 to 5.33. Thus, the normalization by maximum roof drift did not change the shape of the distribution by much.
2. With few exceptions, the distribution and the values are similar for the 10/50 and 2/50 sets of ground motions, indicating little sensitivity to the severity of the records. The notable exception is the LA 20-story structure, where the data for the 2/50 set of ground motions shows a migration of large drift demands to the bottom of the structure. Two reasons can be quoted for this migration, one being the P-delta effect which is larger for the more severe ground motions, and the other being the pulse-like nature of many of the 2/50 records.
3. The Boston structures exhibit very large ratios of story drift to roof drift near the top of the structure, demonstrating the great importance of higher mode effects generated by the Boston ground motions. The values for the upper stories are almost identical to the values for the ratio of maximum story drift (over height of structure) to roof drift, as shown in Figure 7.21, indicating that the maximum story drift is confined to a few upper stories of the structure.
4. For all nine structures the presented ratios are larger than 1.0 for most or all stories, and in many cases much larger than 1.0. This implies that the median story drift angle is larger than the roof drift angle in almost all stories. This has an implication for the pushover analysis, as discussed in the next section.
5. The patterns identified at the median level are closely followed at the 84^{th} percentile level, as can be observed by comparing Figures 7.25 and 7.26.

The great differences in the distributions of the medians of the ratio of story drift to roof drift for the nine structures lead to the important albeit discouraging conclusion that there is no common distribution that can be generalized, neither for a given number of stories nor for a given location. The distribution depends on configuration, design decisions, and on the ground motion characteristics. The sensitivity to ground motion characteristics can be evaluated only through time history analysis, which may lead to consistent but ground motion dependent patterns that potentially can be generalized. The sensitivity to the design decisions can possibly be evaluated from a static pushover analysis. This issue is addressed in the next section.

7.3.3 Use of Pushover Analysis to Estimate Story Drift Demands

A pushover analysis is often used to evaluate the performance of structures. The presently practiced process is to predict a target displacement, which constitutes the best estimate of the roof displacement caused by the design ground motion, push the structure under a predetermined or adaptive load pattern to this target displacement, and compare the element or story force and deformation demands computed at the target displacement to available capacities. Implicit in this process is the assumption that the element and story demands computed at the target displacement are reasonable surrogates of the maximum demands experienced by the structure in the "design earthquake".

There are several issues of concern in this process. One is the ability to predict with reasonable accuracy the roof displacement caused by the design ground motion. Based on information in the literature, and confirmed in this study for regular SMRF structures, this can be achieved with good confidence provided that the roof displacement is controlled by the first mode and that the P-delta sensitive range is not entered. Another concern is the ability to predict maximum dynamic story drift demands over the height at a given target displacement. This issue is addressed later. The third concern is the validity of using the roof displacement caused by the design ground motion as the target displacement. This concern is addressed next.

As stated previously, for all nine structures the median ratios of story drift to roof drift are larger than 1.0 for most or all stories, and in many cases much larger than 1.0. The reason is that maximum story drifts do not occur simultaneously. Thus, the sum of

maximum story displacements is always larger than the roof displacement. If the pushover is to capture all maximum story drifts over the height of the structure, then the target displacement needs to be bigger than the roof displacement associated with the design ground motion. The analysis carried out in this study provide specific information on the amount by which the roof displacement should be increased.

Table 7.1 presents relevant information obtained for the 9 pre-Northridge structures and all sets of ground motions. It shows in the last column estimates of the factor by which the median observed roof displacement needs to be increased in order to equal the sum of medians of the observed maximum story displacements. Supporting data from which this factor is derived are shown in the other two columns. For the 3-story LA and Seattle structures this factor is close to unity, but for all other structures it is significantly larger. It is particularly large for structures that are dominated by higher mode effects. To some degree this factor is compensated for in the FEMA 273 approach by neglecting the inelasticity factor (see Section 7.2.2) in the estimate of the target displacement, but for structures with large higher mode effects this compensation is insufficient. The conclusion is that for structures with significant higher mode effects the story drift demands will be underestimated by a pushover analysis even if the drift demand distribution over the height is accurately simulated in the pushover.

The information from the analysis carried out in this study can be used also to evaluate the pushover's potential to predict maximum dynamic story drift demands over the height for a given target displacement. A pushover analysis will provide a unique answer even though the relationship between dynamic story drifts and roof drift will never be unique except for a single ground motion. Thus, the quality of a pushover prediction can only be measured "in average", using representative sets of ground motions. Examples of the scatter in the relationship between story drifts and roof drift are shown in Figures 7.27 and 7.28, using a typical upper story (story 8) and a typical lower story (story 3) of the LA 9-story structure for illustration. The data points represent the response to all 60 records contained in the 50/50, 10/50, and 2/50 record sets. The scatter is very large, particularly for story 8, but the data show the opposite trend for the two stories. For the upper story (Figure 7.27) the ratio of story drift to roof drift is mostly larger than 1.0 for small roof drifts and smaller than 1.0 for large roof drifts. The reason is that under small intensity ground motions (low ductility demands) the higher mode effects lead to larger than average drifts in the upper stories whereas under large intensity ground motions (high ductility demands) the large drift demands migrate to the lower

stories. Thus, in the graph for story 3 (Figure 7.28) the story drift becomes larger than the roof drift at large values of roof drift.

This pattern is consistently observed for the LA 9- and 20-story structures. To capture this pattern and to define a representative relationship between story drifts and roof drift, a regression analysis is performed using the following form to relate the two quantities:

$$\theta_{st,i} = a_i \left(\theta_{roof}\right)^{b_i} \tag{7.5}$$

where $\theta_{st,i}$ is the story drift angle for story i, θ_{roof} is the roof drift angle, and a_i and b_i are coefficients obtained from a regression analysis using the data points obtained from the nonlinear dynamic analysis of the structures subjected to all 60 records. The coefficients a_i and b_i are determined by minimizing the least square error between the observed and predicted values.

The main advantage of using the relationship given in Equation 7.5 is that it permits capture of the patterns described before. As illustrated in Figure 7.29, a value of $b < 1$ implies a decrease in the ratio of story drift to roof drift with increasing roof drift, whereas a value of $b > 1$ implies the opposite. The values for the coefficients a and b for several structures are given in Table 7.2. The stories that are much affected by higher mode effects have "low" b values, whereas stories much affected by P-delta effects or near-fault pulse-like ground motions have b values that are greater than 1.0. Another advantage of the particular form of the equation is that it ties in directly with the formulation used for developing the drift hazard curves in Section 5.5.2.

An assessment of the goodness of story drift predictions from a pushover analysis can be achieved by comparing the regressed dynamic story drift to roof drift relationships with the relationships obtained from the pushover analysis. Representative results are shown in Figures 7.30 to 7.35. As expected, a comparison of Figures 7.30 and 7.31 reveals a very good match for the LA 3-story structure. A similar match is also obtained for the Seattle 3-story structure.

A comparison between Figures 7.32 and 7.33 shows only fair agreement between the results of the pushover analysis and the regression analysis for the LA 20-story structure. The trends are similar (except for story 1) but the quantitative values differ significantly, particularly for stories 7 and 9 in which the pushover analysis severely underestimates the regressed drift demands due to a reduction in applied horizontal load after the development of a post-yield negative stiffness in the structure. It is important to note that for this structure the pushover does capture the large demands imposed on most of the lower stories due to the large P-delta effects.

It has been emphasized several times that the pushover analysis provides inadequate story drift demand predictions for structures that are significantly affected by higher mode effects. An example to this effect is seen by comparing Figures 7.34 and 7.35, which show the results obtained for the Seattle 9-story structure. The values and patterns for the story drift demands are very different between the regression analysis and the pushover predictions, and the differences increase with increasing roof drift. The comparison becomes worse for the Seattle 20-story structure.

In conclusion, the estimation of story drift demands over the height of the structure as a function of the roof drift is difficult to carry out on account of the dependence of the relationship on a multitude of factors, including relative strength and stiffness of the stories, higher mode and P-delta effects, and characteristics of the ground motions. The pushover analysis procedure is useful in estimating this relationship for many cases. It will provide good predictions for low-rise structures and will provide much insight into structural behavior in many other cases. For instance, it is very useful in assessing the importance of P-delta effects by providing good estimates of the drift demand associated with the onset of negative stiffness. However, it is not a good means for predicting drift demands in structures subjected to ground motions that cause significant higher mode effects.

7.4 Estimation of Element Deformation Demands [a_{ELM}]

In the previous sections factors and processes have been discussed that permit an estimate of maximum story drift demands. This section presents a simplified procedure that transforms story drift demand estimates into estimates of the element plastic

deformation demands at each floor level. This process involves the following two steps: 1) estimating the story plastic deformation demand (i.e., estimating the story yield drift and subtracting it from the total story drift demand), and 2) relating the story plastic deformation demand to the element (beams, panel zone) plastic deformation demands. The latter process assumes that plastic rotations in columns are negligible.

7.4.1 Estimation of Story Plastic Drift Angle

The story plastic drift angle can be obtained by subtracting the story yield drift angle from the total story drift angle. An estimate of the story yield drift is greatly facilitated if the following simplifying assumptions on elastic behavior can be made:

1. The inflection points are at mid-heights of the columns and mid-spans of the beams. This is a reasonable assumption for structures that do not have a severe stiffness discontinuity between adjacent stories.
2. The story yield drift is associated with yielding in either beams or panel zones, i.e., the columns are stronger than the beams and/or the panel zone. This is a reasonable assumption for code designed structures in which the strong column-weak beam/panel zone criterion is followed.
3. The effects of gravity loading on yielding in beams and panel zones can be neglected. This is an important assumption that is violated if the beam gravity moment constitutes an important fraction of the beam bending strength.
4. The story elevation has regular geometry and uniform section properties (i.e., the standard portal method assumption can be made).
5. Second order effects and lateral deflection due to axial column deformations can be neglected.
6. Dynamic interaction between adjacent stories has little effect on the story yield drift.

For cases in which these assumptions hold, the story yield drift is not expected to be significantly different between adjacent stories, and the substructure shown in Figure 7.36 represents all essential behavior aspects. The story yield drift can be estimated as follows:

Step 1: Assume that the beams framing into the typical subassembly shown in Figure 7.36 are the first elements to yield at the connection. The corresponding shear force in

the columns, V_{col}, can be estimated using the assumption of midpoint inflection points, by the following equation:

$$V_{col} = \frac{\Delta M}{h\left[1 - \frac{d_c}{l}\right]} = \frac{2 \times M_{pb}}{h\left[1 - \frac{d_c}{l}\right]} \tag{7.6}$$

in which M_{pb} is the plastic moment of the beam, d_c is the depth of the column, h the height between the two inflection points in the columns, and l the distance between the inflection points in the beams framing into the connection. Using this estimate for the shear force in the column, the shear force in the panel zone can be estimated using Equation 3.5, which is reproduced here for completeness:

$$V_{pz} = \left(\frac{\Delta M}{d_b} - V_{col}\right) = \left(\frac{2 \times M_{pb}}{d_b} - V_{col}\right) \tag{7.7}$$

This shear force demand for the panel zone is compared to the yield strength of the panel zone, $V_{y,pz}$, given by Equation 3.1. If the computed demand is less than the yield strength given by Equation 3.1, then the assumption made at the beginning of Step 1 holds true. If not, then the panel zone yields before the beams and then the shear force in the column is estimated from the following equation:

$$V_{y,pz} = \frac{1}{d_b}\left[V_{col} \times h\left(1 - \frac{d_c}{l}\right)\right] - V_{col} \tag{7.8}$$

Thus, at the end of Step 1, the shear force in the column, V_{col}, associated with first yielding at the connection, has been determined.

Step 2: Using the geometry of the subassembly, basic element properties, and the estimated shear force in the column corresponding to the first yield at the connection, the associated drift components can be computed. The lateral drift from beam flexural deformations, d_b, from column flexural deformations, d_c, and from panel zone shear deformations, d_{pz}, is computed as follows:

$$d_b = \frac{1}{2} \times \frac{V_{col} \times h^2 \left(1 - \frac{d_c}{l}\right)}{\left(\frac{6EI_b}{l - d_c}\right)} \tag{7.9}$$

$$d_c = V_{col} \times \frac{(h - d_b)^3}{12EI_c} \tag{7.10}$$

$$d_{pz} = V_{col} \times \frac{(h - d_b) \times \left(\frac{h}{d_b} - 1\right)}{Gt_p d_c} \tag{7.11}$$

where I_b and I_c denote the moment of inertia for the beams and columns, d_b and d_c denote the depth of the beam and column sections, E is the elasticity modulus of steel, G is the shear modulus of steel, and t_p is the thickness of the panel zone.

The story yield drift angle, $q_{y,st}$, and consequently the story plastic deformation, $q_{p,st}$ can then be evaluated as:

$$q_{y,st} = \frac{\left(d_b + d_c + d_{pz}\right)}{h} \tag{7.12}$$

$$q_{p,st} = q_{total,st} - q_{y,st} \tag{7.13}$$

The formulations presented in Equations 7.6 to 7.13 can easily be modified for cases in which the beam sections framing into the connection are not the same on either side of the connection. Using this procedure for the cases for which the assumptions made

previously are valid, a good estimate for the story yield drift and the story plastic drift demand can be obtained.

7.4.2 Relating Story and Element Plastic Deformation Demands

The distribution of element plastic deformation demands as a function of the story plastic drift demand can be calculated using a procedure similar to that adopted for estimating the story yield drift. The process works on the premise given by the following equation (again, the possibility of plastic hinging in the columns is neglected in this approach):

$$h \times q_{p,st} = h \times q_{p,b} + (h - d_b) \times q_{p,pz} \tag{7.14}$$

where the subscript *p* denotes plastic deformation, *b* denotes the beam, *pz* the panel zone, and *st* the story. Again, it must be emphasized that this equation is reasonable only if the gravity moments in the beams are small compared to M_{pb}.

The initial assumption is made that plastic deformation is existing in both the beams and the panel zone forming the connection. For such cases, the moment in the beam, M_b, can be written as:

$$M_b = M_{pb} + a\left(\frac{6EI_b}{l}\right) \times q_{p,b} \tag{7.15}$$

where M_{pb} is the plastic moment for the beam, and a is the associated strain-hardening in the moment-rotation relationship. Using Equation 7.15 and Equation 7.6 where *DM* is now equal to $2M_b$, the shear force in the column is estimated. Then the shear force demand for the panel zone can be evaluated as follows:

$$V_{pz} = 2 \times M_b \left[\frac{1}{d_b} - \frac{1}{h\left(1 - \frac{d_c}{l}\right)}\right] \tag{7.16}$$

V_{pz} can be related to the yield shear force, $V_{y,pz}$, for the panel zone and the plastic shear distortion using the following equation:

$$V_{pz} = V_{y,pz} + bK_{pz}q_{p,pz} \tag{7.17}$$

where b denotes the effective strain-hardening for the second slope of the trilinear shear-force shear distortion relationship, K_{pz} is the elastic shear stiffness of the panel zone, and q_{pz} is the plastic shear distortion in the panel zone. Equating Equations 7.16 and 7.17 and eliminating the V_{pz} term results in the following expression for the panel zone plastic shear distortion as a function of the moment in the beam:

$$q_{p,pz} = \frac{2 \times M_b \left[\frac{1}{d_b} - \frac{1}{h\left(1 - \frac{d_c}{l}\right)} \right] - V_{y,pz}}{bK_{pz}} \tag{7.18}$$

Substituting Equation 7.18 in Equation 7.14 and rearranging the terms yields the following expression for the beam plastic deformation demand as a function of the story plastic drift demand:

$$q_{p,b} = \frac{q_{p,st} \times bK_{pz}\left(\frac{h}{h - d_b}\right) - 2 \times M_{pb}\left[\frac{1}{d_b} - \frac{1}{h\left(1 - \frac{d_c}{l}\right)} \right] + V_{y,pz}}{2 \times a\left(\frac{6EI_b}{l}\right) \times \left[\frac{1}{d_b} - \frac{1}{h\left(1 - \frac{d_c}{l}\right)} \right] + bK_{pz}\left(\frac{h}{h - d_b}\right)} \tag{7.19}$$

Using the value for the beam plastic deformation obtained from Equation 7.19 and substituting in Equation 7.15, the moment in the beam can be evaluated. This value for the beam moment, when substituted in Equation 7.18 yields the corresponding plastic

deformation in the panel zone. Alternatively, substituting the beam plastic deformation in Equation 7.14 yields the panel zone plastic deformation.

Thus, this process permits the estimation of the element plastic deformation demands from the story plastic drift demand. There are two important considerations that need to be highlighted:

1. If the panel zone is the only yielding element at the connection, then Equation 7.19 will return a negative value for the beam plastic deformation demand, indicating that the moment in the beam is less than the beam plastic moment. For such cases the value for the panel zone plastic deformation needs to be recomputed using Equation 7.14, with $q_{p,b}$ equal to zero. If only one element at the connection yields then Equation 7.14 provides a complete solution for estimation of element plastic deformation demands.
2. If the value obtained for the panel zone plastic shear distortion is greater than 3 times the yield distortion (typically about 0.003 or 0.3% for A-572 steel), i.e., the panel zone reaches the third slope of the trilinear relationship, then Equation 7.21 has to be modified to reflect the third branch of the shear force-shear distortion relationship. For estimated values not much larger than $3q_{y,pz}$, a modification may not be necessary as the idea is only to get an estimate of the plastic deformation. However, if the value obtained for the panel zone plastic distortion is large compared to $3q_{y,pz}$, then a modification is required. This can be achieved by modifying Equation 7.17 as follows:

$$V_{pz} = V_{y,pz} + \left(bK_{pz} \times 3q_{y,pz}\right) + \left(b_1 K_{pz} \times \left(q_{p,pz} - 3q_{y,pz}\right)\right) \tag{7.20}$$

where b_1 represents the slope of the third branch of the shear force–shear distortion relationship for the panel zone. This equation can then be transformed into the following equivalent form (similar to Equation 7.17):

$$V_{pz} = V'_{y,pz} + b'K_{pz}q_{p,pz} \tag{7.21}$$

where

$$V'_{y,pz} = V_{y,pz} + (b - b_1) \times K_{pz} \times 3q_{y,pz} \quad (7.22)$$

and

$$b' = b_1 \quad (7.23)$$

Equation 7.21 replaces Equation 7.17, the value of $V_{y,pz}$ is changed to $V'_{y,pz}$, and b is replaced by b' in Equation 7.18 and Equation 7.19.

7.4.3 Verification of Procedure

The adequacy of the simplified procedure for the estimation of element plastic deformation demands from given story drift demands is evaluated by means of several examples. The median story drift demands obtained from the time history analysis are used as the starting point. At the floor level a floor drift angle is calculated as the average of the adjoining two stories drift angles. The story yield and plastic drifts are computed from Equations 7.6 to 7.13. The procedure outlined by Equations 7.14 through 7.21 is employed to estimate the element plastic deformation demands, which are then compared to the median results obtained from the nonlinear dynamic analysis. Results of comparisons are shown in Figures 7.37 to 7.40.

Figure 7.37 pertains to an interior column line of the LA 9-story structure and the 2/50 set of ground motions. The estimated beam and panel zone plastic deformation demands are compared to the median of the observed dynamic analysis results. For floor 7 the first estimate for the beam plastic deformation was 0.005 while the estimated panel zone plastic deformation was 0.02. These estimates needed to be revised because the panel zone has reached the third slope of its shear force – shear distortion relationship at a plastic deformation of about 0.009. This modification is carried out using Equations 7.20 through 7.23. Equation 7.19 is recomputed, which returns a negative value for the beam plastic deformation, indicating that the moment in the beam is below beam plastic moment. Then Equation 7.14 is used to return a value of 0.02 for panel zone plastic deformation.

Also shown in Figure 7.37 are the floor drift angles (average of drift angles of adjacent stories) and the corresponding yield drift angles computed from the procedure. The simplified procedure provides very good estimates for the element plastic

deformation demands, given the story drift demand. The estimated demands capture the distribution of demands between the beams and panel zone, as well as the absolute values very well.

The procedure has been developed with several simplifying assumptions, such as no plastification in the columns. Though a reasonable assumption for many cases, under certain conditions this assumption and others (e.g., midpoint inflection points) may be far from reality. Even for such cases (e.g., LA 20-story structure under the 2/50 set of ground motions) the simplified procedure provides good element deformation estimates at the median drift level (Figures 7.38 and 7.39) and also at very large drift levels (Figure 7.40, for the LA30 ground motion). In the latter case the column exhibits plastic deformation demand in the time history analysis, which in the simplified procedure is distributed to the beam and/or panel zone plastic deformation demands. In the example shown in Figure 7.40 this did not lead to a very large error.

7.5 Conclusions

In this chapter a simplified procedure for the estimation of seismic deformation demands in steel moment resisting frame structures has been presented. The procedure utilizes elastic spectral displacement demand information and basic structural properties to obtain estimates for roof drifts, story drifts, and ultimately, beam and panel zone plastic deformation demands. The procedure is facilitated by the use of a pushover analysis with an appropriate analytical model of the structure. The procedure is based on data obtained from extensive linear and nonlinear static and dynamic analysis of typical steel frame structures, and on additional data available in the literature.

The first part of the procedure, which transforms the elastic spectral displacement demand at the first mode period of the analytical model to the inelastic roof drift angle demand (inclusive of “mild” P-delta effects), is based on statistical observations from the analysis of the model buildings. The modification factors developed for the SAC model structures are in good agreement with similar factors given in the literature for simplified cases/scenarios. Thus, this step reinforces the generality of the developed factors. The factors are based on sets of ground motions of differing intensity. Furthermore, the study shows that the effect of inelasticity in the structures can often be estimated using single-degree-of-freedom systems. For structures with a fundamental period exceeding one

second the inelasticity factor is insensitive to period and structure strength properties (except for soft soil ground motions). The same cannot be said for P-delta effects. The modification for structure P-delta effects is found to be very sensitive once the structure attains the negative post-yield stiffness region. A pushover analysis helps to identify the cases in which the structure might attain the negative post-yield stiffness. For structures in which a positive post-yield stiffness is maintained, the effects of P-delta are well contained.

The second part of the procedure relates the roof drift to the maximum story drift and the distribution of story drifts over the height of the structure. The ratio of maximum story drift to roof drift has been evaluated statistically, and representative modification factors, which depend on height and location of the structure, are suggested. The distribution of story drifts over height depends strongly on structural and ground motion characteristics. Representative patterns are presented, but no simple rules for the generation of distributions could be developed. Here, a pushover analysis is helpful to provide insight into structural behavior, and in specific cases quantitative information. The potential and limitations of the pushover analysis are summarized.

The third and final part of the procedure relates the story drift demand to the element plastic deformation demands. This is achieved by utilizing basic element strength and stiffness characteristics and representative substructures. The story yield drift is estimated first, and element plastic deformation demands are then obtained from the plastic story drift, with due consideration given to the relative strength of beams and panel zones at a connection.

Thus, the procedure can be used to obtain quick estimates for the seismic deformation demands for SMRFs subjected to different types and intensities of ground motions. The estimates of the seismic deformation demands can then be compared to capacity estimates, at the element or system level, to yield an assessment of the performance of the structure.

The procedure has been developed primarily to simplify seismic demand evaluation. It can easily be used to address the conjugate problem of conceptual design. Given a certain limit on the level of plastic deformation demands at the element level, the story drift limit can be estimated followed by an estimation of the roof drift limit. This roof drift limit can then be related to spectral displacement demands. Coupled with

information from other studies (Krawinkler et al, 1991, 1997) an estimate for the strength and stiffness of the structure can be obtained, which can then be used for preliminary sizing of members.

The main advantage of the developed procedure lies in its simplicity in providing an estimate of deformation demands for structural performance evaluation, assistance in conceptual designs, and identification of cases in which more refined analysis may be necessary. For regular (no apparent abnormalities) structures the developed procedure should provide reasonable and conservative estimates of seismic deformation demands for SMRFs. At different stages of the development, however, several simplifying assumptions have been made, which may invalidate demand estimates for structures and ground motions far outside the range used in this study.

Table 7.1 Ratio of Average of Median Story Drift Angles to Median of Roof Drift Angles for All Structures; All Sets of Records

Location	Structure	Hazard Level	Average of Median of Story Drift Angles	Median of Roof Drift Angles	Ratio: Story/Roof
LA	3-story	2/50 Set	0.04070	0.03930	1.04
		10/50 Set	0.01970	0.01870	1.05
		50/50 Set	0.01190	0.01100	1.08
	9-story	2/50 Set	0.03080	0.02522	1.22
		10/50 Set	0.01665	0.01352	1.23
		50/50 Set	0.01001	0.00741	1.35
	20-story	2/50 Set	0.02014	0.01461	1.38
		10/50 Set	0.01193	0.00838	1.42
		50/50 Set	0.00638	0.00390	1.64
Seattle	3-story	2/50 Set	0.04329	0.04084	1.06
		10/50 Set	0.01725	0.01550	1.11
	9-story	2/50 Set	0.02452	0.01699	1.44
		10/50 Set	0.01412	0.00941	1.50
	20-story	2/50 Set	0.01388	0.00822	1.69
		10/50 Set	0.00842	0.00524	1.61
Boston	3-story	2/50 Set	0.01226	0.00938	1.31
		10/50 Set	0.00457	0.00342	1.34
	9-story	2/50 Set	0.00709	0.00376	1.89
		10/50 Set	0.00272	0.00131	2.08
	20-story	2/50 Set	0.00414	0.00216	1.92
		10/50 Set	0.00152	0.00075	2.03

Table 7.2 Values for coefficients “a” and “b” in Equation 7.5, for LA 3-, 9-, and 20-story and Seattle 9-story Structures

	Coefficients	Story 1	Story 2	Story 3	Story 4	Story 5	Story 6	Story 7	Story 8	Story 9	Story 10
LA 3-story	a	1.040	0.922	0.821							
	b	1.027	0.956	0.916							
LA 9-story	a	0.822	1.765	2.051	1.781	1.064	0.624	0.338	0.179	0.106	
	b	0.933	1.092	1.123	1.083	0.972	0.854	0.678	0.505	0.405	
LA 20-story	a	1.489	3.015	4.334	5.143	4.170	1.914	0.858	0.446	0.237	0.160
	b	1.008	1.101	1.172	1.210	1.182	1.046	0.896	0.775	0.657	0.579
	Coefficients	Story 11	Story 12	Story 13	Story 14	Story 15	Story 16	Story 17	Story 18	Story 19	Story 20
	a	0.165	0.199	0.186	0.123	0.061	0.047	0.048	0.053	0.056	0.052
	b	0.569	0.588	0.574	0.503	0.379	0.334	0.328	0.327	0.324	0.313
Seattle 9-story	a	0.356	0.413	0.558	0.703	0.571	0.536	0.412	0.255	0.228	
	b	0.729	0.751	0.837	0.872	0.793	0.750	0.660	0.540	0.535	

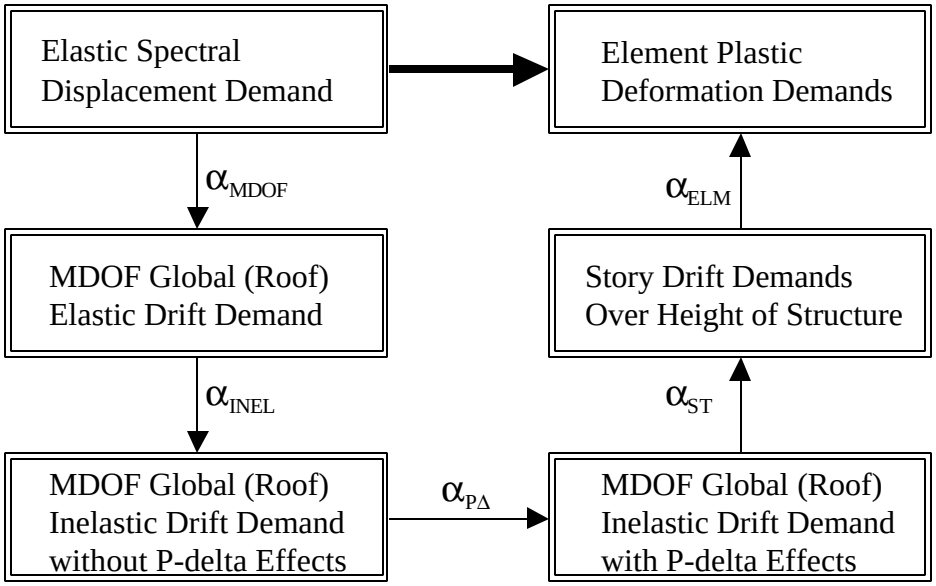

Figure 7.1 Simplified Procedure for Estimation of Seismic Deformation Demands for Steel Moment Resisting Frame Structures

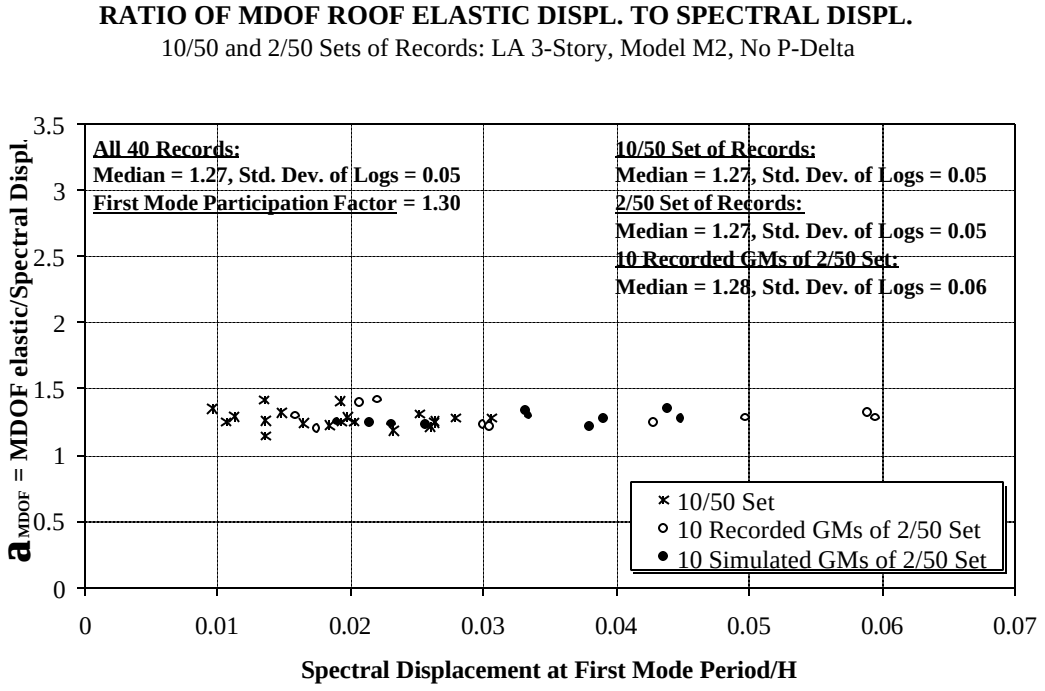

Figure 7.2 MDOF Modification Factor for LA 3-story Structure; 10/50 and 2/50 Sets of Ground Motions

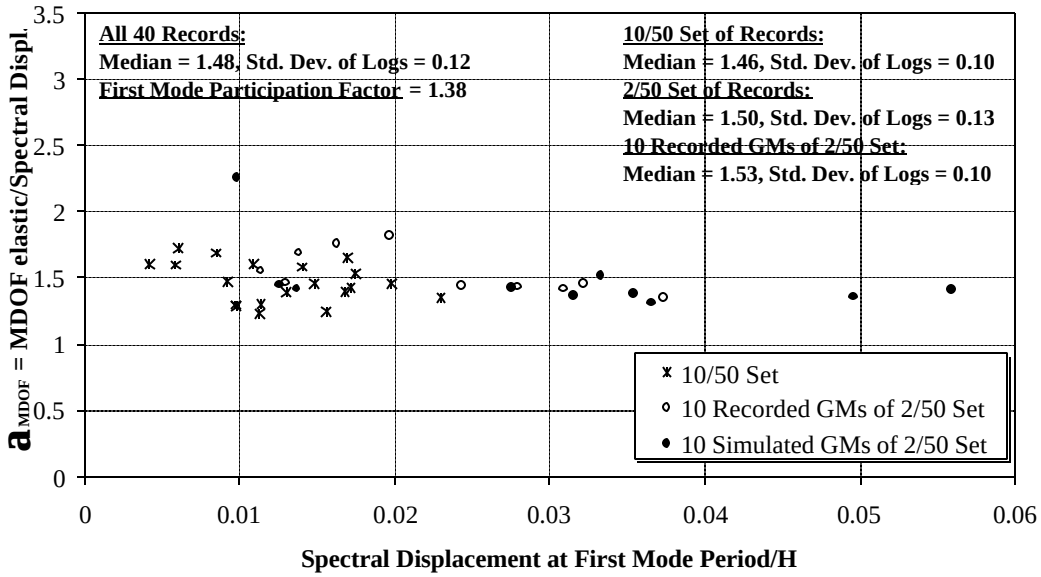

Figure 7.3 MDOF Modification Factor for LA 9-story Structure; 10/50 and 2/50 Sets of Ground Motions

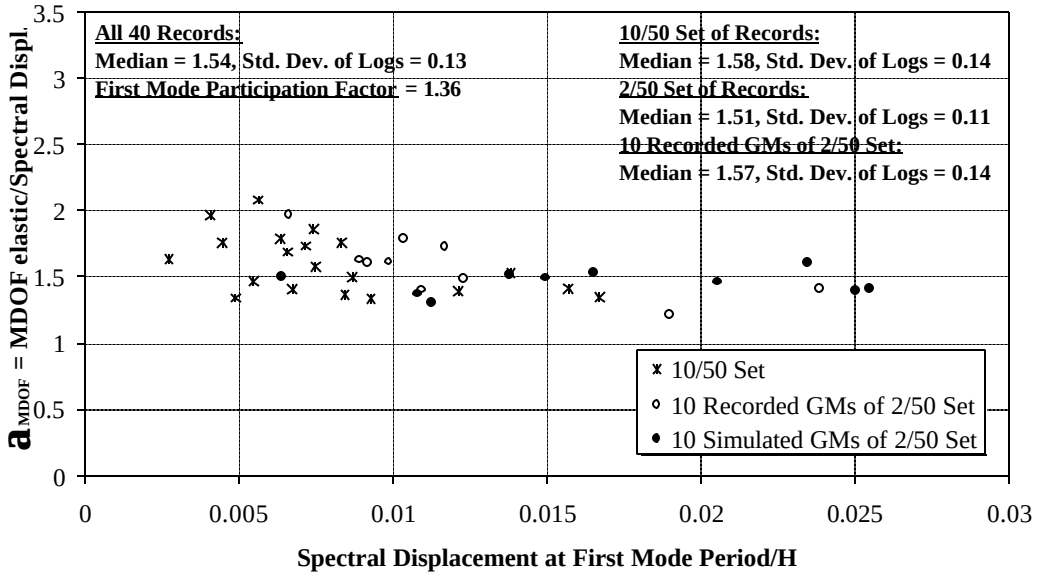

Figure 7.4 MDOF Modification Factor for LA 20-story Structure; 10/50 and 2/50 Sets of Ground Motions

RATIO OF MDOF ROOF ELASTIC DISPL. TO SPECTRAL DISPL.

10/50 and 2/50 Sets of Records: BO 9-Story, Model M2, No P-Delta

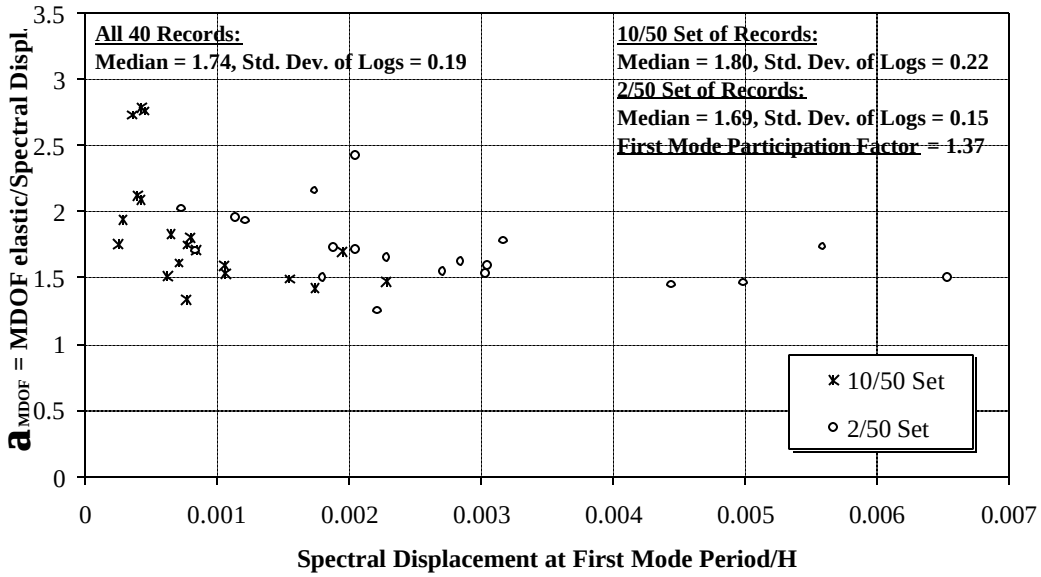

Figure 7.5 MDOF Modification Factor for Boston 9-story Structure; 10/50 and 2/50 Sets of Ground Motions

RATIO OF MDOF ROOF ELASTIC DISPL. TO SPECTRAL DISPL.

10/50 and 2/50 Sets of Records: BO 20-Story, Model M2, No P-Delta

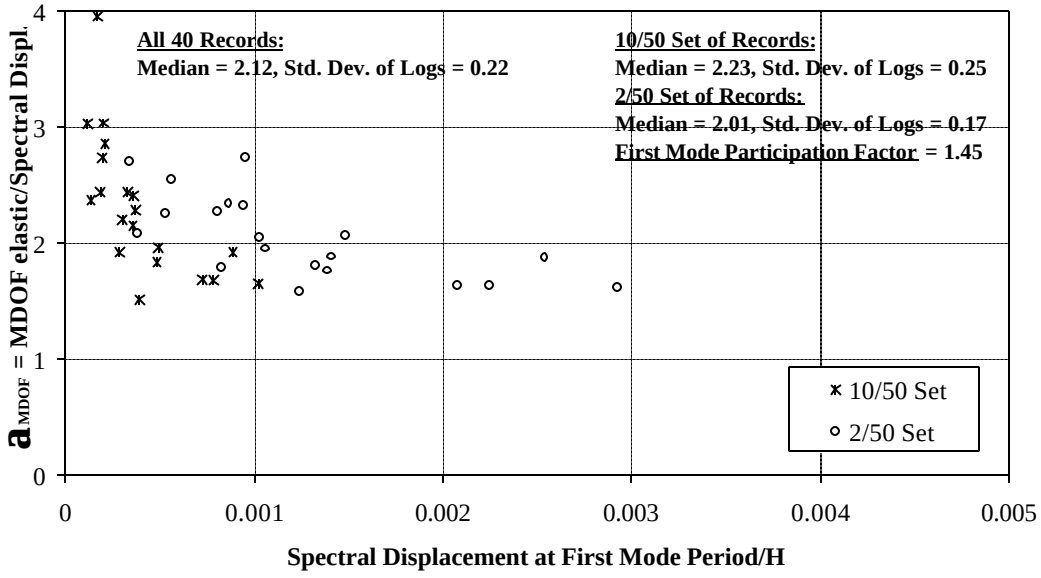

Figure 7.6 MDOF Modification Factor for Boston 20-story Structure; 10/50 and 2/50 Sets of Ground Motions

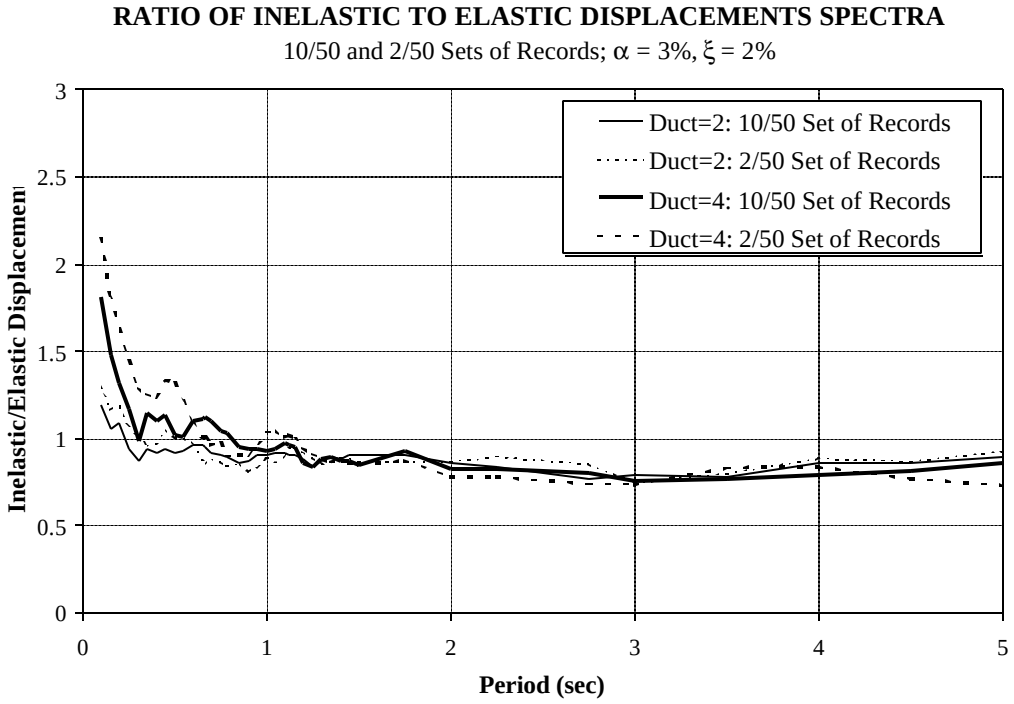

Figure 7.7 Median Values for Inelastic/Elastic Displacements for SDOF Systems, α = 3%, ξ = 2%; 10/50 and 2/50 Sets of LA Ground Motions

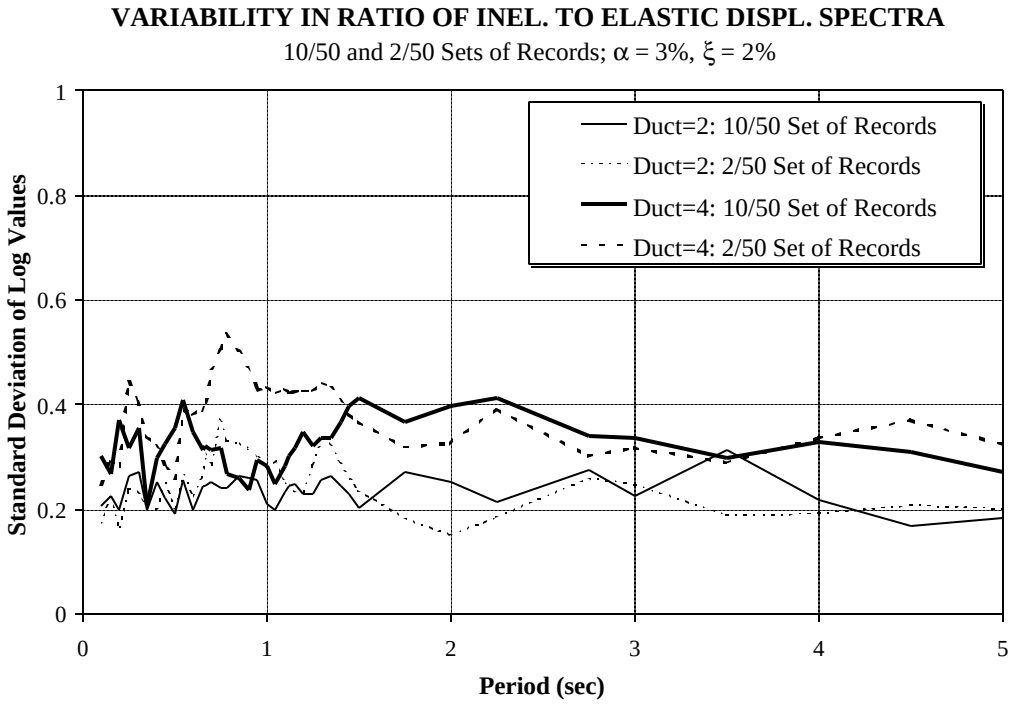

Figure 7.8 Dispersion Associated with Values for Inelastic/Elastic Displacements for SDOF Systems, α = 3%, ξ = 2%; 10/50 and 2/50 Sets of LA Ground Motions

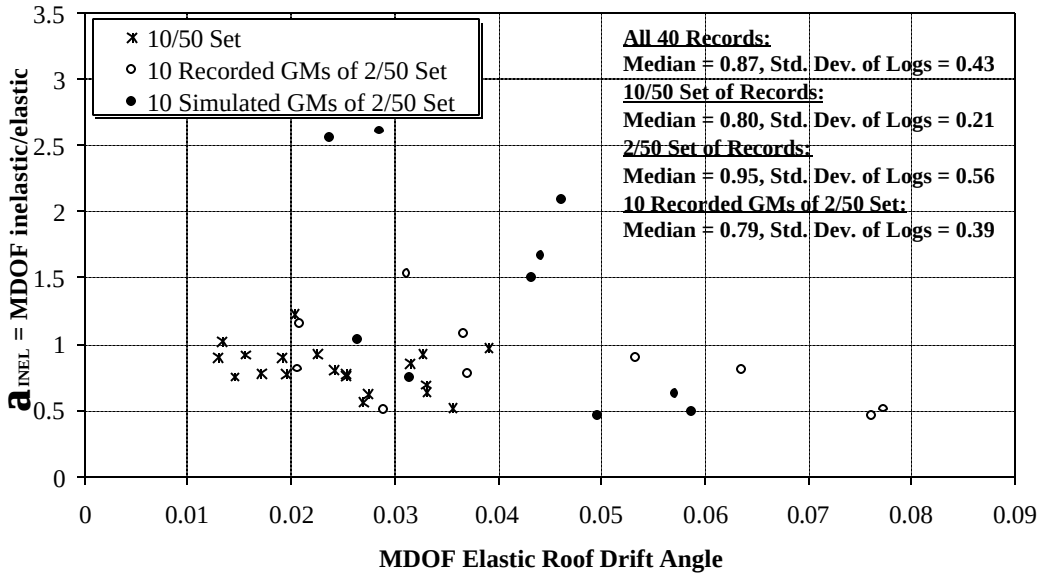

Figure 7.9 Inelasticity Modification Factor for LA 3-story Structure; 10/50 and 2/50 Sets of Ground Motions

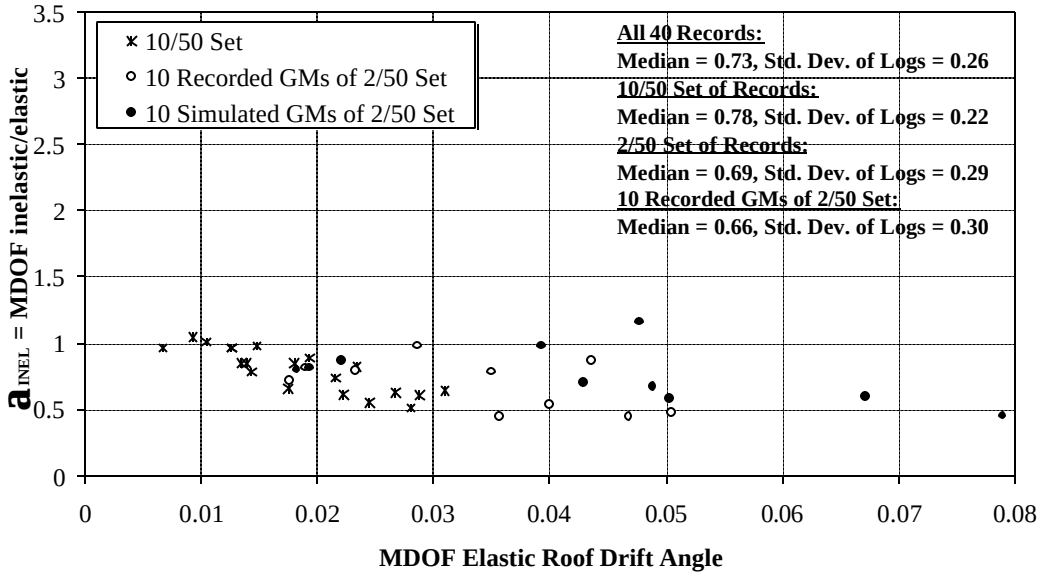

Figure 7.10 Inelasticity Modification Factor for LA 9-story Structure; 10/50 and 2/50 Sets of Ground Motions

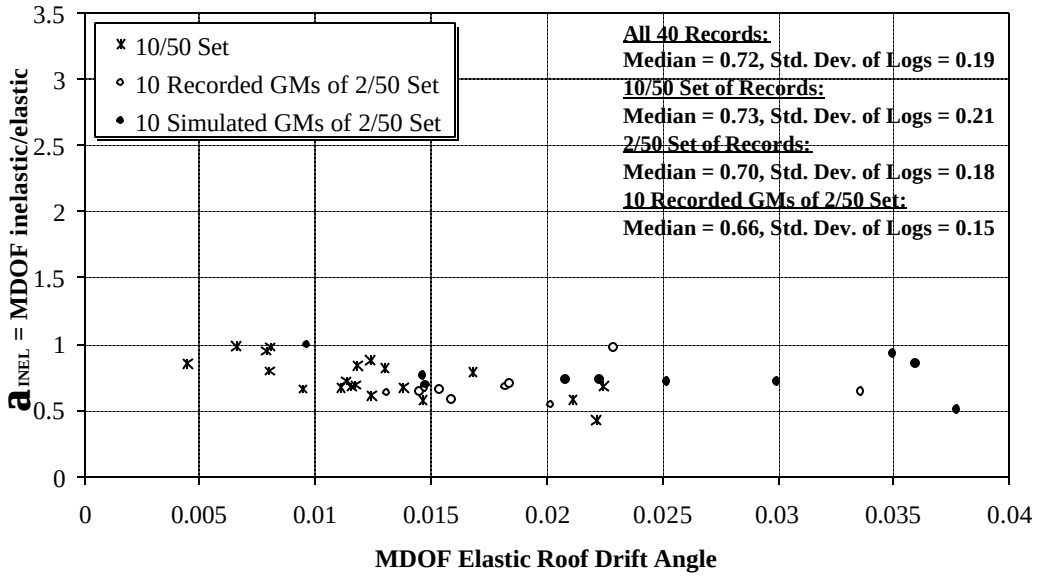

Figure 7.11 Inelasticity Modification Factor for LA 20-story Structure; 10/50 and 2/50 Sets of Ground Motions

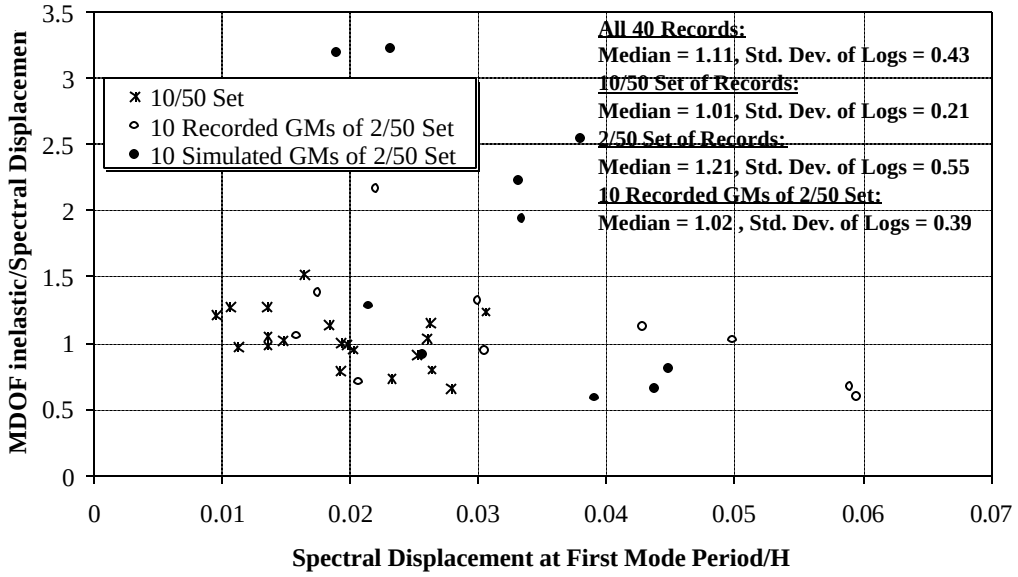

Figure 7.12 Product of MDOF and Inelasticity Modification Factors for LA 3-story Structure; 10/50 and 2/50 Sets of Ground Motions

RATIO OF MDOF ROOF INELASTIC DISPL. TO SPECTRAL DISPL.

10/50 and 2/50 Sets of Records: LA 9-Story, Model M2, No P-Delta

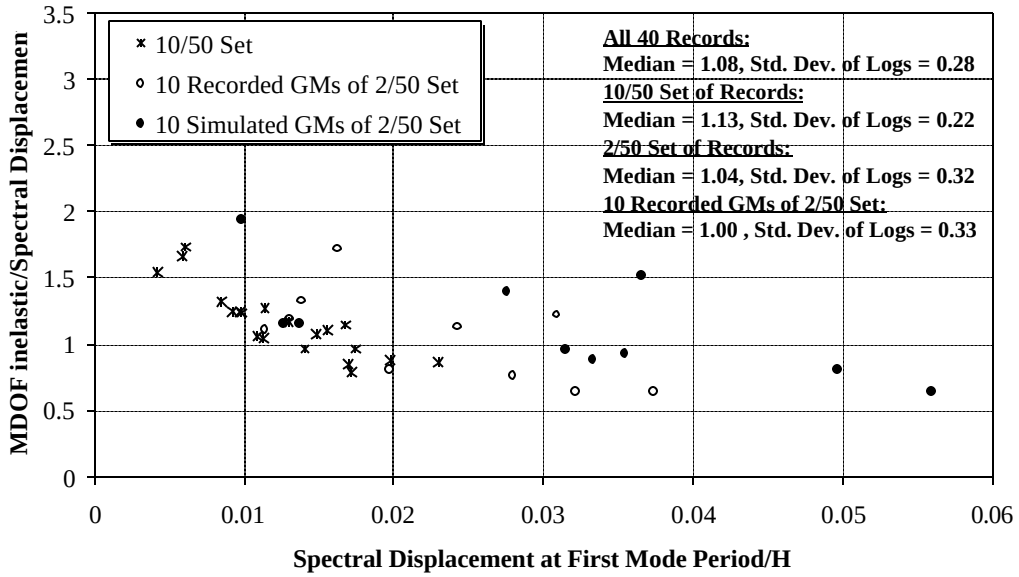

Figure 7.13 Product of MDOF and Inelasticity Modification Factors for LA 9-story Structure; 10/50 and 2/50 Sets of Ground Motions

RATIO OF MDOF ROOF INELASTIC DISPL. TO SPECTRAL DISPL.

10/50 and 2/50 Sets of Records: LA 20-Story, Model M2, No P-Delta

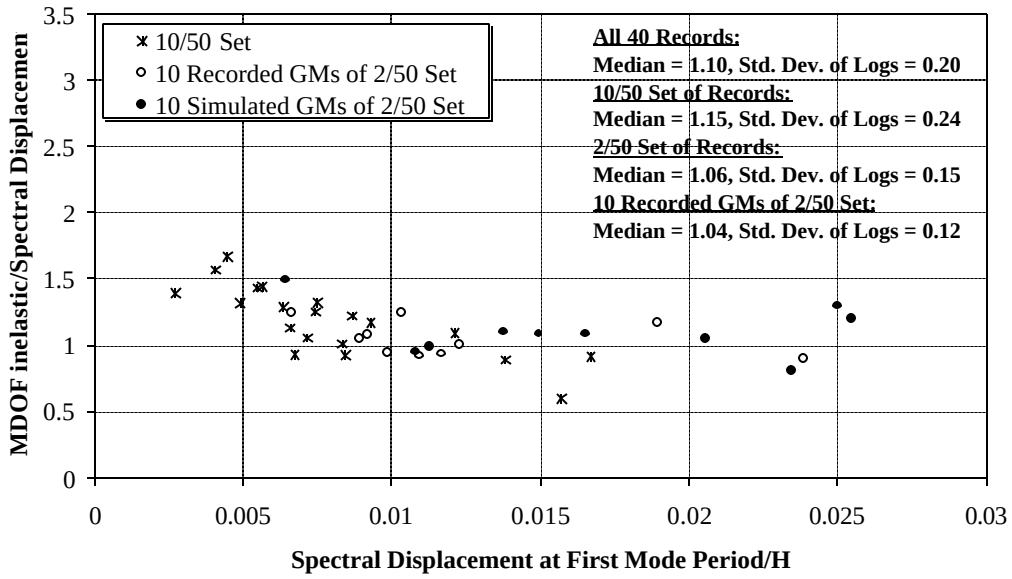

Figure 7.14 Product of MDOF and Inelasticity Modification Factors for LA 20-story Structure; 10/50 and 2/50 Sets of Ground Motions

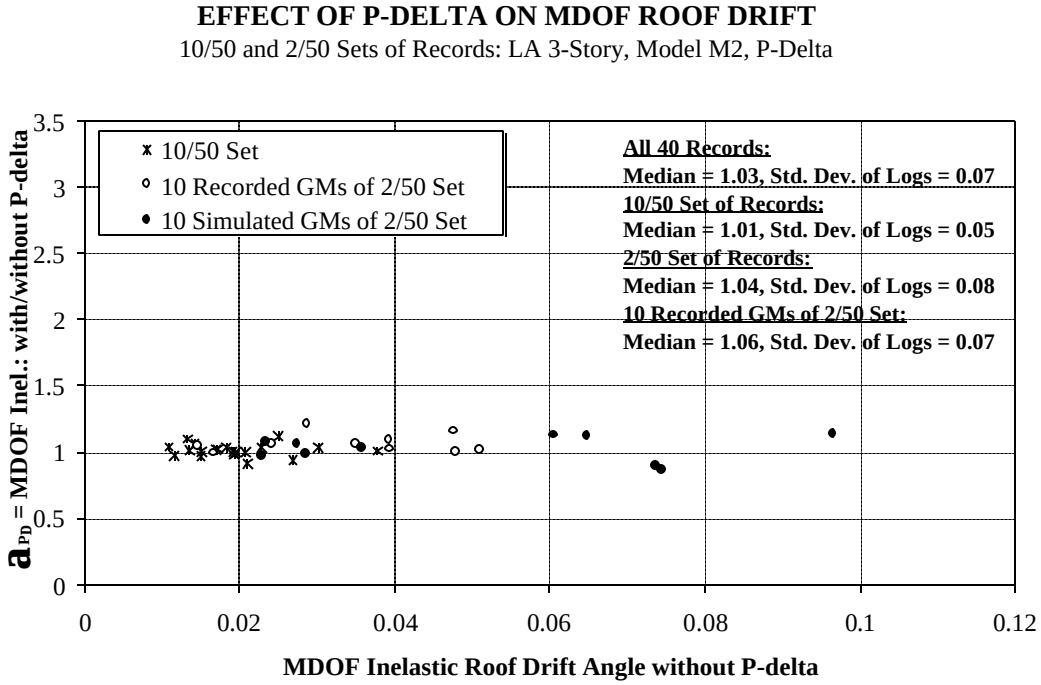

Figure 7.15 P-Delta Modification Factor for LA 3-story Structure; 10/50 and 2/50 Sets of Ground Motions

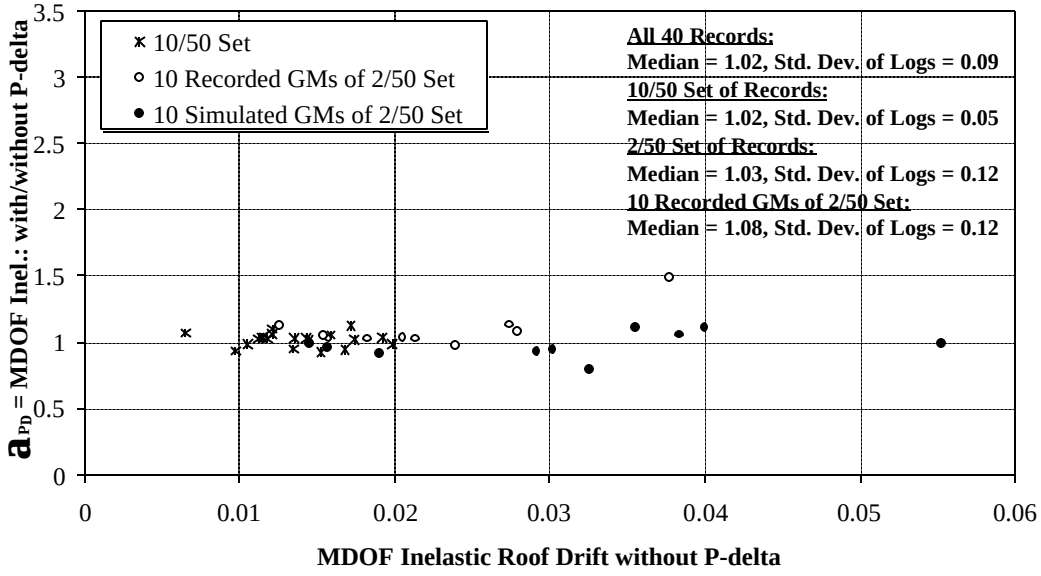

Figure 7.16 P-Delta Modification Factor for LA 9-story Structure; 10/50 and 2/50 Sets of Ground Motions

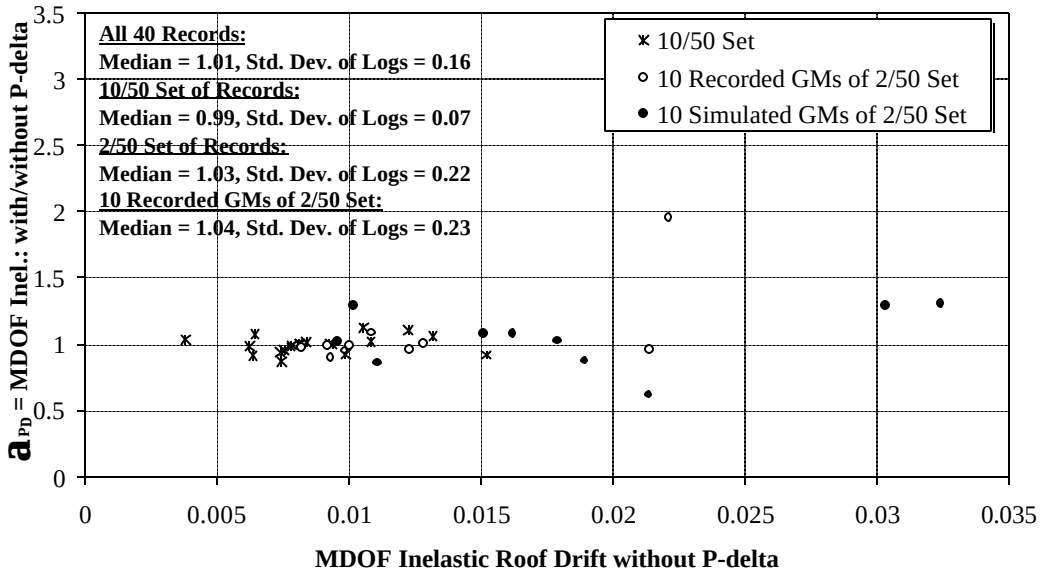

Figure 7.17 P-Delta Modification Factor for LA 20-story Structure; 10/50 and 2/50 Sets of Ground Motions

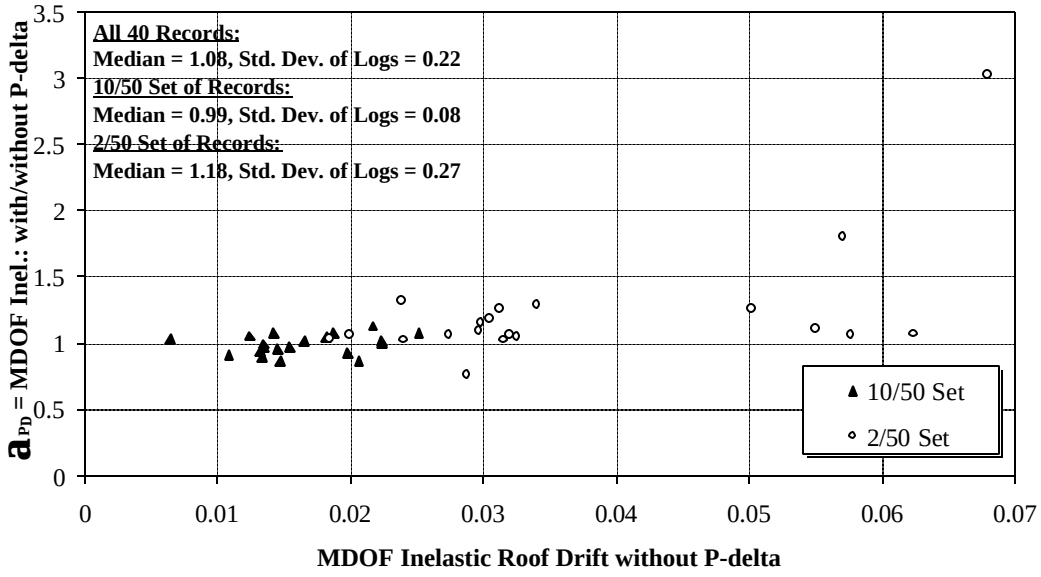

Figure 7.18 P-Delta Modification Factor for Seattle 3-story Structure; 10/50 and 2/50 Sets of Ground Motions

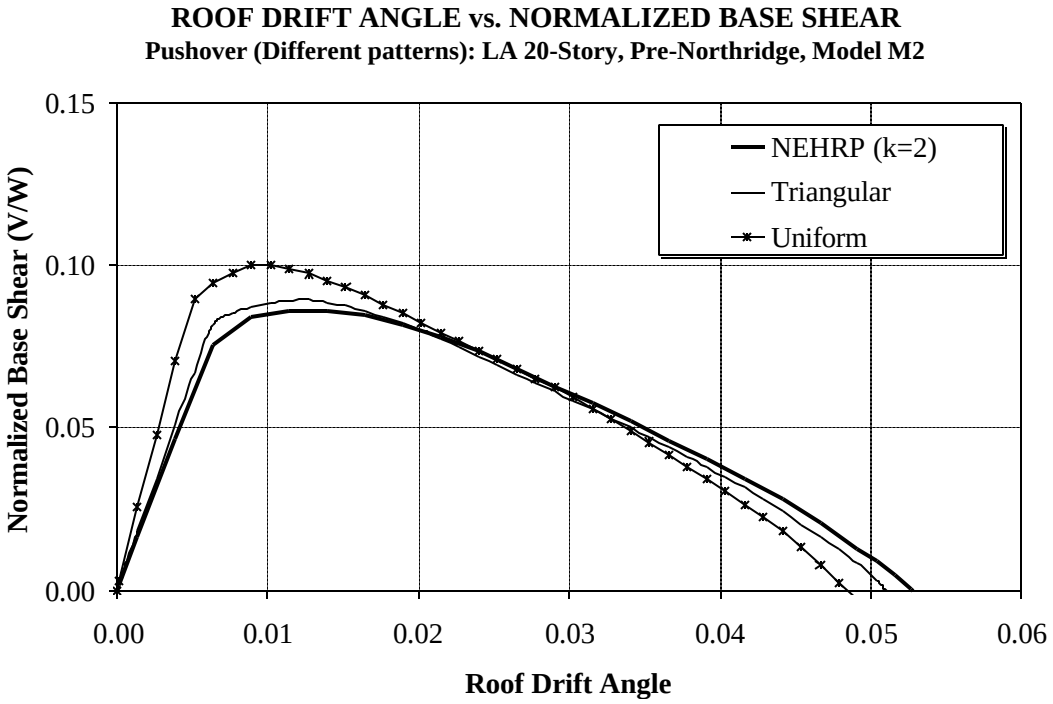

Figure 7.19 Effect of Load Pattern on Global (Roof) Pushover Response for LA 20-story Structure, Model M2

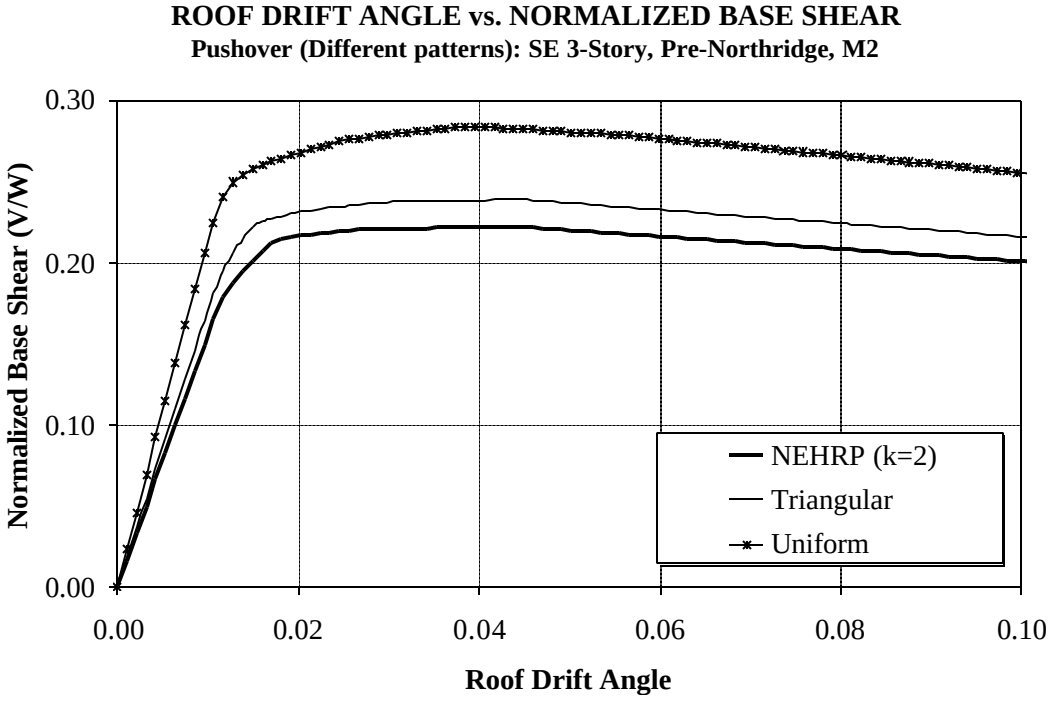

Figure 7.20 Effect of Load Pattern on Global (Roof) Pushover Response for Seattle 3-story Structure, Model M2

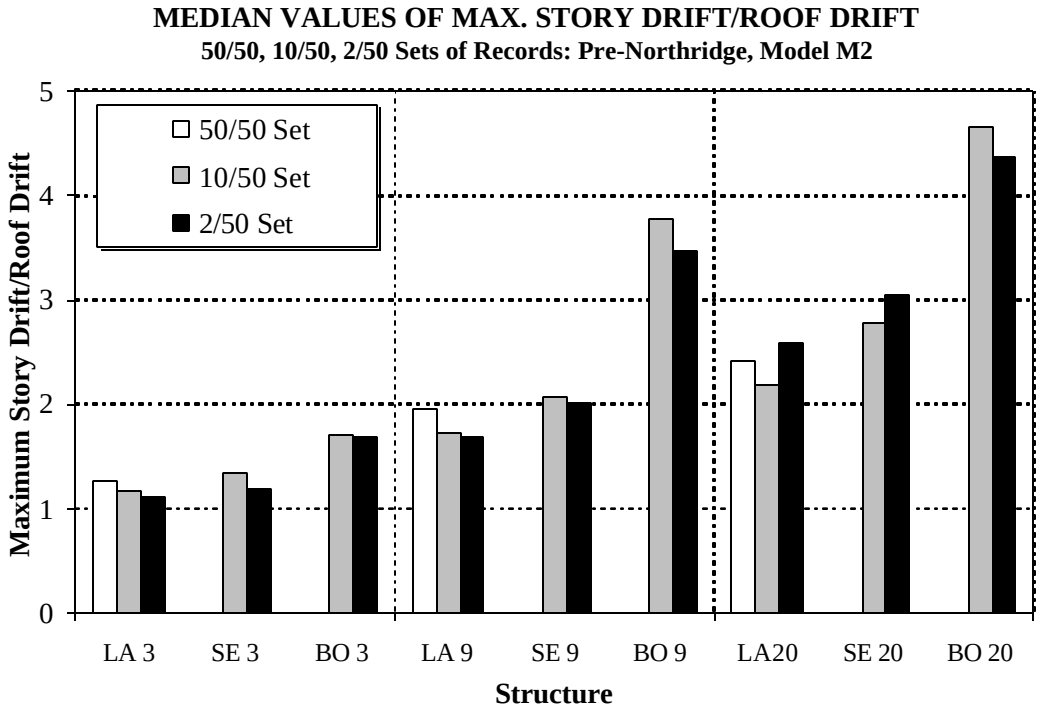

Figure 7.21 Median Values for Ratio of Max. Story Drift to Roof Drift for All Structures; All Sets of Records

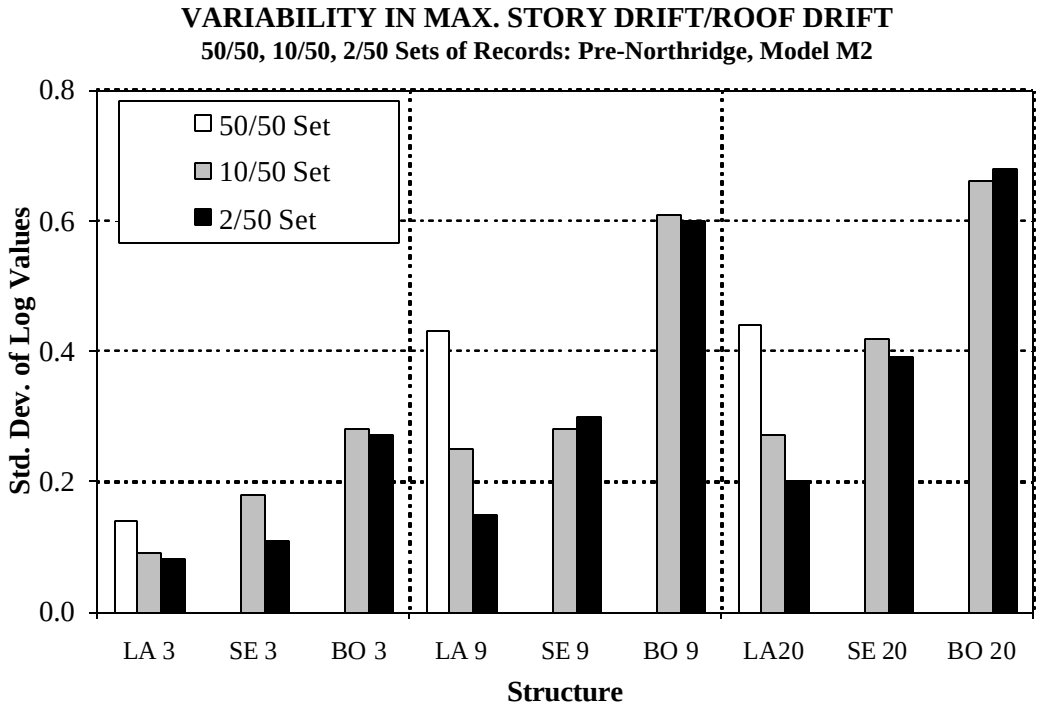

Figure 7.22 Dispersion Associated with Ratio of Max. Story Drift to Roof Drift for All Structures; All Sets of Records

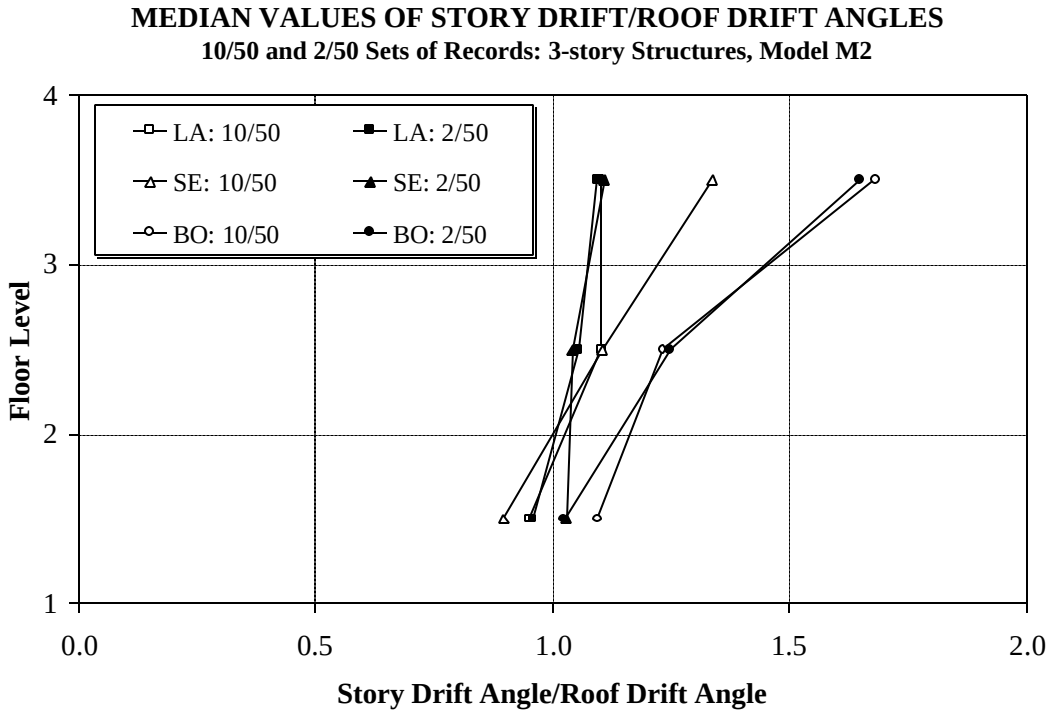

Figure 7.23 Median Values for Ratio of Story Drift Angle to Roof Drift Angle for All 3-story Structures; 10/50 and 2/50 Sets of Records

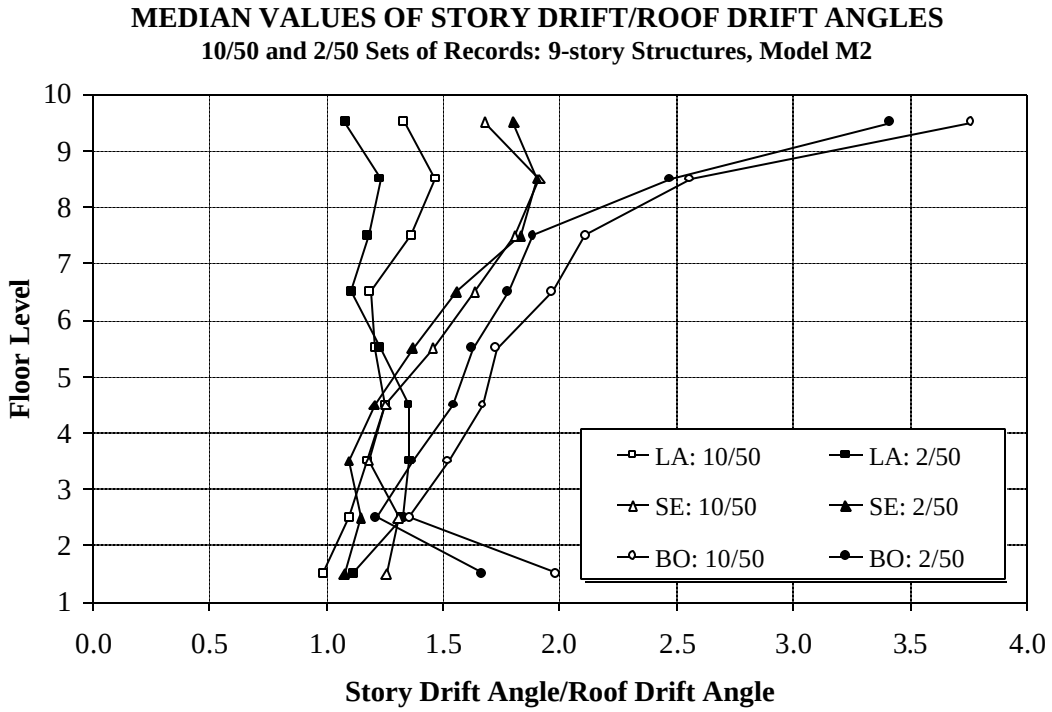

Figure 7.24 Median Values for Ratio of Story Drift Angle to Roof Drift Angle for All 9-story Structures; 10/50 and 2/50 Sets of Records

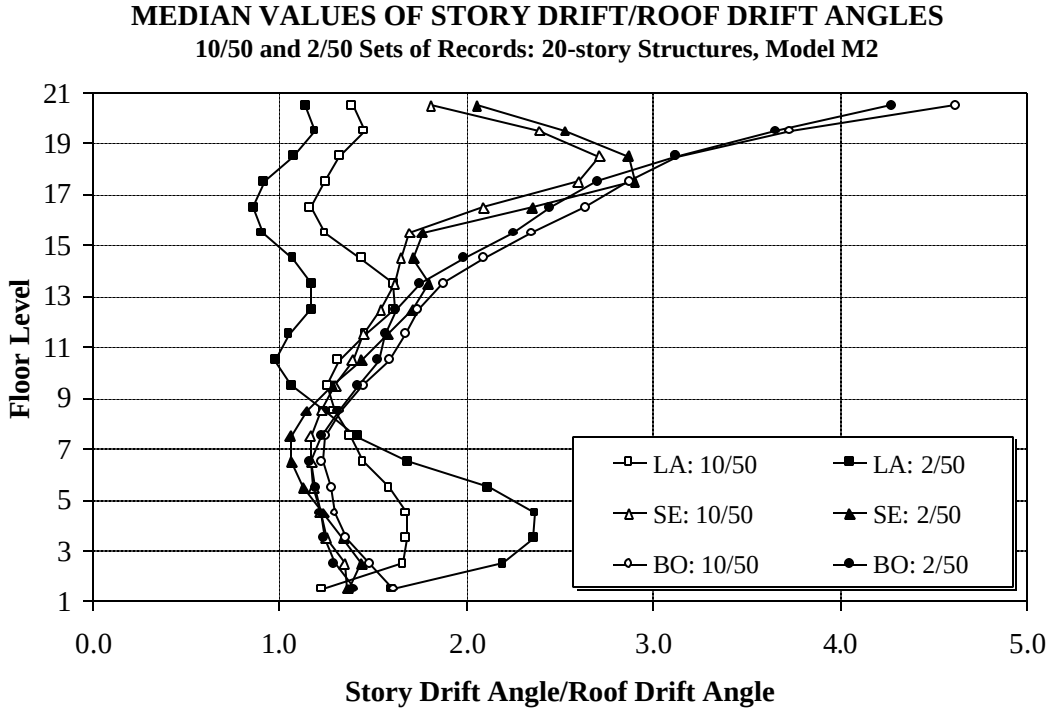

Figure 7.25 Median Values for Ratio of Story Drift Angle to Roof Drift Angle for All 20-story Structures; 10/50 and 2/50 Sets of Records

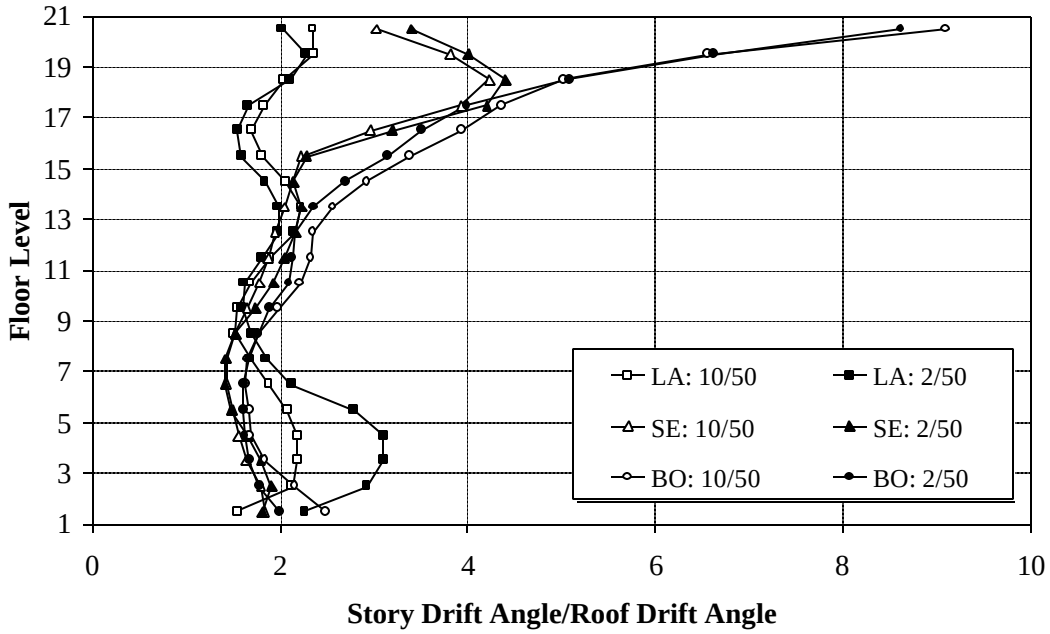

Figure 7.26 84th Percentile Values for Ratio of Story Drift Angle to Roof Drift Angle for LA, Seattle, and Boston 20-story Structures; 10/50 and 2/50 Sets of Records

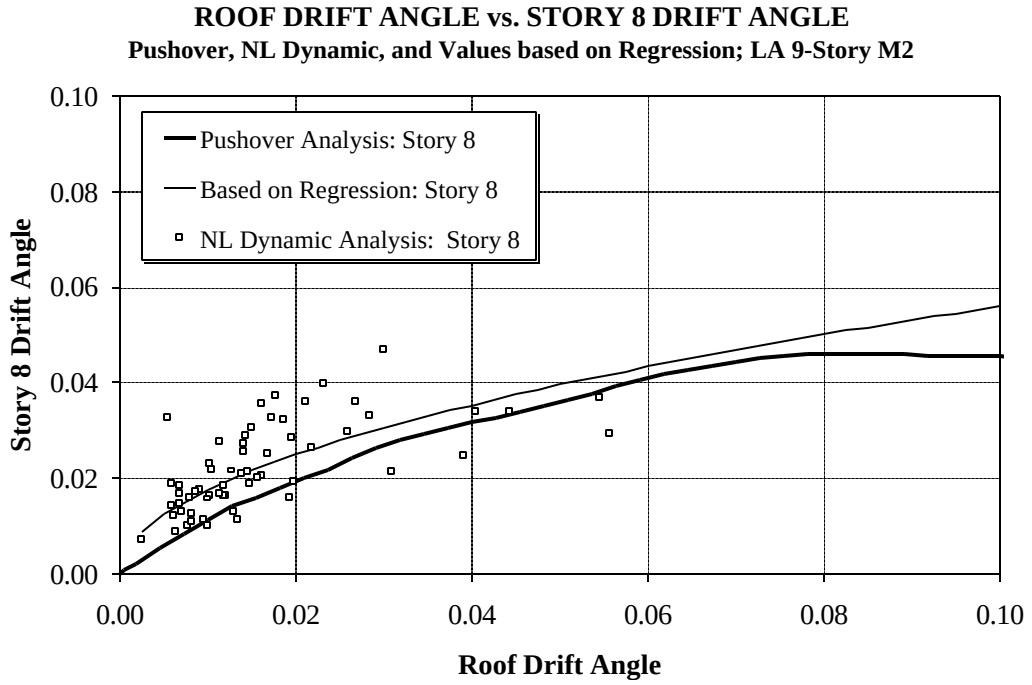

Figure 7.27 Story 8 Drift Angle as a Function of Roof Drift Angle for LA 9-story Structure; Data Points, Pushover Curve, and Regression Curve; All LA Records

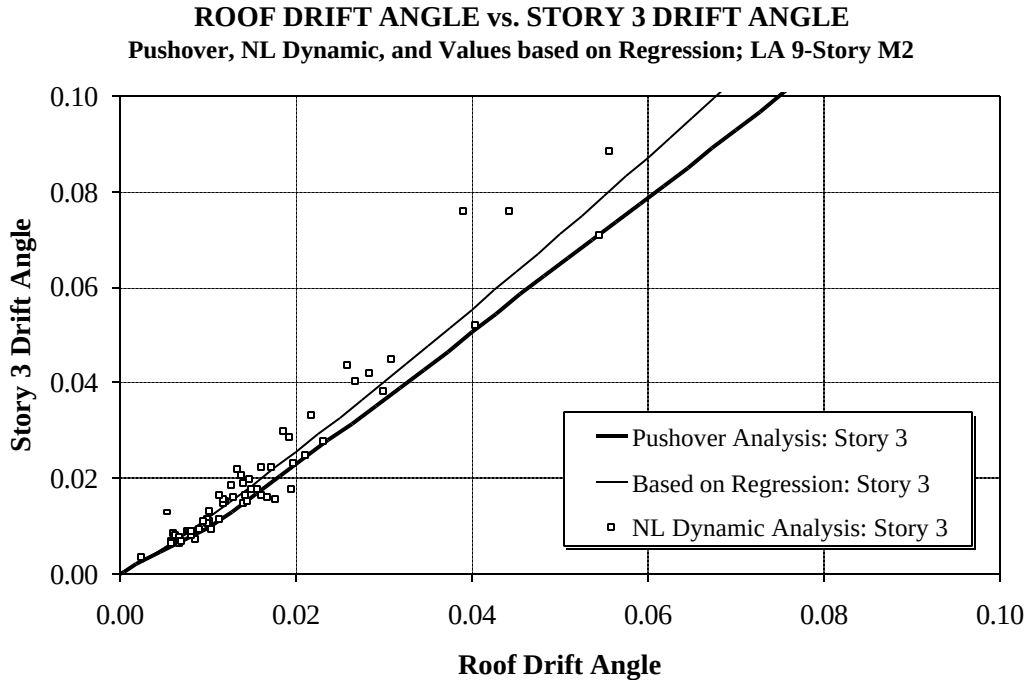

Figure 7.28 Story 3 Drift Angle as a Function of Roof Drift Angle for LA 9-story Structure; Data Points, Pushover Curve, and Regression Curve; All LA Records

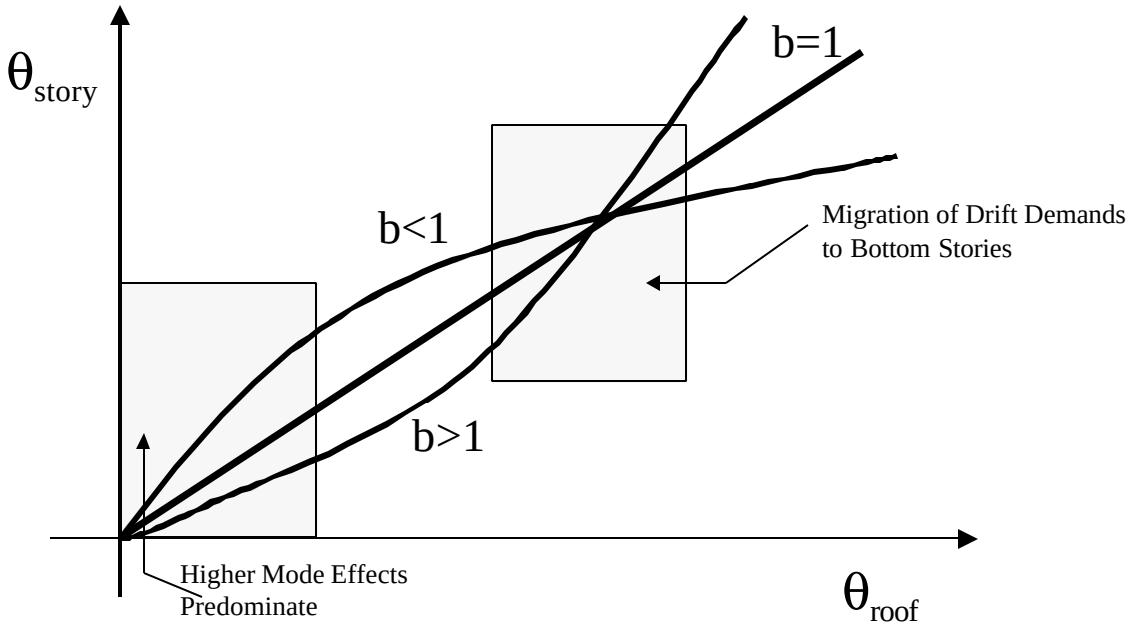

Figure 7.29 General Form of Equation 7.5 for
Relating Story Drift Angles to Roof Drift Angle

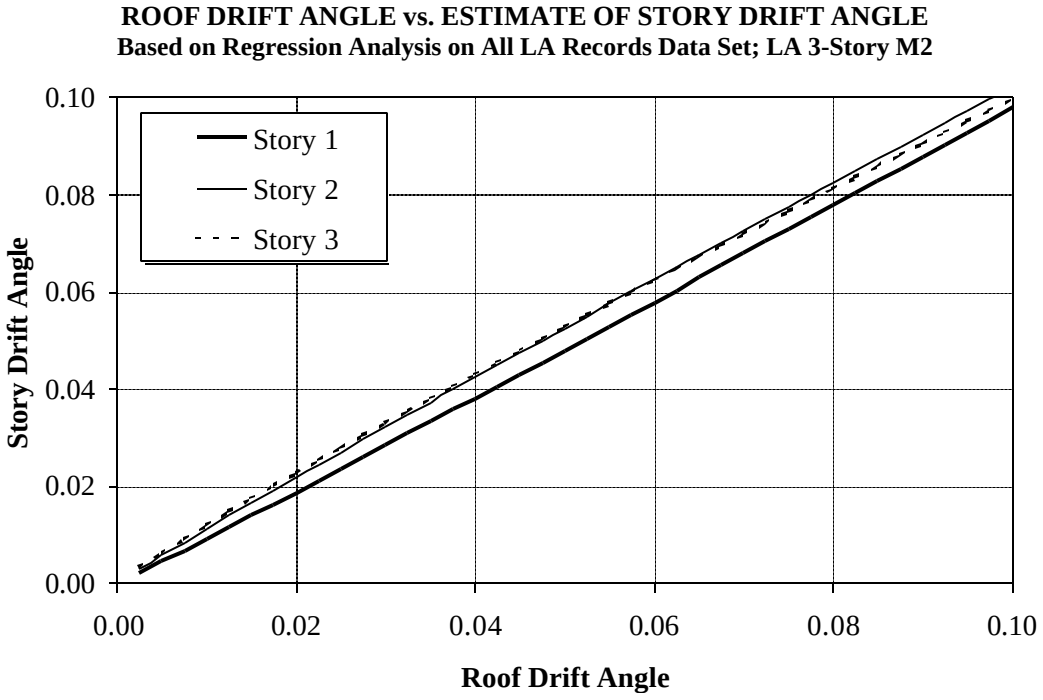

Figure 7.30 Relationship Between Story Drift Angles and Roof Drift Angle for LA 3-story Structure, Based on Regression Analysis; All LA Records

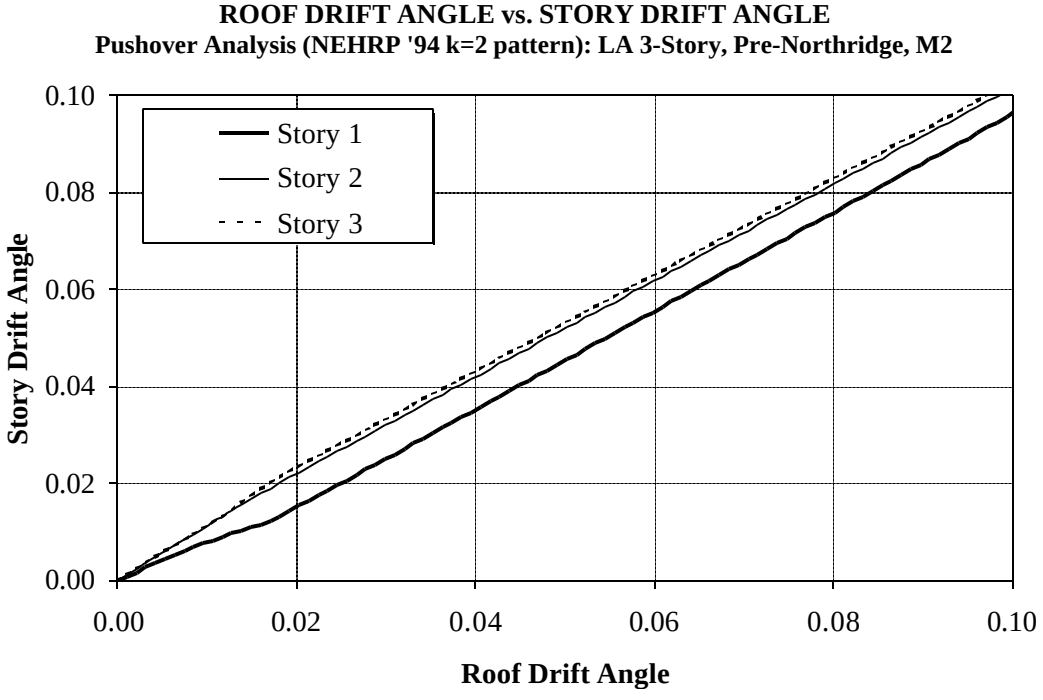

Figure 7.31 Relationship Between Story Drift Angles and Roof Drift Angle for LA 3-story Structure, Based on Pushover Analysis

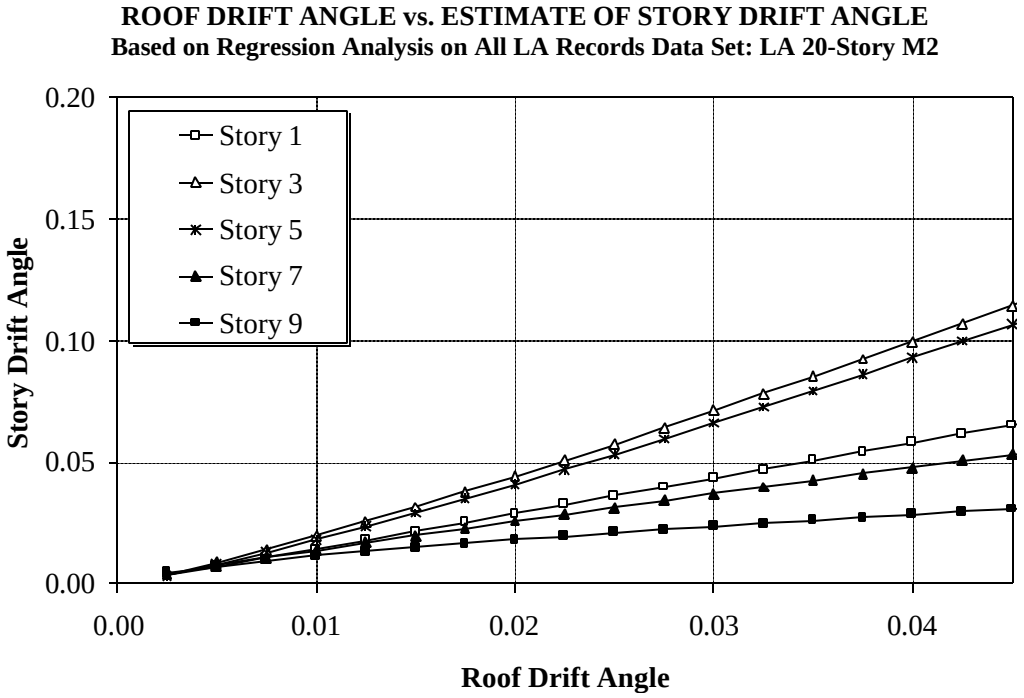

Figure 7.32 Relationship Between Story Drift Angles and Roof Drift Angle for LA 20-story Structure, Based on Regression Analysis; All LA Records

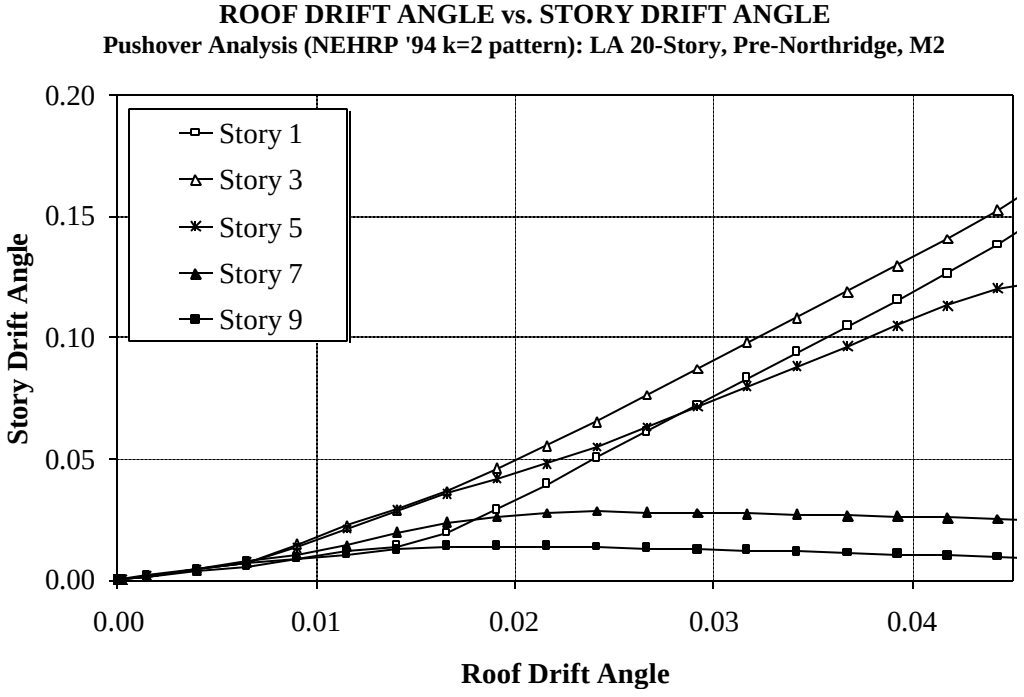

Figure 7.33 Relationship Between Story Drift Angles and Roof Drift Angle for LA 20-story Structure, Based on Pushover Analysis

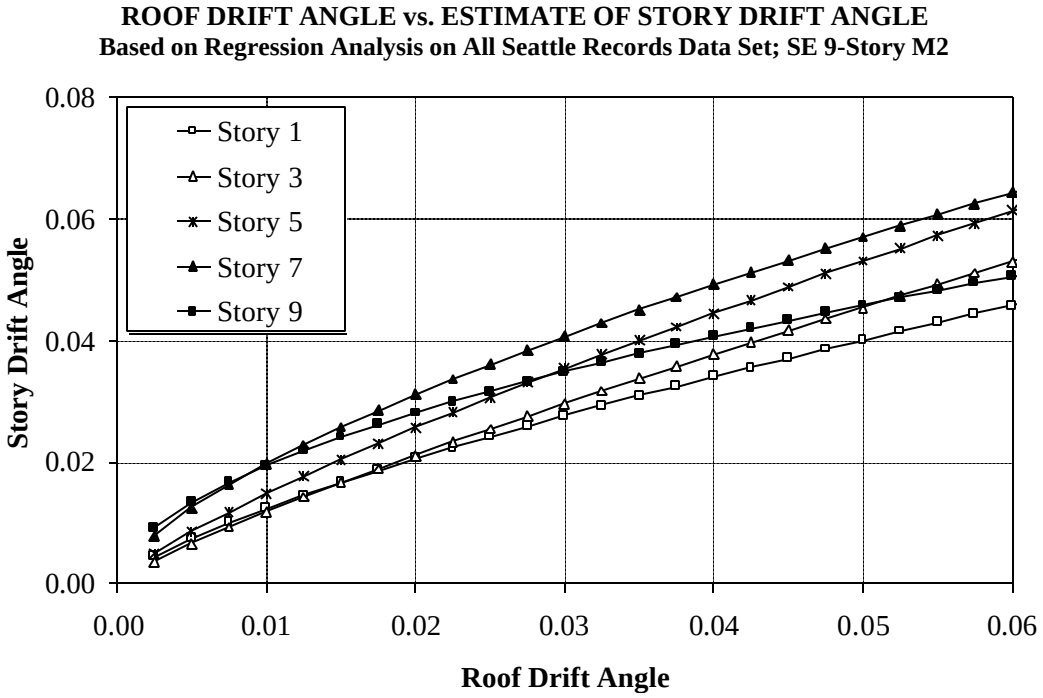

Figure 7.34 Relationship Between Story Drift Angles and Roof Drift Angle for SE 9-story Structure, Based on Regression Analysis; All Seattle Records

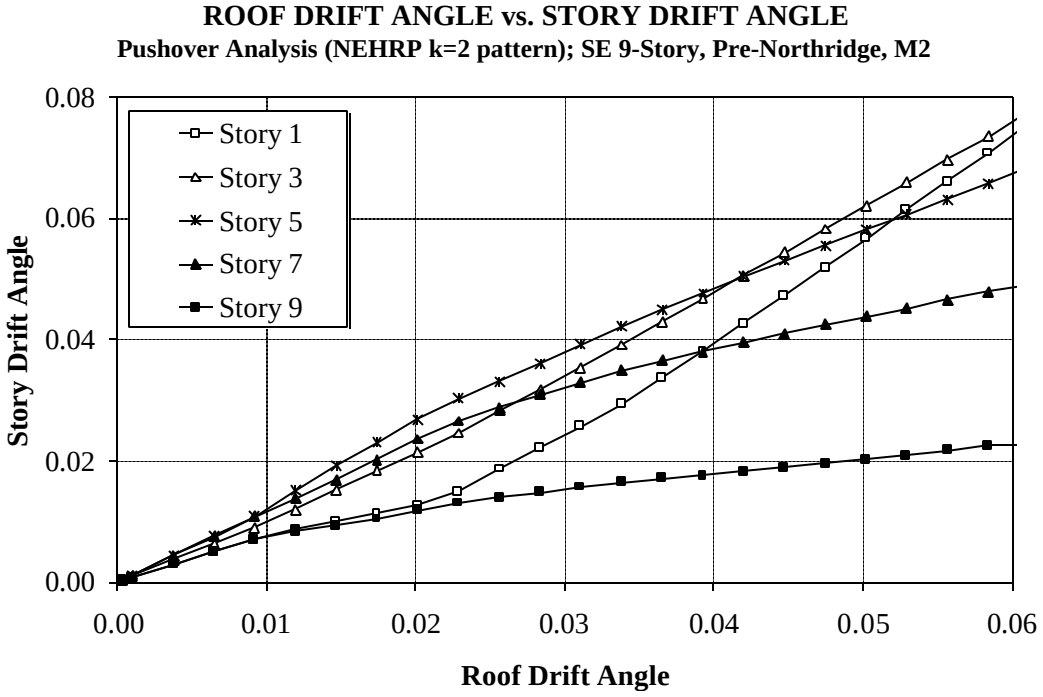

Figure 7.35 Relationship Between Story Drift Angles and Roof Drift Angle for SE 9-story Structure, Based on Pushover Analysis

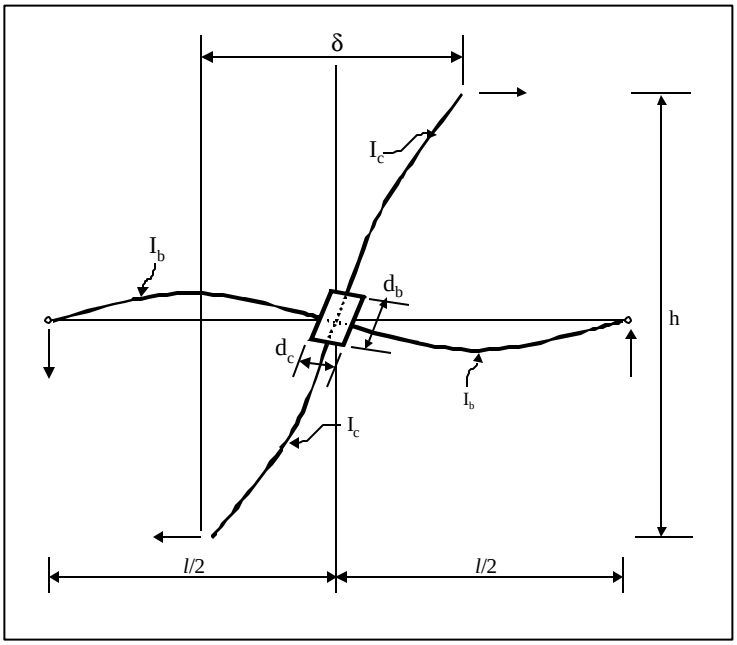

Figure 7.36 Components of Lateral Deflection in Beam-Column Subassembly at an Interior Column [from Krawinkler, 1978]

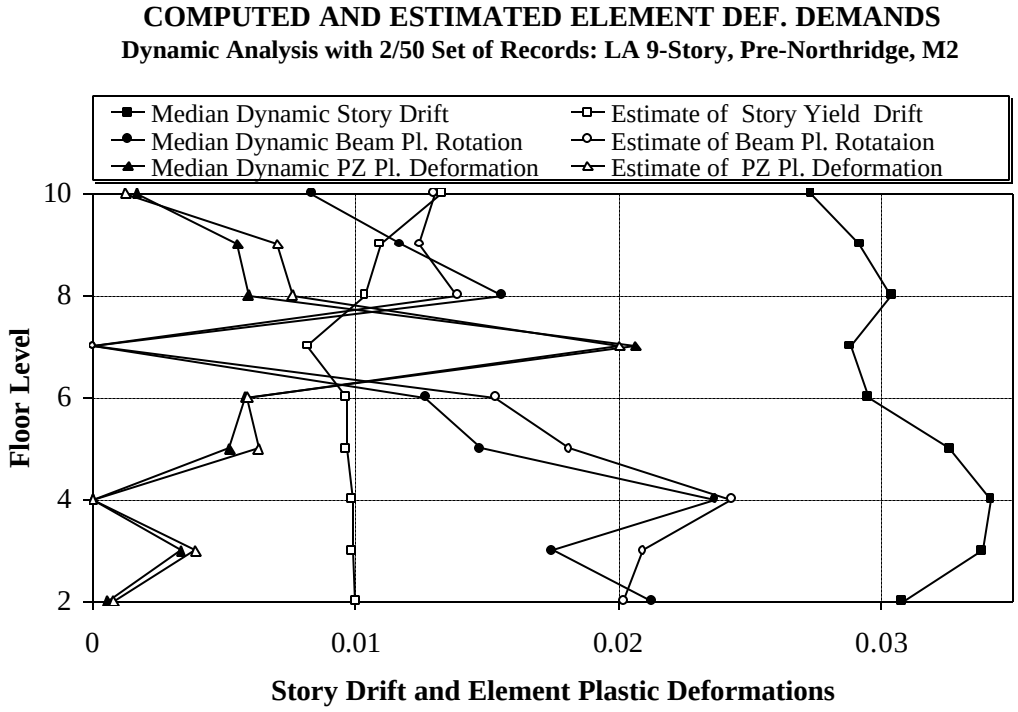

Figure 7.37 Comparison of Element Plastic Deformation Demands From Simplified Procedure and Inelastic Analysis, LA 9-story Structure; 2/50 Set of Records

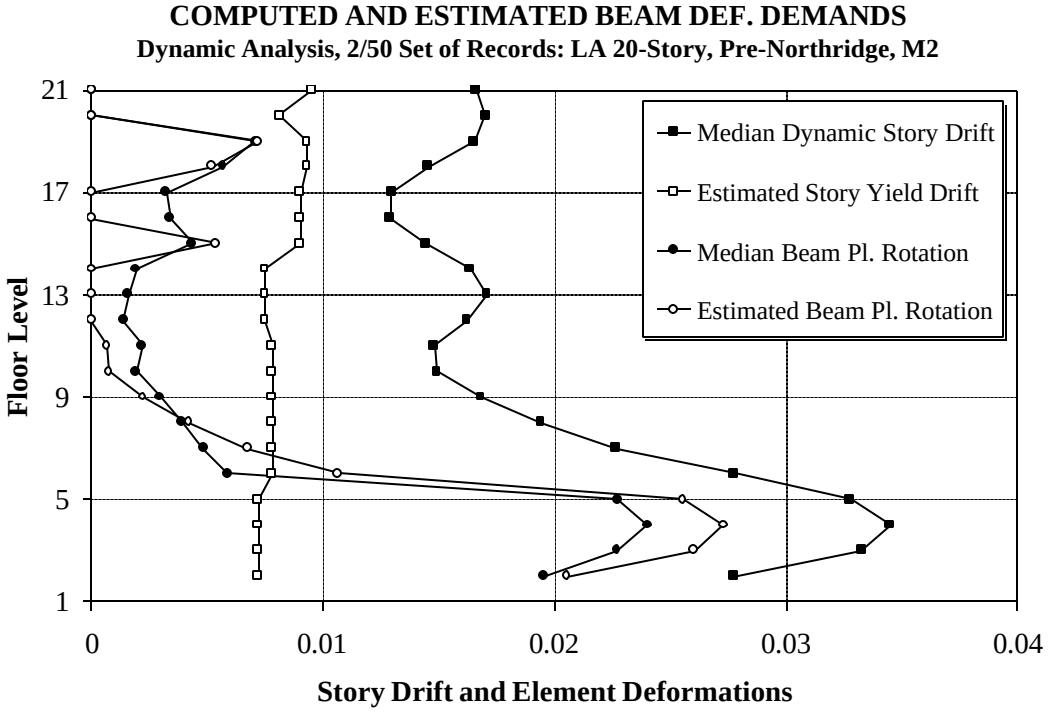

Figure 7.38 Comparison of Beam Plastic Rotation Demands From Simplified Procedure and Inelastic Analysis, LA 20-story Structure; 2/50 Set of Records

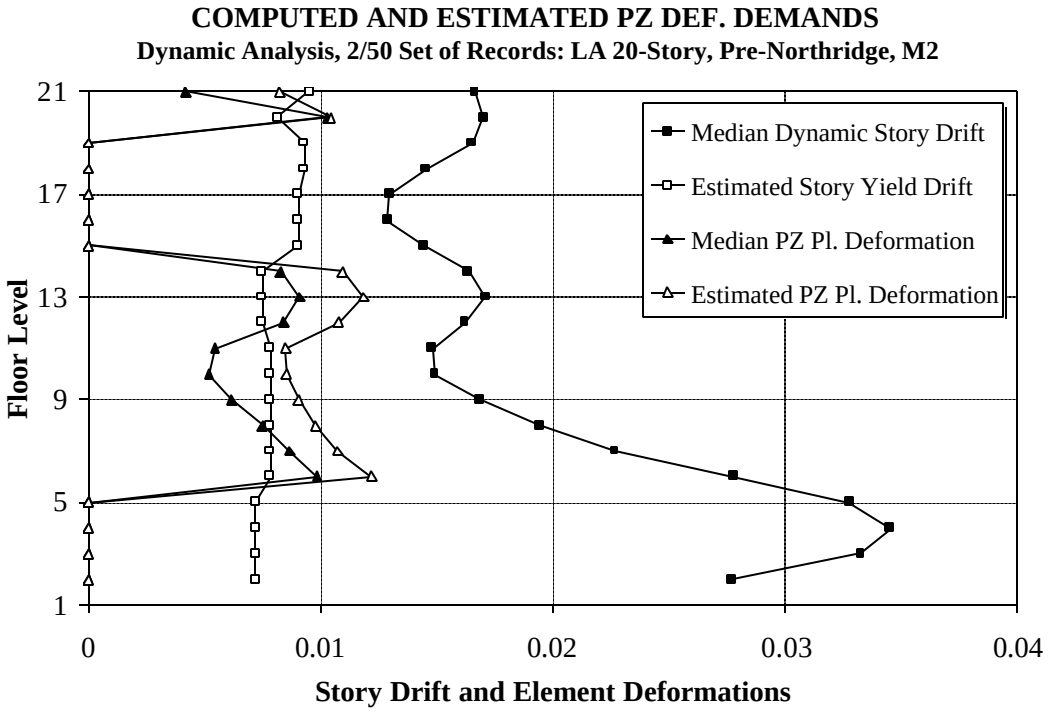

Figure 7.39 Comparison of Panel Zone Plastic Deformation Demands From Simplified Procedure and Inelastic Analysis, LA 20-story Structure; 2/50 Set of Records

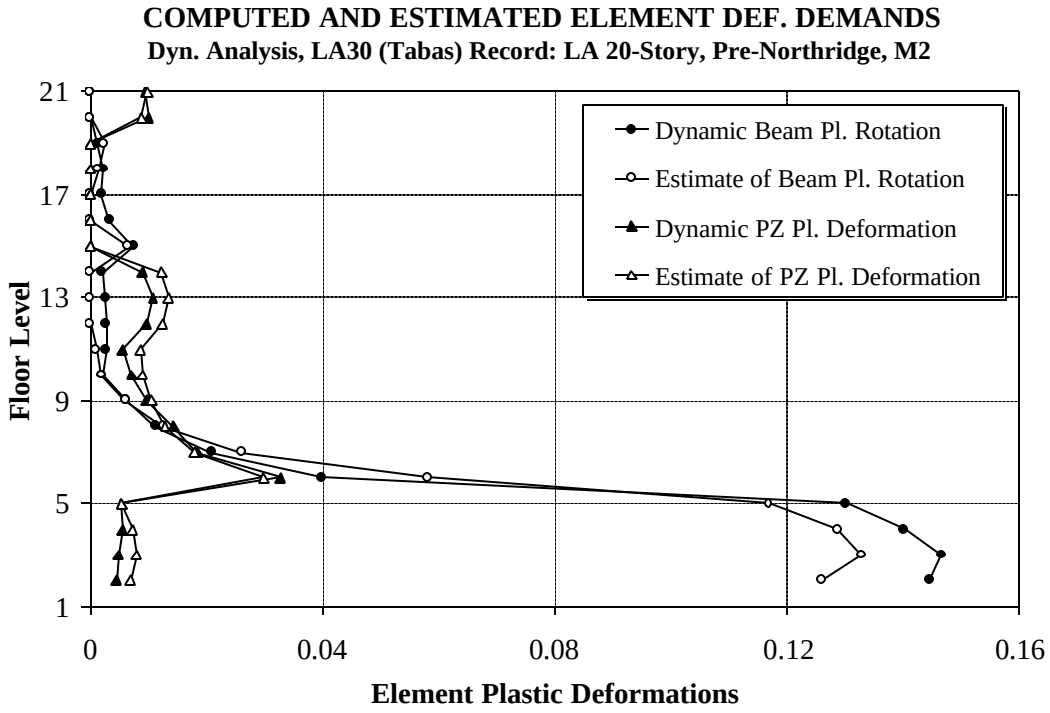

Figure 7.40 Comparison of Element Plastic Deformation Demands From Simplified Procedure and Inelastic Analysis, LA 20-story Structure; LA30 (Tabas) Record

CHAPTER 8

SENSITIVITY STUDIES

8.1 Introduction

The seismic demands for steel moment resisting frame structures, presented in the previous chapters and used for development of the simplified demand assessment procedure, have been based on certain assumptions concerning the element and structure level modeling. For example, a value of 3% has been ascribed for strain-hardening for all the elements, and 2% Rayleigh damping has been chosen for all the structures. The response of the structure is influenced by these decisions, as well as a multitude of other factors. The focus of this chapter is on an evaluation of the sensitivity of the response of SMRFs to the following different factors:

- Strain-hardening assumptions in force-deformation relationships for elements,
- Stiffness degradation in beams, which is represented through severe pinching of the moment-rotation relationship for beam springs,
- Level of damping (as a percentage of critical) in the structure,
- Strength of material, which deals with the difference between expected yield strength of and nominal yield strength of material,
- Variations in initial period of the structure due to the contribution to elastic stiffness from the non-structural elements in the structure, and
- Configuration and Redundancy, which is described in terms of changes in bay width and/or number of moment resisting connections per frame per floor level.

A wide range of values and representative configurations, which attempt to bound the possible extent for these different factors, are used in order to evaluate their possible

effect on the demands the structure might be subjected to during seismic excitation. The sensitivity of the response of the structure is evaluated primarily in terms of the global (roof) and story drift angle demands. As shown in Chapter 7, the story drift angle demand value can be converted to element plastic deformation demand values, thereby providing an estimate for the sensitivity at the element level, if required.

The sensitivity studies are carried out using the 2/50 sets of ground motions and representative subsets of the basic pre-Northridge structures; structures for which the factor under study is expected to influence the response most significantly. The analytical representation that includes panel zones (model M2) is adopted for all the sensitivity studies, except for the sensitivity study related to stiffness degradation in Section 8.3. Three redesigns of the LA 9-story structure, all of which conform to UBC '94 requirements, (see Appendix B) are evaluated. The redesigns vary from a code compliant version for the original configuration (response for which was discussed in Chapter 6), to code compliant designs which have reduced bay width (15 feet) and/or a different number of moment resisting connections per moment resisting frame (6, 9, or 18 connections) per floor.

8.2 Strain-Hardening Assumptions

There are two major assumptions involved in the analytical modeling for the post-yield stiffness of the element. The first assumption is concerning the use of a bilinear force-deformation relationship, which is an approximation for the complex cyclic force-deformation relationship of the element (see Section 3.2). The second assumption is the value ascribed to the post-yield stiffness, as a function of the elastic stiffness, for the bilinear relationship. The focus in this section is on the second assumption; the sensitivity analysis is carried out by using a set of strain-hardening values of 0%, 3% (reference level), 5%, and 10%, with the same value being used for all the elements in the structure. These values are expected to be representative of the range of possible strain-hardening values for the different structural elements.

The response of single-degree-of-freedom (SDOF) systems has been shown to be very sensitive to a change in the value of strain-hardening (and consequently the post-yield stiffness) for systems which show a negative post-yield stiffness (see Figures 4.3 and 4.4). The systems with –5% strain-hardening exhibit a significantly more unstable

response and higher displacement amplification factors than the systems with –3% strain-hardening. A similar conclusion has been drawn by Rahnama and Krawinkler (1993), using a different set of ground motions. The response for systems with a positive post-yield stiffness is, however, not as greatly affected by similar changes in the strain-hardening value. Detailed observations comparing many different parameters for generic multi-degree-of-freedom (MDOF) moment resisting frame structures spanning a wide range of periods, with strain-hardening values of 0% and 5% (P-delta effects not included) are given in Seneviratna and Krawinkler (1997). Their results indicate that the response of MDOF structures is not very sensitive to the change in strain-hardening value, for structures having non-negative post-yield stiffness.

The two pre-Northridge structures, which show a large negative post-yield stiffness due to severe P-delta effects are the Seattle 3-story and the LA 20-story structures (see Chapter 4). The deformation demands for these two structures are also evaluated to be very large, especially under a few records from the 2/50 sets of ground motions. Thus, these two structures are expected to show maximum sensitivity to the value for strain-hardening chosen for the force-deformation relationship at the element level. Consequently these two structures are chosen to evaluate the sensitivity of the response of MDOF structures to the element strain-hardening value.

Seattle 3-story Structure

The global pushover response for the SE 3-story structure, model M2, with the different strain-hardening values is presented in Figure 8.1. The original 3% model attained a negative post-yield slope (α = -2.2%) at about 0.045 global drift. The 0% model has a steeper (more negative, α = -5.5%) slope as compared to the 3% model, and also attains the negative slope at a lower global drift value of approximately 0.025. The 5% model shows only a marginal negative slope, while the 10% model clearly has a positive post-yield slope. The global stability factor, or the reduction in strain-hardening due to P-delta effect, is approximately 0.06 (or 6%).

The dynamic analysis is carried out using the 2/50 set of Seattle ground motion records. The 0% model collapsed (story drift reaching a value at which the lateral resistance of the story is zero) under the two ground motion records (SE27 and SE31), which resulted in exceedingly high drift demands also for the 3% model (see Chapter 4). Thus, statistical values are not being presented for the 0% model. For the other models

the median and 84th percentile story drift angle demands are shown in Figure 8.2. The result to note is that the difference between the demands for the 3% and 5% models is much larger than the difference in demands between the 5% and 10% models. The reason is the sensitivity of the response to the presence and magnitude of a negative post-yield stiffness. A small change in the negative post-yield stiffness may greatly affect the response of the structure, whereas an equal change in strain-hardening in the positive range has a much smaller effect. This feature is clearly reflected by comparing the maximum global drift angle demand values between the different models. The 3% model has a maximum global drift of 0.205, which drastically reduces to 0.076 for the 5% model, while only marginally reducing to 0.067 for the 10% model (see Table 8.1). Thus, the effect is most pronounced for the records which induce very severe drift demands (the tendency for the structure to drift to one side is greatly reduced). This is also indicated by the pushover analysis, wherein till about 0.025 global drift angle the response is very similar for all the models, but the differences increase rapidly for higher global drift angle demands.

Another important observation is the reduction in the scatter (reflected through the standard deviation of the log values) from 0.58 for the 3% model to 0.39 for the 10% model (see Table 8.1). The reason, again, being that with increasing strain-hardening value, not only fewer ground motions are able to push the structure into the sensitive negative post-yield range, but also that the models with lower negative (more positive) post-yield stiffness are more stable as is also indicated by the results for the SDOF systems. Consequently the resulting drift demands are much better bounded.

LA 20-story Structure

The global pushover curves for the LA 20-story structure with different element strain-hardening values are shown in Figure 8.3. Similar behavior, as seen for the Seattle structure is observed in terms of the effect of change in strain-hardening values on the roof drift angle-base shear curves. Since the LA 20-story structure is subject to severe P-delta effects (global stability factor is approximately 0.08), the post-yield slope is negative for the 5% model also, and is attained at about 0.030 global drift value.

The median and 84th percentile values for the story drift angles, under the 2/50 set of LA records, with 3%, 5%, and 10% element strain-hardening are shown in Figure 8.4. The 0% model collapsed under 4 out of the set of 20 records. The difference in the story

drift demands at the median level is not very significant as very few ground motions of the set of 20 records push the structure into the range of significant negative post-yield stiffness. For this reason, the effect is more pronounced at the 84th percentile level. Again, the reduction in demands is larger between the 3% and 5% models as compared to the reduction between the 5% and 10% models. The statistical values for the global drift angle demands are given in Table 8.1 for the different models. The reduction in maximum global drift demands may not seem significant, but when seen in context of where the particular drift demand places the structure on the global pushover curve, can reflect a significant change in the response of the structure. Again, the scatter associated with the drift demands decreases with an increase in strain-hardening, indicating a more stable response of the structure.

This short discussion shows that the response of structures can be very sensitive to the value for element strain-hardening, for cases where the structure attains a negative post-yield stiffness and is subjected to high drift demands, or is subjected to long duration ground motions (several of the Seattle records) under which the structure tends to progressively drift to one side. For other cases where the structure stays on the strength plateau or has a hardening post-yield slope, the effect of a change in strain-hardening value is quite benign, as is also indicated by the Seneviratna and Krawinkler (1997) study. Thus, for certain structures under a few ground motions, the strain-hardening assumption could be critical for response prediction, which could vary from predicted "collapse" to demand values well within acceptable ranges.

8.3 Stiffness Degradation

The use of bilinear force-deformation relationships for different elements ignores the presence of strength deterioration (e.g., due to element local buckling) and stiffness degradation (e.g., due to slip in bolts in partially-restrained connections) in the structure (see Section 3.2). The effect of strength deterioration has been documented in Rahnama and Krawinkler (1993) for SDOF systems, over a wide range of periods. The focus in this section is on evaluation of the effects of stiffness degradation, represented through a pinching hysteresis loop as shown in Figure 8.5 (details for the model are given in Rahnama and Krawinkler, 1993). A severe case of stiffness degradation is presented, wherein the F_p (pinching strength) is 25% of the plastic strength of the element. The pinching characteristics are modeled in the beam springs. The response of the LA 9-story

structure under the 2/50 set of ground motions is presented. Additionally, the feasibility of using SDOF systems as indicators for the effect of stiffness degradation on real MDOF structures is evaluated.

Four cases for the structure are evaluated: 1) Bilinear force-deformation characteristics (referred to as the bilinear model) with P-delta effects, 2) Bilinear model without P-delta effects, 3) Pinching model with P-delta effects, and 4) Pinching model without P-delta effects. The mean story drift angle demands over the height of the structure are shown in Figure 8.6. The statistical values for the ratios of story drift angles between the pinching and bilinear models are shown in Figure 8.7. The story drift amplification due to pinching, without P-delta effects, varies from about 1.0 in the first story to about 1.75 in the uppermost story. This increase in amplification over height is attributed to the variation of the number of cycles (total, and inelastic) with the height. The total number of cycles (counted for the bilinear model) increased, on average, from 15 in story 1 to 25 in story 9; the corresponding inelastic cycles increased from 4 to 8. Since the severity of the effect of pinching is directly related to the number of cycles, the story drift demand increases accordingly.

When P-delta effects are introduced in the structure, the amplification in drift demands in the lower stories is almost identical for the bilinear and pinching models. However, there is a larger de-amplification in the upper stories for the pinching model. These observations suggest that in the lower stories, where the number of cycles is small, the effect of stiffness degradation in the form of pinching of the hysteresis loop is not very important, whether or not P-delta effects are present. The effect in the upper stories could be significant depending on the characteristics of the structures, and ground motions. For example, if there is inelasticity in the upper stories of the structure (like in the Seattle 20-story structure), and the structure is subjected to severe higher mode effects and/or long duration ground motions, which result in a large number of cycles, then the amplification due to pinching could be quite significant.

An important observation to note is that the effect of stiffness degradation needs to be considered at each individual story level; comparing the maximum demands over height could be very misleading. For example, at the mean level, the ratio of the maximum story drift angles (over height) for the pinching and bilinear models (with P-delta) is about 1.0, while the maximum story level drift angle ratio is about 1.4 in story 9.

The other issue of interest in the context of stiffness degradation is the assessment of the feasibility of using SDOF systems as indicators for the response of the structures. The mean of the ratio between displacements for pinching models with –3% strain-hardening to displacements for pinching models with 0% strain-hardening, for SDOF systems, is shown in Figure 8.8. The effect of negative strain-hardening is almost negligible in the long period range, but increases sharply for short periods. These results are in sharp contrast with similar results for the bilinear models (Figures 4.3 and 4.4), which show much larger displacement amplification coupled with unstable behavior at short periods due to drifting of the response to one side (Figure 4.2). The response of the pinching models is better on account of a more symmetric response for these models, which is described using the hysteresis curve concept in MacRae (1994).

The results discussed above, along with results for three 3-story structures presented in Gupta and Krawinkler (1998), indicate that the effect of P-delta on the response of the pinching models (both SDOF and MDOF) is usually (but not always) smaller than the effect on the response for bilinear models. For tall structures, an amplification in the demand in the upper stories is to be expected on account of the stiffness degradation in the force-deformation relationship for the beam elements. A direct correlation between the SDOF and MDOF responses could not be established, except that the first mode SDOF systems indicate similar trends as the MDOF systems. The lack of direct correlation is attributed to the influence of higher mode effects, which directly influence the severity of the pinching characteristics, and which cannot be captured by the single-degree-of-freedom systems. The results discussed here have been based on model M1 (due to limitations associated with incorporating the pinching hysteresis model into the analysis program) and nominal strength of material.

8.4 Level of Damping in Structure

The level of damping (as a percentage of critical) used for the response assessment of structures is at best an approximation based on engineering judgement. In this study 2% Rayleigh damping has been used, which is fixed at the first mode period and a period of 0.2 seconds for the 3- and 9-story structures, and first and fifth mode periods for the 20-story structures. The choice of these particular period points to calculate the damping coefficients ensures that the significant modes of the structure are not excluded from the response of the structure due to excessive damping. The sensitivity of the response of the

structure to the assumption related to the level of damping is evaluated in this section. Four different values of damping are considered, 2% (reference level), 5%, 10%, and 20%. The sensitivity of the response for the 3-story LA structure (short duration ground motions, no negative post-yield stiffness) and the 3-story Seattle structure (long duration ground motions, significant negative post-yield stiffness) is evaluated.

The median story drift angle demand values for the LA 3-story structure, under the 2/50 set of ground motions, are shown in Figure 8.9, with the corresponding 84^{th} percentile values shown in Figure 8.10. Results for the Seattle 3-story structure are shown in Figures 8.11 and 8.12. The relative reduction in story drift angle demands with increasing level of structural damping for the two structures is very similar. The exception is observed for the reduction between the 2% and 5% models at the 84^{th} percentile, where the reduction is larger for the Seattle structure. The reason for this larger reduction is that the tendency of the structure to drift to one side (ratcheting) is reduced, specifically under the two ground motions that push the reference structure (2% damping) to very large drift demands. This effect can also be seen from the global drift angle demands shown in Table 8.2, wherein the maximum global drift for the Seattle structure is significantly reduced by increasing the damping to 5%. As with increasing values of strain-hardening, the scatter associated with the data reduces with increasing levels of structural damping.

These observations, in general, indicate that the effect of change in damping value on structural response is not very sensitive to the ground motion characteristics (LA versus Seattle records). To further confirm this lack of dependency on ground motion characteristics, a pilot study using a set of 20 near-field ground motions (Somerville et al., 1997) was carried out for the LA structure. The effect of change in damping on structural response for this set was observed to be very similar to the effect observed for the 2/50 set of ground motions. Furthermore, the effect was also very similar between the 10 fault-normal and 10-fault parallel components of the set of records.

These observations are reinforced by results presented in Krawinkler and Seneviratna (1997) for single-degree-of-freedom systems with damping values ranging from 0-20% of critical, for a different set of 15 ground motions. Their results also indicate that the effect of damping is not significantly affected by the period of the SDOF system, except at very shot periods. Their results indicate that the effect of change in structural damping is well represented by the SDOF systems.

The important conclusions, which can be drawn from this brief discussion concerning the effect of the level of structural damping on the structural response, are that 1) the effect is not significantly influenced by ground motion characteristics, unless the structure has a tendency to progressively drift to one side, in which case an increase in structural damping (which could be artificially induced, also) may improve the structural response quite significantly, and 2) for structures responding primarily in the first mode, SDOF systems are able to well predict the effect of a change in the level of damping on the structural response. These conclusions are based on the response of the 3-story structures and the information in the referenced study.

8.5 Strength of Material

The effect of the difference between nominal and expected strength of material has been discussed for the LA 9-story structure under Section 6.2, where the focus was primarily on the distribution of demands between the elements at typical connections. This section complements the information in Section 6.2, with an evaluation of the effect of expected strength versus nominal strength of steel, for the LA 3- and 20-story structures subjected to the 2/50 set of ground motions. The LA structures use A36 ksi beams (nominal strength is 36 ksi, expected strength is 49.2 ksi) and A572 Gr. 50 ksi columns (nominal strength is 50 ksi, expected strength is 57.6 ksi). The emphasis is on global and story drift angle demands, only. The effect on element demands is similar to the effect discussed in Section 6.2.

The global pushover curves for the LA 3-story structure, with expected and nominal strength of steel, are shown in Figure 8.13. As the beams are relatively weaker than the panel zones and yield first, the increase in strength of the structure is proportional to the increase in strength of the beams. Thus, the yielding pattern is similar between the two models, and consequently the global pushover curves are similar. The statistical values for the global drift demands are given in Table 8.3, and the story drift angle demands are shown in Figure 8.14. The demands for the model with nominal strength of steel are higher, but not by a large amount.

The global pushover curves for the LA 20-story models are shown in Figure 8.15, and the dynamic story drift angle demands are shown in Figure 8.16. At the outset the results for the 20-story seem to portray similar trends as observed for the 3-story structure.

There is, however, a critical difference; the 20-story structure with nominal steel strength collapses under the two severe records (LA30 and LA36, see Chapter 4), while the model with expected steel strength does not (though it has very high story drift demands, in excess of 0.10 radians). The statistical values are based on 18 out of the 20 records for both models. The model with nominal strength properties attains a state of zero lateral resistance sooner (roughly 0.043 roof drift angle) as against the model with expected strength (roughly 0.052 roof drift angle). Thus, even though the severity of the P-delta effect is identical for the two models, the model with nominal strength of steel attains the negative post-yield slope at a slightly lower roof drift angle (see Figure 8.15) and consequently reaches collapse conditions sooner. The global drift demands shown in Table 8.3 also indicate that the model with nominal strength of steel is close to collapse under another record (LA35), which induces a maximum roof drift angle of 0.0423.

The possibility exists that addition of all other contributions to the model (resulting in a model such as model M2A, see Section 3.4) may prevent the collapse of the model with nominal strength properties. However, the important result to note is the likelihood of obtaining very different response of the structure, on account of a difference in the steel strength. This observation reiterates the necessity of employing the most accurate model possible (in terms of analytical modeling and properties of elements), for cases which exhibit unacceptable response with simpler models and structural properties. For other cases simpler models and estimates of structural properties may be adequate to provide a fair estimate for the structural response.

A change in material strength properties affects the local distribution of demands (where different types of steel are used for the beams and columns), as observed in Section 6.2, but does not affect the story and global drift angle demands very significantly. This conclusion holds true for structures, which do not develop negative post-yield stiffness and/or are not subjected to very severe drift demands. Under such conditions the response of the structure becomes very sensitive to any change in strength of the structure. For this reason, the Seattle 3-story structure is expected to show higher drift demands when modeled using nominal strength properties. The other Seattle structures and Boston structures are not expected to be significantly influenced by a change in material strength properties.

8.6 Period of Structure

The response of the structure is affected by the presence of cladding, partition walls, and other non-structural elements. These elements are expected to increase the elastic stiffness of the structure, but by an amount that depends greatly on architectural considerations. Their contribution to the post-yield stiffness and strength of the structure is expected to be small and is ignored in this study. The effect on the elastic stiffness, however, cannot be ignored as the increased stiffness results in a shift in the period of the structure, which may result in very different drift demands for the structure. In order to assess the range of effect the stiffness of non-structural elements may have on the seismic response, the first mode period of the structure is reduced by factors of 1.25, 1.50, and 2.00. This is achieved by increasing the elastic stiffness of all columns, beams, and panel zone elements by the same proportions. The strain-hardening for the elements is adjusted accordingly, to result in the same post-yield stiffness as that for the original structure. The caveat of this procedure is that the unloading stiffness of the structure, which equals the elastic stiffness, is now higher than that for the original structure. This may not be very accurate, especially if the structure is subjected to large inelastic demands during which the non-structural elements are damaged to an extent that there is no further contribution to the stiffness of the structure from these elements.

The global pushover curves for the LA 3-story structure, with different first mode periods are shown in Figure 8.17. Since the post-yield stiffness is being kept unchanged by adjusting the strain-hardening ratio, the global pushover curves only vary in the elastic range. The global pushover curves for the other structures show similar trends. The statistical values for the story drift angle demands for the different 3-story models are shown in Figure 8.18. The median and 84th percentile story drift angle demands for the LA 9-story structure are shown in Figures 8.19 and 8.20, respectively, and similar results for the LA 20-story structure are shown in Figures 8.21 and 8.22. The global drift angle demands for the three structures are given in Table 8.4.

The median and 84th percentile drift angle demands decrease with a decrease in the first mode period of the structure, though that is not the case for each individual record, i.e., for some cases the demands increase with a decrease in period on account of the spectral characteristics of the ground motion. In general, the decrease in median global drift demands is not proportional to the decrease in the median elastic spectral displacement demands, even for the 3-story structure, for this set of ground motions.

This is attributed to the influence of higher mode effects, which may change disproportionately depending on the period shift in the structure coupled with the shape of the elastic response spectrum for the ground motion.

Even though the median elastic displacement demand spectrum is fairly constant for the range of periods swept for the LA 20-story structure, the drift demands are lower for the shorter period 20-story structures. This is because even though the median spectral displacements do not change by much, the individual displacement demand spectrum for a few records change quite significantly (e.g., LA30 ground motion – see Figure 4.12). This reduction in spectral displacement demand results in a reduction for the structure P-delta effect, compounding the reduction in the structural drift demand to the extent that it is reflected in the median values also. This effect is clearly seen from the following example: for the LA30 ground motion the global drift angle demand reduces from 0.043 for the original model to 0.018 (58% reduction) for the model with T/1.50 first mode period, while the elastic spectral displacement demand only decreases from 59.9 inches to 36.4 inches (39% reduction). Consequently, the differences are larger at the 84^{th} percentile level of demands, as compared to the median level. The LA 9-story shows similar results. The pattern for story drift demands over height is not much affected by the period shifts for the 3- and 20-story structures, while the 9-story drift pattern changes with a larger reduction in demands being observed for the upper stories. This is due to the fact that the lower stories are designed primarily for stiffness (drift control) while the upper stories are designed more on the basis of strength requirements. An increase in the stiffness, thus affects the upper stories more significantly. This effect is not as significant for the 20-story structure because of the inherent weakness in the lower stories of the structure due to structure P-delta effects.

The contribution of non-structural elements to the strength (minor) and elastic stiffness (major) cannot be quantified accurately, and may vary from structure to structure on account of aesthetic and functional requirements of the structure. The general conclusion is that conventional models in which the contributions of the non-structural elements to the elastic stiffness are ignored, will result in an overestimation of the drift demands for the structure. The extent of the overestimation depends on the characteristics of the structural and non-structural elements, and the ground motion characteristics. This conclusion needs to be kept in mind when results from time history analysis with conventional models are interpreted. However, representing the stiffening effect by an increase in elastic stiffness may overestimate the decrease in drift demands

because of the cyclic stiffness degradation of non-structural elements. The elastic demand spectra provide an estimate for the change in drift demands, but may not be able to capture the full effect of the change in structural period on the dynamic response of the structure when higher mode and P-delta effects become important.

8.7 Configuration and Redundancy

The emphasis in this section is on evaluation of sensitivity of the structural response to the configuration and redundancy of the system. Configuration issues relate to the bay width and the location of moment resisting (MR) connections on a floor level, among others. Redundancy issues relate to the number of MR connections at a floor level, which have to sustain the demands imposed by the seismic excitation. Consider the simplest form of the relationship, described in Section 7.4, between the story drift angle demand and the element deformation demands at a connection where the beam is much weaker than the panel zone (and column). For such a case the relationship between the beam plastic rotation, and story drift angle and story yield drift angle, can be written as:

$$q_{beam,\,plastic} \approx q_{st,\,plastic} \approx q_{st,total} - q_{st,\,yield} \tag{8.1}$$

This equation suggests that all beams on that floor are subjected to the same level of inelastic deformation irrespective of the number of beams on the floor, i.e., irrespective of the bay width or redundancy in the system (provided that gravity moments are small).

A change in the configuration and/or redundancy of the system usually results in a change in the size of members for the structure. For example, shorter bay widths will typically result in the use of lighter (shallower) beam sections. This change in beam depth might be significant, especially in the context of fracture of the welded beam-column connections, as shown by Roeder and Foutch (1996), wherein they present a correlation between the beam depth and the likelihood of fracture (larger beam depth being more susceptible to fracture). Since the focus of this study is on the response of ductile SMRFs, the issue related to correlation between beam depth and probability of fracture is not addressed here. The reader is referred to a study by Cornell and Luco (1998), which addresses this particular issue.

The focus in this section is on the different kinds of designs that may be obtained based on decisions concerning the configuration and number of MR connections in a structure, and their effect on the static and dynamic response of the structures. For this purpose, three redesigns for the LA 9-story structure are carried out (the structure height, plan dimensions, and weight are kept constant; see Appendix B for details) using the computer program BERT (Fuyama et al., 1993). The designs are based on nominal strength of steel to relate to the original LA 9-story design process, but the evaluation is carried out using expected strength of steel. BERT designs code (UBC) compliant structures based on a weight efficiency at the story sub-structure level. The three redesigns are described below:

1. R1-LA9: Weight efficient version for the original configuration of the LA 9-story structure, i.e., 30' bays and 9 FR connections/frame/floor. The response of this structure has been discussed previously in Chapter 6.
2. R2-LA9: The bay width is reduced to 15', resulting in 10 bays of which 9 are moment-resisting, resulting in 18 FR connections/frame/floor.
3. R3-LA9: The bay width is kept constant at 30', however, only 3 bays are moment-resisting, resulting in 6 FR connections/frame/floor.

The R1 redesign resulted in a much lighter structure (about 23% lighter) as compared to the original LA 9-story structure, on account of a significant reduction in column sizes at the small expense of an increase in beam sections (more efficient to control drift through beams, rather than columns). The R2 redesign uses much lighter beam sections on account of the shorter bay width, and also lighter column sections. The R3 redesign has heavier beam sections (maximum depth of beams was constrained as 36 inches) and lighter columns. The redesigns meet the code drift criterion and the strong column-weak panel zone criterion (due to use of expected strength properties, the beams became relatively stronger than the columns at many connections).

The modal characteristics for the three redesigns and the original LA 9-story structure are given in Table 8.5. The R1 and R3 redesigns are more flexible than the original LA 9-story design, on account of conforming more closely (less margin) to the code drift criterion. The R2 design is only slightly more flexible on account of the design being controlled closely by both strength and stiffness requirements.

The redesigns are significantly weaker than the original structure, as can be seen from Figure 8.23, which shows the global pushover curves for the four structures. The strength of the redesigns is controlled by yielding in the panel zones, which prevent the development of bending strength in beams and columns. Thus, even though the beam sections are similar between the original design and the R1 and R3 redesigns, the redesigns exhibit much lower strength. All the redesigns (especially R1 and R3) show desirable inelastic characteristics, insofar that the pushover curves are characterized by wide strength plateaus, i.e., the lateral strength does not decrease significantly until the roof drift angle reaches about 0.06 radians. The reduction in lateral strength of the R2 redesign at about 0.06 radians global drift demand is attributed to the development of negative post-yield stiffness in the middle stories of the structure.

The median and 84th percentile story drift angle demands under the 2/50 set of LA ground motions, for the four structures are shown in Figures 8.24 and 8.25, respectively. The global drift angle demands are given in Table 8.6. The median global (roof) drift demands between the different designs are comparable, though differences of the order of 0.01 are observed at the 84th percentile level. One possible reason for the higher global drift is the longer periods for the structures. For R2, the differences are due to the development of the post-yield negative stiffness in the middle stories at high global drift demand values (in excess of 0.06). This effect is also reflected in the story drift demand values, wherein demands for the R1 and R3 redesigns have similar patterns and slightly higher demands than demands for the original structure, while the R2 model shows a bulge in the middle stories drift angle demands.

The conclusion to be drawn from this brief discussion on effect of configuration and redundancy on the response of SMRFs is that very different designs can be obtained for the same structure, based on the design decisions. The differences can be in terms of the bay widths, number of moment-resisting connections, member properties, and combined structural characteristics. The response of ductile SMRFs is not expected to vary significantly with these changes in configuration and redundancy, unless the change induces a weakness in the structure (like the one observed for the R2 redesign). The effect on the response of the structure may be more critical when fracture of welded beam-column joints is introduced, on account of the documented relationship between beam depth and likelihood of fracture.

8.8 Conclusions

This chapter focused on the sensitivity of the static and dynamic response to assumptions introduced in the modeling of the structures (e.g., element strain-hardening, structural damping), or due to effects which cannot be directly accounted for in conventional models (e.g., period shifts on account of non-structural components). The conclusions which can be drawn from the sensitivity analysis studies discussed in this chapter are as follows:

- Strain-hardening: The structural response is observed to be sensitive to the element strain-hardening assumption for cases in which the structure is pushed into the negative post-yield stiffness region, as the value of element strain-hardening directly affects the onset and slope of the negative post-yield range. The reduced negative post-yield stiffness on account of increased strain-hardening may also reduce the tendency of the structure to ratchet to one side, especially under long duration ground motions. The effect of a change in element strain-hardening for other cases (positive post-yield slopes) is not found to be very significant. The SDOF systems are indicative of the effect of changes in strain-hardening on the response for MDOF structures.

- Stiffness Degradation: The effect of stiffness degradation, which is addressed using a pinching hysteresis loop for the beam springs, increases for upper stories, and is often related to the number of inelastic cycles experienced by the structure. Lower stories, which are usually more affected by the P-delta effect, are not severely influenced by stiffness degradation. In general, stiffness degradation decreases the P-delta effect. The SDOF systems are not able to capture the effect of stiffness degradation on the response of MDOF structures very well.

- Structural Damping: The effect of structural damping is observed to be not very sensitive on the ground motion characteristics. Increased levels of damping reduce the tendency of structures to drift to one side, like for structures with negative post-yield stiffness subjected to long duration ground motions. In general, an increase in structural damping may provide a convenient means for controlling the response of critical structures. The SDOF systems are able to predict well the change in response of short structures due to changes in the level of structural damping.

- Strength of Material: The effect of changes in the strength of steel at the element level and the structure level, for the LA 9-story structures, have been discussed in Chapter 6. The conclusion was that the change in strength usually has a benign effect at the structure level, except for certain sensitive cases where the change (reduction) in strength might drive the structure near collapse. This conclusion is reinforced in this chapter through observations for the LA 3- and 20-story structures. A change in material strength may greatly affect element behavior; plastic deformations may shift partially or totally from one element to another.

- Configuration and Redundancy: A change in bay width (configuration) and/or redundancy (number of moment-resisting connections per frame per floor) will result in a change in member properties. However, if the change does not induce a weakness in a particular story or at the structure level, then the response is expected to be similar.

The list of factors considered in this chapter is by no means exhaustive. The structural response is affected by a multitude of factors, some of which can be quantified and others cannot be as easily ascertained or quantified. For certain cases, a better representation of the element and structural characteristics may significantly alter the calculated response, to the extent that predicted "collapse" could change to an acceptable level of performance. This chapter provides information on the effect of a few of these factors on the structural response of typical SMRF structures, subjected to severe ground shaking hazard. The effect on the structural response, at the global and story drift level, is not expected to be as significant at lower levels of ground shaking.

Table 8.1 Sensitivity of Global Drift Angle Demands with Element Strain-Hardening, Seattle 3-story and LA 20-story Structures; 2/50 Sets of Ground Motions

Seattle 3-Story

	a = 0%	**a = 3%**	**a = 5%**	**a = 10%**
Maximum	Model Collapsed Under 2/20 Records	0.2054	0.0761	0.0671
84th Percentile		0.0726	0.0558	0.0522
Median		0.0408	0.0365	0.0355
Minimum		0.0190	0.0190	0.0189
Std.Dev. Of Logs		0.58	0.42	0.39

LA 20-Story

	a = 0%	**a = 3%**	**a = 5%**	**a = 10%**
Maximum	Model Collapsed Under 4/20 Records	0.0432	0.0367	0.0324
84th Percentile		0.0247	0.0220	0.0213
Median		0.0146	0.0140	0.0139
Minimum		0.0080	0.0080	0.0080
Std. Dev. Of Logs		0.53	0.45	0.43

Table 8.2 Sensitivity of Global Drift Angle Demands with Structural Damping, LA and Seattle 3-story Structures; 2/50 Sets of Ground Motions

LA 3-Story

	x = 2%	**x = 5%**	**x = 10%**	**x = 20%**
Maximum	0.1095	0.0942	0.0761	0.0533
84th Percentile	0.0658	0.0582	0.0490	0.0371
Median	0.0393	0.0356	0.0313	0.0251
Minimum	0.0152	0.0141	0.0134	0.0114
Std.Dev. Of Logs	0.52	0.49	0.45	0.39

Seattle 3-Story

	x = 2%	**x = 5%**	**x = 10%**	**x = 20%**
Maximum	0.2054	0.1281	0.0758	0.0509
84th Percentile	0.0726	0.0592	0.0464	0.0349
Median	0.0408	0.0358	0.0301	0.0240
Minimum	0.0190	0.0183	0.0169	0.0144
Std.Dev. Of Logs	0.58	0.50	0.43	0.38

Table 8.3 Sensitivity of Global Drift Angle Demands with Strength of Material, LA 3-, 9-, and 20-story Structures; 2/50 Set of Ground Motions

	LA 3-Story		LA 9-Story		LA 20-Story*	
	Exp. Fy	Nom. Fy	Exp. Fy	Nom. Fy	Exp. Fy	Nom. Fy
Maximum	0.1095	0.1251	0.0558	0.0577	0.0421	0.0423
84th Percentile	0.0637	0.0705	0.0391	0.0400	0.0196	0.0212
Median	0.0382	0.0426	0.0252	0.0247	0.0130	0.0134
Minimum	0.0152	0.0153	0.0142	0.0124	0.0080	0.0074
Std. Dev. Of Logs	0.51	0.50	0.44	0.48	0.41	0.46

* Values for LA 20-story structure are based on 18 records only (LA30 and LA36 have been excluded due to collapse of model with nominal strength properties)

Table 8.4 Sensitivity of Global Drift Angle Demands with First Mode Period of Structure, LA 3-, 9-, and 20-story Structures; 2/50 Set of Ground Motions

LA 3-Story

	T	**T/1.25**	**T/1.50**	**T/2.00**
Maximum	0.1095	0.0838	0.0642	0.0494
84th Percentile	0.0658	0.0579	0.0528	0.0432
Median	0.0393	0.0354	0.0323	0.0268
Minimum	0.0152	0.0131	0.0112	0.0100
Std.Dev. Of Logs	0.52	0.49	0.49	0.48

LA 9-Story

	T	**T/1.25**	**T/1.50**	**T/2.00**
Maximum	0.0558	0.0506	0.0461	0.0390
84th Percentile	0.0391	0.0341	0.0300	0.0271
Median	0.0252	0.0231	0.0198	0.0168
Minimum	0.0142	0.0130	0.0096	0.0057
Std.Dev. Of Logs	0.44	0.39	0.42	0.48

LA 20-Story

	T	**T/1.25**	**T/1.50**
Maximum	0.0432	0.0373	0.0307
84th Percentile	0.0247	0.0211	0.0188
Median	0.0146	0.0127	0.0117
Minimum	0.0080	0.0061	0.0053
Std.Dev. Of Logs	0.53	0.51	0.48

Table 8.5 Modal Characteristics of Original and Redesigned LA 9-story Structures

		Mode 1	Mode 2	Mode 3
SAC LA 9-Story, 30' bays and 9 MR conn./frame	Period (sec.)	2.241	0.836	0.467
	Modal Mass %age	82.1	11.1	4.1
R1 LA 9-Story, 30' bays and 9 MR conn./frame		Mode 1	Mode 2	Mode 3
	Period (sec.)	2.666	0.985	0.574
	Modal Mass %age	82.1	11.3	3.8
R2 LA 9-Story, 15' bays and 18 MR conn./frame		Mode 1	Mode 2	Mode 3
	Period (sec.)	2.356	0.866	0.502
	Modal Mass %age	79.0	13.4	4.3
R3 LA 9-Story, 30' bays and 6 MR conn./frame		Mode 1	Mode 2	Mode 3
	Period (sec.)	2.678	0.984	0.560
	Modal Mass %age	81.3	12.0	3.8

Table 8.6 Global Drift Angle Demands for Original and Redesigned LA 9-story Structures; 2/50 Set of Ground Motions

	SAC LA9-Story, 30' bays, 9 MR/frame	R1 LA9-Story, 30' bays, 9 MR/frame	R2 LA9-Story, 15' bays, 18 MR/frame	R3 LA9-Story, 15' bays, 6 MR/frame
Maximum	0.0558	0.0624	0.0662	0.0622
84th Percentile	0.0391	0.0461	0.0489	0.0456
Median	0.0252	0.0253	0.0283	0.0284
Minimum	0.0142	0.0122	0.0089	0.0120
Std. Dev. Of Logs	0.44	0.47	0.55	0.47

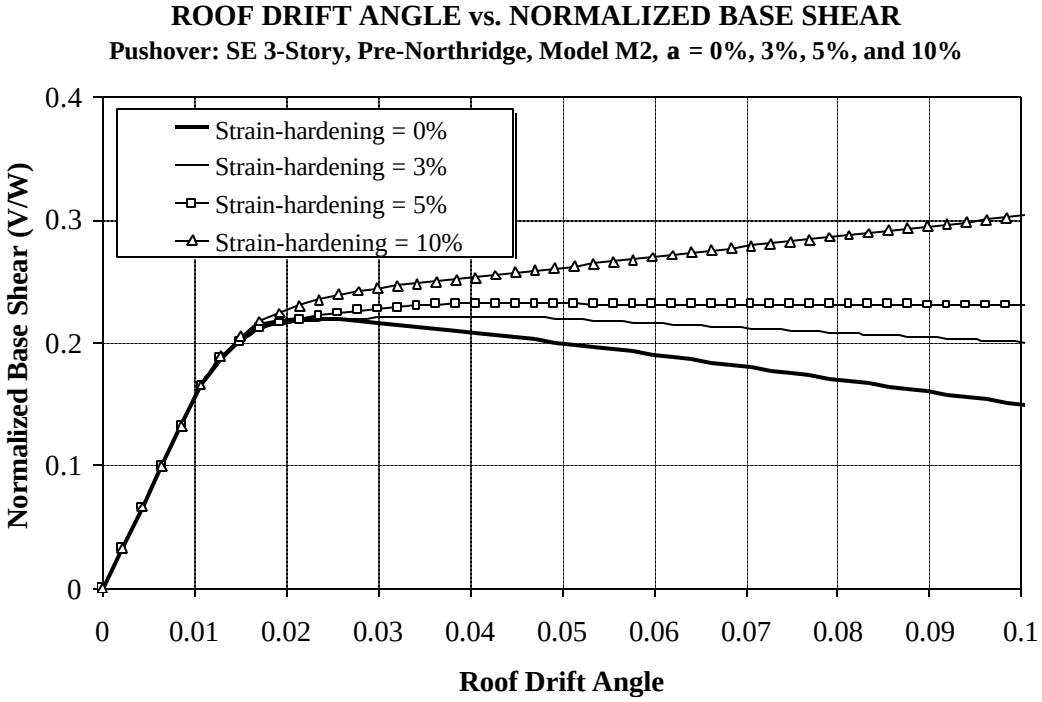

Figure 8.1 Sensitivity of Global Pushover Curves to Element Strain-Hardening, Seattle 3-story Structure; Pushover Analysis

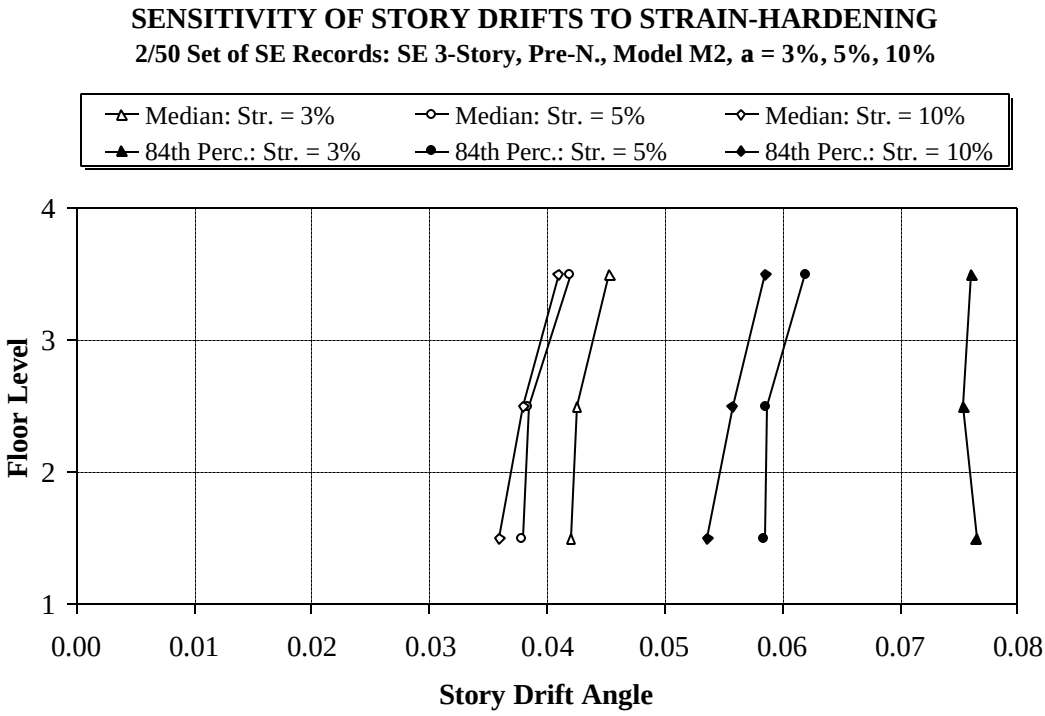

Figure 8.2 Sensitivity of Story Drift Angle Demands to Element Strain-Hardening, Seattle 3-story Structure; 2/50 Set of Ground Motions

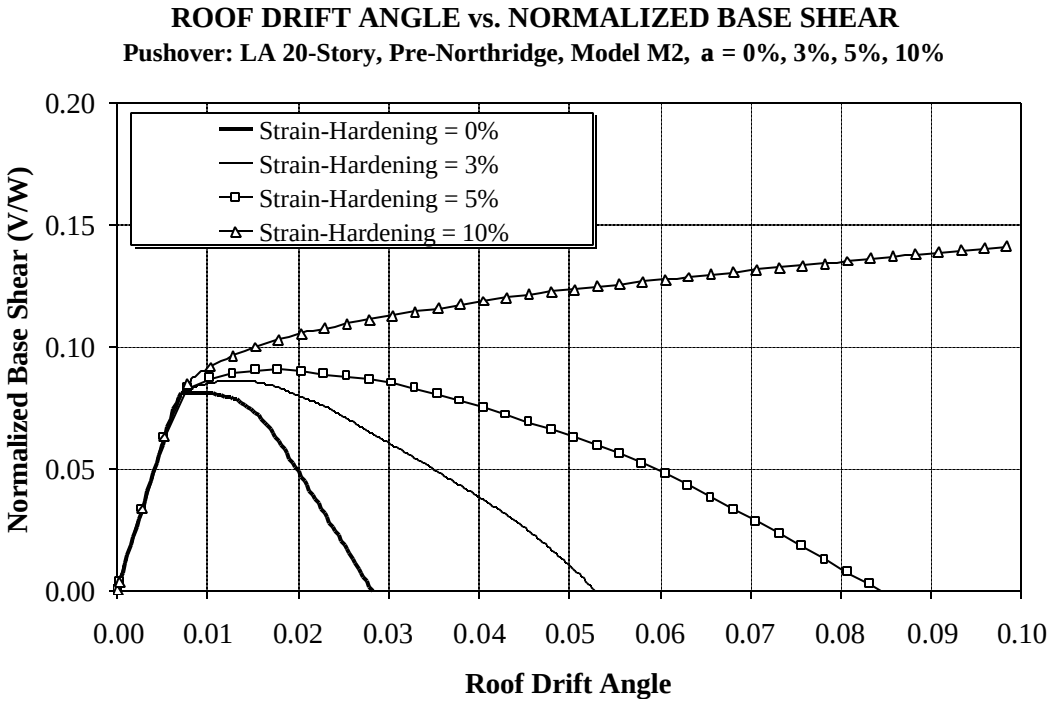

Figure 8.3 Sensitivity of Global Pushover Curves to Element Strain-Hardening, LA 20-story Structure; Pushover Analysis

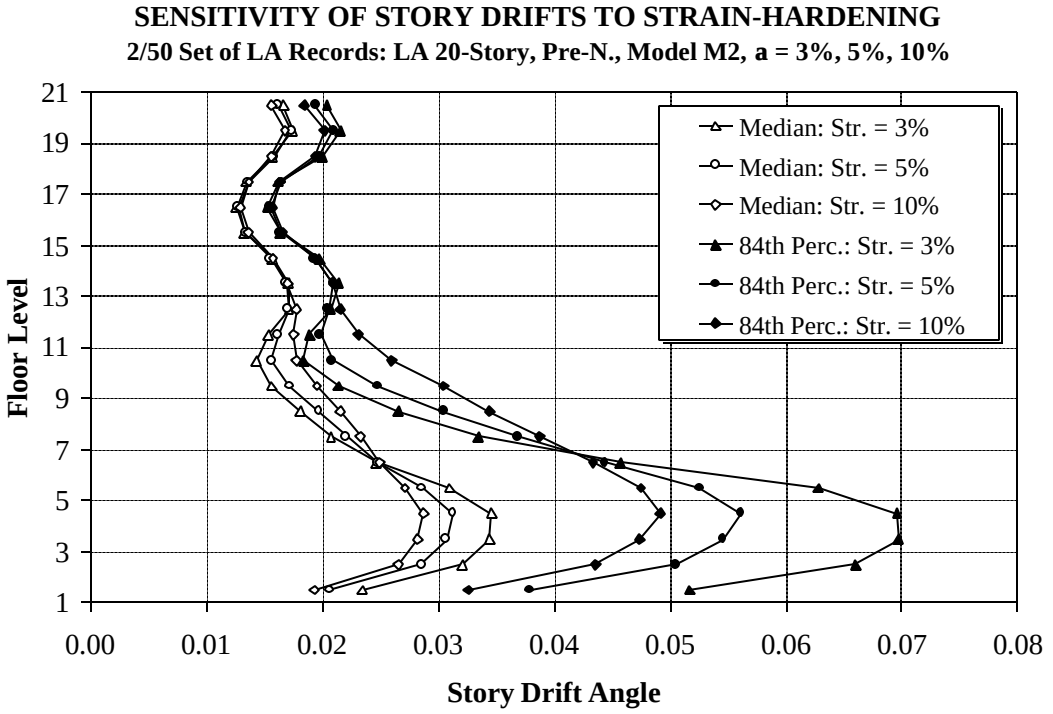

Figure 8.4 Sensitivity of Story Drift Angle Demands to Element Strain-Hardening, LA 20-story Structure; 2/50 Set of Ground Motions

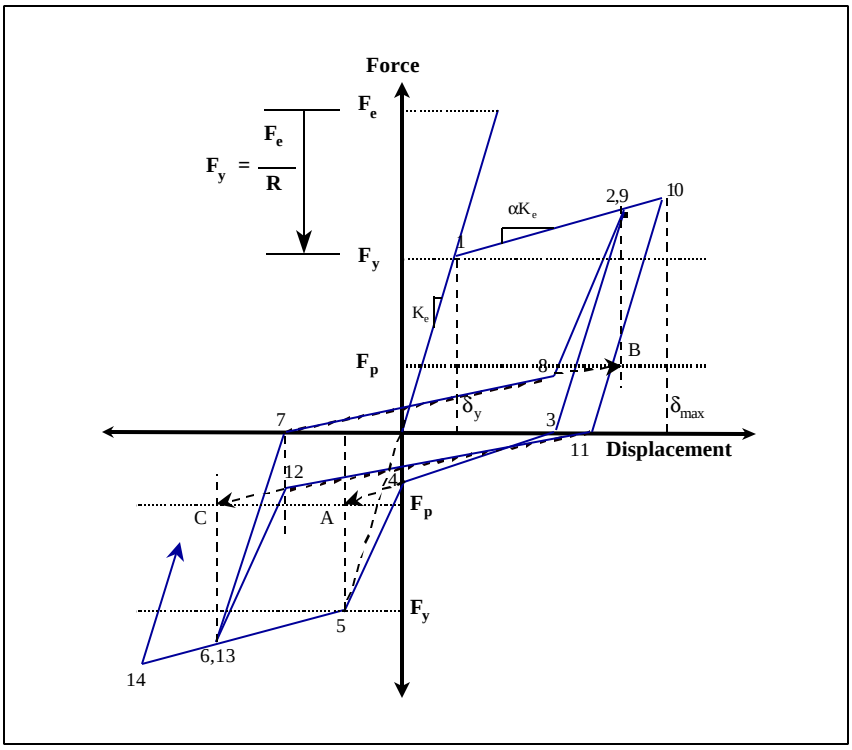

Figure 8.5 Stiffness Degrading (Pinching) Model; (Rahnama and Krawinkler, 1993)

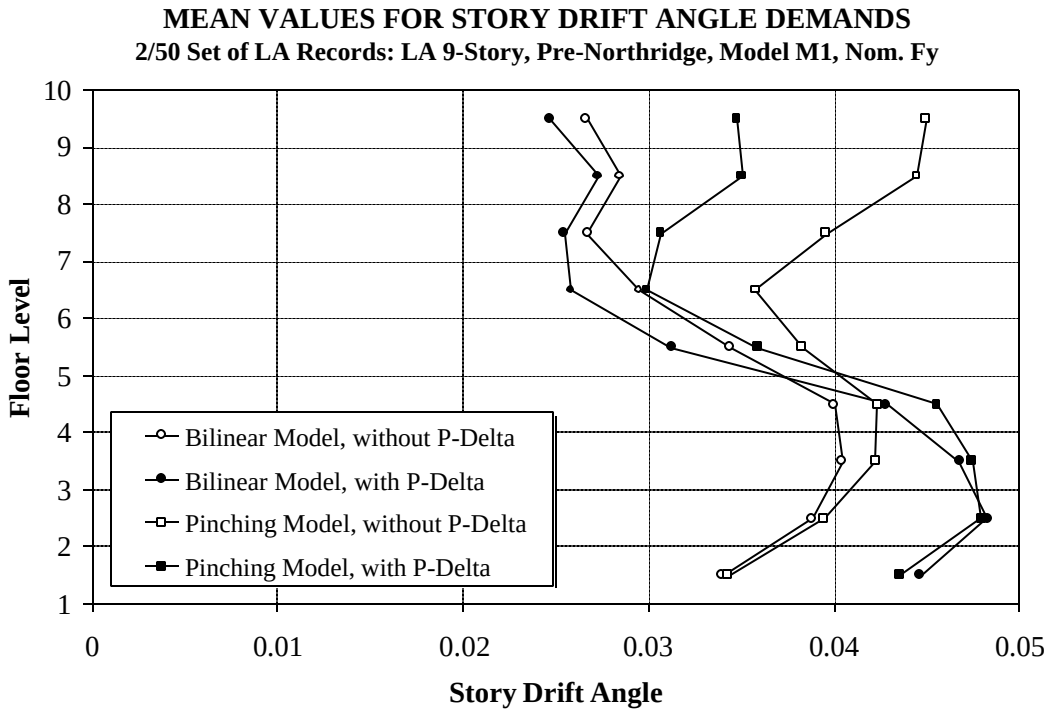

Figure 8.6 Sensitivity of Story Drift Angle Demands to Stiffness Degradation, LA 9-story Structure; 2/50 Set of Ground Motions

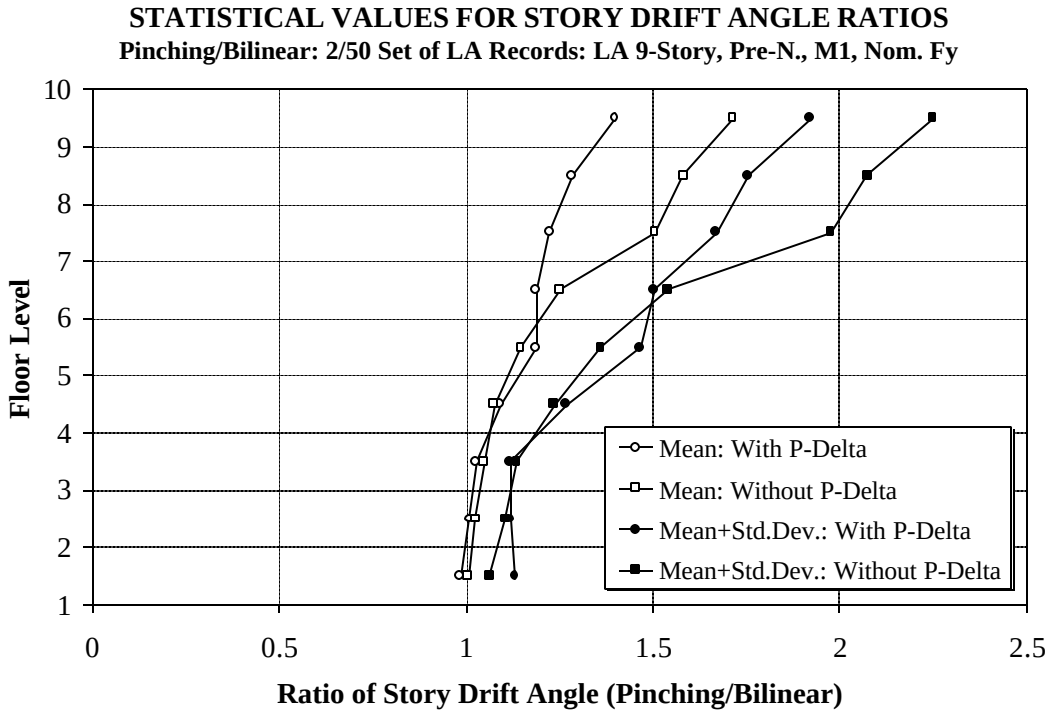

Figure 8.7 Story Drift Angle Ratios (Pinching Model/Bilinear Model) with and without P-delta Effect, LA 9-story Structure; 2/50 Set of Ground Motions

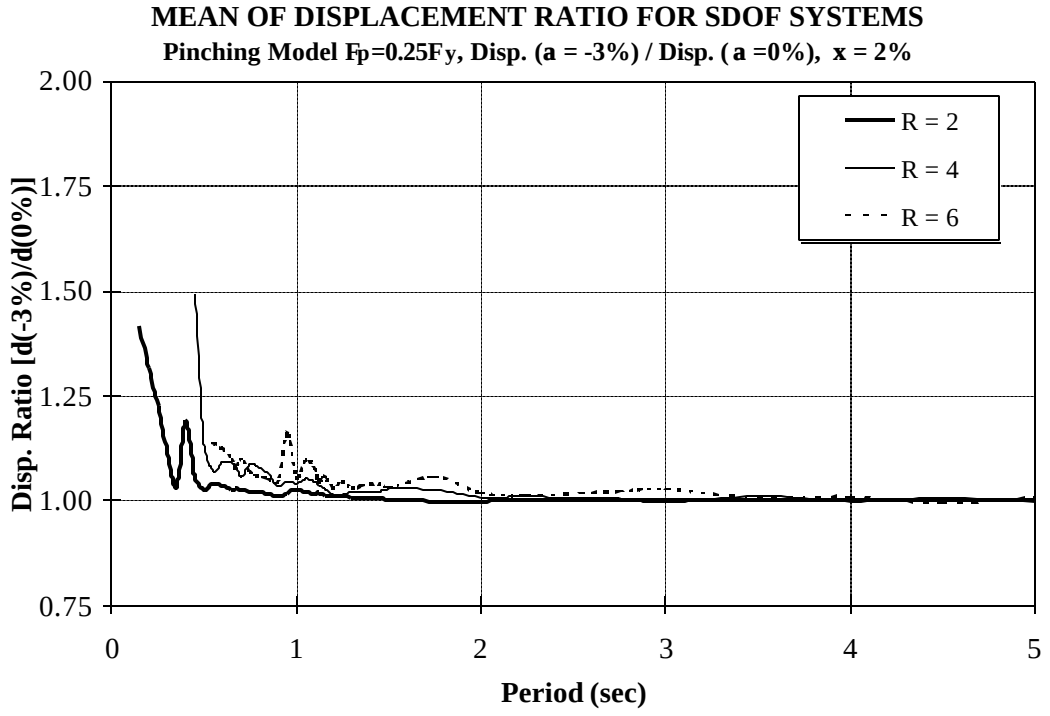

Figure 8.8 Effect of P-delta on Displacement Demands for SDOF Systems with Stiffness Degradation (75% Pinching); 2/50 Set of Ground Motions

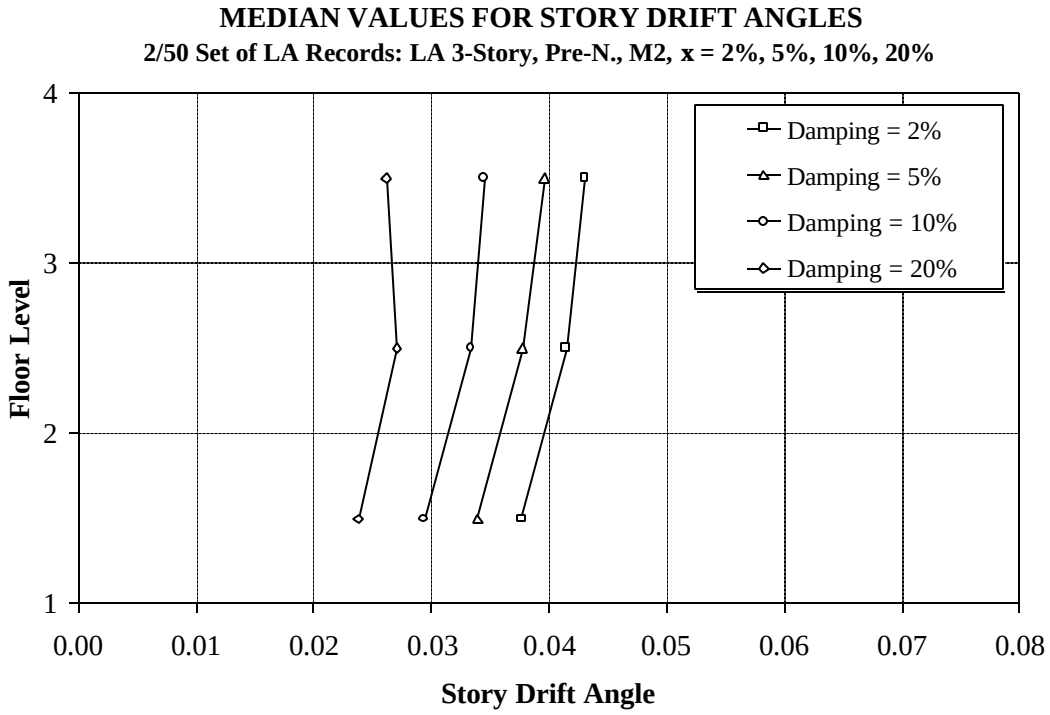

Figure 8.9 Sensitivity of Story Drift Angle Demands (Median Values) to Structural Damping, LA 3-story Structure; 2/50 Set of Ground Motions

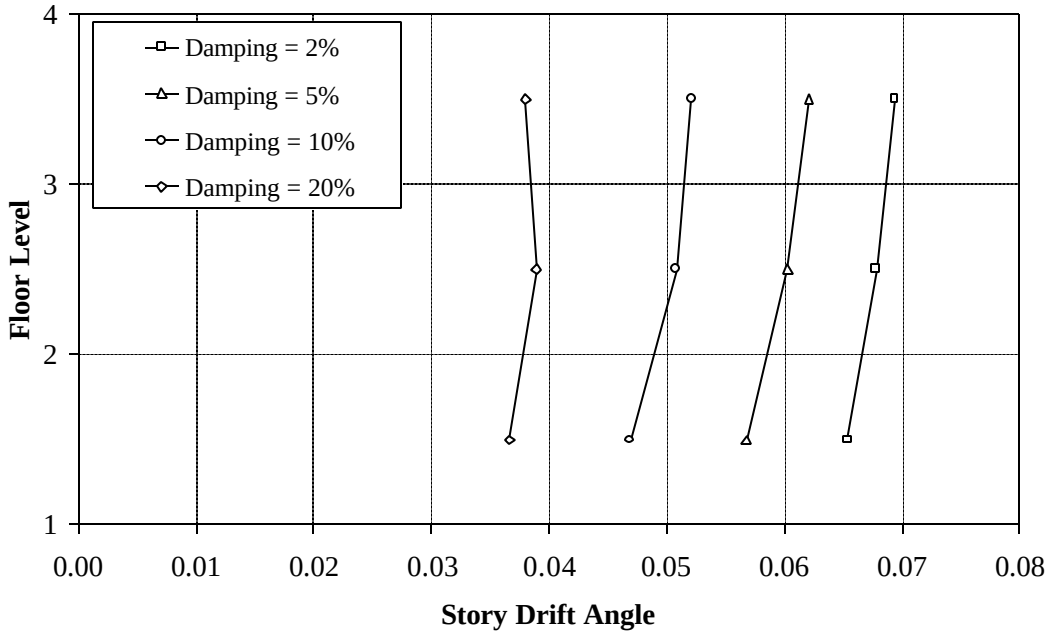

Figure 8.10 Sensitivity of Story Drift Angle Demands (84th Percentile Values) to Structural Damping, LA 3-story Structure; 2/50 Set of Ground Motions

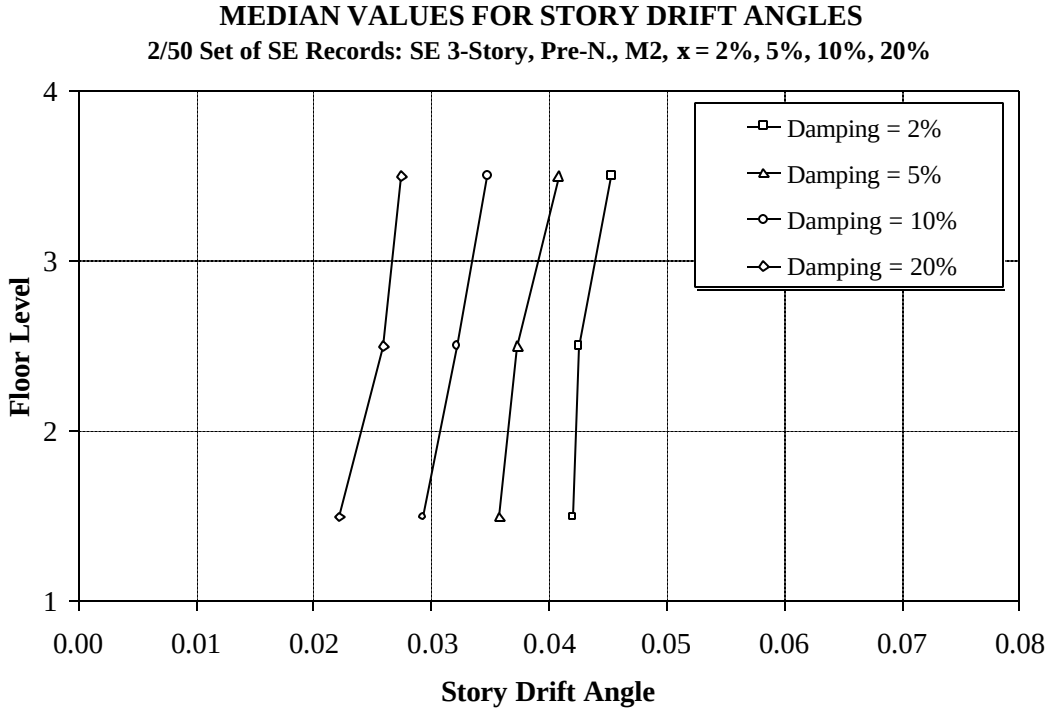

Figure 8.11 Sensitivity of Story Drift Angle Demands (Median Values) to Structural Damping, Seattle 3-story Structure; 2/50 Set of Ground Motions

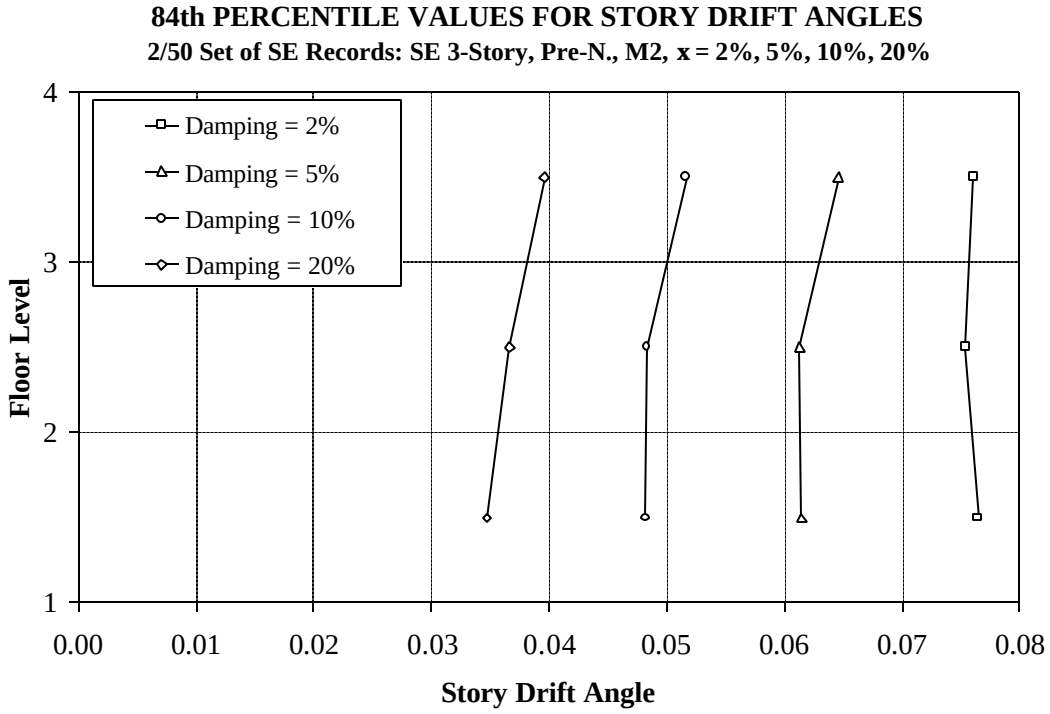

Figure 8.12 Sensitivity of Story Drift Angle Demands (84th Percentile Values) to Structural Damping, Seattle 3-story Structure; 2/50 Set of Ground Motions

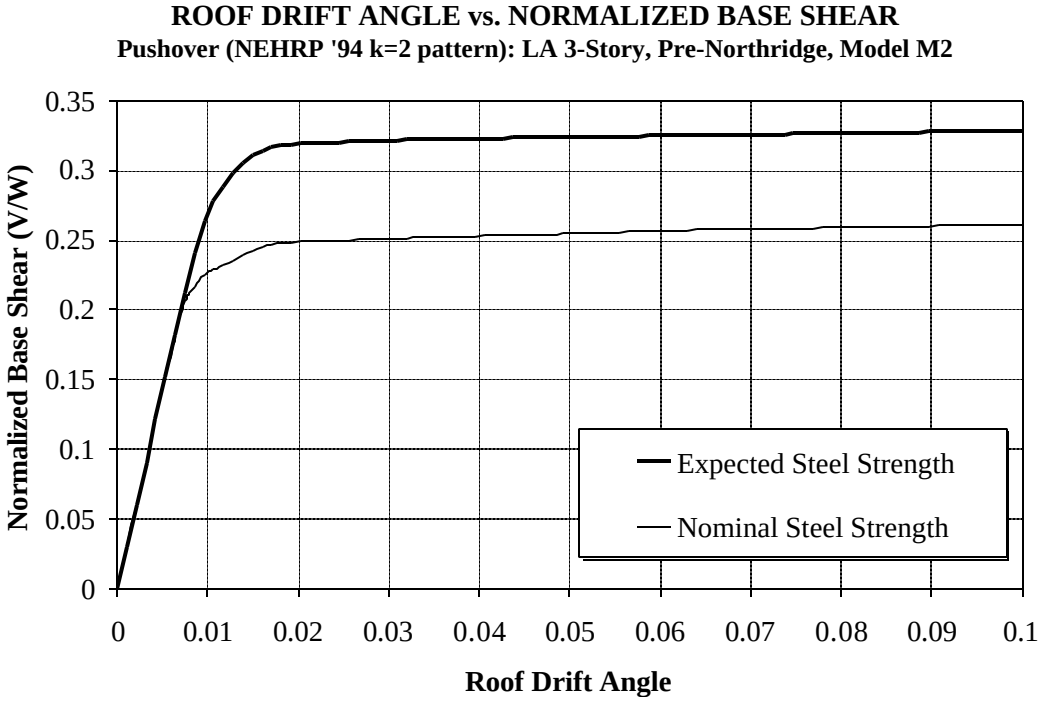

Figure 8.13 Sensitivity of Global Pushover Curves to Strength of Material, LA 3-story Structure; Pushover Analysis

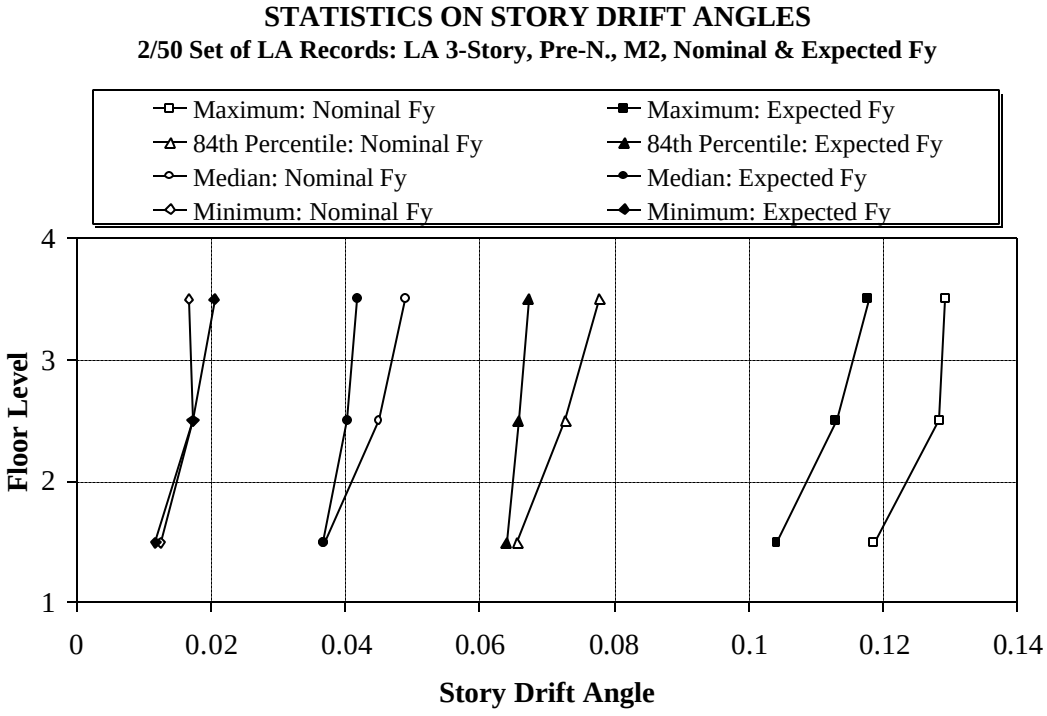

Figure 8.14 Sensitivity of Story Drift Angle Demands to Strength of Material, LA 3-story Structure; 2/50 Set of Ground Motions

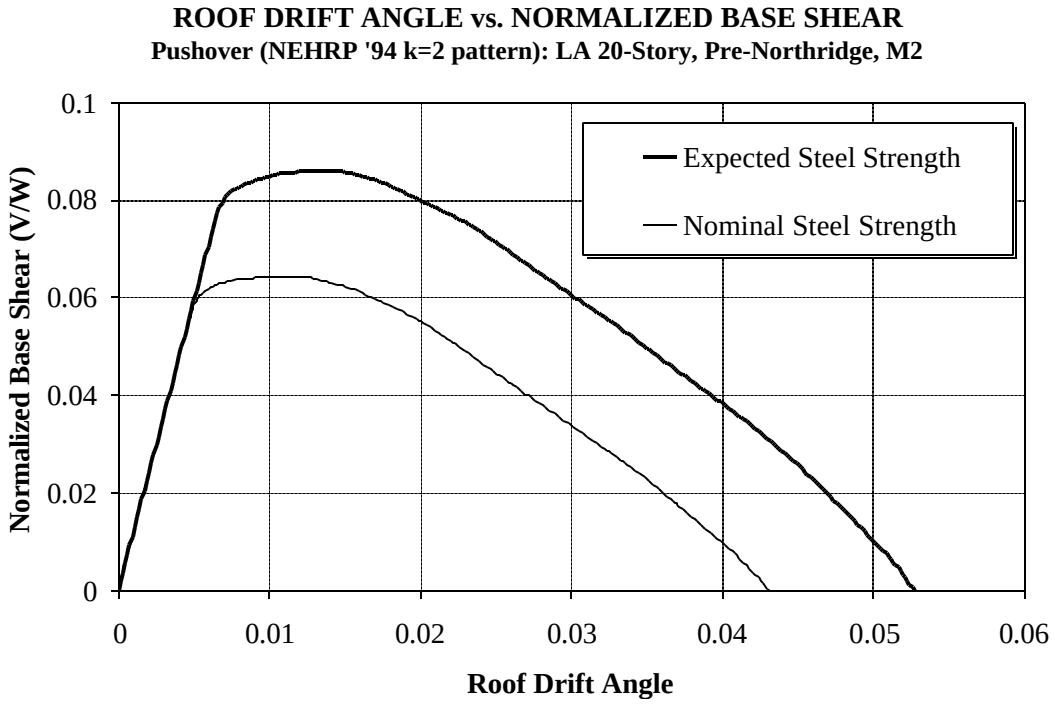

Figure 8.15 Sensitivity of Global Pushover Curves to Strength of Material, LA 20-story Structure; Pushover Analysis

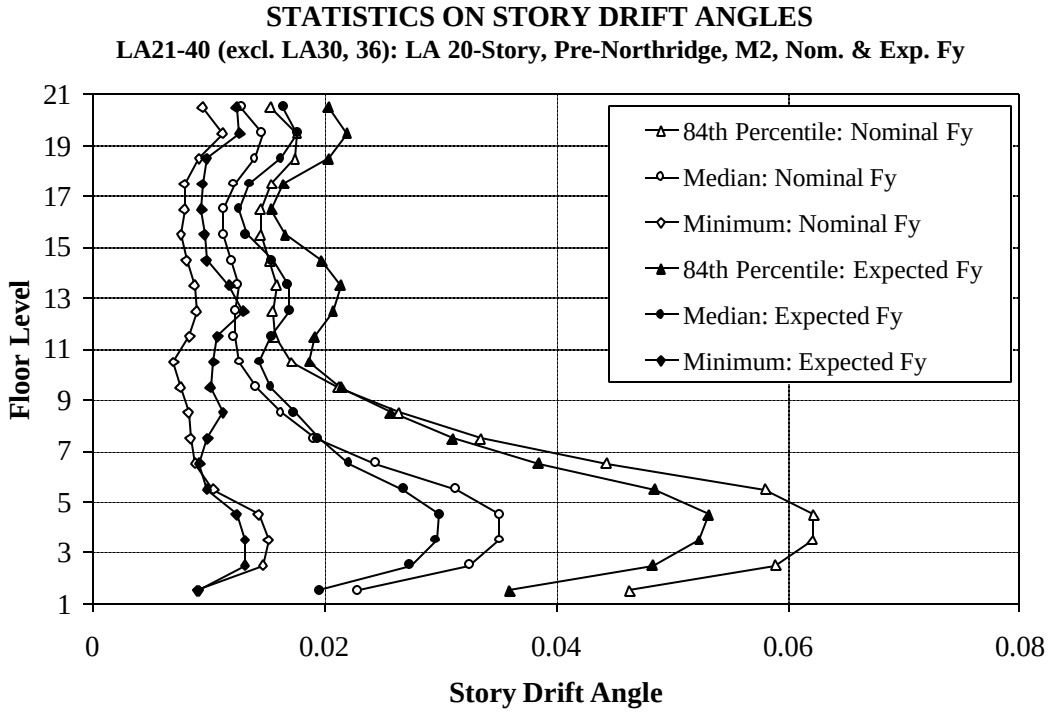

Figure 8.16 Sensitivity of Story Drift Angle Demands to Strength of Material, LA 20-story Structure; 2/50 Set of Ground Motions

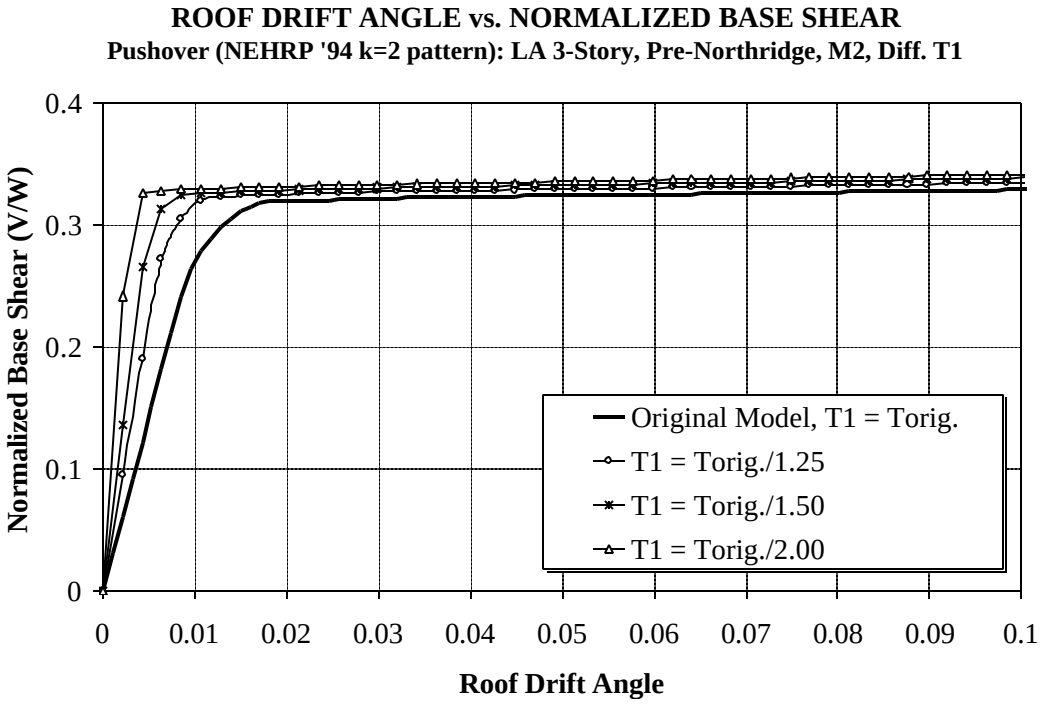

Figure 8.17 Sensitivity of Global Pushover Curves to Period of Structure, LA 3-story Structure; Pushover Analysis

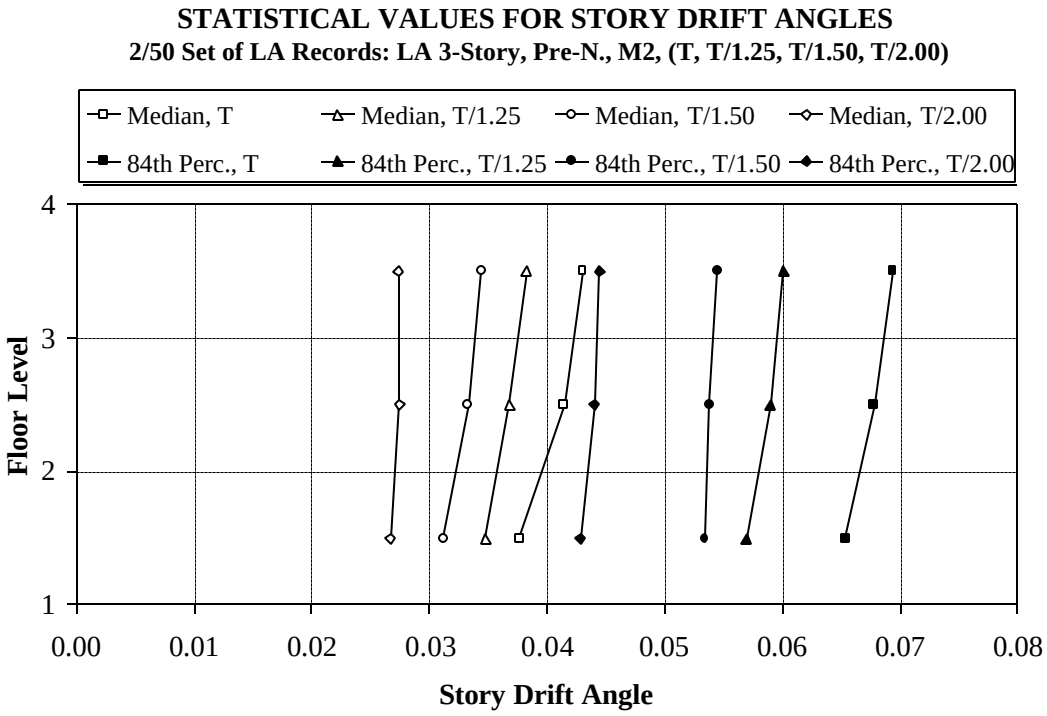

Figure 8.18 Sensitivity of Story Drift Angle Demands to Period of Structure, LA 3-story Structure; 2/50 Set of Ground Motions

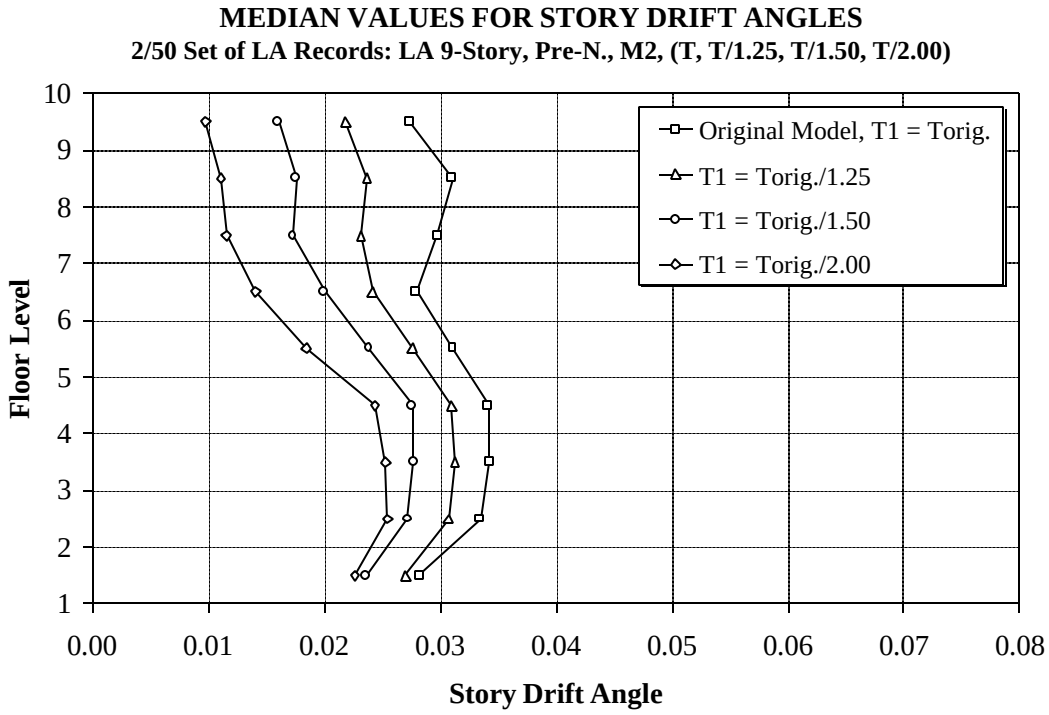

Figure 8.19 Sensitivity of Story Drift Angle Demands (Median Values) to Period of Structure, LA 9-story Structure; 2/50 Set of Ground Motions

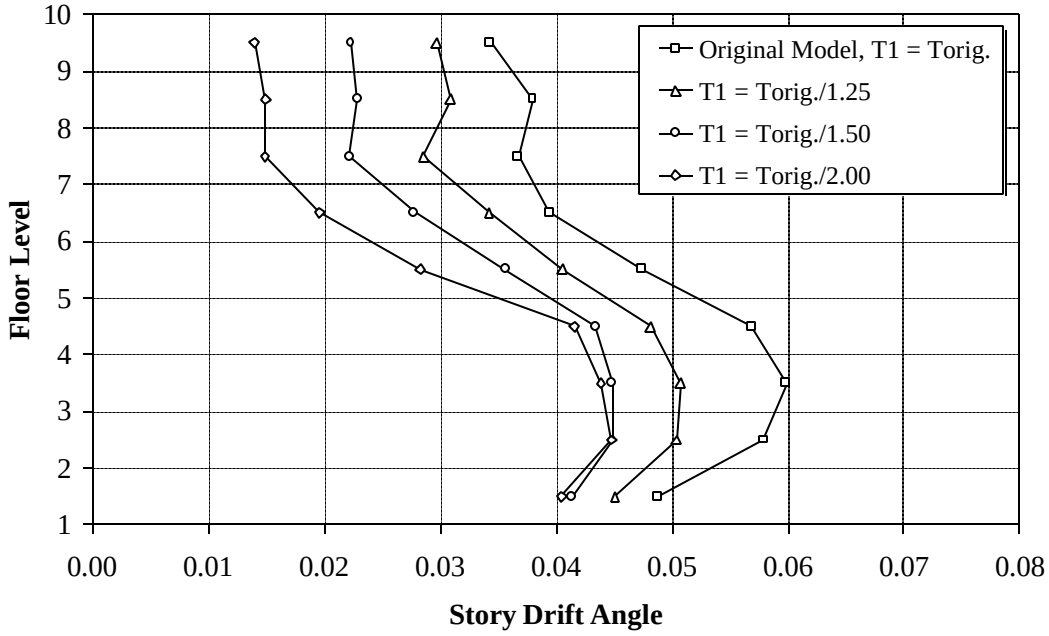

Figure 8.20 Sensitivity of Story Drift Angle Demands (84^{th} Percentile Values) to Period of Structure, LA 9-story Structure; 2/50 Set of Ground Motions

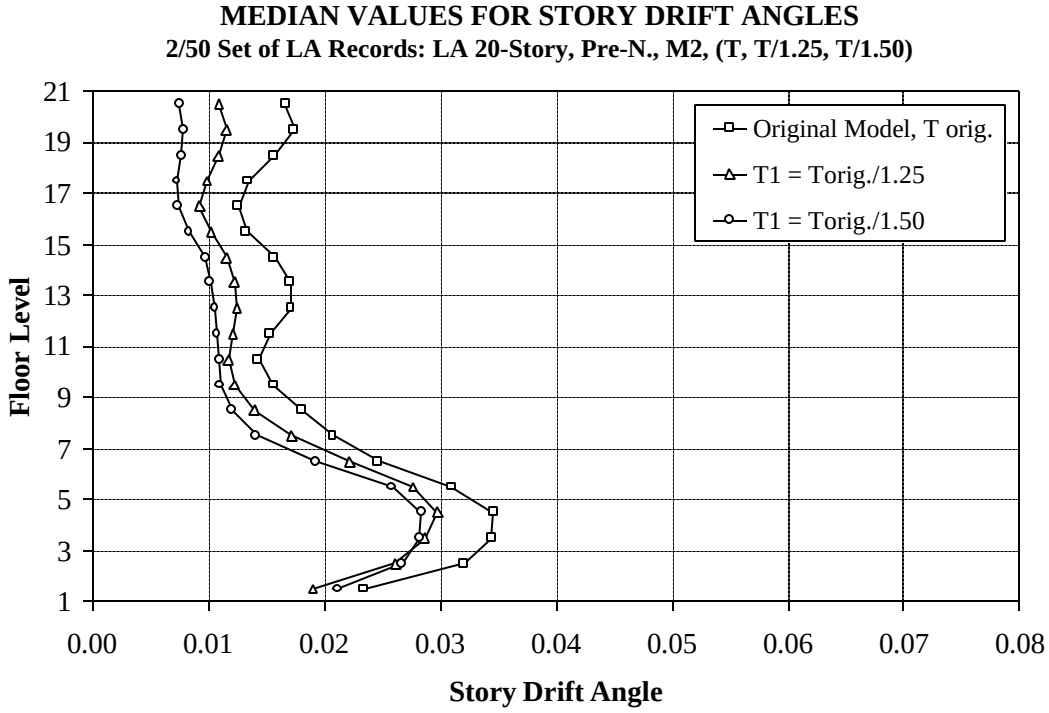

Figure 8.21 Sensitivity of Story Drift Angle Demands (Median Values) to Period of Structure, LA 20-story Structure; 2/50 Set of Ground Motions

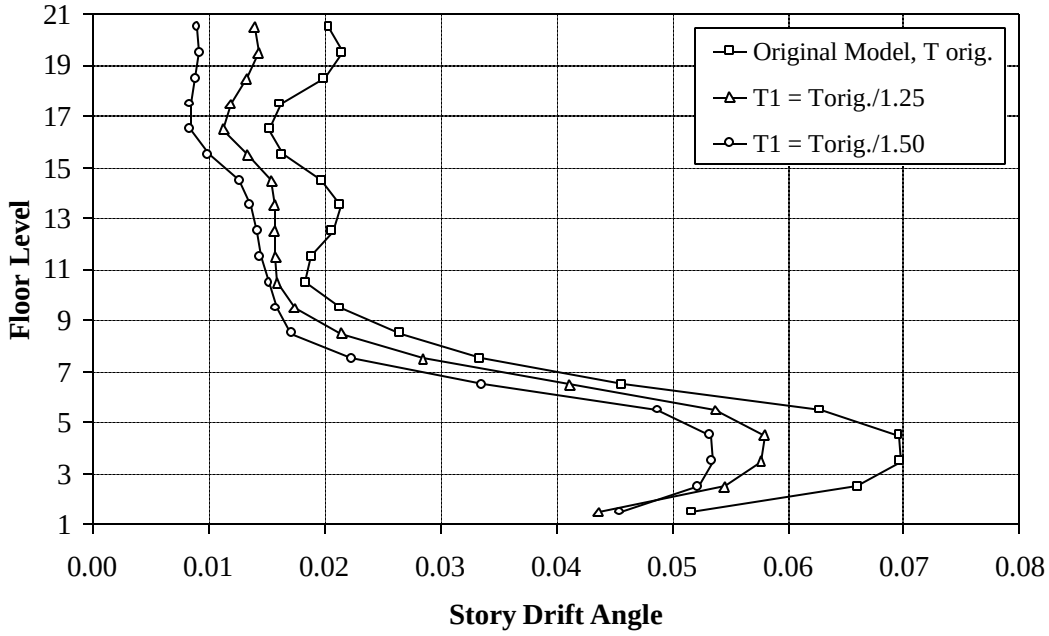

Figure 8.22 Sensitivity of Story Drift Angle Demands (84th Percentile Values) to Period of Structure, LA 20-story Structure; 2/50 Set of Ground Motions

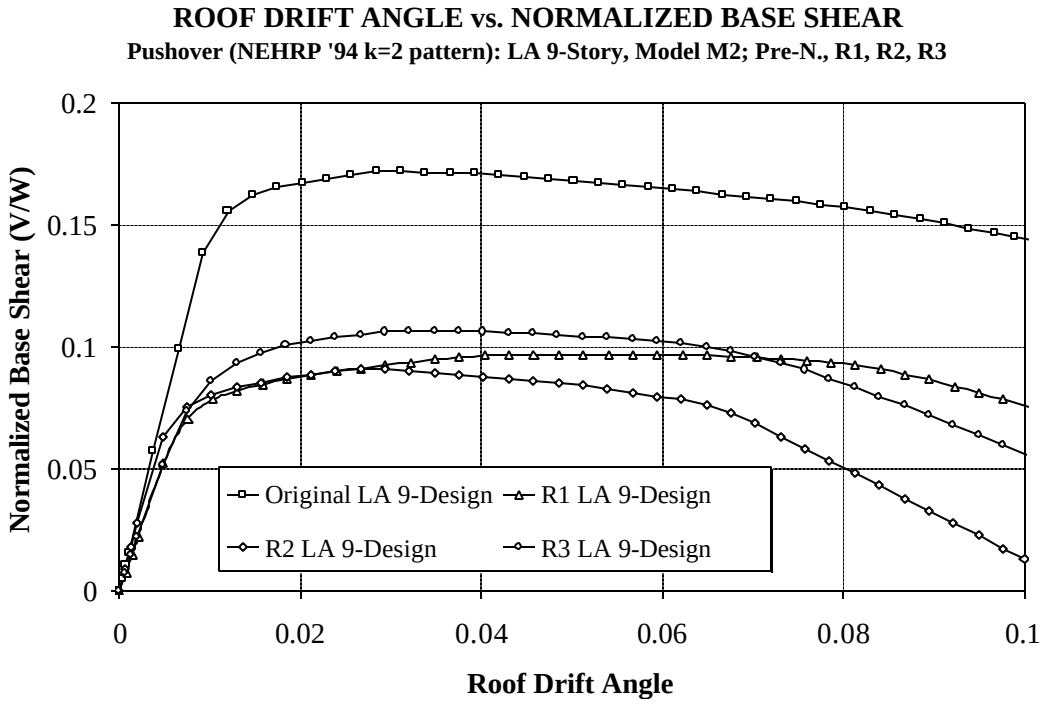

Figure 8.23 Global Pushover Curves for Original and Redesigned LA 9-story Structures; Pushover Analysis

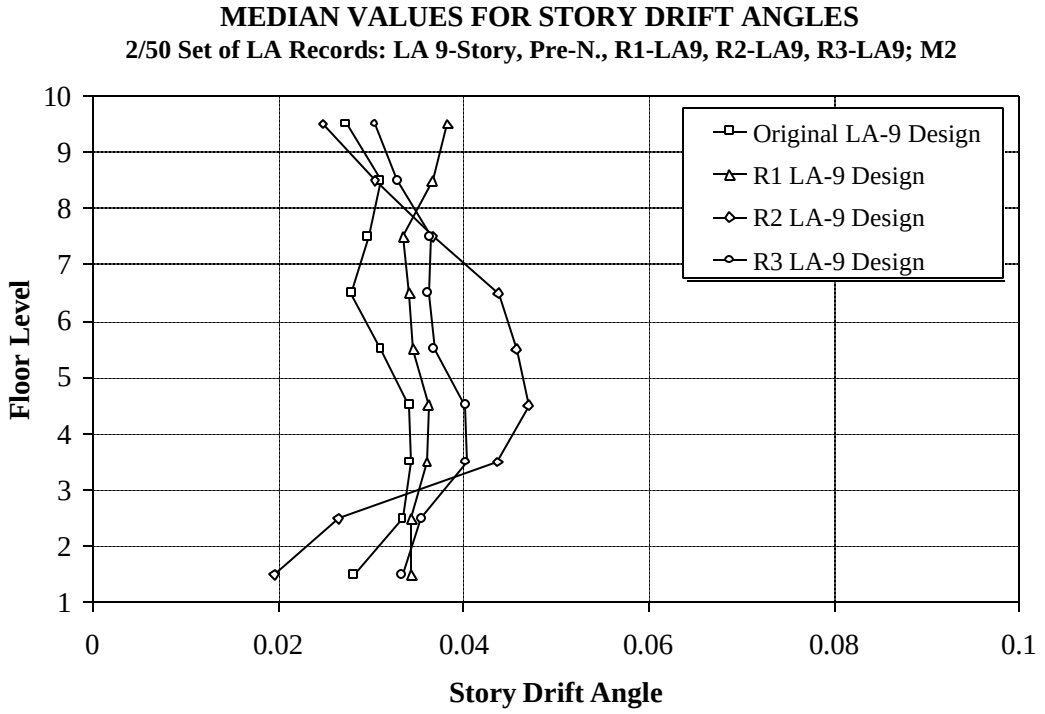

Figure 8.24 Median Story Drift Angle Demands for Original and Redesigned LA 9-story Structures; 2/50 Set of Ground Motions

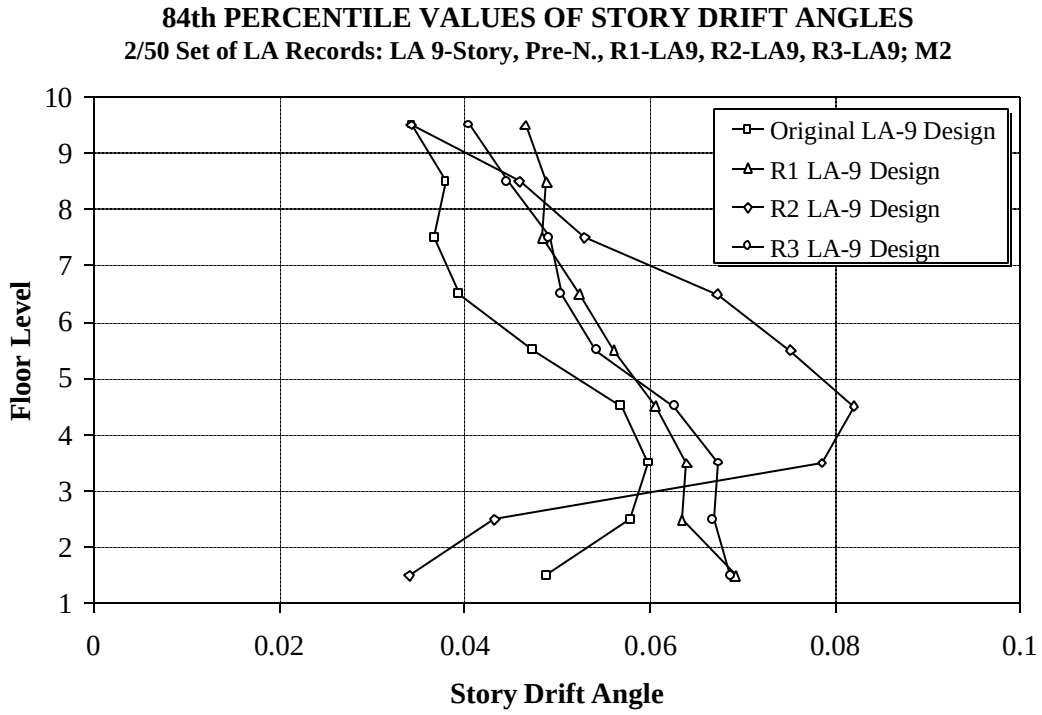

Figure 8.25 84th Percentile Story Drift Angle Demands for Original and Redesigned LA 9-story Structures; 2/50 Set of Ground Motions

CHAPTER 9

SUMMARY AND CONCLUSIONS

The primary objective of the research discussed in this report is to develop an understanding of the critical issues controlling the inelastic behavior and response of steel moment resisting frame structures, for different levels of seismic hazard. Behavior characteristics at the element level are utilized to study system behavior and response through a detailed seismic demand and performance evaluation for a multitude of steel moment resisting frame structures, which are representative of typical buildings and design practices in the US. Suites of ground motions representative of the seismicity of different geographic locations are used for demand and performance evaluation of the SMRF structures. This assessment provides information on the expected demands for existing typical structures as well as for structures being designed using new connection types that attempt to mitigate the likelihood of weld fractures. The results from the comprehensive seismic demand evaluation provide the background for the development of a simplified seismic demand estimation procedure for steel moment resisting frame structures. The developed procedure provides a convenient vehicle for estimation of structure and element level deformation demands, using ground motion spectral information and basic characteristics of the structure as the primary input. The capacity issue for a demand/capacity performance evaluation process is not addressed here, but basic information on cumulative demand parameters, which needs to be considered in the capacity evaluation, is provided for many of the structures studied in this research.

Analytical Modeling

The starting point for this research work is the development of representative analytical models for steel frame structures. The use of overly complex element models

is not considered essential on account of the many uncertainties involved in demand and capacity estimation. However, the models need to represent the major characteristics of the elements and the structures. Where necessary, bounds on the structural response were obtained through sensitivity studies. The main conclusions relating to analytical modeling of elements and structures are as follows:

- The global response can be significantly affected by modeling assumptions at the structure level (e.g., inclusion of gravity columns, floor slab effects, shear connections, non-structural components, etc.). This conclusion holds true especially for cases in which a change in basic mechanism occurs (e.g., development of a weak story) due to a change in structure modeling, or if the structure is driven into a range of negative post-yield stiffness. For specific cases the computed response may vary from predicted "collapse" to a response well within "acceptable" limits, depending on the accuracy of the analytical model.

- Gross approximations in the analytical modeling (such as the centerline model M1) may result in a very erroneous evaluation of the seismic demands at the element level, and in many cases at the system level. A model that captures the behavior of all important elements of the structure (albeit in an approximate manner, e.g., bilinear force-deformation relationships), is intrinsic to a reliable estimation of seismic demands for SMRF structures.

- The element deformation demands are greatly affected by the choice of the analytical model. Panel zones of beam-to-column connections are important structural elements whose strength and stiffness need to be represented in analytical models. A model that ignores panel zone deformations will concentrate the deformation demands in the beams or the column. The use of cover-plated beam flanges or reduced beam sections, which move the plastic hinge away from the face of the column, induces additional forces on the panel zone due to the shear at the plastic hinge location working on the distance between the plastic hinge and the face of the column. This reinforces the need for an analytical model that includes panel zones.

- Analytical models for the panel zone can be developed from standard beam-column and rotational spring elements, which are available in most nonlinear analysis programs. The model used in this study is able to represent the major

characteristics of the panel zone rather well, and is a better representation than the "scissors" type representation of the panel zone.

Element Behavior Issues

All conclusions drawn on element behavior are based on the M2 analytical model, which incorporates panel zone elements. The main conclusions are as follows:

- The distribution of deformation demands between the elements at a typical connection is found to be very sensitive to a host of factors, including subjective design decisions (choice of member sections, choice of weak element at connection), material strength, and choice of basic connection types (standard pre-Northridge connection, cover-plated beam flange connection, or reduced beam section). Depending on these factors, the plastic deformation demands at a connection may be concentrated entirely in the beams or panel zones, or may be distributed amongst the elements at the connection, including the column. The expectation that beams attract most of the plastic deformation demands does not hold true in many cases, even at the exterior column line of the structure. Thus, the state of stress and strain at a connection may be very different from usual expectations.

- Distribution of demands between elements at a connection may vary not only between different designs, but within the same design also. The influence of the distribution of element deformation demands at the connection level on the system response is, however, not very significant in most cases. The exceptions are cases in which a change in choice of connection properties results in a significant change in global structural properties. For example, the reduced beam section design has a significantly lower strength and is driven to very large drift demands under two ground motions of the 2/50 set of records.

- The level of plastic rotation in the beams, for cases in which the beams are the weak elements at the connection, is approximately equal to the story plastic drift angle demand. For cases in which the panel zones are the weak elements, the plastic shear distortion angle in the panel zone is approximately 20-30% higher than the story plastic drift angle demand. The reason is that story drift caused by panel zone

shear distortion is proportional to the clear height of the column rather than the centerline (story) height.

- The "strong-column" concept may not prevent the development of plastic hinges in the columns, even when the strength of the column is significantly higher than the strength of the weak element at the connection. The strong-column concept assumes equal column moments above and below the connection (mid-height inflection points in the columns). However, the bending moment diagram for the column may change significantly after yielding of beams at a connection. This is due to the additional demands imposed on the column on account of global bending of the column in the deformed shape of the structure. The inflection point moves closer to the base of the column, resulting in a potential for plastic hinge formation at the top of the column. The formation of plastic hinges in the columns was observed for many ground motions for the LA and Seattle 9- and 20-story structures. The change in moment distribution over the height of the column is amplified where severe discontinuities exist between the story drift demands in adjacent stories. These discontinuities can arise due to P-delta effects, higher mode effects, or design characteristics of the structure (e.g., presence of weak stories).

- Significant axial force demands (compressive and tensile) have to be expected in the exterior columns of tall structures due to high overturning moment demands for the structure. This is especially true for structures with high story shear strengths. For example, the first story exterior columns in the LA 20-story structure, under the 2/50 set of records, have a median axial force demand of 40% (compressive) and 19% (tensile) of their axial yield strength. The high axial forces may significantly reduce the bending moment capacity of the columns, increasing the potential for plastic hinge development. The high axial forces together with the migrating point of inflection in the column indicate that the point-plastic-hinge concept may not be appropriate for columns, due to member P-delta effects. The column behavior issue requires a much more detailed investigation.

- Significant plastic deformation demands can be expected at the base of the columns at the ground floor level. This holds true for columns that can be considered fixed-at the ground floor, and also for columns that continue into a basement. The median values range from zero to 0.03 radians for a 2/50 hazard level, for the LA structures.

- Column splices, which can be a source of brittle failure if partial penetration welds are used, may be subjected to severe axial force and bending moment demands. Detailed research is required to evaluate the behavior and response of column splices and the consequences of splice fractures on the system performance.

System Behavior Issues

A comprehensive evaluation of the seismic demands for 3-, 9-, and 20-story structures in three seismic zones of the US (zones 2A, 3, and 4), under sets of ground motions representative of hazard levels with return periods of 72, 475, and 2475 years was carried out. The main conclusions drawn from the demand evaluation and subsequent performance assessment for these structures are summarized as follows:

- The bare steel moment resisting frames for the structures are very flexible, with first mode periods of 1.0 to 1.9 seconds for 3-story structures, 2.2 to 3.3 seconds for the 9-story structures, and 3.0 to 4.0 seconds for the 20-story structures. These periods are significantly higher than those estimated using code equations. Typically, the LA structures are the least flexible, except for the 20-story structures, where the Seattle structure is comparable, and the Boston structure significantly stiffer than the LA structure. Furthermore, the strength of the Boston 20-story structure is more than 50% higher than that for the LA structure. This difference arises because wind effects control the design for the Seattle and Boston 20-story structures. All structures show significant overstrength with respect to the allowable stress design level. The designs are also slightly stiffer than would be required for code drift control requirements.

- Structure P-delta effects may greatly influence the response of the structures due to the development of a negative post-yield stiffness in specific stories of the structure. P-delta stability is a serious concern in a few code compliant structures (LA 20-story and Seattle 3-story) if subjected to very severe ground motions. This is the case for severe pulse-type ground motions and long duration motions resulting in a progressive drift of the structure onto one side. The response of a structure, if sensitive to P-delta effects, is strongly influenced by modeling assumptions, especially those assumptions that result in a delay or acceleration of the development of a negative post-yield story stiffness. A potential solution to the P-delta problem exists in the form of a flexible secondary system (such as stiff gravity

columns) that add to the stiffness of the structure after the primary system has yielded, thereby widening the stable strength plateau region of the pushover curve.

- Elastic static and dynamic analysis is found to be incapable of identifying the P-delta induced hazard for a structure. The stories in which a negative post-yield stiffness may develop, and the associated drift limits, cannot be captured by an elastic analysis.

- The use of the code prescribed stability coefficient is inadequate to safeguard against the formation of a negative post-yield stiffness in the structures. P-delta effects have to be assessed based on an inelastic representation for the structure. The value of the stability coefficient coupled with the appropriate strain-hardening value for the elements, however, provides a preliminary indication of the importance of the story P-delta effect.

- Presuming that the SAC model structures and ground motions are representative of typical conditions, the following conclusions can be drawn on story drift demands:

  1. The 50/50 ground motions in LA (72 year return period) induce drift angle demands of about 1% in average, but in some events the demands may become larger than 2%. These records cause very small inelastic behavior in average, but ductility demands larger than 2 are noted in some events and locations.
  2. For LA and Seattle the 10/50 ground motions cause drift demands of about 2% in average; except for the 20-story structures where the demands are clearly lower. In some cases the demands approach 3%. The demands for Seattle are often but not always somewhat smaller than for Los Angeles. A clear decrease in demands for Seattle compared to Los Angeles is not evident, particularly for the 3-story structure.
  3. In rare events, represented by the 2/50 set of records, all LA structures and the 3-story Seattle structure may experience very high drift demands. For a few ground motions drift angles in excess of 10% are computed. The median drift demands are in the order of 4%.
  4. For the LA and Seattle 3-story structures the distribution of story drift over the height of the structure is rather uniform. These structures vibrate primarily in the first mode. For the 9-story structures the distribution over height is also rather uniform although higher mode effects are becoming evident in the Seattle

structure. For the LA 20-story structure the drift distribution over height is also rather uniform for small and moderate ground motions, but a clear drift bulge in the bottom stories is evident once the ground motions are sufficiently severe to cause significant P-delta effects. For the Seattle 20-story structure the drift demands show a clear bulge in the top stories, which is caused primarily by the relatively weak shear strength of the top stories due to wind design considerations.

5. The drift demands seem to decrease with the height of the structure, with the 20-story structures showing (relatively) the lowest demands. This observation does not hold true if the structure is subjected to very severe ground shaking and is affected by high P-delta effects, as is the case for the LA 20-story structure.
6. The performance of the code designed steel moment resisting frame structures used in this study is deemed to be in fair agreement with general expectations for conventional design events (10/50 ground motions) and more frequent events. However, for rare events (2/50 ground motions) larger than expected inelastic deformations may be experienced and the potential for unacceptable performance is not negligible.
7. The Boston 9- and 20-story structures are subjected to ground motions whose spectral displacement demands at the first mode period are much smaller than those represented by the NEHRP spectrum. As a consequence, the first mode effects for these structures are small. Nevertheless, yielding in the upper stories is observed in several of the analyses of the 9- and 20-story structures due to higher mode effects. Story ductility demands higher than 2 are computed in some cases. This yielding occurs even though the structures have significant overstrength due to wind effects that control the design.

- A potential collapse hazard exists for structures in which a negative post-yield story stiffness may form and which are subjected to very severe ground motions. The presence of response outliers may not be adequately reflected in statistical values. The issue of outliers is of serious concern and needs to be addressed in detail.

- The structural response, especially of structures experiencing negative post-yield stiffness due to P-delta effects and structures subjected to long duration ground motions, is sensitive to various degrees to:

1. Element strain-hardening assumptions. A small change in the extent of the negative post-yield stiffness can result in a very large change in the dynamic response. Similar changes in positive post-yield stiffness cases have a much smaller effect on the response. Single-degree-of-freedom systems (SDOF) can be used as indicators for the effect of changes in strain-hardening on structural response, but may not be able to predict the extent of the influence on the dynamic demands for the multi-degree-of-freedom (MDOF) systems in the case of P-delta sensitive structures.
2. Structural damping values. The effect of damping is found to be quite independent of ground motion characteristics. SDOF systems are good indicators of the extent of the influence of structural damping on the response of the MDOF structures.
3. Material strength properties. These properties can influence the distribution of demands at the connection level quite severely. A change in basic mechanism may be induced, in which case the structural response may also be altered significantly. For other cases the effect on global structural response is not very significant.
4. Influence of nonstructural elements. If the stiffness of these elements is maintained, the reduction in period results (usually) in a reduction in story drift demands. This reduction for MDOF structures is, however, not necessarily proportional to the reduction in first mode spectral displacement demands because of higher mode effects and potential P-delta effects.

- Stiffness degradation at the element level leads to amplification in story drift demands. The amplification increases for upper stories on account of the larger number of inelastic cycles. The amplification may be large for structures with significant inelasticity in the upper stories subjected to long duration ground motions. The P-delta effect, in general, reduces the amplification due to stiffness degradation. SDOF systems can be used as indicators for the effect of stiffness degradation on the global (roof) drift of MDOF structures, but they may under-predict the amplification at the story level.

- Configuration (changing bay width and/or beam size) and redundancy (changing the number of moment resisting connections) by themselves have a benign effect on the response of structures without fractured connections, other than effects attributed to basic design differences (strength, stiffness). Since elements at a floor

level experience similar levels of plastic deformation demands provided that gravity moments are small, the effect of redundancy or change in beam depths will not be significant, unless the capacity of elements or connections changes. This issue needs special attention for structures in which the potential for connection fracture exists.

- The statistical values of global and story drift angle demands for the post-Northridge structures (cover-plated beam flanges) are similar to the demands for the pre-Northridge (standard connections) structures. Some differences under particular records are observed due to differences in design details, with the demands being somewhat lower for the post-Northridge structures,.

- The designs using reduced beam sections (RBS) have lower strength than comparable pre-Northridge designs. The pre-Northridge designs can be modified to an RBS design without changing member sections, as the primary designs are stiffness controlled and have significant overstrength. The element deformation demands are primarily concentrated in the beam plastic hinge locations since the demands on the panel zones become smaller. For most records the global and story drift demands are similar to those for the other models.

Cumulative Demand Parameters

The element and structure behavior assessment and demand estimation focused primarily on the maxima of demand parameters, which by themselves do not describe the complete response of the structure. The damage to an element and the structure is a function of all the inelastic cycles the structure experiences. The capacities of elements and the structure are, therefore, related to the amplitude and number of inelastic cycles. Thus, an estimate of the cumulative deformation demands (also represented by energy demands) becomes important for a comprehensive performance evaluation process. The element and story level cumulative deformation and energy demands are evaluated for representative structures under severe (2/50 sets of ground motions) loading conditions. The conclusions that can be drawn from the results are:

- The cumulative story drift angle demands show a very different distribution over the height of the structure than the maximum value parameters, with the cumulative demands in the upper stories usually being significantly higher than the demands in

the lower stories. This effect is more pronounced for the Seattle structures, in which the cumulative plastic drift demands in the upper stories of the 9-story structure are about 10 times the demands in the lower stories. The reasons are higher mode effects and the very long strong-motion duration of Seattle ground motions. These results indicate that the cumulative deformation capacity has to be significantly higher for the upper stories. Furthermore, the identification for the critical story in the structure may change depending on the parameters being used. A similar conclusion can be drawn from the distribution of hysteretic energy demands over the height of the 9-story structures.

- The relationship between cumulative plastic story drift demand and maximum drift demand depends strongly on the structure height (number of stories), the location of the story (top versus bottom story), and the type of ground motion (e.g., pulse-type versus long duration). Thus, in an experimental capacity evaluation program much attention needs to be paid in the applied loading history to the great variation in the ratio of cumulative to maximum demand.

- The energy input imparted to an MDOF structure may be very different from input energy estimates obtained from the first mode SDOF system. The difference between the SDOF and MDOF energy demands increases very rapidly with increasing structural period, due to higher mode effects. The amplification can be particularly severe for ground motions with low energy content at the first mode of the MDOF structure, for instance in the Seattle 9- and 20-story structures. The ratio of the hysteretic energy to the input energy is quite stable and well represented by the SDOF systems, for a particular set of records. The ratio may vary between different sets of records, depending on the duration and frequency characteristics of the records.

- Columns at the base of the structure can be expected to be called upon to dissipate a sizeable portion of the structure hysteretic energy. For other floors the energy demands are distributed primarily between the beams and panel zones, depending on the relative strength of the elements. The distribution of hysteretic energy dissipation over the height of the structure is similar to the distribution of cumulative plastic deformation demands.

- A direct comparison of the cumulative plastic deformation and energy demands between different stories can be misleading on account of different cumulative capacities of elements. A better comparison for cumulative demand assessment can be obtained by normalizing the element energy demands to their yield energy demands (yield strength times yield deformation). The normalization of energy values permits a direct comparison not only between similar elements on different floor levels but also between different elements (beams versus panel zones).

Global Strength Issues

For a low performance level such as collapse prevention, structural behavior assessment and performance evaluation need to focus on deformation and energy demands, but not exclusively. For specific issues of concern, such as overturning moment demands and vertical strength irregularities (weak stories), global strength consideration become critical. The main conclusions on story shear strength and overturning moment demands are as follows:

- The nonlinear static analysis provides low estimates of the base and story shear strengths compared to values recorded in nonlinear dynamic analyses. This is on account of the pushover analysis being tagged to a fixed load pattern. Furthermore, the pushover analysis provides a constant lever arm (centroid of applied loads over the height of the structure) for overturning moments, which depends on the applied load pattern but in the case of triangular or similar lateral load patterns is significantly higher than the lever arm obtained from dynamic analysis. This is on account of higher mode effects, which affect structures to varying degrees depending on the number of stories and the frequency characteristics of the ground motion.

- In an estimation of maximum overturning moments from the pushover analysis two compensating errors occur. The story shears are underestimated, but the lever arm of the lateral loads is overestimated. For the structures studied this compensation has resulted in a good estimate of the overturning moments close to the bottom of the structures, when the maximum moments from the pushover analysis are compared to the maximum moments from the time history analyses. This observation cannot be generalized, but it clearly shows that it is inappropriate to

apply an overturning moment reduction factor to the maximum moments obtained from the pushover analysis.

Assessment of Pushover Analysis

Nonlinear dynamic analysis, with realistic analytical models for the structures and subjected to representative ground motion time histories, is viewed as the most accurate means for seismic behavior and demand assessment of structures. However, in many practical cases, and particularly in the conceptual design phase, the use of a complex analysis cannot be justified and the use of an approximate method becomes a matter of necessity. The use of an equivalent single-degree-of-freedom system and the use of nonlinear static analysis are two options in this direction. Both these techniques are associated with many caveats, and results from such prediction methods have to be interpreted with great caution. This study has extensively used the nonlinear static analysis as a supplemental analysis technique to better understand the structural behavior, rationalize the dynamic response, and in the process assess the adequacy (or lack thereof) of the pushover analysis in structural evaluation. The major conclusions from this part of the research are as follows:

- The pushover analysis identifies important behavioral aspects for the structures very well, except for cases in which the response is dominated by higher mode effects. The analysis is particularly useful for structures subjected to severe P-delta effects, as the analysis is able to identify and capture the weakness in the structure due to the P-delta effect. For the cases studied the pushover curves (global base shear - roof displacement curves and more so the story shear - interstory drift curves) clearly identify the drift demands around which the structure may be severely affected by P-delta effects. The analysis is also able to identify the stories contributing disproportionately to the global drift of the structure. From this viewpoint the use of a pushover analysis is invaluable in identifying potential problems associated with the structure.

- The pushover analysis is also a very useful tool for element behavior evaluation and for identification of relative distribution of demands between elements. The analysis is able to predict the locations of plastic hinges in the structures fairly well. Again, this conclusion does not hold true for structures influenced by severe higher

mode effects. Within a story, however, the relative distribution of demands between elements is closely captured by the pushover analysis.

- The main advantage of the pushover analysis technique is identification of problems and typical behavior patterns, and not so much the quantification of demands. In this respect the estimate may range from fairly accurate to very inaccurate, depending on the parameter evaluated and on the importance of higher mode effects.

- Except for the 3-story structures, whose response is dominated by first mode vibration, the story drift predictions obtained by pushing the structure to the roof displacement obtained from the SDOF spectral displacement (or for that matter from the MDOF inelastic analysis) are generally poor. The reasons are that the pushover load pattern does not capture dynamic effects and that the maximum dynamic story drifts occur at different times.

Simplified Demand Evaluation

The comprehensive quantification of seismic demands for typical steel moment resisting frame structures provided a basis for the development of a simplified seismic demand estimation procedure for SMRF structures. Parts of this procedure have been developed previously, but these developments have used generic structures with predetermined failure modes. This study reinforces past results through the use of real structures, and complements the procedure by extending it to include the estimation of element deformation demands, using spectral information and basic structural characteristics as the primary input. The major conclusions are as follows:

- With one exception, the roof drift angle demand for elastic MDOF structures can be well predicted using the first mode elastic spectral displacement demand for the ground motion and the first mode participation factor of the structure. The exception occurs when the ground motion has very little energy content at the first mode period and the response is strongly dominated by higher mode effects (Boston records). For such cases an elastic dynamic analysis is recommended to ascertain the roof drift angle demand.

- The elastic roof drift angle can be modified for inelasticity in the structure by either using information based on single-degree-of-freedom systems, or empirical factors derived on the basis of statistical evaluations for the structures.

- The effect of P-delta on the structural response is sensitive to the ground motion characteristics. When the range of negative post-yield stiffness is not entered, P-delta effects may increase or decrease the roof drift demands, but the P-delta factor is small in average and for the cases studied does not exceed 1.3 for individual ground motions. When the negative post-yield stiffness range (stability sensitive range) is entered, drift amplifications may become very large, and only a time history analysis will tell the amount of amplification. Thus, a small P-delta modification factor can be used for the former case, and the latter case should be prevented whenever possible.

- The global (roof) drift to story drift transformation is dependent on the structural characteristics, and there is no unique process to estimate this relationship. Approximate empirical factors, which are structure height dependent, may be used coupled with engineering judgement as to the location and values for the maximum story drift demands as a function of the roof drift demand. A pushover analysis provides an indication for the locations of large story drifts; it may be used to supplement the empirical factors.

- The transformation from story drift demand to element plastic deformation demand is based on the strength and stiffness properties of the elements at a connection at the floor, with the underlying assumption of no plastification in the columns and mid height inflection points. Both of these assumptions may not hold true in severe inelastic cases, however, one of the purposes of the simplified assessment is to identify the critical cases for more detailed analysis. For essentially "regular" cases where the assumptions hold, the procedure provides reasonable estimates for the demands. For cases in which plastification in the columns contributes to the story drift, the procedure will distribute the column plastic demand to the beam and/or panel zone.

Concluding Remarks

The conclusions and results presented in this study are applicable only within the conditions identified in each chapter, and are based on a particular set of structures and ground motions. Thus, the quantitative results are representative primarily for structures conforming to similar design details, and subjected to similar sets of ground motions. The behavior issues are, however, generic to steel structures in general, as is the simplified seismic demand estimation procedure. The research described in this report has attempted to answer the important questions related to the behavior and expected response of typical steel moment resisting frame structures in different geographic locations, when subjected to different hazard level ground motions.

This research forms part of a much larger research program, which addresses many other critical issues central to the demand estimation for steel moment resisting frame structures. Much work remains to be done in the area of behavior identification (fracture conditions, column hinging, splices, among others) and response and performance assessment (especially capacity assessment) to launch the move towards a performance based seismic design and analysis procedure. It is a long order, but the process itself and the knowledge developed move the profession closer to the eventual goal. This research is intended to contribute towards this goal.

APPENDIX A

CHARACTERISTICS AND DESCRIPTION OF SEISMIC INPUT

A.1 Description of Sets of Ground Motions

Sets of ground motions representative of different hazard levels have been assembled for the three geographic locations (Los Angeles, Seattle, and Boston) as part of the SAC steel research project (Somerville et al., 1997). The sets consist of recorded and simulated ground motions and represent return periods of 475 years (10% probability of being exceeded in 50 years; referred to as the 10/50 sets), and 2475 years (2% probability of being exceeded in 50 years; referred to as the 2/50 sets). In addition, the Los Angeles structures are also subjected to a set representative of a 72 year return period (50% probability of being exceeded in 50 years; referred to as the 50/50 set). Each set of ground motions consists of 20 time histories; 10 ground motions each with 2 orthogonal components. The individual components of all the records have been rotated to 45^{o} degrees with respect to the fault in order to minimize directivity effects.

The ground motions are scaled (same scaling factor is used for the two components of a ground motion) such that, on average, their spectral values match with a least square error fit to the United States Geological Survey's (USGS) mapped values at 0.3, 1.0, and 2.0 seconds, and an additional predicted value at 4.0 seconds (Somerville et al., 1997). The weights ascribed to the four period points are 0.1 at the 0.3 second period point and 0.3 for the other three period points. The target spectra provided by USGS are for the S_B/S_C soil type boundaries, which have been modified to be representative for soil type S_D (stiff soil - measured shear wave velocity between 600 to 1200 ft/sec). Details concerning the modification factors used to transform the target response spectra to be

representative of soil type S_D, and the scaling factors used for the individual ground motions are given in Somerville et al. (1997). The target response spectra values for soil type S_D are reproduced in Table A.1. Tables A.2 to A.4 provide basic information for the individual earthquake records constituting the different sets of ground motions for Los Angeles, Seattle, and Boston, respectively. The duration of the ground motion records, given in Tables A.2 to A.4, signifies the total length of the time history. The entire length of the time history is used for analysis, i.e., the time history is not curtailed to reflect only the strong motion duration of the record.

A.2 Spectral Characteristics of Ground Motions

The median elastic displacement spectra and the associated dispersion in the data for the different sets of ground motions are shown in Figures 5.15 to 5.18 (for 2% damping). An idea of the relative seismic hazard in the different regions can be obtained from these figures.

The elastic strength demand (acceleration) and displacement demand spectra for the individual ground motions constituting the different sets of ground motions are shown in Figures A.1 to A.6 for Los Angeles, Figures A.7 to A.10 for Seattle, and Figures A.11 to A.14 for Boston. Overlaid on these graphs are the median and 84^{th} percentile values for the particular set of ground motions. The differences in the spectral characteristics of the sets of ground motions and a comparison with NEHRP spectra are presented in Section 5.3.

Table A.1 Target Response Spectra Values for Soil Type S_D for 5% Damping Level (from Somerville et al., 1997)

Location	Hazard Level	Period			
		0.3	1.0	2.0	4.0
Los Angeles	2/50	1.610	1.190	0.540	0.190
	10/50	1.070	0.680	0.330	0.123
	50/50	0.514	0.288	0.149	0.069
Seattle	2/50	1.455	1.000	0.410	0.164
	10/50	0.710	0.390	0.180	0.072
Boston	2/50	0.340	0.160	0.077	0.030
	10/50	0.120	0.052	0.028	0.0108

Table A.2 Basic Characteristics of Los Angeles Ground Motion Records

50/50 Set of Records (72 years Return Period)						
Designation	*Record Information*	*Duration (sec.)*	*Magnitude Mw*	*R (km)*	*Scale*	*PGA (in/sec^2)*
LA41	Coyote Lake, 1979	39.38	5.7	8.8	2.28	227.7
LA42	Coyote Lake, 1979	39.38	5.7	8.8	2.28	128.7
LA43	Imperial Valley, 1979	39.08	6.5	1.2	0.40	55.4
LA44	Imperial Valley, 1979	39.08	6.5	1.2	0.40	43.1
LA45	Kern, 1952	78.60	7.7	107.0	2.92	55.7
LA46	Kern, 1952	78.60	7.7	107.0	2.92	61.4
LA47	Landers, 1992	79.98	7.3	64.0	2.63	130.4
LA48	Landers, 1992	79.98	7.3	64.0	2.63	118.8
LA49	Morgan Hill, 1984	59.98	6.2	15.0	2.35	123.0
LA50	Morgan Hill, 1984	59.98	6.2	15.0	2.35	211.0
LA51	Parkfield, 1966, Cholame 5W	43.92	6.1	3.7	1.81	301.4
LA52	Parkfield, 1966, Cholame 5W	43.92	6.1	3.7	1.81	243.8
LA53	Parkfield, 1966, Cholame 8W	26.14	6.1	8.0	2.92	267.7
LA54	Parkfield, 1966, Cholame 8W	26.14	6.1	8.0	2.92	305.1
LA55	North Palm Springs, 1986	59.98	6.0	9.6	2.75	199.8
LA56	North Palm Springs, 1986	59.98	6.0	9.6	2.75	146.3
LA57	San Fernando, 1971	79.46	6.5	1.0	1.30	97.7
LA58	San Fernando, 1971	79.46	6.5	1.0	1.30	89.2
LA59	Whittier, 1987	39.98	6.0	17.0	3.62	296.7
LA60	Whittier, 1987	39.98	6.0	17.0	3.62	184.7

Table A.2 (cont'd.) Basic Characteristics of Los Angeles Ground Motion Records

10/50 Set of Records (475 years Return Period)						
Designation	*Record Information*	*Duration (sec.)*	*Magnitude Mw*	*R (km)*	*Scale*	*PGA (in/sec^2)*
LA01	Imperial Valley, 1940	39.38	6.9	10.0	2.01	178.0
LA02	Imperial Valley, 1940	39.38	6.9	10.0	2.01	261.0
LA03	Imperial Valley, 1979	39.38	6.5	4.1	1.01	152.0
LA04	Imperial Valley, 1979	39.38	6.5	4.1	1.01	188.4
LA05	Imperial Valley, 1979	39.08	6.5	1.2	0.84	116.4
LA06	Imperial Valley, 1979	39.08	6.5	1.2	0.84	90.6
LA07	Landers, 1992	79.98	7.3	36.0	3.20	162.6
LA08	Landers, 1992	79.98	7.3	36.0	3.20	164.4
LA09	Landers, 1992	79.98	7.3	25.0	2.17	200.7
LA10	Landers, 1992	79.98	7.3	25.0	2.17	139.1
LA11	Loma Prieta, 1989	39.98	7.0	12.4	1.79	256.9
LA12	Loma Prieta, 1989	39.98	7.0	12.4	1.79	374.4
LA13	Northridge, 1994, Newhall	59.98	6.7	6.7	1.03	261.8
LA14	Northridge, 1994, Newhall	59.98	6.7	6.7	1.03	253.7
LA15	Northridge, 1994, Rinaldi	14.95	6.7	7.5	0.79	206.0
LA16	Northridge, 1994, Rinaldi	14.95	6.7	7.5	0.79	223.9
LA17	Northridge, 1994, Sylmar	59.98	6.7	6.4	0.99	219.9
LA18	Northridge, 1994, Sylmar	59.98	6.7	6.4	0.99	315.5
LA19	North Palm Springs, 1986	59.98	6.0	6.7	2.97	393.5
LA20	North Palm Springs, 1986	59.98	6.0	6.7	2.97	380.9

2/50 Set of Records (2475 years Return Period)						
Designation	*Record Information*	*Duration (sec.)*	*Magnitude Mw*	*R (km)*	*Scale*	*PGA (in/sec^2)*
LA21	1995 Kobe	59.98	6.9	3.4	1.15	495.3
LA22	1995 Kobe	59.98	6.9	3.4	1.15	355.4
LA23	1989 Loma Prieta	24.99	7.0	3.5	0.82	161.4
LA24	1989 Loma Prieta	24.99	7.0	3.5	0.82	182.6
LA25	1994 Northridge	14.95	6.7	7.5	1.29	335.3
LA26	1994 Northridge	14.95	6.7	7.5	1.29	364.3
LA27	1994 Northridge	59.98	6.7	6.4	1.61	357.8
LA28	1994 Northridge	59.98	6.7	6.4	1.61	513.4
LA29	1974 Tabas	49.98	7.4	1.2	1.08	312.4
LA30	1974 Tabas	49.98	7.4	1.2	1.08	382.9
LA31	Elysian Park (simulated)	29.99	7.1	17.5	1.43	500.5
LA32	Elysian Park (simulated)	29.99	7.1	17.5	1.43	458.1
LA33	Elysian Park (simulated)	29.99	7.1	10.7	0.97	302.1
LA34	Elysian Park (simulated)	29.99	7.1	10.7	0.97	262.8
LA35	Elysian Park (simulated)	29.99	7.1	11.2	1.10	383.1
LA36	Elysian Park (simulated)	29.99	7.1	11.2	1.10	424.9
LA37	Palos Verdes (simulated)	59.98	7.1	1.5	0.90	274.7
LA38	Palos Verdes (simulated)	59.98	7.1	1.5	0.90	299.7
LA39	Palos Verdes (simulated)	59.98	7.1	1.5	0.88	193.1
LA40	Palos Verdes (simulated)	59.98	7.1	1.5	0.88	241.4

Table A.3 Basic Characteristics of Seattle Ground Motion Records

10/50 Set of Records (475 years Return Period)						
Designation	*Record Information*	*Duration (sec.)*	*Magnitude Mw*	*R (km)*	*Scale*	*PGA (in/sec^2)*
SE01	Long Beach, Vernon CMD Bldg.	39.08	6.5	1.2	0.49	67.1
SE02	Long Beach, Vernon CMD Bldg.	39.08	6.5	1.2	0.49	52.2
SE03	Morgan Hill, Gilroy	59.98	6.2	15.0	2.84	149.1
SE04	Morgan Hill, Gilroy	59.98	6.2	15.0	2.84	255.8
SE05	West, Washington, Olympia	79.98	6.5	56.0	1.86	148.1
SE06	West, Washington, Olympia	79.98	6.5	56.0	1.86	135.9
SE07	West, Washington, Seattle Army B.	66.68	6.5	80.0	5.34	113.9
SE08	West, Washington, Seattle Army B.	66.68	6.5	80.0	5.34	150.1
SE09	North Palm Springs	59.98	6.0	6.7	1.71	226.9
SE10	North Palm Springs	59.98	6.0	6.7	1.71	219.7
SE11	Puget Sound, Wa., Olympia	81.82	7.1	80.0	4.30	290.5
SE12	Puget Sound, Wa., Olympia	81.82	7.1	80.0	4.30	230.1
SE13	Puget Sound, Wa., Federal OFC B.	74.08	7.1	61.0	5.28	142.6
SE14	Puget Sound, Wa., Federal OFC B.	74.08	7.1	61.0	5.28	117.0
SE15	Eastern Wa., Tacoma County	59.98	7.1	60.0	8.68	112.1
SE16	Eastern Wa., Tacoma County	59.98	7.1	60.0	8.68	221.8
SE17	Llolleo, Chile 3/3/85	99.98	8.0	42.0	1.24	269.4
SE18	Llolleo, Chile 3/3/85	99.98	8.0	42.0	1.24	259.0
SE19	Vinadel Mar, Chile	99.98	8.0	42.0	1.69	209.1
SE20	Vinadel Mar, Chile	99.98	8.0	42.0	1.69	148.4

2/50 Set of Records (2475 years Return Period)						
Designation	*Record Information*	*Duration (sec.)*	*Magnitude Mw*	*R (km)*	*Scale*	*PGA (in/sec^2)*
SE21	1992 Mendocino	59.98	7.1	8.5	0.98	291.8
SE22	1992 Mendocino	59.98	7.1	8.5	0.98	187.5
SE23	1992 Erzincan	20.78	6.7	2.0	1.27	233.7
SE24	1992 Erzincan	20.78	6.7	2.0	1.27	208.3
SE25	1949 Olympia	79.98	6.5	56.0	4.35	345.8
SE26	1949 Olympia	79.98	6.5	56.0	4.35	317.2
SE27	1965 Seattle	81.82	7.1	80.0	10.04	678.1
SE28	1965 Seattle	81.82	7.1	80.0	10.04	537.3
SE29	1985 Valpariso	99.98	8.0	42.0	2.90	632.1
SE30	1985 Valpariso	99.98	8.0	42.0	2.90	607.7
SE31	1985 Valpariso	99.98	8.0	42.0	3.96	490.6
SE32	1985 Valpariso	99.98	8.0	42.0	3.96	348.2
SE33	Deep Interplate (simulation)	79.98	7.9	65.0	3.84	307.6
SE34	Deep Interplate (simulation)	79.98	7.9	65.0	3.84	249.7
SE35	1978 Miyagi-oki	79.98	7.4	66.0	1.78	234.3
SE36	1978 Miyagi-oki	79.98	7.4	66.0	1.78	302.6
SE37	Shallow Interplate (simulation)	79.98	7.9	15.0	0.94	217.5
SE38	Shallow Interplate (simulation)	79.98	7.9	15.0	0.94	206.5
SE39	Shallow Interplate (simulation)	79.98	7.9	15.0	1.49	223.3
SE40	Shallow Interplate (simulation)	79.98	7.9	15.0	1.49	289.5

Table A.4 Basic Characteristics of Boston Ground Motion Records

10/50 Set of Records (475 years Return Period)						
Designation	*Record Information*	*Duration (sec.)*	*Magnitude Mw*	*R (km)*	*Scale*	*PGA (in/sec^2)*
BO01	Simulation, hanging wall	29.99	6.5	30.0	0.39	48.0
BO02	Simulation, hanging wall	29.99	6.5	30.0	0.39	28.7
BO03	Simulation, foot wall	29.99	6.5	30.0	0.54	55.7
BO04	Simulation, foot wall	29.99	6.5	30.0	0.54	43.2
BO05	New Hampshire, 1982	19.23	4.3	8.4	10.75	222.4
BO06	New Hampshire, 1982	19.23	4.3	8.4	10.75	121.9
BO07	Nahanni, 1985	20.34	6.9	9.6	0.09	34.0
BO08	Nahanni, 1985	20.34	6.9	9.6	0.09	32.0
BO09	Nahanni, 1985	18.76	6.9	6.1	0.20	23.4
BO10	Nahanni, 1985	18.76	6.9	6.1	0.20	28.4
BO11	Nahanni, 1985	19.02	6.9	18.0	0.92	51.5
BO12	Nahanni, 1985	19.02	6.9	18.0	0.92	52.4
BO13	Saguenay, 1988	17.74	5.9	96.0	1.57	77.4
BO14	Saguenay, 1988	17.74	5.9	96.0	1.57	112.0
BO15	Saguenay, 1988	29.57	5.9	98.0	3.21	202.2
BO16	Saguenay, 1988	29.57	5.9	98.0	3.21	95.9
BO17	Saguenay, 1988	39.05	5.9	118.0	3.25	70.7
BO18	Saguenay, 1988	39.05	5.9	118.0	3.25	87.8
BO19	Saguenay, 1988	33.24	5.9	132.0	3.34	68.1
BO20	Saguenay, 1988	33.24	5.9	132.0	3.34	105.2

2/50 Set of Records (2475 years Return Period)						
Designation	*Record Information*	*Duration (sec.)*	*Magnitude Mw*	*R (km)*	*Scale*	*PGA (in/sec^2)*
BO21	simulation, foot wall	29.99	6.5	30.0	0.99	122.0
BO22	simulation, foot wall	29.99	6.5	30.0	0.99	140.6
BO23	simulation, foot wall	29.99	6.5	30.0	0.84	129.4
BO24	simulation, foot wall	29.99	6.5	30.0	0.84	92.6
BO25	simulation, foot wall	29.99	6.5	30.0	0.63	112.0
BO26	simulation, foot wall	29.99	6.5	30.0	0.63	119.2
BO27	Nahanni, 1985 Station 1	20.34	6.9	9.6	0.27	97.2
BO28	Nahanni, 1985 Station 1	20.34	6.9	9.6	0.27	91.5
BO29	Nahanni, 1985 Station 2	18.76	6.9	6.1	0.56	67.0
BO30	Nahanni, 1985 Station 2	18.76	6.9	6.1	0.56	81.4
BO31	Nahanni, 1985 Station 3	19.02	6.9	18.0	2.63	147.2
BO32	Nahanni, 1985 Station 3	19.02	6.9	18.0	2.63	150.0
BO33	Saguenay, 1988	17.74	5.9	96.0	4.48	221.4
BO34	Saguenay, 1988	17.74	5.9	96.0	4.48	302.4
BO35	Saguenay, 1988	29.57	5.9	98.0	9.21	580.7
BO36	Saguenay, 1988	29.57	5.9	98.0	9.21	275.6
BO37	Saguenay, 1988	39.05	5.9	118.0	9.30	202.4
BO38	Saguenay, 1988	39.05	5.9	118.0	9.30	251.5
BO39	Saguenay, 1988	33.24	5.9	132.0	9.58	195.1
BO40	Saguenay, 1988	33.24	5.9	132.0	9.58	301.4

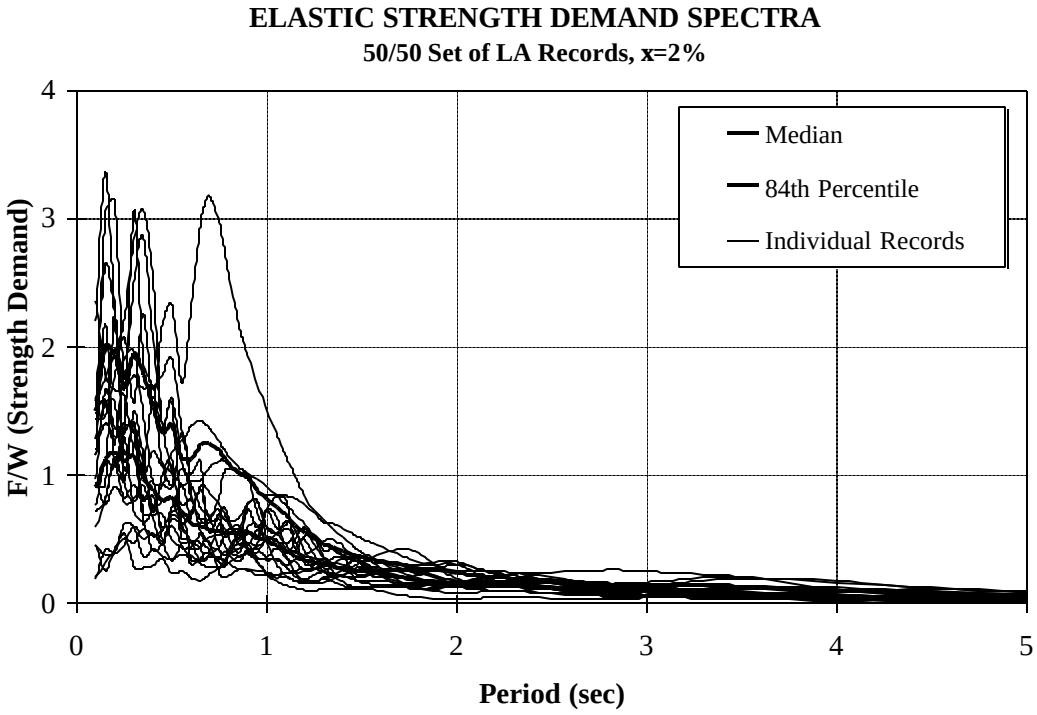

Figure A.1 Elastic Strength Demand (Acceleration) Spectra,
50/50 Set of LA Ground Motions

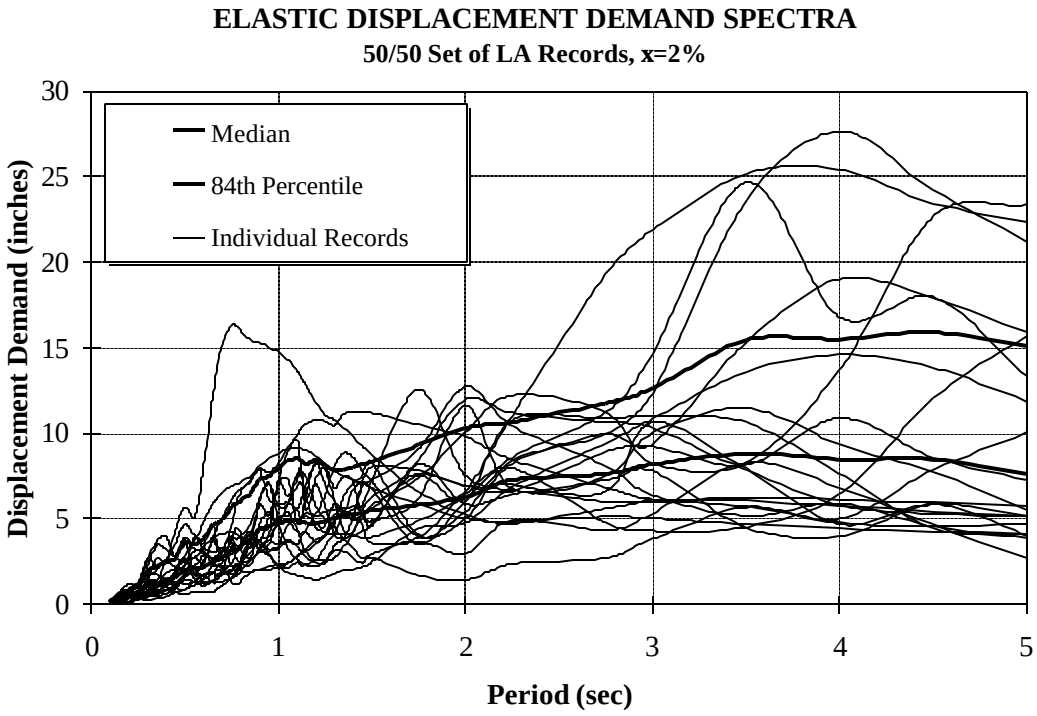

Figure A.2 Elastic Displacement Demand Spectra,
50/50 Set of LA Ground Motions

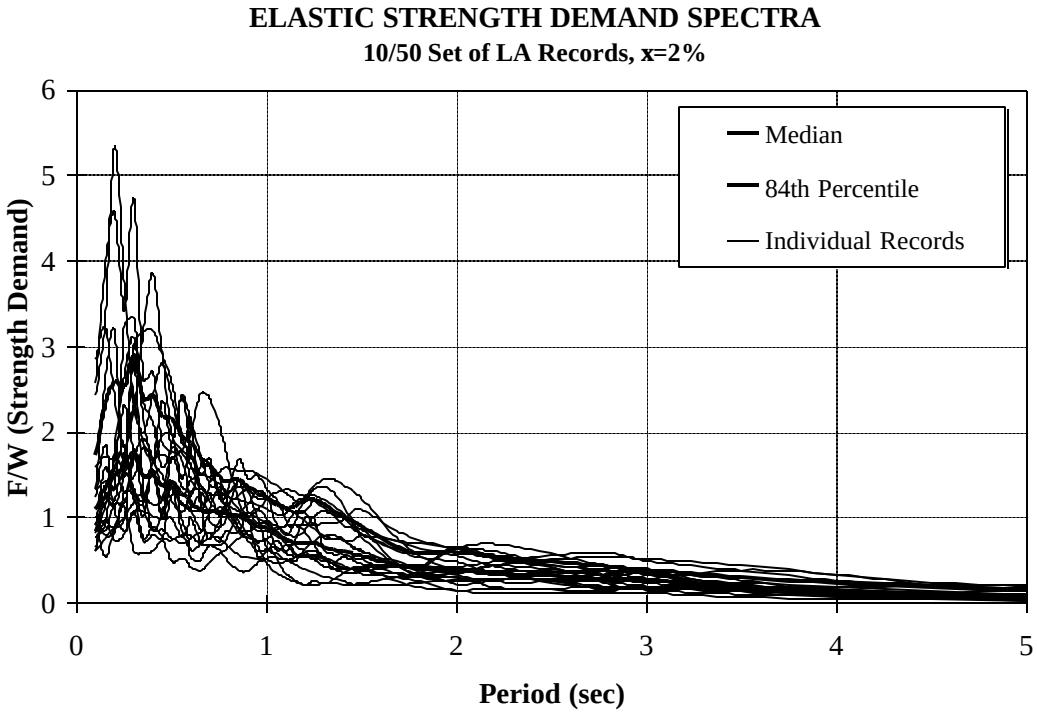

Figure A.3 Elastic Strength Demand (Acceleration) Spectra,
10/50 Set of LA Ground Motions

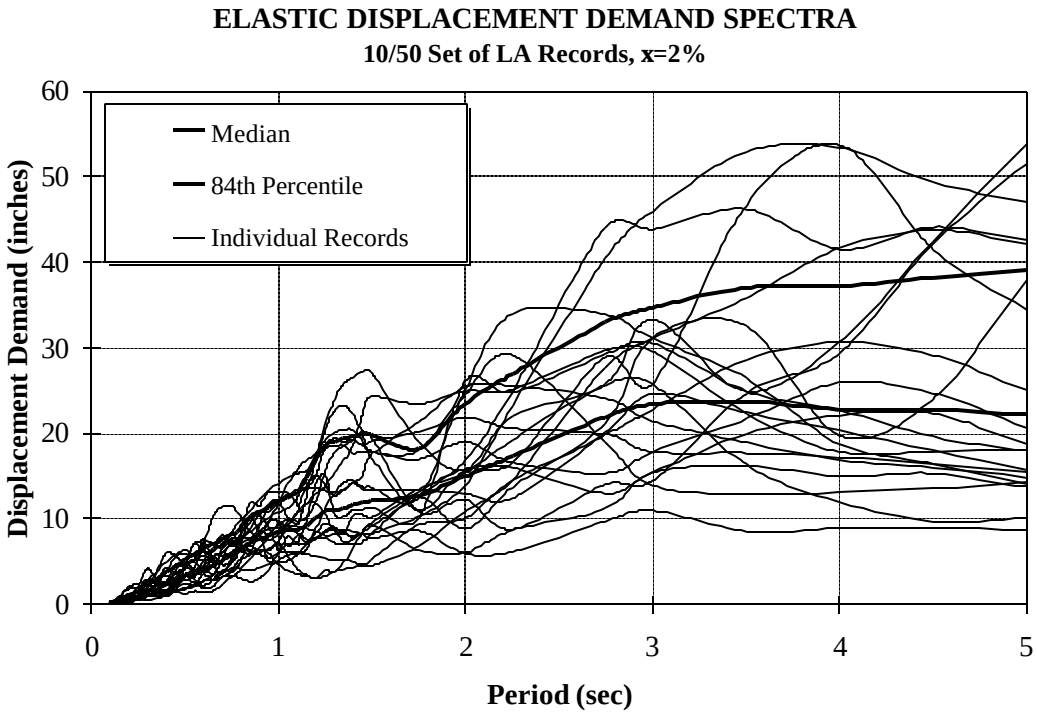

Figure A.4 Elastic Displacement Demand Spectra,
10/50 Set of LA Ground Motions

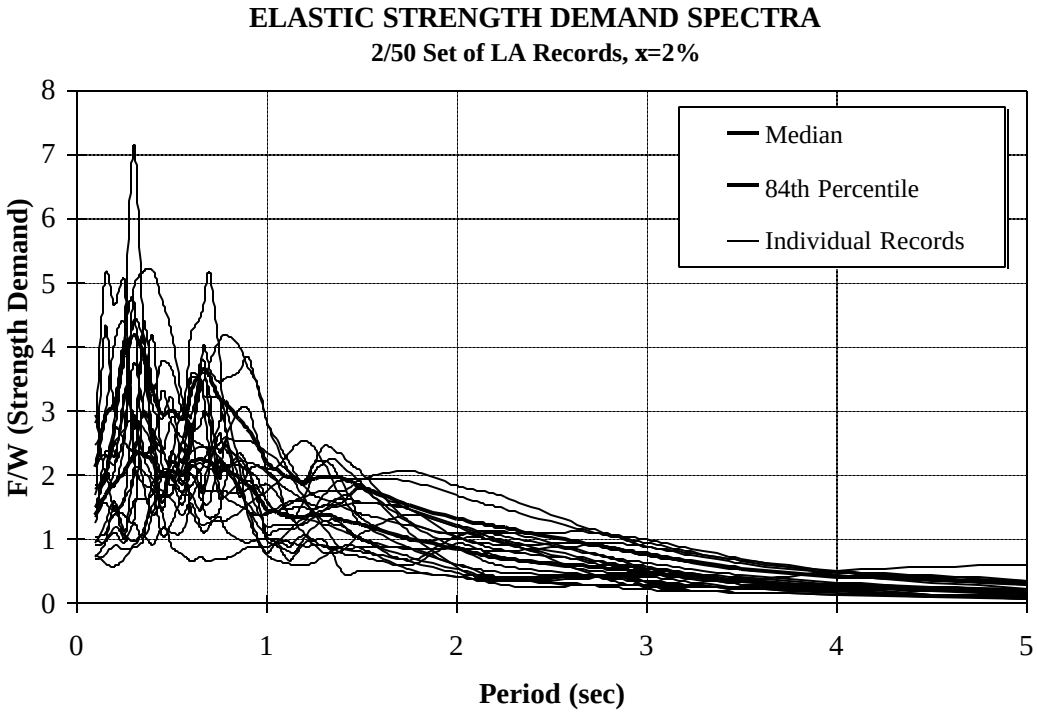

Figure A.5 Elastic Strength Demand (Acceleration) Spectra,
2/50 Set of LA Ground Motions

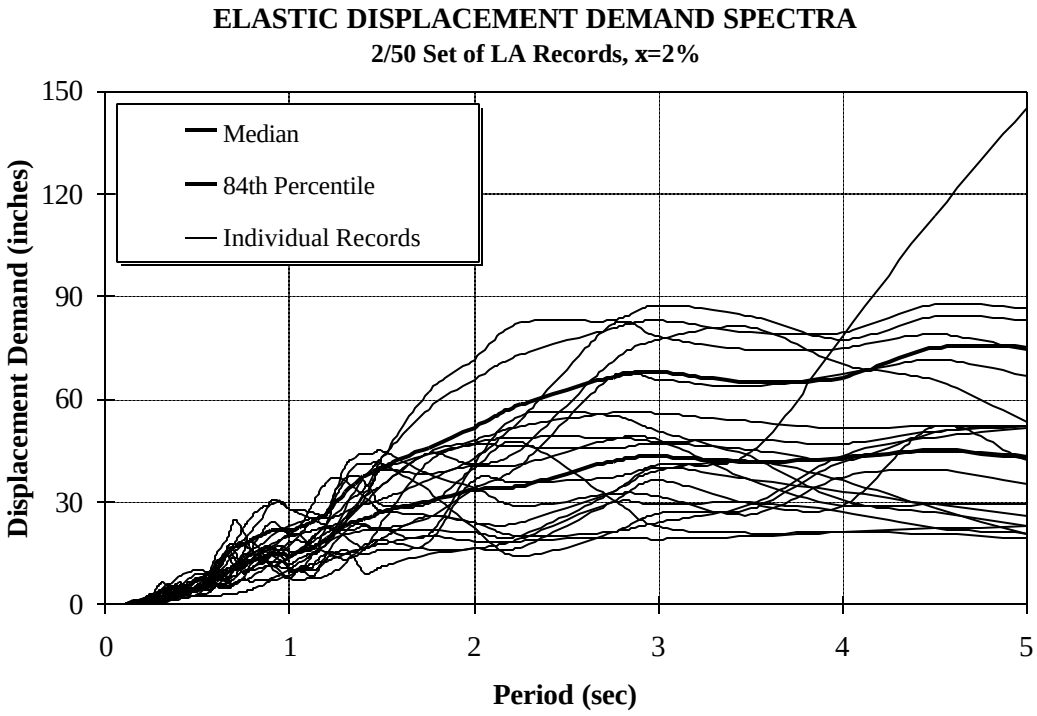

Figure A.6 Elastic Displacement Demand Spectra,
2/50 Set of LA Ground Motions

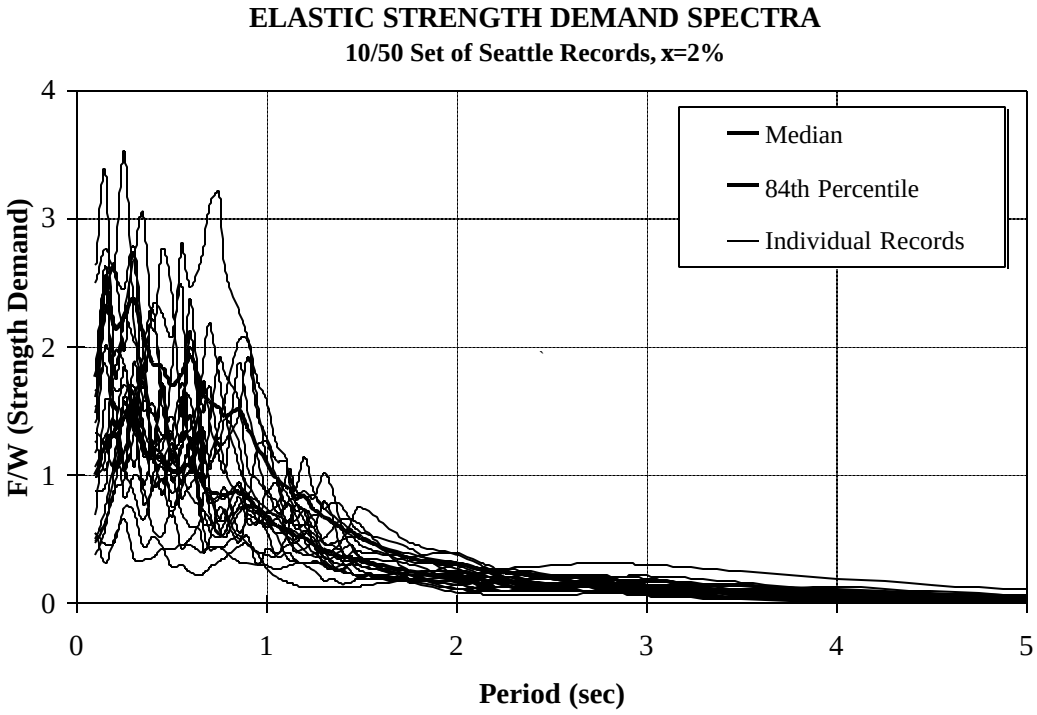

Figure A.7 Elastic Strength Demand (Acceleration) Spectra,
10/50 Set of Seattle Ground Motions

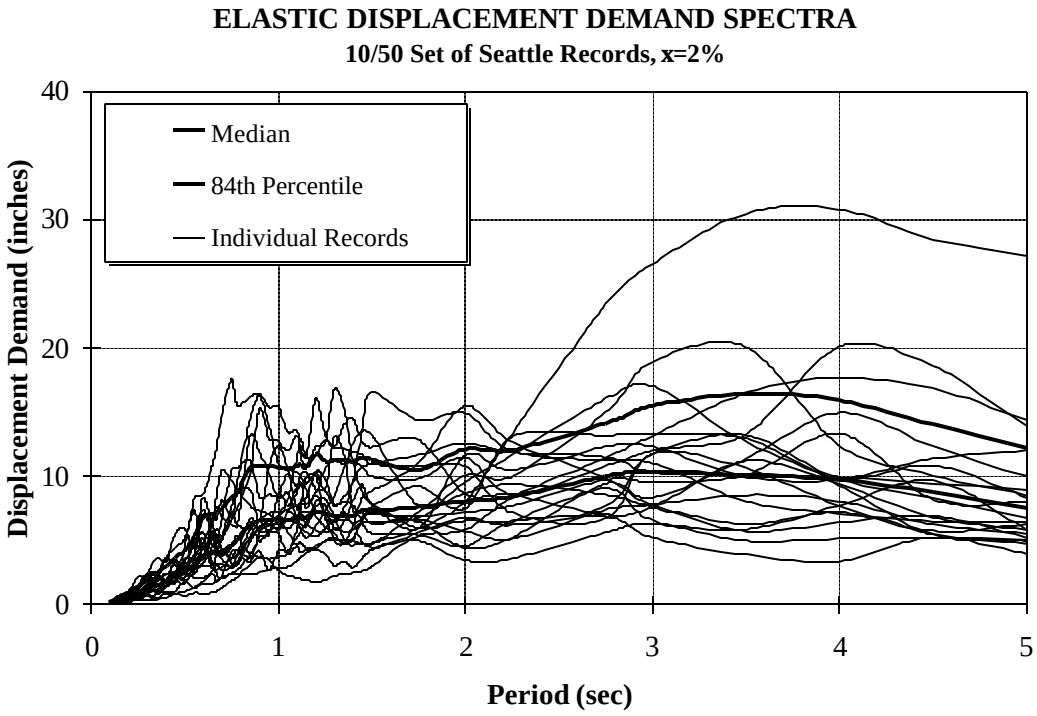

Figure A.8 Elastic Displacement Demand Spectra,
10/50 Set of Seattle Ground Motions

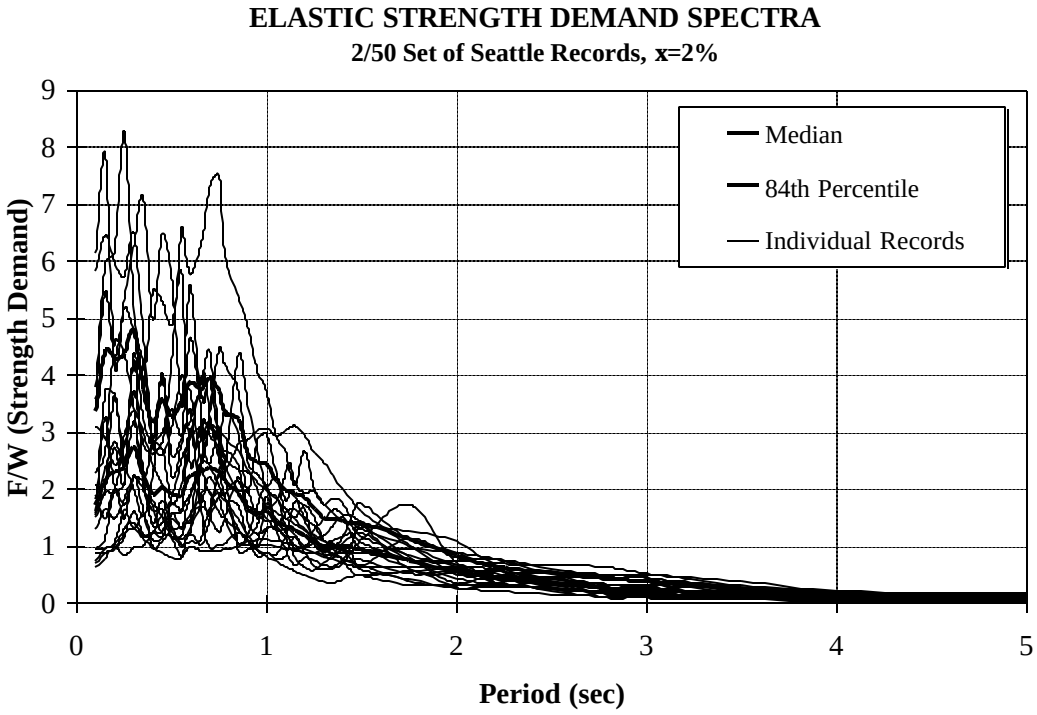

Figure A.9 Elastic Strength Demand (Acceleration) Spectra,
2/50 Set of Seattle Ground Motions

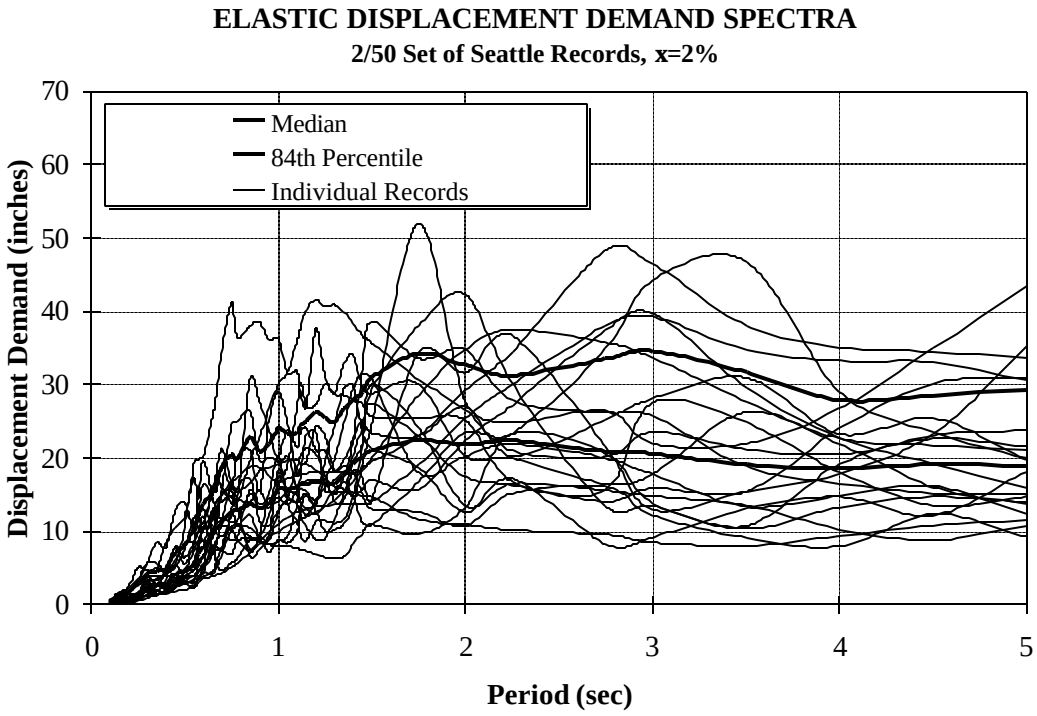

Figure A.10 Elastic Displacement Demand Spectra,
2/50 Set of Seattle Ground Motions

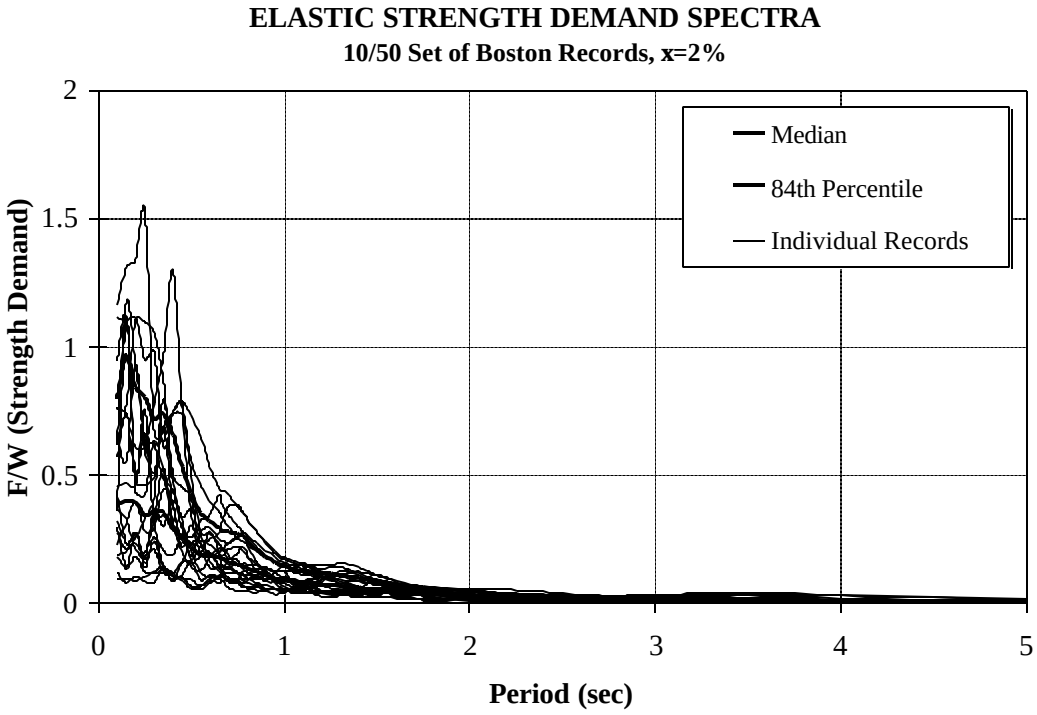

Figure A.11 Elastic Strength Demand (Acceleration) Spectra, 10/50 Set of Boston Ground Motions

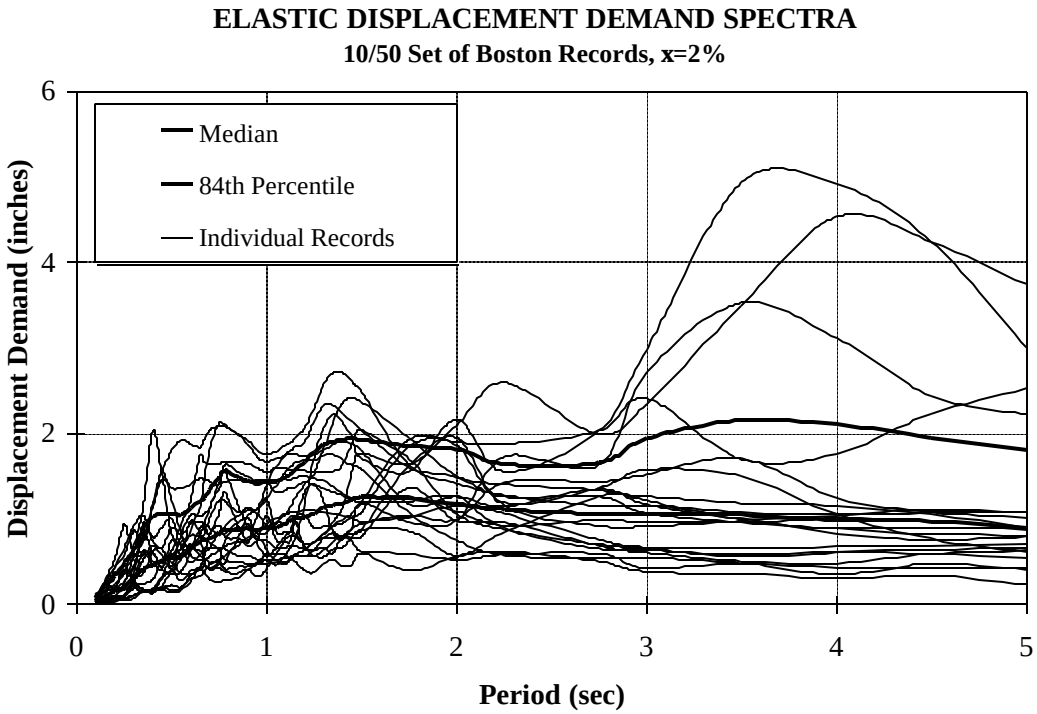

Figure A.12 Elastic Displacement Demand Spectra, 10/50 Set of Boston Ground Motions

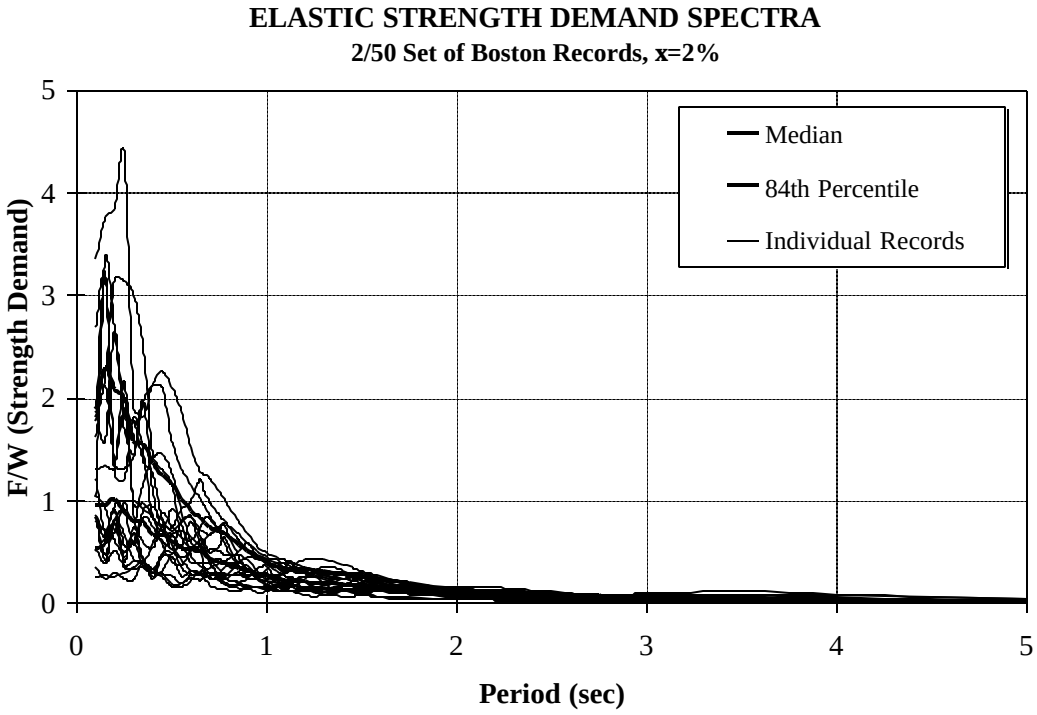

Figure A.13 Elastic Strength Demand (Acceleration) Spectra,
2/50 Set of Boston Ground Motions

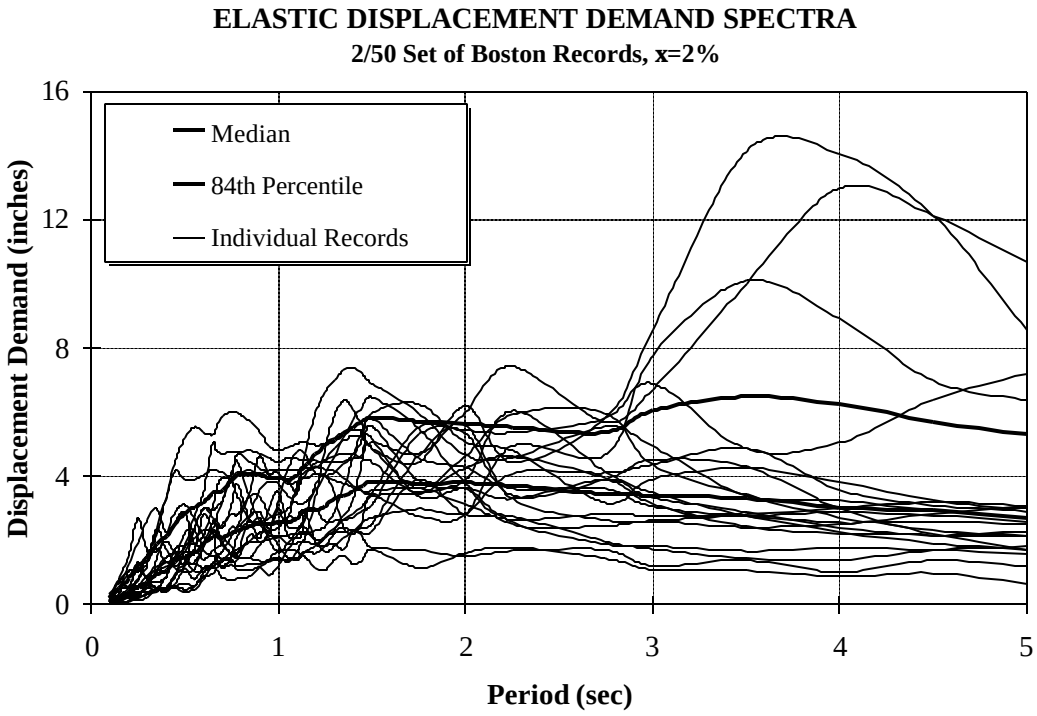

Figure A.14 Elastic Displacement Demand Spectra,
2/50 Set of Boston Ground Motions

APPENDIX B

DESCRIPTION OF MODEL BUILDINGS

B.1 Description of Buildings and Basic Loading Conditions

As part of the SAC steel project three consulting firms were commissioned to perform code designs for 3-, 9-, and 20-story model buildings, following the local code requirements for the following three cities: Los Angeles (UBC 1994), Seattle (UBC 1994) and Boston (BOCA 1993). All prevailing code requirements for gravity, wind, and seismic design needed to be considered. The buildings were to be designed as standard office buildings situated on stiff soil (soil type S2 as per UBC '94 and BOCA '93 definitions).

The floor plans and elevations for the buildings were preset, as shown in Figure B.1. The shaded area indicates the penthouse location. Gravity frame columns are located only below the penthouse in the 20-story buildings, resulting in 2 bays of 40 feet bounding a 20 feet bay in the gravity frames. The column bases in the 3-story buildings are considered as fixed. The 9-story buildings have a single-level basement, and the 20-story buildings have a 2-level basement. The buildings were required to conform to a drift limit of h/400, where "h" is the story height. The loading information provided was the following:

Steel framing:	as designed
Floors and Roof:	3 inch metal decking with 2.5 inches of normal weight concrete fill and fireproofing
Roofing:	7 psf average
Ceilings/Flooring:	3 psf average, including fireproofing

Mechanical/Electrical:	7 psf average for all floors, additionally 40 psf over penthouse area for equipment
Partitions:	as per code requirements (10 psf for seismic load, 20 psf for gravity design)
Exterior Wall:	25 psf of wall surface average, including any penthouses. Assume 2 feet from perimeter column lines to edge of building envelope. Include 42 inch parapet at main roof level, none at penthouse roof.
Live Load:	typical code values for office occupancy (50 psf everywhere)
Wind Load:	as per code requirements, assuming congested area (exposure B as per UBC '94 definition)
Seismic Load:	as per code requirements.

Based on this basic information, the consulting firms were asked to carry out three types of structural designs:

1. Pre-Northridge Designs: These designs were based on design practices prevalent before the Northridge earthquake, i.e., without consideration of the FEMA 267 (1995) document. These designs had the standard beam-to-column welded connection details.
2. Post-Northridge Designs: These designs were to additionally conform to the provisions of FEMA 267 (1995). The designers decided on the use of cover-plated beam flanges in order to move the location of the plastic hinge in the beam away from the face of the column.
3. Special Designs: Two types of special designs were carried out for the 9-story post-Northridge structures in all three geographic locations. The first special design involved the use of reduced beam sections, while the other design involved the use of a higher strength steel (A913) for the columns.

Thus, the basic definitions for the buildings were kept constant between the different regions, but no other constraints concerning the design of the buildings (e.g., number of moment resisting connections, choice of member sections, etc.) were imposed. The buildings so designed can be considered as being representative of typical steel moment frame structures in the three geographic locations, designed according to either pre- or post-Northridge design practice.

All three design offices selected perimeter moment resisting frames as the structural system. In all cases the design of the moment frames in the two orthogonal directions was either identical or very similar, thus, only half of the structure is considered in the analysis. The ordinary difference between the NS and East-West (EW) direction comes from the difference in gravity load effects on account of the orientation of the gravity beams and sub-beams. Both the beams and sub-beams are oriented in the NS direction. However, as the gravity loading on the girders of the perimeter SMRFs is small and has almost negligible effect on the seismic response, the decision to analyze the structure only in the NS direction is justified.

The loading used for the analysis of the frames is based on the details given before, which result in the following floor load distribution (steel weight is assumed as 13 psf for all designs):

Floor dead load for weight calculations:	96 psf
Floor dead load for mass calculations:	86 psf
Roof dead load excluding penthouse:	83 psf
Penthouse dead load:	116 psf
Reduced live load per floor and for roof:	20 psf

Cladding and parapet loads are based on the surface area of the structures. Based on these loading definitions the seismic mass for the structures is as follows (the values are for the entire structure):

<u>3-story Structures:</u>

Roof:	70.90 kips-sec^2/ft
Floor 3 and Floor 2:	65.53 kips-sec^2/ft

<u>9-story Structures:</u>

Roof:	73.10 kips-sec^2/ft
Floor 9 to Floor 3:	67.86 kips-sec^2/ft
Floor 2:	69.04 kips-sec^2/ft

<u>20-story Structures:</u>

Roof:	40.06 kips-sec^2/ft
Floor 20 to Floor 3:	37.76 kips-sec^2/ft
Floor 2:	38.63 kips-sec^2/ft

The design details (member sections, doubler plates, design basis, etc.) for the different structures are summarized in the following sections.

B.2 Los Angeles (LA) Structures

The lateral load design of all LA structures was controlled by seismic load considerations. The location of the moment resisting frames is shown by the bold lines in Figure B.2. All the columns in the perimeter moment frames bend about the strong axis. The strong axis of the gravity frame columns' is oriented in the NS direction.

In the 9-story building, one of the exterior bays has only one moment resisting connection to avoid bi-axial bending in the corner column. In the 20-story buildings all the exterior connections are moment resisting connections and box columns are used at the corners to resist bi-axial bending. The design yield strength of the beams and girders is 36 ksi and of the columns is 50 ksi. Most of the girder sizes are controlled by drift rather than strength considerations. The sections used in the NS frames of the pre-Northridge and post-Northridge designs are summarized in Table B.1.

Panel zone doubler plates have been used to conform to the minimum panel zone shear strength code requirement. The thickness for the doubler plates are shown in Table B.1. The first number represents the thickness of the doubler plate for the exterior columns, while the second number represents the thickness of the doubler plates for the interior columns of the SMRF. The doubler plates have the same nominal yield strength as the columns.

In the post-Northridge designs cover plates are welded to the top and bottom of the girder flanges. The dimensions of the cover plates used are given in Table B.2. "W1" denotes the width of the top cover plate next to the column face, and "T1" denotes the thickness of the top cover plate. The top cover plate extends for a length of 18 inches from the face of the column and ends with a width of 3 inches with uniform tapering from the face of the column to the end of the cover plate. The bottom cover plate is rectangular in shape with a width of "W2" and a thickness of "T2". The cover plates have the same nominal yield strength as the girders.

Addition of cover plates to girder flanges increases the stiffness of the girders. The increase is, however, not large enough to induce a major change in the global properties of the structure (see Table 5.1) and hence the member sections in the pre- and post-Northridge designs are very similar. Some small differences observed in the member properties in some parts of the buildings, can be explained as follows:

1. the designer specified A36 steel for beams and girders in the pre-Northridge design, while using Dual Grade A36 Gr. 50 steel for the post-Northridge design. As the dual grade steel has a higher nominal yield strength (50 ksi as against 36 ksi for A36), the gravity beams and to some extent the SMRF girder sizes could be reduced. [The expected yield strength of the both the steel types is, however, very close, and a common value of 49.2 ksi is used in the analysis in this work.]
2. the increase in girder moment at the face of the column may be responsible for the use of slightly heavier column sections in some locations, to maintain the strong column – weak girder concept.

Based on the member properties of the pre- and post-Northridge structures, the global response of same height structures is expected to be similar. Differences are expected at the local level, i.e., in the distribution of demands between the beam, panel zone, and the column.

B.3 Seattle (SE) Structures

The design of the Seattle 3- and 9-story structures was governed by seismic loads, however, the design of the 20-story structure was controlled by wind loads (based on a wind speed of 80 mph). The wind design base shear for the 20-story structure is almost identical to the seismic design base shear for the LA 20-story structure, resulting in the stiffness of the two structures being similar (see Table 5.1). A572 Gr. 50 (nominal yield strength of 50 ksi, expected yield strength 57.6 ksi) steel has been used for all column, beam and girder sections in all Seattle designs.

The position of the moment resisting frames is shown by the bold lines in Figure B.3. The strong axis of the gravity frame columns' is oriented in the NS direction. The layout of the moment resisting frame is observed to be slightly different from the layout of the MR frames for the LA buildings. The member sections for the pre-Northridge design,

post-Northridge design, and the design employing reduced beam sections (RBS) are given in Table B.3.

The dimensions of the cover plates used for the post-Northridge designs are given in Table B.4, where "L" denotes the length of the cover plate, "W" the width, and "T" the thickness. The bottom cover plate has a rectangular cross section. The top cover plate has a width equal to "W1" at the face of the column, maintains this width for 2-1/2 inches from the column face, and then tapers uniformly to a width of 3-1/2 inches at the end of the cover plate.

The choice of the girder sections in the post-Northridge designs was influenced by detailing considerations; the length of the cover plate is taken as half the depth of the girder, and the thickness equal to the girder flange thickness (or $1/8^{th}$ inch thicker for the top cover plate). This criterion resulted in the selection of girders which are typically shallower with wider, thicker flanges. In order to offset the additional demand generated at the column due to movement of the plastic hinge away from the face of the column, the column sizes were increased in the post-Northridge designs. The increased demands also resulted in the use of thicker doubler plates for the panel zones. The global stiffness of the pre- and post-Northridge designs is almost identical, again indicating that the change in design criteria is likely to affect only the local distribution of demands at the connections.

The requirement of limiting the weld stress at the beam-to-column complete penetration weld to 40 ksi, resulted in the use of cover plates even in the reduced beam section design. The cover plate dimensions for the design employing the reduced beam section details are given in Table B.5. For all post-Northridge and RBS designs, the cover plates are of the same yield strength as the girders. The doubler plates have the same yield strength as the columns.

The cover plate geometry is similar to the geometry used in the post-Northridge designs, with the exception of the end of the cover plate being 3 inches wide instead of 3-1/2 inches wide. The geometry of the reduced beam section is given in Table B.6. The designers used a curved cutout pattern for the reduced beam section, with the maximum allowable flange reduction of 50% being utilized. The RBS starts at a distance of L minus 0.5L(RBS) from the face of the column and extends for a length of L(RBS). The minimum width of W(RBS) is at the midsection of the RBS.

The RBS design has member sizes that are similar to those of the pre-Northridge design, in most areas. The only major difference observed is in the use of lighter sections for the exterior columns in the RBS design, due to a reduction in the maximum force demand transferred from the beam onto the column. Again, the global characteristics of the different designs are similar and differences in response are expected primarily at the local level.

B.4 Boston (BO) Structures

The location of the moment resisting connections in the Boston 3- and 20-story structures is identical to the location of the MR connections in the Seattle 3- and 20-story structures (see Figure B.3). The placement of the MR connections in the 9-story structure is identical to the placement in the LA 9-story structure (see Figure B.2). The strong axis of the gravity frame columns' is oriented in the NS direction. The design of the 3-story structure is controlled by seismic loads, while the designs for the 9- and 20-story structures are wind controlled designs. The member sections for the pre- and post-Northridge designs are given in Table B.7. A572 Gr. 50 steel has been used for both beams and columns in the Boston designs.

The dimensions for the cover plates used in the Boston post-Northridge designs are given in Table B.8. "T" stands for the thickness of the plates, and "L" for the length of the plates. The top cover plates have a width equal to "W1" at the face of the column, maintain this width for 2 inches from the column face, and then taper uniformly to a width of "W2". The bottom cover plate has a rectangular cross section with a width of "W".

There are striking differences between the pre- and post-Northridge designs for Boston. Boston lies in seismic Zone 2A, thus the pre-Northridge designs are not required to comply with specific panel zone strength requirements or the strong column criterion, which are binding in seismic Zones 3 and 4. The post-Northridge designs, however, have to comply with both a minimum panel zone shear strength requirement as well as the strong column concept, in accordance with FEMA 267 (1995), thereby resulting in the use of significantly heavier column sections and extensive use of doubler plates.

B.5 Redesigned LA 9-story Structures

Three redesigns of the LA pre-Northridge 9-story structure were carried out using the computer program BERT (Building Engineering Reasoning Tool) developed by Fuyama et al. (1993). The program performs code compliant designs with an emphasis on reducing weight but paying attention to constructability. Beams and girders were designed using A36 steel, while A 572 Gr. 50 steel was used for the design of columns. The floor plans for the three redesigns (designated as R1-, R2-, and R3-LA9), showing the changes in bay width and/or the number of moment resisting connections per floor with respect to the original LA 9-story design, are shown in Figure B.4. The member sections for the redesigns are given in Table B.9. Only the NS moment resisting frame sections are shown.

For the original configuration redesign (R1-LA9), a significant reduction in column sizes is observed at the cost of a small increase in girder sizes. This reduction in the column sizes is primarily on account of the strong column criterion being satisfied on the basis of the strong column – weak panel zone concept rather than the strong column – weak girder concept. The R2 redesign has lighter girder sections on account of the reduced span of the beams. The R3 redesign has heavier girders but lighter columns as compared to the original LA pre-Northridge structure. The three redesigns conform to the code drift requirements and satisfy the minimum panel zone shear strength requirement as well as the strong column criterion (in many cases through weak panel zones).

Table B.1 Beam and Column Sections, and Doubler Plate Thickness for Los Angeles Model Buildings

PRE-NORTHRIDGE DESIGNS

NS Moment Resisting Frame — NS Gravity Frames

3-story Building

Story/Floor	COLUMNS		DOUBLER	GIRDER	COLUMNS		BEAMS
	Exterior	Interior	PLATES (in)		Below penthouse	Others	
1/2	W14X257	W14X311	0,0	W33X118	W14X82	W14X68	W18X35
2/3	W14X257	W14X311	0,0	W30X116	W14X82	W14X68	W18X35
3/Roof	W14X257	W14X311	0,0	W24X68	W14X82	W14X68	W16X26

9-story Building

Story/Floor	COLUMNS		DOUBLER	GIRDER	COLUMNS		BEAMS
	Exterior	Interior	PLATES (in)		Below penthouse	Others	
-1/1	W14X370	W14X500	0,0	W36X160	W14X211	W14X193	W21X44
1/2	W14X370	W14X500	0,0	W36X160	W14X211	W14X193	W18X35
2/3	W14X370, W14X370	W14X500, W14X455	0,0	W36X160	W14X211, W14X159	W14X193, W14X145	W18X35
3/4	W14X370	W14X455	0,0	W36X135	W14X159	W14X145	W18X35
4/5	W14X370, W14X283	W14X455, W14X370	0,0	W36X135	W14X159, W14X120	W14X145, W14X109	W18X35
5/6	W14X283	W14X370	0,0	W36X135	W14X120	W14X109	W18X35
6/7	W14X283, W14X257	W14X370, W14X283	0,0	W36X135	W14X120, W14X90	W14X109, W14X82	W18X35
7/8	W14X257	W14X283	0,0	W30X99	W14X90	W14X82	W18X35
8/9	W14X257, W14X233	W14X283, W14X257	0,0	W27X84	W14X90, W14X61	W14X82, W14X48	W18X35
9/Roof	W14X233	W14X257	0,0	W24X68	W14X61	W14X48	W16X26

Notes:
1. Column line A has exterior column sections oriented about strong axis,
   Column line F has exterior column sections oriented about weak axis
   Column lines B,C,D, and E have interior column sections

20-story Building

Story/Floor	COLUMNS		DOUBLER	GIRDER	COLUMNS	BEAMS	
	Exterior	Interior	PLATES (in)			40 feet span	20 feet span
-2/-1	15X15X2.00	W24X335	0,0	W14X22	W14X550	W21X50	W14X22
-1/1	15X15X2.00	W24X335	0,0	W30X99	W14X550	W24X68	W16X26
1/2	15X15X2.00	W24X335	0,0	W30X99	W14X550	W21X50	W14X22
2/3	15X15X2.00, 15X15X1.25	W24X335, W24X335	0,0	W30X99	W14X550, W14X455	W21X50	W14X22
3/4	15X15X1.25	W24X335	0,0	W30X99	W14X455	W21X50	W14X22
4/5	15X15X1.25	W24X335	0,0	W30X99	W14X455	W21X50	W14X22
5/6	15X15X1.25, 15X15X1.00	W24X335, W24X229	0,0	W30X108	W14X455, W14X370	W21X50	W14X22
6/7	15X15X1.00	W24X229	0,0	W30X108	W14X370	W21X50	W14X22
7/8	15X15X1.00	W24X229	0,0	W30X108	W14X370	W21X50	W14X22
8/9	15X15X1.00, 15X15X1.00	W24X229, W24X229	0,0	W30X108	W14X370, W14X311	W21X50	W14X22
9/10	15X15X1.00	W24X229	0,0	W30X108	W14X311	W21X50	W14X22
10/11	15X15X1.00	W24X229	0,0	W30X108	W14X311	W21X50	W14X22
11/12	15X15X1.00, 15X15X1.00	W24X229, W24X192	0,0	W30X99	W14X311, W14X257	W21X50	W14X22
12/13	15X15X1.00	W24X192	0,0	W30X99	W14X257	W21X50	W14X22
13/14	15X15X1.00	W24X192	0,0	W30X99	W14X257	W21X50	W14X22
14/15	15X15X1.00, 15X15X0.75	W24X192, W24X131	0,5/8	W30X99	W14X257, W14X176	W21X50	W14X22
15/16	15X15X0.75	W24X131	0,5/8	W30X99	W14X176	W21X50	W14X22
16/17	15X15X0.75	W24X131	0,5/8	W30X99	W14X176	W21X50	W14X22
17/18	15X15X0.75, 15X15X0.75	W24X131, W24X117	0,5/8	W27X84	W14X176, W14X108	W21X50	W14X22
18/19	15X15X0.75	W24X117	0,5/8	W27X84	W14X108	W21X50	W14X22
19/20	15X15X0.75, 15X15X0.50	W24X117, W24X84	0,0	W24X62	W14X108	W21X50	W14X22
20/Roof	15X15X0.50	W24X84	0,0	W21X50	W14X108, W14X43	W21X44	W12X16

Notes:
1. The basement floor (-1 level) has simple connections

General Notes
1. There are a total of 6 column lines below the penthouse for the 3- and 9-story buildings, and 4 for the 20-story building
2. For doubler plate thickness, the first number signifies the value for the exterior columns, the second for the interior columns
3. Splices are located 6 feet above the floor centerline in stories where 2 column sections are given (below splice, above splice)

Table B.1 (continued) Beam and Column Sections, and Doubler Plate Thickness for Los Angeles Model Buildings

POST-NORTHRIDGE DESIGNS

NS Moment Resisting Frame — NS Gravity Frames

3-story Building

Story/Floor	COLUMNS		DOUBLER	GIRDER	COLUMNS		BEAMS
	Exterior	Interior	PLATES (in)		Below penthouse	Others	
1/2	W14X257	W14X311	0,0	W30X116	W14X82	W14X68	W16X26
2/3	W14X257	W14X311	0,0	W30X116	W14X82	W14X68	W16X26
3/Roof	W14X257	W14X311	0,0	W24X62	W14X82	W14X68	W14X22

9-story Building

Story/Floor	COLUMNS		DOUBLER	GIRDER	COLUMNS		BEAMS
	Exterior	Interior	PLATES (in)		Below penthouse	Others	
-1/1	W14X370	W14X500	0,0	W36X150	W14X211	W14X193	W18X35
1/2	W14X370	W14X500	0,0	W36X150	W14X211	W14X193	W16X26
2/3	W14X370, W14X370	W14X500, W14X455	0,0	W36X150	W14X211, W14X159	W14X193, W14X145	W16X26
3/4	W14X370	W14X455	0,0	W33X141	W14X159	W14X145	W16X26
4/5	W14X370, W14X283	W14X455, W14X370	0,0	W33X141	W14X159, W14X120	W14X145, W14X109	W16X26
5/6	W14X283	W14X370	0,0	W33X141	W14X120	W14X109	W16X26
6/7	W14X283, W14X257	W14X370, W14X283	0,1/2	W33X130	W14X120, W14X90	W14X109, W14X82	W16X26
7/8	W14X257	W14X283	0,0	W27X102	W14X90	W14X82	W16X26
8/9	W14X257, W14X233	W14X283, W14X257	0,1/2	W27X94	W14X90, W14X61	W14X82, W14X48	W16X26
9/Roof	W14X233	W14X257	0,0	W24X62	W14X61	W14X48	W14X22

Notes:
1. Column line A has exterior column sections oriented about strong axis,
   Column line F has exterior column sections oriented about weak axis
   Column lines B,C,D, and E have interior column sections

20-story Building

Story/Floor	COLUMNS		DOUBLER	GIRDER	COLUMNS	BEAMS	
	Exterior	Interior	PLATES (in)			40 feet span	20 feet span
-2/-1	15X15X2.00	W24X335	0,0	W14X22	W14X550	W18X40	W14X22
-1/1	15X15X2.00	W24X335	0,0	W30X99	W14X550	W24X55	W14X22
1/2	15X15X2.00	W24X335	0,0	W30X99	W14X550	W18X40	W14X22
2/3	15X15X2.00, 15X15X1.25	W24X335, W24X335	0,0	W30X99	W14X550, W14X455	W18X40	W14X22
3/4	15X15X1.25	W24X335	0,0	W30X99	W14X455	W18X40	W14X22
4/5	15X15X1.25	W24X335	0,0	W30X99	W14X455	W18X40	W14X22
5/6	15X15X1.25, 15X15X1.00	W24X335, W24X279	0,0	W30X108	W14X455, W14X370	W18X40	W14X22
6/7	15X15X1.00	W24X279	0,0	W30X108	W14X370	W18X40	W14X22
7/8	15X15X1.00	W24X279	0,0	W30X108	W14X370	W18X40	W14X22
8/9	15X15X1.00, 15X15X1.00	W24X279, W24X279	0,0	W30X108	W14X370, W14X311	W18X40	W14X22
9/10	15X15X1.00	W24X279	0,0	W30X108	W14X311	W18X40	W14X22
10/11	15X15X1.00	W24X279	0,0	W30X108	W14X311	W18X40	W14X22
11/12	15X15X1.00, 15X15X1.00	W24X279, W24X229	0,0	W30X99	W14X311, W14X257	W18X40	W14X22
12/13	15X15X1.00	W24X229	0,0	W30X99	W14X257	W18X40	W14X22
13/14	15X15X1.00	W24X229	0,0	W30X99	W14X257	W18X40	W14X22
14/15	15X15X1.00, 15X15X0.75	W24X229, W24X162	0,5/8	W30X99	W14X257, W14X176	W18X40	W14X22
15/16	15X15X0.75	W24X162	0,5/8	W30X99	W14X176	W18X40	W14X22
16/17	15X15X0.75	W24X162	0,5/8	W30X99	W14X176	W18X40	W14X22
17/18	15X15X0.75, 15X15X0.75	W24X162, W24X117	0,5/8	W27X84	W14X176, W14X108	W18X40	W14X22
18/19	15X15X0.75	W24X117	0,5/8	W27X84	W14X108	W18X40	W14X22
19/20	15X15X0.75, 15X15X0.50	W24X117, W24X94	0,1/2	W24X62	W14X108	W18X40	W14X22
20/Roof	15X15X0.50	W24X94	0,0	W21X50	W14X108, W14X43	W18X35	W12X14

Notes:
1. The basement floor (-1 level) has simple connections

Table B.2 Cover Plate Details for LA post-Northridge Model Buildings

TOP AND BOTTOM FLANGE COVER PLATE DETAILS

Girder Section		W21X44	W24X55	W24X62	W24X84	W24X94	W27X94
Top Plate	W1x T1	5" x 1/2"	5" x 3/4"	5" x 3/4"	7" x 3/4"	7" x 3/4"	8" x 3/4"
Bottom Plate	W2 x T2	8" x 1/2"	9" x 3/8"	9" x 1/2"	11" x 5/8"	12" x 5/8"	11" x 5/8"

Girder Section		W27X102	W30X108	W30X116	W33X130	W33X141	W36X150
Top Plate	W1x T1	8-1/2" x 3/4"	9" x 3/4"	9" x 3/4"	9" x 1"	9" x 1"	10" x 1"
Bottom Plate	W2 x T2	12" x 5/8"	12" x 5/8"	12" x 3/4"	13" x 3/4"	13" x 3/4"	14" x 3/4"

Table B.3 Beam and Column Sections, and Doubler Plate Thickness for Seattle Model Buildings

PRE-NORTHRIDGE DESIGNS

NS Moment Resisting Frame | NS Gravity Frames

3-story Building

Story/Floor	COLUMNS		DOUBLER PLATES (in)	GIRDER	COLUMNS		BEAMS
	Exterior	Interior			Below penthouse	Others	
1/2	W14X159	W14X176	0,1/4	W24X76	W10X77	↑	W16X26
2/3	W14X159	W14X176	0,9/16	W24X84	W10X77, W10X60	Same as below penthouse	W16X26
3/Roof	W14X159	W14X176	0,0	W18X40	W10X60	↓	W14X22

9-story Building

Story/Floor	COLUMNS		DOUBLER PLATES (in)	GIRDER	COLUMNS		BEAMS
	Exterior	Interior			Below penthouse	Others	
-1/1	W24X229	↑	0,0	W30X108	W14X159	↑	W16X31
1/2	W24X229		0,0	W30X108	W14X159		W16X26
2/3	W24X229, W24X229		0,1/4	W30X116	W14X159, W14X132		W16X26
3/4	W24X229		0,0	W30X108	W14X132		W16X26
4/5	W24X229, W24X207	Same as Exterior Columns	0,0	W27X94	W14X132, W14X109	Same as below penthouse	W16X26
5/6	W24X207		0,0	W27X94	W14X109		W16X26
6/7	W24X207, W24X162		0,1/4	W24X76	W14X109, W14X90		W16X26
7/8	W24X162		0,1/4	W24X76	W14X90		W16X26
8/9	W24X162, W24X131		0,1/4	W24X62	W14X90, W14X61		W16X26
9/Roof	W24X131	↓	0,1/4	W24X62	W14X61	↓	W14X22

Notes:
1. Column lines A though E have column sections oriented about strong axis,
   Column line F has column sections oriented about weak axis

20-story Building

Story/Floor	COLUMNS		DOUBLER PLATES (in)	GIRDER	COLUMNS	BEAMS	
	Exterior	Interior				40 feet span	20 feet span
-2/-1	W24X229	↑	0,0	W12X14	W14X426	W21X44	W12X14
-1/1	W24X229		0,1/4	W30X132	W14X426	W21X50	W12X16
1/2	W24X229, W24X229		0,1/4	W30X132	W14X426, W14X398	W21X44	W12X14
2/3	W24X229		0,1/4	W30X132	W14X398	W21X44	W12X14
3/4	W24X229, W24X229		0,1/4	W30X132	W14X398, W14X342	W21X44	W12X14
4/5	W24X229		0,1/4	W30X132	W14X342	W21X44	W12X14
5/6	W24X229, W24X192		0,1/2	W30X132	W14X342, W14X311	W21X44	W12X14
6/7	W24X192		0,1/2	W30X132	W14X311	W21X44	W12X14
7/8	W24X192, W24X192		0,1/2	W30X132	W14X311, W14X257	W21X44	W12X14
8/9	W24X192		0,1/4	W30X116	W14X257	W21X44	W12X14
9/10	W24X192, W24X192	Same as Exterior Columns	0,1/4	W30X116	W14X257, W14X233	W21X44	W12X14
10/11	W24X192		0,1/4	W27X114	W14X233	W21X44	W12X14
11/12	W24X192, W24X192		0,1/4	W27X114	W14X233, W14X193	W21X44	W12X14
12/13	W24X192		0,1/4	W27X94	W14X193	W21X44	W12X14
13/14	W24X192, W24X162		0,1/4	W27X94	W14X193, W14X159	W21X44	W12X14
14/15	W24X162		0,1/4	W27X94	W14X159	W21X44	W12X14
15/16	W24X162, W24X162		0,1/4	W27X94	W14X159, W14X120	W21X44	W12X14
16/17	W24X162		0,0	W24X62	W14X120	W21X44	W12X14
17/18	W24X162, W24X131		0,0	W24X62	W14X120, W14X90	W21X44	W12X14
18/19	W24X131		0,0	W21X57	W14X90	W21X44	W12X14
19/20	W24X131, W24X131		0,0	W21X57	W14X90, W14X61	W21X44	W12X14
20/Roof	W24X131	↓	0,0	W21X57	W14X61	W18X35	W12X14

Notes:
1. The basement floor (-1 level) has simple connections

General Notes
1. For doubler plate thickess, the first number signifies the value for the exterior columns, the second for the interior columns
2. Splices are located 6 feet above the floor centerline in stories where 2 column sections are given (below splice, above splice)

Table B.3 (continued) Beam and Column Sections, and Doubler Plate Thickness for Seattle Model Buildings

POST-NORTHRIDGE DESIGNS

NS Moment Resisting Frame

NS Gravity Frames

3-story Building

Story/Floor	COLUMNS		DOUBLER PLATES (in)	GIRDER	COLUMNS		BEAMS
	Exterior	Interior			Below penthouse	Others	
1/2	W14X342	W14X398	0,3/8	W33X141	W10X77	↑	W16X26
2/3	W14X342, W14X159	W14X398, W14X159	0,5/8	W21X62	W10X77, W10X60	Same as below penthouse	W16X26
3/Roof	W14X159	W14X159	0,7/8	W21X62	W10X60	↓	W14X22

9-story Building

Story/Floor	COLUMNS		DOUBLER PLATES (in)	GIRDER	COLUMNS		BEAMS
	Exterior	Interior			Below penthouse	Others	
-1/1	W24X229	↑	0,7/16	W27X114	W14X159	↑	W16X31
1/2	W24X229		0,7/16	W27X114	W14X159		W16X26
2/3	W24X229, W24X229		0,7/16	W27X114	W14X159, W14X132		W16X26
3/4	W24X229		0,3/8	W27X94	W14X132		W16X26
4/5	W24X229, W24X207	Same as Exterior Columns	0,3/8	W27X94	W14X132, W14X109	Same as below penthouse	W16X26
5/6	W24X207		0,3/8	W27X94	W14X109		W16X26
6/7	W24X207, W24X162		0,3/8	W24X76	W14X109, W14X90		W16X26
7/8	W24X162		0,3/8	W21X62	W14X90		W16X26
8/9	W24X162, W24X131		0,3/8	W21X62	W14X90, W14X61		W16X26
9/Roof	W24X131	↓	0,7/16	W21X62	W14X61	↓	W14X22

Notes:

1. Column lines A though E have column sections oriented about strong axis, Column line F has column sections oriented about weak axis

20-story Building

Story/Floor	COLUMNS		DOUBLER PLATES (in)	GIRDER	COLUMNS	BEAMS	
	Exterior	Interior				40 feet span	20 feet span
-2/-1	W24X306	↑	0,0	W12X14	W14X426	W21X44	W12X14
-1/1	W24X306		0,3/8	W27X129	W14X426	W21X50	W12X16
1/2	W24X306, W24X306		0,3/8	W27X129	W14X426, W14X398	W21X44	W12X14
2/3	W24X306		0,3/8	W27X129	W14X398	W21X44	W12X14
3/4	W24X306, W24X306		0,3/8	W27X129	W14X398, W14X342	W21X44	W12X14
4/5	W24X306		0,3/8	W27X129	W14X342	W21X44	W12X14
5/6	W24X306, W24X279		0,3/8	W27X129	W14X342, W14X311	W21X44	W12X14
6/7	W24X279		0,3/8	W27X129	W14X311	W21X44	W12X14
7/8	W24X279, W24X279		0,3/8	W27X129	W14X311, W14X257	W21X44	W12X14
8/9	W24X279		0,3/8	W27X129	W14X257	W21X44	W12X14
9/10	W24X279, W24X279	Same as Exterior Columns	0,3/8	W24X103	W14X257, W14X233	W21X44	W12X14
10/11	W24X279		0,3/8	W24X103	W14X233	W21X44	W12X14
11/12	W24X279, W24X229		0,3/8	W24X103	W14X233, W14X193	W21X44	W12X14
12/13	W24X229		0,3/8	W24X103	W14X193	W21X44	W12X14
13/14	W24X229, W24X192		0,3/8	W24X84	W14X193, W14X159	W21X44	W12X14
14/15	W24X192		0,3/8	W24X84	W14X159	W21X44	W12X14
15/16	W24X192, W24X162		0,1/2	W24X84	W14X159, W14X120	W21X44	W12X14
16/17	W24X162		0,3/8	W21X62	W14X120	W21X44	W12X14
17/18	W24X162, W24X131		0,3/8	W21X62	W14X120, W14X90	W21X44	W12X14
18/19	W24X131		0,3/8	W21X62	W14X90	W21X44	W12X14
19/20	W24X131, W24X131		0,3/8	W21X62	W14X90, W14X61	W21X44	W12X14
20/Roof	W24X131	↓	0,7/16	W21X62	W14X61	W18X35	W12X14

Notes:

1. The basement floor (-1 level) has simple connections

Table B.3 (continued) Beam and Column Sections, and Doubler Plate Thickness for Seattle Model Buildings

REDUCED BEAM SECTION - POST-NORTHRIDGE DESIGN

NS Moment Resisting Frame

NS Gravity Frames

9-story Building

Story/Floor	COLUMNS		DOUBLER PLATES (in)	GIRDER
	Exterior	Interior		
-1/1	W24X176	W24X229	0,1/4	W30X108
1/2	W24X176	W24X229	0,1/4	W30X116
2/3	W24X176, W24X176	W24X229, W24X229	0,1/4	W30X116
3/4	W24X176	W24X229	0,0	W30X108
4/5	W24X176, W24X176	W24X229, W24X207	0,0	W27X94
5/6	W24X176	W24X207	0,0	W27X94
6/7	W24X176, W24X131	W24X207, W24X162	0,1/4	W24X84
7/8	W24X131	W24X162	0,0	W24X76
8/9	W24X131, W24X94	W24X162, W24X131	0,0	W24X55
9/Roof	W24X94	W24X131	0,0	W21X44

COLUMNS		BEAMS
Below penthouse	Others	
W14X159	↑	W16X31
W14X159		W16X26
W14X159, W14X132		W16X26
W14X132		W16X26
W14X132, W14X109	Same as below penthouse	W16X26
W14X109		W16X26
W14X109, W14X90		W16X26
W14X90		W16X26
W14X90, W14X61		W16X26
W14X61	↓	W14X22

Notes:

1. Column lines A though E have exterior column sections oriented about strong axis,
   Column line F has exterior column sections oriented about weak axis
   Column lines B,C, and D have interior column sections

Table B.4 Cover Plate Details for Seattle post-Northridge Model Buildings

TOP AND BOTTOM FLANGE COVER PLATE DETAILS

Girder Section		W21X62	W24X76	W24X84	W24X103
Top Plate	L x W1x T1	11 x 8-1/4 x 3/4	12 x 9 x 3/4	12 x 9 x 7/8	12 x 9 x 1-1/8
Bottom Plate	L x W2 x T2	11 x 10-1/4 x 5/8	12 x 11 x 5/8	12 x 11 x 3/4	12 x 11 x 1

Girder Section		W27X94	W27X129	W33X141	
Top Plate	L x W1x T1	14 x 10 x 7/8	14 x 10 x 1-1/4	17 x 11-1/2 x 1-1/8	
Bottom Plate	L x W2 x T2	14 x 12 x 3/4	14 x 12 x 1-1/8	17 x 13-1/2 x 1	

Table B.5 Cover Plate Details for Seattle post-Northridge RBS Model Building

TOP AND BOTTOM FLANGE COVER PLATE DETAILS (RBS DESIGN)

Girder Section		W21X44	W24X55	W24X76	W24X84
Top Plate	L x W1x T1	10 x 6-1/2 x 3/8	11 x 7 x 3/8	11 x 9 x 5/16	11 x 9 x 3/8
Bottom Plate	L x W2 x T2	10 x 8-1/2 x 1/4	11 x 9 x 5/16	11 x 11 x 1/4	11 x 11 x 5/16

Girder Section		W27X94	W30X108	W30X116	
Top Plate	L x W1x T1	13 x 10 x 3/8	14 x 10-1/2 x 7/16	14 x 10-1/2 x 7/16	
Bottom Plate	L x W2 x T2	13 x 12 x 5/16	14 x 12-1/2 x 3/8	14 x 12-1/2 x 3/8	

Table B.6 Reduced Beam Section Details for Seattle post-Northridge RBS Model Building

REDUCED BEAM SECTION GEOMETRY

Girder Section	W21X44	W24X55	W24X76	W24X84
L x L(RBS) x W(RBS)	18-1/2 x 15-1/2 x 3-1/4	21 x 18 x 3-1/2	21 x 18 x 4-/2	21 x 18 x 5

Girder Section	W27X94	W30X108	W30X116	
L x L(RBS) x W(RBS)	24 x 20-1/4 x 5	26-1/2 x 22-1/2 x 5-1/4	26-1/2 x 22-1/2 x 5-1/4	

Table B.7 Beam and Column Sections, and Doubler Plate Thickness for Boston Model Buildings

PRE-NORTHRIDGE DESIGNS

NS Moment Resisting Frame

NS Gravity Frames

3-story Building

Story/Floor	COLUMNS		DOUBLER PLATES (in)	GIRDER	COLUMNS		BEAMS
	Exterior	Interior			Below penthouse	Others	
1/2	W14X74	W14X99	0,0	W18X35	4-W12X65 & 2-W12X72	W12X58	W16X26
2/3	W14X74	W14X99	0,0	W21X57	4-W12X65 & 2-W12X72	W12X58	W16X26
3/Roof	W14X74	W14X99	0,0	W21X62	4-W12X65 & 2-W12X72	W12X58	W14X22

9-story Building

Story/Floor	COLUMNS		DOUBLER PLATES (in)	GIRDER	COLUMNS		BEAMS
	Exterior	Interior			Below penthouse	Others	
-1/1	W14X211	W14X283	0,0	W24X68	4-W14X145 & 2-W14X159	W14X145	W16X26
1/2	W14X211	W14X283	0,0	W36X135	4-W14X145 & 2-W14X159	W14X145	W16X26
2/3	W14X211, W14X159	W14X283, W14X233	0,0	W33X118	see note 3	W14X145, W12X120	W16X26
3/4	W14X159	W14X233	0,0	W30X116	4-W14X120 & 2-W14X132	W12X120	W16X26
4/5	W14X159, W14X132	W14X233, W14X211	0,0	W30X116	see note 4	W12X120, W14X90	W16X26
5/6	W14X132	W14X211	0,0	W30X108	4-W14X99 & 2-W12X106	W14X90	W16X26
6/7	W14X132, W14X99	W14X211, W14X176	0,0	W30X99	see note 5	W14X90, W12X65	W16X26
7/8	W14X99	W14X176	0,0	W27X94	6-W12X79	W12X65	W16X26
8/9	W14X99, W14X61	W14X176, W14X120	0,0	W24X76	see note 6	W12X65, W8X48	W16X26
9/Roof	W14X61	W14X120	0,0	W18X40	4-W12X53 & 2-W12X58	W8X48	W14X22

Notes:

1. Column line A has exterior column sections oriented about strong axis,
   Column line F has exterior column sections oriented about weak axis; W14X61 changes to W14X68
   Column lines B,C,D, and E have interior column sections
2. For the bay with only 1 MR connection the girder sections are (from Floor 1 to Roof) the following:
   W24X68, W27X94, W27X84, W27X84, W24X76, W24X76, W24X68, W24X62, W24X55, and W18X40
3. 4-W14X145 change at splice to 4-W14X120, 2-W14X159 change at splice to 2-W14X132
4. 4-W14X120 change at splice to 4-W14X99, 2-W14X132 change at splice to 2-W12X106
5. 4-W14X99 change at splice to 4-W12X79, 2-W12X106 change at splice to 2-W12X79
6. 4-W12X79 change at splice to 4-12X53, 2-W12X79 change at splice to 2-W12X58

20-story Building

Story/Floor	COLUMNS			DOUBLER PLATES (in)	GIRDER	COLUMNS	BEAMS	
	Exterior	Next to Exterior	Interior				40 feet span	20 feet span
-2/-1	W14X370	W36X194	W36X260	0,0	W12X14	4-W14X311 & 2-W14X211	W18X40	W12X16
-1/1	W14X370	W36X194	W36X260	0,0	W27X94	4-W14X311 & 2-W14X211	W18X40	W12X19
1/2	W14X370, W14X370	W36X194, W36X194	W36X260, W36X260	0,0	W36X182	4-W14X311 & 2-W14X211 (splice in story)	W18X40	W12X19
2/3	W14X370	W36X194	W36X260	0,0	W36X160	4-W14X311 & 2-W14X211	W18X40	W12X19
3/4	W14X370, W14X311	W36X194, W36X182	W36X260, W33X221	0,0	W36X160	4-W14X311 to 4-W14X257 & 2-W14X211 to 2-W14X176	W18X40	W12X19
4/5	W14X311	W36X182	W33X221	0,0	W36X150	4-W14X257 & 2-W14X176	W18X40	W12X19
5/6	W14X311, W14X283	W36X182, W36X170	W33X221, W33X201	0,0	W36X150	4-W14X257 to 4-W14X233 & 2-W14X176 to 2-W14X159	W18X40	W12X19
6/7	W14X283	W36X170	W33X201	0,0	W36X150	4-W14X233 & 2-W14X159	W18X40	W12X19
7/8	W14X283, W14X233	W36X170, W36X160	W33X201, W33X201	0,0	W36X135	4-W14X233 to 4-W14X211 & 2-W14X159 to 2-W14X145	W18X40	W12X19
8/9	W14X233	W36X160	W33X201	0,0	W36X135	4-W14X211 & 2-W14X145	W18X40	W12X19
9/10	W14X233, W14X193	W36X160, W36X150	W33X201, W30X173	0,0	W33X130	4-W14X211 to 4-W14X176 & 2-W14X145 to 2-W14X120	W18X40	W12X19
10/11	W14X193	W36X150	W30X173	0,0	W33X130	4-W14X176 & 2-W14X120	W18X40	W12X19
11/12	W14X193, W14X159	W36X150, W36X135	W30X173, W30X173	0,0	W33X130	4-W14X176 to 4-W14X145 & 2-W14X120 to 2-W14X109	W18X40	W12X19
12/13	W14X159	W36X135	W30X173	0,0	W33X118	4-W14X145 & 2-W14X109	W18X40	W12X19
13/14	W14X159, W14X132	W36X135, W30X116	W30X173, W27X161	0,0	W33X118	4-W14X145 to 4-W14X120 & 2-W14X109 to 2-W14X90	W18X40	W12X19
14/15	W14X132	W30X116	W27X161	0,0	W30X116	4-W14X120 & 2-W14X90	W18X40	W12X19
15/16	W14X132, W14X109	W30X116, W30X99	W27X161, W27X146	0,0	W30X108	4-W14X120 to 4-W12X96 & 2-W14X90 to 2-W12X72	W18X40	W12X19
16/17	W14X109	W30X99	W27X146	0,0	W30X99	4-W12X96 & 2-W12X72	W18X40	W12X19
17/18	W14X109, W14X82	W30X99, W27X84	W27X146, W24X131	0,0	W27X94	4-W12X96 to 4-W12X72 & 2-W12X72 to 2-W10X60	W18X40	W12X19
18/19	W14X82	W27X84	W24X131	0,0	W27X84	4-W12X72 & 2-W10X60	W18X40	W12X19
19/20	W14X82, W14X61	W27X84, W24X68	W24X131, W24X68	0,0	W24X68	4-W12X72 to 4-W10X49 & 2-W10X60 to 2-W8X48	W18X40	W12X19
20/Roof	W14X61	W24X68	W24X68	0,0	W18X35	4-W10X49 & 2-W8X48	W18X40	W14X22

Notes:

1. The basement floor (-1 level) has simple connections

General Notes

1. There are a total of 6 column lines below the penthouse for the 3- and 9-story buildings
2. For doubler plate thickess, the first number signifies the value for the exterior columns, the second for the interior columns
3. Splices are located 6 feet above the floor centerline in stories where 2 column sections are given (below splice, above splice)
4. 4-W14X99, 2-W12X106 signfies four columns of W14X99 and 2 columns of W12X106 below the penthouse

Table B.7 (continued) Beam and Column Sections, and Doubler Plate Thickness for Boston Model Buildings

POST-NORTHRIDGE DESIGNS

NS Moment Resisting Frame

NS Gravity Frames

3-story Building

Story/Floor	COLUMNS		DOUBLER	GIRDER	COLUMNS		BEAMS
	Exterior	Interior	PLATES (in)		Below penthouse	Others	
1/2	W14X82	W14X145	3/8, 2 x 1/2	W21X62	4-W12X65 & 2-W12X72	W12X58	W16X26
2/3	W14X82	W14X145	3/8, 2 x 1/2	W21X62	4-W12X65 & 2-W12X72	W12X58	W16X26
3/Roof	W14X82	W14X145	3/8,3/8	W14X48	4-W12X65 & 2-W12X72	W12X58	W14X22

9-story Building

Story/Floor	COLUMNS		DOUBLER	GIRDER	COLUMNS		BEAMS
	Exterior	Interior	PLATES (in)		Below penthouse	Others	
-1/1	W14X283	W14X500	0,0	W12X53	4-W14X145 & 2-W14X159	W14X145	W16X26
1/2	W14X283	W14X500	3/8,0	W33X141	4-W14X145 & 2-W14X159	W14X145	W16X26
2/3	W14X283, W14X257	W14X500, W14X455	3/8,3/8	W33X141	see note 3	W14X145, W12X120	W16X26
3/4	W14X257	W14X455	0,0	W21X101	4-W14X120 & 2-W14X132	W12X120	W16X26
4/5	W14X257, W14X211	W14X455, W14X398	3/8,0	W21X101	see note 4	W12X120, W14X90	W16X26
5/6	W14X211	W14X398	3/8,0	W21X101	4-W14X99 & 2-W12X106	W14X90	W16X26
6/7	W14X211, W14X159	W14X398, W14X311	1/2,7/16	W21X101	see note 5	W14X90, W12X65	W16X26
7/8	W14X159	W14X311	7/16,3/8	W18X97	6-W12X79	W12X65	W16X26
8/9	W14X159, W14X109	W14X311, W14X193	3/8,9/16	W16X67	see note 6	W12X65, W8X48	W16X26
9/Roof	W14X109	W14X193	3/8,3/8	W12X53	4-W12X53 & 2-W12X58	W8X48	W14X22

Notes:

1. Column line A has exterior column sections oriented about strong axis,
   Column line F has exterior column sections oriented about weak axis
   Column lines B,C,D, and E have interior column sections
2. For the bay with only 1 MR connection the girder sections are (from Floor 1 to Roof) the following:
   W12X53, W16X67, W16X67, W16X67, W16X67, W14X61, W12X58, W12X58, W12X53, W12X53
3. 4-W14X145 change at splice to 4-W14X120, 2-W14X159 change at splice to 2-W14X132
4. 4-W14X120 change at splice to 4-W14X99, 2-W14X132 change at splice to 2-W12X106
5. 4-W14X99 change at splice to 4-W12X79, 2-W12X106 change at splice to 2-W12X79
6. 4-W12X79 change at splice to 4-12X53, 2-W12X79 change at splice to 2-W12X58

20-story Building

Story/Floor	COLUMNS			DOUBLER	GIRDER	COLUMNS	BEAMS	
	Exterior	Next to Exterior	Interior	PLATES (in)			40 feet span	20 feet span
-2/-1	W14X455	W36X393	W36X485	0,0,0	W12X14	4-W14X311 & 2-W14X211	W18X40	W12X16
-1/1	W14X455	W36X393	W36X485	0,0,0	W16X67	4-W14X311 & 2-W14X211	W18X40	W12X19
1/2	W14X455, W14X455	W36X393, W36X393	W36X485, W36X485	0,3/8,0	W33X141	4-W14X311 & 2-W14X211 (splice in story)	W18X40	W12X19
2/3	W14X455	W36X393	W36X485	0,3/8,0	W33X141	4-W14X311 & 2-W14X211	W18X40	W12X19
3/4	W14X455, W14X370	W36X393, W36X328	W36X485, W36X393	0,7/16,3/8	W33X141	4-W14X311 to 4-W14X257 & 2-W14X211 to 2-W14X176	W18X40	W12X19
4/5	W14X370	W36X328	W36X393	0,7/16,3/8	W33X141	4-W14X257 & 2-W14X176	W18X40	W12X19
5/6	W14X370, W14X342	W36X328, W36X300	W36X393, W36X359	0,5/8,3/8	W33X141	4-W14X257 to 4-W14X233 & 2-W14X176 to 2-W14X159	W18X40	W12X19
6/7	W14X342	W36X300	W36X359	0,1/2,3/8	W24X131	4-W14X233 & 2-W14X159	W18X40	W12X19
7/8	W14X342, W14X342	W36X300, W36X300	W36X359, W36X359	0,1/2,3/8	W24X131	4-W14X233 to 4-W14X211 & 2-W14X159 to 2-W14X145	W18X40	W12X19
8/9	W14X342	W36X300	W36X359	0,1/2,3/8	W24X131	4-W14X211 & 2-W14X145	W18X40	W12X19
9/10	W14X342, W14X311	W36X300, W36X260	W36X359, W36X300	0,11/16,1/2	W24X131	4-W14X211 to 4-W14X176 & 2-W14X145 to 2-W14X120	W18X40	W12X19
10/11	W14X311	W36X260	W36X300	0,11/16,1/2	W24X131	4-W14X176 & 2-W14X120	W18X40	W12X19
11/12	W14X311, W14X283	W36X260, W36X260	W36X300, W36X300	3/8,11/16,1/2	W24X131	4-W14X176 to 4-W14X145 & 2-W14X120 to 2-W14X109	W18X40	W12X19
12/13	W14X283	W36X260	W36X300	0,1/2,3/8	W24X117	4-W14X145 & 2-W14X109	W18X40	W12X19
13/14	W14X283, W14X283	W36X260, W36X260	W36X300, W36X280	0,1/2,7/16	W24X117	4-W14X145 to 4-W14X120 & 2-W14X109 to 2-W14X90	W18X40	W12X19
14/15	W14X283	W36X260	W36X280	0,3/8,3/8	W24X104	4-W14X120 & 2-W14X90	W18X40	W12X19
15/16	W14X283, W14X193	W36X260, W36X182	W36X280, W36X210	3/8,9/16,7/16	W24X104	4-W14X120 to 4-W12X96 & 2-W14X90 to 2-W12X72	W18X40	W12X19
16/17	W14X193	W36X182	W36X210	3/8,9/16,7/16	W24X104	4-W12X96 & 2-W12X72	W18X40	W12X19
17/18	W14X193, W14X159	W36X182, W36X150	W36X210, W36X150	9/16,11/16,11/16	W21X101	4-W12X96 to 4-W12X72 & 2-W12X72 to 2-W10X60	W18X40	W12X19
18/19	W14X159	W36X150	W36X150	3/8,1/2,1/2	W18X86	4-W12X72 & 2-W10X60	W18X40	W12X19
19/20	W14X159, W14X109	W36X150, W24X117	W36X150, W24X131	9/16,7/16, 2 x 3/8	W18X76	4-W12X72 to 4-W10X49 & 2-W10X60 to 2-W8X48	W18X40	W12X19
20/Roof	W14X109	W24X117	W24X131	3/8,3/8,3/8	W12X53	4-W10X49 & 2-W8X48	W18X40	W14X22

Notes:

1. The basement floor (-1 level) has simple connections

General Notes

1. There are a total of 6 column lines below the penthouse for the 3- and 9-story buildings
2. For doubler plate thickess, the first number signifies the value for the exterior columns, the second for the interior columns
3. Splices are located 6 feet above the floor centerline in stories where 2 column sections are given (below splice, above splice)
4. 4-W14X99, 2-W12X106 signfies four columns of W14X99 and 2 columns of W12X106 below the penthouse

Table B.8 Cover Plate Details for Boston post-Northridge Model Buildings

TOP AND BOTTOM FLANGE COVER PLATE DETAILS

3-story Building

Girder Section		W21X62	W14X48	
Top Plate	T x W1 x W2 x L	3/4 x 7-3/4 x 2-1/2 x 15	5/8 x 6-7/8 x 6-7/8 x 13	
Bottom Plate	T x W x L	5/8 x 9-1/2 x 15	1/2 x 9 x 13	

9-story Building

Girder Section		W33X141	W21X101	W18X97
Top Plate	T x W1 x W2 x L	1 x 11-1/2 x 5-1/2 x 20	13/16 x 12 x 6 x 14	7/8 x 11 x 5 x 12
Bottom Plate	T x W x L	1 x 13-1/2 x 20	11/16 x 14 x 14	3/4 x 13 x 12

Girder Section		W16X67	W12X58	W12X53
Top Plate	T x W1 x W2 x L	11/16 x 10 x 4 x 11	11/16 x 9-1/2 x 3-1/2 x 9	11/16 x 9-1/2 x 3-1/3 x 9
Bottom Plate	T x W x L	9/16 x 11-1/2 x 11	9/16 x 11-1/2 x 9	9/16 x 11-1/2 x 9

20-story Building

Girder Section		W33X141	W24X131	W24X117
Top Plate	T x W1 x W2 x L	1-3/16 x 11-1/2 x 5-1/2 x 20	1-1/16 x 12-1/2 x 6-1/2 x 15	1 x 12-1/2 x 6-1/2 x 15
Bottom Plate	T x W x L	1-3/16 x 13-1/2 x 20	15/16 x 15 x 15	13/16 x 15 x 15

Girder Section		W24X104	W21X101	W18X86
Top Plate	T x W1 x W2 x L	7/8 x 12-1/2 x 6-1/2 x 15	7/8 x 12 x 6 x 14	7/8 x 11 x 5 x 12
Bottom Plate	T x W x L	3/4 x 14-1/2 x 15	3/4 x 14 x 14	3/4 x 13 x 12

Girder Section		W18X76	W16X67	W12X53
Top Plate	T x W1 x W2 x L	3/4 x 11 x 5 x 12	3/4 x 10 x 4 x 11	3/4 x 9-1/2 x 3-1/2 x 9
Bottom Plate	T x W x L	5/8 x 12-1/2 x 12	5/8 x 12 x 11	9/16 x 11-1/2 x 9

Table B.9 Beam and Column Sections for Redesigned LA 9-story pre-Northridge Buildings

REDESIGNED LA 9-STORY DESIGNS

R1-LA9, original configuration, 9 MR connections/frame/floor

Story/Floor	COLUMNS		GIRDER
	Exterior	Interior	
-1/1	W14X283	W14X311	W36X210
1/2	W14X283	W14X311	W36X210
2/3	W14X283, W14X211	W14X311, W14X233	W36X210
3/4	W14X211	W14X233	W36X150
4/5	W14X211, W14X193	W14X233, W14X193	W36X150
5/6	W14X193	W14X193	W36X135
6/7	W14X193, W14X145	W14X193, WW14X145	W36X135
7/8	W14X145	W14X145	W33X118
8/9	W14X145, W14X90	W14X145, W14X90	W33X118
9/Roof	W14X90	W14X90	W24X68

R2-LA9, 15 feet bay width, 18 MR connections/frame/floor

Story/Floor	COLUMNS		GIRDER
	Exterior	Interior	
-1/1	W14X233	▲	W33X118
1/2	W14X233		W33X118
2/3	W14X233, W14X145		W30X99
3/4	W14X145		W27X94
4/5	W14X145, W14X132	Same as Exterior Columns	W27X102
5/6	W14X132		W24X84
6/7	W14X132, W14X109		W27X84
7/8	W14X109		W24X62
8/9	W14X109, W14X74		W24X62
9/Roof	W14X74	▼	W18X35

R3-LA9, original configuration, 6 MR connections/frame/floor

Story/Floor	COLUMNS		GIRDER
	Exterior	Interior	
-1/1	W14X342	W14X426	W36X256
1/2	W14X342	W14X426	W36X256
2/3	W14X342, W14X283	W14X426, W14X283	W36X210
3/4	W14X283	W14X283	W36X210
4/5	W14X283, W14X233	W14X283, W14X257	W36X182
5/6	W14X233	W14X257	W36X182
6/7	W14X233, W14X193	W14X257, W14X211	W33X141
7/8	W14X193	W14X211	W33X130
8/9	W14X193, W14X159	W14X211, W14X159	W30X116
9/Roof	W14X159	W14X159	W24X94

General Notes

1. No doubler plates were required;
   Designs are fully code (UBC 1994) compliant
2. Splices are located 6 feet above the floor centerline in stories where 2 column sections are given (below splice, above splice)

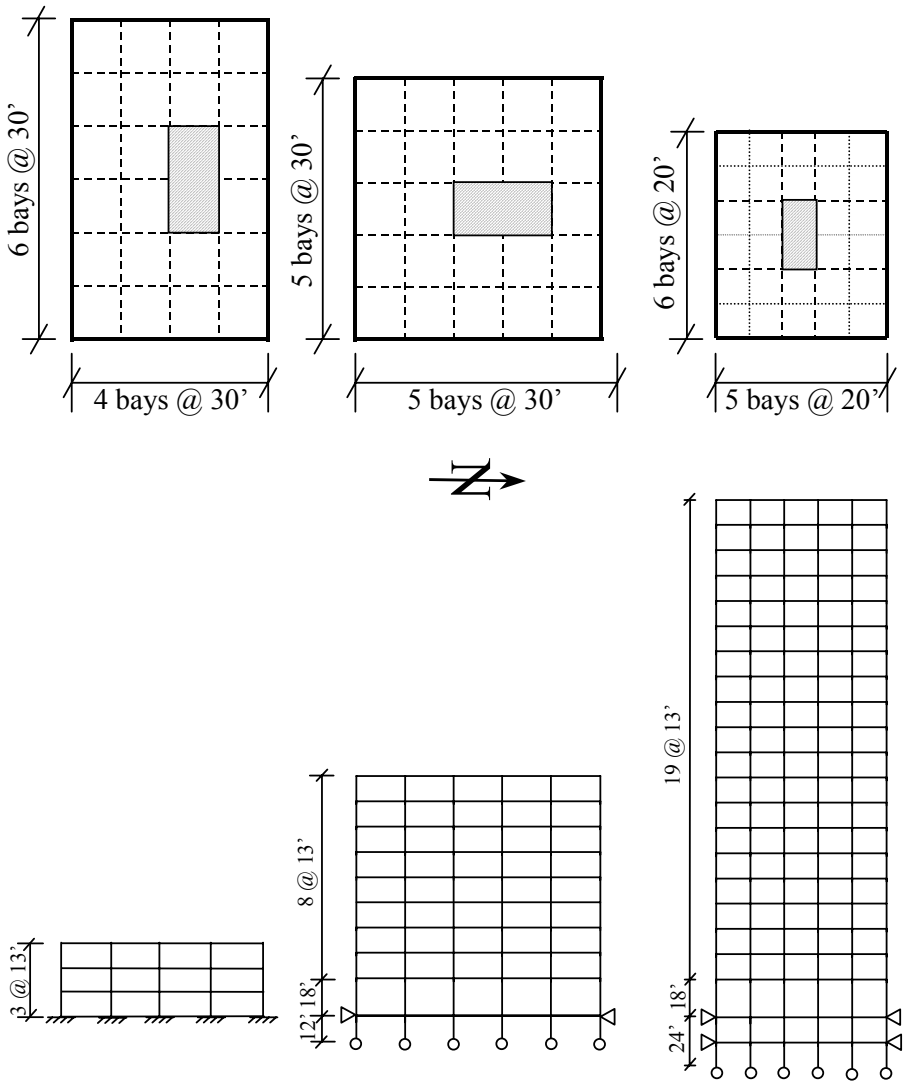

Figure B.1 Floor Plans and Elevations for Model Buildings

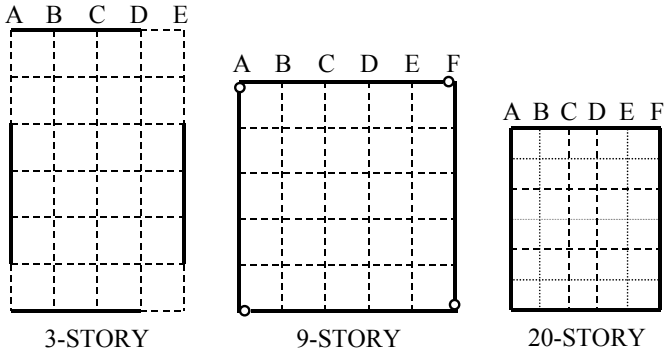

Figure B.2 Floor Plans Showing Layout of Moment Resisting Frames for LA Model Buildings

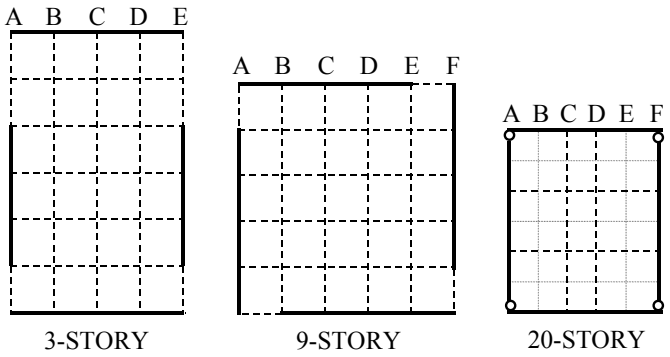

Figure B.3 Floor Plans Showing Layout of Moment Resisting Frames for Seattle Model Buildings

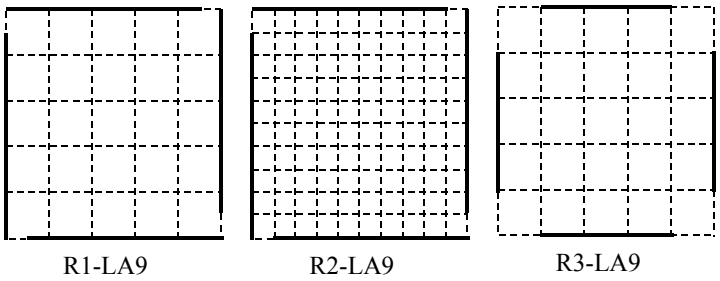

Note:
R1-LA9: 30 feet bay width
R2-LA9: 15 feet bay width, gravity frame design unchanged from R1-LA9
R3-LA9: 30 feet bay width

Figure B.4 Floor Plans Showing Layout of Moment Resisting Frames for Redesigned LA 9-story Buildings

REFERENCES

ATC-3 (1978). "Tentative provisions for the development of seismic regulations for buildings," *Applied Technology Council, NBS Special Publication 510*

ATC-40 (1996). "Methodology for seismic evaluation and upgrade of concrete structures," *Applied Technology Council*

Allahabadi, R., and Powell, G. H. (1988). "DRAIN-2DX user guide," *Report No. UCB/EERC-88/06*, Earthquake Engineering Research Center (EERC), University of California at Berkeley.

Astaneh, A. (1989). "Demand and supply of ductility in steel shear connections," *Journal of Construct. Steel Research*, Vol. 14

Astaneh, A., McMullin, K. M., and Call, S. M. (1993). "Behavior and design of steel single plate shear connections," *Journal of Structural Engineering*, Vol. 119, No. 8

Bernal, D. (1987). "Amplification factors for inelastic dynamic p-Δ effects in earthquake analysis," *Earthquake Engineering and Structural Dynamics.*, Vol. 15, pp. 635-651.

Bertero R. D., and Bertero, V. V. (1992). "Tall reinforced concrete buildings: conceptual earthquake resistant design methodology," *Report No. UCB/EERC-92/16*, Earthquake Engineering Research Center (EERC), University of California at Berkeley.

Bertero, V. V., Anderson, J. C., Krawinkler, H., and Miranda, E. (1991). "Design guidelines for ductility and drift limits," *Report No. UCB/EERC-91/15*, Earthquake Engineering Research Center (EERC), University of California at Berkeley.

Bertero, V. V., Anderson, J. C., and Krawinkler, H. (1994). "Performance of steel buildings structures during the Northridge earthquake," *Report No. UCB/EERC-94/09*, Earthquake Engineering Research Center (EERC), University of California at Berkeley.

Bertero, V. V., and Uang, C. M. (1992). "Issues and future directions in the use of an energy approach for seismic-resistant design of structures," *Nonlinear Seismic Analysis and Design of Reinforced Concrete Buildings*, Edited by P. Fajfar and H. Krawinkler, Elsevier Applied Science, London and New York.

Bertero, V. V. (1997). "Performance-based seismic engineering: A critical review of proposed guidelines," *Seismic Design Methodologies for the Next Generation of Codes*, Edited by P. Fajfar and H. Krawinkler, A. A. Balkema, Rotterdam

Blackman, B., and Popov, E. P. (1995). "Studies in steel moment resisting beam-to-column connections for seismic-resistant design," *Report No. UCB/EERC-95/11*, Earthquake Engineering Research Center (EERC), University of California at Berkeley.

BOCA (1993). "National Building Code," *12th Edition. Building Officials & Code Administrators International, Inc.*

Bondy, D. K. (1996). "A more rational approach to capacity design of seismic moment frame columns," *Earthquake Spectra*, Vol. 12, No. 3.

Bruneau, M., Mahin, S. A., and Popov, E. P. (1987). "Ultimate behavior of butt welded splices in heavy rolled steel sections," *Report No. UCB/EERC-87/10*, Earthquake Engineering Research Center (EERC), University of California at Berkeley.

Cai, C. S., Liu, X. L., and Chen, W.F. (1991). "Further verification of beam-column strength equations," *Journal of Struct. Engrg.*, ASCE, Vol. 117, No. 2.

Carr, A. J. (1996). "RUAOMOKO, user guide," *University of Canterbury, New Zealand*.

Chen, P. F., and Powell, G. H. (1982). "Generalized plastic hinge concepts for 3D beam-column elements," *Report No. UCB/EERC-82/20*, Earthquake Engineering Research Center (EERC), University of California at Berkeley.

Chen, W. F., and Atsuta, T. (1976). *"Theory of beam-columns,"* Vols. 1 and 2, McGraw-Hill, New York.

Chopra, A. K. (1995). *"Dynamics of Structures: Theory and Applications to Earthquake Engineering,"* Prentice Hall, New Jersey

Chung, Y. S. et al. (1988). "A new damage model for reinforced concrete structures," *Proc. of 9th World Conf. On Earthquake Engineering*, Vol. V, Tokyo, Japan

Collins, K. R. (1995) "A reliability-based dual level seismic design procedure for building structures," *Earthquake Spectra*, Vol. 11, No. 3.

Collins, K. R., Wen, Y. K., and Foutch, D. A. (1996). "An alternative seismic design procedure for standard buildings," *Proc. Eleventh World Conference on Earthquake Engineering*, Acapulco, Mexico.

Cornell, C. A. (1996a). "Calculating building seismic performance reliability; A basis for multi-level design norms," *Proc. Eleventh World Conference on Earthquake Engineering*, Acapulco, Mexico.

Cornell, C. A. (1996b). "Reliability-based earthquake-resistant design; the future," *Proc. Eleventh World Conference on Earthquake Engineering*, Acapulco, Mexico.

Cornell, C. A., and Luco, N. (1999). "Effect of connection fractures on the safety and reliability of steel moment-resisting frames," *part of FEMA phase II SAC project*, NISEE - University of California at Berkeley.

Deierlein, G. G., and Yhao D. (1992). "Static and dynamic analysis of steel frames with nonlinear connections and joint effects," *Proceedings of Structures Congress 1992*, ASCE.

Duan, L., and Chen, W.F. (1989). "Design interaction equations for steel beam-columns," *Journal of Struct. Engrg.*, ASCE, Vol. 115, No. 5.

Elwood, K. J., and Wen, Y. K. (1996). "Evaluation of a dual-level design approach for the earthquake resistant design of buildings," *Proc. Eleventh World Conference on Earthquake Engineering*, Acapulco, Mexico.

Fajfar, P., and Fischinger, M. (1988). "N2 - a method for non-linear seismic analysis of regular structures," *Proceedings of the 9th World Conference on Earthquake Engineering*, Vol. 5, Tokyo, Japan

Fajfar, P., and Krawinkler, H. (1992). *"Nonlinear Seismic Analysis and Design of Reinforced Concrete Buildings,"* Elsevier Applied Science, London and New York.

Fajfar, P. Editor (1996). "Towards a new seismic design methodology for buildings," *Research at the University of Ljubljana*, Univerza v Ljubljani (publisher)

FEMA 222A (1995). "*1994 Edition: NEHRP recommended provisions for seismic regulations for new buildings*," Federal Emergency Management Agency.

FEMA 223A (1995). "*1994 Edition: NEHRP recommended provisions for seismic regulations for new buildings, Part 2 - Commentary*," Federal Emergency Management Agency.

FEMA 267. (1995). *"Interim guidelines: evaluation, repair, modification and design of welded steel moment frame structures*," Federal Emergency Management Agency.

FEMA 267A. (1997). *"Interim guidelines advisory No. 1,"* Federal Emergency Management Agency.

FEMA 273 (1997). *"NEHRP Guidelines for the seismic rehabilitation of buildings,"* Federal Emergency Management Agency.

FEMA 274 (1997). *"NEHRP Commentary on the Guidelines for the seismic rehabilitation of buildings,"* Federal Emergency Management Agency.

FEMA 288 (1997). *"Background reports: Metallurgy, Fracture Mechanics, Welding, Moment Connections and Frame Systems Behavior,"* Federal Emergency Management Agency.

FEMA 302 (1997) *"1997 Edition: NEHRP recommended provisions for seismic regulations for new buildings"*, Federal Emergency Management Agency

FEMA 303 (1997) *"1997 Edition: NEHRP recommended provisions for seismic regulations for new buildings, Part 2 - Commentary"*, Federal Emergency Management Agency

Fuchs, H. O., and Stephens, R. I. (1980). *"Metal Fatigue in Engineering,"* John Wiley & Sons

Fuyama, H., Krawinkler, H., and Law, K. H. (1993). "Computer assisted conceptual structural design of steel buildings," *John A. Blume Earthquake Engineering Research Center Report No. 107,* Department of Civil Engineering, Stanford University.

Goel, R. K., and Chopra, A. K. (1997). "Period formulas for moment-resisting frame buildings," *Journal of Struct. Engrg.*, ASCE, Vol. 123, No. 11.

Gupta, A., and Krawinkler, H. (1998). "Effect of stiffness degradation on deformation demands for SDOF and MDOF structures," *Proceedings of the 6th US National Conference on Earthquake Engineering*, May 31 - June 4, 1998, Seattle, Washington.

Kasai, K., and Maison, B. (1999). "Investigation of alternative framing systems with partially restrained connections," *part of FEMA phase II SAC project,* NISEE – University of California at Berkeley.

Kato, B., Aoki, H., and Tagawa, Y. (1984). "Seismic behavior of steel frames with composite girders," *Proceedings, 8th World Conference on Earthquake Engineering*, San Francisco, Vol. VI.

Kilic, S. A. (1996). "Stability issues in frames under lateral loads," *Ph.D. Dissertation*, Department of Civil Engineering, Stanford University, 1996.

Kim, K., and Engelhardt, M. D. (1995). "Development of analytical models for earthquake analysis of steel moment frames," *Report No. PMFSEL 95-2*, Dept. of Civil Engrg., Univ. of Texas at Austin.

Krawinkler, H., Bertero, V. V., and Popov, E. P. (1971). "Inelastic behavior of steel beam-to-column sub-assemblages," *Report No. UCB/EERC-71/07*, Earthquake Engineering Research Center (EERC), University of California at Berkeley.

Krawinkler, H. (1978). "Shear design of steel frame joints," *Engineering Journal*, AISC, Vol. 15, No. 3.

Krawinkler, H., et al. (1983). "Recommendations for experimental studies on the seismic behavior of steel components and materials," *John A. Blume Earthquake Engineering Center*, Report No. 61, Department of Civil Engineering, Stanford University.

Krawinkler, H., and Zohrei, M. (1983). "Cumulative damage in steel structures subjected to earthquake ground motions," *Journal on Computers and Structures*, Vol. 16, No. 1-4.

Krawinkler, H., and Mohasseb, S. (1987). "Effects of panel zone deformations on seismic response," *Journal of Constructional Steel Research*, Elsevier Applied Science Publishers, England, Vol. 8.

Krawinkler, H. (1994). "New trends in seismic design methodology," *Proceedings of the 10th European Conference in Earthquake Engineering*, Vienna, Austria.

Krawinkler, H. et al. (1995). "Seismic demand evaluation for a 4-story steel frame structure damaged in the Northridge earthquake," *The Structural Design of Tall Buildings*, Vol. 5, Number 1, March 1996, pp. 1-27, John Wiley & Sons.

Krawinkler, H., and Gupta, A. (1997). "Deformation and ductility demands in steel moment frame structures," *Proceedings of the 5th International Colloquium on Stability and Ductility of Steel Structures*, Nagoya, Japan, July 29-31, 1997, pp. 57-68.

Krawinkler, H., and Seneviratna, G. D. P. K. (1997). "Pros and cons of a pushover analysis for seismic performance evaluation," *Journal of Engineering Structures*, Vol. 20, No. 4-6, April-June 1998, pp. 452-464

Krawinkler, H., Alavi, B. (1998). "Development of Improved Design Procedures for Near Fault Ground Motions. *SMIP98 Seminar on Utilization of Strong-Motion Data*, Oakland, Sept. 15, 1998.

Krawinkler, H., (1998). Presentation at the *Structural Engineers World Congress*, San Francisco 1998 for paper "Issues and Challenges in Performance Based Seismic Design"

Krawinkler, H., Gupta, A., Luco, N., and Medina, R. (1999). "SAC Testing Programs and Loading Histories", *part of FEMA SAC Phase II project.* NISEE – University of California at Berkeley.

Lawson, R. S., Vance, V. and Krawinkler, H. (1994). "Nonlinear static push-over analysis - why, when, and how?", *Proceedings of the 5th U. S. Conference in Earthquake Engineering*, Vol. 1, Chicago, IL.

Lee, S. J., and Lu, L. W. (1989). "Cyclic tests of full-scale composite joint subassemblages," *Journal of Struct. Engrg.*, ASCE, Vol. 115, No. 8.

Leon, R. T., and Forcier, G. P. (1991). "Performance of semi-rigid composite frames," *Proceedings of the 1991 Annual Technical Session, SSRC*.

Leon, R. T., Hajjar, J. F., and Gustafson, M. A. (1997). "Seismic response of composite moment-resisting connections," *J. of Structural Engineering, to be published*

Liew, J. Y. R., and Chen, W. F. (1995). "Analysis and design of steel frames considering panel joint deformations," *Journal of Struct. Engrg.*, ASCE, Vol. 121, No. 10.

Liew, J. Y. R., White, D. W., and Chen, W.F. (1993a). "Second-order refined plastic-hinge analysis for frame design. Part I," *J. of Struct. Engrg.*, ASCE, Vol. 119, No. 11.

Liew, J. Y. R., White, D. W., and Chen, W.F. (1993b). "Second-order refined plastic-hinge analysis for frame design. Part II," *J. of Struct. Engrg.*, ASCE, Vol. 119, No. 11.

LRFD (1994). "Manual of Steel Construction, Load & Resistance Factor Design, volume I - seismic provisions for structural steel buildings," *American Institute of Steel Construction*, Chicago, IL.

Lu, L. W., Wang, S. J., and Lee, S. J. (1988). "Cyclic behavior of steel and composite joints with panel zone deformation," *Proceedings of the 9th World Conference on Earthquake Engineering*, Vol. IV, Tokyo-Kyoto, Japan.

Luco, N., and Cornell, C. A. (1998). "Effects of random connection fractures on the demands and reliability for a 3-story pre-Northridge SMRF structure," *Proc. of the Sixth US National Conference on Earthquake Engineering*. Seattle, Washington.

MacRae, G. A. (1994). "p-Δ effects on single-degree-of-freedom structures in earthquakes," *Earthquake Spectra*, Vol. 10, No. 3.

MacRae, G. A. (1999). "Effect of ground motion intensity and dynamic characteristics," *part of FEMA phase II SAC Project*, NISEE – University of California at Berkeley.

McCabe, S. L., and Hall, W. J. (1989). "Assessment of seismic structural damage," *Journal of Structural Engineering, Vol. 115, No. 9*

Miranda, E. (1997). "Estimation of maximum interstory drift demands in displacement-based design," *Seismic Design Methodologies for the Next Generation of Codes*, Edited by P. Fajfar and H. Krawinkler, A. A. Balkema, Rotterdam

Nakashima, M. (1991). "Statistical evaluation of strength of steel beam columns," *Journal of Struct. Engrg.*, ASCE, Vol. 117, No. 11.

Nakashima, M. (1994). "Variation of ductility capacity of steel beam-columns," *Journal of Struct. Engrg.*, ASCE, Vol. 120, No. 7.

Nassar, A. A., and Krawinkler, H. (1991). "Seismic demands for SDOF and MDOF systems," *John A. Blume Earthquake Engineering Center Report No. 95*, Department of Civil Engineering, Stanford University.

Osteraas, J. D. and Krawinkler, H. (1990). "Strength and ductility considerations in seismic design," *John A. Blume Earthquake Engineering Research Center Report No. 90*, Department of Civil Engineering, Stanford University.

Park, R., and Paulay, T.(1975). "*Reinforced Concrete Structures*," John Wiley & Sons.

Park, Y. J., Ang, A. H. -S., and Wen, Y. K. (1984). "Seismic damage analysis and damage-limiting design of R.C. buildings," *Structural Engineering Research Series No. 516*, Civil Engineering Studies, University of Illinois at Urbana-Champaign

Popov, E. P., and Stephen, R. M. (1976). "Tensile capacity of partial penetration welds," *Report No. UCB/EERC-76/03*, Earthquake Engineering Research Center (EERC), University of California at Berkeley.

Popov, E. P., Blondet, M., and Stepanov, L. (1996). "Application of dog-bones for improvement of seismic behavior of steel connections," *Report No. UCB/EERC-96/05*, Earthquake Engineering Research Center (EERC), University of California at Berkeley.

Qi, X., and Moehle, J. P. (1991). "Displacement design approach for reinforced concrete structures subjected to earthquakes," *Report No. UCB/EERC-91/02*, Earthquake Engineering Research Center (EERC), University of California at Berkeley.

Rahnama, M., and Krawinkler, H. (1993). "Effects of soft soils and hysteresis models on seismic design spectra," *John A. Blume Earthquake Engineering Center*, Report No. 108, Department of Civil Engineering, Stanford University.

Reinhorn, A., and Naiem, F. (1998). "Effect of deterioration of hysteretic characteristics," *part of FEMA phase II SAC project*, NISEE – University of California at Berkeley.

Ren, W. X., and Zeng, Q. Y. (1997). "Interactive buckling behavior and ultimate load of I-section steel columns," *Journal of Structural Engineering, Vol. 123, No. 9*

Roeder, C. W., Schneider, S. P., and Carpenter, J. E. (1993). "Seismic behavior of moment-resisting steel frames: analytical study," *Journal of Struct. Engrg.*, ASCE, Vol. 119, No. 6.

Roeder, C. W., and Foutch, D. (1996). "Experimental results for seismic resistant steel moment frame connections," *Journal of Structural Engineering, Vol. 122, No. 6*

SAC 95-04, Parts 1 and 2 (1995). "Technical report: Analytical and field investigations of buildings affected by the Northridge earthquake of January 17, 1994," *part of FEMA phase I SAC project, Report No. 95-04*

SAC 95-06 (1995). "Technical report: Surveys and assessment of damage to buildings affected by the Northridge earthquake of July 17, 1994," *part of FEMA phase I SAC project, Report No. 95-06*

SAC 96-01, Parts 1 and 2 (1996). "Technical report: Experimental investigations of beam-column subassemblages," *part of FEMA phase I SAC project, Report No. 96-01*

Saiidi, M. and Sozen, M. A. (1981). "Simple nonlinear seismic analysis of R/C structures," *Journal of the Structural Division,* ASCE, Vol. 107, No. 5.

Schneider, S. P., and Amidi, A. (1998). "Seismic behavior of steel frames with deformable panel zones," *Journal of Struct. Engrg.*, ASCE, Vol. 124, No. 1.

Seneviratna, G. D. P. K., and Krawinkler, H. (1997). "Evaluation of inelastic MDOF effects for seismic design," *John A. Blume Earthquake Engineering Center Report No. 120*, Department of Civil Engineering, Stanford University.

Shome, N, et al. (1997). "Earthquake records and nonlinear MDOF responses," *Report No. RMS-29*, Dept. of Civil Engineering, Stanford University.

Somerville, P., Smith, N., Punyamurthula, S., and Sun, J. (1997). "Development of ground motion time histories for phase 2 of the FEMA/SAC steel project," *SAC Background Document, Report No. SAC/BD-97/04*.

SSPC (1994). "Statistical analysis of tensile data for wide flange structural shapes," Steel Shape Producers Council.

SSRC (1988). "*Guide to stability design criteria for metal structures*," Structural Stability Research Council, 4th Ed., J. Wiley & Sons, New York.

Standards New Zealand (1995). "Concrete structures standard, part I – the design of concrete structures, part II – commentary on the design of concrete structures".

Tagawa, Y., Kato, B., and Aoki, H. (1989). "Behavior of composite beams in steel frame under hysteretic loading," *Journal of Struct. Engrg.*, ASCE, Vol. 115, No. 8.

Tsai, K. C., and Popov, E. P. (1988). "Steel beam-column joints in seismic moment resisting frames," *Report No. UCB/EERC-88/19*, Earthquake Engineering Research Center (EERC), University of California at Berkeley.

Tsai, K. C., and Popov, E. P. (1990). "Seismic panel zone design effect on seismic story drift in steel frames," *Journal of Struct. Engrg.*, ASCE, Vol. 116, No. 12.

UBC (1994). "Structural Engineering Design Provisions," *Uniform Building Code*, Vol. 2, International Conference of Building Officials.

UBC (1997). "Structural Engineering Design Provisions," *Uniform Building Code*, Vol. 2, International Conference of Building Officials.

SEAOC Vision 2000 (1995). "A framework for performance based design, Volumes I, II, & III," *Structural Engineers Association of California (SEAOC).*

Wen, Y. K. (1995). "Building reliability and code calibration," *Earthquake Spectra*, Vol. 11, No. 2.

Wen, Y. K., and Foutch, D. A. (1997). "Proposed statistical and reliability framework for comparing and evaluating predictive models for evaluation and design, and critical issues in developing such framework," *SAC Background Document, Report No. SAC/BD-97/03*.

Wen, Y. K., and Han, S. W. (1997). "Method of reliability-based seismic design. I: Equivalent nonlinear systems," *Journal of Structural Engineering, Vol. 123, No. 3*

Yura, J. A. (1971). "The effective length of columns in unbraced frames," *Engineering Journal*, AISC, April 1971.

Ziemian, R. D., McGuire, W., and Deierlein, G. G. (1992a). "Inelastic limit states design. Part I: Planar frame studies," *Journal of Struct. Engrg.*, ASCE, Vol. 118, No. 9.

Ziemian, R. D., McGuire, W., and Deierlein, G. G. (1992b). "Inelastic limit states design. Part II: Three-dimensional frame study," *J. of Struct. Engrg.*, ASCE, Vol. 118, No. 9.